DOKTORSAVHANDLINGAR
VID
CHALMERS TEKNISKA HÖGSKOLA
Nr 40

CONTRIBUTIONS TO THE KNOWLEDGE OF FLEXURAL CRITICAL SPEEDS

BY

INGEMAR FERNLUND

GÖTEBORG 1963

DOKTORSAVHANDLINGAR
VID
CHALMERS TEKNISKA HÖGSKOLA

CONTRIBUTIONS TO THE KNOWLEDGE OF FLEXURAL CRITICAL SPEEDS

BY

INGEMAR FERNLUND

GÖTEBORG
ELANDERS BOKTRYCKERI AKTIEBOLAG
1963

The following papers are included in this dissertation:

I. "Critical Speeds of a Shaft with Thin Discs". Ingemar Fernlund. Transactions of Chalmers University of Technology, No 260, 1962.

II. "On the Whirling of a Rotor." Ingemar Fernlund. Transactions of Chalmers University of Technology, No 276, 1963.

III. "Running through the Critical Speed of a Rotor." Ingemar Fernlund. Transactions of Chalmers University of Technology, No 277, 1963.

IV. "Notes on Critical Speeds". Ingemar Fernlund. Transactions of Chalmers University of Technology, No 278, 1963.

CONTRIBUTIONS TO THE KNOWLEDGE OF FLEXURAL CRITICAL SPEEDS

AV

INGEMAR FERNLUND

AKADEMISK AVHANDLING

SOM MED TILLSTÅND AV CHALMERS TEKNISKA HÖGSKOLA FRAMLÄGGES TILL OFFENTLIG GRANSKNING FÖR TEKNISK DOKTORSGRADS VINNANDE LÖRDAGEN DEN 14 DECEMBER 1963 KL. 10 Å HÖRSALEN I ADMINISTRATIONSBYGGNADEN VID CHALMERS TEKNISKA HÖGSKOLA, SVEN HULTINS GATA GÖTEBORG.

GÖTEBORG
ELANDERS BOKTRYCKERI AKTIEBOLAG
1963

Correction list

Page /line	Stands	Ought to stand
15/11	[5]	[7]
49/last line	och	and
103/5	51,4448 56,1558	51,5548 56,1448

Preface

The dissertation presents the results from research work on flexural critical speeds during the years 1959—62. It was made at the *Institute of Machine Elements, Chalmers University of Technology, Gothenburg, Sweden*. The Head of the Institute is Professor *B. Jakobsson*. The work has to some extent been sponsored by the *Swedish Technical Research Council, Chalmersska Forskningsfonden*, and *Ogradueräde Forskares Fond*.

I am very much indebted to Professor *Jakobsson* who put me into this interesting field, and I give him my warmest thanks for his great interest in the subject and for many inspiring discussions about the problems.

I thank the *Swedish Technical Research Council, Chalmersska Forskningsfonden, Ogradueräde Forskares Fond*, and the *Publications Committee of Chalmers University of Technology* for their sponsorship.

I have been exceedingly fortunate in getting valuable assistance from numerous members of the staff of the institute. Especially I thank Mr *Bengt Håkansson* for teaching me programming on the digital computer *Alwac III E* in Gothenburg.

Best thanks also to the personnel at *"Institutet för automatisk databehandling"* in Gothenburg for good co-operation.

Ingemar Fernlund

Introduction

Suppose that the machine designer has to control the dynamic properties of the seemingly simple construction in fig. 1, in which all geometrical data, weights, and motor properties are known.

The shaft will run at the speed n_0 (r.p.m.) at which the load torque is M_0 (Nm). The bearing A is a single row deep groove ball bearing and the bearing B a cylindrical roller bearing.

The designer may check the construction in the following way:

1. At a certain motor speed $n = n_c$ the shaft will probably have a rough motion. This speed is called the ordinary critical speed. The shaft whirls around the bearings as a skipping-rope with the angular velocity $N = N_c = n_c$. The shaft deflection and the corresponding shaft stresses at this speed and in its vicinity ought to be determined.

The reports [I] and [IV] give methods for predicting the ordinary critical speed.

2. Knowing the ordinary critical speed n_c he knows if the rotor will work at a sub-critical or post-critical speed. Suppose that the shaft has to run at a post-critical speed n_0. Then it must be controlled if the motor is capable of bringing the shaft through its critical speed.

Hereby report [III] is useful.

3. At the steady state the motor has to supply the rotor with the torque M_0. But besides this torque the motor can give "torque-tones" such as $M_{1s} \sin q_s \omega_0 t$ and $M_{2s} \cos q_s \omega_0 t$, where

M_{1s}, M_{2s} = Amplitudes of the "torque-tone" of order s

q_s = Constant depending on the motor type

t = Time (sec.)

$\omega_0 = \frac{\pi}{30} n_0$ = Angular velocity of the shaft $\left(\frac{\text{rad}}{\text{sec}}\right)$.

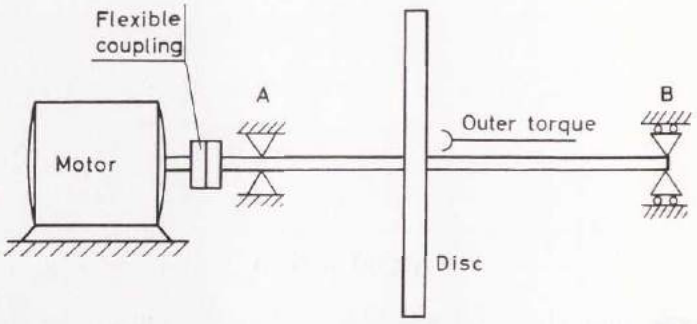

Fig. 1

These "torque-tones" force the shaft to whirl with

$$K = \frac{n}{N} = \frac{1}{1 \mp q_s}$$

With these K-values the shaft has critical whirl speeds N_{cs1} and N_{cs2} and they occur at the motor speeds $n_{cs1} = \frac{N_{cs1}}{1-q_s}$ and $n_{cs2} = \frac{N_{cs2}}{1+q_s}$ respectively.

Hence, it must be controlled if n_0 is such a "secondary" critical speed with a great "torque-tone-amplitude". Such an amplitude can give rise to large shaft deflections and stresses. The influence of such disturbing "torque-tones" is studied in [II].

4. Suppose that n_0 is not a secondary critical speed. In spite of this the shaft can be unable to work satisfactory. In a system as in fig. 1 two kinds of damping can be separated. The construction consists of both rotating and fixed elastic sections. The friction between the stationary and the rotating parts is called e x t e r n a l friction and the friction within the rotating parts i n t e r n a l friction. It can be shown [5, 21] that the hysteresis effect of the shaft material has the same action as internal friction. In this dissertation both kinds of damping are approximated to be viscous. The damping coefficients can be looked upon as "equivalent" coefficients [4]. The external damping always limits the shaft deflection or the deflection of the centre of gravity. On the contrary the internal damping under certain conditions can increase these deflections.

Thus, it may happen that the speed n_0 is in a region where the motion of the disc is unstable. Such cases are treated in [II] and [III].

The example shows the main problems concerning the control of the dynamic properties of a rotor.

Of course, it has not been possible to point out all phenomena treated in the reports [I], [II], [III], and [IV]. Therefore, some special matters from the contents of these reports are given a more exhaustive account.

Determination of the Flexural Critical Speeds of a Rotor

In the introduction a special bearing arrangement was supposed and it was mentioned that the ordinary critical speed could be calculated with the aid of [I]. Also other bearing arrangements are considered there and a survey is given in tab. 2. It is shown that the critical whirling speeds of such shafts can be written

$$N_{ci} = \frac{30}{\pi} \sqrt{\frac{1}{A^{**}} \cdot \frac{EI}{ML^3}} \qquad (i = 1, 2, 3, \ldots) \text{ (r.p.m.)}$$

Here

E = Modulus of elasticity in tension and compression $\left(\frac{\mathrm{N}}{\mathrm{m}^2}\right)$

I = Moment of inertia of the cross section of the shaft (m^4)

M = Mass of the disc (kg)

L = Length of the shaft (m)

The value A^{**} is obtained from

$$A^{**} = \frac{m}{M} \cdot \frac{1}{\lambda^4}$$

where m is the mass of the shaft (kg) and λ is solved from the equations

$$\left.\begin{aligned} \frac{m}{M} &= \lambda \cdot \frac{A(\lambda) + \Theta^* \lambda^3 B(\lambda)}{C(\lambda) + \Theta^* \lambda^3 D(\lambda)} \\ \Theta^* &= \frac{2\gamma I_p}{mL^2} \\ \gamma &= \frac{1}{2}\left(K - \frac{1}{2}\right) \end{aligned}\right\}$$

The functions $A(\lambda)$, $B(\lambda)$, $C(\lambda)$, and $D(\lambda)$ can be found in tab. 2 for some kinds of supports. Concerning further notations reference is made to [I].

Order	Kind of support	A	B	C	D
1	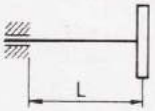	$\sin\lambda\,\mathrm{ch}\lambda-\cos\lambda\,\mathrm{ch}\lambda$	$1-\cos\lambda\,\mathrm{ch}\lambda$	$1+\cos\lambda\,\mathrm{ch}\lambda$	$\sin\lambda\,\mathrm{ch}\lambda+\cos\lambda\,\mathrm{ch}\lambda$
2	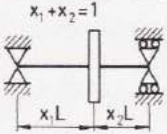	$\frac{1}{2}\left\{\frac{1}{\cot\varphi+\cot\psi}-\frac{1}{\mathrm{cth}\varphi+\mathrm{cth}\psi}\right\}$	$\frac{1}{4}\cdot\frac{(\mathrm{tg}\varphi-\mathrm{tgh}\varphi)\ (\mathrm{tg}\psi-\mathrm{tgh}\psi)}{(\mathrm{tg}\varphi+\mathrm{tg}\psi)\ (\mathrm{tgh}\varphi+\mathrm{tgh}\psi)}$	1	$-\frac{1}{2}\left\{\frac{1}{\mathrm{tg}\varphi+\mathrm{tg}\psi}-\frac{1}{\mathrm{tgh}\varphi+\mathrm{tgh}\psi}\right\}$
3	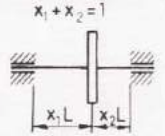	$(N^2+KP)\ (RU-ST)+$ $+(S^2+RT)\ (KQ-NP)$	$(N^2+KP)\ (S^2+RT)$	$(N^2+KP)(U^2+RT)+(S^2+RT)\times$ $(Q^2+KP)+(NP-KQ)\ (RS-$ $-TU)+(KN-PQ)\ (ST-RU)$ $-(P^2+NQ)\ (R^2+SU)-$ $-(K^2+NQ)\ (T^2+SU)$	$-(N^2+KP)\ (RS-TU)+$ $+(S^2+RT)\ (PQ-KN)$
4	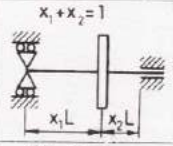	$(N_0P_0-K_0Q_0)\ (RU-ST)-$ $-2K_0N_0(S^2+RT)$	$(N_0P_0-K_0Q_0)\ (S^2+RT)$	$N_0P_0(R^2-S^2-T^2+U^2)+$ $+K_0Q_0(R^2+S^2-T^2-U^2)+$ $+2P_0Q_0(ST-RU)+2K_0N_0\times$ $(RS-TU)$	$-(N_0P_0-K_0Q_0)\ (RS-TU)$ $-2P_0Q_0(S^2+RT)$
5	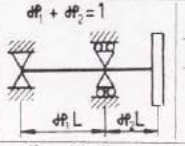	$-2\left\{K_1N_1(S_0T_0-R_0U_0)-\right.$ $\left.-(K_1-N_1)R_0T_0\right\}$	$K_1N_1\left\{(S_0-U_0)^2+R_0^2-T_0^2\right\}-$ $-(K_1-N_1)\ (S_0T_0-R_0U_0)$	$K_1N_1\left\{(S_0+U_0)^2+R_0^2-T_0^2\right\}+$ $+(K_1-N_1)\ (S_0T_0-R_0U_0)$	$2\left\{K_1N_1(R_0U_0+S_0T_0)+\right.$ $\left.+(K_1-N_1)S_0U_0\right\}$
6	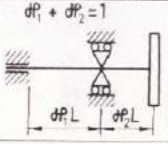	$2\left\{(N_0N-Q_0K)\ (T_0S-U_0R)+\right.$ $\left.+R_0T_0(N^2+KP)\right\}$	$-(N_0N-Q_0K)\ (S^2+RT)+$ $+(S_0R-R_0S)\ (N^2+KP)$	$-(N_0N-Q_0K)\ [U^2+2(T_0T-$ $-T_0^2)+RT-4T_0^2]+(N^2+$ $+KP)\ (S_0T_0-R_0U_0)$	$2\left\{S_0U_0(N^2+KP)-\right.$ $\left.-(N_0N-Q_0K)\ (U_0T+T_0S)\right\}$

Tab. 2 (Part I: p. 107)

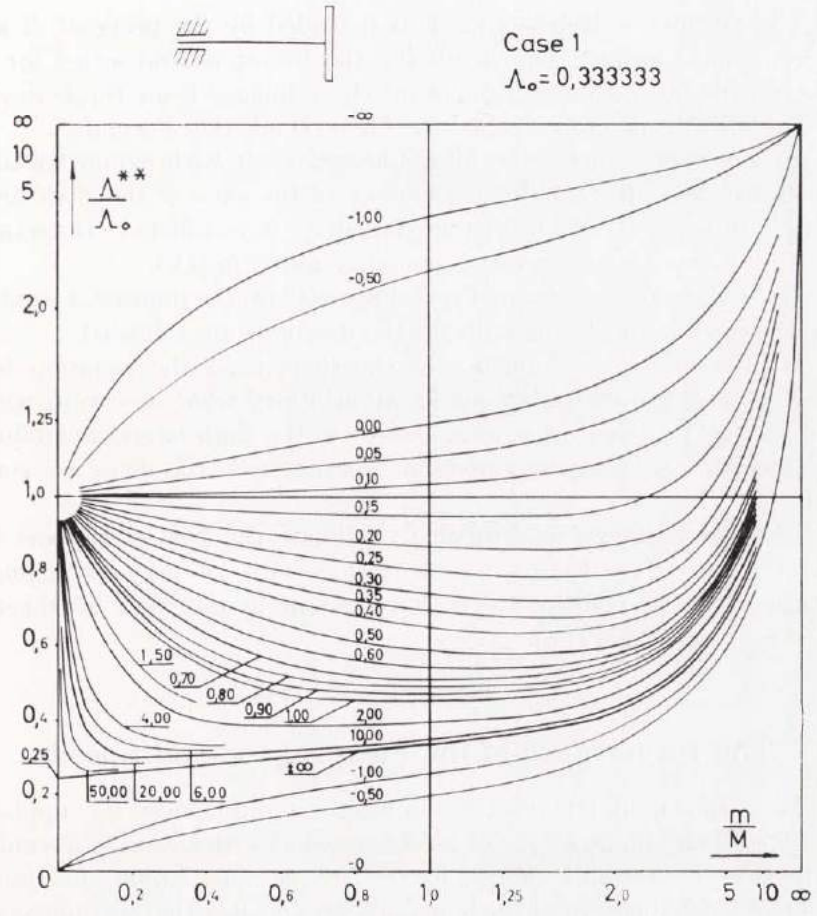

Fig. 3 (Part I: p. 118)

In [I] diagrams are drawn with $\frac{\Lambda^{**}}{\Lambda_0}$ as a function of $\frac{m}{M}$ for different values of the "gyroscopic" parameter Θ^*. The "non-dimensional critical speed" Λ_0 is obtained by neglecting the mass of the shaft and the gyroscopic effect (elementary value). For $\Theta^* > 0$ only the first critical speed is considered but for $\Theta^* < 0$ the first two critical speeds are accounted for. The diagrams can be used for any kind of whirl. An example of such a diagram is given in fig. 3. The curves are valid for the clamped-free rotor shown in the vignette of the figure.

In 1961 *Wojnowski* and *Faucette* [23] presented the solution of Case 2 in tab. 2. In their diagrams the gyroscopic effect was not considered.

The use of the diagrams in [I] is extended by the proposal of an approximate formula for calculating the lowest critical speed for a shaft with several discs. Because of the influence from Dunkerley's well-known formula it is called the "New Dunkerley Formula".

In one case, viz. for the hinged-hinged shaft with symmetrically mounted discs, the simultaneous action of the mass of the shaft and the gyroscopic effects from two thin discs is considered. Diagrams for rapid calculations in this case can be found in [IV].

In "Tables for Calculating Critical Speeds" [8] the numerical results which are the underlying stuff for the diagrams are collected.

By neglecting the influence of the shaft mass the equation for determining the critical speeds for an arbitrary whirl of a rotor with an arbitrary number of discs is derived in [I]. Both lateral flexibility of the bearings and the gyroscopic actions from the discs are considered.

In practice it can be difficult to estimate the kind of support in an accurate way. Hence, a bearing has both lateral and angular stiffness. These matters are to some extent investigated by theory and experiments in [IV].

The Importance of the Flexural Critical Speeds

It is shown in [II] that an unbalanced rotor must be supplied with a certain input torque to be able to whirl with a certain K-value. The shaft deflection is limited by the "torque-tone" amplitude. But a perfectly balanced rotor without any friction has the possibility to whirl with an arbitrary K-value with an arbitrary deflection of the shaft at zero input torque. This is shown in [IV]. It is also derived that an increase of the shaft deflection demands an outer force. If such a force is applied the change in kinetic energy is equal to the change in potential energy.

Tests were carried out for studying the whirling [II] and the test apparatus is principally sketched in fig. 4.

With capacitive pick-ups mounted in two perpendicular directions the motion of the disc centre could be seen on an oscilloscope screen. At some critical states the traces of the disc centre are drawn in fig. 5 and a visible comparison between theory and tests can be done. The figures are taken from [II] in which also other "whirl curves" are presented.

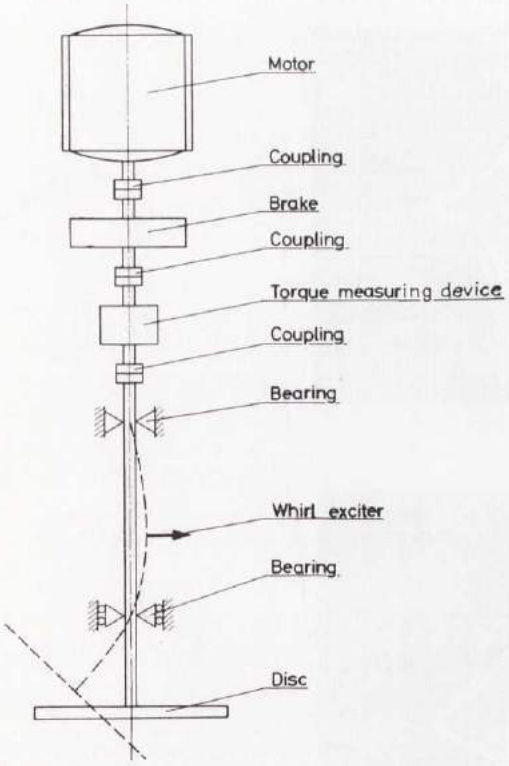

Fig. 4 (Part II: p. 62)

For the ordinary critical speed ($K = 1$) two cases must be separated. The input torque for maintaining the whirl of an unbalanced rotor at a non-critical state is zero. Only at the critical state an input torque is required. Then the demand for torque increases with time and so does the shaft deflection. The result can be interpreted as follows. Because the motor has a limited capacity of supplying torque it can maintain the whirl only when the torque needed can be supplied. In other cases the whirl must change.

If, on the other hand, a rotor with external damping is considered, a certain constant torque must maintain the whirl. This torque is different at different speeds and is proportional to the shaft deflection.

It must be emphasized that it is not dangerous to run a rotor at its critical speeds if the shaft stress is lower than the yield point stress. This statement is settled for dispersing the mysticism around the conception "critical speeds". It is evident that there are cases at which these speeds hardly ought to be named critical.

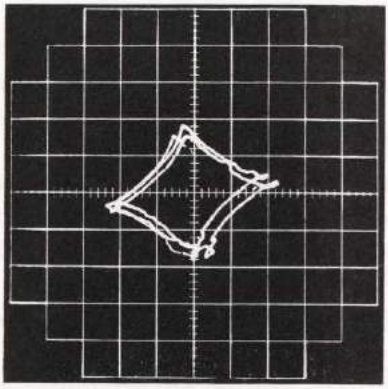

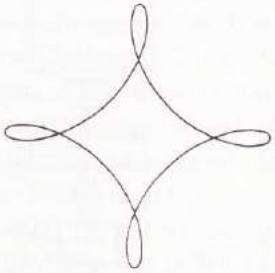

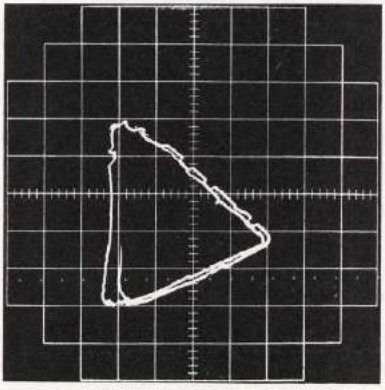

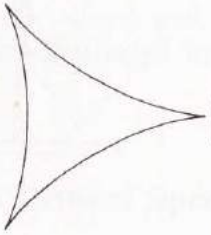

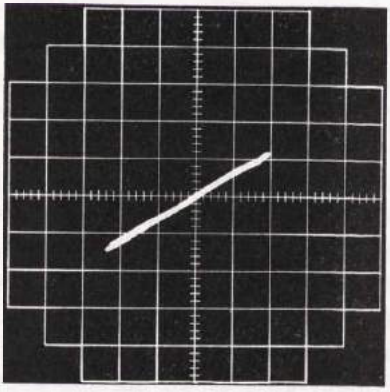

Fig. 5 (Part II: p. 68)

On Passing the Flexural Critical Speed

When starting or stopping a rotor it must pass an infinite number of critical speeds corresponding to a series of K-values. As has been mentioned only a limited number occur at uniform motor speeds. The behaviour of a rotor when it is accelerated or decelerated through secondary critical states and the ordinary critical speed is investigated theoretically by assuming u n i f o r m acceleration or deceleration or a l i n e a r l y varying deceleration. As could be expected no pecularities could be seen at the secondary critical states.

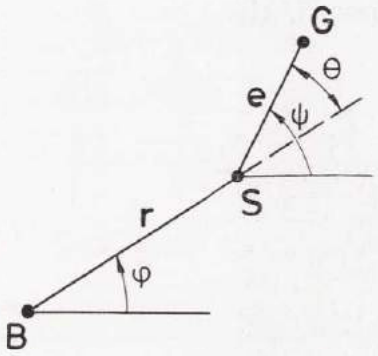

Fig. 6

Test have been carried out for verifying the theories. In some tests the relative positions of the points B, S, and G were photographed by a "slow motion camera" when the rotor passed its ordinary critical speed [III].

Fig. 6 is obtained by cutting the disc in fig. 1 by a plane through the disc.

The notations are:

B = Centre line between the bearings
S = Centre of the shaft
G = Centre of gravity of the disc

e = Eccentricity
r = Shaft deflection
φ = "Whirl" angle
ψ = "Motor" angle
ϑ = $\psi - \varphi$

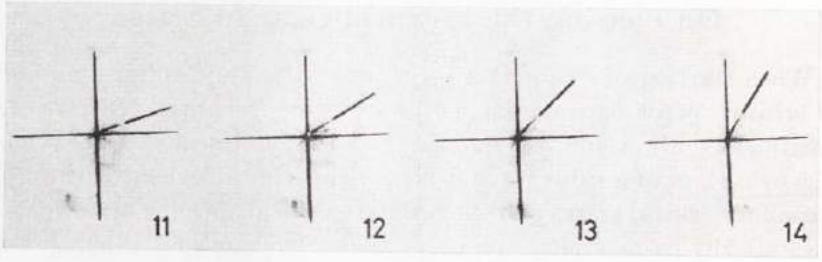

Sub-critical constant speed ($\theta = 0°$) (11—14).

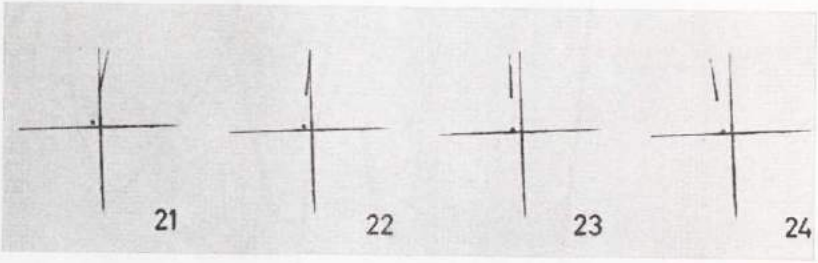

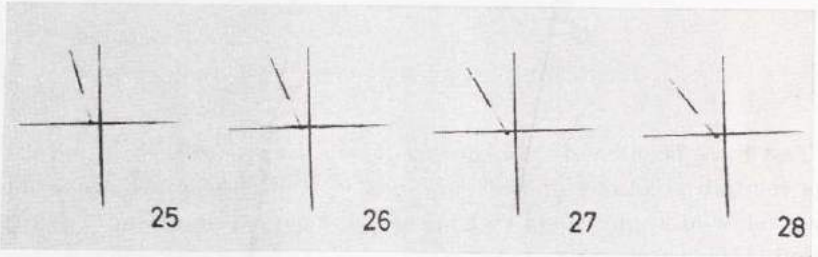

Post-critical speeds just above the critical speed ($\theta \approx 90°$) (21—28).

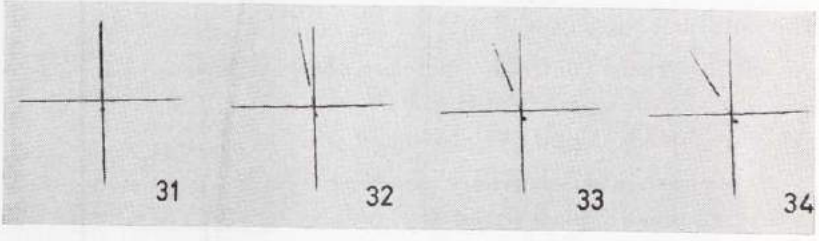

Post-critical constant speed ($\theta = 180°$) (31—34).

Fig. 7 (Part III: p. 49)

A hinged-hinged-free rotor was filmed during acceleration through its ordinary critical state. The shaft was accelerated from 900 r.p.m. The critical speed was 1158 r.p.m. Three characteristic pieces from this film are shown in fig. 7. The "hair-cross" is the point B and the broken line indicates the direction of the line SG.

This test and others are accounted for in [III]. There diagrams are also collected showing the shaft deflection during different accelerations (decelerations), start speeds, and external damping coefficients.

In [III] also the action of a deflection limiter is investigated. Hereby the remarkable result was obtained that the most important property of the deflection limiter was that of producing tangential forces on the shaft. A deflection limiter without friction will act as an amplifier for the shaft deflection.

References

1. Aitken, A. C.: Determinants and Matrices. Oliver and Boyd, 1959.
2. Biezeno-Grammel: Technische Dynamik. Julius Springer, 1939.
3. Capello, Andrea: Transients in Simple Undamped Oscillators Under Inertial Disturbances. Journal of Applied Mechanics, March, 1960.
4. Den Hartog: Mechanical Vibrations. Mc Graw-Hill, 1956.
5. Dimentberg, F. M.: Flexural Vibrations of Rotating Shafts. Butterworths, 1961.
6. Dornig, Antongiulio: Transients in Simple Undamped Oscillators Under Inertial Disturbances. Journal of Applied Mechanics, June, 1959.
7. Ellington, I. P. and Mc Callion, H.: On Running a Machine through its Resonant Frequency. Journal of the Royal Aeronautical Society, September, 1956, Vol. 60.
8. Fernlund, I.: Tables for Calculating Critical Speeds of a Shaft with Thin Discs. (Available only at the Library of Chalmers University of Technology, Gothenburg, Sweden), 1960.
9. Grammel, R.: Der Kreisel. Springer-Verlag, 1950.
10. Hahn, E.: Note sur la vitesse critique des arbres et la Formule de Dunkerley. Schweiz, Bauztg., Bd 72, 1918.
11. Jakobsson, B.: The Semi-Inverted Diagram, Engineers' Digest January, Volume 5, No. 1, 1948.
12. Kamke, E.: Differential Gleichungen. Akademische Verlagsgesellschaft, Leipzig, 1943.
13. Kane, T. R.: An Addition to the Theory of Whirling. Journal of Applied Mechanics, Sept., 1961.
14. Kopal, Z.: Numerical Analysis. Chapman & Hull Ltd, London, 1955.
15. Lewis, F. M.: Vibration During Acceleration Through a Critical Speed. Transactions A. S. M. E., 54, 1932.
16. Malmqvist, Stenström, Danielsson: Matematisk Analys. Natur och Kultur, 1952.
17. Palmgren, A.: Ball and Roller Bearing Engineering, 3rd Edition. 1959.
18. Schröder, Paul: Die kritischen Zustände zweiter Art raschumlaufender Wellen. Dissertation, Stuttgart, 1924.
19. Stodola, A.: Dampfturbinen, 6. Auflage. Springer, 1924.
20. Timoshenko, S.: Strength of Materials, Part II. D. van Nostrand Company, Inc., New York.
21. Timoshenko, S. and Young, D. H.: Vibration Problems in Engineering.
22. Watson, G. N.: Bessel Functions. Cambridge, 1944.
23. Wojnowski, Reyton and Faucett, Thomas: Critical Speeds of Two Bearing Machines with Overhung Weight. Journal of Engineering for Industry, November, 1961.
24. Zurmühl, R.: Matrizen. Springer-Verlag, 1958.

GÖTEBORG 1963
ELANDERS BOKTRYCKERI AKTIEBOLAG

CHALMERS TEKNISKA HÖGSKOLAS HANDLINGAR
TRANSACTIONS OF CHALMERS UNIVERSITY OF TECHNOLOGY
GOTHENBURG, SWEDEN
Nr 260 (Avd. Maskinteknik 27) 1962

CRITICAL SPEEDS OF A SHAFT WITH THIN DISCS

BY

INGEMAR FERNLUND

Report No. 19 from the Institute of Machine Elements
Chalmers University of Technology
Gothenburg, Sweden
1962

Av Chalmers Tekniska Högskolas Handlingar hava tidigare utkommit:

Fullständig förteckning över Chalmers Tekniska Högskolas Handlingar
lämnas av Chalmers Tekniska Högskolas Bibliotek, Göteborg.

175. Zimen, K. E., *Diffusion von Edelgasatomen die durch Kernreaktion in festen Stoffen gebildet werden.* 7 s. 1956. Kr. 2: —. (Institutionen för Kärnkemi. 1.)
176. Inthoff, W., und Zimen, K. E., *Kinetik der Diffusion radioaktiver Edelgase aus festen Stoffen nach Bestrahlung.* 16 s. 1956. Kr. 4: —. (Institutionen för Kärnkemi. 2.)
177. Granholm, Hjalmar, *Puts och lättbetong.* 45 s. 1956. Kr. 3: —. (Avd. Väg- och Vattenbyggnad. Byggnadsteknik. 24.)
178. Olving, Sven, *A new method for space charge wave interaction studies. I.* 12 s. 1956. Kr. 3: —. (Avd. Elektroteknik. 51.)
179. Hansbo, Sven, *The critical load of rectangular frames analysed by convergence methods.* 47 s. 1956. Kr. 11: —. (Avd. Väg- och Vattenbyggnad. Byggnadsteknik. 25.)
180. Westberg, Vidor, *Measurements of noise radiation at 10 cm. from glow lamps. Preliminary report.* 14 s. 1956. Kr. 4: 50. (Avd. Elektroteknik. 52.)
181. Svensson, S. I., Hellgren, G., and Perers, O., *The Swedish radioscientific solar eclipse expedition to Italy, 1952. Preliminary report.* 30 s. 1956. Kr. 8: —. (Avd. Elektroteknik. 53.)
182. Wax, Nelson, *A note on design considerations for a proposed auroral radar.* 16 s. 1957. Kr. 3: —. (Avd. Elektroteknik. 54.)
183. Joshi, G. H., *The electromagnetic interaction between two crossing electron streams. I.* 31 s. 1957. Kr. 8: —. (Avd. Elektroteknik. 55.)
184. Smith, Bengt, *Dry methods for removing hydrogen sulphide from gases.* 65 s. 1957. Kr. 15: —. (Avd. Kemi och Kemisk Teknologi. 34.)
185. Ekelöf, S., Björk, N., and Davidson, R., *Large signal behaviour of directly heated thermistors.* 31 s. 1957. Kr. 8: —. (Avd. Elektroteknik. 56.)
186. Carlsson, Bengt, und Larsson, Hans, *Wirkungsgrad und Selbsthemmung einfacher Umlaufgetriebe.* 48 s. 1957. Kr. 9: —. (Avd. Maskinteknik. 8.)
187. Aurell, Carl G., *The equivalent transmission line of a linear four-terminal network. Calculations with cascade-connected four-terminal networks.* 39 s. 1957. Kr. 6: —. (Avd. Elektroteknik. 57.)
188. Lundholm, R., *Induced overvoltage-surges on transmission lines and their bearing on the lightning performance at medium voltage networks.* 117 s. 1957. Kr. 19: —. (Avd. Elektroteknik. 58.)
189. Floberg, Leif, *The infinite journal bearing, considering vaporization.* 83 s. 1957. Kr. 13: —. (Avd. Maskinteknik. 9.)
190. Jakobsson, Bengt, and Floberg, Leif, *The finite journal bearing, considering vaporization.* 117 s. 1957. Kr. 19: 50. (Avd. Maskinteknik. 10.)
191. Chako, Nicholas, *Characteristic curves on planes in the image space.* 49 s. 1957. Kr. 15: —. (Avd. Allmänna Vetenskaper. 12.)
192. Ekelöf, Stig, *The development and decay of the magnetic flux in a non-delayed telephone relay.* 50 s. 1957. Kr. 15: —. (Avd. Elektroteknik. 59.)
193. Björklund, Kjell, *Bestämning av porslins draghållfasthet.* 78 s. 1958. Kr. 15: —. (Institutionen för Silikatkemisk Forskning. 39.)
194. Granholm, Per, *Sound insulation of single leaf walls.* 48 s. 1958. Kr. 8: —. (Avd. Väg- och Vattenbyggnad. Byggnadsteknik. 26.)
195. Granholm, Hjalmar, *Om vattengenomslag i murade väggar med särskild hänsyn till tegel som fasadmaterial.* 172 s. 1958. Kr. 16: —. (Avd. Väg- och Vattenbyggnad. Byggnadsteknik. 27.)
196. Meos, Johan, and Olving, Sven, *On the origin of radar echoes associated with auroral activity.* 20 s. 1958. Kr. 5: —. (Avd. Elektroteknik. 60.)
197. Joshi, G. H., *The electromagnetic interaction between two crossing electron streams. II.* 10 s. 1958. Kr. 3: 50. (Avd. Elektroteknik. 61.)
198. Wilhelmsson, Hans, *The interaction between an obliquely incident plane electromagnetic wave and an electron beam. II.* 32 s. 1958. Kr. 7: —. (Avd. Elektroteknik. 62.)
199. Kärrholm, Gunnar, *A method of iteration applied to beams resting on springs.* 50 s. 1958. Kr. 12: —. (Avd. Allm. Vetenskaper. 13.)
200. Jakobsson, Bengt, and Floberg, Leif, *The partial journal bearing.* 60 s. 1958. Kr. 14: —. (Avd. Maskinteknik. 11.)
201. Kärrholm, Gunnar, *Influenced functions of elastic plates divided in strips.* 18 s. 1958. Kr. 4: 50. (Avd. Väg- och Vattenbyggnad. Byggnadsteknik. 28.)

Forts. å omsl. 3:dje sida

CHALMERS TEKNISKA HÖGSKOLAS HANDLINGAR
TRANSACTIONS OF CHALMERS UNIVERSITY OF TECHNOLOGY
GOTHENBURG, SWEDEN
Nr 260 (Avd. Maskinteknik 27) 1962

CRITICAL SPEEDS OF A SHAFT WITH THIN DISCS

BY

INGEMAR FERNLUND

Report No. 19 from the Institute of Machine Elements
Chalmers University of Technology
Gothenburg, Sweden
1962

SCANDINAVIAN UNIVERSITY BOOKS
AKADEMIFÖRLAGET-GUMPERTS, GÖTEBORG

Contents

1. Introduction

To many engineers the conception "critical speed" of a shaft has a deterrent effect. It often depends upon the fact that in most cases these speeds cause much trouble and the determination of them is tedious and cumbersome.

The common procedure is to calculate the lowest critical speed with some approximate method, for example that of Dunkerley, which is explained at the end of the book.

However, most of these methods cannot be used when higher critical speeds are wanted. In these cases this book is intended to be a help for the designer. All waste of time on derivations is avoided. The equations giving the critical speeds are shown in their final form for most of the cases occurring in practice.

The literature on the subject does not develop the theory for flexible bearings. Here is shown that this flexibility of the supports hardly renders any difficulties of the calculation.

Many times it is possible to neglect the gyroscopic effects of the flywheels. On the other hand it must be involved in an accurate computation. The equations for the critical speeds in these cases are also given.

Further it is shown how the simultaneous influence of the inertia of the flywheel and the mass of the shaft affect the critical speeds of a shaft with one flywheel. Diagrams simplify the calculations in this case.

In this book an improved Dunkerley approximation is suggested with the aid of which these diagrams are of value even when the shaft is equipped with several discs.

In the book only thin discs are considered. The theory is also valid in a special case for a thick disc, viz. when the mounting zone is small.

2. Notation

A	Arbitrary constant
B	Arbitrary constant. Centre of bearing
C	Arbitrary constant. Non-dimensional spring constant
D	Arbitrary constant
E	Modulus of elasticity in tension and compression
F	Force
G	Centre of gravity
I	Moment of inertia of a cross section $[L^4]$
I_p	Polar moment of inertia of a disc $[ML^2]$
I_e	Equatorial moment of inertia of a disc $[ML^2]$
L	Length of a shaft
M	Mass. Bending moment
M_{ref}	Reference mass
M_g	Bending moment due to the gyroscopic effect
O	Origin
P	Point
Q	Point on a shaft
R	Radius of a disc
S	Centre of a shaft
c	Spring constant
e	Excentricity
$f = \frac{\omega}{\Omega}$	Ratio
i	Number of order
k	Constant or radius of inertia
l	Distance
n	Number of the discs. R.p.m.
r	Radius
s	Number of order
t	Time
v	Angle
x	Coordinate
y	Deflection
z	Coordinate

Θ	Angle
$\Theta^* = \frac{2\gamma I_p}{mL^2}$	Non-dimensional moment of inertia
$\Theta_M = \frac{M_{ref}\Omega^2}{c} \cdot \Lambda$	Non-dimensional constant
$\Theta_I = \frac{I_{ref}\Omega^2}{L^2 c} \cdot \Lambda$	Non-dimensional constant
$\Lambda = \frac{kEI}{M_{ref}L^3\Omega^2}$	Non-dimensional "critical speed"
Ω	Angular velocity of the whirl
α	Influence number concerning displacements
β	Influence number concerning rotations
$\gamma = \frac{1}{2}\left(\frac{\omega}{\Omega} - \frac{1}{2}\right)$	Constant
δ	Displacement
ε	Number
ζ	Non-dimensional influence number concerning rotations. Coordinate axis
η	Non-dimensional displacement
$\varkappa$	Non-dimensional constant
λ	Non-dimensional constant $\left(\lambda^4 = \frac{mL^3\Omega^2}{EI}\right)$
μ	Non-dimensional weight of a disc $\left(\text{or } \mu = \frac{m}{M}\right)$
$\nu = \frac{2\gamma I_p}{ML^2}$	Non-dimensional moment of inertia $\left(\text{or } \nu = \frac{\lambda^4}{96}\right)$
ξ	Non-dimensional influence number concerning displacements. Coordinate axis
ϱ	Constant
$\varphi = x_1\lambda$	Argument
$\psi = (1-x_1)\lambda$	Argument
ω	Angular velocity of the rotation of the shaft

Indices:

crit	With reference to the critical condition
F	With reference to a force
M	With reference to a moment. (In the connection with Θ M refer to a mass and with I to a moment of inertia)
stat	With reference to a static load

3. The Meaning of Critical Speeds

Before studying the nature of critical speeds the conception influence number is introduced. Consider the beam in fig. 9.1. It is loaded by a unit force at the point Q_1. The deflection under the force is noted by α_{11} and the deflection in another point Q_2 is noted by α_{21}. The first index indicates the position of the deflection and the second one the position of the unit force.

Now place this force in the point Q_2 according to fig. 9.2. The deflection under the unit force is now α_{22} and the one in the point Q_1 is α_{12}.

Maxwell has shown (see for instance [3]), that $\alpha_{12} = \alpha_{21}$ independent of the way of supporting the beam. Observe that this connection only concerns elastic deflections in the beam.

If, on the other hand, the beam is loaded by two unit forces as in fig. 9.3, and the deflection y_3 in the point Q_3 is wanted, the method of superposition is used. The forces Q_1 and Q_2 give in Q_3 the deflections α_{31} and α_{32} respectively. Thus we get

$$y_3 = \alpha_{31} + \alpha_{32}$$

Now the forces in the points Q_1 and Q_2 are changed from unity to F_1 and F_2, the deflection in Q_3 will be

$$y_3 = F_1\alpha_{31} + F_2\alpha_{32}$$

The deflection α_s in a point Q_s of a bar loaded by n forces F_1, F_2, $F_3 \ldots F_n$ is analogously

$$y_s = F_1\alpha_{s1} + F_2\alpha_{s2} + F_3\alpha_{s3} + \ldots + F_n\alpha_{sn}$$

or shorter

$$y_s = \sum_{i=1}^{n} F_i\alpha_{si} \quad \ldots\ldots\ldots\ldots\ldots\ldots\ldots\ldots\ldots\ldots \quad 8.1$$

Turning over to a special example consider the shaft in fig. 10.1. The flywheels are thin and their points of gravity are in one plane.

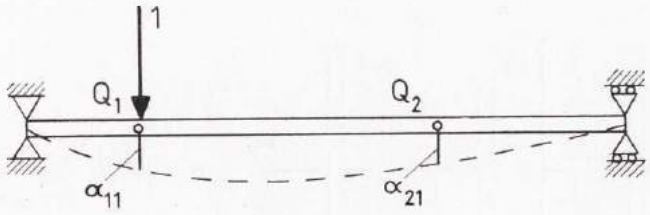

Fig. 9.1

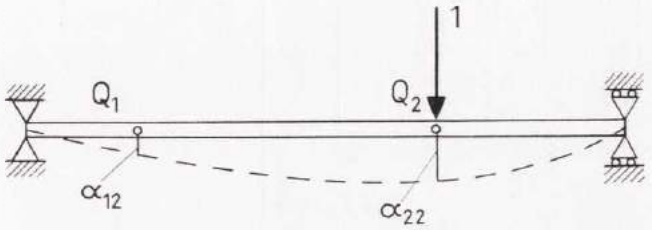

Fig. 9.2

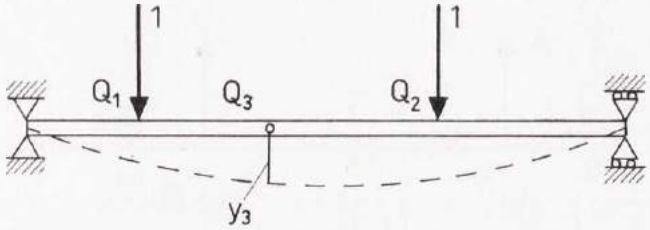

Fig. 9.3

The influence of the inertia forces from the shaft and the gyroscopic effect of the shaft and the flywheels are neglected.

The masses, their locations and the distances between the centres of gravity and the central line of the bearings are shown in the same figure.

When the shaft stands still the resulting torque about the central line of the bearing is

$$\left(\varepsilon Mg \cdot \frac{e}{\varepsilon} - Mg \cdot 2e + \varepsilon Mg \cdot \frac{e}{\varepsilon}\right) \sin v$$

which is identically equal to zero. The plane containing the gravity points makes the angle v with the vertical plane as fig. 10.2 shows. The shaft is said to be statically balanced.

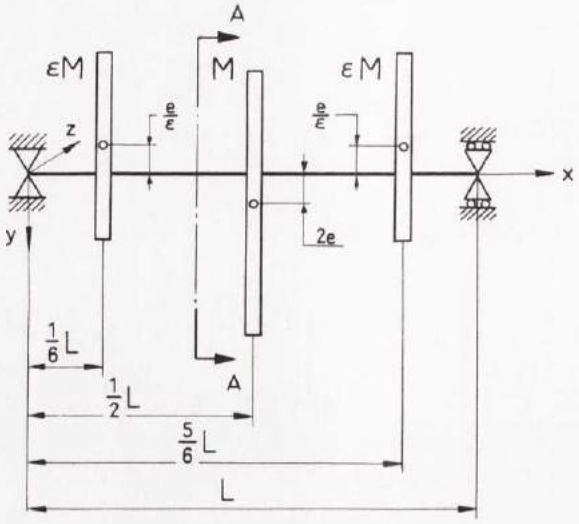

Fig. 10.1

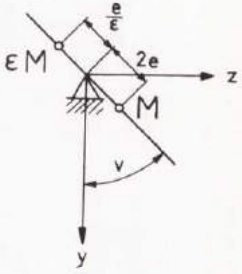

Fig. 10.2

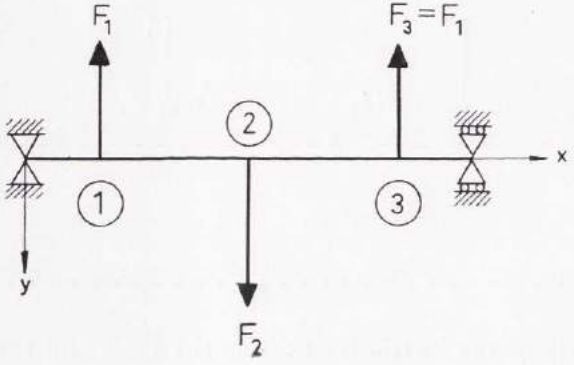

Fig. 10.3

If the shaft is given the angular velocity Ω it will be affected by the forces F_1, F_2, and F_3 according fig. 10.3, where, if the shaft is rigid,

$$\left.\begin{aligned} F_1 = F_3 &= \varepsilon M \cdot \frac{e}{\varepsilon} \cdot \Omega^2 = Me\Omega^2 \\ F_2 &= M \cdot 2e\Omega^2 = 2Me\Omega^2 \end{aligned}\right\}$$

It is assumed that the gravity forces are small in comparison with F_1, F_2, and F_3.

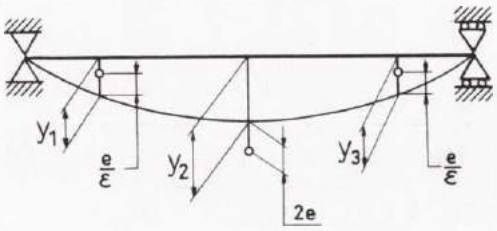

Fig. 11.1

The equations of equilibrium gives

$$\left.\begin{aligned} -(A+B) &= F_1-F_2+F_3 = Me\Omega^2-2Me\Omega^2+Me\Omega^2 \equiv 0 \\ -(A-B)\cdot\frac{L}{2} &= F_1\cdot\left(\frac{L}{2}-\frac{L}{6}\right)-F_3\cdot\left(\frac{L}{2}-\frac{L}{6}\right)\equiv 0 \end{aligned}\right\}$$

where A and B are reaction forces in the bearings.

Thus we get $A = B = 0$.

The shaft is said to be dynamically balanced. However, if the flexibility of the shaft is taken into account other conditions are valid.

If the deflections of the shaft at the flywheels in this case are y_1, y_2, and y_3 respectively, the eq. 8.1, gives with the aid of fig. 11.1,

$$\left.\begin{aligned} y_1 &= F_1\alpha_{11}+F_2\alpha_{12}+F_3\alpha_{13} \\ y_2 &= F_1\alpha_{21}+F_2\alpha_{22}+F_3\alpha_{23} \\ y_3 &= F_1\alpha_{31}+F_2\alpha_{32}+F_3\alpha_{33} \end{aligned}\right\} \quad \ldots\ldots\ldots\ldots \quad 11.2$$

where

$$\left.\begin{aligned} F_1 &= \varepsilon M\left(y_1-\frac{e}{\varepsilon}\right)\Omega^2 \\ F_2 &= M\,(y_2+2e)\Omega^2 \\ F_3 &= \varepsilon M\left(y_3-\frac{e}{\varepsilon}\right)\Omega^2 \end{aligned}\right\} \quad \ldots\ldots\ldots\ldots\ldots \quad 11.3$$

Continuing with the influence numbers we have to calculate the deflections α_{11}, α_{12}, α_{13}, and α_{22} in the figs. 12.1 and 12.2.

By symmetry we get $\alpha_{12} = \alpha_{32}$, and from the reciprocal theorem of Maxwell we get $\alpha_{12} = \alpha_{21}$, $\alpha_{13} = \alpha_{31}$, and $\alpha_{23} = \alpha_{32}$.

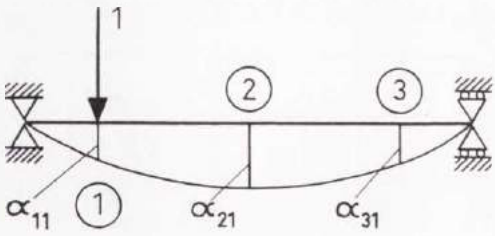

Fig. 12.1

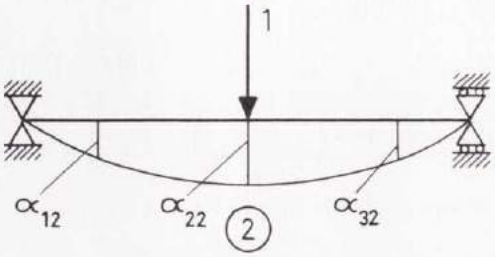

Fig. 12.2

From a handbook is obtained

$$\left.\begin{aligned} \alpha_{11} &= \frac{25}{3888}\cdot\frac{L^3}{EI} \\ \alpha_{12} = \alpha_{21} = \alpha_{32} &= \frac{39}{3888}\cdot\frac{L^3}{EI} \\ \alpha_{13} = \alpha_{31} &= \frac{17}{3888}\cdot\frac{L^3}{EI} \\ \alpha_{22} &= \frac{81}{3888}\cdot\frac{L^3}{EI} \end{aligned}\right\}$$

Substituting

$$\Lambda = 3888\cdot\frac{EI}{ML^3\Omega^2}$$

in the eqs. 11.2 and 11.3 we get

$$\left.\begin{aligned} (25\varepsilon-\Lambda)y_1+39y_2+17\varepsilon y_3 &= -36e \\ 39\varepsilon y_1+(81-\Lambda)y_2+39\varepsilon y_3 &= -84e \\ 17\varepsilon y_1+39y_2+(25\varepsilon-\Lambda)y_3 &= -36e \end{aligned}\right\} \quad \ldots\ldots\ldots \quad 12.3$$

This gives, using CRAMER's rule,

$$\left.\begin{aligned} y_1 = y_3 &= 36e \cdot \frac{(\Lambda-8\varepsilon)\,(\Lambda+10)}{(\Lambda-8\varepsilon)\,(\Lambda-\Lambda_1)\,(\Lambda-\Lambda_3)} \\ y_2 &= 84e \cdot \frac{(\Lambda-8\varepsilon)\left(\Lambda-\frac{60}{7}\varepsilon\right)}{(\Lambda-8\varepsilon)\,(\Lambda-\Lambda_1)\,(\Lambda-\Lambda_3)} \end{aligned}\right\} \quad \ldots\ldots\ 13.1$$

where Λ_1 and Λ_3 satisfy

$$\Lambda^2-(42\varepsilon+81)\Lambda+360\varepsilon = 0 \quad \ldots\ldots\ 13.2$$

The deflections y_1, y_2, and y_3 are infinite when

$$\Lambda = \Lambda_1 \text{ and } \Lambda = \Lambda_3$$

The value $\Lambda_2 = 8\varepsilon$ is of special interest. Substituting in eq. 12.3 we obtain

$$\left.\begin{aligned} 17\varepsilon y_1+39y_2+17\varepsilon y_3 &= -36e \\ 39\varepsilon y_1+(81-8\varepsilon)y_2+39\varepsilon y_3 &= -84e \end{aligned}\right\}$$

and

$$\left.\begin{aligned} y_1+y_3 &= -\frac{36\varepsilon+45}{\varepsilon(17\varepsilon+18)} \cdot e \\ y_2 &= \frac{3}{17\varepsilon+18} \cdot e \end{aligned}\right\} \quad \ldots\ldots\ 13.3$$

The deflections y_1 and y_3 may have any values and must not be equal as eq. 13.1 indicates. The only condition concerns their sum which must have a constant value. The positions of the discs 1 and 3 are indifferent.

One usually says that a shaft with n masses has n critical speeds. (As will be pointed out later, this is a truth with modifications). In this special case the critical speeds are determined by

$$\Lambda = \Lambda_1,\ \Lambda = \Lambda_3, \text{ and } \Lambda = 8\varepsilon$$

However, they are essentially different. The first two give infinite deflections but the third gives an indifferent equilibrium position of the flywheels.

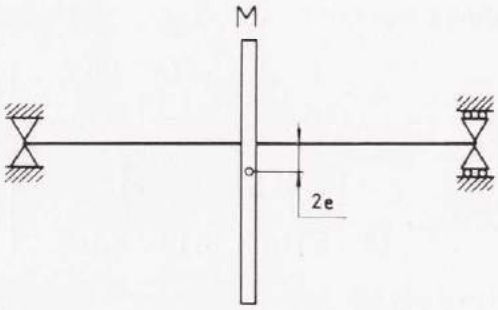

Fig. 14.1

If the eccentricities are equal to zero ($e = 0$) the deflections become indifferent, when $\Lambda = \Lambda_1$, $\Lambda = \Lambda_3$, and $\Lambda = 8\varepsilon$. Thus the critical speeds imply indifferent positions of the flywheels.

A limiting case is obtained by putting $\varepsilon \to 0$. Thus we have from eq. 13.2, that

$$\left.\begin{aligned} \Lambda_3 &= 0 \\ \Lambda_1 &= 81 \end{aligned}\right\}$$

and

$$\Lambda_2 = \lim_{\varepsilon \to 0} 8\varepsilon = 0$$

$\Lambda = 0$ gives, with the aid of eq. 13.1, $y_1 = y_3 = \dfrac{e}{\varepsilon}$ and $y_2 = -2e$, which means that the points of gravity are on the central line of the bearings at infinitely high speed. This is independent of the value of ε.

$\Lambda_1 = 81$ corresponds to the arrangement shown in fig. 14.1.

However, $\Lambda_2 = 0$ gives according to eq. 13.3

$$\left.\begin{aligned} y_1 + y_3 &= \infty \\ y_2 &= \frac{1}{6} e \end{aligned}\right\}$$

This theoretical limit discussion, however, is not brought further. The case of fig. 14.1 is basic standard and has only one critical speed corresponding to $\Lambda_1 = 81$.

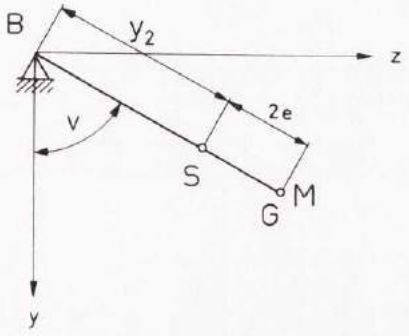

Fig. 15.1

For every flywheel in fig. 10.1 there are three points of importance, viz.

B = the centre of the bearings
S = the centre of the shaft
G = the centre of gravity

The position of these points for the mass on the middle of the shaft is shown in fig. 15.1 in a cross section $A-A$ (see fig. 10.1).

SG is always equal to $2e$, but y_2 and the relative position of the three points will shift depending on the actual value of Λ. With the aid of the eqs. 13.1 these conditions can be studied. The result is seen in fig. 16.1, where the "semi-inverse" diagram method [5] is used. In this case $\varepsilon = 1$, and $\Lambda_1 = 120$, $\Lambda_2 = 8$, $\Lambda_3 = 3$.

The three points BSG are shown at $v = 0°$ and their relative positions below and above the first critical speed are drawn in the same diagram. The deflections y_1 and y_3 are always equal except at $\Lambda = 8$, where $y_1 + y_3 = -\frac{81}{35} e$. They are easily understood by keeping in mind that

B is on the curve
S is on the Λ-axis
The distance between S and G is a constant.

It is remarkable that the gravity centre G_2 below the first critical speed is further away from the centre B_2 than S_2 does, whereas, for

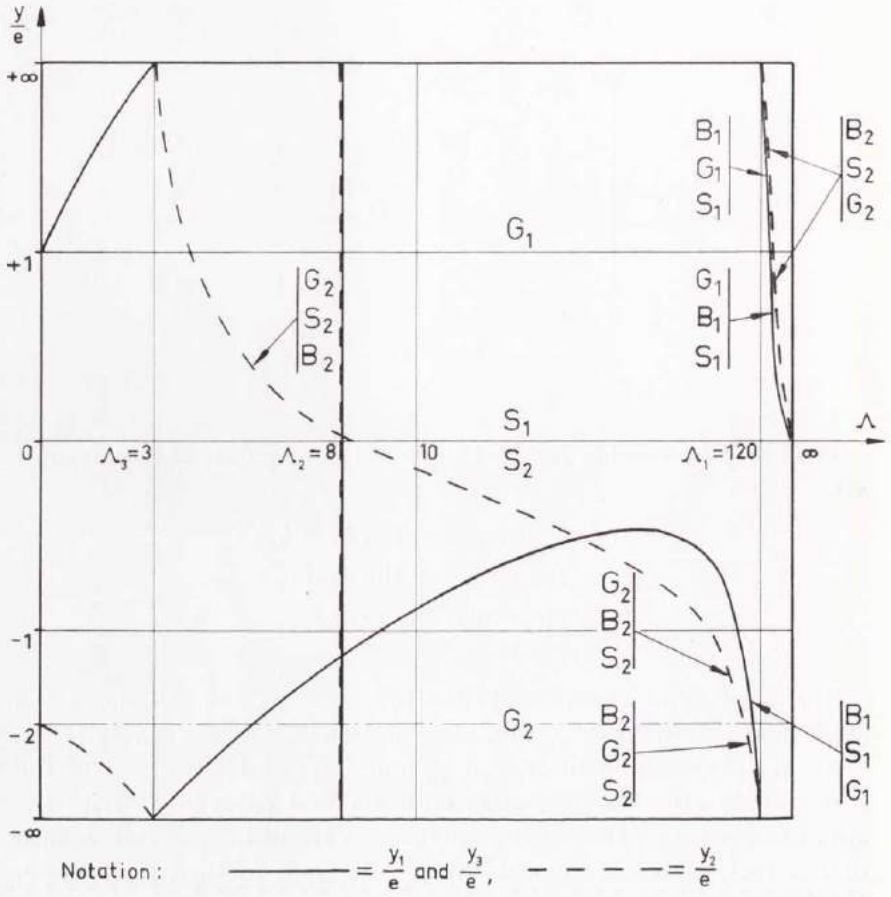

Fig. 16.1

speeds just above the first critical speed, S_2 lies further outside. Analogous things happen to the other flywheels.

If $e = 0$ the fig. 16.1 is not valid. In this case we have the well-known result that the three discs are in indifferent positions at the critical speeds and that certain constant ratios exist between the deflections of the discs. Analogously to fig. 16.1 in this case we obtain fig. 17.1.

At $\quad \Lambda = 120,\ y_1 : y_2 : y_3 = 1 : 2 : 1$

$\Lambda = \quad 8,\ y_1 : y_3 = -1,\ y_2 = 0$

$\Lambda = \quad 3,\ y_1 : y_2 : y_3 = 1 : (-1) : 1$

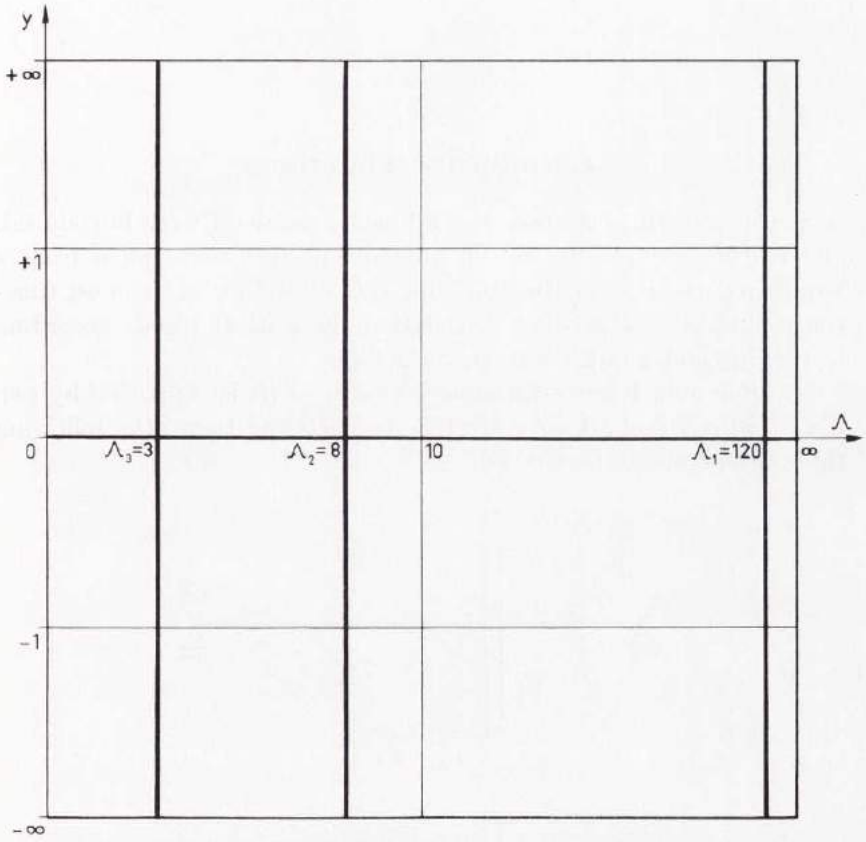

Fig. 17.1

It will be observed that the curves in fig. 17.1 consists of the Λ-axis and three vertical lines.

In this introducing chapter the example has shown the nature of critical speeds. The mass of the shaft and the gyroscopic effects have been neglected.

Infinite deflections were obtained at special "critical" speeds. In practice these infinite deflections, of course, do not occur and furthermore the basic equations are only valid for small deflections.

In spite of this the development in a simple way shows the different tendencies of critical speeds. Thus we can conclude, that a shaft with flywheels being in both static and dynamic balance, or, which is a theoretical case, having no unbalances at all, always has critical speeds.

4. Influence Functions

In the preceding chapter the influence numbers were introduced, and in the exemple the actual numbers needed were taken from a handbook. Because of the fact that this procedure is the most time-consuming procedure when calculating the critical speeds according to this method a quick way is worked out.

Limiting ourselves to the cases when the shaft is supported by two rigid bearings and all discs are situated between them, the following three cases have to be studied:

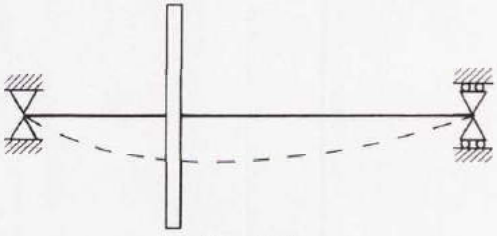

Fig. 18.1

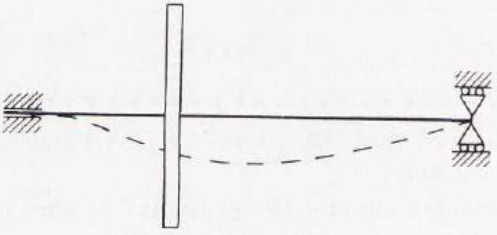

Fig. 18.2

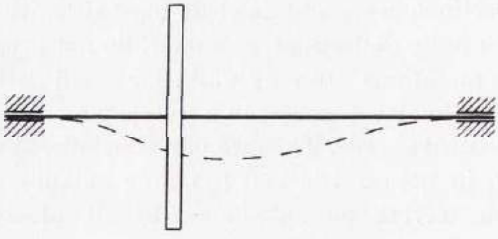

Fig. 18.3

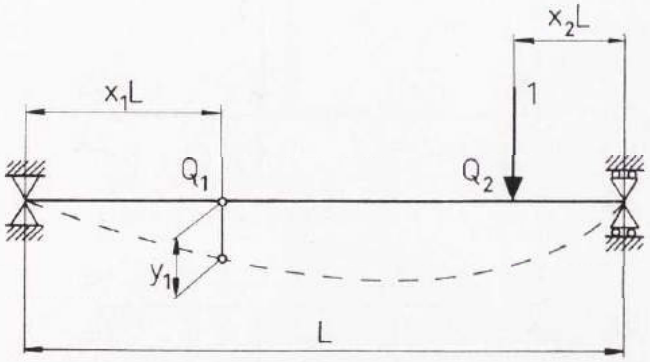

Fig. 19.1

Fig. 18.1 shows two bearings which do not give any bending moments to the shaft. The left hand bearing in fig. 18.2 causes a bending moment, but the right hand bearing does not. In fig. 18.3 both bearings give rise to bending moments. These cases are the only ones that can occur and they are studied in the following where they will be denoted as arrangements with "hinged-hinged" ends, "clamped-hinged" ends, and "clamped-clamped" ends respectively.

Beginning with the case in fig. 18.1 we consider the shaft loaded by a unit force according to fig. 19.1.

The deflection y_1 is wanted. For the forces and bending moment in fig. 19.2, we find that

$$\left.\begin{aligned} A &= x_2 \\ B &= 1-x_2 \end{aligned}\right\}$$

$$M_x = Ax_1L - \underset{x_1>1-x_2}{|1}\,(x_1+x_2-1)\,L$$

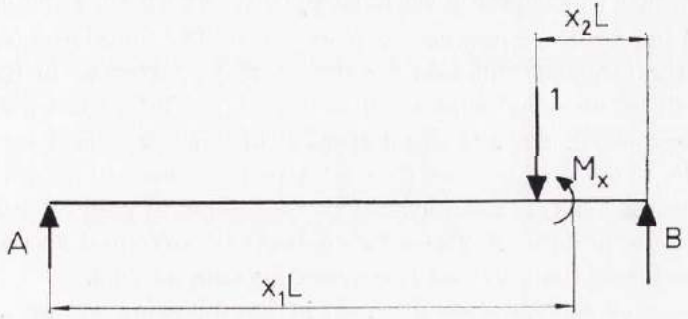

Fig. 19.2

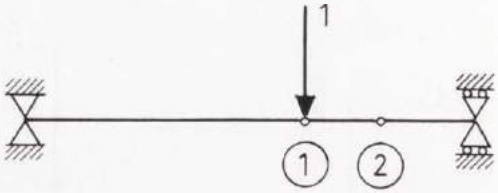

Fig. 20.1

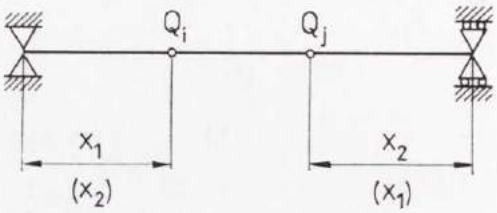

Fig. 20.2

Furthermore we have

$$-EI \cdot \frac{d^2 y_1}{d(x_1 L)^2} = M_x$$

and using the boundary conditions

$$\left.\begin{array}{ll} x_1 = 0 & y_1 = 0 \\ x_1 = 1 & y_1 = 0 \end{array}\right\}$$

we get

$$y_1(x_1, x_2) = \frac{1}{6} x_1 x_2 (1 - x_1^2 - x_2^2) \cdot \frac{L^3}{EI} \quad \ldots\ldots\ldots \quad 20.3$$

In this formula $x_1 \leq (1 - x_2)$ always. Observe that fig. 19.2 does not satisfy this condition.

According to Chapter 3 we have $y_1 = \alpha_{12}$. If we let x_1 be equal to $(1 - x_2)$ the influence number α_{22} is obtained. The function $y_1(x_1, x_2)$ is called the influence function for the shaft supported as in fig. 18.1.

It will be observed that the limit $x_1 \leq (1 - x_2)$ does not affect the usefulness of eq. 20.3. If the deflection in point 2 caused by a unit force in point 1 is wanted (the relative positions are shown in fig. 20.1), instead of this we calculate the deflection in point 1 caused by a unit force in point 2. These two deflections are equal according to MAXWELL and the last case is covered by formula 20.3.

Instead of the notation $y_1(x_1, x_2)$ in the following we use α_{ij}. The indices denote the points studied. See fig. 20.2.

Analogous calculations can be made for the cases shown in the figs. 18.2 and 18.3. The results are given below.

It is important to observe that x_2 in the unsymmetrical case (see fig. 18.2) must be measured from that bearing giving rise to a bending moment. In the symmetrical cases, x_1 and x_2 may be shifted without changing the value of α_{ij}.

Summary:

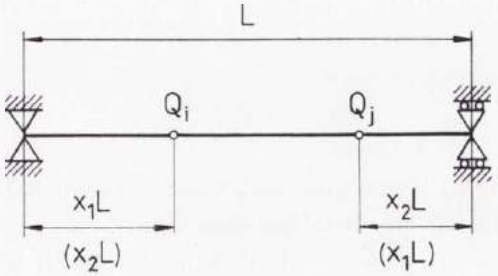

$$\alpha_{ij} = \alpha_{ji} = \frac{1}{6} x_1 x_2 (1 - x_1^2 - x_2^2) \cdot \frac{L^3}{EI}$$

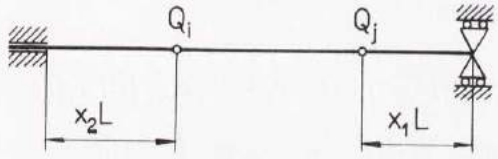

$$\alpha_{ij} = \alpha_{ji} = \frac{1}{6} x_1 x_2^2 \left[\frac{1}{2} (3 - x_1^2)(1 - x_2) - x_1^2 \right] \cdot \frac{L^3}{EI}$$

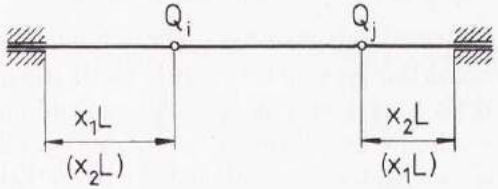

$$\alpha_{ij} = \alpha_{ji} = \frac{1}{6} (x_1 x_2)^2 [3(1 - x_1 - x_2) + 2x_1 x_2] \cdot \frac{L^3}{EI}$$

Fig. 21.1

The treatment above dealt with a shaft supported in both its ends. The cantilever shaft with discs is discussed in Chapter 7 in connection with gyroscopic effects on the critical speeds. The shaft supported by

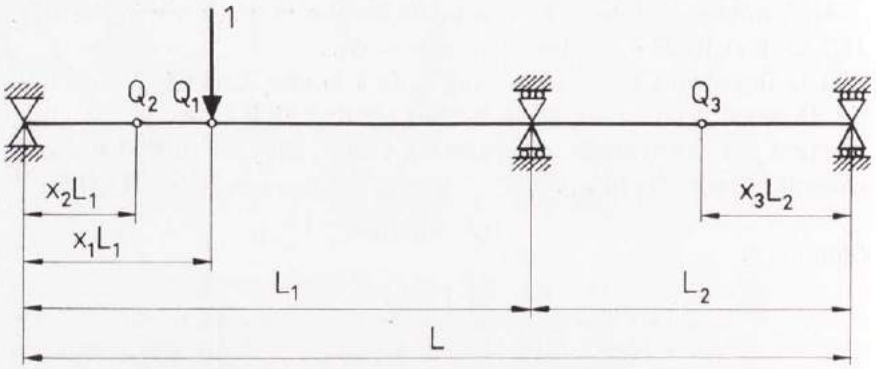

Fig. 22.1

three bearings is an important case. The treatment here premises the bearings not causing any bending moments.

Consider the shaft in fig. 22.1. It is loaded at Q_1 by a unit force. The deflections in the points Q_2 and Q_3 are wanted. The case represents a statically undetermined system. These deflections are easily determined with the aid of the equation of the deflection curve. The final result can be written

$$\left.\begin{aligned} \alpha_{21} &= \frac{1}{6}\,(1-x_1)x_2[(1-x_2^2)-(1-x_1)^2-\tfrac{1}{2}\varkappa_1 x_1\,(1+x_1)\,(1-x_2^2)]\;\varkappa_1^3\cdot\frac{L^3}{EI} \\ \alpha_{31} &= -\frac{1}{12}\,x_1x_3(1-x_1)^2(1-x_3^2)\,(\varkappa_1\varkappa_2)^2\cdot\frac{L^3}{EI} \end{aligned}\right\}$$

where $\varkappa_1 = \dfrac{L_1}{L}$ and $\varkappa_2 = \dfrac{L_2}{L}$. The other symbols are shown in fig. 22.1. Observe that the expression for α_{21} only holds for $x_2 \leq x_1$. When $x_2 > x_1$ the reciprocal theorem of Maxwell is used. If α_{33} is desired the first formula can be used if we put $x_1 = x_2 = x_3$ and change $\varkappa_1$ to $\varkappa_2$.

The treatment is limited to the most usual cases occuring in practice. Further only shafts with the same diameter along all their length are treated. However, the procedure for shafts with variable diameters is described in the next chapter.

Further, in Chapter 14, the influence numbers for a shaft supported by one, two or three rigid bearings are collected. This survey gives also the influence numbers needed for a calculation involving the gyroscopic effect (See Chapter 7) and all thinkable cases for a shaft supported by two rigid bearings are treated.

5. Critical Speeds of a Shaft Supported by Rigid Bearings

In this chapter a shaft with n discs is considered, see fig. 23.2. The shaft may have a variable diameter and the bearings may be hinged or clamped. The mass of the shaft is equal to zero and the gyroscopic effects are neglected.

The masses of the discs are $M_1, M_2, M_3, \ldots M_s \ldots M_n$ respectively. The deflection at the mass no. s is denoted y_s and it is caused by the forces $M_1y_1\Omega^2$, $M_2y_2\Omega^2$, $M_3y_3\Omega^2, \ldots M_sy_s\Omega^2 \ldots$ and $M_ny_n\Omega^2$. Thus we get

$$y_s = M_1y_1\Omega^2\alpha_{s1} + M_2y_2\Omega^2\alpha_{s2} + \ldots + M_sy_s\Omega^2\alpha_{ss} + \ldots + M_ny_n\Omega^2\alpha_{sn}$$

or shorter

$$y_s = \sum_{i=1}^{n} M_iy_i\Omega^2\alpha_{si} \quad \ldots\ldots\ldots\ldots\ldots\ldots \quad 23.1$$

If we introduce a reference mass, M_{ref}, and non-dimensional masses μ_i $(i = 1, 2, 3 \ldots n)$ according to

$$\mu_1 = \frac{M_1}{M_{\text{ref}}}, \quad \mu_2 = \frac{M_2}{M_{\text{ref}}}, \quad \ldots \mu_n = \frac{M_n}{M_{\text{ref}}}$$

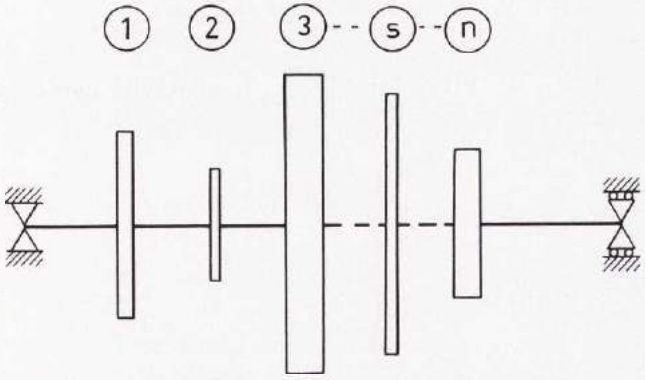

Fig. 23.2

where M_{ref} may be of any kind, as a suggestion

$$M_{\text{ref}} = M_1 + M_2 + \ldots + M_n = \sum_{i=1}^{n} M_i$$

or

$$M_{\text{ref}} = M_i$$

where M_i is chosen in a suitable way.

Now it is possible to write eq. 23.1 as

$$y_s = \sum_{i=1}^{n} \mu_i M_{\text{ref}} y_i \Omega^2 \alpha_{si}$$

or

$$y_s = M_{\text{ref}} \Omega^2 \sum_{i=1}^{n} \mu_i y_i \alpha_{si} \quad \ldots\ldots\ldots\ldots\ldots\ldots \quad 24.1$$

It is always possible to write the influence number α_{si} as

$$\alpha_{si} = \frac{\xi_{si}}{k} \cdot \frac{L^3}{EI}$$

where k is a constant, for example the least common denominator to all the influence numbers. Thus eq. 24.1 becomes

$$y_s = M_{\text{ref}} \Omega^2 \cdot \frac{L^3}{kEI} \sum_{i=1}^{n} \mu_i y_i \xi_{si} \quad \ldots\ldots\ldots\ldots\ldots \quad 24.2$$

Now another quantity is introduced, namely the non-dimensional "critical speed" Λ, where

$$\Lambda = \frac{kEI}{M_{\text{ref}} L^3 \Omega^2}$$

Thus eq. 24.2 will be

$$\Lambda y_s = \sum_{i=1}^{n} \mu_i y_i \xi_{si} \qquad s = 1, 2, 3 \ldots n$$

These equations can be written

$$\left.\begin{array}{l}(\mu_1\xi_{11}-\Lambda)y_1+\mu_2\xi_{12}y_2+\mu_3\xi_{13}y_3+\ldots+\mu_n\xi_{1n}y_n \quad = 0\\ \mu_1\xi_{21}\quad y_1+(\mu_2\xi_{22}-\Lambda)y_2+\mu_3\xi_{23}y_3+\ldots+\mu_n\xi_{2n}y_n = 0\\ \mu_1\xi_{31}\quad y_1+\mu_2\xi_{32}y_2+(\mu_3\xi_{33}-\Lambda)y_3+\ldots+\mu_n\xi_{3n}y_n = 0\\ -\,-\,-\,-\,-\,-\,-\,-\,-\,-\,-\,-\,-\,-\,-\\ \mu_1\xi_{n1}y_1+\mu_2\xi_{n2}y_2+\mu_3\xi_{n3}y_3+\ldots+(\mu_n\xi_{nn}-\Lambda)y_n \quad = 0\end{array}\right\}$$

The condition for this homogenous system not having only a trivial solution is

$$\begin{vmatrix}\mu_1\xi_{11}-\Lambda & \mu_2\xi_{12} & \mu_3\xi_{13} & \ldots\ldots & \mu_n\xi_{1n}\\ \mu_1\xi_{21} & \mu_2\xi_{22}-\Lambda & \mu_3\xi_{23} & \ldots\ldots & \mu_n\xi_{2n}\\ \mu_1\xi_{31} & \mu_2\xi_{32} & \mu_3\xi_{33}-\Lambda & \ldots\ldots & \mu_n\xi_{3n}\\ - & - & - & - & -\\ \mu_1\xi_{n1} & \mu_2\xi_{n2} & \mu_3\xi_{n3} & \ldots\ldots & \mu_n\xi_{nn}-\Lambda\end{vmatrix} = 0 \quad \ldots\ldots \quad 25.1$$

The eq. 25.1 is of order n in Λ and the critical angular velocities are

$$\Omega_i = \sqrt{\frac{kEI}{M_{\text{ref}}L^3\Lambda_i}}\ \text{(rad/s)}\quad i = 1, 2, 3 \ldots n$$

These critical angular velocities are exactly the same as those of transverse vibrations. It depends on the fact that the inertia moments of the discs are neglected. See further about this matter in Chapter 8.

It may be pointed out that the forces on the shaft are caused by the rotation of the discs around the centreline of the bearings and not by the rotation of the discs around the centreline of the shaft. The common case is, however, that the frequencies of these two rotations are equal. In these cases the critical speeds are

$$n_i = \frac{30}{\pi}\sqrt{\frac{kEI}{M_{\text{ref}}L^3\Lambda_i}}\ \text{(r.p.m.)}\quad i = 1, 2, 3 \ldots n \quad \ldots\ldots \quad 25.2$$

But other rotational circumstances are observed. See for instance [3] and [9]. These cases are considered in Chapter 7.

The theory developed above is illustrated by some numerical examples.

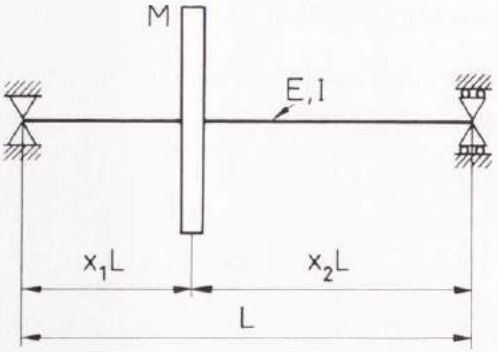

Fig. 26.1

Example 1. Calculate the critical speed for the arrangement in fig. 26.1 if the influence of the mass of the shaft and the gyroscopic effects are neglected.

If $M_{ref} = M$ is $\mu_1 = 1$ and eq. 25.1 gives

$$\mu_1 \xi_{11} - \Lambda = 0$$

or

$$\Lambda = \xi_{11}$$

From fig. 21.1 we get

$$\alpha_{11} = \frac{1}{6} x_1(1-x_1)\,[1-x_1^2-(1-x_1)^2]\frac{L^3}{EI} = \frac{1}{3} \cdot x_1^2(1-x_1)^2 = \frac{1}{3}(x_1x_2)^2\frac{L^3}{EI}$$

Choosing $\xi_{11} = \frac{1}{3}(x_1x_2)^2$ and $k = 1$ eq. 25.2 gives

$$n_{crit} = \frac{30}{\pi}\sqrt{\frac{3EI}{ML^3(x_1x_2)^2}} \text{ (r.p.m.)} \quad \ldots\ldots\ldots\ldots \quad 26.2$$

Analogous formulas may be derived in the other cases of shaft support.

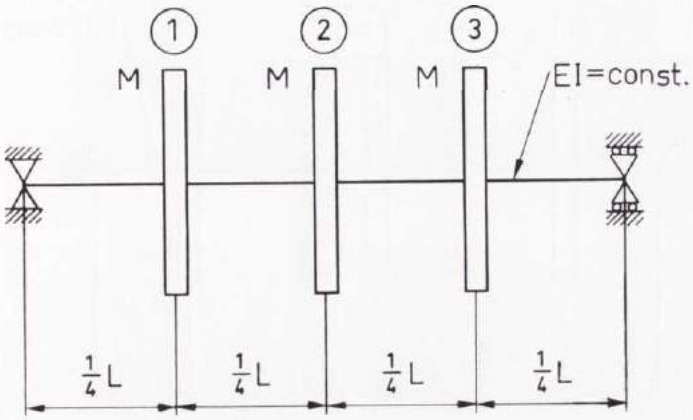

Fig. 27.1

Example 2. Three equal masses are symmetrically placed on a shaft as in fig. 27.1. Determine the critical speeds if the weight of the shaft and the gyroscopic effects are neglected.

From fig. 21.1 we get for this way of supporting

$$\alpha_{ij} = \frac{1}{6} x_1 x_2 (1 - x_1^2 - x_2^2) \cdot \frac{L^3}{EI}$$

and thus

$$\alpha_{33} = \alpha_{11}\left(x_1 = \frac{1}{4};\ x_2 = \frac{3}{4}\right) = \frac{1}{6} \cdot \frac{1}{4} \cdot \frac{3}{4} \cdot \left(1 - \frac{1}{16} - \frac{9}{16}\right) \times$$

$$\times \frac{L^3}{EI} = \frac{1}{6} \cdot \frac{9}{128} \frac{L^3}{EI}$$

$$\alpha_{12} = \alpha_{23} = \alpha_{32} = \alpha_{21}\left(x_1 = \frac{1}{4};\ x_2 = \frac{1}{2}\right) = \frac{1}{6} \cdot \frac{11}{128} \cdot \frac{L^3}{EI}$$

$$\alpha_{13} = \alpha_{31}\left(x_1 = \frac{1}{4};\ x_2 = \frac{1}{4}\right) = \frac{1}{6} \cdot \frac{7}{128} \cdot \frac{L^3}{EI}$$

$$\alpha_{22}\left(x_1 = \frac{1}{2};\ x_2 = \frac{1}{2}\right) = \frac{1}{6} \cdot \frac{16}{128} \cdot \frac{L^3}{EI}$$

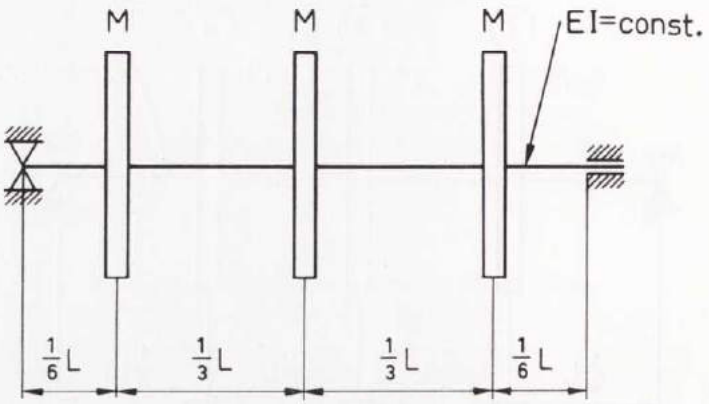

Fig. 28.1

If we choose $k = 6 \cdot 128$ the numerator in the α_{ij} is ξ_{ij}. We get from eq. 25.1, if $M_{\text{ref}} = M$, that

$$\begin{vmatrix} 9-\Lambda & 11 & 7 \\ 11 & 16-\Lambda & 11 \\ 7 & 11 & 9-\Lambda \end{vmatrix} = 0$$

or

$$\Lambda^3 - 34\Lambda^2 + 78\Lambda - 28 = 0$$

The roots are $\Lambda_1 = 16+11\sqrt{2}$, $\Lambda_2 = 2$, $\Lambda_3 = 16-11\sqrt{2}$ and the critical speeds are obtained from eq. 25.2.

Example 3. Three equal masses are placed on a shaft according to fig. 28.1. Determine the critical speeds if the weight of the shaft and the gyroscopic effects are neglected.

For this hinged-clamped bearing arrangement we get from fig. 21.1

$$\alpha_{ij} = \frac{1}{6} x_1 x_2^2 \left[\frac{1}{2} (3-x_1^2)(1-x_2) - x_1^2 \right] \frac{L^3}{EI}$$

Observe that x_1 is measured from the bearing on the left hand side.

Thus

$$\alpha_{11} = \frac{1}{6}\left(\frac{5}{6}\right)^2 \cdot \frac{1}{6}\left[\frac{1}{2} \cdot \frac{1}{6}\left(3 - \frac{1}{36}\right) - \frac{1}{36}\right] \cdot \frac{L^3}{EI} =$$

$$= \frac{2\,375}{12 \cdot 216^2} \cdot \frac{L^3}{EI}$$

$$\alpha_{12} = \alpha_{21} = \frac{1}{6}\left(\frac{1}{2}\right)^2 \cdot \frac{1}{6}\left[\frac{1}{2} \cdot \frac{1}{2}\left(3 - \frac{1}{36}\right) - \frac{1}{36}\right] \cdot \frac{L^3}{EI} =$$

$$= \frac{2\,781}{12 \cdot 216^2} \cdot \frac{L^3}{EI}$$

$$\alpha_{13} = \alpha_{31} = \frac{1}{6}\left(\frac{1}{6}\right)^2 \cdot \frac{1}{6}\left[\frac{1}{2} \cdot \frac{5}{6} \cdot \frac{107}{36} - \frac{1}{36}\right] \cdot \frac{L^3}{EI} =$$

$$= \frac{523}{12 \cdot 216^2} \cdot \frac{L^3}{EI}$$

$$\alpha_{22} = \frac{1}{6}\left(\frac{1}{2}\right)^2 \cdot \frac{1}{2}\left[\frac{1}{2} \cdot \frac{1}{2} \cdot \frac{11}{4} - \frac{1}{4}\right] \cdot \frac{L^3}{EI} = \frac{5\,103}{12 \cdot 216^2} \cdot \frac{L^3}{EI}$$

$$\alpha_{23} = \alpha_{32} = \frac{1}{6}\left(\frac{1}{6}\right)^2 \cdot \frac{1}{2}\left[\frac{1}{2} \cdot \frac{5}{6} \cdot \frac{11}{4} - \frac{1}{4}\right] \cdot \frac{L^3}{EI} =$$

$$= \frac{1\,161}{12 \cdot 216^2} \cdot \frac{L^3}{EI}$$

$$\alpha_{33} = \frac{1}{6}\left(\frac{1}{6}\right)^2 \cdot \frac{5}{6}\left[\frac{1}{2} \cdot \frac{5}{6} \cdot \frac{83}{36} - \frac{25}{36}\right] \cdot \frac{L^3}{EI} = \frac{575}{12 \cdot 216^2} \cdot \frac{L^3}{EI}$$

If we choose $k = 12 \cdot 216^2$ and $M_{\text{ref}} = M$ eq. 25.1 gives

$$\begin{vmatrix} 2\,375-\Lambda & 2\,781 & 523 \\ 2\,781 & 5\,103-\Lambda & 1\,161 \\ 523 & 1\,161 & 575-\Lambda \end{vmatrix} = 0$$

or

$$\Lambda^3 - 8\,053\Lambda^2 + 7\,064\,064\Lambda - 1\,301\,889\,024 = 0$$

This equation has the roots

$$\Lambda_1 = 7\,081,\ \Lambda_2 = 713, \text{ and } \Lambda_3 = 258$$

The critical speeds are obtained from eq. 25.2.

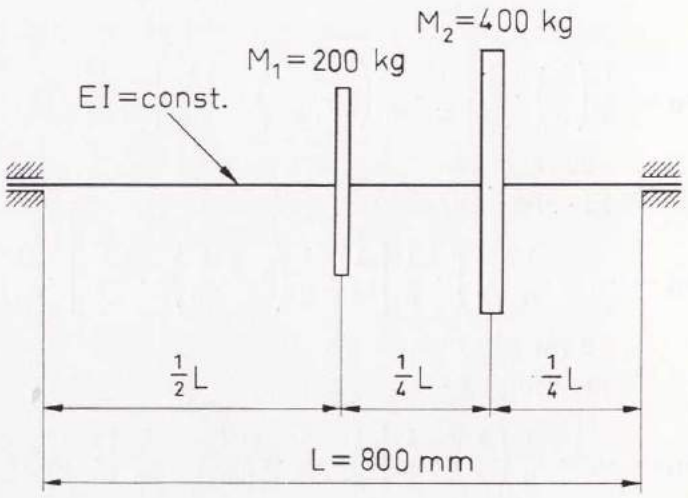

Fig. 30.1

Example 4. A weightless shaft with two discs is supported according to fig. 30.1. Determine the critical speeds if the gyroscopic effects are neglected. The shaft is made of steel and has a diameter ⌀ 70 mm.

From fig. 21.1 we get for this case of supporting

$$\alpha_{ij} = \frac{1}{6}(x_1 x_2)^2[3(1-x_1-x_2)+2x_1x_2]\cdot\frac{L^3}{EI}$$

and thus

$$\alpha_{11} = \frac{1}{6}\left(\frac{1}{2}\cdot\frac{1}{2}\right)^2\left[3\left(1-\frac{1}{2}-\frac{1}{2}\right)+2\cdot\frac{1}{2}\cdot\frac{1}{2}\right]\cdot\frac{L^3}{EI} =$$

$$= \frac{192}{6\cdot 24\cdot 16^2}\cdot\frac{L^3}{EI}$$

$$\alpha_{12} = \alpha_{21} = \frac{1}{6}\left(\frac{1}{2}\cdot\frac{1}{4}\right)^2\left[3\left(1-\frac{1}{2}-\frac{1}{4}\right)+2\cdot\frac{1}{2}\cdot\frac{1}{4}\right]\cdot\frac{L^3}{EI} =$$

$$= \frac{96}{6\cdot 24\cdot 16^2}\cdot\frac{L^3}{EI}$$

$$\alpha_{22} = \frac{1}{6}\left(\frac{3}{4}\cdot\frac{1}{4}\right)^2\left[3\left(1-\frac{3}{4}-\frac{1}{4}\right)+2\cdot\frac{3}{4}\cdot\frac{1}{4}\right]\cdot\frac{L^3}{EI} =$$

$$= \frac{81}{6\cdot 24\cdot 16^2}\cdot\frac{L^3}{EI}$$

If we put $M_{ref} = M_1 = 200$ kg and $k = 6 \cdot 24 \cdot 16^2$ eq. 25.1 gives

$$\begin{vmatrix} 192-\Lambda & 2 \cdot 96 \\ 96 & 2 \cdot 81-\Lambda \end{vmatrix} = 0$$

or

$$\Lambda^2 - 354\Lambda + 12\,672 = 0$$

with the roots

$$\Lambda_1 = 313{,}59 \text{ and } \Lambda_2 = 40{,}41$$

with

$$E = 20{,}6 \cdot 10^{10} \frac{\text{N}}{\text{m}^2}$$

$$I = \frac{\pi d^4}{64} = \frac{\pi}{64} \cdot 70^4 \cdot 10^{-12} \text{ m}^4$$

$$L = 0{,}8 \text{ m}$$

eq. 25.2 gives

$$n_i = \frac{30}{\pi} \sqrt{\frac{6 \cdot 24 \cdot 16^2 \cdot 20{,}6 \cdot 10^{10} \cdot \pi \cdot 70^4 \cdot 10^{-12}}{64 \cdot 200 \cdot 0{,}8^3 \cdot \Lambda_i}}$$

$$n_i = \frac{9\,018}{\sqrt{\Lambda_i}}$$

By inserting the different Λ_i we finally get

$$n_1 = 510 \text{ r.p.m.}$$
$$n_2 = 1\,420 \text{ r.p.m.}$$

Example 5. Determine the critical speeds for a shaft with two masses and supported by three bearings according to fig. 32.1. The gyroscopic effects may be neglected. The shaft is made of steel and has a diameter of 12 mm. In order to take the mass of the shaft into some consideration $\frac{17}{35}$ of the masses of the two sections of the shaft is added to the masses of the discs. See about this assumption in Chapter 9.

The mass of the shaft is 0,62 kg and thus, if $M_{ref} = M_1$,

$$\mu_1 = 1$$

$$\mu_2 = \frac{9{,}37}{5{,}44} = 1{,}72$$

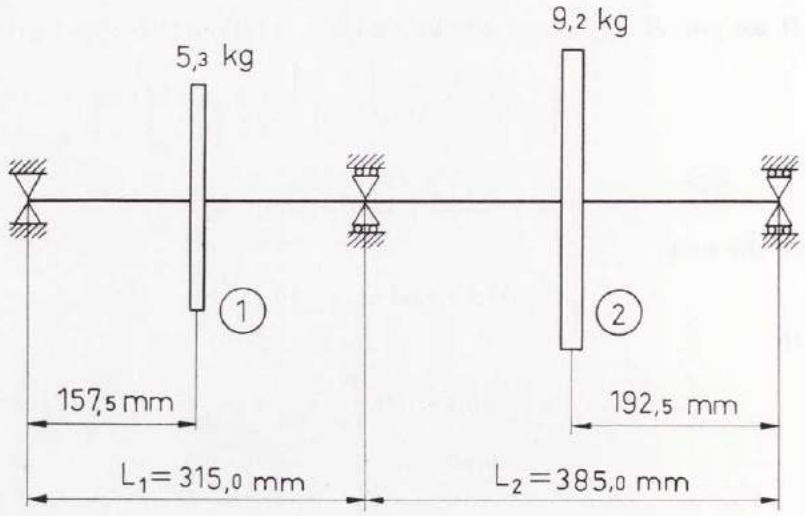

Fig. 32.1

Further we have according to page 22

$$\varkappa_1 = \frac{315}{700} = 0{,}45$$

$$\varkappa_2 = \frac{385}{700} = 0{,}55$$

and

$$\alpha_{11} = \frac{1}{6}\left(1-\frac{1}{2}\right)\cdot\frac{1}{2}\cdot\left[1-\frac{1}{4}-\left(1-\frac{1}{2}\right)^2-\frac{1}{2}\cdot 0{,}45\times\right.$$

$$\left.\times\frac{1}{2}\left(1+\frac{1}{2}\right)\left(1-\frac{1}{4}\right)\right]\cdot 0{,}45^3\cdot\frac{L^3}{EI} = \frac{1{,}36118}{6\cdot 160}\cdot\frac{L^3}{EI}$$

$$\alpha_{12} = \frac{1}{6}\cdot\frac{1}{2}\cdot\frac{1}{2}\cdot\frac{1}{2}\left(1-\frac{1}{2}\right)^2\left(1-\frac{1}{2}\right)^2\cdot(0{,}45\cdot 0{,}55)^2\cdot\frac{L^3}{EI} =$$

$$= \frac{0{,}68913}{6\cdot 160}\cdot\frac{L^3}{EI}$$

$$\alpha_{22} = \frac{1}{6}\left(1-\frac{1}{2}\right)\cdot\frac{1}{2}\cdot\left[1-\frac{1}{4}-\left(1-\frac{1}{2}\right)^2-\frac{1}{2}\cdot 0{,}55\times\right.$$

$$\left.\times\frac{1}{2}\left(1+\frac{1}{2}\right)\left(1-\frac{1}{4}\right)\right]\cdot 0{,}55^3\cdot\frac{L^3}{EI} = \frac{2{,}29805}{6\cdot 160}\cdot\frac{L^3}{EI}$$

Choosing $k = 6 \cdot 160$ the eq. 25.1 gives

$$\begin{vmatrix} 1{,}36118 - \Lambda & 1{,}72 \cdot 0{,}689133 \\ 0{,}689133 & 1{,}72 \cdot 2{,}29805 - \Lambda \end{vmatrix} = 0$$

with the roots $\Lambda_1 = 4{,}24$ and $\Lambda_2 = 1{,}08$. With

$$E = 20{,}6 \cdot 10^{10} \frac{\mathrm{N}}{\mathrm{m}^2}$$

$$I = \frac{\pi d^4}{64} = \frac{\pi}{64} \cdot 12^4 \cdot 10^{-12}\ \mathrm{m}^4$$

$$L = 0{,}7\ \mathrm{m}$$

eq. 25.2 gives

$$n_i = \frac{30}{\pi} \cdot \sqrt{\frac{6 \cdot 160 \cdot 20{,}6 \cdot 10^{10} \cdot \pi \cdot 12^4 \cdot 10^{-12}}{5{,}44 \cdot 64 \cdot 0{,}7^3 \cdot \Lambda_i}} = \frac{3\,137}{\sqrt{\Lambda_i}}$$

and finally

$$n_1 = 1\,524 \text{ r.p.m.}$$
$$n_2 = 3\,022 \text{ r.p.m.}$$

Example 6. A weightless shaft with three discs is supported in three bearings according to fig. 34.1. The shaft is made of steel and has the diameter ⌀ 50 mm. Calculate the critical speeds if the gyroscopic effect is neglected.

We choose $M_{\mathrm{ref}} = 100$ kg and thus $\mu_i = 1$ ($i = 1, 2, 3$). In this case the following influence functions (page 22) are used

$$\alpha_{11} = \alpha_{21}\,(x_1 = x_2) = \frac{1}{6} x_1^2 (1 - x_1)^2 \left[2 - \frac{1}{2} \varkappa_1 (1 + x_1)^2 \right] \varkappa_1^3 \frac{L^3}{EI}$$

$$\alpha_{21} = \frac{1}{6} (1 - x_1)\, x_2 \left[(1 - x_2^2) - (1 - x_1)^2 - \frac{1}{2} \varkappa_1 x_1 (1 + x_1)\,(1 - x_2^2) \right] \varkappa_1^3 \frac{L^3}{EI}$$

$$\alpha_{31} = \frac{1}{6} \cdot \frac{1}{2} x_1 x_3 (1 - x_1)^2 (1 - x_3^2)\,(\varkappa_1 \varkappa_2)^2 \frac{L^3}{EI}$$

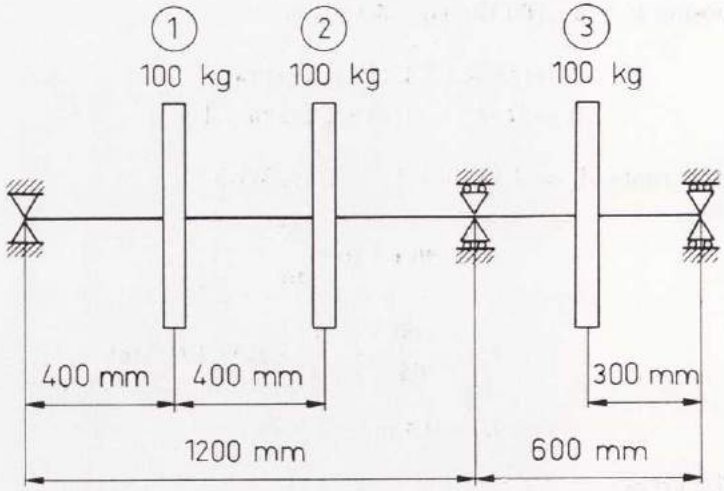

Fig. 34.1

Thus

$$\alpha_{11} = \frac{1}{6}\left(\frac{1}{3}\right)^2\left(1-\frac{1}{3}\right)^2\left[2-\frac{1}{2}\cdot\frac{1\,200}{1\,800}\cdot\left(1+\frac{1}{3}\right)^2\right]\left(\frac{1\,200}{1\,800}\right)^3\cdot\frac{L^3}{EI} =$$

$$= \frac{1\,216}{6\cdot 243^2}\cdot\frac{L^3}{EI}$$

$$\alpha_{12} = \frac{1}{6}\left(1-\frac{2}{3}\right)\cdot\frac{1}{3}\left[1-\left(\frac{1}{3}\right)^2-\left(1-\frac{2}{3}\right)^2-\frac{1}{2}\cdot\frac{1\,200}{1\,800}\times\right.$$

$$\left.\times\frac{2}{3}\left(1+\frac{2}{3}\right)\left(1-\left(\frac{1}{3}\right)^2\right)\right]\cdot\left(\frac{1\,200}{1\,800}\right)^3\cdot\frac{L^3}{EI} = \frac{872}{6\cdot 243^2}\cdot\frac{L^3}{EI}$$

$$\alpha_{22} = \frac{1}{6}\left(\frac{2}{3}\right)^2\left(1-\frac{2}{3}\right)^2\left[2-\frac{1}{2}\cdot\frac{1\,200}{1\,800}\cdot\left(1+\frac{2}{3}\right)^2\right]\left(\frac{1\,200}{1\,800}\right)^3\cdot\frac{L^3}{EI} =$$

$$= \frac{928}{6\cdot 243^2}\cdot\frac{L^3}{EI}$$

$$\alpha_{13} = \frac{1}{6}\cdot\frac{1}{2}\cdot\frac{1}{3}\cdot\frac{1}{2}\left(1-\frac{1}{9}\right)\left(1-\frac{1}{4}\right)\cdot\left(\frac{1\,200}{1\,800}\cdot\frac{600}{1\,800}\right)^2\cdot\frac{L^3}{EI} =$$

$$= \frac{162}{6\cdot 243^2}\cdot\frac{L^3}{EI}$$

$$\alpha_{23} = \frac{1}{6} \cdot \frac{1}{2} \cdot \frac{2}{3} \cdot \frac{1}{2} \left(1 - \frac{4}{9}\right) \left(1 - \frac{1}{4}\right) \left(\frac{1\,200}{1\,800} \cdot \frac{600}{1\,800}\right)^2 \cdot \frac{L^3}{EI} =$$

$$= \frac{202,5}{6 \cdot 243^2} \cdot \frac{L^3}{EI}$$

$$\alpha_{33} = \frac{1}{6} \left(\frac{1}{2}\right)^2 \cdot \left(1 - \frac{1}{2}\right)^2 \cdot \left[2 - \frac{1}{2} \cdot \frac{1}{3} \left(1 + \frac{1}{2}\right)^2\right] \cdot \left(\frac{600}{1\,800}\right)^3 \cdot \frac{L^3}{EI} =$$

$$= \frac{222,1172}{6 \cdot 243^2} \cdot \frac{L^3}{EI}$$

If we take $k = 6 \cdot 243^2 \cdot 10^{-3}$ we have

$$\begin{array}{lll} \xi_{11} = 1,2160 & \xi_{12} = 0,8720 & \xi_{13} = 0,1620 \\ \xi_{21} = 0,8720 & \xi_{22} = 0,9280 & \xi_{23} = 0,2025 \\ \xi_{31} = 0,1620 & \xi_{32} = 0,2025 & \xi_{33} = 0,2221 \end{array}$$

By insertion in eq. 25.1 we get

$$\begin{vmatrix} 1,2160 - \Lambda & 0,8720 & 0,1620 \\ 0,8720 & 0,9280 - \Lambda & 0,2025 \\ 0,1620 & 0,2025 & 0,2221 - \Lambda \end{vmatrix} = 0$$

or

$$\Lambda^3 - 2,3661\Lambda^2 + 0,7770\Lambda - 0,0648 = 0$$

The roots are

$$\left.\begin{array}{l} \Lambda_1 = 1,9925 \\ \Lambda_2 = 0,2348 \\ \Lambda_3 = 0,1388 \end{array}\right\}$$

Then the critical speeds are calculated from eq. 25.2

$$n_i = \frac{30}{\pi} \sqrt{\frac{6 \cdot 243^2 \cdot 10^{-3} \cdot 20,6 \cdot 10^{10} \cdot \pi \cdot 50^4 \cdot 10^{-12}}{64 \cdot 100 \cdot 1,8^3 \cdot \Lambda_i}}$$

and

$$\begin{array}{l} n_1 = 1\,326 \text{ r.p.m.} \\ n_2 = 3\,864 \text{ r.p.m.} \\ n_3 = 5\,025 \text{ r.p.m.} \end{array}$$

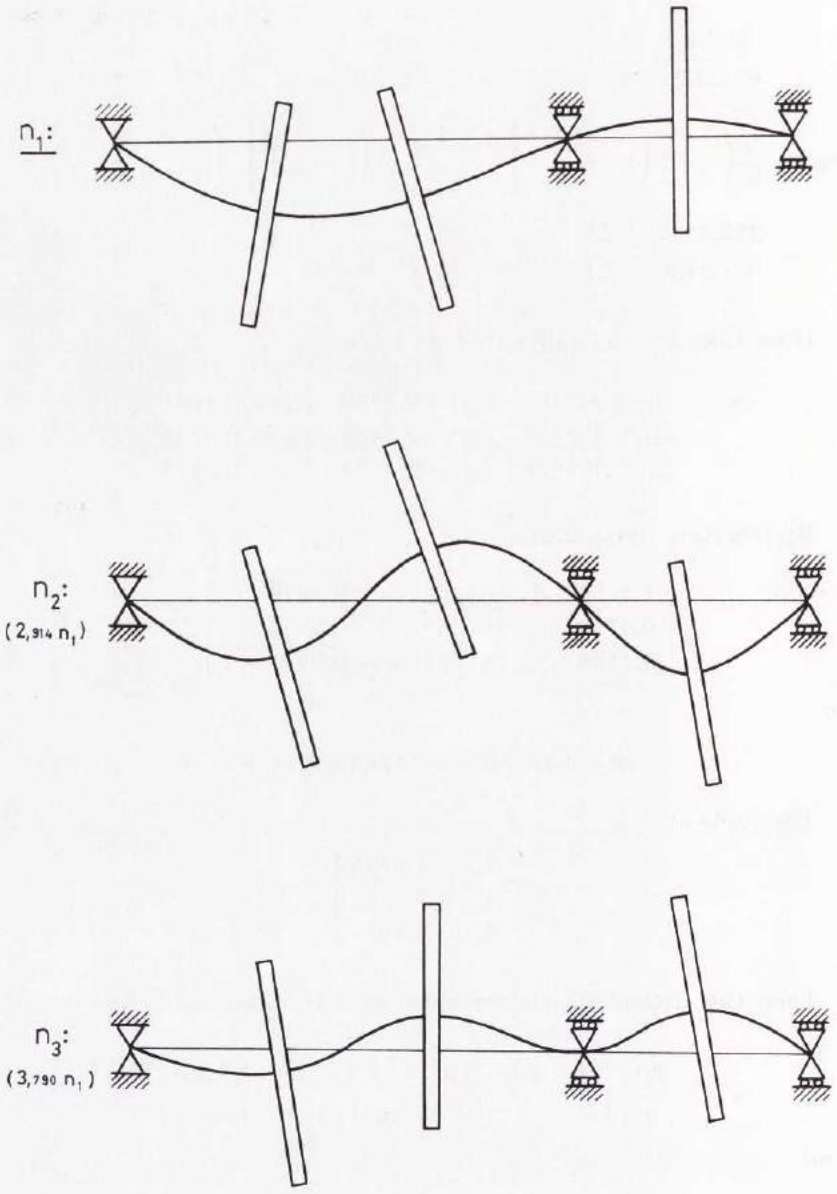

Fig. 36.1

The deflection curves in these three cases can be estimated if the ratios $y_1 : y_2 : y_3$ are known.

From the mathematical theory of determinants it is known that

$$y_1 : y_2 : y_3 = \begin{vmatrix} 0{,}9280-\Lambda & 0{,}2025 \\ 0{,}2025 & 0{,}2221-\Lambda \end{vmatrix} : - \begin{vmatrix} 0{,}8720 & 0{,}2025 \\ 0{,}1620 & 0{,}2221-\Lambda \end{vmatrix} : \begin{vmatrix} 0{,}8720 & 0{,}9280-\Lambda \\ 0{,}1620 & 0{,}2025 \end{vmatrix}$$

With the aid of this expression the following is obtained

$$\begin{aligned} \Lambda_1 &= 1{,}9925 \quad y_2 = 0{,}8552 y_1 \quad y_3 = -0{,}1893 y_1 \\ \Lambda_2 &= 0{,}2348 \quad y_2 = -0{,}8815 y_1 \quad y_3 = -1{,}2912 y_1 \\ \Lambda_3 &= 0{,}1388 \quad y_2 = -1{,}6113 y_1 \quad y_3 = 1{,}9717 y_1 \end{aligned}$$

and the deflection curves can be sketched as shown in figs 36.1 (the deflections are enormously exaggerated).

6. Critical Speeds of a Shaft Supported by Bearings of Lateral Flexibility

In Chapter 5 the shafts carrying the flywheels were supported by rigid bearings. In practice, however, such bearings hardly exist. In most cases they are subjected to elastic deformations. Unfortunately the spring constants occurring are difficult to determine. Moreover the spring constants may be different in different directions.

The usual bearing arrangements (ball-bearings) have the greatest stiffness in the vertical direction and the smallest in the horizontal direction and these conditions are assumed to be valid in the following treatment.

Consider the shaft in fig. 39.1. The bearings are supported in springs with the vertical spring constants being c_1 and c_2.

If we assume that the gyroscopic effect may be neglected the rotational motion can be split up into two oscillations, one in the vertical direction and another in the horizontal one.

Here we study the vertical motion. The left and the right hand springs are depressed y_0^* and $(y_0+y_0^*)$ respectively. In the point Q_i the force F_i is applied. The deflection in Q_s is wanted.

With notations according to fig. 39.1 the total deflection in the point Q_i can be written

$$(y_{\text{tot}})_i = y_i+l_i y_0+y_0^* \quad \ldots\ldots\ldots\ldots\ldots \quad 38.1$$

where y_i is the elastic deflection of the shaft and $(l_i y_0+y_0^*)$ is caused by the springs.

The force in Q_i is thus

$$F_i = M_i(y_{\text{tot}})_i\Omega^2$$

where Ω is the angular velocity of the whirling motion of the shaft. If we consider ordinary critical speeds this velocity is equal to that of the rotation of the discs.

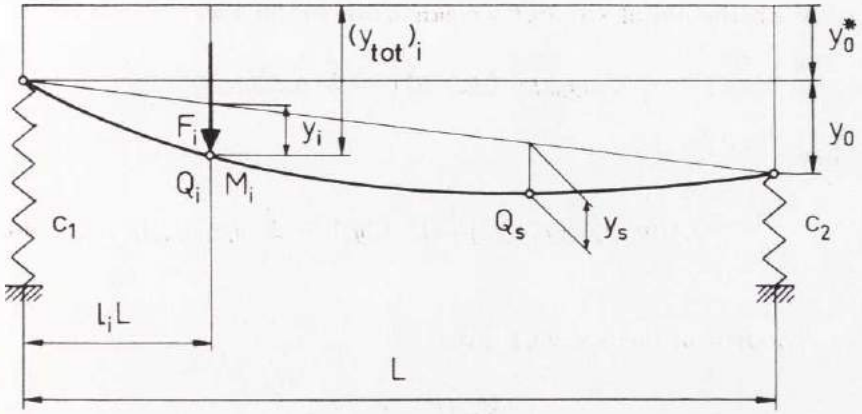

Fig. 39.1

Thus we get for the "elastic" deflection in Q_s

$$y_s = \sum_{i=1}^{n} M_i (y_{tot})_i \Omega^2 \alpha_{si} \quad \ldots\ldots\ldots\ldots\ldots \quad 39.2$$

As in the previous chapter we can put

$$\alpha_{si} = \frac{\xi_{si}}{k} \cdot \frac{L^3}{EI}, \; M_i = \mu_i M_{ref} \text{ and } \Lambda = \frac{kEI}{L^3 M_{ref} \Omega^2}$$

In that way eq. 39.2 becomes

$$\Lambda y_s = \sum_{i=1}^{n} \mu_i \xi_{si} (y_{tot})_i \quad \ldots\ldots\ldots\ldots\ldots \quad 39.3$$

But the equilibrium of the shaft must be fulfilled. Thus

$$\left.\begin{aligned} c_2(y_0 + y_0^*)L - M_{ref}\Omega^2 \sum_{i=1}^{n} \mu_i (y_{tot})_i l_i L = 0 \\ -c_1 y_0^* L + M_{ref}\Omega^2 \sum_{i=1}^{n} \mu_i (y_{tot})_i \, (1 - l_i) L = 0 \end{aligned}\right\} \quad \ldots\ldots\ldots \quad 39.4$$

Addition gives

$$y_0 = M_{ref}\Omega^2 \left(\frac{1}{c_1} + \frac{1}{c_2}\right) \left[\sum_{i=1}^{n} \mu_i l_i (y_{tot})_i - \frac{\dfrac{1}{c_1}}{\dfrac{1}{c_1} + \dfrac{1}{c_2}} \sum_{i=1}^{n} \mu_i (y_{tot})_i \right] \quad 39.5$$

With the aid of eq. 38.1 we can write eq. 39.3 as

$$\Lambda[(y_{tot})_s - l_s y_0 - y_0^*] = \sum_{i=1}^{n} \mu_i \xi_{si} (y_{tot})_i$$

or

$$\Lambda[(y_{tot})_s - (y_0 + y_0^*) + (1 - l_s) y_0] = \sum_{i=1}^{n} \mu_i \xi_{si} (y_{tot})_i \quad \ldots\ldots \quad 40.1$$

The first of the eqs. 39.4 gives

$$y_0 + y_0^* = \frac{M_{ref} \Omega^2}{c} \cdot \frac{c}{c_2} \sum_{i=1}^{n} \mu_i l_i (y_{tot})_i \quad \ldots\ldots\ldots\ldots \quad 40.2$$

If we insert the values of y_0 and $(y_0 + y_0^*)$ according to the eqs. 39.5 and 40.2 respectively in the eq. 40.1 we get by introducing

$$\left.\begin{aligned} \frac{1}{c} &= \frac{1}{c_1} + \frac{1}{c_2} \\ C_1 &= \frac{c}{c_1}; \; C_2 = \frac{c}{c_2} \\ \Theta_M &= \frac{\Lambda M_{ref} \Omega^2}{c} = \frac{k}{c} \cdot \frac{EI}{L^3} \end{aligned}\right\} \quad \ldots\ldots\ldots\ldots \quad 40.3$$

that

$$\Lambda (y_{tot})_s + \Theta_M (1 - l_s - C_2) \sum_{i=1}^{n} \mu_i l_i (y_{tot})_i - \Theta_M (1 - l_s) C_1 \sum_{i=1}^{n} \mu_i (y_{tot})_i -$$

$$- \sum_{i=1}^{n} \mu_i \xi_{si} (y_{tot})_i = 0 \qquad s = 1, 2, 3 \ldots n$$

We have obtained n equations. Only non-dimensional quantities are involved. The unknown variables are $(y_{tot})_1$, $(y_{tot})_2 \ldots . (y_{tot})_n$. The condition for these equations not having only a trivial solution gives the eq. 41.1.

$$\begin{vmatrix} -\Lambda+\mu_1\Theta_M[l_1C_2-(1-l_1)(l_1-C_1)]+\mu_1\xi_{11} & \mu_2\Theta_M[l_2C_2-(1-l_1)(l_2-C_1)]+\mu_2\xi_{12} & \dots & \mu_n\Theta_M[l_nC_2-(1-l_1)(l_n-C_1)]+\mu_n\xi_{1n} \\ \mu_1\Theta_M[l_1C_2-(1-l_2)(l_1-C_1)]+\mu_1\xi_{21} & -\Lambda+\mu_2\Theta_M[l_2C_2-(1-l_2)(l_2-C_1)]+\mu_2\xi_{22} & \dots & \mu_n\Theta_M[l_nC_2-(1-l_2)(l_n-C_1)]+\mu_n\xi_{2n} \\ - - - & - - - & - - - & - - - \\ \mu_1\Theta_M[l_1C_2-(1-l_n)(l_1-C_1)]+\mu_1\xi_{n1} & \mu_2\Theta_M[l_2C_2-(1-l_1)(l_2-C_1)]+\mu_2\xi_{n2} & \dots & -\Lambda+\mu_n\Theta_M[l_nC_2-(1-l_n)(l_n-C_1]+\mu_n\xi_{nn} \end{vmatrix} = 0 \qquad \dots\dots\dots\dots\dots \; 41.1$$

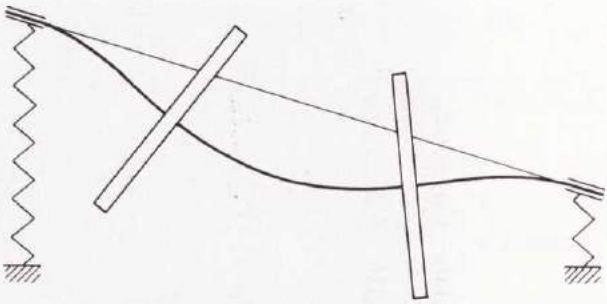

Fig. 42.1

From this equation the A-values are obtained. Then the critical speeds are

$$n_i = \frac{30}{\pi}\sqrt{\frac{kEI}{M_{\text{ref}}L^3A_i}} \quad \ldots\ldots\ldots\ldots\ldots\ldots \quad 42.2$$

For rigid bearings $c_1 = c_2 = \infty$. Thus $c = \infty$, but the values of C_1 and C_2 are finite. For example we can make $c_1 = c_2 \to \infty$. Because of $\frac{1}{c} = \frac{1}{c_1} + \frac{1}{c_2} = \frac{2}{c_1} = \frac{2}{c_2}$ we get $C_1 = C_2 = \frac{1}{2}$. Further $\Theta_M = 0$, and all terms containing Θ_M vanish. The equation 41.1 in this case is identically equal to eq. 25.1.

The choice of the way to calculate the influence numbers depends on the form of the shaft.

If the shaft has but one diameter the influence functions in fig. 21.1 may be used. In other cases graphic methods are advantageous.

It will be observed that the deflection line for a case where the bearings give bending moments will essentially be as in fig. 42.1.

If the spring constants for the bearings are the same in all directions the number of critical speeds is the same as the number of the discs according to the elementary theory. If the spring constants are different in different directions this statement is not correct. The bearing and its neighbourhood are replaced by an infinite number of springs as in fig. 43.1.

These springs have spring constants (per length unit) according to

$$c_\theta = c_1 + (c_2 - c_1)\sin\theta \quad \text{at} \quad 0 \leq \theta \leq \pi$$
$$c_\theta = c_1 - (c_2 - c_1)\sin\theta \quad \text{at} \quad \pi \leq \theta \leq 2\pi$$

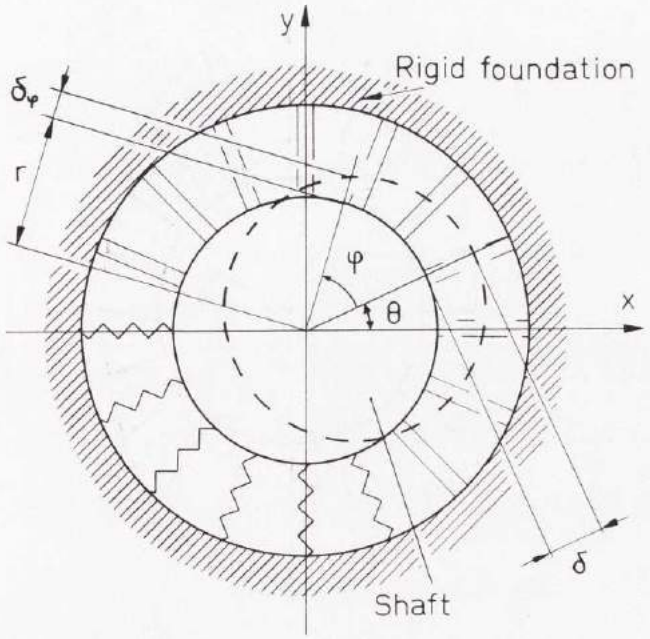

Fig. 43.1

where

c_θ is the spring constant at the angle Θ

c_1 is the spring constant at the angles $\Theta = 0$ and π

c_2 is the spring constant at the angles $\Theta = \frac{\pi}{2}$ and $\frac{3\pi}{2}$

The spring constant function is shown in fig. 44.1. In most machine constructions there is a symmetry concerning the spring constants similar to that one above. Now the shaft is given a displacement δ in the Θ direction shown in figs. 43.1 and 44.1. The problem is to find the direction of the resultant force F. This force may have the components F_x and F_y. Thus we get from the equilibrium equations:

$$\left.\begin{aligned} dF_x &= (c_{\Theta+\varphi}\delta_\varphi r d\varphi) \cdot \cos(\Theta+\varphi) \\ dF_y &= (c_{\Theta+\varphi}\delta_\varphi r d\varphi) \cdot \sin(\Theta+\varphi) \end{aligned}\right\} \quad \ldots\ldots\ldots \quad 43.2$$

It is readily shown that $\delta_\varphi = \delta \cos \varphi$ if $\delta \ll r$.

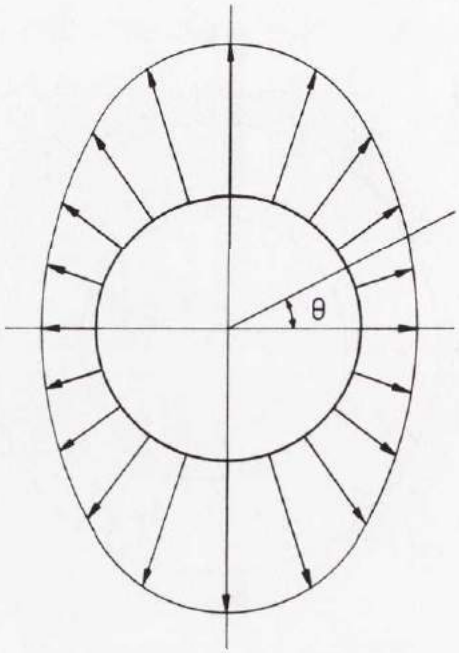

Fig. 44.1

Integration of the eq. 43.2 gives

$$\left.\begin{aligned}
\frac{F_x}{r\delta c_1} &= \int_{-\theta}^{\pi-\theta}\left[1+\left(\frac{c_2}{c_1}-1\right)\sin(\Theta+\varphi)\right]\cos\varphi\cos(\Theta+\varphi)\,d\varphi+\\
&+\int_{\pi-\theta}^{2\pi-\theta}\left[1-\left(\frac{c_2}{c_1}-1\right)\sin(\Theta+\varphi)\right]\cos\varphi\cos(\Theta+\varphi)\,d\varphi\\
\frac{F_y}{r\delta c_1} &= \int_{-\theta}^{\pi-\theta}\left[1+\left(\frac{c_2}{c_1}-1\right)\sin(\Theta+\varphi)\right]\cos\varphi\sin(\Theta+\varphi)\,d\varphi+\\
&+\int_{\pi-\theta}^{2\pi-\theta}\left[1-\left(\frac{c_2}{c_1}-1\right)\sin(\Theta+\varphi)\right]\cos\varphi\sin(\Theta+\varphi)\,d\varphi
\end{aligned}\right\}$$

and from these eqs we get after some calculations

$$\left.\begin{aligned}
\frac{F_x}{r\delta c_1} &= \left[\pi+\frac{4}{3}\left(\frac{c_2}{c_1}-1\right)\right]\cos\Theta\\
\frac{F_y}{r\delta c_1} &= \left[\pi+\frac{8}{3}\left(\frac{c_2}{c_1}-1\right)\right]\sin\Theta
\end{aligned}\right\} \quad \ldots\ldots\ldots \quad 44.2$$

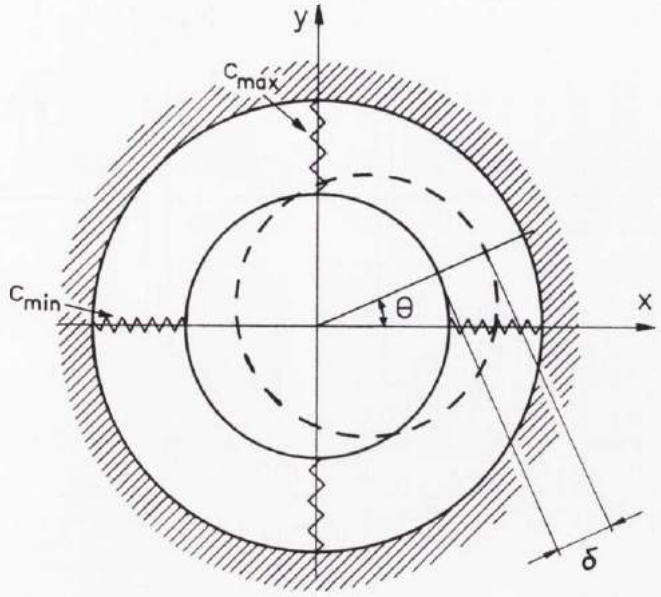

Fig. 45.1

Construct the ratio

$$\frac{F_y}{F_x} = \frac{\pi + \frac{8}{3}\left(\frac{c_2}{c_1} - 1\right)}{\pi + \frac{4}{3}\left(\frac{c_2}{c_1} - 1\right)} \cdot \operatorname{tg} \Theta$$

This expression shows that the resultant force $F = \sqrt{F_x^2 + F_y^2}$ does not have the same direction as the displacement δ except in two cases, viz. $\Theta = 0$ and $\Theta = \frac{\pi}{2}$.

Thus the rotation of the shaft with discs ought to be split up into those directions which have the least and the greatest spring constants. In the case above the maximum and the minimum spring stiffnesses are

$$\left.\begin{aligned} c_{min} &= r\left[\pi c_1 + \frac{4}{3}(c_2 - c_1)\right] \\ c_{max} &= r\left[\pi c_1 + \frac{8}{3}(c_2 - c_1)\right] \end{aligned}\right\} \quad \ldots\ldots\ldots\ldots \quad 45.2$$

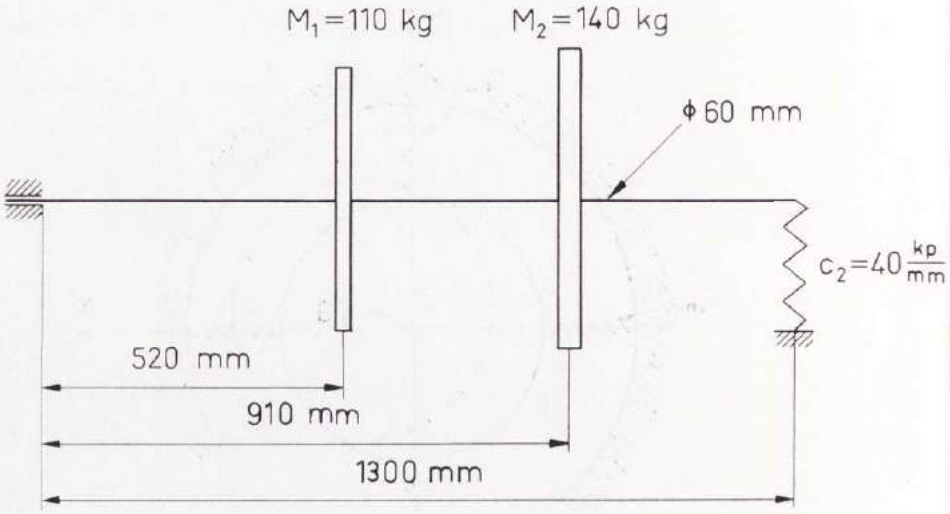

Fig. 46.1

Instead of the spring system in fig. 43.1 we can use the analogous and much simpler one in fig. 45.1.

Giving the shaft the displacement δ in the Θ-direction we get

$$\left.\begin{aligned}\delta_x &= \delta \cos \Theta \\ \delta_y &= \delta \sin \Theta\end{aligned}\right\} \quad \text{and} \quad \left.\begin{aligned}F_x &= c_{\min}\delta_x \\ F_y &= c_{\max}\delta_y\end{aligned}\right\}$$

and finally

$$\left.\begin{aligned}F_x &= c_{\min}\delta \cos \Theta \\ F_y &= c_{\max}\delta \sin \Theta\end{aligned}\right\} \quad \ldots\ldots\ldots\ldots\ldots\ldots \quad 46.2$$

By insertion of $c_{\min}$ and $c_{\max}$ according to eqs. 45.2 we see that the eqs 46.2 are exactly the same as the eqs 44.2.

However, the relative positions of the main directions of the spring constants may vary in the different supporting bearings. Here we limit ourselves to those bearings in which these directions coincide. The usual arrangements are in this way.

The theory is in the following illustrated by numerical examples.

Example 7. Calculate the critical speeds for an arrangement according to fig. 46.1. The discs are thin and the influence of the mass of the shaft and the gyroscopic effect may be neglected. The left hand side bearing is rigid and the right hand side bearing has the same spring

constant in all directions, namely $c_2 = 40$ kp/mm. The diameter of the shaft is 60 mm and $E = 21\,000$ kp/mm².

If we choose $M_{ref} = M_1$ so is $\mu_1 = 1$ and $\mu_2 = \frac{14}{11}$. Further $l_1 = 0{,}4$, $l_2 = 0{,}7$.

For the influence numbers we have

$$\alpha_{ij} = \frac{1}{6} x_1 x_2^2 \left[\frac{1}{2} (3 - x_1^2)(1 - x_2) - x_1^2 \right] \cdot \frac{L^3}{EI}$$

Thus

$$\alpha_{11} = \frac{1}{6} 0{,}4^2 \cdot 0{,}6 \, [0{,}5 \, (1-0{,}4) \, (3-0{,}6^2) - 0{,}6^2] \cdot \frac{L^3}{EI} = \frac{0{,}041472}{6} \cdot \frac{L^3}{EI}$$

$$\alpha_{12} = \frac{1}{6} 0{,}4^2 \cdot 0{,}3 \, [0{,}5 \, (1-0{,}4) \, (3-0{,}6^2) - 0{,}3^2] \cdot \frac{L^3}{EI} = \frac{0{,}037584}{6} \cdot \frac{L^3}{EI}$$

$$\alpha_{22} = \frac{1}{6} 0{,}7^2 \cdot 0{,}3 \, [0{,}5 \, (1-0{,}7) \, (3-0{,}3^2) - 0{,}3^2] \cdot \frac{L^3}{EI} = \frac{0{,}050936}{6} \cdot \frac{L^3}{EI}$$

Taking $k = 600$ we get

$$\xi_{11} = 4{,}1472; \; \xi_{12} = 3{,}7584; \; \xi_{22} = 5{,}0936;$$

$$c_1 = \infty \text{ and } \frac{1}{c} = \frac{1}{c_1} + \frac{1}{c_2} \text{ gives } c = c_2, \; C_1 = 0, \; C_2 = 1$$

Using the MKSA-system

$$\Theta_M = \frac{kEI}{cL^3} = \frac{600 \cdot 21\,000 \cdot 9{,}80665 \cdot 10^6 \cdot \frac{\pi}{64} \cdot 60^4 \cdot 10^{-12}}{40 \cdot 9{,}80665 \cdot 10^3}$$

$$\Theta_M = 91{,}0$$

The eq. 41.1 gives

$$\begin{vmatrix} -A + 1 \cdot 91{,}0[0{,}4 - 0{,}6 \cdot 0{,}4] + 4{,}1472 & \frac{14}{11}\{91{,}0[0{,}7 - 0{,}6 \cdot 0{,}7] + 3{,}7584\} \\ 91{,}0[0{,}4 - 0{,}3 \cdot 0{,}4] + 3{,}7584 & -A + \frac{14}{11}\{91{,}0[0{,}7 - 0{,}3 \cdot 0{,}7] + 5{,}0936\} \end{vmatrix} = 0$$

..... 47.1

or

$$\Lambda^2 - 81{,}95\Lambda + 94{,}9076 = 0$$

The roots are

$$\left.\begin{aligned}\Lambda_1 &= 80{,}80\\ \Lambda_2 &= 1{,}18\end{aligned}\right\}$$

From eqs 40.3 and 41.1 we get

$$n_i = \frac{30}{\pi}\sqrt{\frac{kEI}{M_{\text{ref}}L^3}}\cdot\frac{1}{\sqrt{\Lambda_i}} = \frac{30}{\pi}\sqrt{\frac{kEI}{cL^3}\cdot\frac{c}{M_{\text{ref}}}}\cdot\frac{1}{\sqrt{\Lambda_i}} =$$

$$= \frac{30}{\pi}\sqrt{\frac{\Theta_M C}{M_{\text{ref}}}}\cdot\frac{1}{\sqrt{\Lambda_i}}$$

and in this special case

$$n_i = \frac{30}{\pi}\sqrt{\frac{91{,}0\cdot 40\cdot 9{,}80665\cdot 10^3}{110}}\cdot\frac{1}{\sqrt{\Lambda_i}}$$

or

$$\left.\begin{aligned}n_1 &= 610 \text{ r.p.m.}\\ n_2 &= 5\,000 \text{ r.p.m.}\end{aligned}\right\}$$

If both of the bearings are rigid we get $\Theta_M = 0$ and from eq. 47.1

$$\begin{vmatrix} -\Lambda + 4{,}1472 & \dfrac{14}{11}\cdot 3{,}7584 \\ 3{,}7584 & -\Lambda + \dfrac{14}{11}\cdot 5{,}0936 \end{vmatrix} = 0$$

with the roots $\Lambda_1 = 9{,}714$ and $\Lambda_2 = 0{,}917$ corresponding to $n_1 =$ $= 1\,750$ r.p.m. and $n_2 = 5\,700$ r.p.m.

Thus the flexibility at the bearing lowers the first critical speed from 1 750 r.p.m. to 610 r.p.m. and the second one from 5 700 r.p.m. to 5 000 r.p.m.

If the left bearing in fig. 46.1 also has the spring constant $c_1 = 40$ kp/mm we get the following.

$$c = \frac{c_1}{2} = \frac{c_2}{2} = 20 \text{ kp/mm}$$

$$\Theta_M = 2 \cdot 91{,}0 = 182$$

By inserting in eq. 41.1 we get

$$\begin{vmatrix} -\Lambda + 182[0{,}4 \cdot 0{,}5 - 0{,}6(0{,}4 - 0{,}5)] + 4{,}1472 & 1{,}273\{182[0{,}7 \cdot 0{,}5 - 0{,}6(0{,}7 - 0{,}5)] + 3{,}7584\} \\ 182[0{,}4 \cdot 0{,}5 - 0{,}3(0{,}4 - 0{,}5)] + 3{,}7584 & -\Lambda + 1{,}273\{182[0{,}7 \cdot 0{,}5 - 0{,}3(0{,}7 - 0{,}5)] + 5{,}0936\} \end{vmatrix}$$

or

$$\Lambda^2 - 223{,}4203\Lambda + 5529{,}52 = 0$$

The roots are

$$\left.\begin{aligned} \Lambda_1 &= 195{,}08 \\ \Lambda_2 &= 28{,}34 \end{aligned}\right\}$$

and these values correspond to the critical speeds

$$\left.\begin{aligned} n_1 &= 390 \text{ r.p.m.} \\ n_2 &= 1\,025 \text{ r.p.m.} \end{aligned}\right\}$$

Thus the critical speeds are further lowered. These results are in line with the general theory saying that the greater the deflections the lower the critical speeds.

Example 8. Calculate the critical speeds for the arrangement in fig. 50.1. The disc is thin and the influence of the mass of the shaft and the gyroscopic effect may be neglected. The shaft is equipped with springs at the ends according to the fig. The spring constants are $c_{2\text{hor}} = 20$ kp/mm and $c_{2\text{vert}} = 40$ kp/mm. The diameter of the shaft is 60 mm och $E = 21\,000$ kp/mm^2.

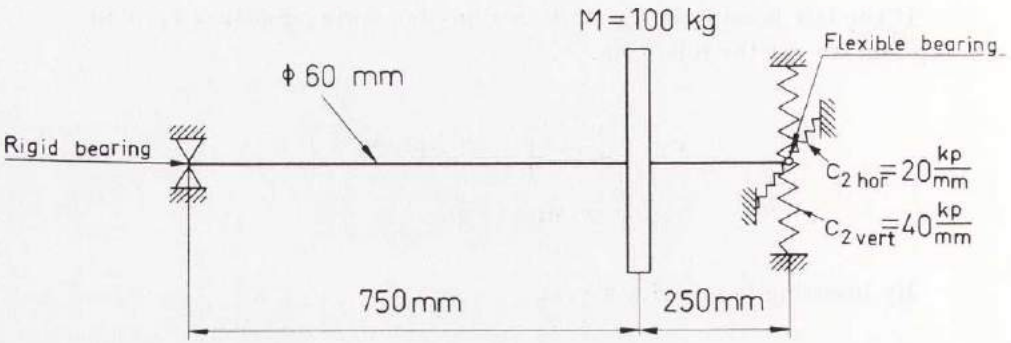

Fig. 50.1

For the influence number we get

$$\alpha_{ij} = \frac{1}{3}(x_1 x_2)^2 \cdot \frac{L^3}{EI} \quad \text{(See page 215)}$$

and here is $l_1 = x_1 = \frac{3}{4}$ and $l_2 = x_2 = \frac{1}{4}$ giving $\alpha_{11} = \frac{3}{256} \cdot \frac{L^3}{EI}$.

Further we choose $M_{ref} = M = 100$ kg. Thus $\mu_1 = \mu = 1$.
For the "vertical motion" we have

$$\frac{1}{c_{vert}} = \frac{1}{\infty} + \frac{1}{40}$$

Thus $c_{vert} = 40$ and $C_{1vert} = \frac{c_{vert}}{c_{1vert}} = 0$, $C_{2vert} = \frac{c_{vert}}{c_{2vert}} = 1$.

For the "horisontal motion" we have

$$\frac{1}{c_{hor}} = \frac{1}{\infty} + \frac{1}{c_{2hor}}$$

Thus $c_{hor} = 20$ and $C_{1hor} = \frac{c_{hor}}{c_{1hor}} = 0$, $C_{2hor} = \frac{c_{hor}}{c_{2hor}} = 1$.

Further choose $k = 256$. Thus $(\Theta_M)_{vert} = 42{,}67$ and $(\Theta_M)_{hor} = 85{,}33$.

The eq. 41.1 gives

$$-\Lambda_{\text{vert}} + 42{,}67\left[\frac{3}{4}\cdot 1 - \frac{1}{4}\left(\frac{1}{4} - 0\right)\right] + 1 \cdot 3 = 0$$

$$\Lambda_{\text{vert}} = 32{,}33$$

and

$$-\Lambda_{\text{hor}} + 85{,}33\left[\frac{3}{4}\cdot 1 - \frac{1}{4}\left(\frac{1}{4} - 0\right)\right] + 1 \cdot 3 = 0$$

$$\Lambda_{\text{hor}} = 62{,}67$$

The corresponding critical speeds are $n_{\text{vert}} = 687$ r.p.m. and $n_{\text{hor}} = 494$ r.p.m.

Without springs we get $\Lambda_{\text{vert}} = \Lambda_{\text{hor}} = 3$ and $n = 2\,256$ r.p.m.

7. The Gyroscopic Effect

In the calculations of the previous chapters no account has been taken to those moments which occur due to the gyroscopic effect. This is done in this chapter.

Consider the disc in fig. 52.1. The deflection line is magnified for clearness. The arrangement is studied at a critical speed. The whirl around the axis AA' has the angular velocity Ω. Now at first suppose that the motor gives to the shaft the same angular velocity. The cross-section BB' in fig. 53.1 shows that a point P on the shaft always will be outwards. This case is the only one of all possible rotational cases without fatigue.

Thus the shaft rotates around O_{11} with the angular velocity Ω.

If the motor delivers an angular velocity of $\omega = \Omega + \omega'$ on the same time as the whirl occurs with velocity Ω instead of fig. 53.1 we get fig. 53.2.

The task is to determine in which way the disc will act on the shaft apart from the centrifugal force. Consider the shaft in fig. 53.3. The disc is assumed to be in a steady whirling motion while the motor runs and it moves around a point on the centreline. The coordinate system ξ, η, ζ rotates with the disc and the eccentricity of the disc is e. The gravity point of the disc is on a line parallel to the ξ-axis.

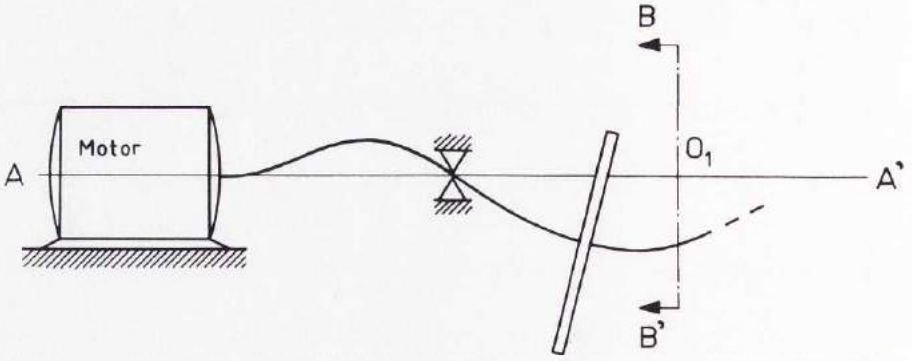

Fig. 52.1

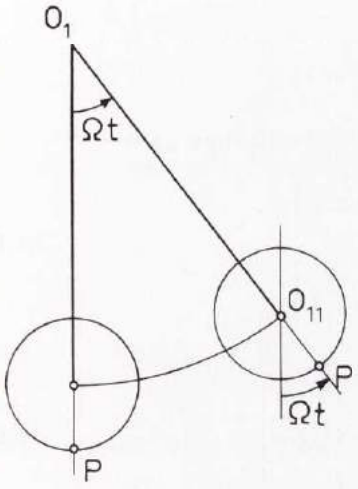

Fig. 53.1

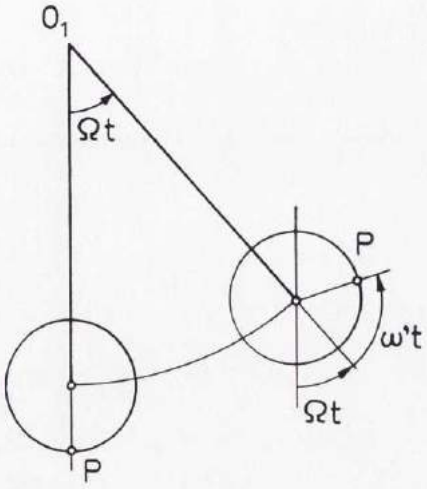

Fig. 53.2

By projection

$$\left.\begin{aligned} \omega_\xi &= \Omega \sin\alpha \cos\omega' t \\ \omega_\eta &= -\Omega \sin\alpha \sin\omega' t \\ \omega_\zeta &= \Omega \cos\alpha + \omega' = \omega'' \end{aligned}\right\}$$

The circumstances for the motions give

$$\omega = \Omega + \omega'$$

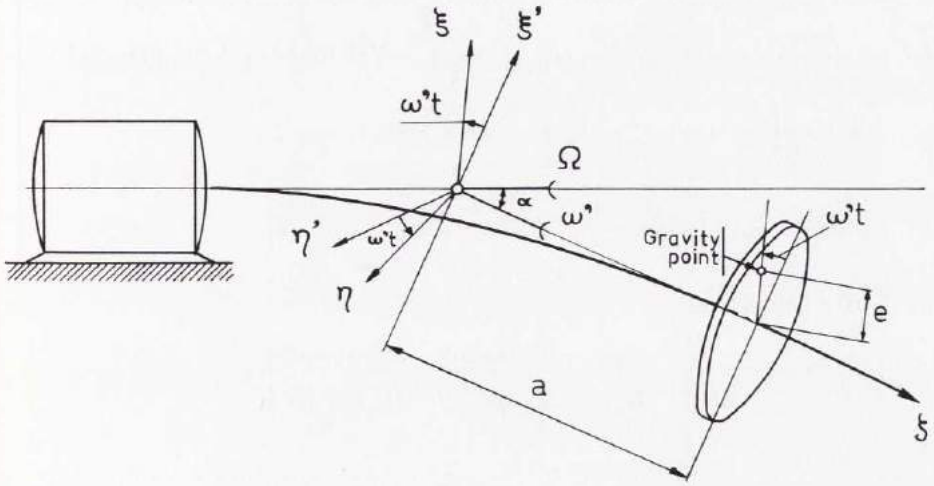

Fig. 53.3

and thus

$$\omega'' = \omega - \Omega\,(1-\cos\alpha)$$

From mechanics the moments (with usual notations) are

$$\left.\begin{aligned} M_\xi &= \dot{U}_\xi - U_\eta\omega_\zeta + U_\zeta\omega_\eta \\ M_\eta &= \dot{U}_\eta - U_\zeta\omega_\xi + U_\xi\omega_\zeta \\ M_\zeta &= \dot{U}_\zeta - U_\xi\omega_\eta + U_\eta\omega_\xi \end{aligned}\right\} \quad \ldots\ldots\ldots\ldots\ldots \quad 54.1$$

and

$$\left.\begin{aligned} U_\xi &= I_\xi\omega_\xi - D_{\xi\eta}\omega_\eta - D_{\xi\zeta}\omega_\zeta \\ U_\eta &= I_\eta\omega_\eta - D_{\eta\zeta}\omega_\zeta - D_{\xi\eta}\omega_\xi \\ U_\zeta &= I_\zeta\omega_\zeta - D_{\xi\zeta}\omega_\xi - D_{\eta\zeta}\omega_\eta \end{aligned}\right\} \quad \ldots\ldots\ldots\ldots \quad 54.2$$

Further

$$\left.\begin{aligned} I_\xi &= I_e + Ma^2 \\ I_\eta &= I_e + M(a^2+e^2) \\ I_\zeta &= I_p + Me^2 \end{aligned}\right\} \qquad \left.\begin{aligned} D_{\xi\eta} &= 0 \\ D_{\xi\zeta} &= Mea \\ D_{\eta\zeta} &= 0 \end{aligned}\right\}$$

Insertion of the actual values in eqs 54.1 and 54.2 gives

$$\left.\begin{aligned} M_\xi &= -\Omega\sin\alpha\sin\omega' t\,\{I_\xi\omega' + (I_p - I_\xi)\omega''\} + \frac{1}{2}\,Mea\,\Omega^2\sin^2\alpha\sin 2\omega' t \\ M_\eta &= -\Omega\sin\alpha\cos\omega' t\,\{I_\xi\omega' + (I_p - I_\xi)\omega''\} - Me^2\Omega(\omega'+\omega'')\sin\alpha\cos\omega' t + \\ &\quad + Mea\left(\frac{\Omega^2}{2}\sin^2\alpha - \omega''^2\right) + \frac{1}{2}\,Mea\Omega^2\sin^2\alpha\cos 2\omega' t \\ M_\zeta &= -Me\Omega^2\sin\alpha\left(a\cos\alpha\sin\omega' t + \frac{1}{2}\,e\sin\alpha\sin 2\omega' t\right) \end{aligned}\right\} \quad 54.3$$

By projection

$$\left.\begin{aligned} M_{\xi'} &= M_\xi\cos\omega' t - M_\eta\sin\omega' t \\ M_{\eta'} &= M_\xi\sin\omega' t + M_\eta\cos\omega' t \end{aligned}\right\}$$

and further

$$M_{\text{motor}} = M_\zeta\cos\alpha + M_{\xi'}\sin\alpha$$

In the special case $e = 0$

$$M_{\xi'} = 0$$

$$M_{\eta'} = -\Omega \sin \alpha \, (I_p \omega'' - I_e \Omega \cos \alpha) + M \, (a \sin \alpha) \Omega^2 \, (a \cos \alpha)$$

$$M_{\text{motor}} = 0$$

The last term in $M_{\eta'}$ means the moment of the "centrifugal force". The moment at the disc, M_g, must be reduced by this amount. Thus by putting $\sin \alpha = \text{tg } \alpha$ and $\cos \alpha = 1$ because α is a small angle we get

$$M_g = -\Omega^2 \left\{ I_p \frac{\omega}{\Omega} - I_e \right\} y'$$

For a thin disc $I_e = \frac{1}{2} I_p$ and consequently

$$M_g = -I_p \Omega^2 \left\{ \frac{\omega}{\Omega} - \frac{1}{2} \right\} y' \quad \ldots\ldots\ldots\ldots \quad 55.1$$

With forward whirl $\frac{\omega}{\Omega} = 1$ and

$$M_{gf} = -\frac{1}{2} I_p \Omega^2 y'$$

With reverse whirl $\frac{\omega}{\Omega} = -1$ and

$$M_{gr} = \frac{3}{2} I_p \Omega^2 y'$$

Observe that the calculated moments are those acting from outside on the disc. Consequently the disc acts on the shaft with moments of the same value but with opposite signs. In that way it is easily seen that M_{gf} tries to bring the shaft back to the centerline but M_{gr} has the opposite action.

Generally the ratio $\frac{\omega}{\Omega} = f$ is not specified to ± 1. It has been seen during tests [3] that under certain circumstances f may have the

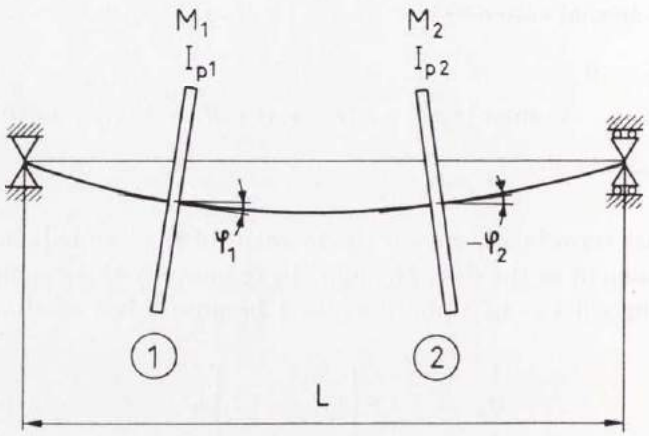

Fig. 56.1

values $+\frac{1}{2}$ and $+\frac{1}{3}$ and theoretically speaking there is no obstacle to f taking any value. But the most common case is $f = +1$ and the practical importance of other possibilities is probably not great. However, at the end of this chapter different critical speeds of a certain arrangement are discussed.

First we consider the shaft with two thin flywheels in fig. 56.1.

The flywheels are perfectly balanced and have the polar inertias I_{p1} and I_{p2}. The inclinations of the shaft at the flywheels are φ_1 and φ_2 at a certain speed.

Then the shaft is affected by forces and moments as in fig. 56.2.

Further we assume that the whirling motion of the shaft around the line between the two bearings has the angular velocity $\Omega \frac{1}{s}$.

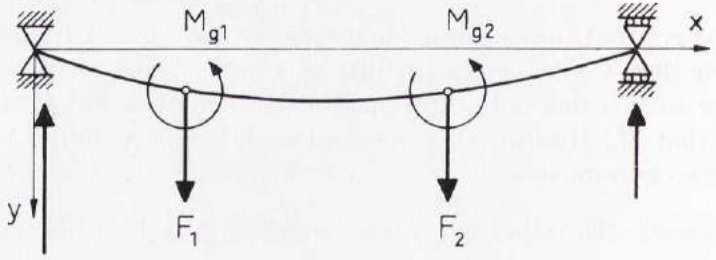

Fig. 56.2

If the rotation around the shaft has the same velocity we get

$$\left.\begin{aligned} F_1 &= M_1 y_1 \Omega^2 \\ F_2 &= M_2 y_2 \Omega^2 \\ M_{g1} &= \frac{1}{2} I_{p1} \Omega^2 \varphi_1 \\ M_{g2} &= \frac{1}{2} I_{p2} \Omega^2 \varphi_2 \end{aligned}\right\} \quad \ldots\ldots\ldots\ldots\ldots 57.1$$

Introduce the following notations:

α_{Fij} = the displacement at a point Q_i on the shaft caused by a unit force at a point Q_j.

α_{Mij} = the displacement at a point Q_i on the shaft caused by a unit moment at a point Q_j.

β_{Fij} = the angle at a point Q_i on the shaft caused by a unit force at a point Q_j.

β_{Mij} = the angle at a point Q_i on the shaft caused by a unit moment in a point Q_j.

The points Q_i and Q_j are arbitrarily choosen. We get

$$\left.\begin{aligned} y_1 &= \alpha_{F11} F_1 + \alpha_{F12} F_2 + \alpha_{M11} M_{g1} + \alpha_{M12} M_{g2} \\ y_2 &= \alpha_{F21} F_1 + \alpha_{F22} F_2 + \alpha_{M21} M_{g1} + \alpha_{M22} M_{g2} \\ \varphi_1 &= \beta_{F11} F_1 + \beta_{F12} F_2 + \beta_{M11} M_{g1} + \beta_{M12} M_{g2} \\ \varphi_2 &= \beta_{F21} F_1 + \beta_{F22} F_2 + \beta_{M21} M_{g1} + \beta_{M22} M_{g2} \end{aligned}\right\} \quad \ldots\ldots\ldots 57.2$$

The eqs 57.1 and 57.2 give

$$\left.\begin{aligned} \left(\alpha_{F11} - \frac{1}{M_1 \Omega^2}\right) F_1 + \alpha_{F12} F_2 + \alpha_{M11} M_{g1} + \alpha_{M12} M_{g2} &= 0 \\ \alpha_{F21} F_1 + \left(\alpha_{F12} - \frac{1}{M_2 \Omega^2}\right) F_2 + \alpha_{M21} M_{g1} + \alpha_{M22} M_{g2} &= 0 \\ \beta_{F11} F_1 + \beta_{F12} F_2 + \left(\beta_{M11} - \frac{2}{I_{p1} \Omega^2}\right) M_{g1} + \beta_{M12} M_{g2} &= 0 \\ \beta_{F21} F_1 + \beta_{F22} F_2 + \beta_{M21} M_{g1} + \left(\beta_{M22} - \frac{2}{I_{p2} \Omega^2}\right) M_{g2} &= 0 \end{aligned}\right\}$$

These equations have not only a trivial solution if

$$\begin{vmatrix} \alpha_{F11} - \dfrac{1}{M_1\Omega^2} & \alpha_{F12} & \alpha_{M11}L & \alpha_{M12}L \\ \alpha_{F21} & \alpha_{F22} - \dfrac{1}{M_2\Omega^2} & \alpha_{M21}L & \alpha_{M22}L \\ \beta_{F11}L & \beta_{F12}L & \left(\beta_{M11} - \dfrac{2}{I_{p1}\Omega^2}\right)L^2 & \beta_{M12}L^2 \\ \beta_{F21}L & \beta_{F22}L & \beta_{M21}L^2 & \left(\beta_{M22} - \dfrac{2}{I_{p2}\Omega^2}\right)L^2 \end{vmatrix} = 0 \quad \ldots\ldots\ldots\ldots\ldots\ldots 58.1$$

The two last rows and columns are multiplied by the length of the shaft L in order to bring the same dimension to all the influence numbers.

Every term in the equation above is then multiplied by $\dfrac{kEI}{L^3}$, where k is an arbitrary constant giving simple numbers in the determinant. Further introduce

$$A = \frac{kEI}{L^3} \cdot \frac{1}{M_{\text{ref}}\Omega^2} \quad \ldots\ldots\ldots\ldots\ldots\ldots 58.2$$

as in Chapter 5. Thus, as an example,

$$\left(\alpha_{F11} - \frac{1}{M_1\Omega^2}\right) \cdot \frac{kEI}{L^3} = \frac{kEI}{L^3} \cdot \alpha_{F11} - \frac{kEI}{L^3} \cdot \frac{1}{M_1\Omega^2} =$$

$$= \frac{kEI}{L^3} \cdot \frac{\xi_{F11}}{k} \cdot \frac{L^3}{EI} - \frac{kEI}{L^3} \cdot \frac{1}{M_{\text{ref}}\Omega^2} \cdot \frac{M_{\text{ref}}}{M_1} = \xi_{F11} - A\mu_1^{-1}$$

where

$$\xi_{F11} = \alpha_{F11} \cdot \frac{kEI}{L^3} \quad \text{(Compare the notation in Chapter 5)}$$

and

$$\mu_1 = \frac{M_1}{M_{\text{ref}}}$$

In a similar way we may proceed with other terms.

For example we get

$$\left(\beta_{M11} - \frac{2}{I_{p1}\Omega^2}\right) L^2 \cdot \frac{kEI}{L^3} = \zeta_{M11} - \Lambda\nu_1^{-1}$$

where

$$\zeta_{M11} = \beta_{M11} \cdot \frac{kEI}{L}$$

and

$$\nu_1 = \frac{I_{p1}}{2M_{\text{ref}}L^2}$$

We finally get

$$\begin{vmatrix} \xi_{F11} - \Lambda\mu_1^{-1} & \xi_{F12} & \xi_{M11} & \xi_{M12} \\ \xi_{F21} & \xi_{F22} - \Lambda\mu_2^{-1} & \xi_{M21} & \xi_{M22} \\ \zeta_{F11} & \zeta_{F12} & \zeta_{M11} - \Lambda\nu_1^{-1} & \zeta_{M12} \\ \zeta_{F21} & \zeta_{F22} & \zeta_{M21} & \zeta_{M22} - \Lambda\nu_2^{-1} \end{vmatrix} = 0 \quad \ldots \quad 59.1$$

where

$$\left.\begin{aligned} \xi_{Fij} &= \alpha_{Fij} \cdot \frac{kEI}{L^3} \\ \xi_{Mij} &= \alpha_{Mij} \cdot \frac{kEI}{L^2} \\ \zeta_{Fij} &= \beta_{Fij} \cdot \frac{kEI}{L^2} \\ \zeta_{Mij} &= \beta_{Mij} \cdot \frac{kEI}{L} \end{aligned}\right\} \quad \ldots\ldots\ldots\ldots\ldots\ldots \quad 59.2$$

and due to Maxwell's theorem and the definitions of the influence numbers

$$\begin{aligned} \xi_{F12} &= \xi_{F21} & \xi_{M21} &= -\zeta_{F12} \\ \xi_{M11} &= -\zeta_{F11} & \xi_{M22} &= -\zeta_{F22} \\ \xi_{M12} &= -\zeta_{F21} & \zeta_{M12} &= \zeta_{M21} \end{aligned}$$

Thus the determinant is symmetrical with respect to one of its diagonals after multiplying the two lowest rows with -1.

The generalization of eq. 59.1 for n discs is evident.

$$
\begin{array}{cccccc}
(\xi_{F11}-\Lambda\mu_1^{-1}) & \xi_{F12}\cdots & \xi_{F1n} & \xi_{M11} & \xi_{M12}\cdots & \xi_{M1n} \\
\xi_{F21} & (\xi_{F22}-\Lambda\mu_2^{-1})\cdots & \xi_{F2n} & \xi_{M21} & \xi_{M22}\cdots & \xi_{M2n} \\
\hline
\xi_{Fn1} & \xi_{Fn2}\cdots & (\xi_{Fnn}-\Lambda\mu_n^{-1}) & \xi_{Mn1} & \xi_{Mn2}\cdots & \xi_{Mnn} \\
\zeta_{F11} & \zeta_{F12}\cdots & \zeta_{F1n} & (\zeta_{M11}-\Lambda\nu_1^{-1}) & \zeta_{M12}\cdots & \zeta_{M1n} \\
\zeta_{F21} & \zeta_{F22}\cdots & \zeta_{F2n} & \zeta_{M21} & (\zeta_{M22}-\Lambda\nu_2^{-1}) & \zeta_{M2n} \\
\hline
\zeta_{Fn1} & \zeta_{Fn2}\cdots & \zeta_{Fnn} & \zeta_{Mn1} & \zeta_{Mn2}\cdots & (\zeta_{Mnn}-\Lambda\nu_n^{-1})
\end{array}
= \quad \ldots\ldots\ldots\ldots\ldots\ldots \quad 60
$$

If we denote the angular velocity of the whirling Ω, and that of the shaft about its centreline ω, we now have treated the case $\Omega = \omega$.

In general the moments in fig. 56.2 may be written

$$
\left.
\begin{aligned}
M_{g1} &= (I_{p1}\omega - I_{e1}\Omega)\,\Omega \sin\varphi_1 \\
M_{g2} &= (I_{p2}\omega - I_{e2}\Omega)\,\Omega \sin\varphi_2
\end{aligned}
\right\}
$$

where I_e denotes the lateral inertias of the discs. Thus we get

$$
\nu_i = \frac{(I_{pi}\omega - I_{ei}\Omega)\Omega}{M_{\mathrm{ref}}\Omega^2 L^2} = \frac{I_{pi}\cdot\dfrac{\omega}{\Omega} - I_{ei}}{M_{\mathrm{ref}}L^2} = \left(\frac{\omega}{\Omega} - \frac{I_{ei}}{I_{pi}}\right)\cdot\frac{I_{pi}}{M_{\mathrm{ref}}L^2} \quad \ldots \quad 60.2
$$

If $\dfrac{\omega}{\Omega} = 1$ (forward whirl or ordinary critical speed), and the disc is thin, viz. $I_{ei} = \dfrac{1}{2} I_{pi}$, we get

$$
\nu_i = \frac{I_{pi}}{2M_{\mathrm{ref}}L^2} \quad \ldots\ldots\ldots\ldots\ldots\ldots \quad 60.3
$$

If $\dfrac{\omega}{\Omega} = -1$ (reverse whirl) we get for the same disc

$$
\nu_i = -3\cdot\frac{I_{pi}}{2M_{\mathrm{ref}}L^2} \quad \ldots\ldots\ldots\ldots\ldots\ldots \quad 60.4
$$

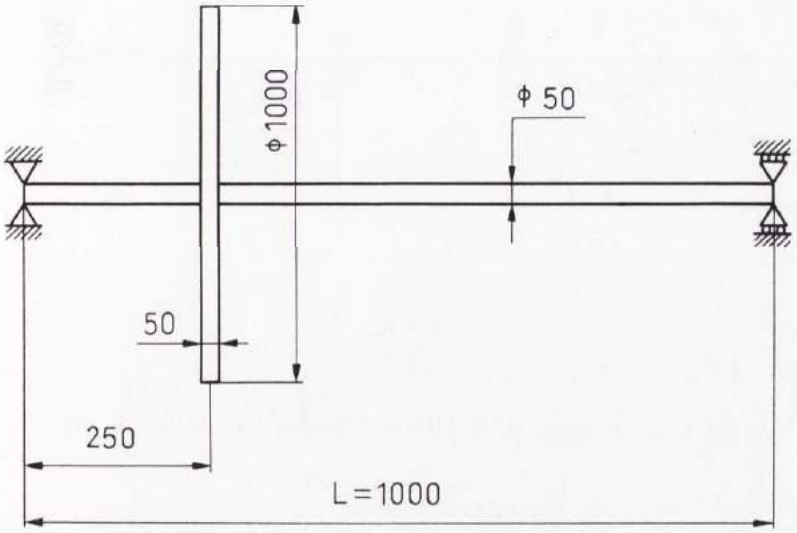

Fig. 61.1

However, the eq. 60.1 is valid in all cases which may occur if ν_i is defined as in eq. 60.2. Observe that the influence numbers must suit the kind of bearings used.

Further we see from eq. 60.2 that n discs give an equation in Λ of order $2n$. Biezeno-Grammel [2] have shown that the equation has n real roots if $\frac{\omega}{\Omega} = 1$ and $2n$ real roots if $\frac{\omega}{\Omega} = -1$.

In the following the use of eq. 60.1 is illustrated by some numerical examples. From these the general conclusion can be made that in bearing arrangements or shafts giving large inclinations to the discs the gyroscopic effect has an obvious influence. In other bearing arrangements its action is smaller.

Example 9. Calculate the critical speeds for the arrangement in fig. 61.1. The ratio $\frac{\omega}{\Omega}$ is thought to be able to vary between the limits $+\infty$ and $-\infty$. The mass of the shaft may be neglected. The shaft and the disc are made of steel.

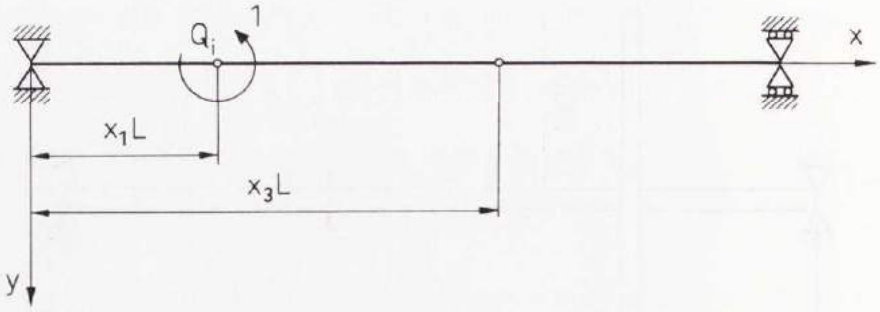

Fig. 62.1

For an arrangement with "hinged-hinged" ends we have

$$\left.\begin{aligned} \alpha_{Fij} &= \frac{1}{6}\, x_1 x_2 (1 - x_1^2 - x_2^2) \cdot \frac{L^2}{EI} \\ \beta_{Fij} &= \frac{d\alpha_{ij}}{d(x_1 L)} = \frac{1}{6} \cdot x_2 (1 - 3x_1^2 - x_2^2) \cdot \frac{L^2}{EI} \end{aligned}\right\}$$

In this case $x_2 = (1 - x_1)$. This gives

$$\left.\begin{aligned} \alpha_{Fii} &= \frac{1}{3}\, (x_1 x_2)^2 \cdot \frac{L^3}{EI} \\ \beta_{Fii} &= \frac{1}{3}\, x_1 x_2 (x_2 - x_1) \cdot \frac{L^2}{EI} \end{aligned}\right\}$$

However, the influence numbers α_{Mij} and β_{Mij} still remain to be determined. Consider the beam in fig. 62.1. A unit bending moment is applied to the beam in Q_i. We seek the deflection and the inclination in this point.

The equation for the elastic deflection line is

$$-EI \frac{d^2 y}{d(x_3 L)^2} = x_3 - \{x_3 - x_1\}^0$$

The boundary conditions are

$$\begin{aligned} x_3 &= 0 \qquad y = 0 \\ x_3 &= 1 \qquad y = 0 \end{aligned}$$

After some simple calculations we get

$$\alpha_{Mij} = \frac{1}{6}\{-x_3^3+3(x_3-x_1)^2-x_3[3(1-x_1)^2-1]\}\frac{L^2}{EI}$$

$$\beta_{Mij} = \frac{1}{6}\{-3x_3^2+6(x_3-x_1)+1-3(1-x_1)^2\}\cdot\frac{L}{EI}$$

and if $x_3 = x_1$ these equations are reduced to

$$\alpha_{Mii} = -\frac{1}{3}(2x_1^3-3x_1^2+x_1)\cdot\frac{L^2}{EI}$$

$$\beta_{Mii} = -\left(x_1^2-x_1+\frac{1}{3}\right)\cdot\frac{L}{EI}$$

In the actual case $x_1 = \frac{1}{4}$ gives

$$\alpha_{F11} = \frac{1}{3}\left(\frac{1}{4}\cdot\frac{3}{4}\right)^2\cdot\frac{L^3}{EI} = \frac{3}{256}\cdot\frac{L^3}{EI}$$

$$\beta_{F11} = \frac{1}{3}\cdot\frac{1}{4}\cdot\frac{3}{4}\left(\frac{3}{4}-\frac{1}{4}\right)\cdot\frac{L^2}{EI} = \frac{1}{32}\cdot\frac{L^2}{EI}$$

$$\alpha_{M11} = -\frac{1}{3}\left\{2\cdot\frac{1}{64}-3\cdot\frac{1}{16}+\frac{1}{4}\right\}\cdot\frac{L^2}{EI} = -\frac{1}{32}\cdot\frac{L^2}{EI}$$

$$\beta_{M11} = -\left(\frac{1}{16}-\frac{1}{4}+\frac{1}{3}\right)\cdot\frac{L}{EI} = -\frac{7}{48}\cdot\frac{L}{EI}$$

Choosing $k = 768$ we get from eq. 59.2

$$\xi_{F11} = 768\cdot\frac{3}{256} = 9$$

$$\zeta_{F11} = 768\cdot\frac{1}{32} = 24$$

$$\xi_{M11} = -24$$

$$\zeta_{M11} = -768\cdot\frac{7}{48} = -112$$

By definition, if $M_{ref} = M$,

$$r_1 = \frac{I_{p1}\left(\frac{\omega}{\Omega}-\frac{1}{2}\right)}{ML^2}$$

or

$$r_1 = \frac{1}{2} \cdot \frac{MR^2}{2 \cdot ML^2} \cdot \left(2\,\frac{\omega}{\Omega} - 1\right) = \left(\frac{R}{2L}\right)^2 \left(2\,\frac{\omega}{\Omega} - 1\right) = \frac{1}{16}\left(2\,\frac{\omega}{\Omega} - 1\right)$$

where R is the radius of the disc. By insertion in eq. 60.1 we get

$$\begin{vmatrix} 9-\Lambda & 24 \\ -24 & -112 - \dfrac{16\Lambda}{2\,\dfrac{\omega}{\Omega} - 1} \end{vmatrix} = 0$$

and from here we can solve

$$\frac{\omega}{\Omega} = \frac{\Lambda^2 - 16\Lambda + 27}{-14\Lambda + 54}$$

This second degree curve is a hyperbola and in fig. 65.1 the ratio $\frac{\omega}{\Omega}$ is drawn as a function of Λ.

The usual critical speed $\left(\frac{\omega}{\Omega} = +1\right)$ corresponds to the point P_1 in fig. 65.1. In this point $\Lambda = \left(1+\sqrt{28}\right) \approx 6{,}2915$. For the reverse whirl $\frac{\omega}{\Omega} = -1$ we get $\Lambda_1 = 3$ and $\Lambda_2 = 27$. Observe that even special forward precessions, viz. such in the range $0 \leq \frac{\omega}{\Omega} \leq \frac{1}{2}$, give two critical speeds. In the figure the points P_2 and P_3 correspond to the two critical speeds at $\frac{\omega}{\Omega} = +\frac{1}{4}$.

The point P_5 is of special interest. In this point $\omega = 0$ and $\Lambda_5 = \left(8+\sqrt{37}\right) \approx 14{,}08$. If, as often happens in practice, the usual critical speed is determined with the aid of a vibration exciter a frequency corresponding to Λ_5-value is obtained. It is seen in the figure that the right value is $\Lambda = 6{,}2915$. The error in this case is 33 % ($\Omega_5 = 0{,}67\ \Omega_1$). Further, another frequency may be obtained, namely that corresponding to the point P_4 $\left(\Lambda = \left(8-\sqrt{37}\right) \simeq 1{,}92\right)$. See more about these matters in Chapter 10.

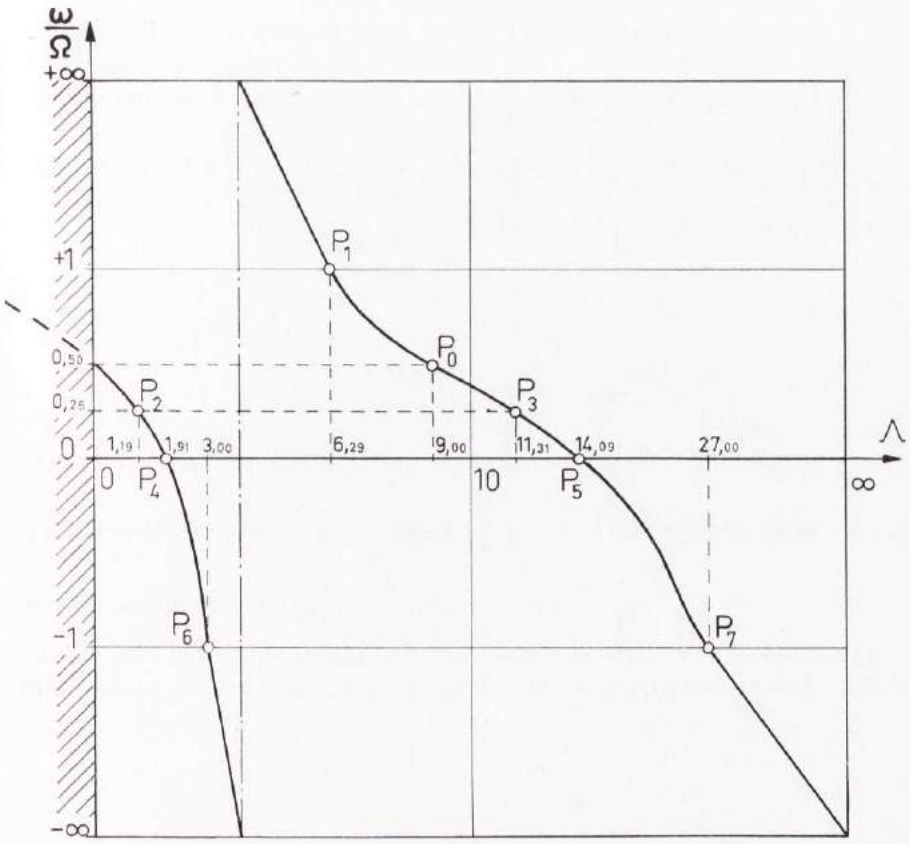

Fig. 65.1

If the gyroscopic effect is neglected we get $\Lambda = 9$. This value can be obtained in fig. 65.1 for $\frac{\omega}{\Omega} = \frac{1}{2}$ giving $\nu_1 = 0$. See point P_0. Thus one could say that $\Lambda = 9$ corresponds to the critical speed for a point mass ($I_p = 0$) or to the special rotational mode $\frac{\omega}{\Omega} = \frac{1}{2}$ for a thin disc. It may be pointed out that $\Lambda = 9$ is always obtained for a point mass independent of the value of the ratio $\frac{\omega}{\Omega}$. The motion of a point mass can be thought of as the result of two lateral oscillations with the same frequency and amplitude with phase angle $\frac{\pi}{2}$

rad and with their directions perpendicular to each other. For a disc, however, only the whirl can be described in that way. To this whirl then the shaft rotation must be added in order to describe the motion completely.

Denoting the critical speed corresponding to $\Lambda = 9$ by n_0 we get

$$\left(\frac{n_1}{n_0}\right)^2 = \frac{\sqrt{28}-1}{3} = 1{,}4305$$

Thus

$$\frac{n_0}{n_1} = 0{,}836$$

The simple calculation gives an error of 16 %. If $\frac{\omega}{\Omega} = +\infty$ one gets from the fig. 65.1 $\Lambda = 3\frac{6}{7}$ while $\frac{\omega}{\Omega} = -\infty$ gives two values of Λ, namely $\Lambda = 3\frac{6}{7}$ and $\Lambda = \infty$. The last one corresponds to $\Omega = 0$ and is trivial. Thus we conclude that if the angular velocity of the shaft is infinite there is only one critical whirl, viz. the one corresponding to $\Lambda = 3\frac{6}{7}$.

The weight of the disc is

$$M = \frac{\pi}{4} \cdot 1{,}0^2 \cdot 0{,}05 \cdot 7\,850 \text{ kg} = 308 \text{ kg}$$

With $E = 20{,}6 \cdot 10^{10} \frac{\text{N}}{\text{m}^2}$ is

$$\Omega_i^2 = \frac{768EI}{ML^3} \cdot \frac{1}{\Lambda_i} = \frac{768 \cdot 20{,}6 \cdot 10^{10} \cdot \pi \cdot 50^4 \cdot 10^{-12}}{64 \cdot 308 \cdot 1{,}0^3 \cdot \Lambda_i}$$

and

$$n_i = \frac{3791}{\sqrt{\Lambda_i}}$$

With easily understood notations we get

$n_0 = 1\,264$ r.p.m. $\quad n_4 = 2\,738$ r.p.m. $\quad n_6 = 2\,189$ r.p.m.
$n_1 = 1\,512$ r.p.m. $\quad n_5 = 1\,010$ r.p.m. $\quad n_7 = \quad 730$ r.p.m.

In order to get a rough conception of the mode of the deflection curves we use the equations

$$\left.\begin{aligned} &(9-\Lambda)\,F_1-24\cdot\frac{M_{g1}}{L}=0\\ &y_1=\frac{F_1}{M\Omega^2}\\ &\varphi_1=\frac{M_{g1}}{\frac{1}{2}I_{p1}\Omega^2} \end{aligned}\right\}$$

Forward whirl $\left(\frac{\omega}{\Omega}=+1\right)$ $\Lambda=6{,}2915$; if $F_1>0$, $M_{g1}>0$

Reverse whirl $\left(\frac{\omega}{\Omega}=-1\right)$ $\Lambda=27$; if $F_1>0$, $M_{g1}<0$

$\Lambda=3$; if $F_1>0$, $M_{g1}>0$

Now we are able to sketch the different deflection curves:

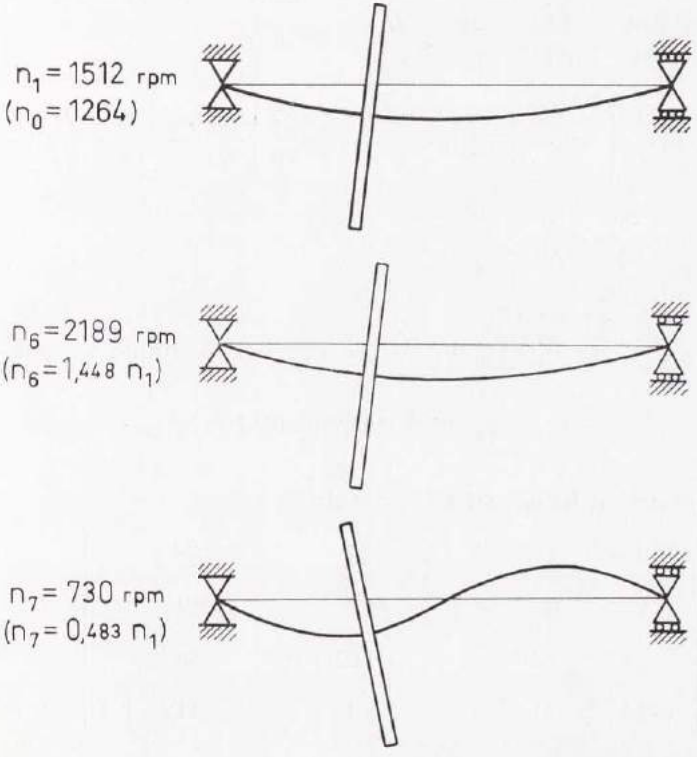

Example 10. Two discs are arranged according to fig. 69.1. Calculate the critical speed at forward and reverse whirl. The mass of the shaft may be neglected. (Compare with Example 9 in this chapter.)

According to the previous example we get

$$\alpha_{F11} = \alpha_{F22} = \frac{3}{256} \cdot \frac{L^3}{EI} = \frac{9}{3 \cdot 256} \cdot \frac{L^3}{EI}$$

$$\beta_{F11} = -\beta_{F22} = -\alpha_{M11} = +\alpha_{M22} = \frac{1}{32} \cdot \frac{L^2}{EI} = \frac{24}{3 \cdot 256} \cdot \frac{L^2}{EI}$$

$$-\beta_{M11} = -\beta_{M22} = \frac{7}{48} \cdot \frac{L}{EI} = \frac{112}{768} \cdot \frac{L}{EI}$$

$$\alpha_{F12} = \alpha_{F21} = \frac{1}{6} \cdot \frac{1}{4} \cdot \frac{1}{4} \left(1 - \frac{1}{16} - \frac{1}{16}\right) \frac{L^3}{EI} = \frac{7}{768} \cdot \frac{L^3}{EI}$$

$$\alpha_{M12} = -\alpha_{M21} = \beta_{F12} = -\beta_{F21} = \frac{1}{6} \cdot \frac{1}{4} \left(1 - \frac{3}{16} - \frac{1}{16}\right) \frac{L^2}{EI} =$$

$$= \frac{1}{32} \cdot \frac{L^2}{EI} = \frac{24}{768} \cdot \frac{L^2}{EI}$$

$$\beta_{M12} = \frac{1}{6} \left\{ -3 \cdot \frac{9}{16} + 6 \cdot \frac{1}{2} + 1 - \frac{27}{16} \right\} \frac{L}{EI} = \frac{5}{48} \cdot \frac{L}{EI} =$$

$$= \frac{80}{768} \cdot \frac{L}{EI}$$

Choose $k = 768$; $M_{\text{ref}} = M_1$

Thus $\mu_1 = 1$; $\mu_2 = 2$. From the previous example we get

$$\nu_1 = \frac{1}{16} \text{ and consequently } \nu_2 = \frac{1}{8}.$$

By insertion in eq. 60.1 we obtain

$$\begin{vmatrix} 9-\Lambda & 7 & -24 & 24 \\ 7 & 9-\frac{1}{2}\Lambda & -24 & 24 \\ 24 & 24 & -112-16\Lambda & 80 \\ -24 & -24 & 80 & -112-8\Lambda \end{vmatrix} \quad \ldots\ldots \quad 68.1$$

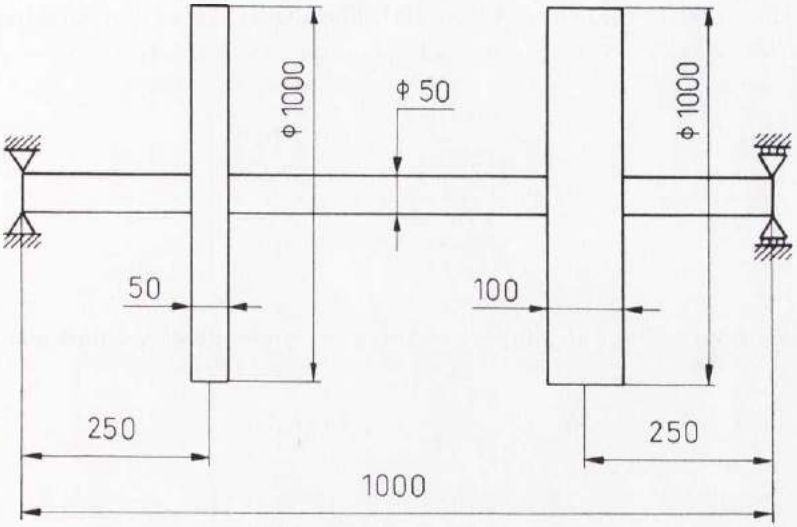

Fig. 69.1

The development of this determinant gives

$$\Lambda^4 - 6\Lambda^3 - 131\Lambda^2 + 48\Lambda + 768 = 0$$

With the aid of Cartesii theorem about the signs we may see that this equation has two or none positive roots. (The theorem states that the number of positive roots of an algebraic equation is equal to the number of sign changes in the equation or this number reduced by two [8].)

Approximative values are obtained if the gyroscopic effect is neglected. Thus from eq. 68.1

$$\begin{vmatrix} 9-\Lambda & 7 \\ 7 & 9-\frac{1}{2}\Lambda \end{vmatrix} = 0$$

and from here $\Lambda_1 = 24{,}374$ and $\Lambda_2 = 2{,}626$. Then calculation with Horner's scheme is advantageous. The result becomes

$$\Lambda_1 = 14{,}535 \quad \Lambda_3 < 0$$
$$\Lambda_2 = 2{,}522 \quad \Lambda_4 < 0$$

Only positive values of Λ are valid. The negative ones give imaginary critical speeds. From the previous example we can write

$$\left.\begin{aligned} n_1 &= \frac{3\,791}{\sqrt{14{,}535}} = 994 \text{ r.p.m.} \\ n_2 &= \frac{3\,791}{\sqrt{2{,}522}} = 2\,387 \text{ r.p.m.} \end{aligned}\right\}$$

Without taking any notice of the gyroscopic effect we had got

$$\left.\begin{aligned} n_1 &= \frac{3\,791}{\sqrt{24{,}374}} = 768 \text{ r.p.m.} \\ n_2 &= \frac{3\,791}{\sqrt{2{,}626}} = 2\,339 \text{ r.p.m.} \end{aligned}\right\}$$

The error in the first critical speed is 23 per cent and in the second one 2 per cent. Both of them are too low.

At reverse whirl we instead of eq. 68.1 get

$$\begin{vmatrix} 9-\Lambda & 7 & -24 & 24 \\ 7 & 9-\frac{1}{2}\Lambda & -24 & 24 \\ 24 & 24 & -112-\frac{16}{3}\Lambda & 80 \\ -24 & -24 & 80 & -112-\frac{8}{3}\Lambda \end{vmatrix} = 0$$

or

$$\Lambda^4-90\Lambda^3+1\,225\Lambda^2-5\,328\Lambda+6\,912 = 0$$

This equation has the following roots

$$\Lambda_1 = 74{,}50 \quad \Lambda_2 = 8{,}549 \quad \Lambda_3 = 4{,}582 \quad \Lambda_4 = 2{,}3685$$

corresponding to the four critical speeds

$n_1 = 439$ r.p.m. $n_2 = 1\,297$ r.p.m. $n_3 = 1\,771$ r.p.m. $n_4 = 2\,463$ r.p.m.

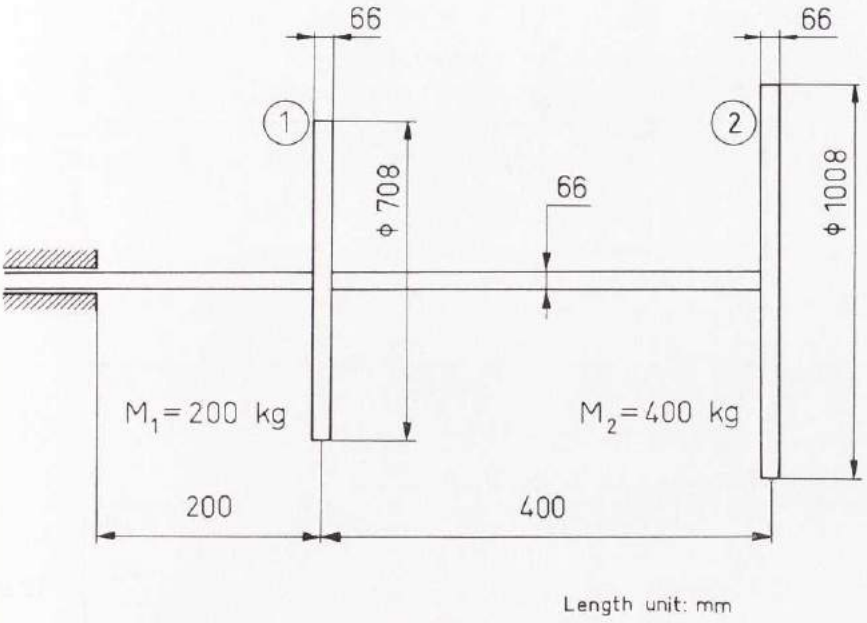

Fig. 71.1

Example 11. Two steel discs are put up on a cantilever steel shaft according to fig. 71.1. Calculate the critical speeds during forward and reverse whirl. The mass of the shaft may be neglected.

First we calculate the influence numbers from the case in fig. 72.1.

For the left part of the shaft we have

$$-EI\frac{d^2y_2}{d(x_2L)} = -(x_2L)\cdot 1$$

The boundary conditions are: $x_2 = x_1 \quad y_2 = 0 \quad y_2' = 0.$

Integration and use of these conditions give

$$\left.\begin{aligned} \alpha_{Fij} = y_2(x_1, x_2) &= \frac{1}{6}(x_2^3 - 3x_1^2x_2 + 2x_1^3)\cdot\frac{L^3}{EI} \\ \beta_{Fij} = y_2'(x_1, x_2) &= \frac{1}{2}(x_1^2 - x_2^2)\cdot\frac{L^2}{EI} \end{aligned}\right\} \quad \ldots\ldots \quad 71.2$$

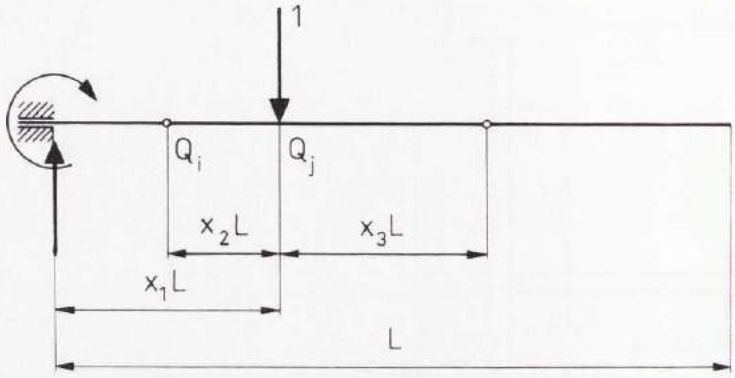

Fig. 72.1

For the right part of the shaft we get

$$\left.\begin{aligned} \alpha_{Fij} &= y_3(x_1, x_3) = y_2(x_1, 0) + (x_3 L)\beta_{Fij} = \frac{1}{6}\, x_1^2(2x_1 + 3x_3) \cdot \frac{L^3}{EI} \\ \beta_{Fij} &= y_2'(x_1, 0) = \frac{x_1^2}{2} \cdot \frac{L^2}{EI} \end{aligned}\right\} \quad 72.2$$

The influence number for a unit bending moment is also needed. For the left part in fig. 73.1 we get

$$-EI\,\frac{d^2 y_2}{d(x_2 L)} = 1$$

The boundary conditions are $x_2 = x_1$; $y_2 = 0$; $y_2' = 0$. After some simple calculations we get

$$\left.\begin{aligned} \alpha_{Mij} &= y_2(x_1, x_2) = -\frac{1}{2}\,(x_1 - x_2)^2 \cdot \frac{L^2}{EI} \\ \beta_{Mij} &= -(x_1 - x_2) \cdot \frac{L}{EI} \end{aligned}\right\} \quad \ldots\ldots\ 72.3$$

For the right part of the shaft we have

$$\left.\begin{aligned} \alpha_{Mij} &= -\frac{1}{2} \cdot x_1(x_1 + 2x_3) \cdot \frac{L^2}{EI} \\ \beta_{Mij} &= -x_1 \cdot \frac{L}{EI} \end{aligned}\right\} \quad \ldots\ldots\ 72.4$$

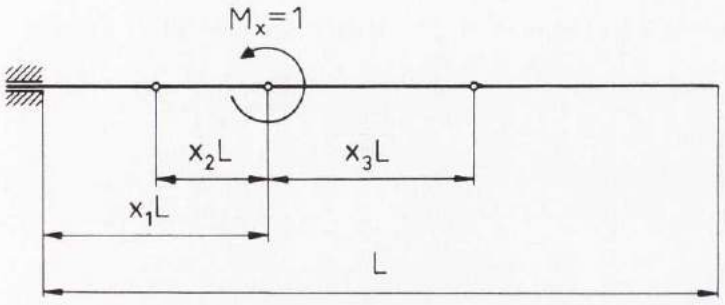

Fig. 73.1

Applying the formulas 71.2, 72.2, 72.3, and 72.4 to the case in question we get

$$\alpha_{F11} = \frac{1}{6} \cdot 2 \cdot \frac{1}{27} \cdot \frac{L^3}{EI} = \frac{2}{162} \cdot \frac{L^3}{EI}$$

$$\alpha_{F22} = \frac{1}{6} \cdot 2 \cdot \frac{L^3}{EI} = \frac{54}{162} \cdot \frac{L^3}{EI}$$

$$\alpha_{F12} = \alpha_{F21} = \frac{1}{6}\left(\frac{8}{27} - 2 + 2\right)\frac{L^3}{EI} = \frac{4}{3 \cdot 27} \cdot \frac{L^3}{EI} = \frac{8}{162} \cdot \frac{L^3}{EI}$$

$$\alpha_{M11} = -\frac{1}{2} \cdot \frac{1}{9} \cdot \frac{L^2}{EI} = -\frac{9}{162} \cdot \frac{L^2}{EI}$$

$$\alpha_{M12} = -\frac{1}{2}\left(1 - \frac{2}{3}\right)^2 \cdot \frac{L^2}{EI} = -\frac{1}{18} \cdot \frac{L^2}{EI} = -\frac{9}{162} \cdot \frac{L^2}{EI}$$

$$\alpha_{M21} = -\frac{1}{2} \cdot \frac{1}{3}\left(\frac{1}{3} + \frac{4}{3}\right) \cdot \frac{L^2}{EI} = -\frac{45}{162} \cdot \frac{L^2}{EI}$$

$$\alpha_{M22} = -\frac{1}{2} \cdot \frac{L^2}{EI} = -\frac{81}{162} \cdot \frac{L^2}{EI}$$

$$\beta_{M11} = -\frac{1}{3} \cdot \frac{L}{EI} = -\frac{54}{162} \cdot \frac{L}{EI}$$

$$\beta_{M22} = -\frac{L}{EI} = -\frac{162}{162} \cdot \frac{L}{EI}$$

$$\beta_{M12} = -\left(1 - \frac{2}{3}\right)\frac{L}{EI} = -\frac{1}{3} \cdot \frac{L}{EI} = -\frac{54}{162} \cdot \frac{L}{EI}$$

Choosing $k = 162$ and $M_{ref} = M_2$ for forward whirl we get

$$\left.\begin{aligned} \Lambda &= \frac{162EI}{M_2L^3\Omega^2} \\ \mu_1 &= 0{,}5 \\ \mu_2 &= 1 \end{aligned}\right\} \qquad \left.\begin{aligned} \nu_1 &= \frac{M_1R_1^2}{2\cdot 2M_{ref}L^2} = \frac{1}{8}\cdot\left(\frac{R_1}{L}\right)^2 = \frac{0{,}59^2}{8} = \frac{1}{23{,}0} \\ \nu_2 &= \frac{M_2R_2^2}{2\cdot 2M_{ref}L^2} = \frac{1}{4}\cdot\left(\frac{R_2}{L}\right)^2 = \frac{0{,}84^2}{4} = \frac{1}{5{,}67} \end{aligned}\right\}$$

The eq. 60.1 now gives

$$\begin{vmatrix} 2-2\Lambda & 8 & -9 & -9 \\ 8 & 54-\Lambda & -45 & -81 \\ +9 & +45 & -54-23\Lambda & -54 \\ +9 & +81 & -54 & -162-5{,}67\Lambda \end{vmatrix} = 0 \ldots \quad 74.1$$

This equation can be written

$$\Lambda^4 - 24{,}08\Lambda^3 - 379{,}75\Lambda^2 - 88{,}74\Lambda + 44{,}72 = 0$$

with the roots

$$\left.\begin{aligned} \Lambda_1 &= 35{,}00 \\ \Lambda_2 &= 0{,}244 \end{aligned}\right\} \qquad \left.\begin{aligned} \Lambda_3 &< 0 \\ \Lambda_4 &< 0 \end{aligned}\right\}$$

So the two critical speeds are

$$\left.\begin{aligned} n_1 &= \quad 940 \text{ r.p.m.} \\ n_2 &= 11\,300 \text{ r.p.m.} \end{aligned}\right\}$$

Without the gyroscopic effect we get from eq. 74.1

$$\begin{vmatrix} 2-2\Lambda & 8 \\ 8 & 54-\Lambda \end{vmatrix} = 0$$

and

$$\left.\begin{aligned} \Lambda_1 &= 54{,}60 \\ \Lambda_2 &= 0{,}403 \end{aligned}\right\} \text{ giving } \left.\begin{aligned} n_1 &= \quad 760 \text{ r.p.m.} \\ n_2 &= 8\,760 \text{ r.p.m.} \end{aligned}\right\}$$

The first value is 19 per cent and the second one 22,5 per cent too low.

For reverse whirl we get from eq. 60.1 (the coefficients for Λ in the lower part of the principal diagonal in eq. 74.1 are divided by -3 as seen from the formulas 60.3 and 60.4)

$$\begin{vmatrix} 2-2\Lambda & 8 & 9 & 9 \\ 8 & 54-\Lambda & 45 & 81 \\ 9 & 45 & 54-\frac{23}{3}\Lambda & 54 \\ 9 & 81 & 54 & 162-\frac{5,67}{3}\Lambda \end{vmatrix} = 0$$

This equation has the roots

$$\Lambda_1 = 131,57 \quad \Lambda_2 = 14,94 \quad \Lambda_3 = 1,06 \quad \Lambda_4 = 0,19$$

with the corresponding four critical speeds

$n_1 = 393$ r.p.m. $n_2 = 1\,165$ r.p.m. $n_3 = 4\,240$ r.p.m. $n_4 = 10\,300$ r.p.m.

8. Critical Speeds of a Shaft Supported by Bearings of Lateral Flexibility Considering the Gyroscopic Effect

We have already studied both the influence of flexible bearings and the gyroscopic effect on critical speeds but not when they act simultaneously. In this chapter, however, such a treatment is carried out.

Consider the arrangement in fig. 77.1. The two bearings have the radial spring constants c_1 and c_2 respectively. The discs are thin. It is assumed that the shaft is perfectly balanced. In that way there are no deflections save at some special speeds, the critical ones.

The deflection y_s and the inclination φ_s in a point Q_s on the shaft can be written

$$\left.\begin{aligned} y_s &= \sum_{i=1}^{n} F_i\alpha_{Fsi} + \sum_{i=1}^{n} M_{gi}\alpha_{Msi} \\ \varphi_s &= \sum_{i=1}^{n} F_i\beta_{Fsi} + \sum_{i=1}^{n} M_{gi}\beta_{Msi} \end{aligned}\right\} \quad \ldots\ldots\ldots\ 76.1$$

where $F_i = M_i(y_{\text{tot}})_i\Omega^2$ and $M_{gi} = \frac{1}{2} I_{pi}\Omega^2(\varphi_{\text{tot}})_i$ for forward whirl.

The notations are the same as in Chapter 7. Further we have from fig. 77.1

$$\left.\begin{aligned} (y_{\text{tot}})_s &= y_0^* + l_s y_0 + y_s \\ (\varphi_{\text{tot}})_s &= \varphi_s + \frac{y_0}{L} \end{aligned}\right\} \quad \ldots\ldots\ldots\ 76.2$$

The angle φ_s is measured from the centre line of the bearings. In fig. 78.1 the different angles are shown separately.

Further the equilibrium gives

$$\left.\begin{aligned} c_1 y_0^* L - \sum_{i=1}^{n} M_i(y_{\text{tot}})_i\Omega^2(1-l_i)L - \sum_{i=1}^{n} \frac{1}{2} I_{pi}\Omega^2(\varphi_{\text{tot}})_i &= 0 \\ c_2(y_0 + y_0^*)L - \sum_{i=1}^{n} M_i(y_{\text{tot}})_i\Omega^2 l_i L + \sum_{i=1}^{n} \frac{1}{2} I_p\Omega^2(\varphi_{\text{tot}})_i &= 0 \end{aligned}\right\} \quad \ldots\ldots\ 76.3$$

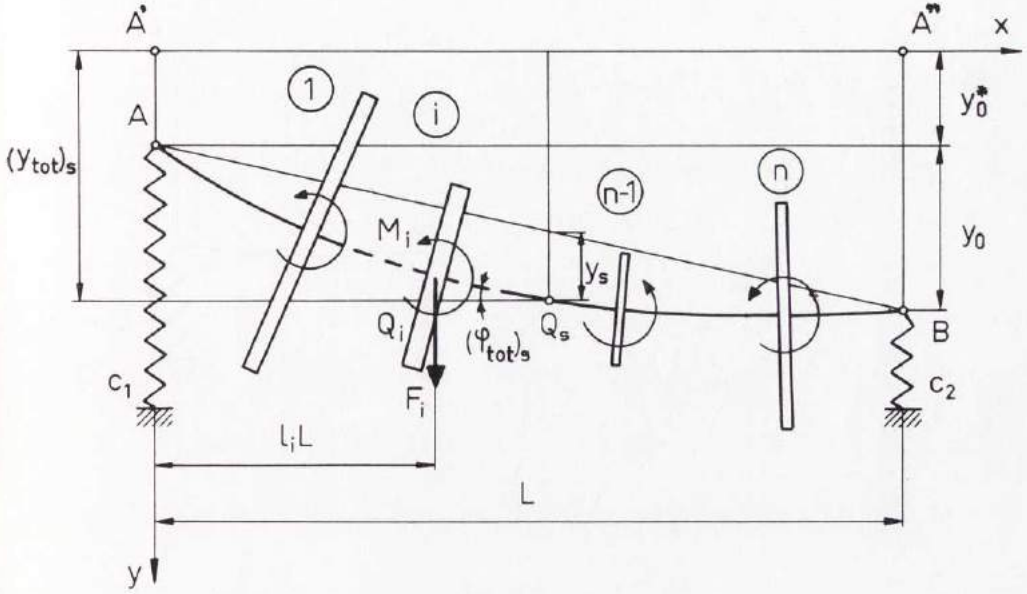

Fig. 77.1

Now introduce $M_i = \mu_i M_{\text{ref}}$ and $\frac{1}{2} I_{pi} = \gamma_i I_{\text{ref}}$, where M_{ref} and I_{ref} may be choosen arbitrarily. Thus, if $y = \eta L$, the eqs 76.3 become

$$\left.\begin{aligned} c_1\eta_0^* &= M_{\text{ref}}\Omega^2 \sum_{i=1}^{n} \mu_i(1-l_i)\,(\eta_{\text{tot}})_i + \frac{I_{\text{ref}}\Omega^2}{L^2} \sum_{i=1}^{n} \gamma_i(\varphi_{\text{tot}})_i \\ c_2(\eta_0+\eta_0^*) &= M_{\text{ref}}\Omega^2 \sum_{i=1}^{n} \mu_i l_i(\eta_{\text{tot}})_i - \frac{I_{\text{ref}}\Omega^2}{L^2} \sum_{i=1}^{n} \gamma_i(\varphi_{\text{tot}})_i \end{aligned}\right\}$$

and

$$\left.\begin{aligned} \eta_0^* &= \frac{M_{\text{ref}}\Omega^2}{c_1} \sum_{i=1}^{n} \mu_i(1-l_i)\,(\eta_{\text{tot}})_i + \frac{I_{\text{ref}}\Omega^2}{L^2 c_1} \sum_{i=1}^{n} \gamma_i(\varphi_{\text{tot}})_i \\ \eta_0 &= \frac{M_{\text{ref}}\Omega^2}{c_2} \sum_{i=1}^{n} \mu_i l_i(\eta_{\text{tot}})_i - \frac{I_{\text{ref}}\Omega^2}{L^2 c_2} \sum_{i=1}^{n} \gamma_i(\varphi_{\text{tot}})_i - \\ &\quad - \frac{M_{\text{ref}}\Omega^2}{c_1} \sum_{i=1}^{n} \mu_i(1-l_i)\,(\eta_{\text{tot}})_i - \frac{I_{\text{ref}}\Omega^2}{L^2 c_1} \sum_{i=1}^{n} \gamma_i(\varphi_{\text{tot}})_i \end{aligned}\right\} \quad \ldots\ldots\ 77.2$$

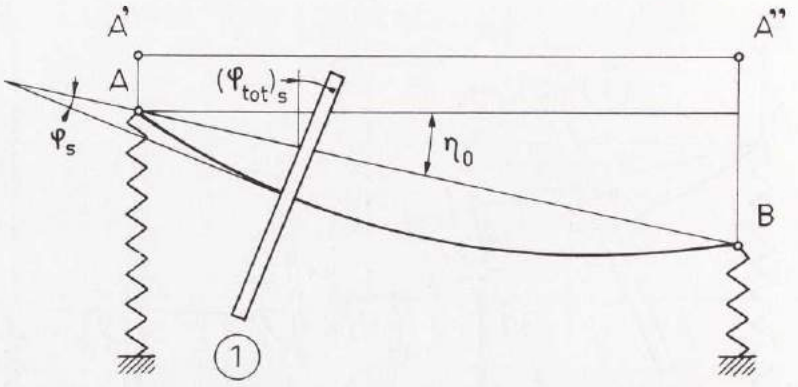

Fig. 78.1

Now we have from Chapter 6 that

$$\left.\begin{aligned} \frac{1}{c} &= \frac{1}{c_1} + \frac{1}{c_2} \\ C_1 &= \frac{c}{c_1};\quad C_2 = \frac{c}{c_2} \end{aligned}\right\}$$

Using these notations and

$$\left.\begin{aligned} \Theta_M &= \frac{M_{\text{ref}}\Omega^2}{c}\cdot\Lambda \\ \Theta_I &= \frac{I_{\text{ref}}\Omega^2}{L^2c}\cdot\Lambda \\ \Lambda &= \frac{kEI}{M_{\text{ref}}L^3\Omega^2} \end{aligned}\right\}$$

we can write the eqs 77.2 as

$$\left.\begin{aligned} \Lambda\eta_0^* &= C_1\Theta_M \sum_{i=1}^{n} \mu_i(1-l_i)\,(\eta_{\text{tot}})_i + C_1\Theta_I \sum_{i=1}^{n} \gamma_i(\varphi_{\text{tot}})_i \\ \Lambda\eta_0 &= \Theta_M \sum_{i=1}^{n} \mu_i l_i(\eta_{\text{tot}})_i - C_1\Theta_M \sum_{i=1}^{n} \mu_i(\eta_{\text{tot}})_i - \Theta_I \sum_{i=1}^{n} \gamma_i(\varphi_{\text{tot}})_i \end{aligned}\right\} \quad \ldots\ 78.2$$

Writing the eqs 76.2 in a non-dimensional form we get

$$\left.\begin{aligned}(\eta_{\mathrm{tot}})_s &= \eta_0^* + l_s\eta_0 + \eta_s \\ \varphi_s &= (\varphi_{\mathrm{tot}})_s - \eta_0\end{aligned}\right\}$$

or

$$\left.\begin{aligned}\eta_s &= (\eta_{\mathrm{tot}})_s - \eta_0^* - l_s\eta_0 \\ \varphi_s &= (\varphi_{\mathrm{tot}})_s - \eta_0\end{aligned}\right\} \quad \ldots\ldots\ldots\ldots\ldots \quad 79.1$$

With the aid of eq. 78.2 we may write

$$\begin{aligned}\Lambda\eta_s = {} & \Lambda(\eta_{\mathrm{tot}})_s - C_1\Theta_M\Sigma\mu_i(1-l_i)\,(\eta_{\mathrm{tot}})_i - C_1\Theta_I\Sigma\gamma_i(\varphi_{\mathrm{tot}})_i - \\ & - l_s\Theta_M\Sigma\mu_i l_i(\eta_{\mathrm{tot}})_i + C_1 l_s\Theta_M\Sigma\mu_i(\eta_{\mathrm{tot}})_i + l_s\Theta_I\Sigma\gamma_i(\varphi_{\mathrm{tot}})_i\end{aligned}$$

or

$$\begin{aligned}\Lambda\eta_s = {} & \Lambda(\eta_{\mathrm{tot}})_s + (C_1 - l_s)\Theta_M\Sigma\mu_i l_i(\eta_{\mathrm{tot}})_i - (1-l_s)C_1\Theta_M\Sigma\mu_i(\eta_{\mathrm{tot}})_i - \\ & - (C_1 - l_s)\Theta_I\Sigma\gamma_i(\varphi_{\mathrm{tot}})_i \quad \ldots\ldots\ldots\ldots\ldots\ldots\ldots\ldots\ldots\ldots \quad 79.2\end{aligned}$$

The eqs 76.1 can be written

$$\left.\begin{aligned}\eta_s &= M_{\mathrm{ref}}\Omega^2\Sigma\mu_i(\eta_{\mathrm{tot}})_i\alpha_{Fsi} + \frac{I_{\mathrm{ref}}\Omega^2}{L}\,\Sigma\gamma_i(\varphi_{\mathrm{tot}})_i\alpha_{Msi} \\ \varphi_s &= M_{\mathrm{ref}}\Omega^2 L\Sigma\mu_i(\eta_{\mathrm{tot}})_i\beta_{Fsi} + I_{\mathrm{ref}}\Omega^2\Sigma\gamma_i(\varphi_{\mathrm{tot}})_i\beta_{Msi}\end{aligned}\right\}$$

By introducing

$$\left.\begin{aligned}\alpha_{Fsi} &= \xi_{Fsi}\cdot\frac{L^3}{kEI} \\ \alpha_{Msi} &= \xi_{Msi}\cdot\frac{L^2}{kEI} \\ \beta_{Fsi} &= \zeta_{Fsi}\cdot\frac{L^2}{kEI} \\ \beta_{Msi} &= \zeta_{Msi}\cdot\frac{L}{kEI}\end{aligned}\right\} \quad \text{and} \quad \nu = \frac{I_{\mathrm{ref}}}{M_{\mathrm{ref}}L^2}$$

we get

$$\left.\begin{aligned}\Lambda\eta_s &= \Sigma\mu_i(\eta_{\mathrm{tot}})_i\xi_{Fsi} + \nu\Sigma\gamma_i(\varphi_{\mathrm{tot}})_i\xi_{Msi} \\ \Lambda\varphi_s &= \Sigma\mu_i(\eta_{\mathrm{tot}})_i\zeta_{Fsi} + \nu\Sigma\gamma_i(\varphi_{\mathrm{tot}})_i\zeta_{Msi}\end{aligned}\right\} \quad \ldots\ldots\ldots \quad 79.3$$

By insertion of the eq. 79.2 and the last of the eqs 79.1 we obtain

$$\left.\begin{aligned} &\Lambda(\eta_{\mathrm{tot}})_s+(C_1-l_s)\Theta_M\Sigma\mu_i l_i(\eta_{\mathrm{tot}})_i-(1-l_s)C_1\Theta_M\Sigma\mu_i(\eta_{\mathrm{tot}})_i- \\ &-(C_1-l_s)\Theta_I\Sigma\gamma_i(\varphi_{\mathrm{tot}})_i-\Sigma\mu_i\xi_{Fsi}(\eta_{\mathrm{tot}})_i-\nu\Sigma\gamma_i\xi_{Msi}(\varphi_{\mathrm{tot}})_i=0 \\ &\Sigma\mu_i(\eta_{\mathrm{tot}})_i\zeta_{Fsi}+\nu\Sigma\gamma_i(\varphi_{\mathrm{tot}})_i\zeta_{Msi}=\Lambda(\varphi_{\mathrm{tot}})_s-\Theta_M\Sigma\mu_i l_i(\eta_{\mathrm{tot}})_i+ \\ &+C_1\Theta_M\Sigma\mu_i(\eta_{\mathrm{tot}})_i+\Theta_I\Sigma\gamma_i(\varphi_{\mathrm{tot}})_i \end{aligned}\right\}$$

or

$$\left.\begin{aligned} &\Lambda(\eta_{\mathrm{tot}})_s+(C_1-l_s)\Theta_M\sum_i\mu_i l_i(\eta_{\mathrm{tot}})_i-(1-l_s)C_1\Theta_M\sum_i\mu_i(\eta_{\mathrm{tot}})_i- \\ &-\sum_i\mu_i\xi_{Fsi}(\eta_{\mathrm{tot}})_i-(C_1-l_s)\Theta_I\sum_i\gamma_i(\varphi_{\mathrm{tot}})_i-\nu\sum_i\gamma_i\xi_{Msi}(\varphi_{\mathrm{tot}})_i=0 \\ &C_1\Theta_M\sum_i\mu_i(\eta_{\mathrm{tot}})_i-\Theta_M\sum_i\mu_i l_i(\eta_{\mathrm{tot}})_i-\sum_i\mu_i\zeta_{Fsi}(\eta_{\mathrm{tot}})_i+\Lambda(\varphi_{\mathrm{tot}})_s+ \\ &+\Theta_I\sum_i\gamma_i(\varphi_{\mathrm{tot}})_i-\nu\sum_i\gamma_i\zeta_{Msi}(\varphi_{\mathrm{tot}})_i=0 \end{aligned}\right\}$$

In order to get non-trivial solutions the following eq. must be valid

$$\begin{vmatrix} -\Lambda+A_{11} & A_{12} & \dots & A_{1n} & B_{11} & B_{12} & \dots & B_{1n} \\ A_{21} & -\Lambda+A_{22} & \dots & A_{2n} & B_{21} & B_{22} & \dots & B_{2n} \\ \dots & \dots & \dots & \dots & \dots & \dots & \dots & \dots \\ A_{n1} & A_{n2} & \dots & -\Lambda+A_{nn} & B_{n1} & B_{n2} & \dots & B_{nn} \\ C_{11} & C_{12} & \dots & C_{1n} & -\Lambda+D_{11} & D_{12} & \dots & D_{1n} \\ C_{21} & C_{22} & \dots & C_{2n} & D_{21} & -\Lambda+D_{22} & \dots & D_{2n} \\ \dots & \dots & \dots & \dots & \dots & \dots & \dots & \dots \\ C_{n1} & C_{n2} & \dots & C_{nn} & D_{n1} & D_{n2} & \dots & -\Lambda+D_{nn} \end{vmatrix} = 0$$

..... 80.1

where

$$\left.\begin{aligned} A_{si}&=\mu_i\Theta_M[l_iC_2-(1-l_s)\,(l_i-C_1)]+\mu_i\xi_{Fsi} \\ B_{si}&=\gamma_i\Theta_I(C_1-l_s)+\nu\gamma_i\xi_{Msi} \\ C_{si}&=-\mu_i\Theta_M(C_1-l_i)+\mu_i\zeta_{Fsi} \\ D_{si}&=-\gamma_i\Theta_I+\nu\gamma_i\zeta_{Msi} \end{aligned}\right\} \quad \dots\dots \quad 80.2$$

From eq. 80.1 we can solve Λ and then the eq. 58.2 gives the critical speeds. The theory is illustrated by an example.

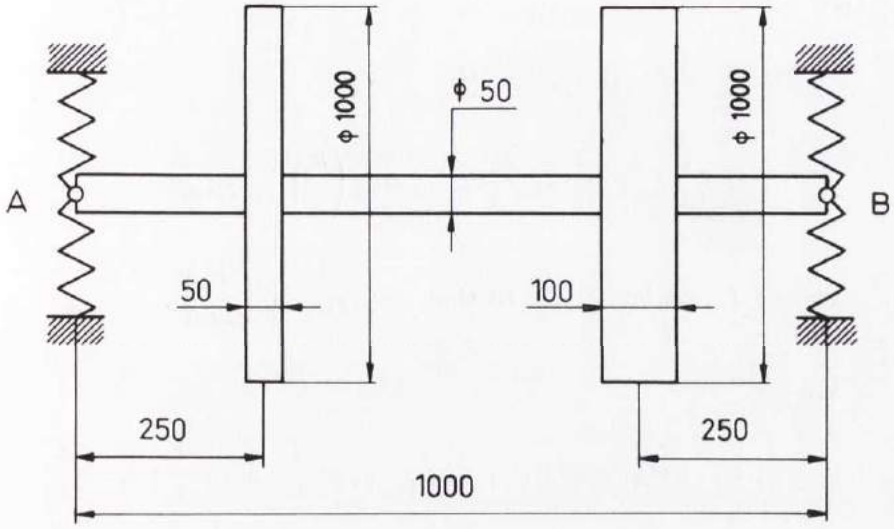

Fig. 81.1

Example 12. The shaft in Chapter 7, Example 10, is equipped with two equal "radial" springs at the bearings as in fig. 81.1. The spring constant is 100 kp/mm.

From Example 10 we have

$$\begin{aligned} \xi_{F11} &= \xi_{F22} = 9 & -\xi_{M11} &= \xi_{M22} = 24 \\ \xi_{F12} &= \xi_{F21} = 7 & \xi_{M12} &= -\xi_{M21} = 24 \\ \zeta_{F11} &= -\zeta_{F22} = 24 & -\zeta_{M11} &= -\zeta_{M22} = 112 \\ \zeta_{F12} &= -\zeta_{F21} = 24 & \zeta_{M12} &= \zeta_{M21} = 80 \end{aligned}$$

$k = 768$; $M_{\text{ref}} = M_1$; $\mu_1 = 1$; $\mu_2 = 2$

Further we get

$$\Theta_M = \frac{kEI}{cL^3} = \frac{768 \cdot 21\,000 \cdot 9{,}80665 \cdot 10^6 \cdot \dfrac{\pi}{64} \cdot 50^4 \cdot 10^{-12}}{100 \cdot 9{,}80665 \cdot 10^3}$$

$\Theta_M = 49{,}48$ Say $\Theta_M = 50{,}0$

and

$$\Theta_I = \Theta_M \cdot \frac{I_{\text{ref}}}{M_{\text{ref}} L^2} = \varkappa \Theta_M$$

$$\frac{1}{2} I_{pi} = \frac{1}{2} M_i \frac{R_i^2}{2} = \mu_i M_{\text{ref}} \left(\frac{R_i}{2}\right)^2 = \gamma_i I_{\text{ref}}$$

Choose I_{ref} to be $M_{\text{ref}} L^2$. In that way $\gamma_i = \mu_i \left(\frac{R_i}{2L}\right)^2$.

We get

$$r = 1\,;\ \Theta_I = \Theta_M = 50{,}0\,;\ \gamma_1 = \frac{1}{16}\,;\ \gamma_2 = \frac{1}{8}\,;\ l_1 = \frac{1}{4}\,;\ l_2 = \frac{3}{4}$$

By definition

$$\frac{1}{c} = \frac{1}{c_1} + \frac{1}{c_2}$$

and $c_1 = c_2$ gives $C_1 = C_2 = \frac{1}{2}$.

From the eqs 80.2

$$A_{11} = 1 \cdot 50 \left[\frac{1}{4} \cdot \frac{1}{2} - \left(1 - \frac{1}{4}\right)\left(\frac{1}{4} - \frac{1}{2}\right)\right] + 1 \cdot 9 = \frac{788}{32}$$

$$A_{12} = 2 \cdot 50 \left[\frac{3}{4} \cdot \frac{1}{2} - \left(1 - \frac{1}{4}\right)\left(\frac{3}{4} - \frac{1}{2}\right)\right] + 2 \cdot 7 = \frac{1\,048}{32}$$

$$A_{21} = 1 \cdot 50 \left[\frac{1}{4} \cdot \frac{1}{2} - \left(1 - \frac{3}{4}\right)\left(\frac{1}{4} - \frac{1}{2}\right)\right] + 1 \cdot 7 = \frac{524}{32}$$

$$A_{22} = 2 \cdot 50 \left[\frac{3}{4} \cdot \frac{1}{2} - \left(1 - \frac{3}{4}\right)\left(\frac{3}{4} - \frac{1}{2}\right)\right] + 2 \cdot 9 = \frac{1\,576}{32}$$

$$B_{11} = \frac{1}{16} \cdot 50 \left(\frac{1}{2} - \frac{1}{4} \right) + 1 \cdot \frac{1}{16} (-24) = - \frac{23}{32}$$

$$B_{12} = \frac{1}{8} \cdot 50 \left(\frac{1}{2} - \frac{1}{4} \right) + 1 \cdot \frac{1}{8} \cdot 24 = \frac{146}{32}$$

$$B_{21} = \frac{1}{16} \cdot 50 \left(\frac{1}{2} - \frac{3}{4} \right) + 1 \cdot \frac{1}{16} (-24) = - \frac{73}{32}$$

$$B_{22} = \frac{1}{8} \cdot 50 \left(\frac{1}{2} - \frac{3}{4} \right) + 1 \cdot \frac{1}{8} \cdot 24 = \frac{46}{32}$$

$$C_{11} = 1 \cdot 50 \left(\frac{1}{4} - \frac{1}{2} \right) + 1 \cdot 24 = \frac{368}{32}$$

$$C_{12} = 2 \cdot 50 \left(\frac{3}{4} - \frac{1}{2} \right) + 2 \cdot 24 = \frac{2\,336}{32}$$

$$C_{21} = 1 \cdot 50 \left(\frac{1}{4} - \frac{1}{2} \right) + 1 \, (-24) = - \frac{1\,168}{32}$$

$$C_{22} = 2 \cdot 50 \left(\frac{3}{4} - \frac{1}{2} \right) + 2 \, (-24) = - \frac{736}{32}$$

$$D_{11} = - \frac{1}{16} \cdot 50 + 1 \cdot \frac{1}{16} (-112) = - \frac{324}{32}$$

$$D_{12} = - \frac{1}{8} \cdot 50 + 1 \cdot \frac{1}{8} \cdot 80 = \frac{120}{32}$$

$$D_{21} = - \frac{1}{16} \cdot 50 + 1 \cdot \frac{1}{16} \cdot 80 = \frac{60}{32}$$

$$D_{22} = - \frac{1}{8} \cdot 50 + 1 \cdot \frac{1}{8} (-112) = - \frac{648}{32}$$

By putting $32\Lambda = \varrho$ the eq. 80.1 gives

$$\begin{vmatrix} -\varrho+788 & 1\,048 & -23 & 146 \\ 524 & -\varrho+1\,576 & -73 & 46 \\ 368 & 2\,336 & -\varrho-324 & 120 \\ -1\,168 & -736 & 60 & -\varrho-648 \end{vmatrix} = 0 \ldots \quad 84.1$$

or

$$\varrho^4 - 1\,392\varrho^3 - 1\,018\varrho^2 + 82\,673\,644\varrho + 42\,328\,915\,968 = 0$$

with the roots $\varrho_1 = 1\,899{,}5$ and $\varrho_2 = 217{,}54$. The other roots are complex numbers. Thus $\Lambda_1 = 59{,}36$ and $\Lambda_2 = 6{,}798$. The corresponding critical speeds are $n_1 = 492$ r.p.m. and $n_2 = 1\,454$ r.p.m. The deflection lines may be drawn with the aid of the equations given in this chapter.

If the gyroscopic effect is neglected from eq. 84.1 we get

$$\begin{vmatrix} -\varrho+788 & 1\,048 \\ 524 & -\varrho+1\,576 \end{vmatrix} = 0$$

with the roots $\varrho_1 = 2\,021$ and $\varrho_2 = 343$ and thus $\Lambda_1 = 63{,}156$ and $\Lambda_2 = 10{,}719$ giving $n_{01} = 477$ r.p.m. and $n_{02} = 1\,158$ r.p.m.

In the same way it is possible to find the critical speeds for the shaft when the spring constant is varied between 0 and ∞. The result is collected in table 84.2.

Spring constant kp/mm	1st critical speed. Gyroscopic effect considered r.p.m.	1st critical speed. Gyroscopic effect neglected r.p.m.	Increase due to the gyroscopic effect per cent	2nd critical speed. Gyroscopic effect considered r.p.m.	2nd critical speed. Gyroscopic effect neglected r.p.m.	Increase due to the gyroscopic effect per cent
0	0	0	0	0	0	0
10	187	187	~ 0	875	416	110,34
40	347	344	0,87	1 244	794	56,68
50	380	375	1,33	1 249	875	42,74
100	492	477	3,14	1 454	1 158	25,56
500	761	669	13,75	1 947	1 839	5,87
1 000	850	713	19,21	2 113	2 044	3,38
2 500	926	744	24,45	2 257	2 207	2,27
5 000	958	756	26,72	2 317	2 270	2,07
∞	994	768	29,43	2 387	2 339	2,05

Table 84.2

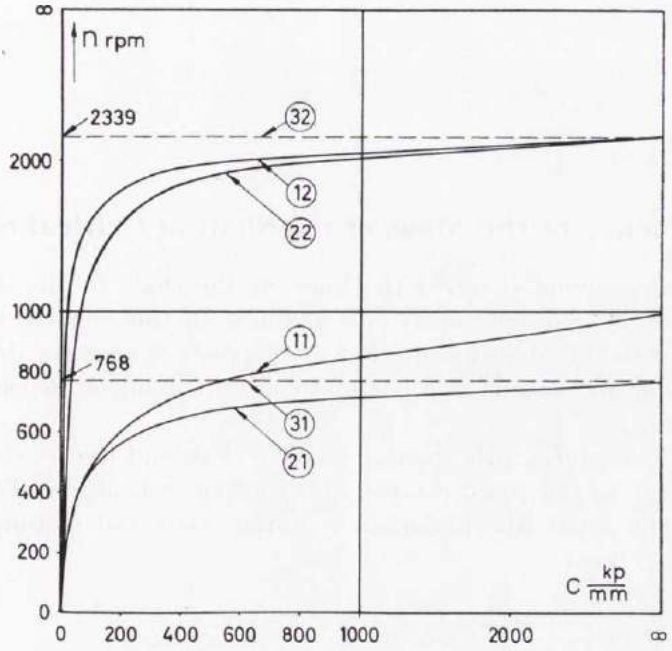

Fig. 85.1

Curve 11: 1st critical speed. Gyroscopic effect considered
Curve 12: 2nd critical speed. Gyroscopic effect considered
Curve 21: 1st critical speed. Gyroscopic effect neglected
Curve 22: 2nd critical speed. Gyroscopic effect neglected
Curve 31: 1st critical speed. Stiff bearings. Gyroscopic effect neglected
Curve 32: 2nd critical speed. Stiff bearings. Gyroscopic effect neglected

The values are plotted in fig. 85.1. The conclusion is that the gyroscopic effect is considerable at the first critical speed if stiff springs are used and at the second critical speed if weak springs are used.

9. Influence of the Mass of the Shaft at Critical Speeds

In the previous chapters the mass of the shaft in the different arrangements was not taken into account. In this chapter and the next a method is shown to do that with a shaft of constant diameter.

Consider an element of a shaft of constant diameter according to fig. 87.1.

The shaft whirls with angular velocity Ω around the x-axis at the same time as the shaft rotates with angular velocity ω. Then the equilibrium gives (the disturbance of the tangential motion is not considered here)

$$\left.\begin{aligned} &\frac{m}{L}\cdot dxy\Omega^2+\frac{mg}{L}\cdot dx\cos\varphi+T+\frac{\partial T}{\partial x}\cdot dx-T=0 \\ &dM_g+\frac{mg}{L}\cdot dx\cos\varphi\cdot\frac{dx}{2}\quad -Tdx+M+\frac{\partial M}{\partial x}\cdot dx-M=0 \end{aligned}\right\}$$

or after neglecting small terms

$$\left.\begin{aligned} &\frac{\partial T}{\partial x}+\frac{m}{L}\cdot y\Omega^2+\frac{mg}{L}\cdot\cos\varphi=0 \\ &T=\frac{dM}{dx}+\frac{dM_g}{dx} \end{aligned}\right\} \quad \ldots\ldots\ldots \quad 86.1$$

From these equations, if $dM_g=(2\gamma dI_p\Omega^2)y'$, where $\gamma=\frac{1}{4}$ and $\gamma=-\frac{3}{4}$ at forward and reverse whirl respectively, and

$$M=-EIy''$$

we get that

$$T=-EIy'''+2\gamma\Omega^2\cdot\frac{dI_p}{dx}\cdot y'$$

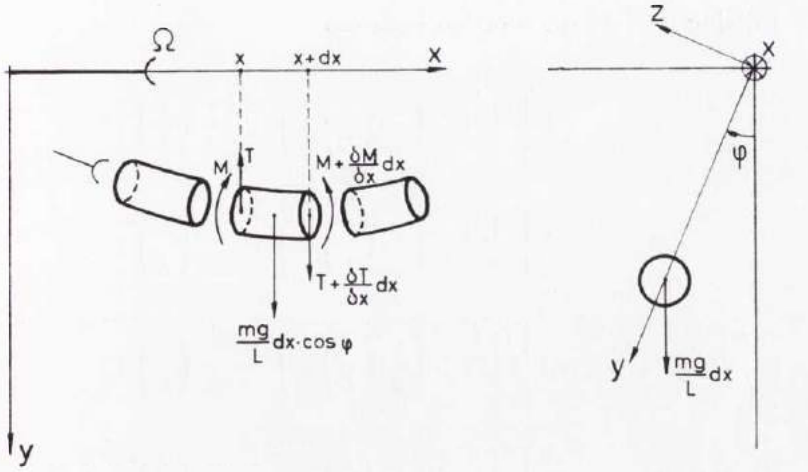

Fig. 87.1

But $dI_p = \frac{dx}{L} \cdot m \cdot \frac{r^2}{2}$, where r is the radius of the shaft. Thus

$$T = -EIy''' + 2\gamma\Omega^2 \cdot \frac{m}{L} \cdot \frac{r^2}{2} \cdot y'$$

Insertion in the first of the eqs. 86.1 gives

$$-EIy^{IV} + 2\gamma\Omega^2 \cdot \frac{m}{L} \cdot \frac{r^2}{2} \cdot y'' + \frac{m}{L}\, y\Omega^2 + \frac{mg}{L} \cos\varphi = 0$$

Now introduce the non-dimensional length $\xi = \frac{x}{L}$. If we neglect the gravity force besides the other forces

$$-EI \frac{d^4y}{d(\xi L)^4} + 2\gamma\Omega^2 \cdot \frac{mr^2}{2L} \cdot \frac{d^2y}{d(\xi L)^2} + \frac{m}{L} \cdot \Omega^2 y = 0$$

$$\frac{d^4y}{d\xi^4} - 2\gamma \cdot \frac{mr^2\Omega^2L^4}{2EIL^3} \cdot \frac{d^2y}{d\xi^2} - \frac{m}{L} \cdot \frac{L^4}{EI} \cdot \Omega^2 y = 0$$

Denoting $\lambda^4 = \frac{mL^3\Omega^2}{EI}$ we get

$$\frac{d^4y}{d\xi^4} - \gamma \left(\frac{r}{L}\right)^2 \lambda^4 \frac{d^2y}{d\xi^2} - \lambda^4 y = 0$$

Putting $y = e^{k\xi}$ the solution becomes

$$k_1 = \quad \lambda \sqrt{\sqrt{1+\left(\frac{\gamma}{2}\left(\frac{r}{L}\right)^2\lambda^2\right)^2} + \frac{\gamma}{2}\left(\frac{r}{L}\right)^2\lambda^2}$$

$$k_2 = -\lambda \sqrt{\sqrt{1+\left(\frac{\gamma}{2}\left(\frac{r}{L}\right)^2\lambda^2\right)^2} + \frac{\gamma}{2}\left(\frac{r}{L}\right)^2\lambda^2}$$

$$k_3 = \quad i\lambda \sqrt{\sqrt{1+\left(\frac{\gamma}{2}\left(\frac{r}{L}\right)^2\lambda^2\right)^2} - \frac{\gamma}{2}\left(\frac{r}{L}\right)^2\lambda^2}$$

$$k_4 = -i\lambda \sqrt{\sqrt{1+\left(\frac{\gamma}{2}\left(\frac{r}{L}\right)^2\lambda^2\right)^2} - \frac{\gamma}{2}\left(\frac{r}{L}\right)^2\lambda^2}$$

The equation of the deflection line for a rotating shaft can now be written as

$$y = \sum_{i=1}^{4} A_i e^{k_i \xi}$$

or using cylindrical and hyperbolic functions and denoting

$$k_1 = \lambda k_h,\ k_2 = -\lambda k_h,\ k_3 = i\lambda k_c,\ k_4 = -i\lambda k_c,$$

we get

$$y = A \sin \lambda k_c \xi + B \sinh \lambda k_h \xi + D \cos \lambda k_c \xi + E \cosh \lambda k_h \xi \quad \ldots\ldots\ldots \quad 88.1$$

The coefficients k_c and k_h are "correction factors" to λ due to the gyroscopic action. In most cases the term $\frac{\gamma}{2}\left(\frac{r}{L}\right)^2 \lambda^2$ can be neglected besides unity and we get $k_c = k_h = 1$. This thing happens exactly when $\Omega = 2\omega$ which is seen from eq. 55.1.

We now have the basic knowledge to calculate the critical speeds of the shaft in fig. 89.1 considering the mass of the shaft and the gyroscopic action of the disc. The gyroscopic action of the shaft is neglected but theoretically there are no obstacles to taking it into account.

In fig. 89.3 the acting forces and moments are shown. Non-dimensional coordinates are used in the radial direction and we need two different systems of coordinates.

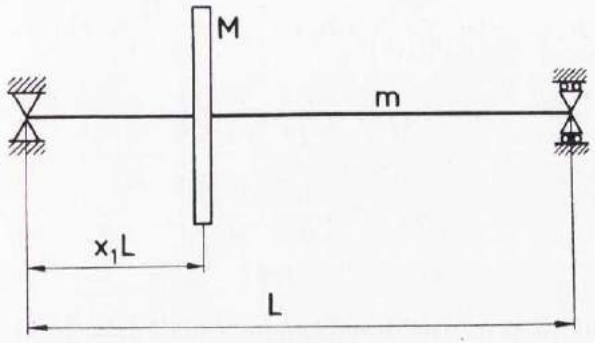

Fig. 89.1

For the two parts of the shaft, if $k_c = k_h = 1$, we get

$$\left.\begin{aligned} y_1 &= A_1 \sin \lambda\xi_1 + B_1 \operatorname{sh} \lambda\xi_1 \\ y_2 &= A_2 \sin \lambda\xi_2 + B_2 \operatorname{sh} \lambda\xi_2 \end{aligned}\right\}$$

Derivation gives

$$\left.\begin{aligned} \frac{1}{\lambda}\cdot\frac{dy_i}{d\xi_i} &= A_i \cos \lambda\xi_i + B_i \operatorname{ch} \lambda\xi_i \\ \frac{1}{\lambda^2}\cdot\frac{d^2y_i}{d\xi_i^2} &= -A_i \sin \lambda\xi_i + B_i \operatorname{sh} \lambda\xi_i \\ \frac{1}{\lambda^3}\cdot\frac{d^3y_i}{d\xi_i^3} &= -A_i \cos \lambda\xi_i + B_i \operatorname{ch} \lambda\xi_i \end{aligned}\right\} \quad \ldots\ldots\ldots \quad 89.2$$

$$i = 1, 2$$

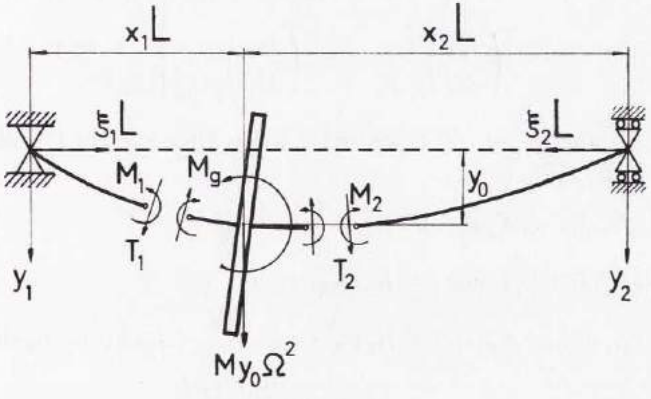

Fig. 89.3

Further $M_i = -EI\dfrac{d^2y_i}{d(\xi_i L)^2}$ and $T_i = \dfrac{dM_i}{d(\xi_i L)}$. Thus

$$\left.\begin{aligned} M_i &= -\frac{EI}{L^2}\cdot\frac{d^2y_i}{d\xi_i^2} \\ T_i &= -\frac{EI}{L^3}\cdot\frac{d^3y_i}{d\xi_i^3} \end{aligned}\right\}$$
$$(i = 1, 2)$$

The equilibrium for the disc demands (small deflection)

$$\left.\begin{aligned} T_1 + T_2 - My_0\Omega^2 &= 0 \\ M_1 - M_2 - M_g &= 0 \end{aligned}\right\}$$

These equations can be written as

$$\left.\begin{aligned} &-\frac{EI}{L^3}\cdot\left(\frac{d^3y_1}{d\xi_1^3}\right)_{\xi_1=x_1} - \frac{EI}{L^3}\cdot\left(\frac{d^3y_2}{d\xi_2^3}\right)_{\xi_2=x_2} - M\Omega^2(y_1)_{\xi_1=x_1} = 0 \\ &-\frac{EI}{L^2}\cdot\left(\frac{d^2y_1}{d\xi_1^2}\right)_{\xi_1=x_1} + \frac{EI}{L^2}\cdot\left(\frac{d^2y_2}{d\xi_2^2}\right)_{\xi_2=x_2} - 2\gamma I_p\Omega^2\left(\frac{dy_1}{d(\xi_1 L)}\right)_{\xi_1=x_1} = 0 \end{aligned}\right\} \quad 90.1$$

where $\gamma = \dfrac{1}{2}\left(\dfrac{\omega}{\Omega} - \dfrac{I_e}{I_p}\right)$. For a thin cylindrical disc of uniform thickness $\gamma = \dfrac{1}{4}$ for forward whirl and $= -\dfrac{3}{4}$ for reverse whirl.

Further

$$\left.\begin{aligned} (y_1)_{\xi_1=x_1} &= (y_2)_{\xi_2=x_2} \\ \left(\frac{dy_1}{d\xi_1}\right)_{\xi_1=x_1} &= -\left(\frac{dy_2}{d\xi_2}\right)_{\xi_2=x_2} \end{aligned}\right\} \quad \ldots\ldots\ldots\ldots \quad 90.2$$

With the aid of eq. 89.2 we may write the eqs. 90.1 and 90.2 if $\lambda x_1 = \varphi$ and $\lambda x_2 = \psi$ as

$$\left.\begin{aligned} &A_1\sin\varphi + B_1\operatorname{sh}\varphi - A_2\sin\psi - B_2\operatorname{sh}\psi = 0 \\ &A_1\cos\varphi + B_1\operatorname{ch}\varphi + A_2\cos\psi + B_2\operatorname{ch}\psi = 0 \\ &A_1\cos\varphi - B_1\operatorname{ch}\varphi + A_2\cos\psi - B_2\operatorname{ch}\psi - \lambda\cdot\frac{M}{m}\left[A_1\sin\varphi + B_1\operatorname{sh}\varphi\right] = 0 \\ &A_1\sin\varphi - B_1\operatorname{sh}\varphi - A_2\sin\psi + B_2\operatorname{sh}\psi - \frac{2\gamma I_p\Omega^2 L}{\lambda EI}\left[A_1\cos\varphi + B_1\operatorname{ch}\varphi\right] = 0 \end{aligned}\right\}$$

These equations have non-trivial solutions only if

$$\begin{vmatrix} \sin\varphi & \operatorname{sh}\varphi & -\sin\psi & -\operatorname{sh}\psi \\ \cos\varphi & \operatorname{ch}\varphi & \cos\psi & \operatorname{ch}\psi \\ \cos\varphi - \lambda\frac{M}{m}\sin\varphi & -\operatorname{ch}\varphi - \lambda\frac{M}{m}\operatorname{sh}\varphi & \cos\psi & -\operatorname{ch}\psi \\ \sin\varphi - \lambda^3\Theta^*\cos\varphi & -\operatorname{sh}\varphi - \lambda^3\Theta^*\operatorname{ch}\varphi & -\sin\psi & \operatorname{sh}\psi \end{vmatrix} = 0 \ldots \quad 91.1$$

where

$$\Theta^* = \frac{1}{\lambda^4}\cdot\frac{2\gamma I_p \Omega^2 L}{EI} = \frac{EI}{mL^3\Omega^2}\cdot\frac{2\gamma I_p\Omega^2 L}{EI}$$

$$\Theta^* = \frac{2\gamma I_p}{mL^2}$$

If the radius of inertia of the disc is k we may write

$$\Theta^* = 2\gamma\cdot\left(\frac{k}{L}\right)^2\cdot\frac{M}{m}$$

and Θ^* may be thought of as a non-dimensional inertia.

Eq. 91.1 can be reduced to the form

$$\frac{m}{M} = \frac{\lambda}{2}\cdot\frac{\left(\dfrac{1}{\cot\varphi+\cot\psi} - \dfrac{1}{\operatorname{cth}\varphi+\operatorname{cth}\psi}\right) + \Theta^*\cdot\dfrac{\lambda^3}{2}\cdot\dfrac{(\operatorname{tg}\varphi-\operatorname{tgh}\varphi)(\operatorname{tg}\psi-\operatorname{tgh}\psi)}{(\operatorname{tg}\varphi+\operatorname{tg}\psi)(\operatorname{tgh}\varphi+\operatorname{tgh}\psi)}}{1-\Theta^*\cdot\dfrac{\lambda^3}{2}\left(\dfrac{1}{\operatorname{tg}\varphi+\operatorname{tg}\psi} - \dfrac{1}{\operatorname{tgh}\varphi+\operatorname{tgh}\psi}\right)} \quad 91.2$$

This equation is mainly of the form

$$\frac{m}{M} = \lambda\cdot\frac{A+\lambda^3\Theta^* B}{1-\lambda^3\Theta^* C} \quad \ldots\ldots\ldots\ldots\ldots\ldots \quad 91.3$$

with easily seen notations. It may be observed that $\dfrac{m}{M}$ is independent of Θ^* if

$$\left.\begin{aligned} B &= At \\ C &= -1\cdot t \end{aligned}\right\} \quad \ldots\ldots\ldots\ldots\ldots\ldots \quad 91.4$$

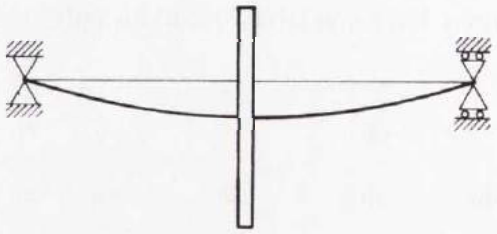

Fig. 92.1

In this case is $\frac{m}{M} = \lambda \cdot \frac{A(1+t\lambda^3\Theta^*)}{1+t\lambda^3\Theta^*} = \lambda \cdot A.$

Further we have $B = -AC$. By insertion we obtain that this connection between the coefficients only occurs at $\varphi = \psi$, viz. when the disc is mounted at the middle of the shaft.

In this case the eq. 91.2 may be simplified to

$$\frac{m}{M} = \frac{\lambda}{4}\left(\operatorname{tg}\frac{\lambda}{2} - \operatorname{tgh}\frac{\lambda}{2}\right) \quad \ldots\ldots\ldots\ldots \quad 92.2$$

We also can solve Θ^* from 91.3 and the result for $\varphi = \psi$ is

$$\lambda^3\Theta^* = \frac{\frac{m}{M} - \lambda \cdot A}{\frac{m}{M} \cdot C + \lambda \cdot B} = \frac{1\left(\frac{m}{M} - \lambda A\right)}{t\left(-\frac{m}{M} + \lambda A\right)} = -\frac{1}{t} = \frac{1}{C}$$

$C\lambda^3\Theta^* = 1$ or

$$\Theta^* = \frac{4}{\lambda^3\left[\cot\frac{\lambda}{2} - \operatorname{coth}\frac{\lambda}{2}\right]} \quad \ldots\ldots\ldots\ldots\ldots\ldots \quad 92.3$$

The formulas 92.2 and 92.3 may also be derived by studying symmetrical and antisymmetrical modes of revolution for a disc at the middle of a shaft.

The eq. 92.2 corresponds to symmetrical modes of rotation as in fig. 92.1 and the eq. 92.3 corresponds to antisymmetrical cases as shown in fig. 93.1.

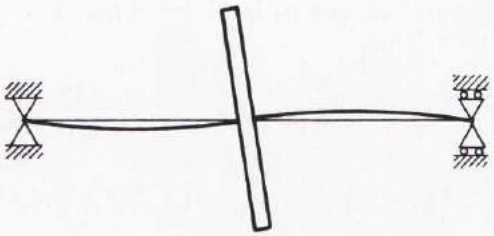

Fig. 93.1

In order to show in a simple way the influence of the mass on the critical speeds the case $x_1 = \frac{1}{2}$ is treated specially. For the first critical speed eq. 92.2 is valid. We may write this eq. as

$$\frac{m}{M} = \frac{\lambda}{4}\left(\operatorname{tg}\frac{\lambda}{2} + i\operatorname{tg}\frac{i\lambda}{2}\right) \quad \ldots\ldots\ldots\ldots \quad 93.2$$

From mathematics it is known that, if $\lambda_0 = \frac{\lambda}{2}$,

$$\operatorname{tg}\lambda_0 = \lambda_0 + \frac{\lambda_0^3}{3} + \frac{2}{15}\lambda_0^5 + \frac{17}{315}\lambda_0^7 + \frac{62}{2\,835}\lambda_0^9 + \frac{1\,382}{155\,925}\lambda_0^{11} + \ldots \qquad |\lambda_0| < \frac{\pi}{2}$$

and

$$\operatorname{tg}\lambda_0 + i\operatorname{tg} i\lambda_0 = 2\left[\frac{1}{3}\lambda_0^3 + \frac{17}{315}\lambda_0^7 + \frac{1\,382}{155\,925}\lambda_0^{11} + \ldots\right]$$

If $\mu = \frac{m}{M}$ and $\lambda_{00} = \lambda_0^4$ we get

$$\mu = \frac{1}{3}\lambda_{00} + \frac{17}{315}\lambda_{00}^2 + \frac{1\,382}{155\,925}\lambda_{00}^3 + \ldots \quad \ldots\ldots \quad 93.3$$

Form the series

$$\lambda_{00} = \sum_{s=0}^{\infty} A_s \mu^s \quad \ldots\ldots\ldots\ldots\ldots\ldots \quad 93.4$$

where the coefficients A_s are to be determined. Put this expression for λ_{00} into eq. 93.3. Thus

$$\mu = \frac{1}{3}\{A_0+A_1\mu+A_2\mu^2+A_3\mu^3+\ldots.\}+\frac{17}{315}\{A_0+A_1\mu+$$

$$+A_2\mu^2+A_3\mu^3+\ldots.\}^2+\frac{1\,382}{155\,925}\{A_0+A_1\mu+A_2\mu^2+$$

$$+A_3\mu^3+\ldots.\}^3+\ldots.$$

The coefficients on both sides of the equal sign must be identically the same. This gives

$$\left.\begin{aligned}
&A_0\left(\frac{1}{3}+\frac{17}{315}+\frac{1\,382}{155\,925}+\ldots.\right)=0\\
&\frac{1}{3}A_1=1\\
&\frac{1}{3}A_2+\frac{17}{315}A_1^2=0\\
&\frac{1}{3}A_3+2\cdot\frac{17}{315}A_1A_2+\frac{1\,382}{155\,925}A_1^3=0\\
&-\ -\ -\ -\ -\ -\ -\ -\ -\ -\ -\ -\ -
\end{aligned}\right\}$$

and from here

$$A_0=0,\ A_1=3,\ A_2=-\frac{51}{35},\ A_3=\frac{376}{539},\ \ldots$$

Eq. 93.4 gives

$$\left(\frac{\lambda}{2}\right)^4=3\mu-\frac{51}{35}\mu^2+\frac{376}{539}\mu^3-\ldots$$

By definition

$$\lambda^4=\frac{mL^3\Omega^2}{EI}=\mu\cdot\frac{ML^3\Omega^2}{EI}$$

and consequently

$$\Omega^2=\frac{48EI}{ML^3}\left(1-\frac{17}{35}\mu+\frac{376}{1\,617}\mu^2-\ldots\right)$$

If the mass of the shaft is neglected we get

$$\Omega^2 = \Omega_0^2 = \frac{48EI}{ML^3} \text{ and}$$

$$\left(\frac{\Omega}{\Omega_0}\right)^2 = 1 - \frac{17}{35}\mu + \frac{376}{1\,617}\mu^2 - \ldots$$

or after a process similar to that above

$$\frac{\Omega}{\Omega_0} = 1 - \frac{17}{70}\mu + \frac{4\,009}{46\,200}\mu^2 - \ldots = 1 - 0{,}2429\mu + 0{,}08677\mu^2 - \ldots .$$

..... 95.1

In many designs the value of μ is low, say $\mu < 0{,}10$.

From the formula 95.1 we conclude that in these cases the first critical speed does not change very much with different values of ordinary values of μ.

A common thumb rule in practice is to bring half the weight of the shaft to the disc and it is an interesting task to compare the result from this assumption with eq. 95.1.

From eq. 26.2 we immediately get

$$\Omega_a^2 = \frac{48EI}{\left(M + \frac{m}{2}\right)L^3}$$

and

$$\left(\frac{\Omega_a}{\Omega_0}\right)^2 = \frac{1}{1 + \frac{\mu}{2}} = 1 - \frac{\mu}{2} + \left(\frac{\mu}{2}\right)^2 - \left(\frac{\mu}{2}\right)^3 + \ldots$$

or after a simple calculation

$$\frac{\Omega_a}{\Omega_0} = 1 - 0{,}25\mu + 0{,}09375\mu^2 -$$

This formula will give a good result. It is seen from eq. 95.1 that if $\frac{17}{35}$ of the weight of the shaft is added to the mass of the disc a very accurate result is obtained.

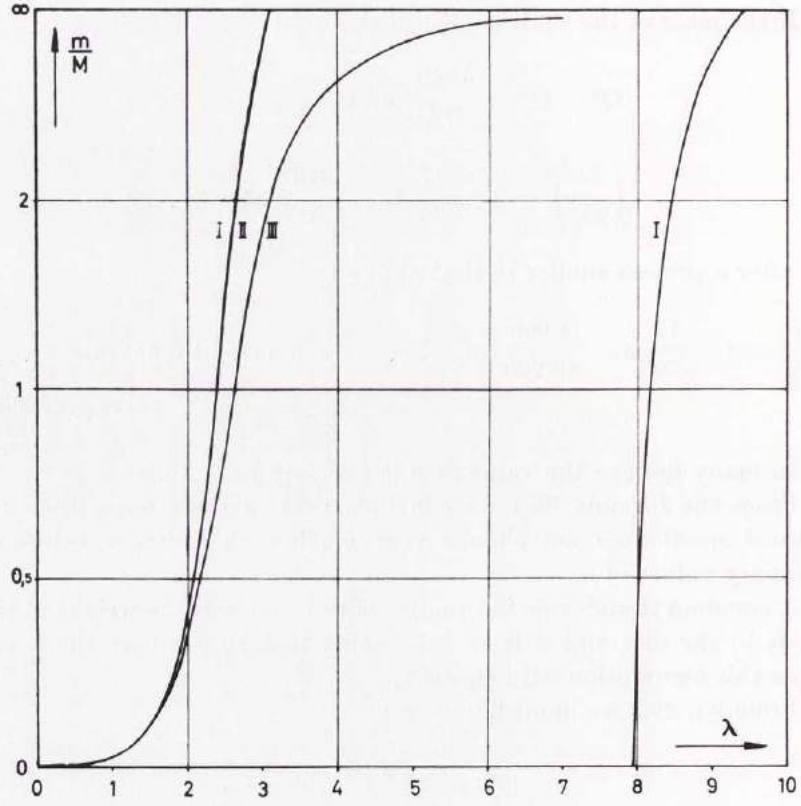

Fig. 96.1

Now we have treated the calculation of the first critical speed with the aid of eq. 92.2. This equation determines all "symmetry modes" of the deflection curve. For every value of μ there is an infinite number of λ-values because of the fact that the equation involves periodic functions. Thus there is also an infinite number of critical speeds. This fact is considered in fig. 96.1 where μ is drawn as a function of λ. In the same figure some other curves are shown for illustrating the degree of accuracy of usual approximations.

Curve I: Exact curve.

Curve II: Curve based on the assumption that half the weight of the shaft can be referred to the disc (coincides practically with the first branch of Curve I).

Curve III: Curve based on the assumption that no part of the mass of the shaft is referred to the disc.

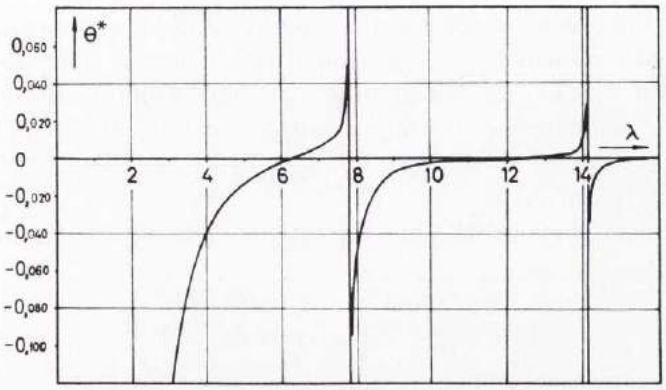

Fig. 97.1

Now we turn over to the antisymmetrical modes of the deflection curve. In these cases eq. 92.3 is valid. The function Θ^* is drawn in fig. 97.1.

Example 13. We now calculate the ordinary critical speed for the arrangement in fig. 61.1 but the disc is placed on the middle of the shaft. For the symmetrical modes we get from the fig. 96.1 or calculations ($\mu = 0{,}050$, $\Theta^* = 1{,}25$) that $\lambda_{1s} = 1{,}230$, $\lambda_{2s} = 2{,}5\pi + \varepsilon_1$ . . . . . and for the antisymmetrical modes we get from fig. 97.1 that $\lambda_{1a} = 2{,}5\pi - \varepsilon_2$, $\lambda_{2a} = 4{,}5\pi - \varepsilon_3$ where ε_i $(i = 1, 2, 3)$ denote a small number. The first corresponding critical speed can be calculated to 930 r.p.m., which is 2,4% lower than the "elementary" value where the mass of the shaft is not considered. The values $\lambda = \pi$, 2π, 3π . . . correspond to the critical speeds for a shaft without disc. Further, $\lambda \cong 2{,}5\pi$, $4{,}5\pi$ . . . corresponds to the antisymmetrical critical speeds for a shaft with a disc of infinite inertia. (The same result as for a "hinged-clamped" shaft without disc and of length $\frac{L}{2}$).

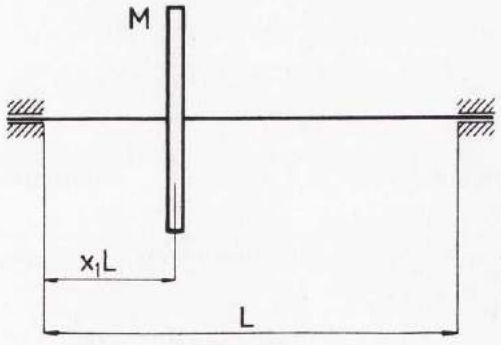

Fig. 97.2

Up to here we have treated the case in fig. 92.1 with bearings free from bending moments. It is evident that analogous calculations can be carried out for other conditions of shaft support. In this book another "symmetrical" bearing arrangement is treated viz. the one giving zero slope to the shaft. We may call it a "clamped-clamped" shaft. See fig. 97.2.

The result is given without derivations. The eq. corresponding to eq. 91.2 is

$$\frac{m}{M} = \lambda \cdot \frac{A+\Theta B}{C+\Theta D}$$

where

$$\begin{aligned}
A &= (N^2+KP)\,(RU-ST)+(S^2+RT)\,(KQ-NP)\\
B &= (N^2+KP)\,(S^2+RT)\\
C &= (N^2+KP)\,(U^2+RT)+(S^2+RT)\,(Q^2+KP)+\\
&\quad +(NP-KQ)\,(RS-TU)+(NK-PQ)\,(ST-RU)-\\
&\quad -(P^2+NQ)\,(R^2+SU)-(K^2+NQ)\,(T^2+SU)\\
D &= (N^2+KP)\,(TU-RS)+(S^2+RT)\,(PQ-KN)
\end{aligned}$$

and

$$\begin{aligned}
K &= \sin\varphi-\operatorname{sh}\varphi & R &= \sin\psi-\operatorname{sh}\psi\\
N &= \cos\varphi-\operatorname{ch}\varphi & S &= \cos\psi-\operatorname{ch}\psi\\
P &= \sin\varphi+\operatorname{sh}\varphi & T &= \sin\psi+\operatorname{sh}\psi\\
Q &= \cos\varphi+\operatorname{ch}\varphi & U &= \cos\psi+\operatorname{ch}\psi
\end{aligned}$$

$$\begin{aligned}
\varphi &= x_1\lambda\\
\psi &= (1-x_1)\lambda\\
\lambda^4 &= \frac{mL^3}{EI}\,\Omega^2\\
\Theta^* &= \left(\frac{\omega}{\Omega}-\frac{I_e}{I_p}\right)\cdot\frac{I_p}{mL^2}\\
\Theta &= \lambda^3\Theta^*
\end{aligned}$$

Especially we get for $\Theta^* = 0$, $\varphi = \psi = \frac{1}{2}$ the equation

$$\frac{m}{M} = \frac{\lambda}{2}\cdot\frac{1-\cos\frac{\lambda}{2}\operatorname{ch}\frac{\lambda}{2}}{\sin\frac{\lambda}{2}\operatorname{ch}\frac{\lambda}{2}+\operatorname{sh}\frac{\lambda}{2}\cos\frac{\lambda}{2}} \qquad \ldots\ldots\ldots \quad 98.1$$

giving all critical speeds at symmetrical deflection curve. Further we have λ independent of $\frac{m}{M}$ if

$$\lambda^3\Theta^* = \frac{A}{B} = \frac{C}{D}$$

and from here

$$\Theta^* = \frac{2}{\lambda^3} \cdot \frac{\sin\frac{\lambda}{2}\operatorname{ch}\frac{\lambda}{2} - \cos\frac{\lambda}{2}\operatorname{sh}\frac{\lambda}{2}}{\cos\frac{\lambda}{2}\operatorname{ch}\frac{\lambda}{2} - 1}$$

giving all critical speeds at antisymmetrical deflection curves. Now the eq. 98.1 will be scrutinized narrowly. Put $\lambda_0 = \frac{\lambda}{2}$. Thus

$$\frac{m}{M} = \lambda_0 \cdot \frac{\frac{1}{\cos\lambda_0 \operatorname{ch}\lambda_0} - 1}{\operatorname{tg}\lambda_0 + \operatorname{tgh}\lambda_0}$$

Further by expansion in series

$$\operatorname{tg}\lambda_0 + \operatorname{tgh}\lambda_0 = \operatorname{tg}\lambda_0 - i\operatorname{tg} i\lambda_0 = 2\left(\lambda_0 + \frac{2}{15}\lambda_0^5 + \frac{62}{2\,835}\lambda_0^9 + \dots\right)$$

and

$$\cos\lambda_0 \operatorname{ch}\lambda_0 = \left(1 - \frac{\lambda_0^2}{2} + \frac{\lambda_0^4}{24} - \frac{\lambda_0^6}{720} + \frac{\lambda_0^8}{40\,320} - \frac{\lambda_0^{10}}{3\,628\,800} + \frac{\lambda_0^{12}}{479\,001\,600}\right)\left(1 + \frac{\lambda_0^2}{2} + \frac{\lambda_0^4}{24} + \frac{\lambda_0^6}{720} + \frac{\lambda_0^8}{40\,320} + \frac{\lambda_0^{10}}{3\,628\,800} + \frac{\lambda_0^{12}}{479\,001\,600} + \dots\right) = 1 - \frac{\lambda_0^4}{6} + \frac{1}{70}\left(\frac{\lambda_0^4}{6}\right)^2 - \frac{1}{34\,650}\left(\frac{\lambda_0^4}{6}\right)^3 + \dots$$

Put $\nu = \frac{\lambda_0^4}{6}$ and we get

$$2 \cdot \frac{m}{M} = \frac{\frac{1}{1 - \left[\nu - \frac{1}{70}\nu^2 + \frac{1}{34\,650}\nu^3 - \dots\right]} - 1}{1 + \frac{4}{5}\nu + \frac{248}{315}\nu^2 + \dots}$$

If the expression within the bracket is less than unity we have, if $\mu = \frac{m}{M}$,

$$2\mu = \left(1 - \frac{4}{5}\nu - \frac{232}{1\,575}\nu^2 - \ldots\right)\left(\nu + \frac{69}{70}\nu^2 + \frac{33\,661}{34\,650}\nu^3 + \ldots\right)$$

or if $\nu = 2\nu_0$

$$\mu = \nu_0 + \frac{13}{35}\nu_0^2 + \frac{274}{1\,925}\nu_0^3 + \ldots \quad \ldots\ldots\ldots\ldots \quad 100.1$$

Now construct the series

$$\nu_0 = \sum_{s=0}^{\infty} A_s \mu^s$$

Putting these series into eq. 100.1 and equating the coefficients we get

$$\nu_0 = \frac{\nu}{2} = \frac{1}{2} \cdot \frac{\lambda_0^4}{6} = \frac{1}{12}\left(\frac{\lambda}{2}\right)^4 = \frac{\lambda^4}{192} = \mu - \frac{13}{35}\mu^2 + \frac{72}{539}\mu^3 + \ldots$$

and

$$\frac{ML^3\Omega^2}{192EI} = 1 - \frac{13}{35}\mu + \frac{72}{539}\mu^2 + \ldots$$

If the mass of the shaft is neglected we get

$$\Omega^2 = \Omega_0^2 = \frac{192EI}{ML^3}$$

and consequently

$$\left(\frac{\Omega}{\Omega_0}\right)^2 = 1 - \frac{13}{35}\mu + \frac{72}{539}\mu^2 + \ldots$$

or

$$\frac{\Omega}{\Omega_0} = 1 - \frac{13}{70}\mu + \frac{109}{2\,200}\mu^2 + \ldots$$

It is immediately seen that a good result is obtained if $\frac{13}{35}$ of the mass of the shaft is added to the mass of the disc and we then compute according to the elementary theory.

The numbers $\frac{17}{35}$ and $\frac{13}{35}$ which occur at the hinged-hinged shaft and the clamped-clamped shaft respectively may be derived with the Rayleigh method. Assuming a deflection line in lateral vibration according to

$$y = f(x) \sin \Omega t$$

the potential energy due to bending stresses can be written

$$E_{\text{pot}} = \int_0^L \frac{\left(-EI \frac{\partial^2 y}{\partial x^2}\right)^2 dx}{2EI} = \frac{1}{2} EI \int_0^L \left(\frac{\partial^2 y}{\partial x^2}\right)^2 dx$$

The kinetic energy is the sum of the kinetic energies of the shaft and the disc. Thus

$$E_{\text{kin}} = \frac{M}{2} \left[\left(\frac{\partial y}{\partial t}\right)_{x=\frac{L}{2}}\right]^2 + \frac{1}{2} \int_0^L \left(\frac{m}{L} dx\right) \left(\frac{\partial y}{\partial t}\right)^2$$

The maximum amounts of E_{pot} and E_{kin} are equal. This condition determines Ω^2. Thus

$$\Omega^2 = \frac{\int_0^L [f''(x)]^2 dx}{M\left[f\left(x = \frac{L}{2}\right)\right]^2 + \frac{m}{L} \int_0^L [f(x)]^2 dx} \cdot EI$$

If $f(x)$ is chosen as a function proportional to the deflection function obtained when a single force is acting on the middle of the shaft we get for example with the aid of the influence functions in Chapter 14.

$$\Omega^2 = \frac{48EI}{M + \frac{17}{35} m}$$

for the hinged-hinged shaft and

$$\Omega^2 = \frac{192EI}{M + \frac{13}{35}m}$$

for the clamped-clamped shaft.

The coefficient before m varies with the position of the disc. We may write this coefficient

$$F_i = \frac{\frac{1}{L}\int_0^L [f(x)]^2 dx}{[f(x = x_1 L)]^2}$$

Calculating with a function $f(x)$ obtained for a force applied at $x = x_1 L$ the functions below were obtained. The results correspond to the first six shaft arrangements shown in Chapter 14.

$$F_1 = \frac{33}{140}x_1 + x_3 + \frac{3}{4}\left(\frac{x_3}{x_1}\right)^2 (x_3 - 2x_1) \qquad [x_1 + x_3 = 1]$$

$$F_2 = \frac{1}{420(x_1x_2)^2}\{35[x_1^3(1+x_2)^2 + x_2^3(1+x_1)^2] + 15(x_1^5 + x_2^5) -$$

$$-42[x_1^4(1+x_2) + x_2^4(1+x_1)]\} \qquad [x_1 + x_2 = 1]$$

$$F_3 = \frac{1}{840(x_1x_2)^2}\{378(x_1^3 + x_2^3) + 30[x_1^3(1+2x_1)^2 + x_2^3(1+$$

$$+2x_2)^2] - 210[x_1^3(1+2x_1) + x_2^3(1+2x_2)]\} \qquad [x_1 + x_2 = 1]$$

$$F_4 = \frac{1}{105(x_1x_2)^2(x_1+3)^2}\{(3-x_1^2)^2(15x_2^3 - 35x_2^2 + 21x_2) +$$

$$+84x_1^4x_2 - 14(3x_1^2 - x_1^4)(6x_2 - 5x_2^2) + x_1^3(15x_1^4 + 60x_1^3 -$$

$$-66x_1^2 - 252x_1 + 315)\} \qquad [x_1 + x_2 = 1]$$

$$F_5 = \frac{1}{420x_1^2}\{99x_1^5 + 8\varkappa_1^5 + 231\varkappa_1x_1^4 + 140\varkappa_1^2x_1^3\} \qquad [x_1 + \varkappa_1 = 1]$$

$$F_6 = \frac{1}{35x_1^2(3+x_1)^2}\{132x_1^5 + 231\varkappa_1x_1^4 + 105\varkappa_1^2x_1^3 + 3\varkappa_1^5\}$$

$$[x_1 + \varkappa_1 = 1]$$

These functions are tabulated in the tables 103.1 and 104.1.

x_1	F_1 $x_1+x_3=1$	F_2 $x_1+x_2=1$	F_3 $x_1+x_2=1$	F_4 $x_1+x_2=1$	F_5 $x_1+x_1=1$	F_6 $x_1+x_1=1$
0,00	∞	∞	∞	∞	∞	∞
0,01	7 131,0991	198,2230	219,3612	100,4354	181,1410	89,9688
0,02	1 693,6926	51,4448	56,1558	26,4666	43,0506	21,2444
0,03	714,4926	23,8311	25,5505	12,3940	18,1842	8,9179
0,04	381,1292	13,9381	14,7182	7,3427	9,7200	4,7396
0,05	231,0992	9,2727	9,6478	4,9475	5,9119	2,8682
0,06	151,9024	6,6920	6,8632	3,6159	3,9027	1,8856
0,07	105,5288	5,1082	5,1660	2,7949	2,7271	1,3138
0,08	76,3214	4,0625	4,0529	2,2504	1,9875	0,9562
0,09	56,9046	3,3334	3,2819	1,8694	1,4965	0,7204
0,10	43,4486	2,8034	2,7249	1,5915	1,1569	0,5585
0,11	33,8110	2,4051	2,3087	1,3820	0,9143	0,4439
0,12	26,7216	2,0974	1,9893	1,2198	0,7364	0,3606
0,13	21,3907	1,8545	1,7384	1,0915	0,6032	0,2989
0,14	17,3076	1,6590	1,5376	0,9881	0,5016	0,2525
0,15	14,1312	1,4991	1,3742	0,9035	0,4231	0,2171
0,16	11,6271	1,3665	1,2395	0,8334	0,3616	0,1899
0,17	9,6303	1,2553	1,1269	0,7746	0,3130	0,1688
0,18	8,0222	1,1610	1,0320	0,7249	0,2743	0,1524
0,19	6,7161	1,0803	0,9511	0,6824	0,2432	0,1396
0,20	5,6471	1,0107	0,8817	0,6459	0,2182	0,1296
0,21	4,7667	0,9503	0,8216	0,6144	0,1979	0,1219
0,22	4,0373	0,8974	0,7693	0,5870	0,1815	0,1160
0,23	3,4301	0,8510	0,7235	0,5631	0,1682	0,1114
0,24	2,9224	0,8100	0,6833	0,5422	0,1574	0,1081
0,25	2,4964	0,7735	0,6476	0,5239	0,1487	0,1056
0,26	2,1379	0,7411	0,6160	0,5078	0,1416	0,1040
0,27	1,8353	0,7122	0,5878	0,4936	0,1360	0,1030
0,28	1,5795	0,6862	0,5627	0,4812	0,1316	0,1025
0,29	1,3628	0,6629	0,5401	0,4703	0,1282	0,1024
0,30	1,1791	0,6419	0,5199	0,4607	0,1256	0,1027
0,31	1,0232	0,6230	0,5017	0,4524	0,1237	0,1034
0,32	0,8909	0,6059	0,4854	0,4452	0,1224	0,1042
0,33	0,7787	0,5905	0,4707	0,4390	0,1216	0,1053
0,34	0,6836	0,5766	0,4574	0,4337	0,1212	0,1066
0,35	0,6032	0,5641	0,4454	0,4294	0,1212	0,1080
0,36	0,5352	0,5527	0,4347	0,4258	0,1216	0,1096
0,37	0,4780	0,5426	0,4250	0,4230	0,1221	0,1112
0,38	0,4301	0,5334	0,4164	0,4209	0,1230	0,1130
0,39	0,3900	0,5253	0,4087	0,4195	0,1240	0,1148
0,40	0,3568	0,5180	0,4018	0,4187	0,1251	0,1167
0,41	0,3294	0,5116	0,3957	0,4186	0,1265	0,1186
0,42	0,3071	0,5059	0,3904	0,4191	0,1279	0,1206
0,43	0,2892	0,5011	0,3858	0,4203	0,1295	0,1226
0,44	0,2750	0,4969	0,3819	0,4220	0,1311	0,1247
0,45	0,2639	0,4934	0,3787	0,4244	0,1328	0,1267
0,46	0,2557	0,4906	0,3760	0,4273	0,1346	0,1288
0,47	0,2498	0,4885	0,3740	0,4309	0,1365	0,1309
0,48	0,2459	0,4869	0,3726	0,4351	0,1384	0,1331
0,49	0,2436	0,4860	0,3717	0,4400	0,1403	0,1352

Table 103.1

x_1	F_1 $x_1+x_3=1$	F_2 $x_1+x_2=1$	F_3 $x_1+x_2=1$	F_4 $x_1+x_2=1$	F_5 $x_1+\varkappa_1=1$	F_6 $x_1+\varkappa_1=1$
0,50	0,2429	0,4857	0,3714	0,4455	0,1423	0,1373
0,51	0,2433	0,4860	0,3717	0,4517	0,1443	0,1395
0,52	0,2447	0,4869	0,3726	0,4586	0,1463	0,1416
0,53	0,2470	0,4885	0,3740	0,4663	0,1483	0,1437
0,54	0,2499	0,4906	0,3760	0,4747	0,1503	0,1459
0,55	0,2533	0,4934	0,3787	0,4840	0,1524	0,1480
0,56	0,2572	0,4969	0,3819	0,4942	0,1544	0,1501
0,57	0,2613	0,5011	0,3858	0,5054	0,1565	0,1523
0,58	0,2657	0,5059	0,3904	0,5175	0,1585	0,1543
0,59	0,2702	0,5116	0,3957	0,5308	0,1606	0,1565
0,60	0,2748	0,5180	0,4018	0,5453	0,1627	0,1586
0,61	0,2793	0,5253	0,4087	0,5610	0,1647	0,1607
0,62	0,2839	0,5334	0,4164	0,5782	0,1668	0,1628
0,63	0,2882	0,5426	0,4250	0,5969	0,1688	0,1649
0,64	0,2925	0,5527	0,4347	0,6174	0,1708	0,1670
0,65	0,2966	0,5641	0,4454	0,6397	0,1728	0,1690
0,66	0,3005	0,5766	0,4574	0,6641	0,1749	0,1711
0,67	0,3042	0,5905	0,4707	0,6908	0,1769	0,1731
0,68	0,3076	0,6059	0,4854	0,7201	0,1789	0,1752
0,69	0,3107	0,6230	0,5017	0,7524	0,1808	0,1772
0,70	0,3135	0,6419	0,5199	0,7879	0,1828	0,1792
0,71	0,3160	0,6629	0,5401	0,8271	0,1848	0,1812
0,72	0,3181	0,6862	0,5627	0,8705	0,1867	0,1832
0,73	0,3200	0,7122	0,5878	0,9188	0,1886	0,1852
0,74	0,3215	0,7411	0,6160	0,9726	0,1905	0,1872
0,75	0,3226	0,7735	0,6476	1,0328	0,1924	0,1892
0,76	0,3234	0,8100	0,6833	1,1005	0,1943	0,1911
0,77	0,3238	0,8510	0,7235	1,1769	0,1962	0,1931
0,78	0,3239	0,8974	0,7693	1,2637	0,1981	0,1950
0,79	0,3236	0,9503	0,8216	1,3627	0,1999	0,1970
0,80	0,3230	1,0107	0,8817	1,4764	0,2018	0,1989
0,81	0,3219	1,0803	0,9511	1,6079	0,2036	0,2008
0,82	0,3205	1,1610	1,0320	1,7612	0,2054	0,2027
0,83	0,3188	1,2553	1,1269	1,9413	0,2072	0,2046
0,84	0,3166	1,3665	1,2395	2,1550	0,2090	0,2065
0,85	0,3142	1,4991	1,3742	2,4114	0,2107	0,2084
0,86	0,3113	1,6590	1,5376	2,7228	0,2125	0,2103
0,87	0,3081	1,8545	1,7384	3,1065	0,2142	0,2121
0,88	0,3046	2,0974	1,9893	3,5870	0,2160	0,2140
0,89	0,3007	2,4051	2,3087	4,2005	0,2177	0,2158
0,90	0,2964	2,8034	2,7249	5,0018	0,2194	0,2177
0,91	0,2918	3,3334	3,2819	6,0776	0,2211	0,2195
0,92	0,2869	4,0625	4,0529	7,5715	0,2228	0,2214
0,93	0,2816	5,1082	5,1660	9,7353	0,2244	0,2232
0,94	0,2760	6,6920	6,8632	13,0460	0,2261	0,2250
0,95	0,2701	9,2727	9,6478	18,4976	0,2277	0,2268
0,96	0,2638	13,9381	14,7182	28,4611	0,2293	0,2286
0,97	0,2573	23,8311	25,5505	49,8293	0,2310	0,2304
0,98	0,2504	51,5548	56,1448	110,4241	0,2326	0,2322
0,99	0,2432	198,2230	219,3612	435,0734	0,2341	0,2339
1,00	0,2357	∞	∞	∞	0,2357	0,2357

Table 104.1

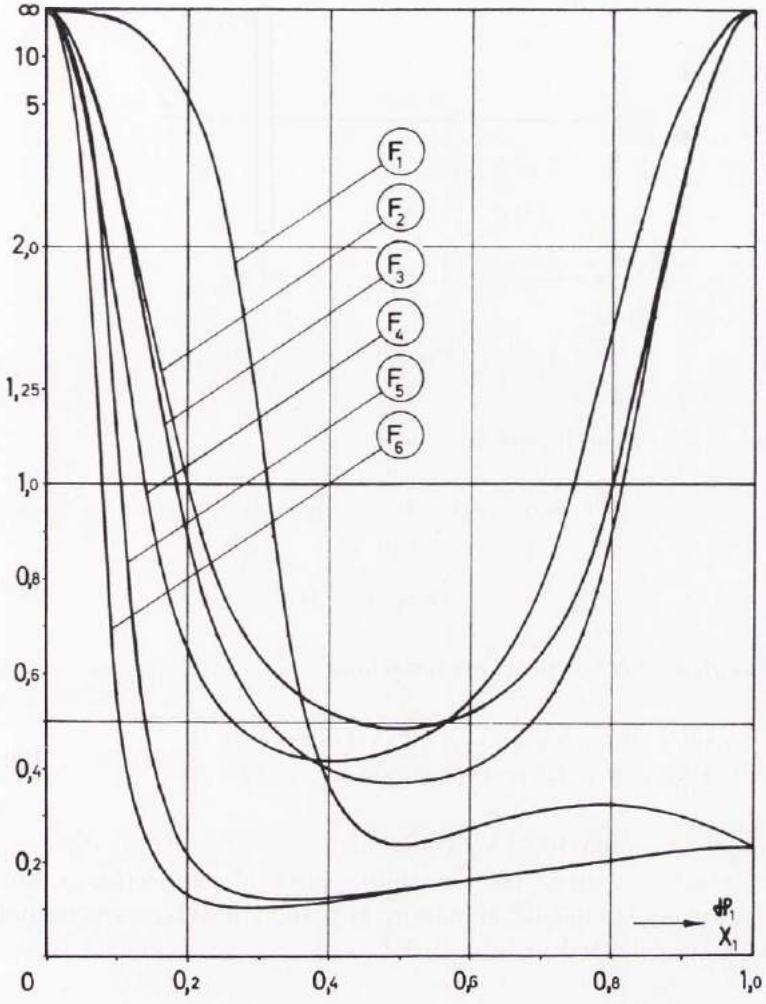

Fig. 105.1

In fig. 105.1 the "correction" functions F_i ($i = 1, 2, 3, \ldots . 6$) are drawn against $x_1(\varkappa_1)$. It is evident that the importance of the mass of the shaft grows rapidly if the disc is mounted near a bearing.

Now turn over to the "clamped-free" case shown in fig. 106.1.

The equation for the deflection line is

$$y = A \sin \lambda\xi + B \operatorname{sh} \lambda\xi + C \cos \lambda\xi + D \operatorname{ch} \lambda\xi$$

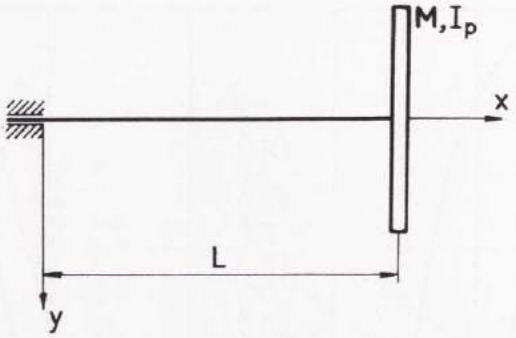

Fig. 106.1

The boundary conditions are

$$\begin{aligned} \xi = 0 \quad & y = 0 \quad && y' = 0 \\ \xi = 1 \quad & -EIy'' && = 2\gamma I_p \Omega^2 y' \\ & -EIy''' && = My\Omega^2 \end{aligned}$$

These give with the previous notations

$$\frac{m}{M} = \lambda \frac{\sin\lambda \operatorname{ch}\lambda - \cos\lambda \operatorname{sh}\lambda + \Theta^* \lambda^3 (1 - \cos\lambda \operatorname{ch}\lambda)}{1 + \cos\lambda \operatorname{ch}\lambda + \Theta^* \lambda^3 (\sin\lambda \operatorname{ch}\lambda + \cos\lambda \operatorname{sh}\lambda)} \quad \ldots\ldots\ldots \quad 106.2$$

In [4] the formula 106.2 is tabulated.

In the same manner the remaining cases of supporting a shaft with one mass by means of one or two rigid bearings are treated. All cases are collected in table 107.1.

The new notations are

$$\begin{aligned} K_0 &= \sin\varphi & R_0 &= \sin\psi & K_1 &= \operatorname{tg}\varphi \\ N_0 &= \operatorname{sh}\varphi & S_0 &= \cos\psi & N_1 &= \operatorname{tgh}\varphi \\ P_0 &= \cos\varphi & T_0 &= \operatorname{sh}\psi & \varphi &= x_1 L \text{ or } \varphi = \varkappa_1 L \\ Q_0 &= \operatorname{ch}\varphi & U_0 &= \operatorname{ch}\psi & \psi &= x_2 L \text{ or } \psi = \varkappa_2 L \end{aligned}$$

and we may write

$$\frac{m}{M} = \lambda \cdot \frac{A + \Theta B}{C + \Theta D}$$

Order	Kind of support	A	B	C	D
1	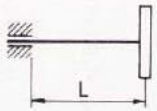	$\sin\lambda\,\mathrm{ch}\lambda-\cos\lambda\,\mathrm{ch}\lambda$	$1-\cos\lambda\,\mathrm{ch}\lambda$	$1+\cos\lambda\,\mathrm{ch}\lambda$	$\sin\lambda\,\mathrm{ch}\lambda+\cos\lambda\,\mathrm{ch}\lambda$
2	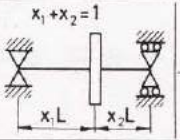	$\frac{1}{2}\left\{\frac{1}{\cot\varphi+\cot\psi}-\frac{1}{\mathrm{cth}\varphi+\mathrm{cth}\psi}\right\}$	$\frac{1}{4}\cdot\frac{(\mathrm{tg}\varphi-\mathrm{tgh}\varphi)\,(\mathrm{tg}\psi-\mathrm{tgh}\psi)}{(\mathrm{tg}\varphi+\mathrm{tg}\psi)\,(\mathrm{tgh}\varphi+\mathrm{tgh}\psi)}$	1	$-\frac{1}{2}\left\{\frac{1}{\mathrm{tg}\varphi+\mathrm{tg}\psi}-\frac{1}{\mathrm{tgh}\varphi+\mathrm{tgh}\psi}\right\}$
3	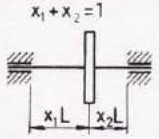	$(N^2+KP)\,(RU-ST)+$ $+(S^2+RT)\,(KQ-NP)$	$(N^2+KP)\,(S^2+RT)$	$(N^2+KP)(U^2+RT)+(S^2+RT)\times$ $(Q^2+KP)+(NP-KQ)\,(RS-$ $-TU)+(KN-PQ)\,(ST-RU)$ $-(P^2+NQ)\,(R^2+SU)-$ $-(K^2+NQ)\,(T^2+SU)$	$-(N^2+KP)\,(RS-TU)+$ $+(S^2+RT)\,(PQ-KN)$
4	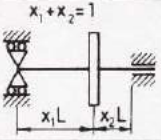	$(N_0P_0-K_0Q_0)\,(RU-ST)-$ $-2K_0N_0(S^2+RT)$	$(N_0P_0-K_0Q_0)\,(S^2+RT)$	$N_0P_0(R^2-S^2-T^2+U^2)+$ $+K_0Q_0(R^2+S^2-T^2-U^2)+$ $+2P_0Q_0(ST-RU)+2K_0N_0\times$ $(RS-TU)$	$-(N_0P_0-K_0Q_0)\,(RS-TU)$ $-2P_0Q_0\,(S^2+RT)$
5	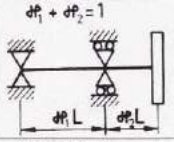	$-2\{K_1N_1(S_0T_0-R_0U_0)-$ $-(K_1-N_1)R_0T_0\}$	$K_1N_1\{(S_0-U_0)^2+R_0^2-T_0^2\}-$ $-(K_1-N_1)\,(S_0T_0-R_0U_0)$	$K_1N_1\{(S_0+U_0)^2+R_0^2-T_0^2\}+$ $+(K_1-N_1)\,(S_0T_0-R_0U_0)$	$2\{K_1N_1(R_0U_0+S_0T_0)+$ $+(K_1-N_1)S_0U_0\}$
6	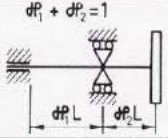	$2\{(N_0N-Q_0K)\,(T_0S-U_0R)+$ $+R_0T_0(N^2+KP)\}$	$-(N_0N-Q_0K)\,(S^2+RT)+$ $+(S_0R-R_0S)\,(N^2+KP)$	$-(N_0N-Q_0K)\,[U^2+2(T_0T-$ $-T_0^2)+RT-4T_0^2]+(N^2+$ $+KP)\,(S_0T_0-R_0U_0)$	$2\{S_0U_0(N^2+KP)-$ $-(N_0N-Q_0K)\,(U_0T+T_0S)\}$

Table 107.1

By definition

$$\Omega^2 = \frac{EI}{mL^3} \cdot \lambda^4$$

or

$$\Omega^2 = \frac{\lambda^4}{\frac{m}{M}} \cdot \frac{EI}{ML^3}$$

It may be observed that the ratio $\Lambda^{**} = \frac{m}{M} : \lambda^4$ corresponds to the value Λ used in the elementary theory neglecting the mass of the shaft. With the electronic computer Alwac III E in Gothenburg Λ^{**} was calculated in the cases shown in table 107.1. The numerical result is found in [4] and diagrams in Chapter 11 in this treatise. As will be seen in next chapter Λ^{**} is of great use even when calculating the first critical speed for a shaft with several discs.

In order to show the applicability of the tables [4] an example is of value.

Example 14. Calculate the first critical speed for the shaft in Example 9 considering the mass of the shaft and the gyroscopic action of the disc.

We have

$$m = 15{,}4 \text{ kg}$$
$$M = 308 \text{ kg}$$
$$\Theta^* = \frac{1}{4}\left(\frac{500}{1\,000}\right)^2 \cdot \frac{308}{15{,}4} = 1{,}25$$
$$\frac{m}{M} = 0{,}050$$
$$x_1 = 0{,}25$$

From the tables is obtained

$\Theta^* = 1{,}20$	$\lambda = 1{,}50$	$\frac{m}{M} = 0{,}044733$	$\frac{m}{M} : \lambda^4 = 0{,}008836$
	$\lambda = 1{,}60$	$\frac{m}{M} = 0{,}055333$	$\frac{m}{M} : \lambda^4 = 0{,}008443$
$\Theta^* = 1{,}30$	$\lambda = 1{,}50$	$\frac{m}{M} = 0{,}044004$	$\frac{m}{M} : \lambda^4 = 0{,}008692$
	$\lambda = 1{,}60$	$\frac{m}{M} = 0{,}054380$	$\frac{m}{M} : \lambda^4 = 0{,}008298$

Linear interpolation gives

$$\frac{m}{M} : \lambda^4 = \frac{1}{2} \; (0{,}496887 \cdot 0{,}008443 + 0{,}503113 \cdot 0{,}008836 +$$

$$+ 0{,}577872 \cdot 0{,}008298 + 0{,}422128 \cdot 0{,}008692) = 0{,}008553$$

The right value is $\frac{m}{M} : \lambda^4 = 0{,}008540$. The interpolated value has an error of only $1{,}5\ ‰$. The critical speed is $n = 1\,462$ r.p.m. Compare the result $n = 1\,512$ r.p.m. obtained in Example 9 when no account was taken of the mass of the shaft. The error in that case is $3{,}4\ \%$.

10. The Improved "Dunkerley" Formula

In the next chapter diagrams for calculating critical speeds are given for a single disc on a shaft. The use of these diagrams can be very much extended which will now be explained.

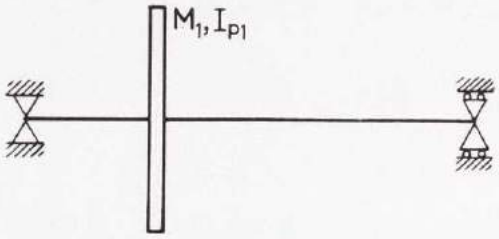

Fig. 110.1

From eq. 60.1 we get for the arrangement in fig. 110.1 with usual notations (see Chapter 7)

$$\begin{vmatrix} \xi_{F11}-\Lambda\mu_1^{-1} & \xi_{M11} \\ \zeta_{F11} & \zeta_{M11}-\Lambda r_1^{-1} \end{vmatrix} = 0$$

or

$$-\Lambda^2+\Lambda(\mu_1\xi_{F11}+r_1\zeta_{M11})-\mu_1 r_1(\xi_{F11}\zeta_{M11}-\zeta_{F11}\xi_{M11}) = 0 \ldots \quad 110.2$$

We now have taken the gyroscopic effect into account. Neglecting it we get

$$-\Lambda^2+\Lambda\mu_1\xi_{F11} = 0$$

and besides $\Lambda = 0$

$$\Lambda = \mu_1\xi_{F11}$$

Now denote $\Lambda_{11} = \mu_1 \xi_{F11}$ and $\Lambda_{12} = \nu_1 \zeta_{M11}$. Eq. 110.2 becomes with the aid of Maxwell's theorem

$$-1 + \frac{1}{\Lambda}(\Lambda_{11} + \Lambda_{12}) - \frac{\mu_1 \nu_1}{\Lambda^2}(\xi_{F11}\zeta_{M11} - \xi^2_{M11}) = 0$$

If

$$\frac{\mu_1 \nu_1}{\Lambda^2}(\xi_{F11}\zeta_{M11} - \xi^2_{M11}) \ll 1 \quad \ldots\ldots\ldots\ldots \quad 111.1$$

we get $\Lambda = \Lambda_1$ where

$$\Lambda_1 = \Lambda_{11} + \Lambda_{12}$$

The condition 111.1 means that the gyroscopic effect is small.

Now put another disc on the shaft. For this case eq. 59.1 is valid. From here

$$\Lambda^4 - \Lambda^3\{\mu_1 \xi_{F11} + \nu_1 \zeta_{M11} + \mu_2 \xi_{F22} + \nu_2 \zeta_{M22}\} + \Lambda^2\{\ldots\} + \ldots = 0$$

Denoting

$$\Lambda_1 = \Lambda_{11} + \Lambda_{12} = \mu_1 \xi_{F11} + \nu_1 \zeta_{M11}$$

$$\Lambda_2 = \Lambda_{21} + \Lambda_{22} = \mu_2 \xi_{F22} + \nu_2 \zeta_{M22}$$

we get

$$1 - \frac{1}{\Lambda}(\Lambda_1 + \Lambda_2) + \frac{1}{\Lambda^2}(\ldots) + \ldots = 0$$

If the sum of the last three terms is much less than unity we get

$$\Lambda = \Lambda_1 + \Lambda_2$$

The generalization is evident. If the shaft is equipped with s discs the first critical speed approximately is

$$\Lambda = \Lambda_1 + \Lambda_2 + \ldots + \Lambda_s \quad \ldots\ldots\ldots\ldots \quad 111.2$$

Because of the fact that Λ is inversely proportional to n^2 we instead of this may write

$$\frac{1}{n^2} = \frac{1}{n_1^2} + \frac{1}{n_2^2} + \ldots + \frac{1}{n_s^2} \quad \ldots\ldots\ldots\ldots \quad 112.1$$

Neglecting the gyroscopic effect we get

$$\Lambda = \Lambda_{11} + \Lambda_{21} + \ldots\ldots + \Lambda_{s1} \quad \ldots\ldots\ldots\ldots \quad 112.2$$

The differential equation for the transversal oscillations of the shaft is

$$\left.\begin{aligned} y_1 &= [-M_1\ddot{y}_1]\left[\xi_{F11}\cdot\frac{L^3}{kEI}\right] + \left[-\frac{I_p}{2}\cdot\ddot{\varphi}_1\right]\left[-\xi_{M11}\cdot\frac{L^2}{kEI}\right] \\ \varphi_1 &= [-M_1\ddot{y}_1]\left[\zeta_{F11}\cdot\frac{L^2}{kEI}\right] + \left[-\frac{I_p}{2}\cdot\ddot{\varphi}_1\right]\left[-\zeta_{M11}\cdot\frac{L}{kEI}\right] \end{aligned}\right\} \quad 112.3$$

Putting

$$y_1 = y_{10}\sin\Omega t$$
$$\varphi_1 = \varphi_{10}\sin\Omega t$$

we obtain after some manipulations

$$\left.\begin{aligned} (\Lambda - \mu_1\xi_{F11})\, y_{10} + \nu_1\xi_{M11}\ (L\varphi_{10}) &= 0 \\ -\mu\zeta_{F11}y_{10} + (\Lambda + \nu_1\zeta_{M11})\ (L\varphi_{10}) &= 0 \end{aligned}\right\}$$

and from here

$$-\Lambda^2 + \Lambda(\mu_1\xi_{F11} - \nu_1\zeta_{M11}) + \mu_1\nu_1(\xi_{F11}\zeta_{M11} - \zeta_{F11}\xi_{M11}) = 0$$

This equation is identical with eq. 110.2 if we change ν_1 to $-\nu_1$. Very often the critical frequency is determined practically from a test where a vibration exciter is used. However, the frequency determined in this way differs from the frequency of the critical speed due to different actions of the moments of inertia in the two cases. The test will always give two low values independent of bearing arrangements. See also Example 9.

Neglecting the influence of moments of inertia the first of the eqs. 112.3 may be written

$$y_{10} = M_1 y_{10} \Omega^2 \alpha_{11}$$

and

$$M_1 \alpha_{11} = \frac{1}{\Omega_{11}^2}$$

The static deflection under the load M_1 in fig. 110.1 is

$$(\delta_1)_{\text{stat}} = M_1 g \alpha_{11}$$

or from above

$$(\delta_1)_{\text{stat}} = \frac{g}{\Omega_{11}^2}$$

and eq. 112.2 can be written

$$\frac{1}{\Omega^2} = \frac{(\delta_1)_{\text{stat}}}{g} + \frac{(\delta_2)_{\text{stat}}}{g} + \dots$$

or

$$\Omega^2 = \frac{g}{\Sigma(\delta_i)_{\text{stat}}}$$

Dunkerley's formula is usually presented in this form. Observe that it is equivalent to eq. 112.2. It may be emphasized that the formula is approximate even if the gyroscopic effect and the mass of the shaft may be neglected except for a shaft with one mass.

In eq. 111.2 the gyroscopic effect is considered to the same degree. This equation may be called the extended Dunkerley formula and was proposed by Hahn [6].

A third possibility is to use the formula

$$\Lambda^* = \Lambda_1^* + \Lambda_2^* + \dots + \Lambda_s^* \quad \dots\dots\dots\dots \quad 113.1$$

where Λ_i^* are the greatest roots of the equation 110.2 and equations analogous to this.

It is easily shown that $\Lambda_i < \Lambda_i^* < \Lambda_{i1}$. Concluding, we have got three kinds of approximate formulas, viz. the ordinary one (eq. 112.2), the extended one (eq. 111.2) and the improved one (eq. 113.1). They are

compared in the example below. We want to compute the first critical speed approximately for the shaft on page 69. We get

$\Lambda = 9+18 = 27$ according to the usual Dunkerley formula
$\Lambda = 9-7+18-14 = 6$ „ „ „ extended „ „
$\Lambda = 3 \cdot 6{,}2915 = 18{,}8745$ „ „ „ improved „ „

The correct value is $\Lambda = 14{,}535$. It may be observed that if $\nu_i = 0$ the three formulas coincide. In spite of extraordinary circumstances the improved formula only gives 14 % higher critical speed than the exact calculation. The other formulas come completely wrong.

At last a fourth possibility is proposed. In order to take the mass of the shaft into some account we have from Chapter 9

$$\Omega^2 = \frac{1}{\frac{m}{M\lambda^4}} \cdot \frac{EI}{ML^3}$$

and from the elementary theory (Chapter 5)

$$\Omega^2 = \frac{1}{\Lambda_0} \cdot \frac{EI}{ML^3}$$

Denoting $\Lambda^{**} = \frac{m}{M\lambda^4}$ the "new Dunkerley formula" valid for s discs can be expressed as

$$\Lambda^{**} = \sum_{i=1}^{s} \mu_i \varkappa_i^3 \cdot \frac{\Lambda_i^{**}}{\Lambda_{oi}} \cdot \Lambda_{oi} \quad \ldots\ldots\ldots\ldots \quad 114.1$$

where

$$\mu_i = \frac{M_i}{M_{\text{ref}}}$$

$$\varkappa_i = \frac{L_i}{L}$$

$$\Omega^2 = \frac{1}{\Lambda^{**}} \cdot \frac{EI}{M_{\text{ref}} L^3}$$

Observe that $\varkappa_i = 1$ if no part of the shaft is a cantilever. The use of eq. 114.1 is illustrated by an example.

Example 15. Calculate the lowest critical speed for the arrangement in Example 11 with the aid of the "new Dunkerley formula". Compare the result with those obtained by ordinary formulas.

We have

$$\frac{m}{M} = \frac{\pi}{4} \cdot 66^2 \cdot 10^{-6} \cdot 600 \cdot 10^{-3} \cdot 7\,850 \text{ kg} = 16{,}11 \text{ kg}$$

$$\left(\frac{m}{M}\right)_1 = \frac{200}{600} \cdot \frac{16{,}11}{200} = 0{,}02685$$

$$\Theta_1^* = \frac{1}{4}\left(\frac{708}{400}\right)^2 \cdot \frac{1}{0{,}02685} = 29{,}17$$

$$\left(\frac{m}{M}\right)_2 = \frac{16{,}11}{400} = 0{,}04028$$

$$\Theta_2^* = \frac{1}{4}\left(\frac{1\,008}{1\,200}\right)^2 \cdot \frac{1}{0{,}04028} = 4{,}379$$

and from here, with the aid of an electronic computer, if $M_{\text{ref}} = M_2 = 400$ kg,

$$\Lambda^{**} = \frac{1}{2} \cdot \frac{1}{27} \cdot 0{,}3503 \cdot \frac{1}{3} + 1 \cdot 1 \cdot 0{,}6778 \cdot \frac{1}{3}$$

Instead of calculating the Λ_i^{**}-values they may be read from the diagram on page 118.

$$n^{**} = 19{,}99 \sqrt{\frac{EI}{M_{\text{ref}} L^3}} = 915 \text{ r.p.m.}$$

Formula 113.1 gives

$$\Lambda^* = \left(0{,}3464 \cdot \frac{1}{2} + 36{,}110 \cdot 1\right) \cdot \frac{1}{162}$$

and

$$n^* = 20{,}18 \sqrt{\frac{EI}{M_{\text{ref}} L^3}} = 924 \text{ r.p.m.}$$

The usual Dunkerley formula gives

$$\Lambda_0 = \left(1 \cdot \frac{1}{2} + 54 \cdot 1\right) \cdot \frac{1}{162}$$

and

$$n_0 = 16{,}46 \sqrt{\frac{EI}{M_{\text{ref}} L^3}} = 753 \text{ r.p.m.}$$

The extended Dunkerley formula fails as

$$\Lambda_{oe} = 1 \cdot \frac{1}{2} - \frac{3 \cdot 54}{23} + 54 \cdot 1 - \frac{3 \cdot 162}{5{,}67} < 0$$

The exact value (with the mass of the shaft neglected) is from page 74

$$n = 20{,}54 \sqrt{\frac{EI}{M_{\text{ref}} L^3}} = 940 \text{ r.p.m.}$$

11. Diagrams for Calculating the First Critical Speed

In this chapter diagrams for calculating the first critical speed for the bearing arrangements shown in fig. 107.1 are presented.

For the "exact" theory we have

$$\Omega^2 = \frac{1}{\Lambda^{**}} \cdot \frac{EI}{ML^3}$$

where $\Lambda^{**} = \frac{m}{M\lambda^4}$ and for the elementary theory we have

$$\Omega^2 = \frac{1}{\Lambda_0} \cdot \frac{EI}{ML^3}$$

In the diagrams the ratio $\frac{\Lambda^{**}}{\Lambda_0}$ is drawn as a function of $\frac{m}{M}$. Semi-inverse diagrams are used [7] for covering all the range of the variables. The value of Λ_0 is given at the top of every diagram.

Each diagram is valid for a certain x_1 or $\varkappa_1$ (see fig. 107.1) and it is calculated for $x_1\ (\varkappa_1) = 0{,}05,\ 0{,}10,\ 0{,}15 \ldots\ldots 0{,}95$. The parameter Θ^* is varied within the interval $-\infty \leq \Theta^* \leq +\infty$.

It may be observed that the diagrams are valid for all rotational circumstances because of

$$\Theta^* = \left(\frac{\omega}{\Omega} - \frac{1}{2}\right) \cdot \frac{I_p}{mL^2}$$

At the ordinary critical speed $\Theta^* = \frac{1}{2} \cdot \frac{I_p}{mL^2}$.

Further it was shown in Chapter 10 that the diagrams in connection with the "new Dunkerley formula" (eq. 114.1) constitute a tool in calculating the first critical speed.

Each diagram is equipped with a number of order indicating the bearing arrangement. These numbers are shown in fig. 107.1.

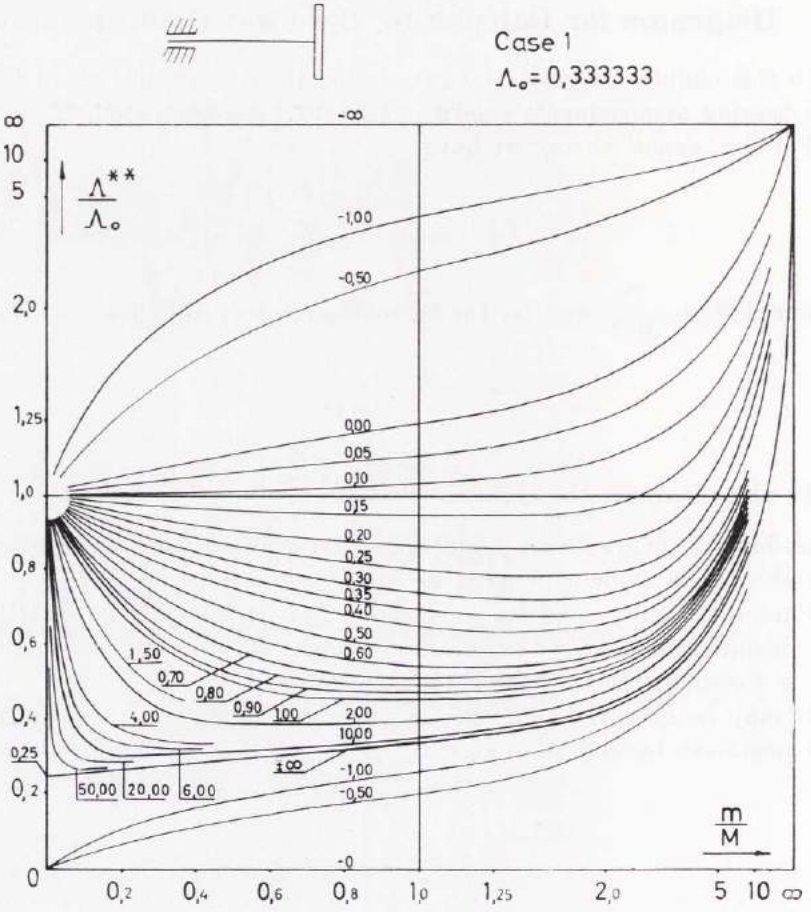
Case 1
$\Lambda_o = 0{,}333333$
$\frac{\Lambda^{**}}{\Lambda_o}$
$\frac{m}{M}$
-∞
-1,00
-0,50
0,00
0,05
0,10
0,15
0,20
0,25
0,30
0,35
0,40
0,50
0,60
0,70
0,80
0,90
1,00
1,50
2,00
4,00
6,00
10,00
20,00
50,00
±∞
-1,00
-0,50
-0
∞
10
5
2,0
1,25
1,0
0,8
0,6
0,4
0,25
0,2
0
0,2
0,4
0,6
0,8
1,0
1,25
2,0
5
10
∞

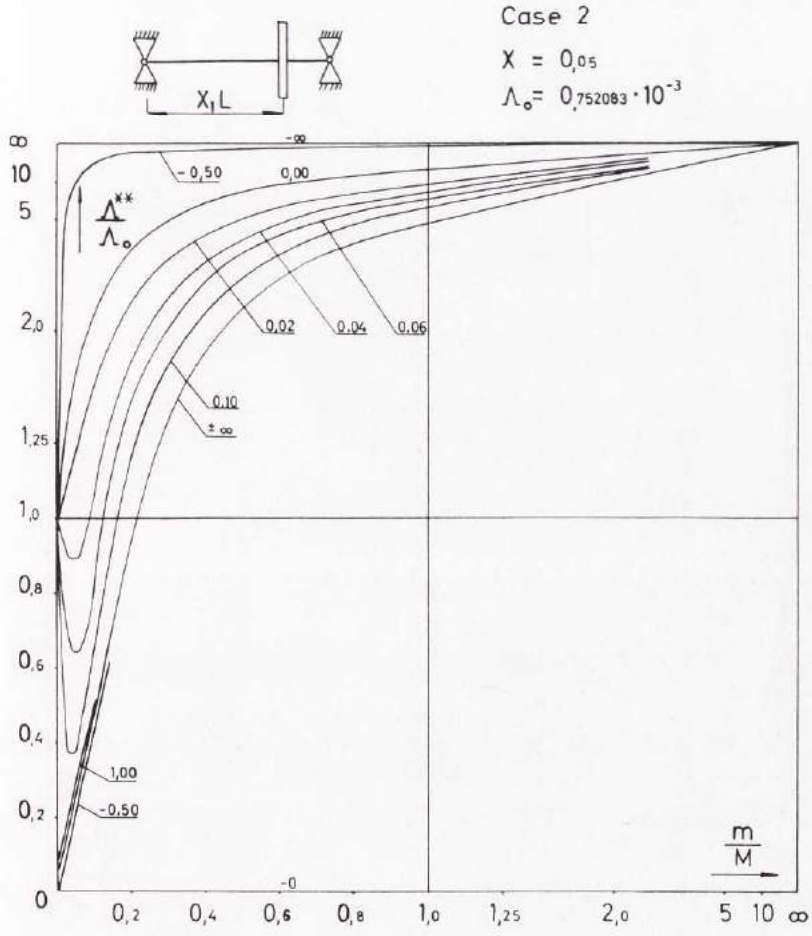
Case 2
X = 0,05
Λ₀ = 0,752083 · 10⁻³
X L
-∞
∞
10
5
2,0
1,25
1,0
0,8
0,6
0,4
0,2
0
-0,50
0,00
0,02
0,04
0,06
0,10
± ∞
1,00
-0,50
-0
0,2
0,4
0,6
0,8
1,0
1,25
2,0
5
10
∞
m/M

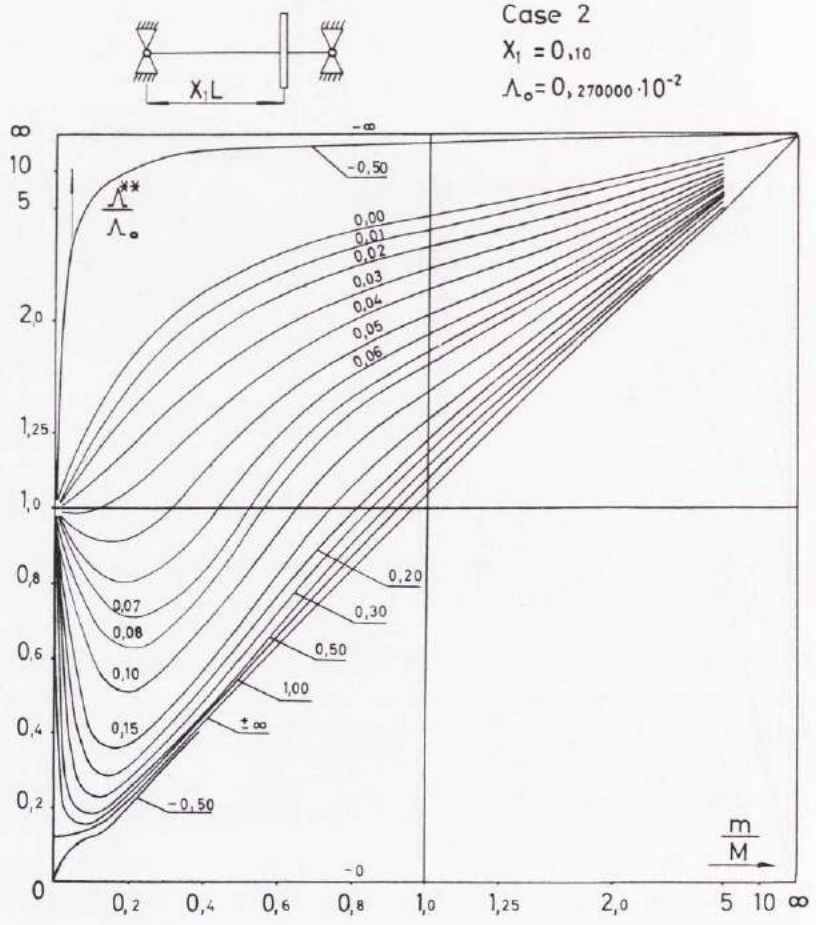
Case 2
$X_1 = 0,10$
$\Lambda_o = 0,270000 \cdot 10^{-2}$
$X_1 L$
$\frac{\Lambda^{**}}{\Lambda_o}$
$\frac{m}{M}$
-∞
-0,50
0,00
0,01
0,02
0,03
0,04
0,05
0,06
0,20
0,30
0,50
1,00
±∞
0,07
0,08
0,10
0,15
-0,50
-0
∞
10
5
2,0
1,25
1,0
0,8
0,6
0,4
0,2
0
0,2
0,4
0,6
0,8
1,0
1,25
2,0
5
10
∞

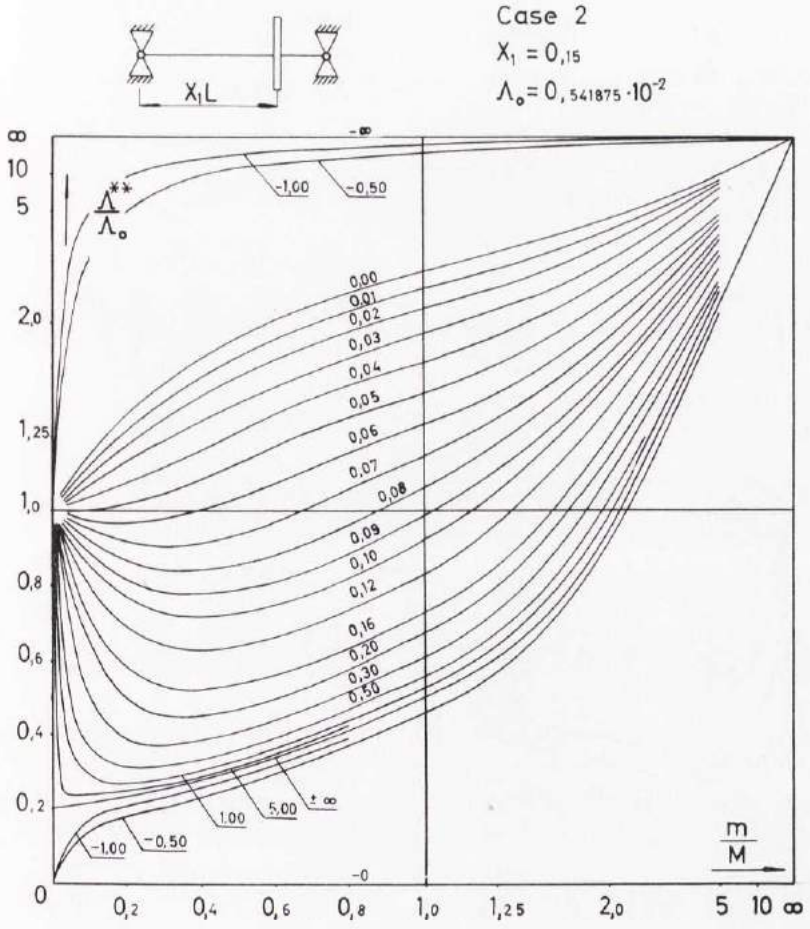
Case 2
$X_1 = 0,15$
$\Lambda_o = 0,541875 \cdot 10^{-2}$
$X_1 L$
Λ^{**}/Λ_o
-1,00
-0,50
0,00
0,01
0,02
0,03
0,04
0,05
0,06
0,07
0,08
0,09
0,10
0,12
0,16
0,20
0,30
0,50
1,00
5,00
± ∞
m/M
∞
10
5
2,0
1,25
1,0
0,8
0,6
0,4
0,2
0
0,2
0,4
0,6
0,8
1,0
1,25
2,0
5
10
∞

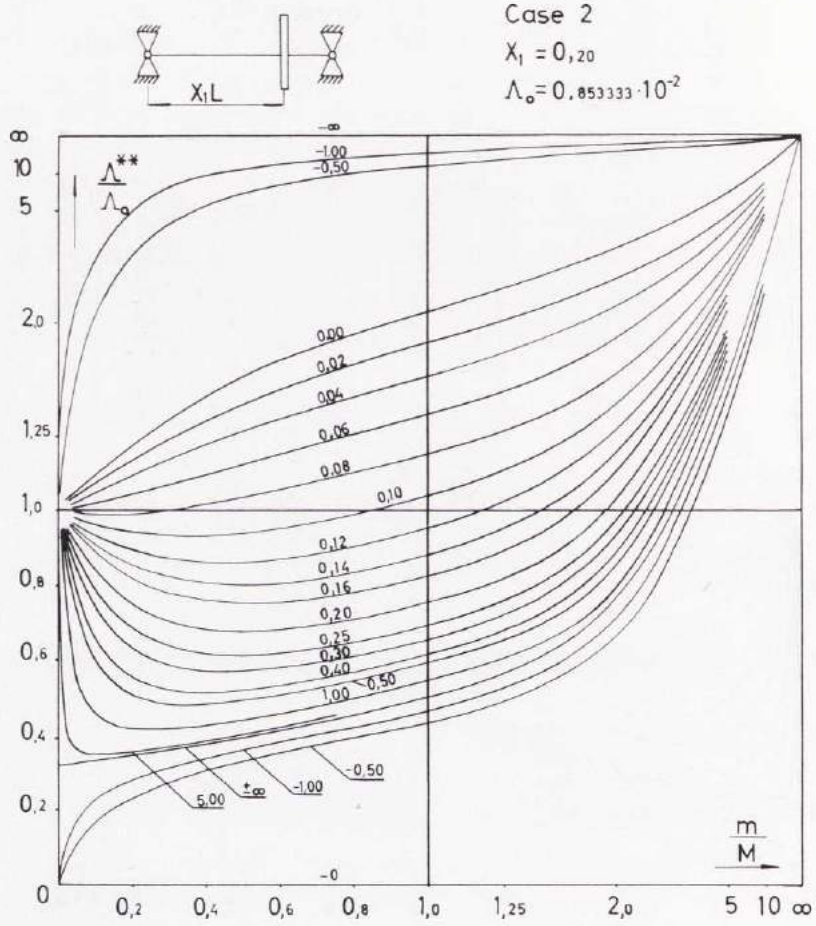
Case 2
$X_1 = 0,20$
$\Lambda_o = 0,853333 \cdot 10^{-2}$
$X_1 L$
$\frac{\Lambda^{**}}{\Lambda_o}$
$\frac{m}{M}$
-∞
-1,00
-0,50
0,00
0,02
0,04
0,06
0,08
0,10
0,12
0,14
0,16
0,20
0,25
0,30
0,40
1,00
-0,50
5,00
±∞
-1,00
-0,50
-0
∞
10
5
2,0
1,25
1,0
0,8
0,6
0,4
0,2
0
0,2
0,4
0,6
0,8
1,0
1,25
2,0
5
10
∞

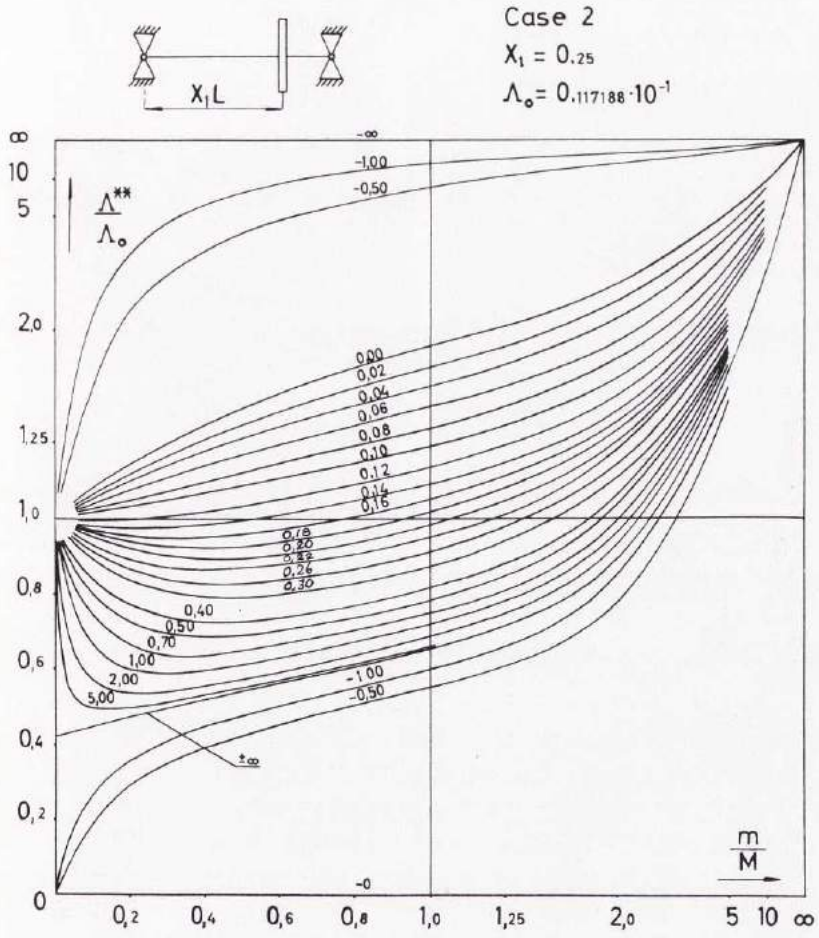
Case 2
$X_1 = 0.25$
$\Lambda_o = 0.117188 \cdot 10^{-1}$
$X_1 L$
$\frac{\Lambda^{**}}{\Lambda_o}$
$\frac{m}{M}$
$\pm\infty$
-∞
-1,00
-0,50
0,00
0,02
0,04
0,06
0,08
0,10
0,12
0,14
0,16
0,18
0,20
0,22
0,24
0,30
0,40
0,50
0,70
1,00
2,00
5,00
-1,00
-0,50
-0
∞
10
5
2,0
1,25
1,0
0,8
0,6
0,4
0,2
0
0,2
0,4
0,6
0,8
1,0
1,25
2,0
5
10
∞

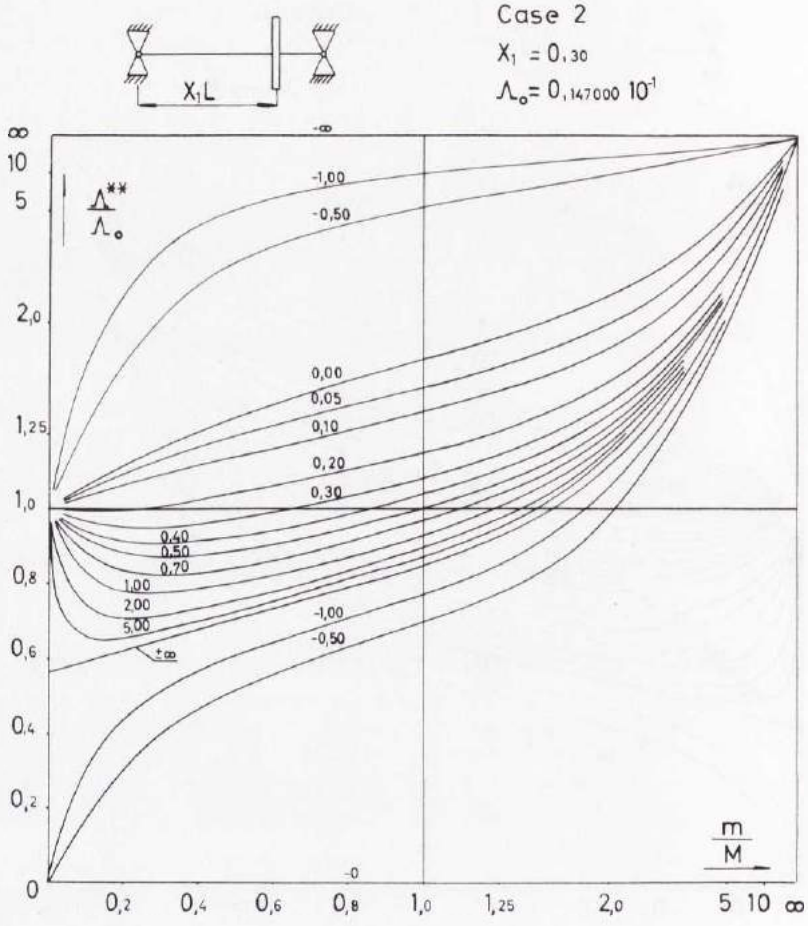
Case 2
$X_1 = 0,30$
$\Lambda_o = 0,147000\ 10^{-1}$
$X_1 L$
$\frac{\Lambda^{**}}{\Lambda_o}$
-∞
-1,00
-0,50
0,00
0,05
0,10
0,20
0,30
0,40
0,50
0,70
1,00
2,00
5,00
±∞
-1,00
-0,50
-0
∞
10
5
2,0
1,25
1,0
0,8
0,6
0,4
0,2
0
0,2
0,4
0,6
0,8
1,0
1,25
2,0
5
10
∞
$\frac{m}{M}$

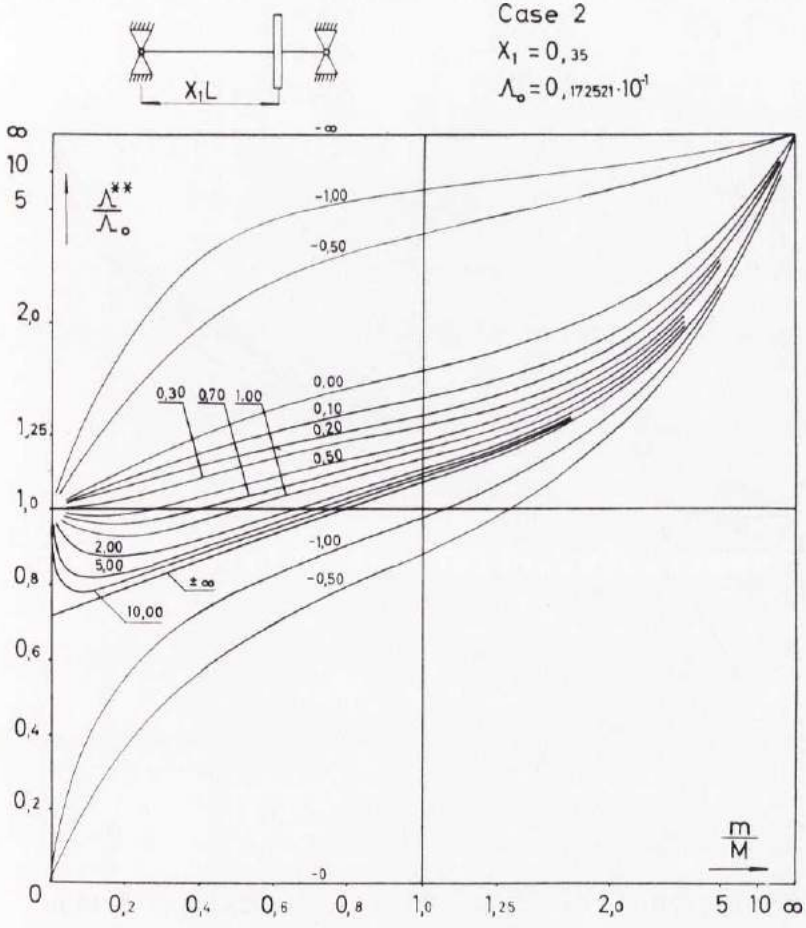
Case 2
$X_1 = 0,35$
$\Lambda_0 = 0,172521 \cdot 10^{-1}$
$X_1 L$
$\frac{\Lambda^{**}}{\Lambda_0}$
$\frac{m}{M}$
-∞
-1,00
-0,50
0,00
0,10
0,20
0,50
0,30
0,70
1,00
2,00
5,00
10,00
±∞
-1,00
-0,50
-0
∞
10
5
2,0
1,25
1,0
0,8
0,6
0,4
0,2
0
0,2
0,4
0,6
0,8
1,0
1,25
2,0
5
10
∞

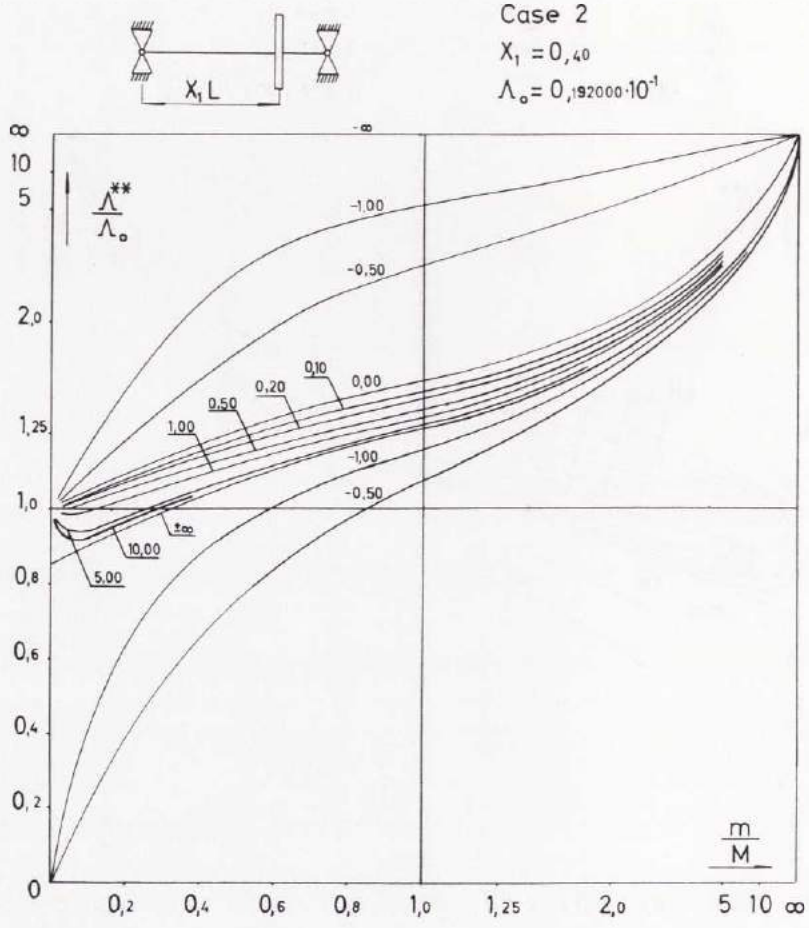
Case 2
X1 = 0,40
Λo = 0,192000·10-1
X1 L
Λ**/Λo
m/M
-∞
-1,00
-0,50
0,10
0,00
0,20
0,50
1,00
-1,00
-0,50
±∞
10,00
5,00
∞
10
5
2,0
1,25
1,0
0,8
0,6
0,4
0,2
0
0,2
0,4
0,6
0,8
1,0
1,25
2,0
5
10
∞

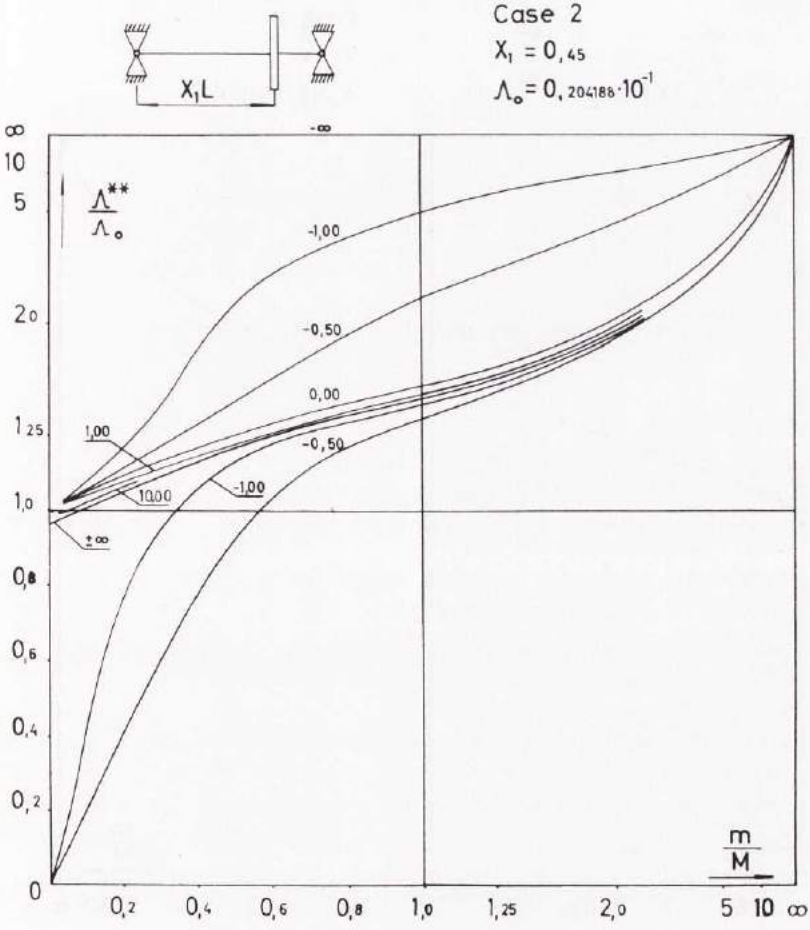
Case 2
$X_1 = 0,45$
$\Lambda_o = 0,204188 \cdot 10^{-1}$
$X_1 L$
$\frac{\Lambda^{**}}{\Lambda_o}$
-∞
-1,00
-0,50
0,00
-0,50
-1,00
1,00
1000
±∞
$\frac{m}{M}$
∞ 10 5 2,0 1,25 1,0 0,8 0,6 0,4 0,2 0
0,2 0,4 0,6 0,8 1,0 1,25 2,0 5 10 ∞

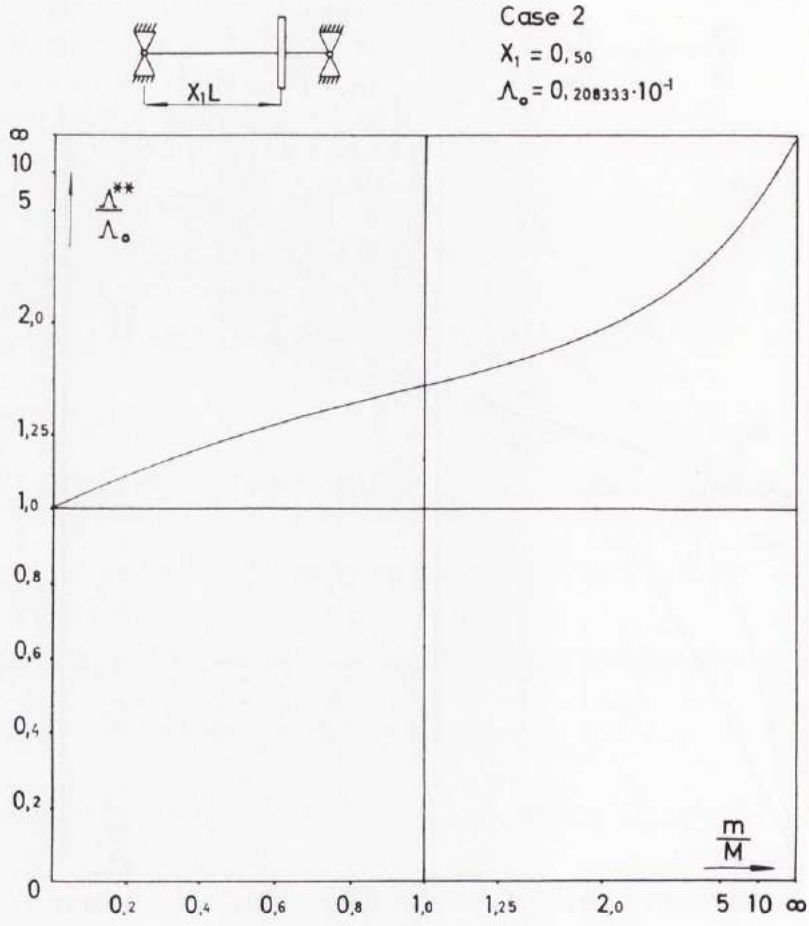
Case 2
$X_1 = 0,50$
$\Lambda_0 = 0,208333 \cdot 10^{-1}$
$X_1 L$
$\frac{\Delta^{**}}{\Lambda_0}$
$\frac{m}{M}$
∞
10
5
2,0
1,25
1,0
0,8
0,6
0,4
0,2
0
0,2
0,4
0,6
0,8
1,0
1,25
2,0
5
10
∞

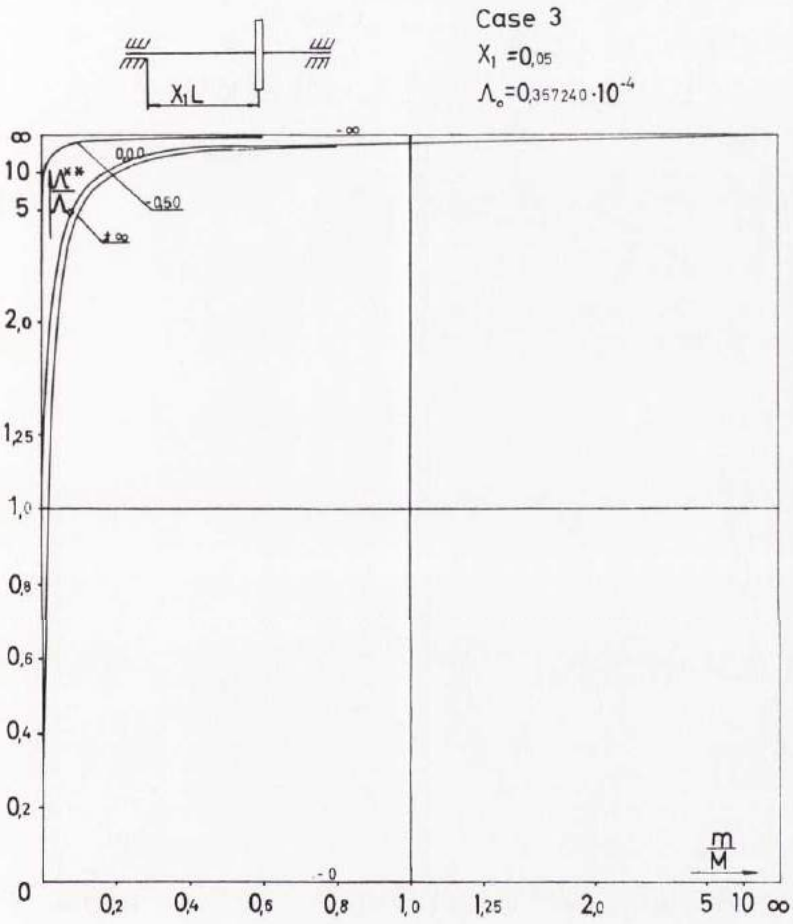
Case 3
X1 =0,05
Λe=0,357240·10⁻⁴
X1 L
∞
10
5
2,0
1,25
1,0
0,8
0,6
0,4
0,2
0
0,2
0,4
0,6
0,8
1,0
1,25
2,0
5
10
∞
- ∞
- 0
000
050
m/M

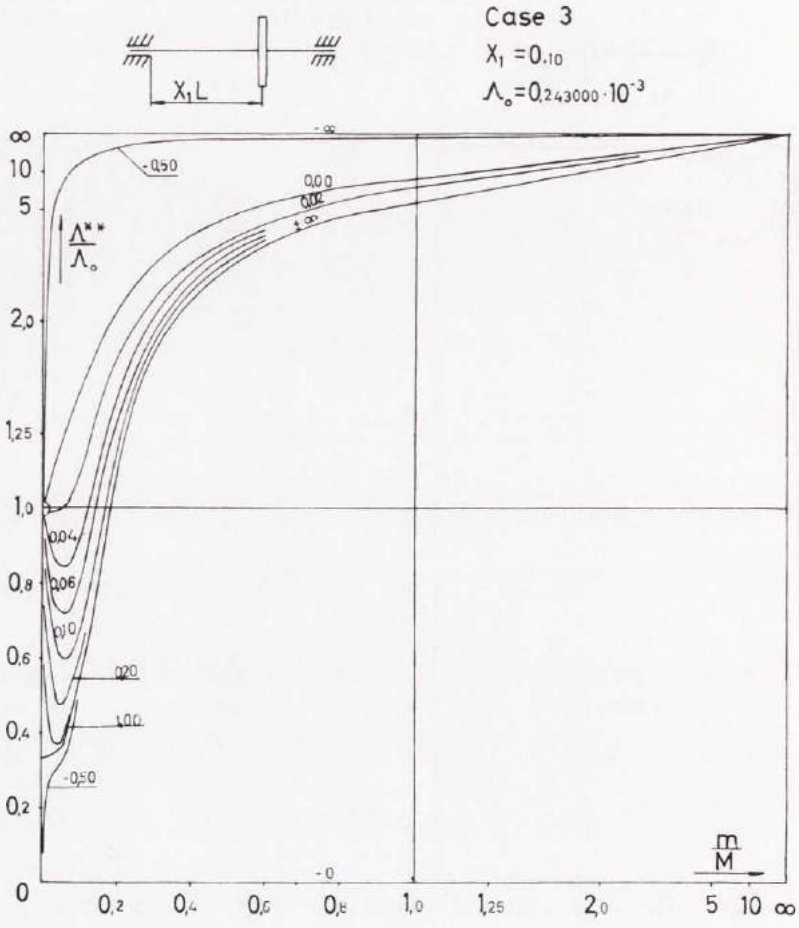
Case 3
X1 = 0.10
Λ0 = 0.243000 · 10⁻³
X1 L
Λ**/Λ0
-0.50
0.00
0.02
+∞
0.04
0.06
0.10
0.20
1.00
-0.50
-0
m/M
∞
10
5
2.0
1.25
1.0
0.8
0.6
0.4
0.2
0
0.2
0.4
0.6
0.8
1.0
1.25
2.0
5
10
∞

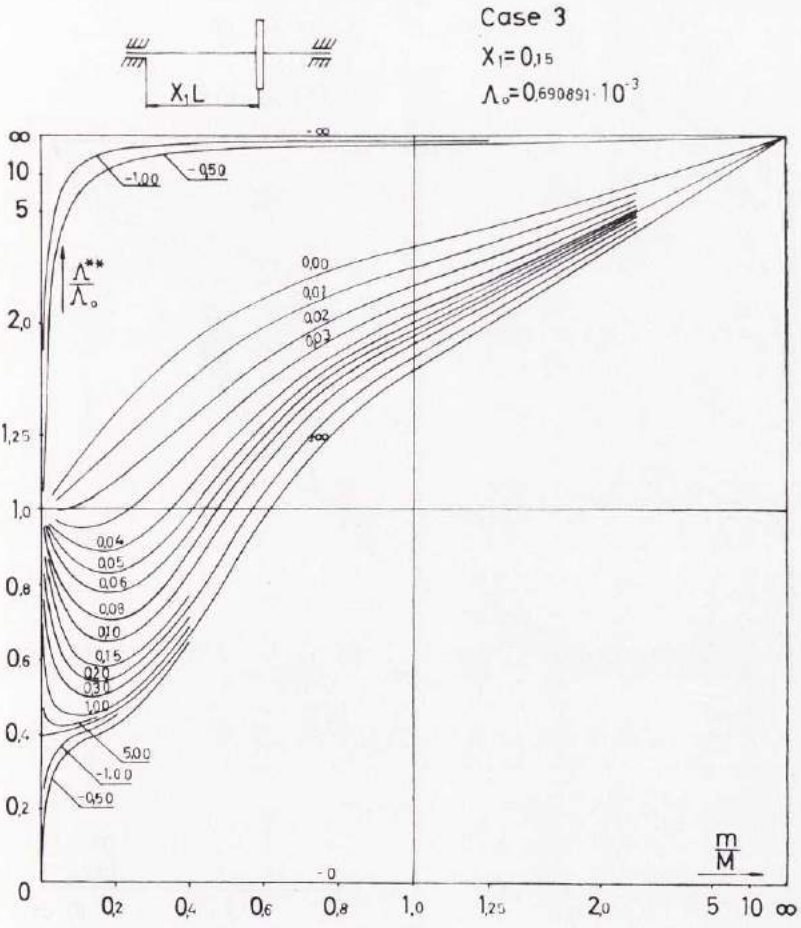
Case 3
X1= 0,15
Λ0= 0,690891 · 10-3
X1 L
∞
10
5
2,0
1,25
1,0
0,8
0,6
0,4
0,2
0
Λ**/Λ0
-∞
-1,00
-0,50
0,00
0,01
0,02
0,03
+∞
0,04
0,05
0,06
0,08
0,10
0,15
0,20
0,30
1,00
5,00
-1,00
-0,50
-0
m/M
0,2
0,4
0,6
0,8
1,0
1,25
2,0
5
10
∞

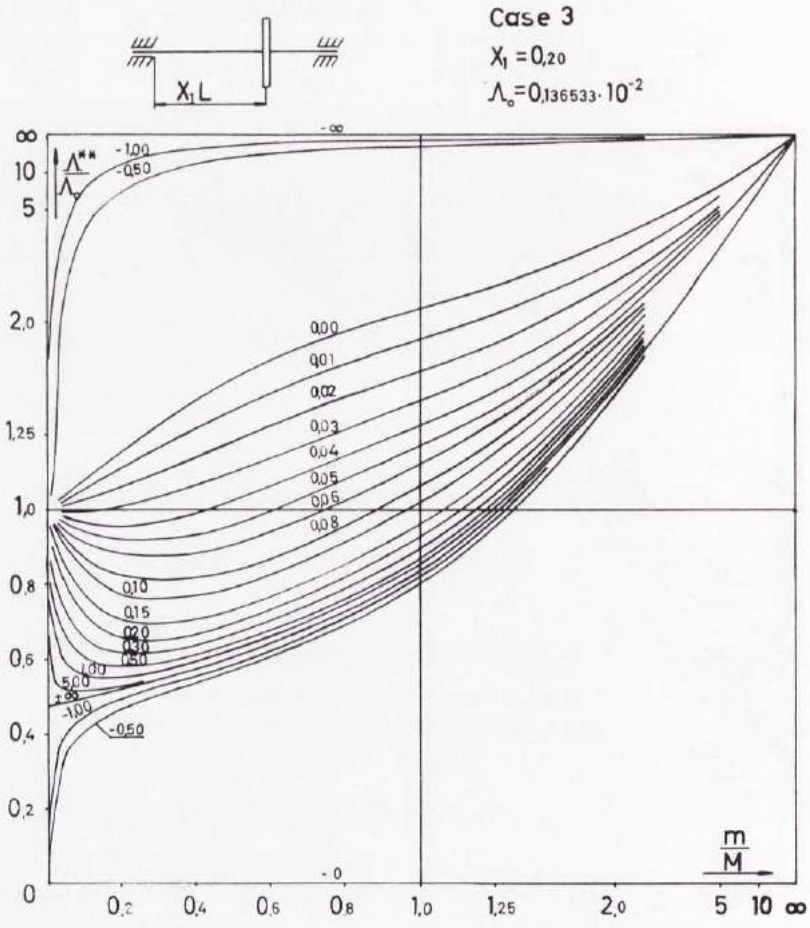
Case 3
$X_1 = 0{,}20$
$\Lambda_o = 0{,}136533 \cdot 10^{-2}$
$X_1 L$
$\frac{\Lambda^{**}}{\Lambda_o}$
$\frac{m}{M}$
-∞
-1,00
-0,50
0,00
0,01
0,02
0,03
0,04
0,05
0,06
0,08
0,10
0,15
0,20
0,25
0,30
0,50
1,00
5,00
+∞
-1,00
-0,50
-0
∞
10
5
2,0
1,25
1,0
0,8
0,6
0,4
0,2
0
0,2
0,4
0,6
0,8
1,0
1,25
2,0
5
10
∞

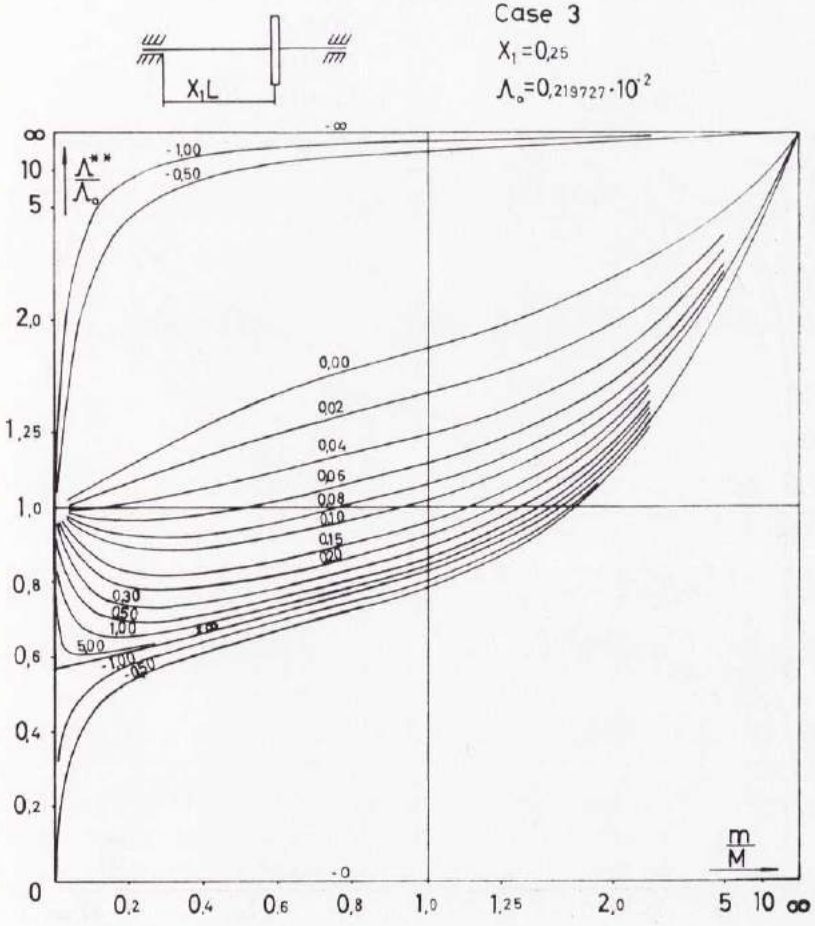
Case 3
$X_1 = 0{,}25$
$\Lambda_o = 0{,}219727 \cdot 10^{-2}$
$X_1 L$
$\frac{\Lambda^{**}}{\Lambda_o}$
$\frac{m}{M}$
-∞
-1,00
-0,50
0,00
0,02
0,04
0,06
0,08
0,10
0,15
0,20
0,30
0,50
1,00
5,00
∞
-1,00
-0,50
-0
∞
10
5
2,0
1,25
1,0
0,8
0,6
0,4
0,2
0
0,2
0,4
0,6
0,8
1,0
1,25
2,0
5
10
∞

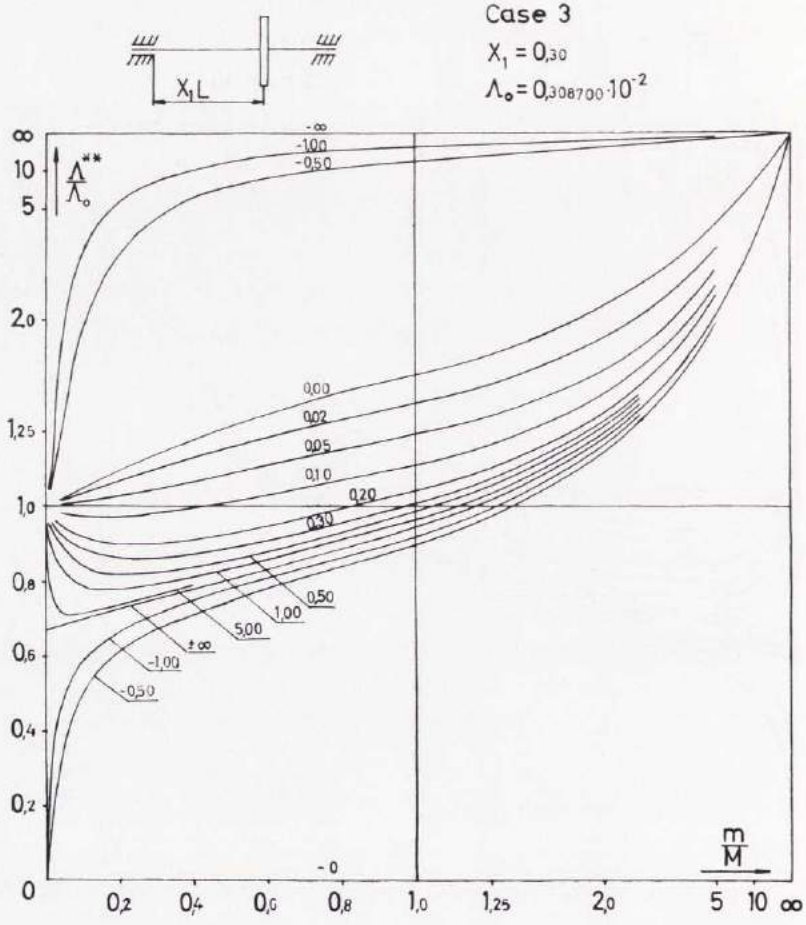
Case 3
X1 = 0,30
Λo = 0,308700·10⁻²
X1L
Λ**/Λo
m/M
-∞
-1,00
-0,50
0,00
0,02
0,05
0,10
0,20
0,30
0,50
1,00
5,00
±∞
-1,00
-0,50
-0
∞
10
5
2,0
1,25
1,0
0,8
0,6
0,4
0,2
0
0,2
0,4
0,6
0,8
1,0
1,25
2,0
5
10
∞

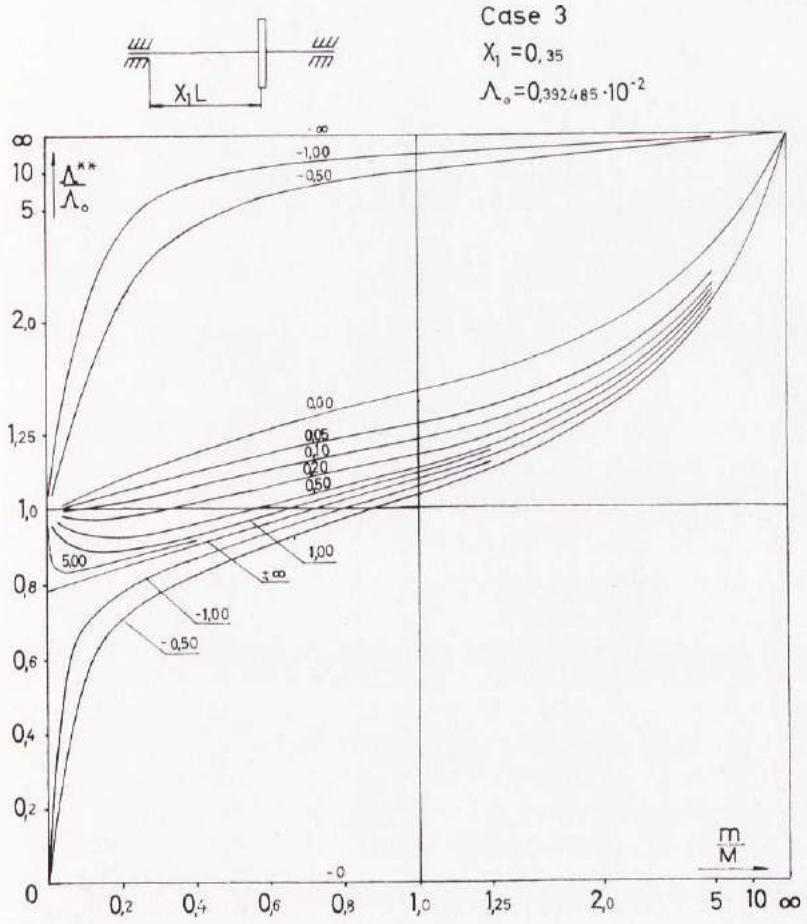
Case 3
$X_1 = 0,35$
$\Lambda_o = 0,392485 \cdot 10^{-2}$
$X_1 L$
$\frac{\Lambda^{**}}{\Lambda_o}$
$\frac{m}{M}$
-1,00
-0,50
0,00
0,05
0,10
0,20
0,50
1,00
5,00
$\pm\infty$
-0
∞
10
5
2,0
1,25
1,0
0,8
0,6
0,4
0,2
0
0,2
0,4
0,6
0,8
1,0
1,25
2,0
5
10
∞

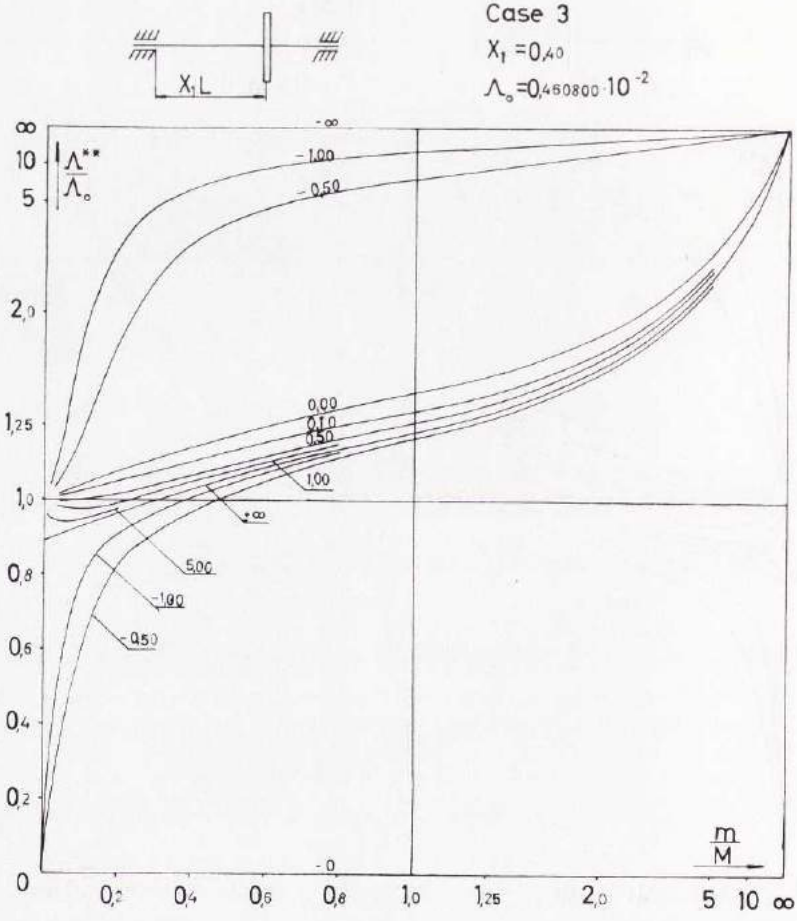
Case 3
X1 =0,40
Λo=0,460800·10-2
X1 L
Λ**/Λo
-∞
-1,00
-0,50
0,00
0,10
0,50
1,00
+∞
5,00
-1,00
-0,50
-0
m/M
∞
10
5
2,0
1,25
1,0
0,8
0,6
0,4
0,2
0
0,2
0,4
0,6
0,8
1,0
1,25
2,0
5
10
∞

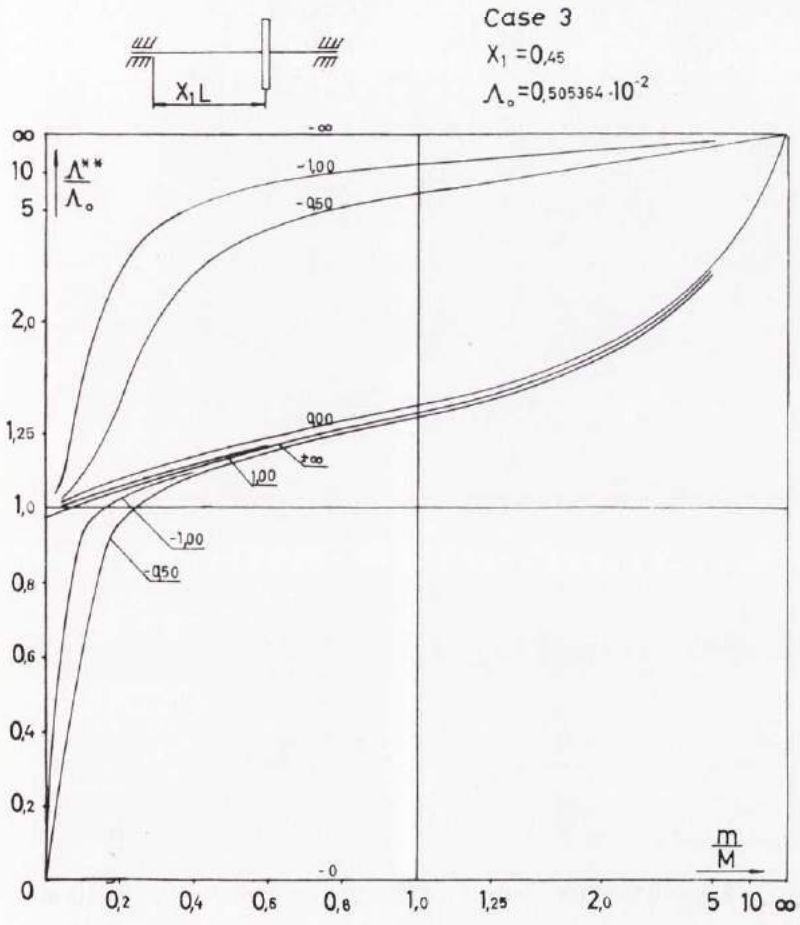
Case 3
X1 = 0,45
Λ0 = 0,505364 · 10⁻²
X1 L
Λ** / Λ0
-∞
-1,00
-0,50
0,00
+∞
1,00
-1,00
-0,50
-0
m / M
∞ 10 5 2,0 1,25 1,0 0,8 0,6 0,4 0,2 0
0,2 0,4 0,6 0,8 1,0 1,25 2,0 5 10 ∞

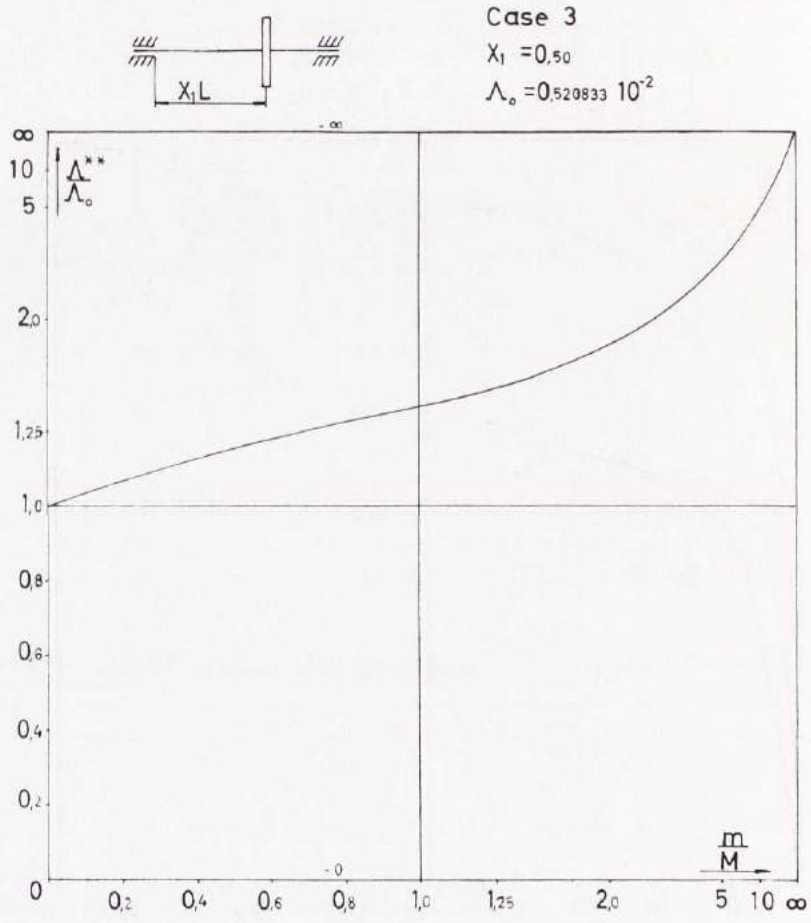
Case 3
$X_1 = 0{,}50$
$\Lambda_o = 0{,}520833\ 10^{-2}$
$X_1 L$
$\frac{\Lambda^{**}}{\Lambda_o}$
∞
10
5
2,0
1,25
1,0
0,8
0,6
0,4
0,2
0
0,2
0,4
0,6
0,8
1,0
1,25
2,0
5
10
∞
$\frac{m}{M}$

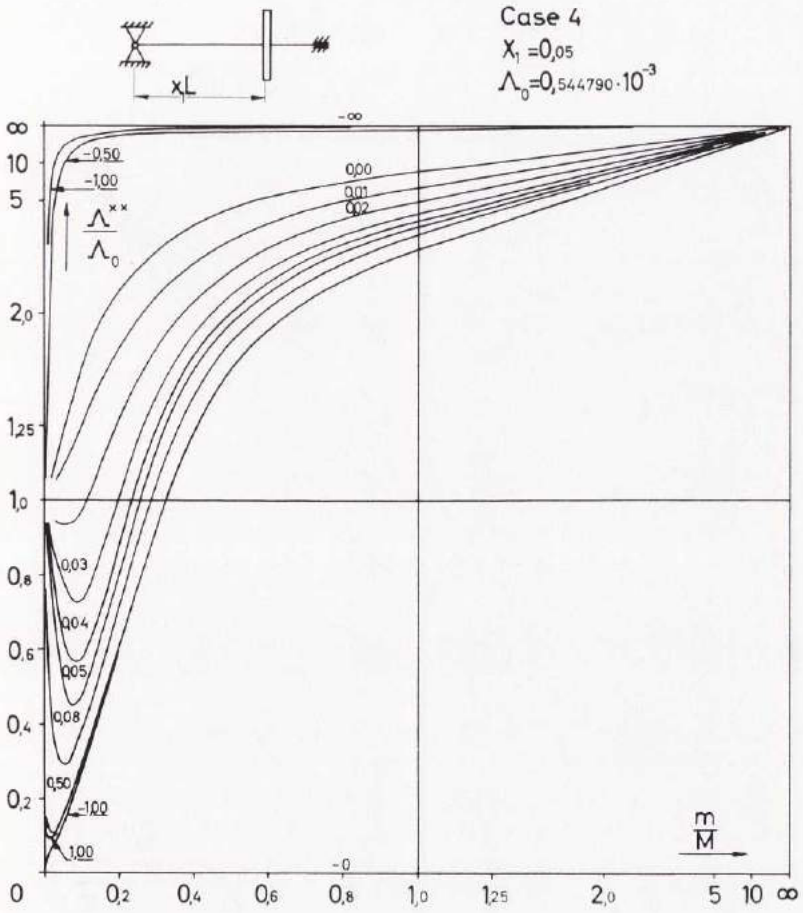
Case 4
$X_1 = 0{,}05$
$\Lambda_0 = 0{,}544790 \cdot 10^{-3}$
x L
$-\infty$
∞
10
5
2,0
1,25
1,0
0,8
0,6
0,4
0,2
0
-0,50
-1,00
0,00
0,01
0,02
$\frac{\Lambda^{xx}}{\Lambda_0}$
0,03
0,04
0,05
0,08
0,50
-1,00
1,00
-0
$\frac{m}{M}$
0,2
0,4
0,6
0,8
1,0
1,25
2,0
5
10
∞

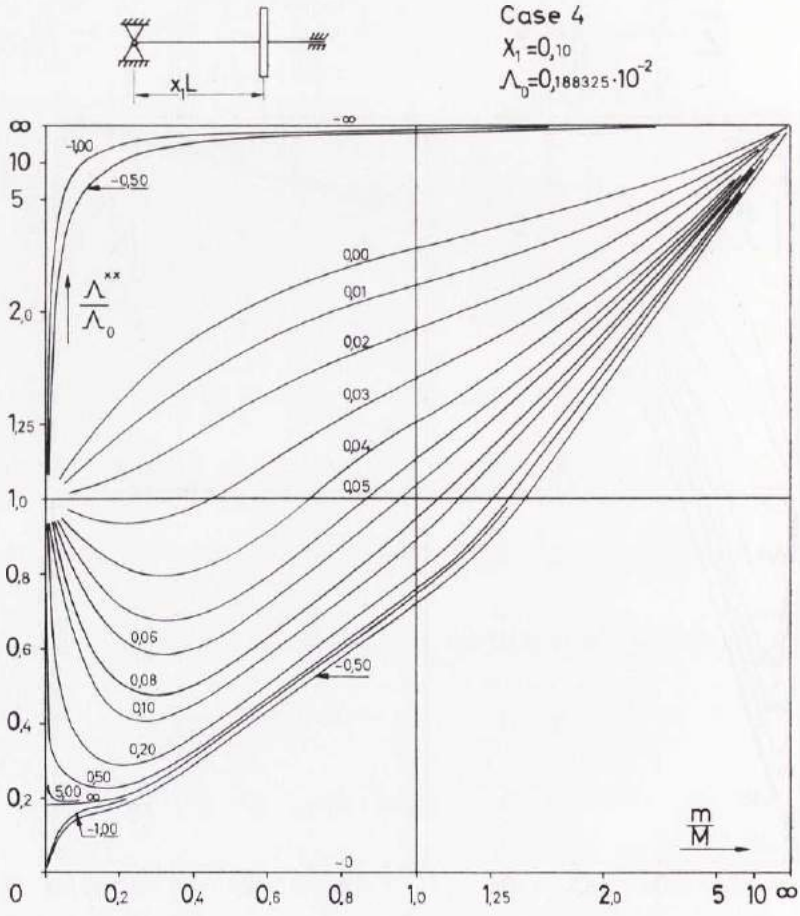
Case 4
$X_1 = 0{,}10$
$\Lambda_0 = 0{,}188325 \cdot 10^{-2}$
x₁L
$\frac{\Lambda^{xx}}{\Lambda_0}$
$\frac{m}{M}$
-∞
-1,00
-0,50
0,00
0,01
0,02
0,03
0,04
0,05
0,06
0,08
0,10
0,20
0,50
5,00
∞
-1,00
-0,50
-0
∞
10
5
2,0
1,25
1,0
0,8
0,6
0,4
0,2
0
0,2
0,4
0,6
0,8
1,0
1,25
2,0
5
10
∞

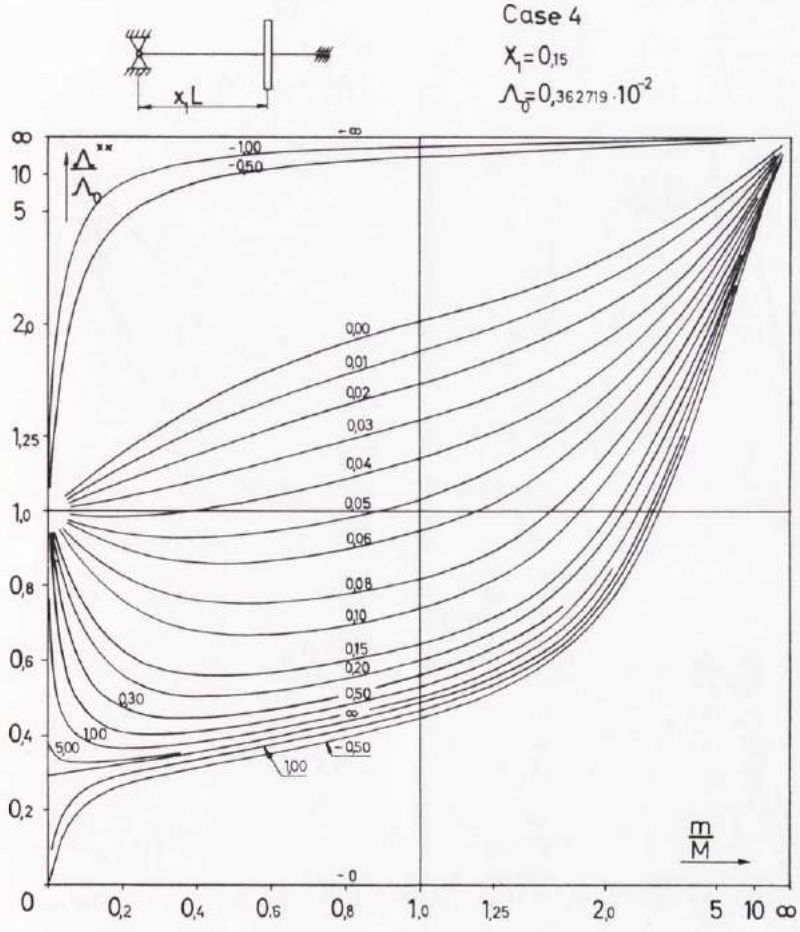
Case 4
$\chi_1 = 0{,}15$
$\Lambda_0 = 0{,}362719 \cdot 10^{-2}$
x₁L
Δ^{xx}/Λ_0
-1,00
-0,50
0,00
0,01
0,02
0,03
0,04
0,05
0,06
0,08
0,10
0,15
0,20
0,50
∞
-0,50
1,00
0,30
1,00
5,00
-0
m/M
∞ 10 5 2,0 1,25 1,0 0,8 0,6 0,4 0,2 0
0,2 0,4 0,6 0,8 1,0 1,25 2,0 5 10 ∞

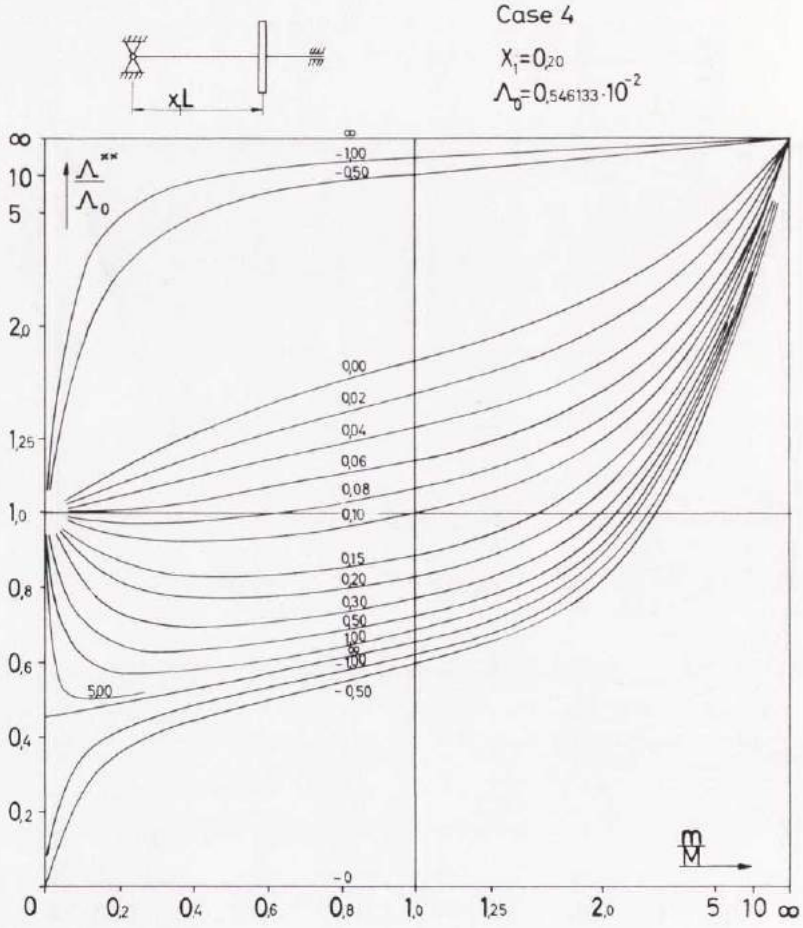
Case 4
$X_1 = 0{,}20$
$\Lambda_0 = 0{,}546133 \cdot 10^{-2}$
x L
$\frac{\Lambda^{**}}{\Lambda_0}$
∞
10
5
2,0
1,25
1,0
0,8
0,6
0,4
0,2
0
-1,00
-0,50
0,00
0,02
0,04
0,06
0,08
0,10
0,15
0,20
0,30
0,50
1,00
-1,00
-0,50
-0
5,00
$\frac{m}{M}$
0,2
0,4
0,6
0,8
1,0
1,25
2,0
5
10
∞

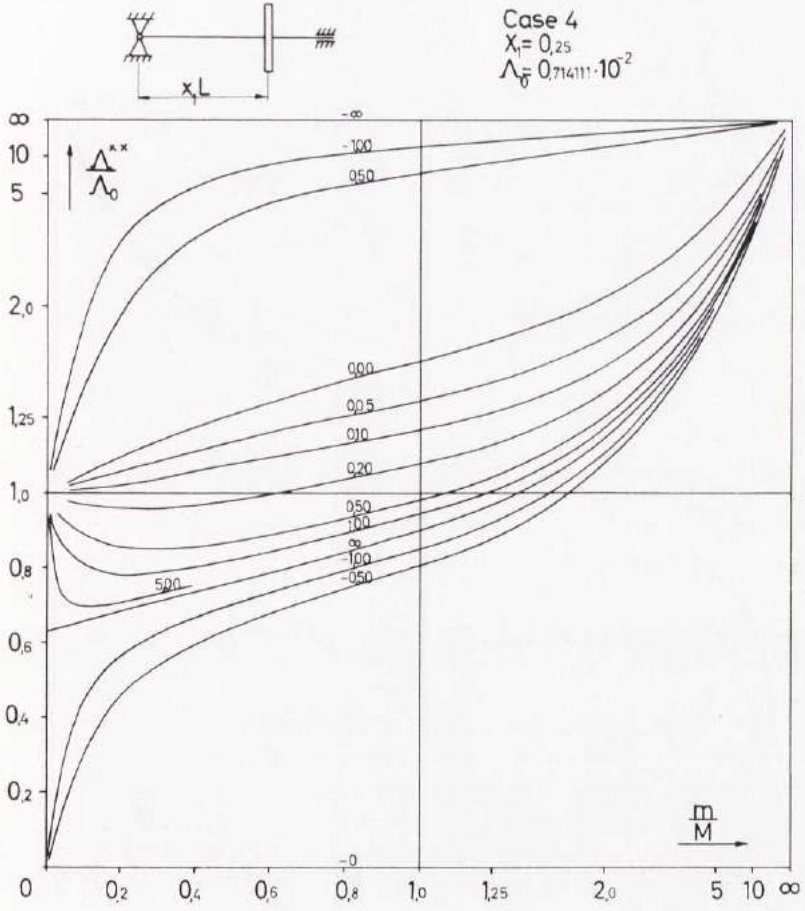
Case 4
$x_1 = 0{,}25$
$\Lambda_0 = 0{,}714111 \cdot 10^{-2}$
$x_1 L$
$\frac{\Delta^{**}}{\Lambda_0}$
∞
10
5
2,0
1,25
1,0
0,8
0,6
0,4
0,2
0
$-\infty$
-100
0,50
0,00
0,05
0,10
0,20
0,50
1,00
∞
-1,00
-0,50
5,00
-0
0,2
0,4
0,6
0,8
1,0
1,25
2,0
5
10
∞
$\frac{m}{M}$

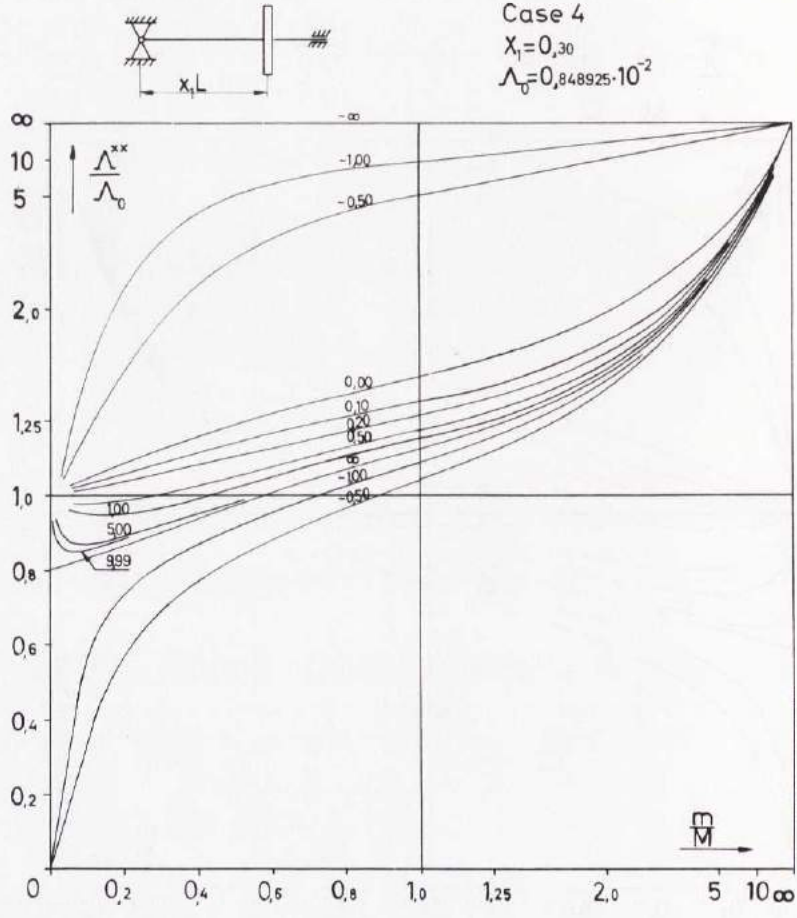
Case 4
$X_1 = 0{,}30$
$\Lambda_0 = 0{,}848925 \cdot 10^{-2}$
$x_1 L$
$\frac{\Lambda^{xx}}{\Lambda_0}$
$\frac{m}{M}$
-∞
-1,00
-0,50
0,00
0,10
0,20
0,50
∞
-100
-0,50
100
500
999
∞
10
5
2,0
1,25
1,0
0,8
0,6
0,4
0,2
0
0,2
0,4
0,6
0,8
1,0
1,25
2,0
5
10
∞

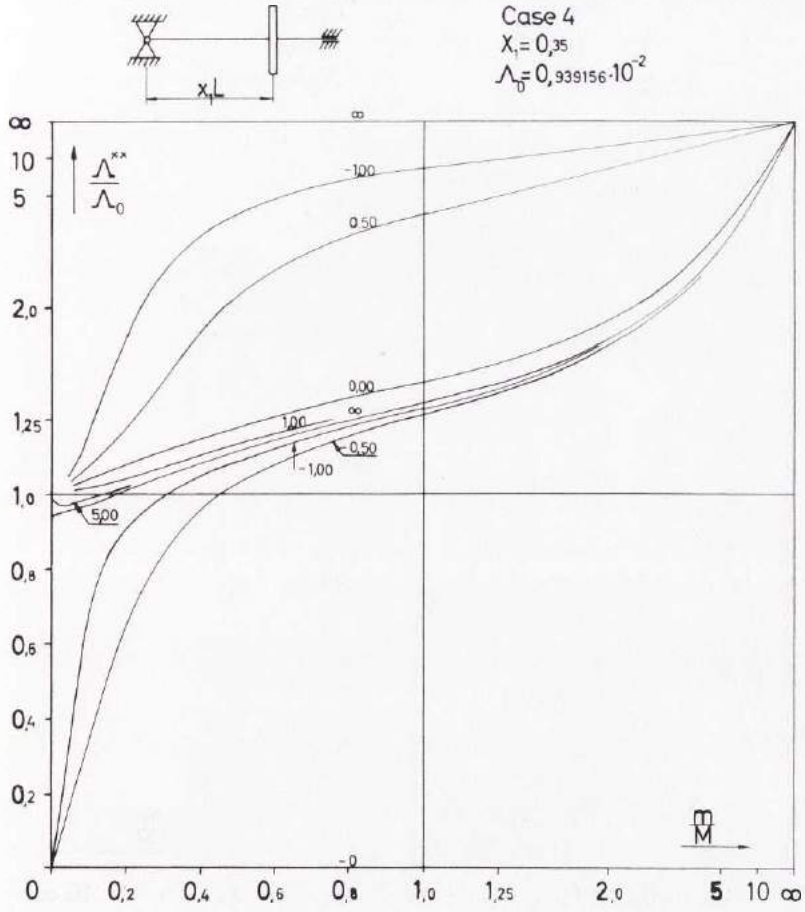
Case 4
X1= 0,35
Λ0= 0,939156·10-2
x1L
Λ**/Λ0
-1,00
0,50
0,00
1,00
∞
-0,50
-1,00
5,00
m/M
∞
10
5
2,0
1,25
1,0
0,8
0,6
0,4
0,2
0
-0
0,2
0,4
0,6
0,8
1,0
1,25
2,0
5
10
∞

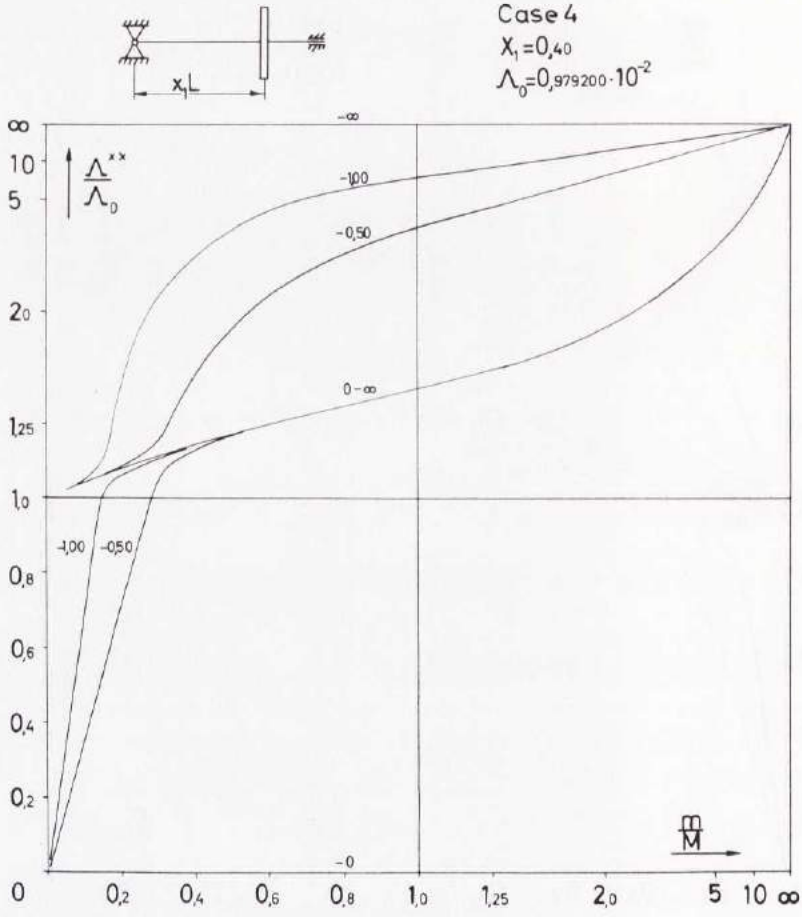
Case 4
X1 = 0,40
Λ0 = 0,979200 · 10-2
x1L
Λ**/Λ0
-∞
-1,00
-0,50
0 -∞
-1,00
-0,50
-0
m/M
∞
10
5
2,0
1,25
1,0
0,8
0,6
0,4
0,2
0
0,2
0,4
0,6
0,8
1,0
1,25
2,0
5
10
∞

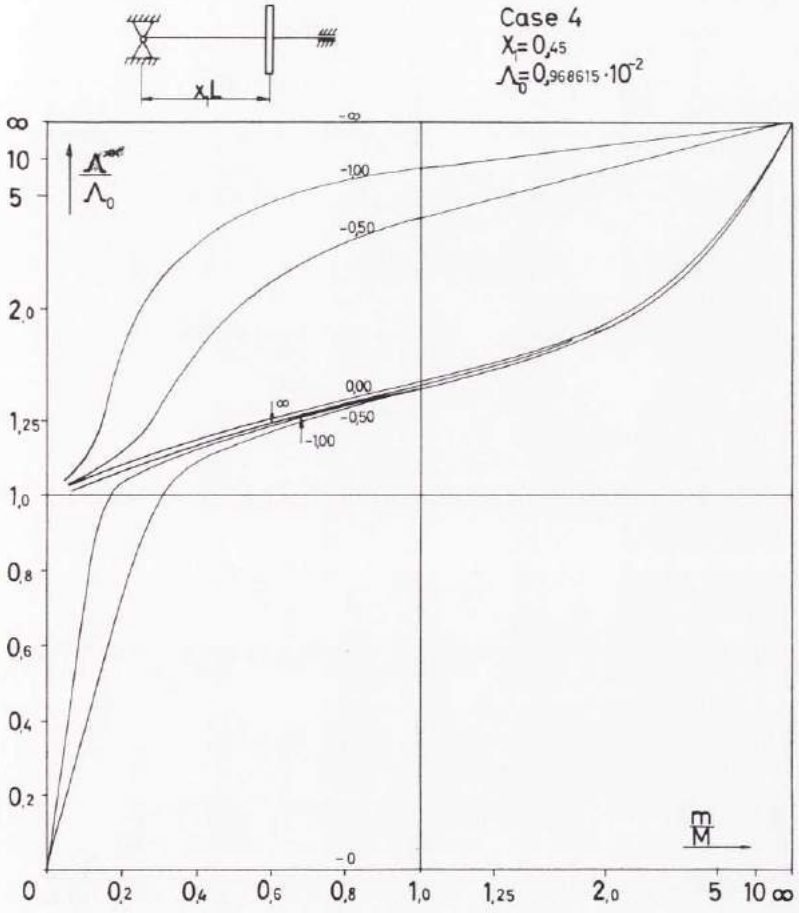
Case 4
$X_1 = 0{,}45$
$\Lambda_0 = 0{,}968615 \cdot 10^{-2}$
x L
$\frac{\Lambda}{\Lambda_0}$
$\frac{m}{M}$
-∞
-1,00
-0,50
0,00
∞
-0,50
-1,00
-0
∞ 10 5 2,0 1,25 1,0 0,8 0,6 0,4 0,2 0
0,2 0,4 0,6 0,8 1,0 1,25 2,0 5 10 ∞

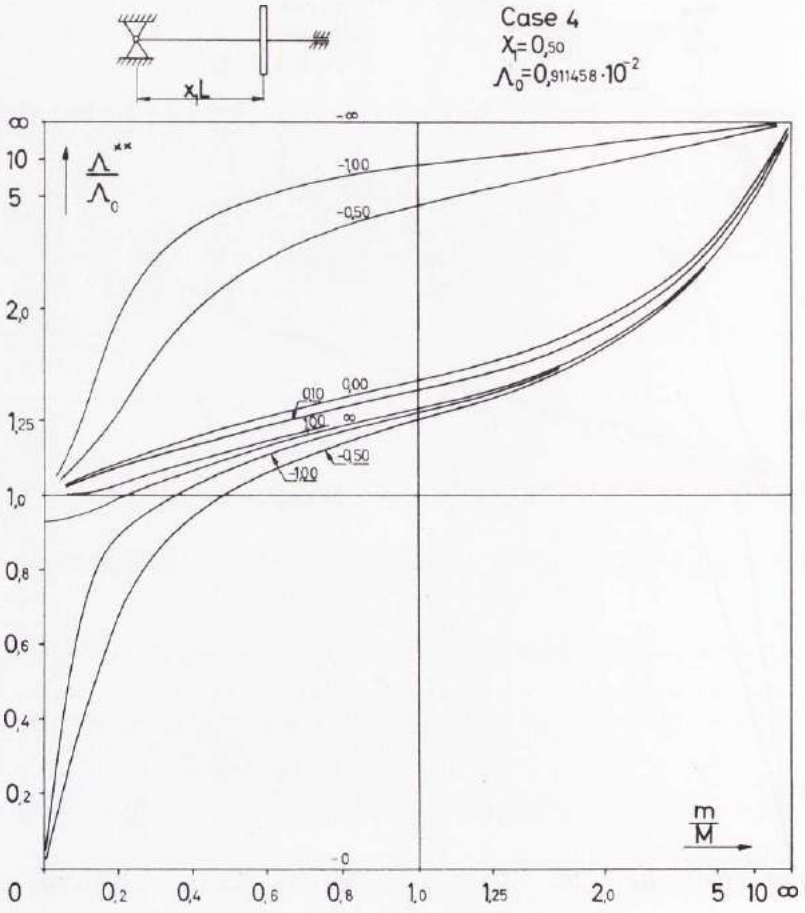
Case 4
$\chi_1 = 0{,}50$
$\Lambda_0 = 0{,}911458 \cdot 10^{-2}$
$x_1 L$
$\frac{\Lambda^{**}}{\Lambda_0}$
$\frac{m}{M}$
-∞
-1,00
-0,50
0,00
0,10
1,00
∞
-0,50
-1,00
-0
∞
10
5
2,0
1,25
1,0
0,8
0,6
0,4
0,2
0
0,2
0,4
0,6
0,8
1,0
1,25
2,0
5
10
∞

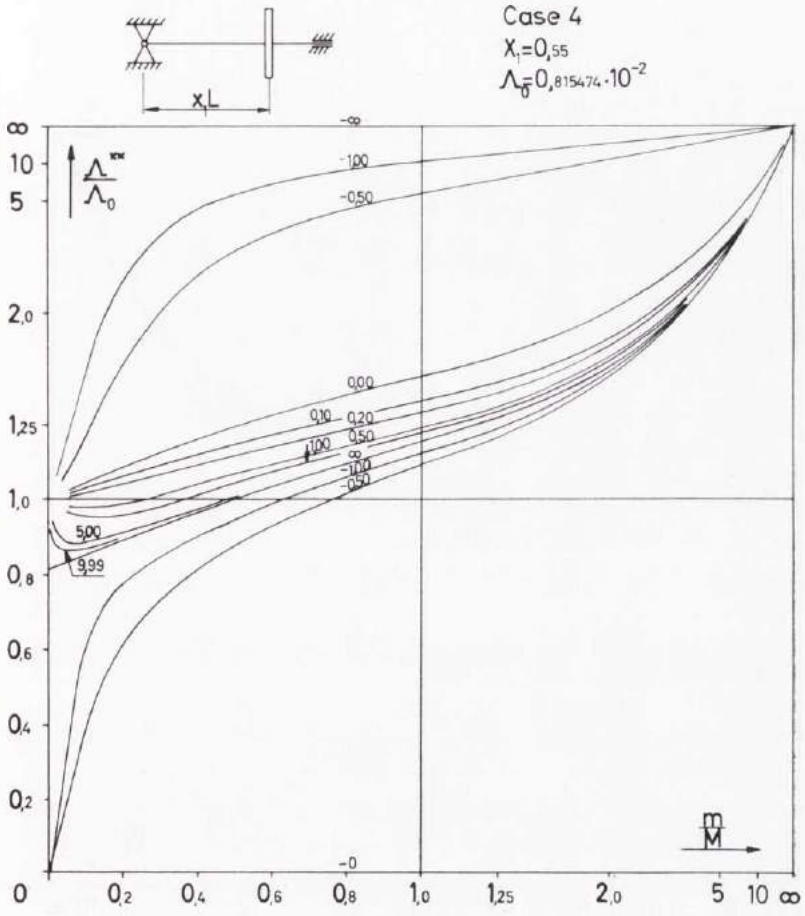
Case 4
X1=0,55
Λ0=0,815474·10⁻²
x/L
Λ*/Λ0
-∞
-1,00
-0,50
0,00
0,10
0,20
0,50
1,00
∞
-1,00
-0,50
5,00
9,99
-0
m/M
∞ 10 5 2,0 1,25 1,0 0,8 0,6 0,4 0,2 0
0,2 0,4 0,6 0,8 1,0 1,25 2,0 5 10 ∞

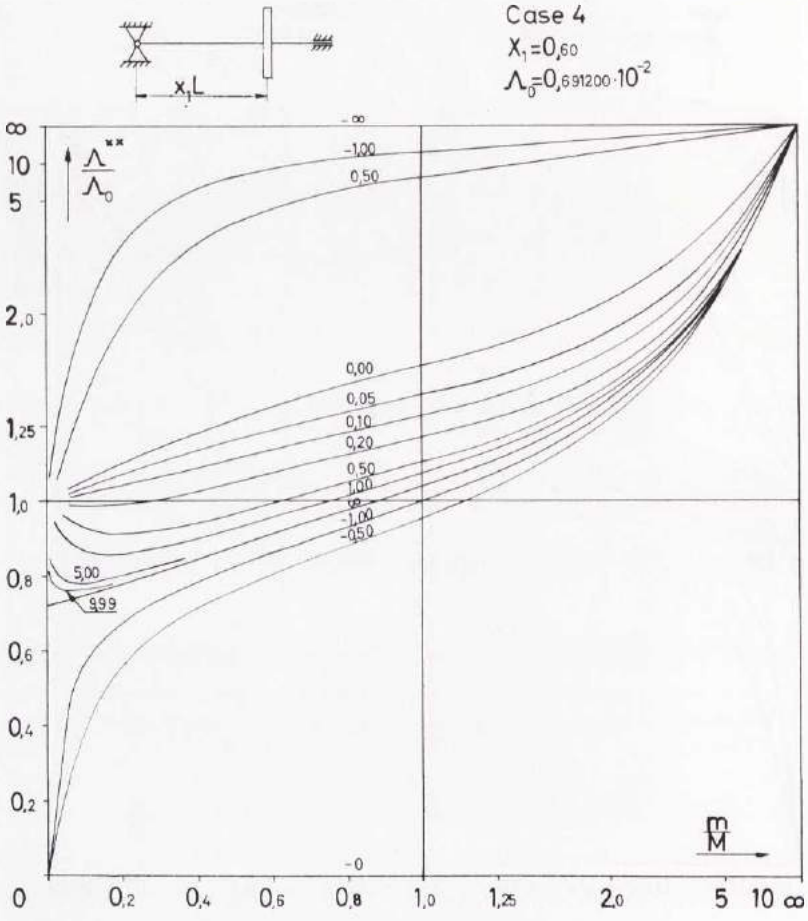
Case 4
$\chi_1 = 0{,}60$
$\Lambda_0 = 0{,}691200 \cdot 10^{-2}$
$x_1 L$
$\frac{\Lambda^{**}}{\Lambda_0}$
$\frac{m}{M}$
-∞
-1,00
0,50
0,00
0,05
0,10
0,20
0,50
1,00
∞
-1,00
-0,50
5,00
9,99
-0
∞
10
5
2,0
1,25
1,0
0,8
0,6
0,4
0,2
0
0,2
0,4
0,6
0,8
1,0
1,25
2,0
5
10
∞

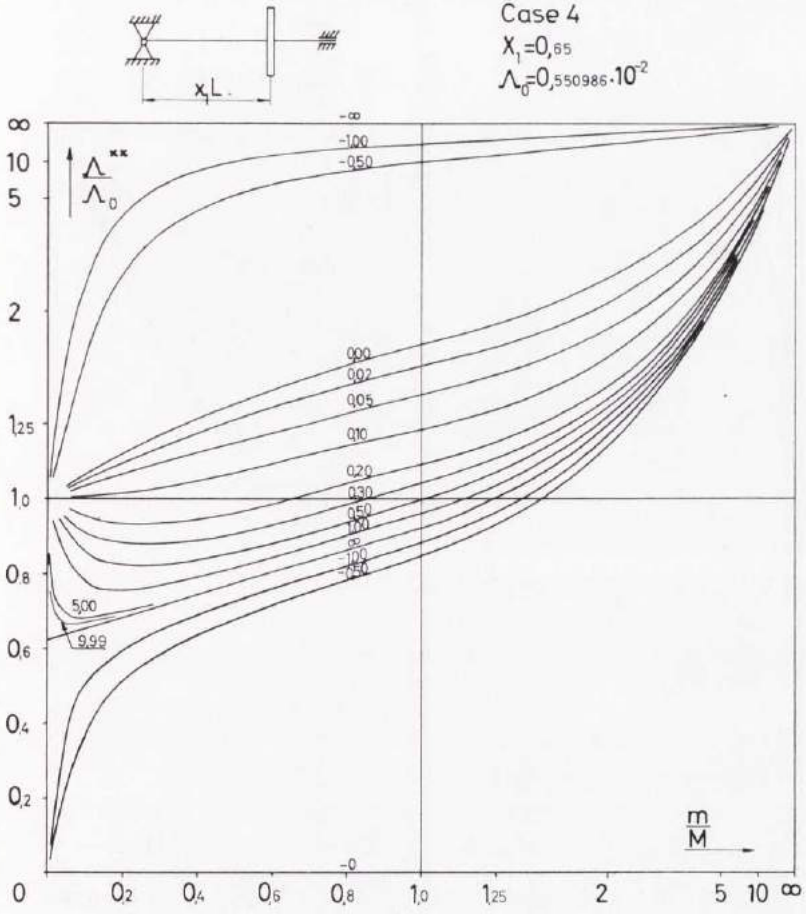
Case 4
X1=0,65
Λ0=0,550986·10-2
x L
Λ**/Λ0
m/M
-∞
-100
-050
000
002
005
010
020
030
050
100
∞
-100
-050
-0
500
999
∞
10
5
2
1,25
1,0
0,8
0,6
0,4
0,2
0
0,2
0,4
0,6
0,8
1,0
1,25
2
5
10
∞

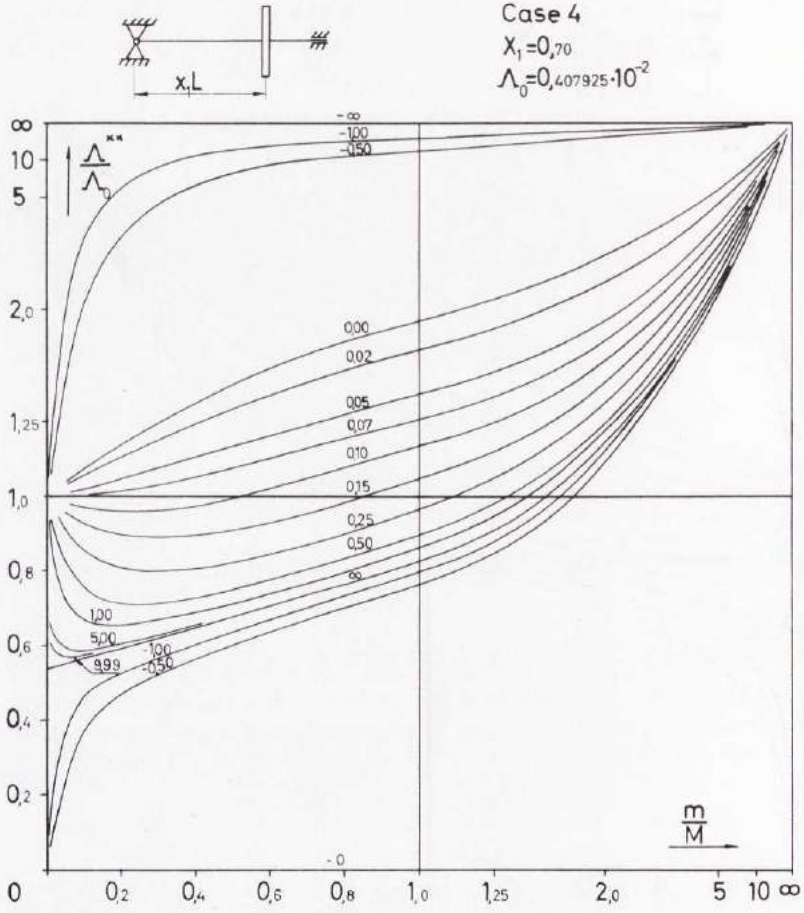
Case 4
$X_1 = 0{,}70$
$\Lambda_0 = 0{,}407925 \cdot 10^{-2}$
x,L
$\frac{\Lambda^{**}}{\Lambda_0}$
$\frac{m}{M}$
-∞
-100
-050
0,00
0,02
0,05
0,07
0,10
0,15
0,25
0,50
∞
1,00
5,00
9,99
-100
-050
-0
∞ 10 5 2,0 1,25 1,0 0,8 0,6 0,4 0,2 0
0,2 0,4 0,6 0,8 1,0 1,25 2,0 5 10 ∞

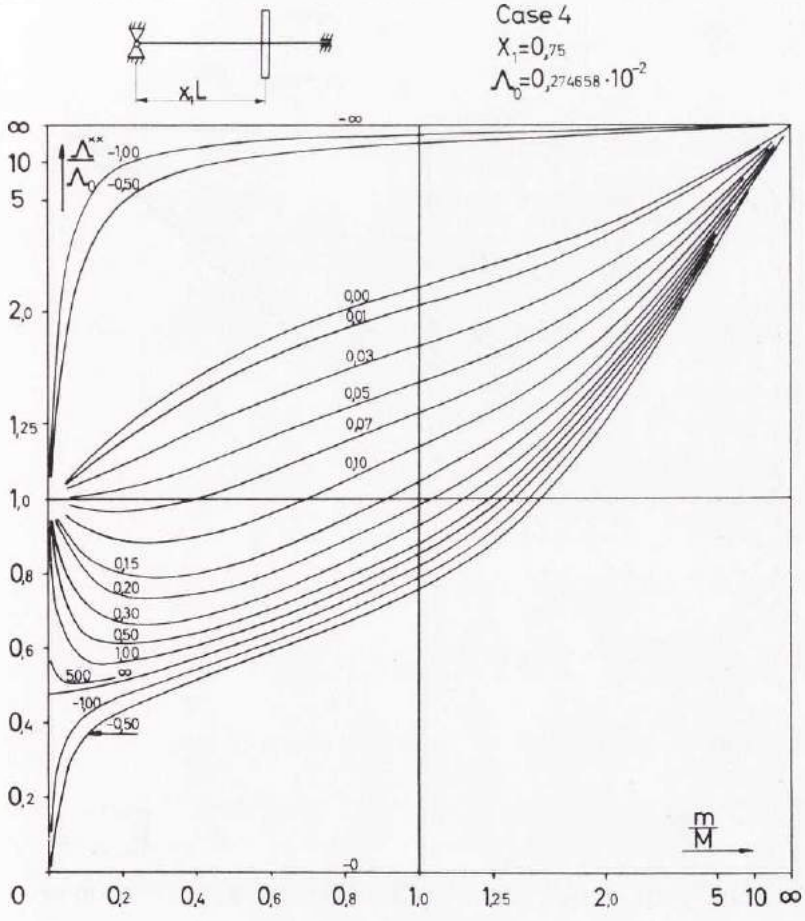
Case 4
X1=0,75
Λ0=0,274658·10-2
x1L
Λ**/Λ0
-1,00
-0,50
0,00
0,01
0,03
0,05
0,07
0,10
0,15
0,20
0,30
0,50
1,00
5,00
∞
-100
-0,50
-∞
-0
m/M
∞
10
5
2,0
1,25
1,0
0,8
0,6
0,4
0,2
0
0,2
0,4
0,6
0,8
1,0
1,25
2,0
5
10
∞

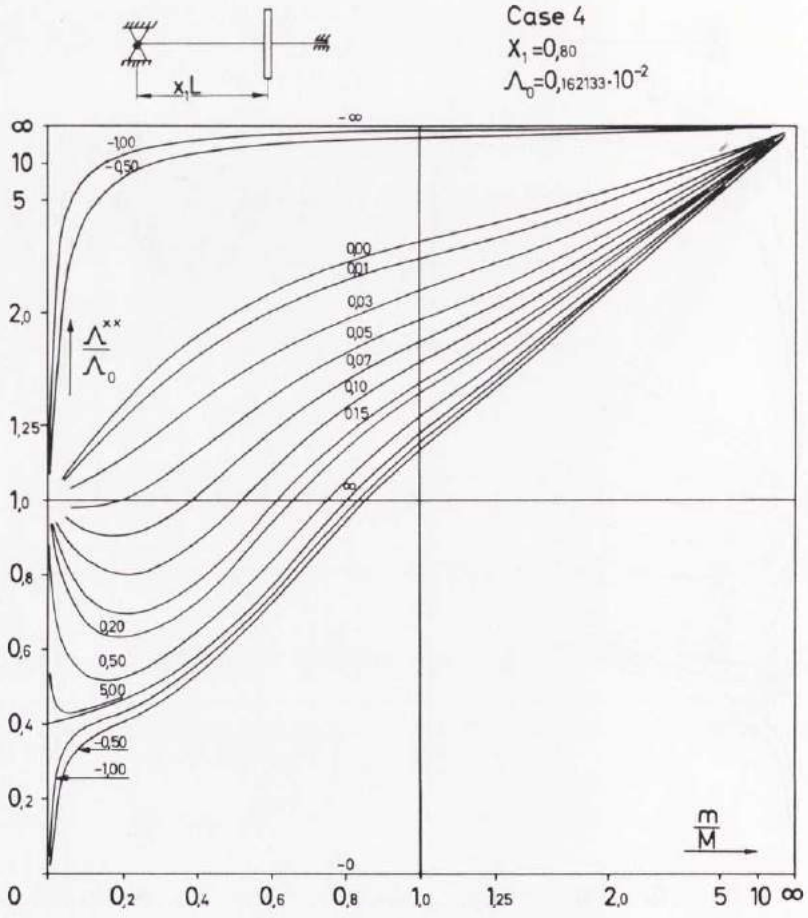
Case 4
$X_1 = 0{,}80$
$\Lambda_0 = 0{,}162133 \cdot 10^{-2}$
$x_1 L$
$\frac{\Lambda^{xx}}{\Lambda_0}$
$\frac{m}{M}$
-∞
-100
-0,50
0,00
0,01
0,03
0,05
0,07
0,10
0,15
∞
0,20
0,50
5,00
-0,50
-1,00
-0
0
0,2
0,4
0,6
0,8
1,0
1,25
2,0
5
10
∞

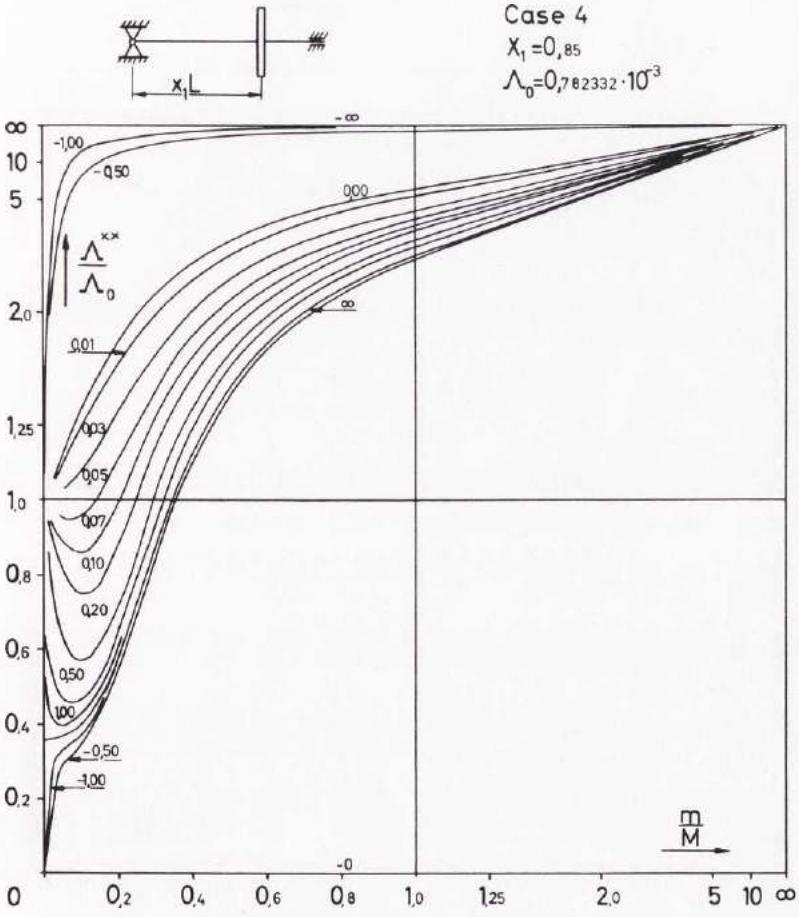
Case 4
X1 =0,85
Λ0=0,782332·10-3
x1L
-∞
-1,00
-0,50
0,00
∞
0,01
0,03
0,05
0,07
0,10
0,20
0,50
1,00
-0,50
-1,00
-0
Λxx/Λ0
m/M
∞
10
5
2,0
1,25
1,0
0,8
0,6
0,4
0,2
0
0,2
0,4
0,6
0,8
1,0
1,25
2,0
5
10
∞

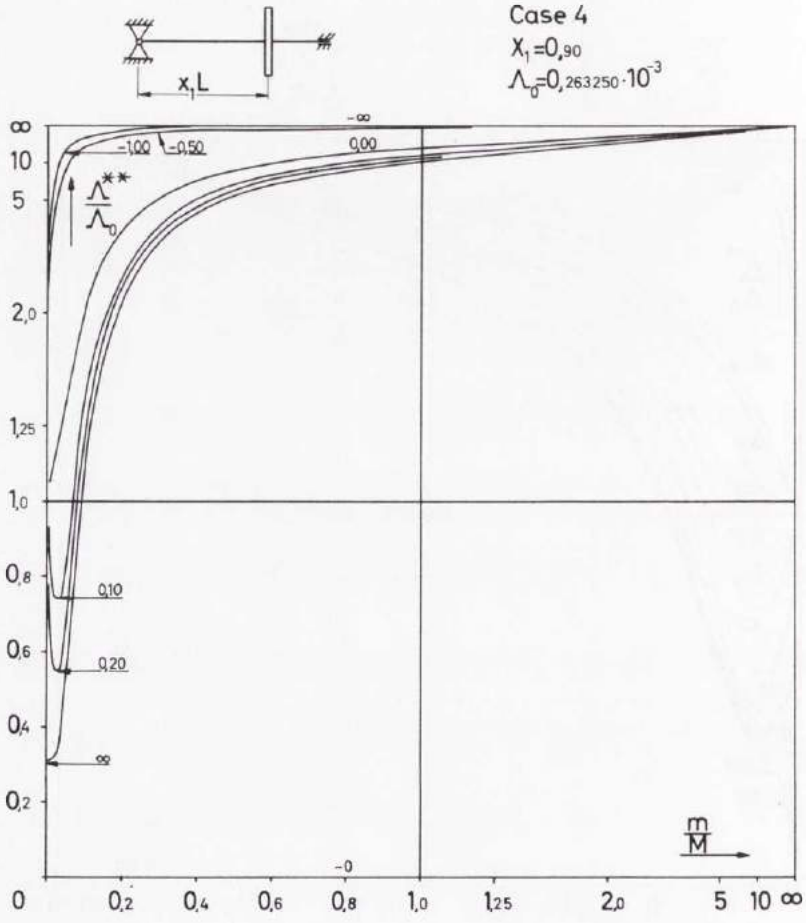
Case 4
$X_1 = 0{,}90$
$\Lambda_0 = 0{,}263250 \cdot 10^{-3}$
x, L
$\frac{\Lambda^{**}}{\Lambda_0}$
-∞
-1,00
-0,50
0,00
0,10
0,20
∞
-0
$\frac{m}{M}$
∞
10
5
2,0
1,25
1,0
0,8
0,6
0,4
0,2
0
0,2
0,4
0,6
0,8
1,0
1,25
2,0
5
10
∞

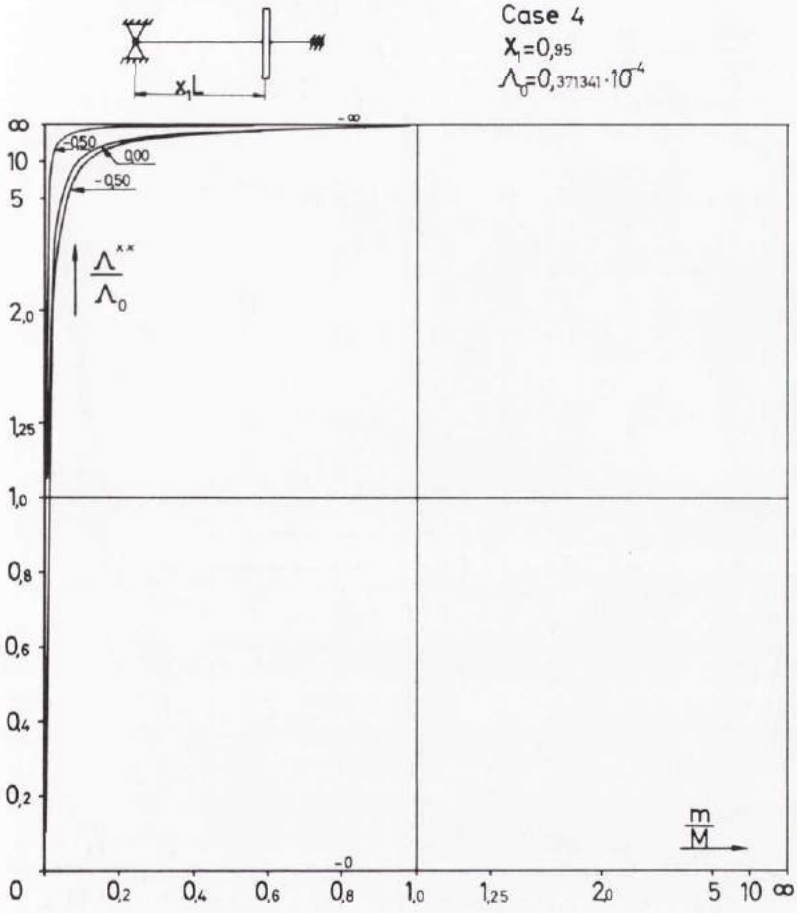
Case 4
$X_1=0,95$
$\Lambda_0=0,371341\cdot10^{-4}$
x_1L
$-\infty$
0,50
0,00
-0,50
$\frac{\Lambda^{**}}{\Lambda_0}$
∞
10
5
2,0
1,25
1,0
0,8
0,6
0,4
0,2
0
-0
0,2
0,4
0,6
0,8
1,0
1,25
2,0
5
10
∞
$\frac{m}{M}$

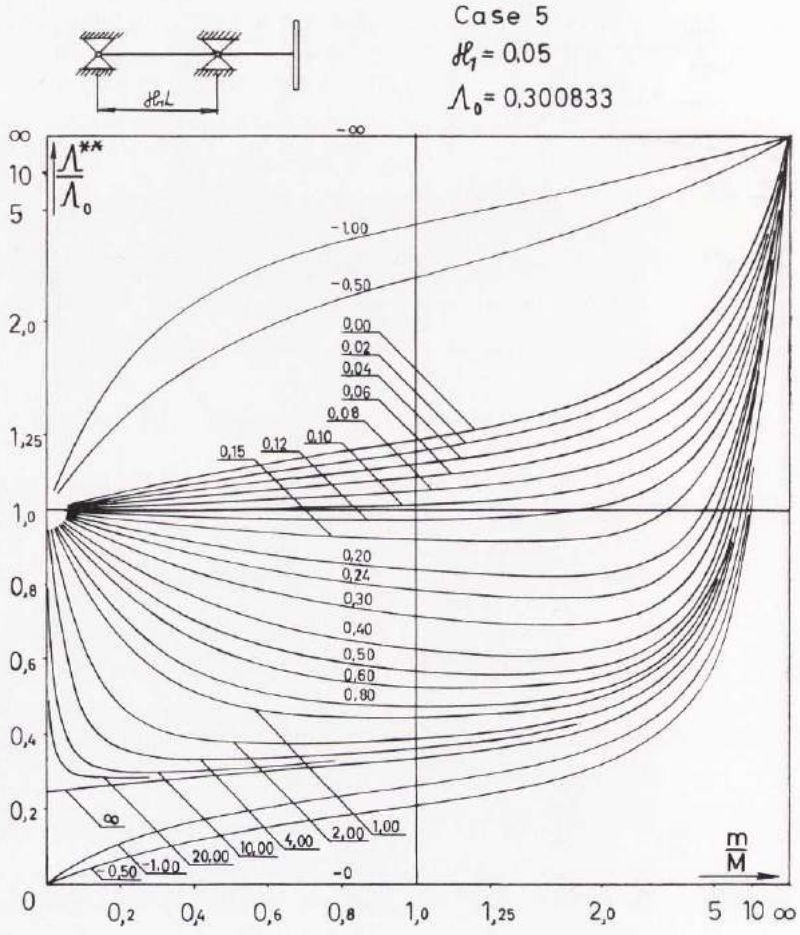
Case 5
$\mathcal{H}_1 = 0.05$
$\Lambda_0 = 0.300833$
$\frac{\Lambda^{**}}{\Lambda_0}$
$\frac{m}{M}$
-∞
-1.00
-0.50
0.00
0.02
0.04
0.06
0.08
0.10
0.12
0.15
0.20
0.24
0.30
0.40
0.50
0.60
0.80
∞
20.00
10.00
4.00
2.00
1.00
-0
∞ 10 5 2,0 1,25 1,0 0,8 0,6 0,4 0,2 0
0,2 0,4 0,6 0,8 1,0 1,25 2,0 5 10 ∞

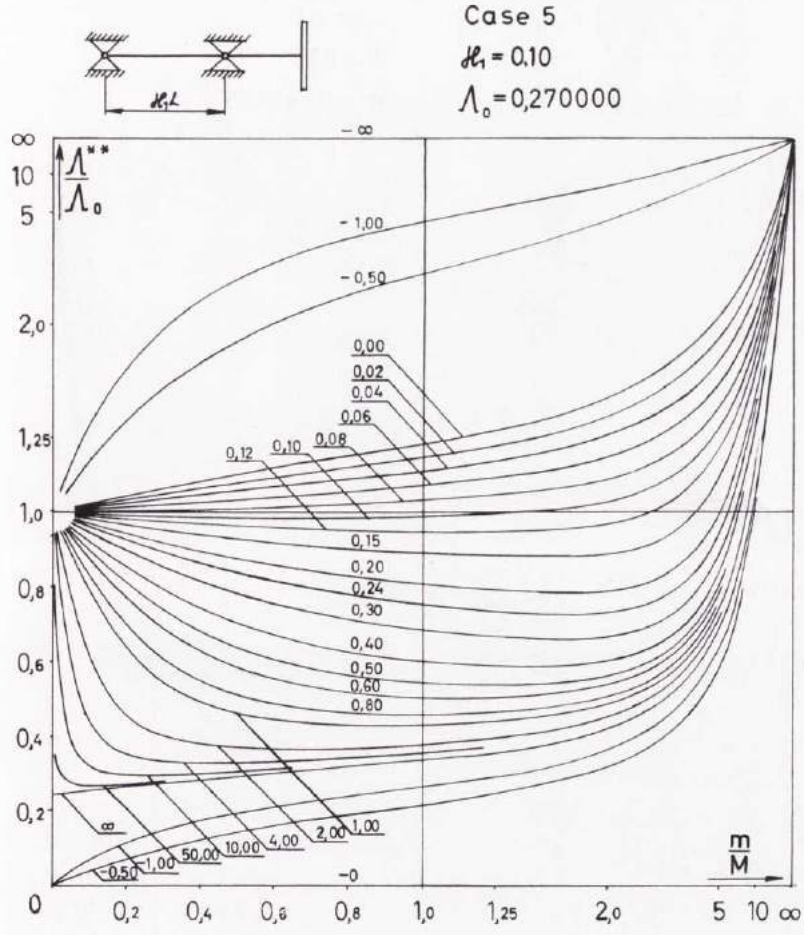
Case 5
$\varkappa_1 = 0.10$
$\Lambda_0 = 0{,}270000$
$\varkappa_1 L$
$\frac{\Lambda^{**}}{\Lambda_0}$
$\frac{m}{M}$
∞
10
5
2,0
1,25
1,0
0,8
0,6
0,4
0,2
0
0,2
0,4
0,6
0,8
1,0
1,25
2,0
5
10
∞
−∞
−1,00
−0,50
0,00
0,02
0,04
0,06
0,08
0,10
0,12
0,15
0,20
0,24
0,30
0,40
0,50
0,60
0,80
∞
50,00
10,00
4,00
2,00
1,00
−0,50
−1,00
−0

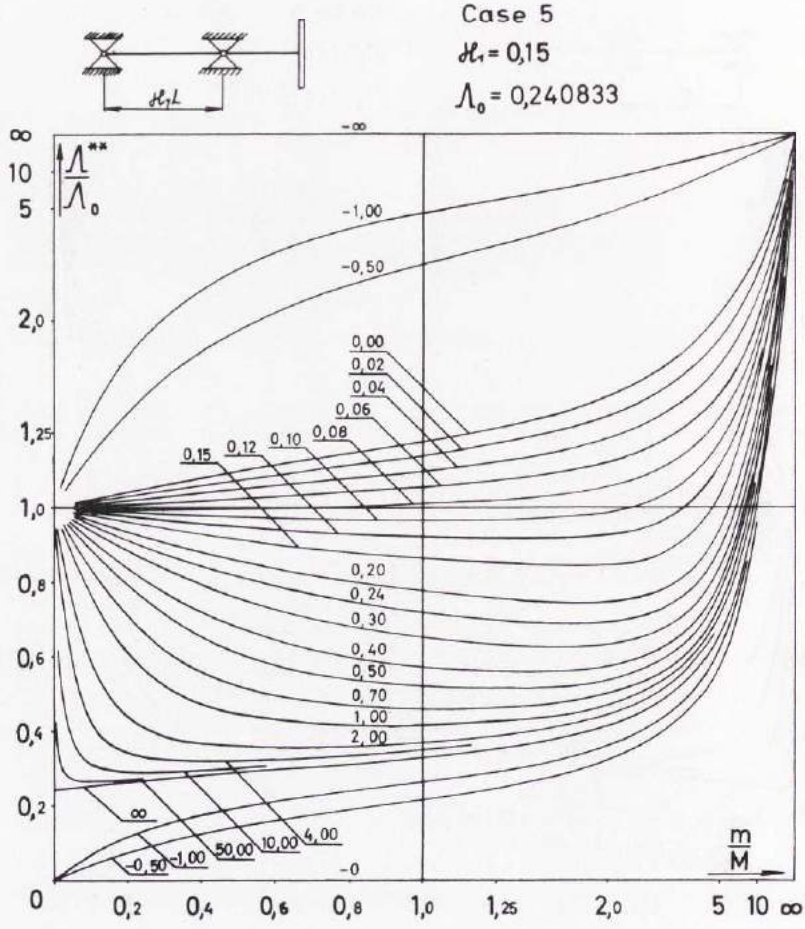
Case 5
$\mathcal{H}_1 = 0{,}15$
$\Lambda_0 = 0{,}240833$
$\mathcal{H}_1 L$
$\frac{\Lambda^{**}}{\Lambda_0}$
$\frac{m}{M}$
-∞
-1,00
-0,50
0,00
0,02
0,04
0,06
0,08
0,10
0,12
0,15
0,20
0,24
0,30
0,40
0,50
0,70
1,00
2,00
∞
-0
-0,50
-1,00
-50,00
-10,00
-4,00
∞ 10 5 2,0 1,25 1,0 0,8 0,6 0,4 0,2 0
0,2 0,4 0,6 0,8 1,0 1,25 2,0 5 10 ∞

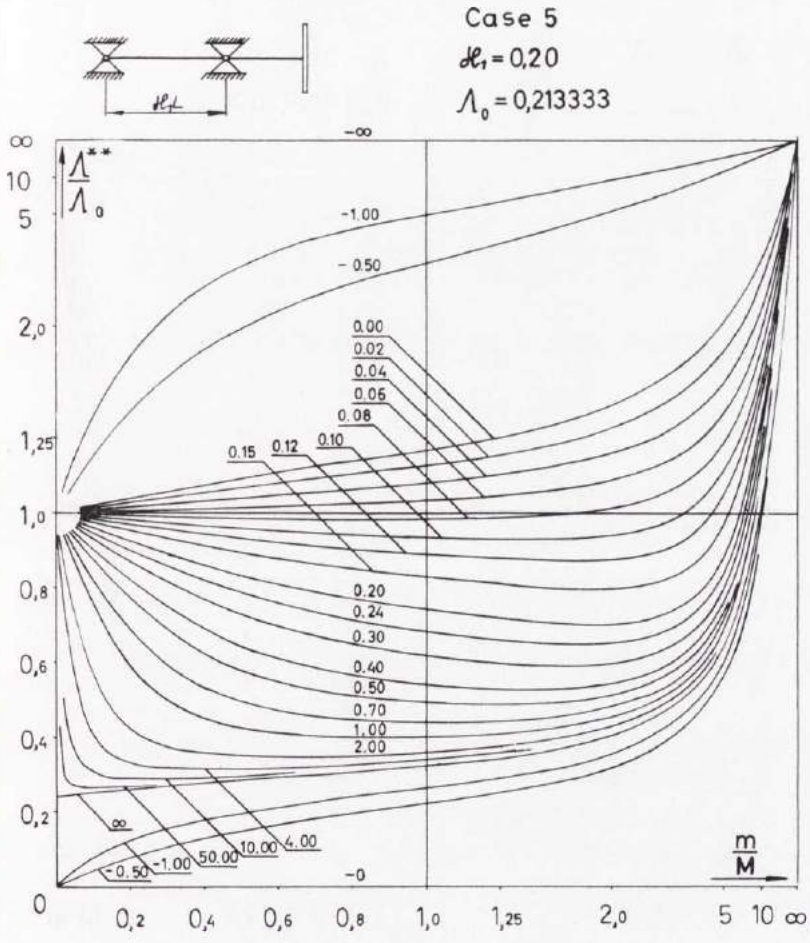
Case 5
$\alpha_1 = 0{,}20$
$\Lambda_0 = 0{,}213333$
$\frac{\Lambda^{**}}{\Lambda_0}$
$\frac{m}{M}$
∞
10
5
2,0
1,25
1,0
0,8
0,6
0,4
0,2
0
−∞
-1.00
- 0.50
0.00
0.02
0.04
0.06
0.08
0.10
0.12
0.15
0.20
0.24
0.30
0.40
0.50
0.70
1.00
2.00
∞
4.00
10.00
50.00
-1.00
- 0.50
−0
0,2
0,4
0,6
0,8
1,0
1,25
2,0
5
10
∞

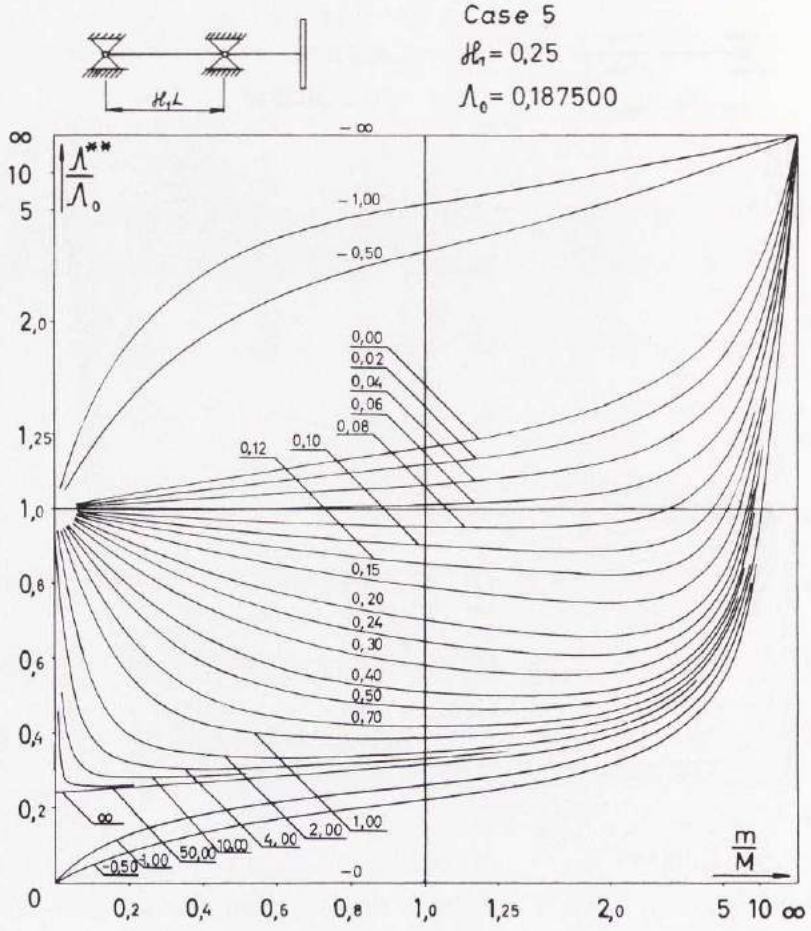
Case 5
$\mathcal{H}_1 = 0{,}25$
$\Lambda_0 = 0{,}187500$
$H_1 L$
$\frac{\Lambda^{**}}{\Lambda_0}$
$-\infty$
$-1{,}00$
$-0{,}50$
0,00
0,02
0,04
0,06
0,08
0,10
0,12
0,15
0,20
0,24
0,30
0,40
0,50
0,70
1,00
2,00
4,00
10,00
50,00
$-3{,}00$
$-0{,}50$
∞
-0
$\frac{m}{M}$
∞ 10 5 2,0 1,25 1,0 0,8 0,6 0,4 0,2 0
0,2 0,4 0,6 0,8 1,0 1,25 2,0 5 10 ∞

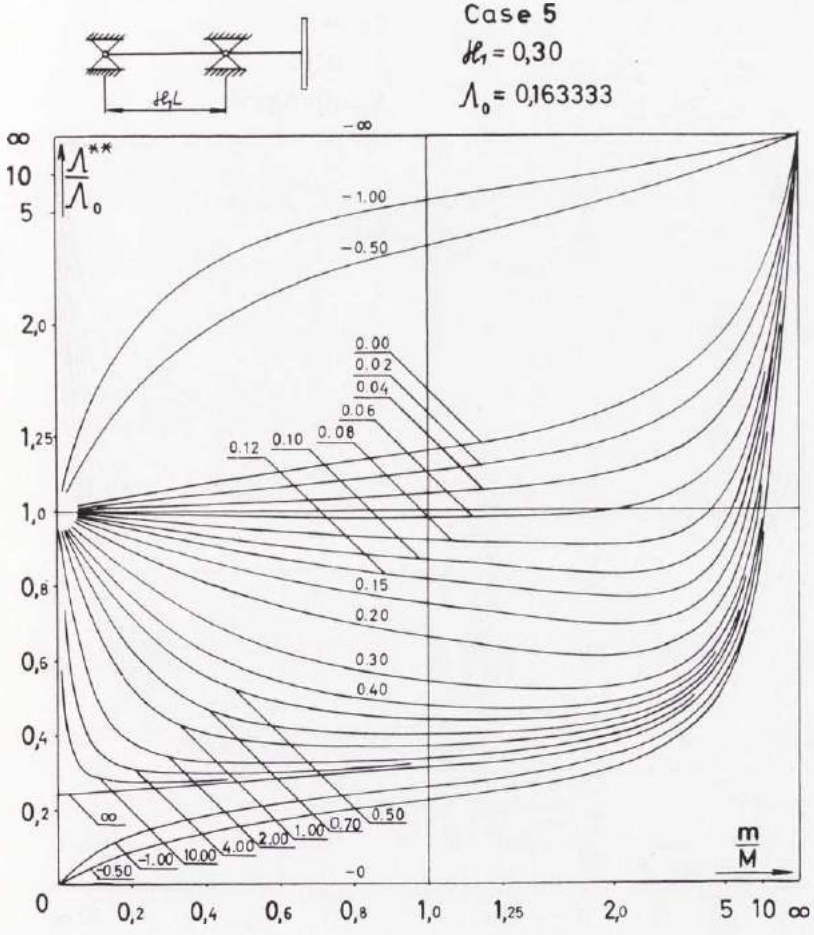
Case 5
$\delta\ell_1 = 0{,}30$
$\Lambda_0 = 0{,}163333$
$\delta\ell_1 L$
$\frac{\Lambda^{**}}{\Lambda_0}$
$\frac{m}{M}$
$-\infty$
-1.00
-0.50
0.00
0.02
0.04
0.06
0.08
0.10
0.12
0.15
0.20
0.30
0.40
0.50
0.70
1.00
2.00
4.00
10.00
∞
-0.50
-1.00
-0
∞ 10 5 2,0 1,25 1,0 0,8 0,6 0,4 0,2 0
0,2 0,4 0,6 0,8 1,0 1,25 2,0 5 10 ∞

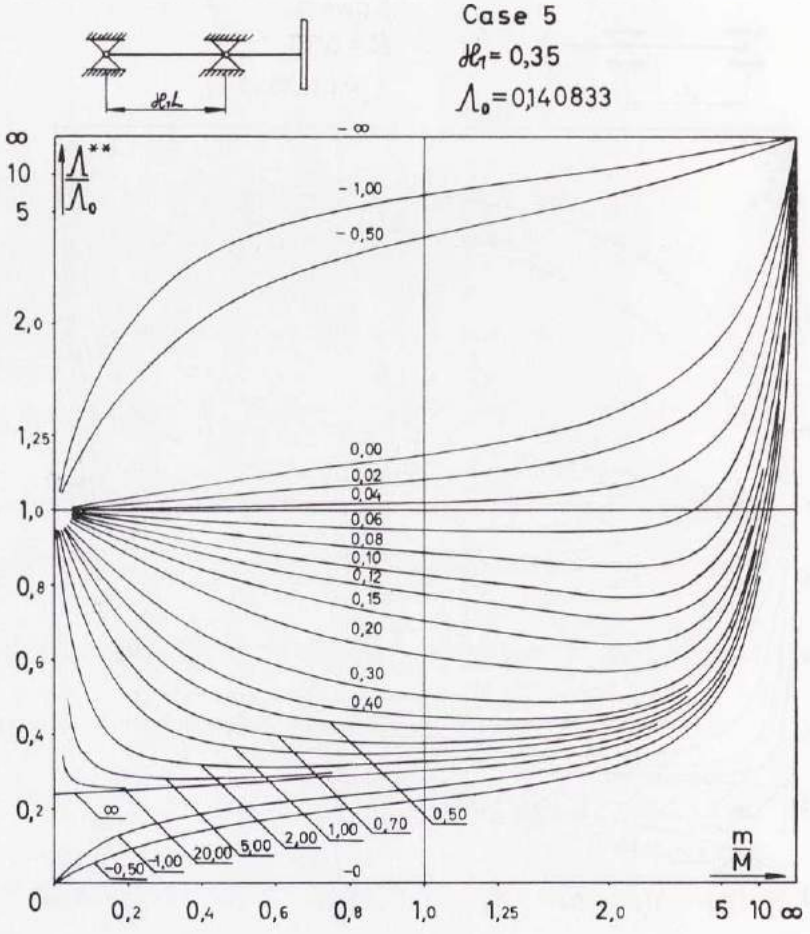
Case 5
$\alpha_1 = 0{,}35$
$\Lambda_0 = 0{,}140833$
$\alpha_1 L$
$\frac{\Lambda^{**}}{\Lambda_0}$
$\frac{m}{M}$
$-\infty$
$-1{,}00$
$-0{,}50$
$0{,}00$
$0{,}02$
$0{,}04$
$0{,}06$
$0{,}08$
$0{,}10$
$0{,}12$
$0{,}15$
$0{,}20$
$0{,}30$
$0{,}40$
$0{,}50$
$0{,}70$
$1{,}00$
$2{,}00$
$5{,}00$
$20{,}00$
∞
$-0{,}50$
$-1{,}00$
-0
∞ 10 5 2,0 1,25 1,0 0,8 0,6 0,4 0,2 0
0,2 0,4 0,6 0,8 1,0 1,25 2,0 5 10 ∞

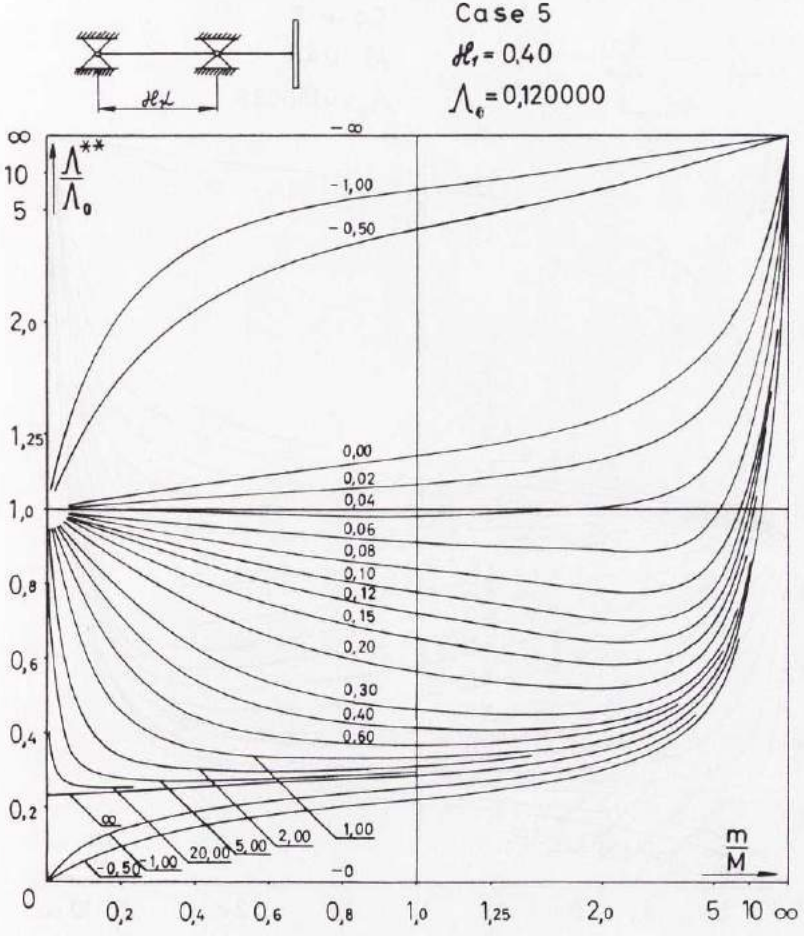
Case 5
$\mathcal{H}_1 = 0.40$
$\Lambda_0 = 0{,}120000$
$\mathcal{H}_1 L$
$\frac{\Lambda^{**}}{\Lambda_0}$
$\frac{m}{M}$
$-\infty$
$-1{,}00$
$-0{,}50$
$0{,}00$
$0{,}02$
$0{,}04$
$0{,}06$
$0{,}08$
$0{,}10$
$0{,}12$
$0{,}15$
$0{,}20$
$0{,}30$
$0{,}40$
$0{,}60$
∞
$20{,}00$
$5{,}00$
$2{,}00$
$1{,}00$
-0
∞ 10 5 2,0 1,25 1,0 0,8 0,6 0,4 0,2 0
0,2 0,4 0,6 0,8 1,0 1,25 2,0 5 10 ∞

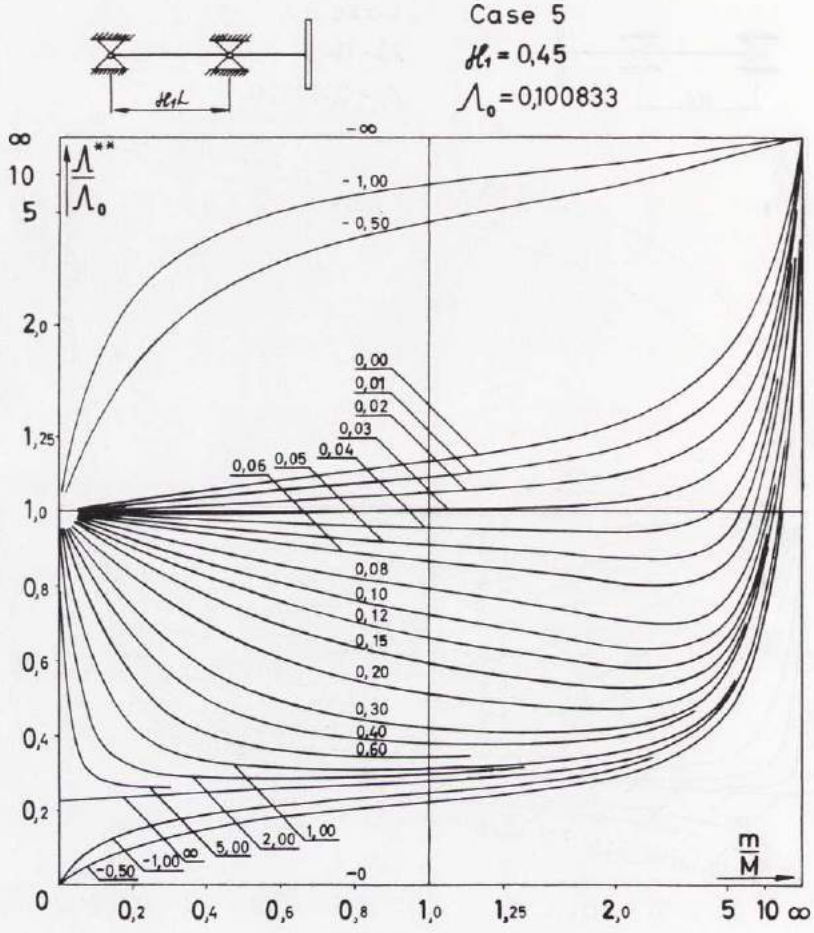
Case 5
$\mathcal{H}_1 = 0{,}45$
$\Lambda_0 = 0{,}100833$
$\mathcal{H}_1 L$
$\frac{\Lambda^{**}}{\Lambda_0}$
$\frac{m}{M}$
∞
10
5
2,0
1,25
1,0
0,8
0,6
0,4
0,2
0
0,2
0,4
0,6
0,8
1,0
1,25
2,0
5
10
∞
−∞
- 1,00
- 0,50
0,00
0,01
0,02
0,03
0,04
0,05
0,06
0,08
0,10
0,12
0,15
0,20
0,30
0,40
0,60
1,00
2,00
5,00
∞
-1,00
-0,50
−0

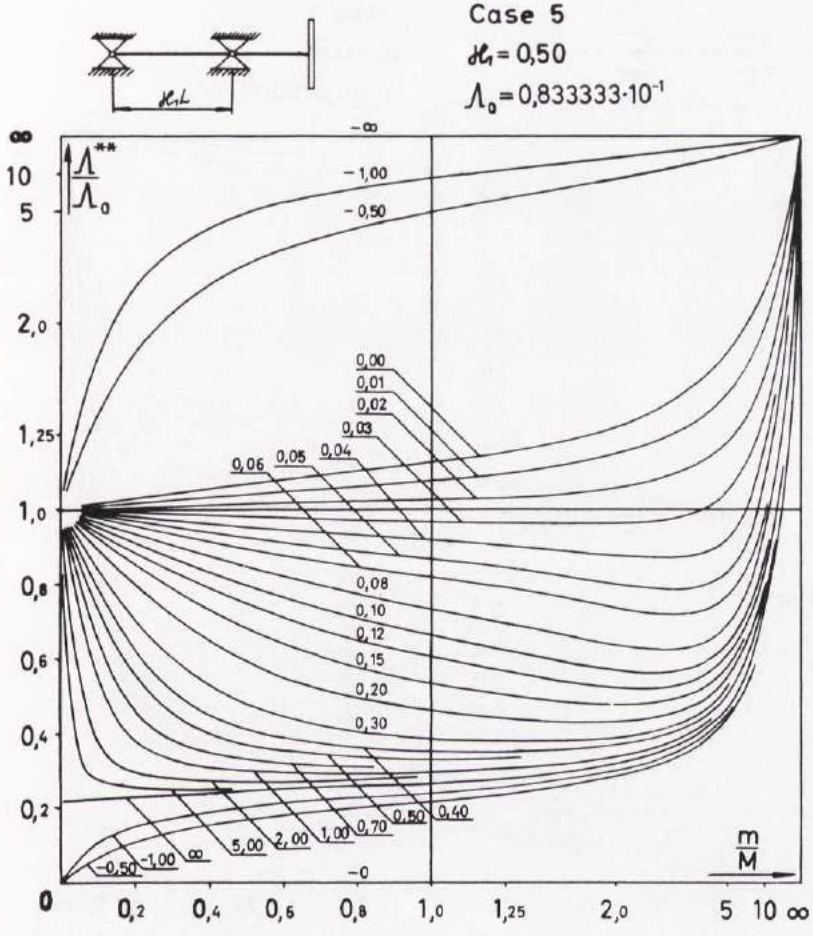
Case 5
$\varkappa_1 = 0{,}50$
$\Lambda_0 = 0{,}833333 \cdot 10^{-1}$
$\varkappa_1 L$
$\frac{\Lambda^{**}}{\Lambda_0}$
$\frac{m}{M}$
$-\infty$
$-1{,}00$
$-0{,}50$
0,00
0,01
0,02
0,03
0,04
0,05
0,06
0,08
0,10
0,12
0,15
0,20
0,30
0,40
0,50
0,70
1,00
2,00
5,00
∞
-0
∞
10
5
2,0
1,25
1,0
0,8
0,6
0,4
0,2
0
0,2
0,4
0,6
0,8
1,0
1,25
2,0
5
10
∞

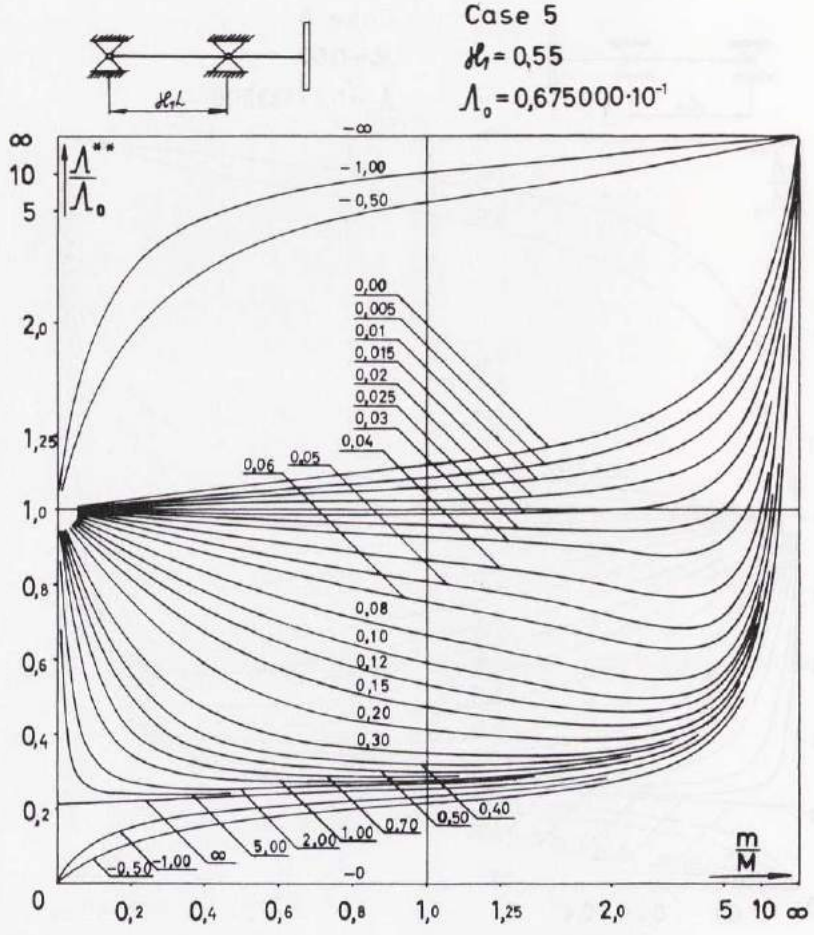
Case 5
$\alpha_1 = 0{,}55$
$\Lambda_0 = 0{,}675000 \cdot 10^{-1}$
$\alpha_1 L$
$\frac{\Lambda^{**}}{\Lambda_0}$
$\frac{m}{M}$
$-\infty$
$-1{,}00$
$-0{,}50$
$0{,}00$
$0{,}005$
$0{,}01$
$0{,}015$
$0{,}02$
$0{,}025$
$0{,}03$
$0{,}04$
$0{,}05$
$0{,}06$
$0{,}08$
$0{,}10$
$0{,}12$
$0{,}15$
$0{,}20$
$0{,}30$
$0{,}40$
$0{,}50$
$0{,}70$
$1{,}00$
$2{,}00$
$5{,}00$
∞
$-1{,}00$
$-0{,}50$
-0
0
0,2
0,4
0,6
0,8
1,0
1,25
2,0
5
10
∞

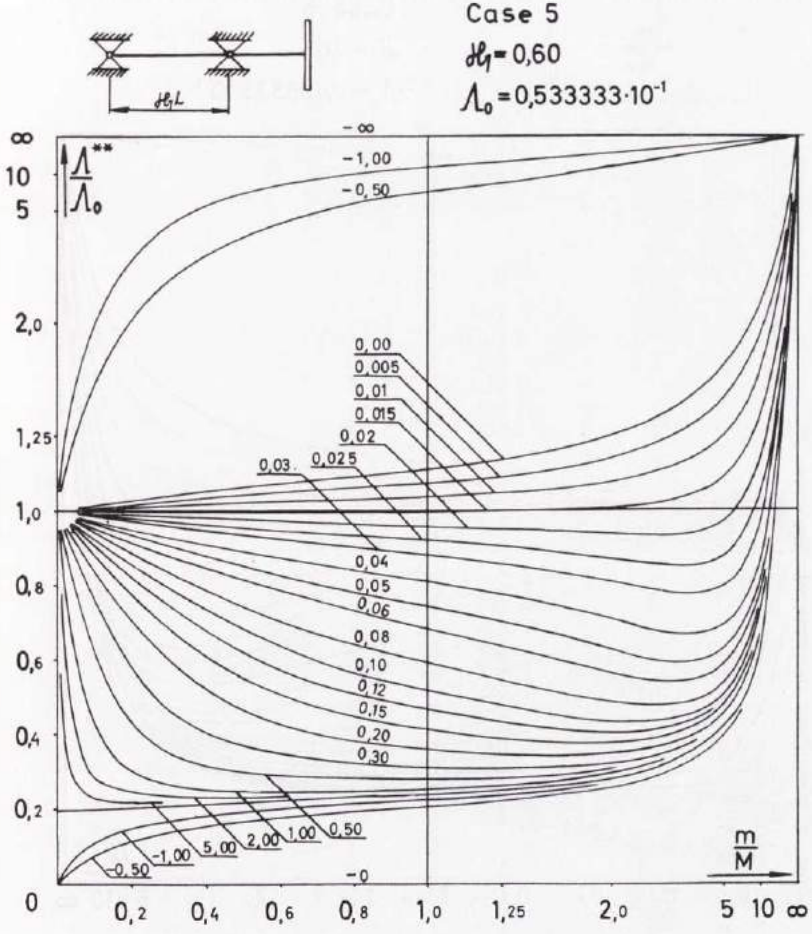
Case 5
$\alpha_1 = 0{,}60$
$\Lambda_0 = 0{,}533333 \cdot 10^{-1}$
$\alpha_1 L$
$\frac{\Lambda^{**}}{\Lambda_0}$
$-\infty$
$-1{,}00$
$-0{,}50$
0,00
0,005
0,01
0,015
0,02
0,025
0,03
0,04
0,05
0,06
0,08
0,10
0,12
0,15
0,20
0,30
0,50
1,00
2,00
5,00
$-1{,}00$
$-0{,}50$
-0
$\frac{m}{M}$
∞
10
5
2,0
1,25
1,0
0,8
0,6
0,4
0,2
0
0,2
0,4
0,6
0,8
1,0
1,25
2,0
5
10
∞

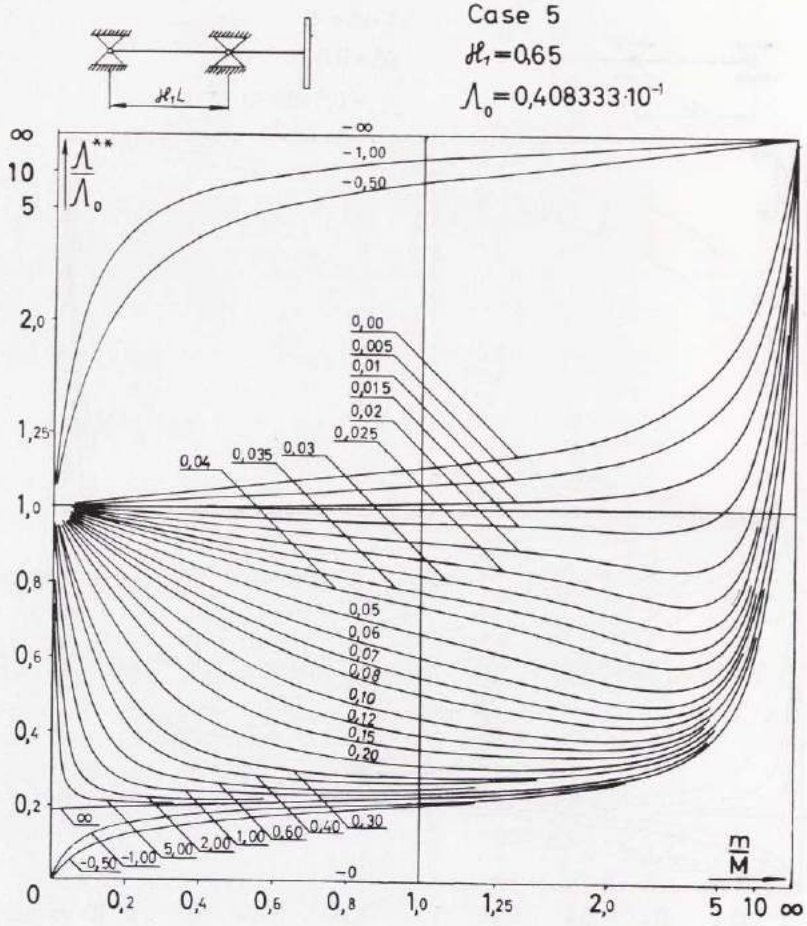
Case 5
$\mathcal{H}_1 = 0{,}65$
$\Lambda_0 = 0{,}408333 \cdot 10^{-1}$
$\mathcal{H}_1 L$
$\frac{\Lambda^{**}}{\Lambda_0}$
$\frac{m}{M}$
$-\infty$
$-1{,}00$
$-0{,}50$
$0{,}00$
$0{,}005$
$0{,}01$
$0{,}015$
$0{,}02$
$0{,}025$
$0{,}03$
$0{,}035$
$0{,}04$
$0{,}05$
$0{,}06$
$0{,}07$
$0{,}08$
$0{,}10$
$0{,}12$
$0{,}15$
$0{,}20$
$0{,}30$
$0{,}40$
$0{,}60$
$1{,}00$
$2{,}00$
$5{,}00$
∞
-0
∞ 10 5 2,0 1,25 1,0 0,8 0,6 0,4 0,2 0
0,2 0,4 0,6 0,8 1,0 1,25 2,0 5 10 ∞

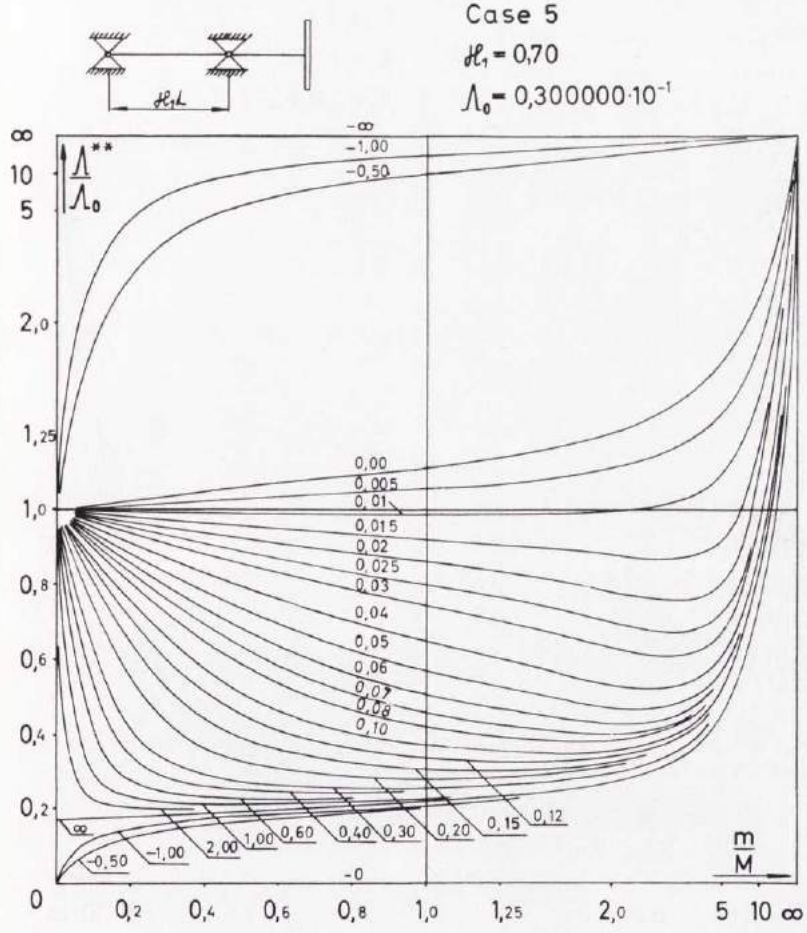
Case 5
$\mu_1 = 0{,}70$
$\Lambda_0 = 0{,}300000 \cdot 10^{-1}$
$\mu_1 L$
$\frac{\Lambda^{**}}{\Lambda_0}$
$\frac{m}{M}$
$-\infty$
-1,00
-0,50
0,00
0,005
0,01
0,015
0,02
0,025
0,03
0,04
0,05
0,06
0,07
0,08
0,10
0,12
0,15
0,20
0,30
0,40
0,60
1,00
2,00
∞
-0
0
0,2
0,4
0,6
0,8
1,0
1,25
2,0
5
10
∞

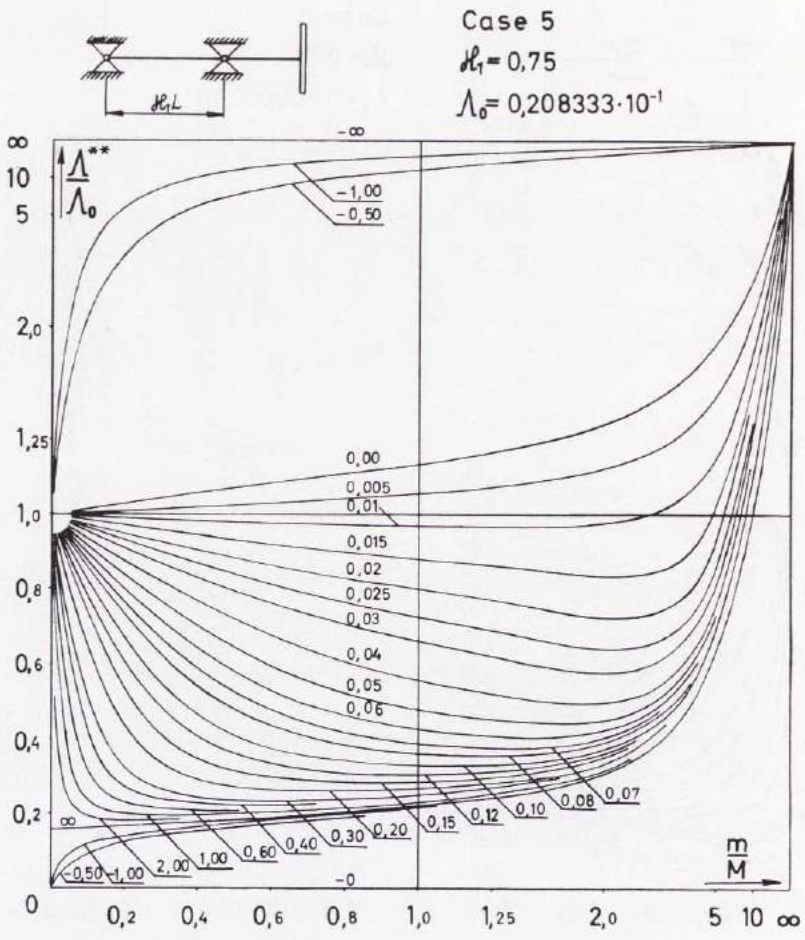
Case 5
$\varkappa_1 = 0{,}75$
$\Lambda_0 = 0{,}208333 \cdot 10^{-1}$
$\varkappa_1 L$
$\frac{\Lambda^{**}}{\Lambda_0}$
$\frac{m}{M}$
$-\infty$
$-1{,}00$
$-0{,}50$
$0{,}00$
$0{,}005$
$0{,}01$
$0{,}015$
$0{,}02$
$0{,}025$
$0{,}03$
$0{,}04$
$0{,}05$
$0{,}06$
$0{,}07$
$0{,}08$
$0{,}10$
$0{,}12$
$0{,}15$
$0{,}20$
$0{,}30$
$0{,}40$
$0{,}60$
$1{,}00$
$2{,}00$
$-0{,}50$
$-1{,}00$
∞
-0
∞ 10 5 2,0 1,25 1,0 0,8 0,6 0,4 0,2 0
0,2 0,4 0,6 0,8 1,0 1,25 2,0 5 10 ∞

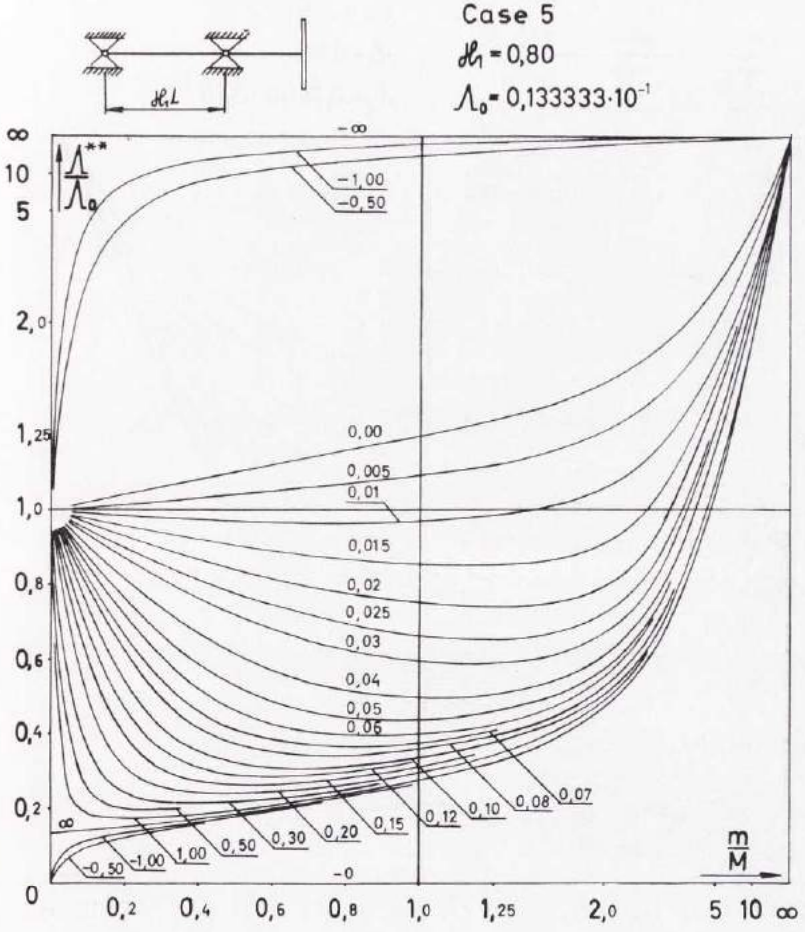
Case 5
$\alpha_1 = 0{,}80$
$\Lambda_0 = 0{,}133333 \cdot 10^{-1}$
$\alpha_1 L$
$\frac{\Lambda^{**}}{\Lambda_0}$
$-\infty$
$-1{,}00$
$-0{,}50$
$0{,}00$
$0{,}005$
$0{,}01$
$0{,}015$
$0{,}02$
$0{,}025$
$0{,}03$
$0{,}04$
$0{,}05$
$0{,}06$
$0{,}07$
$0{,}08$
$0{,}10$
$0{,}12$
$0{,}15$
$0{,}20$
$0{,}30$
$0{,}50$
$1{,}00$
$-0{,}50$
$-1{,}00$
∞
-0
$\frac{m}{M}$
∞ 10 5 2,0 1,25 1,0 0,8 0,6 0,4 0,2 0
0,2 0,4 0,6 0,8 1,0 1,25 2,0 5 10 ∞

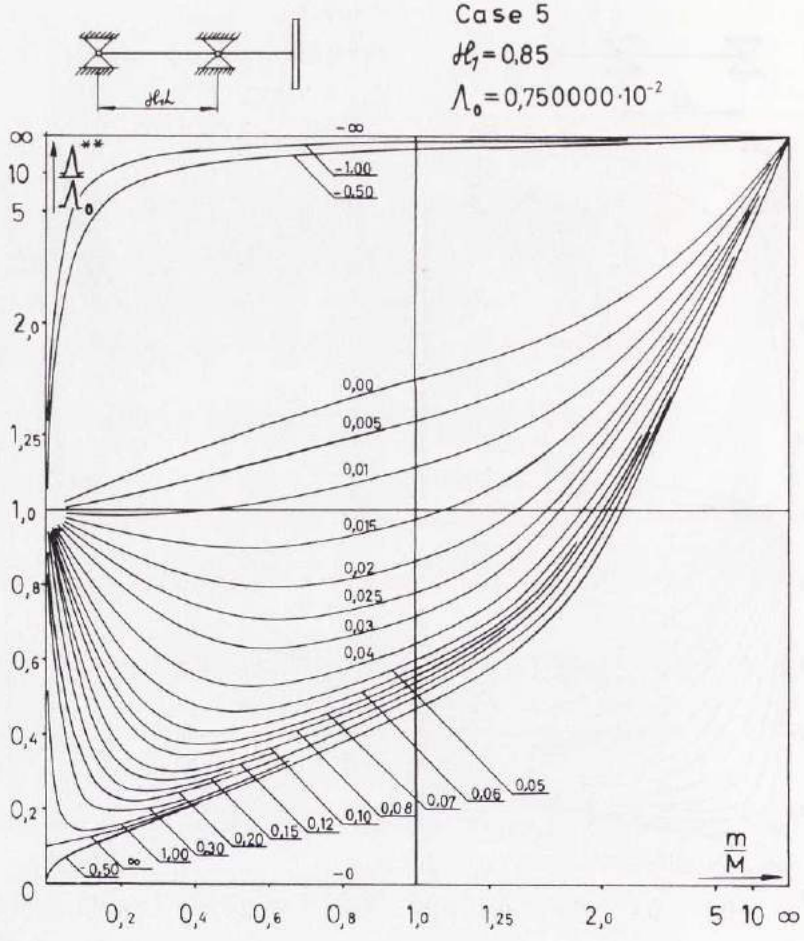
Case 5
$\mathcal{H}_1 = 0{,}85$
$\Lambda_0 = 0{,}750000 \cdot 10^{-2}$
$\mathcal{H}_1 L$
Λ^{**}
Λ_0
$-\infty$
-1,00
-0,50
0,00
0,005
0,01
0,015
0,02
0,025
0,03
0,04
0,05
0,06
0,07
0,08
0,10
0,12
0,15
0,20
0,30
1,00
∞
-0,50
-0
$\frac{m}{M}$
∞ 10 5 2,0 1,25 1,0 0,8 0,6 0,4 0,2 0
0,2 0,4 0,6 0,8 1,0 1,25 2,0 5 10 ∞

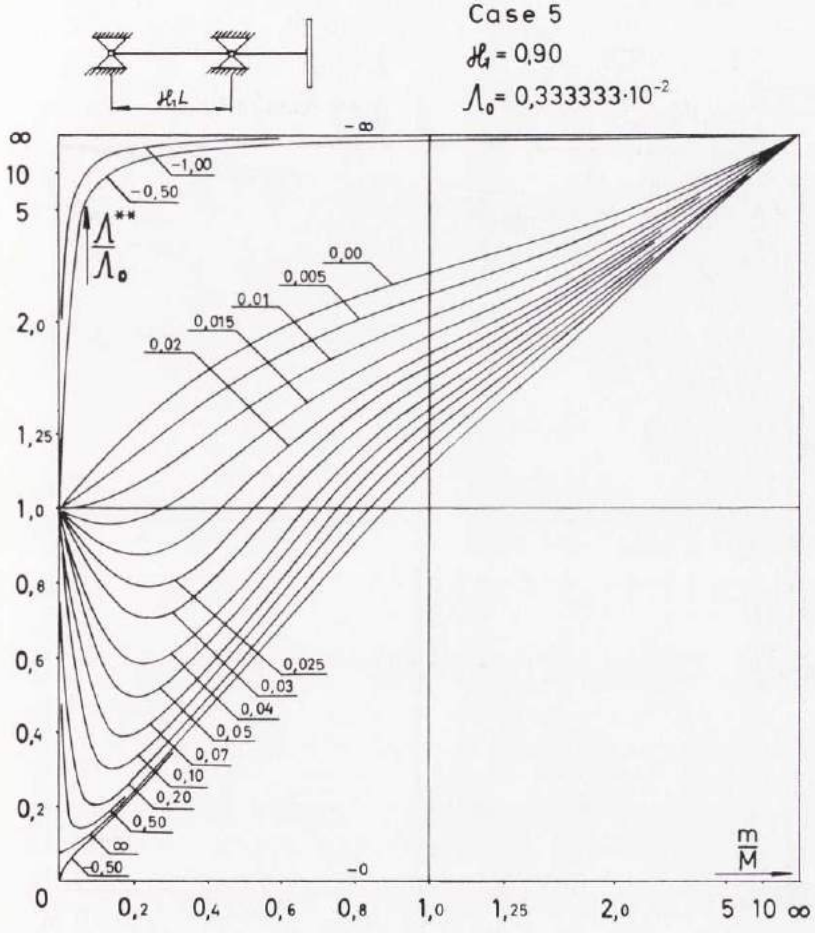
Case 5
$\mathcal{H}_1 = 0{,}90$
$\Lambda_0 = 0{,}333333 \cdot 10^{-2}$
$\mathcal{H}_1 L$
$\frac{\Lambda^{**}}{\Lambda_0}$
$\frac{m}{M}$
$-\infty$
$-1{,}00$
$-0{,}50$
$0{,}00$
$0{,}005$
$0{,}01$
$0{,}015$
$0{,}02$
$0{,}025$
$0{,}03$
$0{,}04$
$0{,}05$
$0{,}07$
$0{,}10$
$0{,}20$
$0{,}50$
∞
$-0{,}50$
-0
∞ 10 5 2,0 1,25 1,0 0,8 0,6 0,4 0,2 0
0,2 0,4 0,6 0,8 1,0 1,25 2,0 5 10 ∞

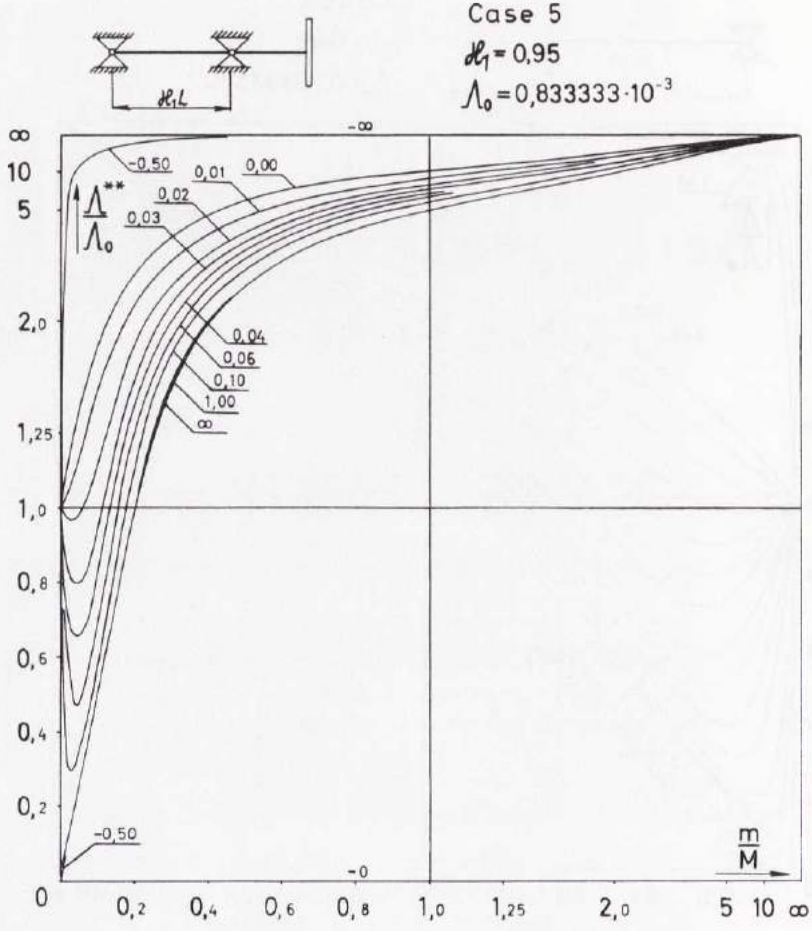
Case 5
$\alpha_1 = 0{,}95$
$\Lambda_0 = 0{,}833333 \cdot 10^{-3}$
$\alpha_1 L$
$\frac{\Lambda^{**}}{\Lambda_0}$
-∞
-0,50
0,01
0,00
0,02
0,03
0,04
0,06
0,10
1,00
∞
-0,50
-0
$\frac{m}{M}$
∞ 10 5 2,0 1,25 1,0 0,8 0,6 0,4 0,2 0
0,2 0,4 0,6 0,8 1,0 1,25 2,0 5 10 ∞

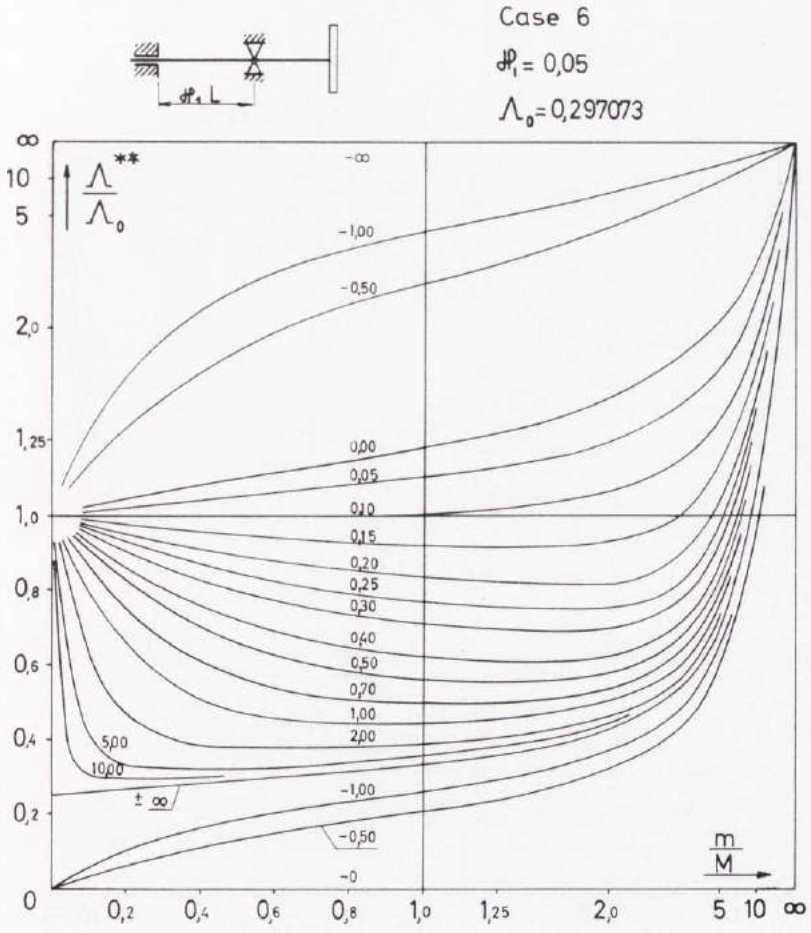
Case 6
$\alpha_1 = 0{,}05$
$\Lambda_0 = 0{,}297073$
$\frac{\Lambda^{**}}{\Lambda_0}$
$\frac{m}{M}$
$-\infty$
-1,00
-0,50
0,00
0,05
0,10
0,15
0,20
0,25
0,30
0,40
0,50
0,70
1,00
2,00
5,00
10,00
$\pm\infty$
-1,00
-0,50
-0
∞
10
5
2,0
1,25
1,0
0,8
0,6
0,4
0,2
0
0,2
0,4
0,6
0,8
1,0
1,25
2,0
5
10
∞

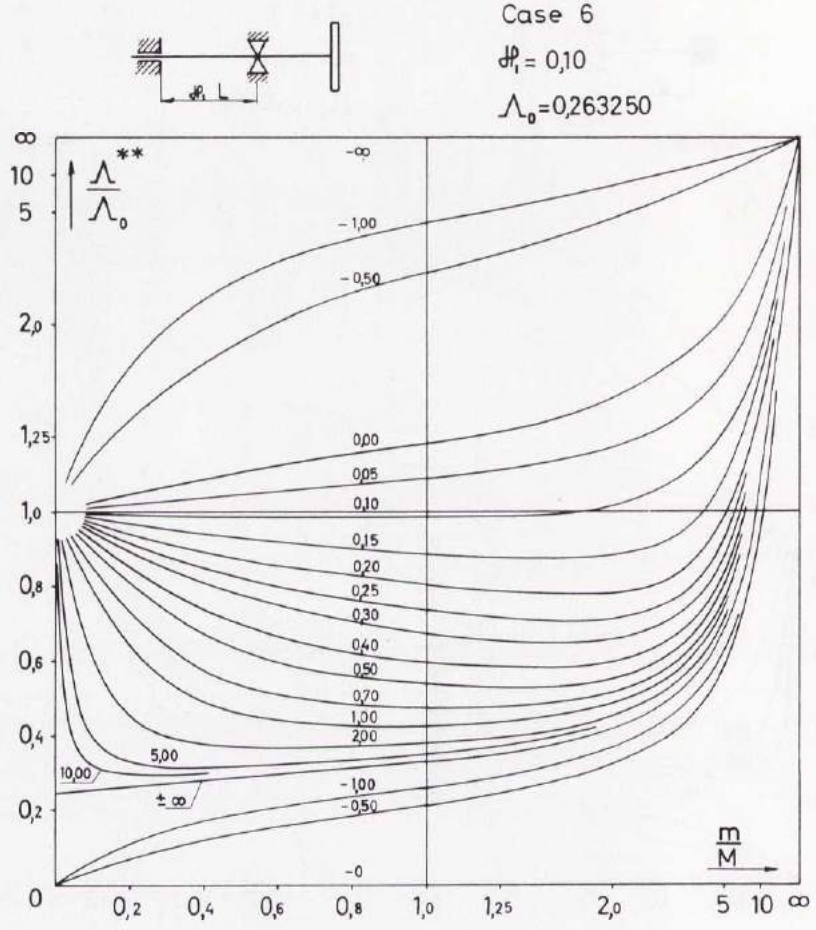
Case 6
$d\beta_1 = 0{,}10$
$\Lambda_0 = 0{,}263250$
$\frac{\Lambda^{**}}{\Lambda_0}$
$\frac{m}{M}$
-∞
-1,00
-0,50
0,00
0,05
0,10
0,15
0,20
0,25
0,30
0,40
0,50
0,70
1,00
2,00
5,00
10,00
± ∞
-1,00
-0,50
-0
∞
10
5
2,0
1,25
1,0
0,8
0,6
0,4
0,2
0
0,2
0,4
0,6
0,8
1,0
1,25
2,0
5
10
∞

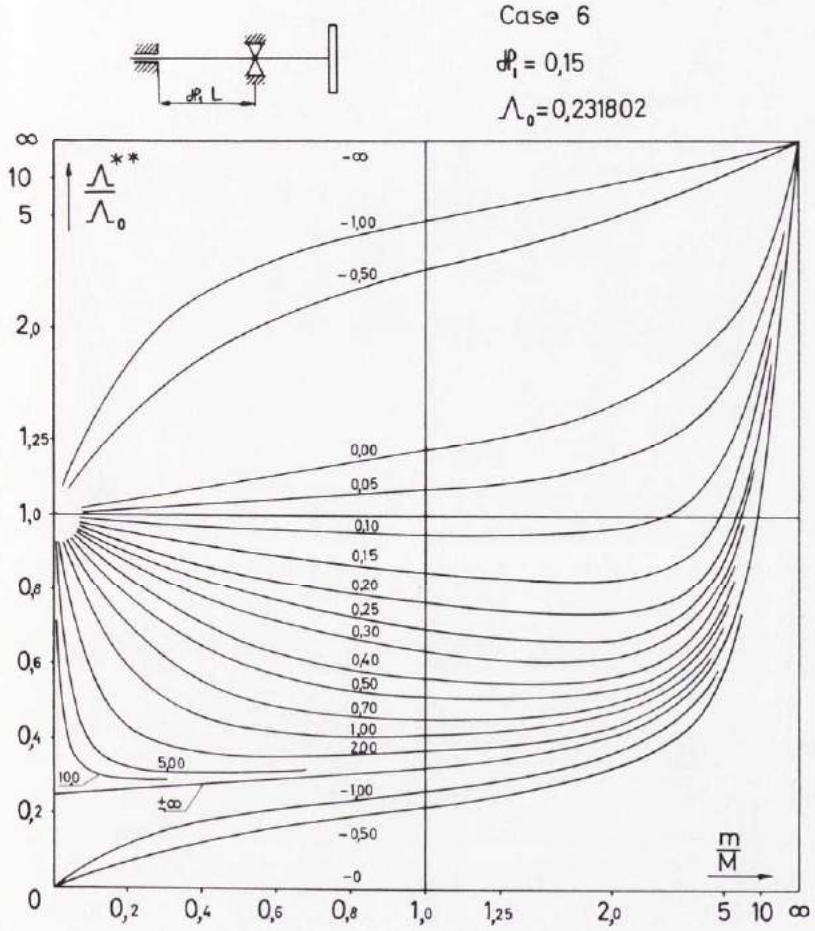
Case 6
dP1 = 0,15
Λ0 = 0,231802
dP1 L
Λ**/Λ0
-∞
-1,00
-0,50
0,00
0,05
0,10
0,15
0,20
0,25
0,30
0,40
0,50
0,70
1,00
2,00
5,00
10,0
±∞
-1,00
-0,50
-0
m/M
∞
10
5
2,0
1,25
1,0
0,8
0,6
0,4
0,2
0
0,2
0,4
0,6
0,8
1,0
1,25
2,0
5
10
∞

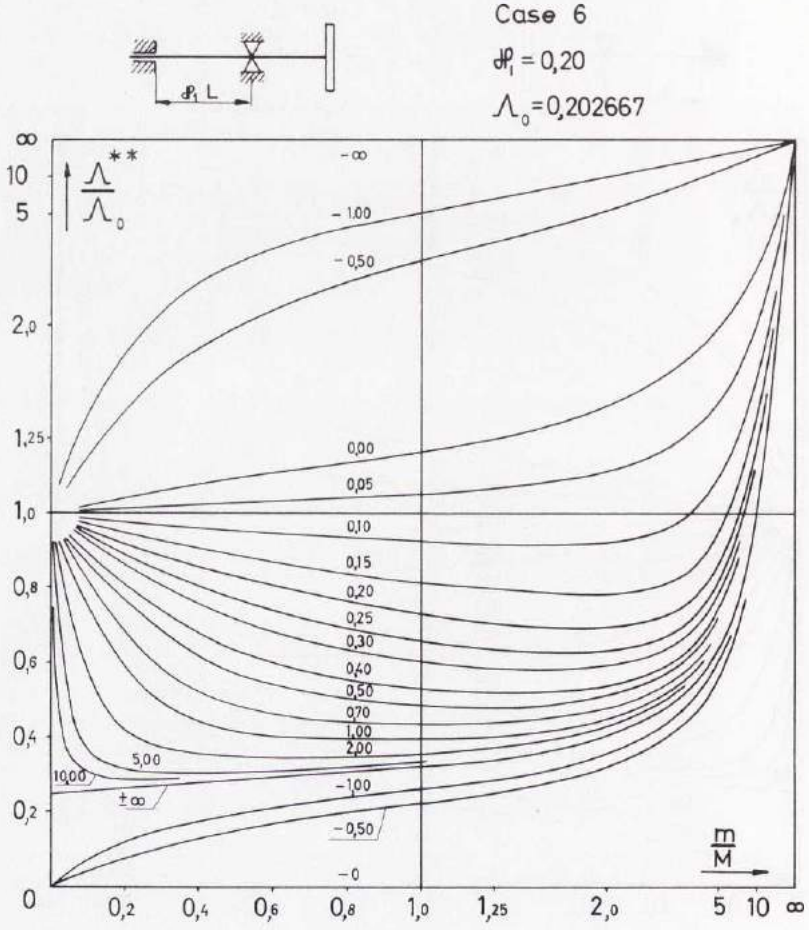
Case 6
$\alpha_1 = 0,20$
$\Lambda_0 = 0,202667$
$\alpha_1 L$
$\frac{\Lambda^{**}}{\Lambda_0}$
$\frac{m}{M}$
$-\infty$
-1,00
-0,50
0,00
0,05
0,10
0,15
0,20
0,25
0,30
0,40
0,50
0,70
1,00
2,00
5,00
10,00
$\pm\infty$
-1,00
-0,50
-0
∞
10
5
2,0
1,25
1,0
0,8
0,6
0,4
0,2
0
0,2
0,4
0,6
0,8
1,0
1,25
2,0
5
10
∞

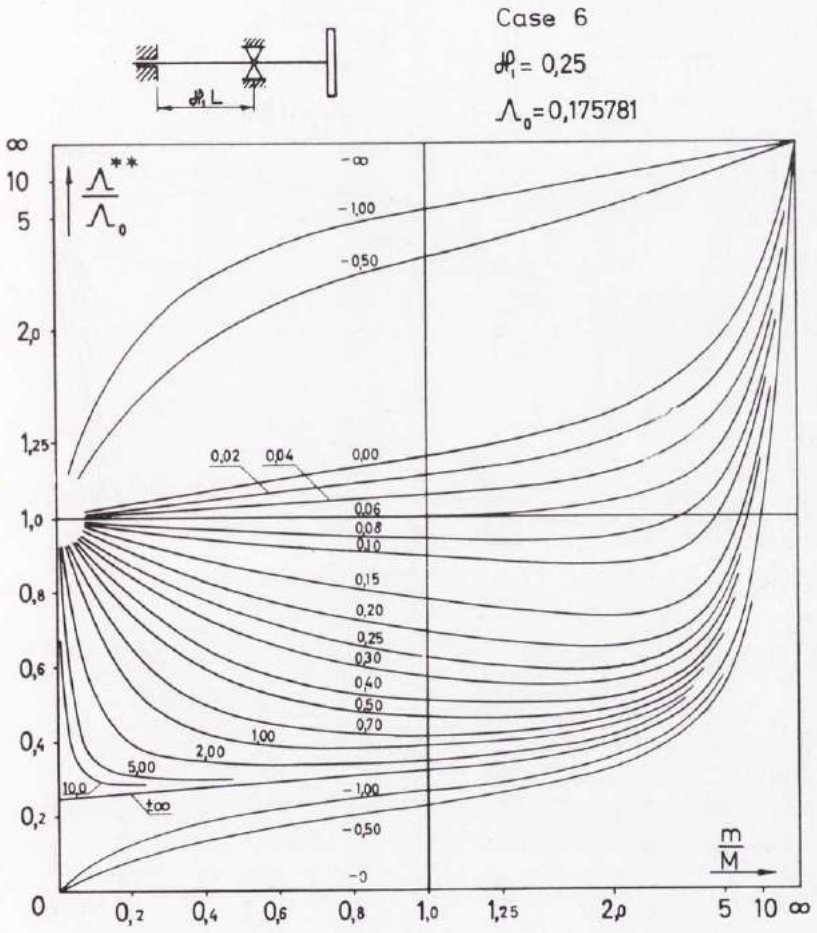
Case 6
$\alpha_1 = 0{,}25$
$\Lambda_0 = 0{,}175781$
$\alpha_1 L$
$\frac{\Lambda^{**}}{\Lambda_0}$
∞
10
5
2,0
1,25
1,0
0,8
0,6
0,4
0,2
0
$-\infty$
-1,00
-0,50
0,02
0,04
0,00
0,06
0,08
0,10
0,15
0,20
0,25
0,30
0,40
0,50
0,70
1,00
2,00
5,00
10,0
∞
-1,00
-0,50
-0
$\frac{m}{M}$
0,2
0,4
0,6
0,8
1,0
1,25
2,0
5
10
∞

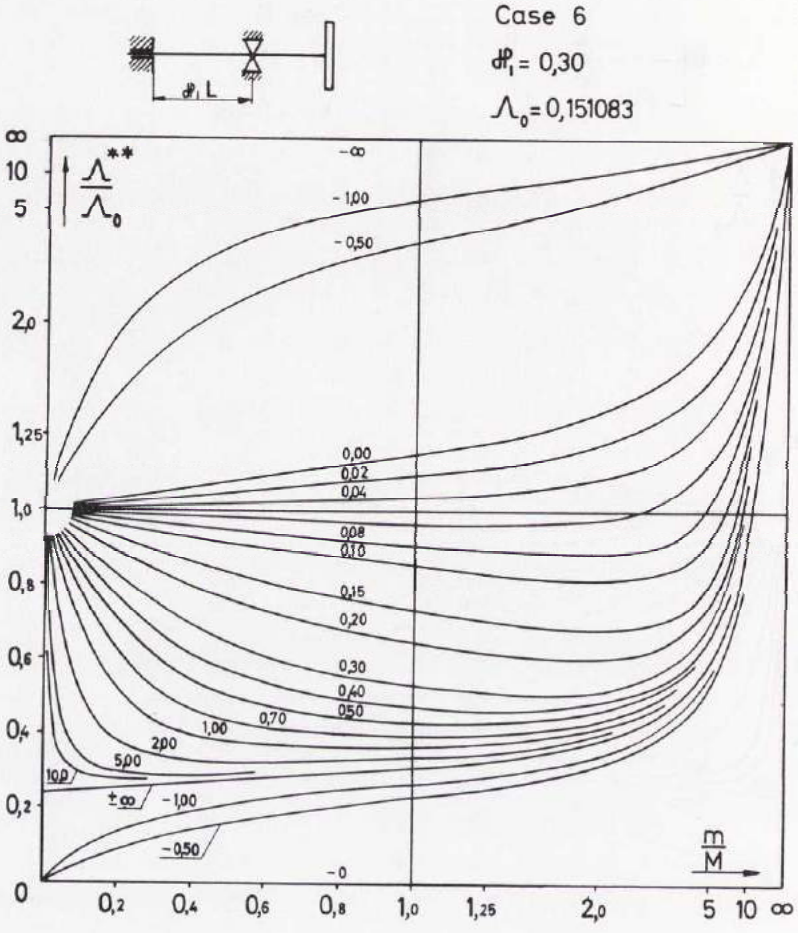
Case 6
$d\beta_1 = 0{,}30$
$\Lambda_0 = 0{,}151083$
$d\beta_1 L$
$\frac{\Lambda^{**}}{\Lambda_0}$
$\frac{m}{M}$
$-\infty$
-1,00
-0,50
0,00
0,02
0,04
0,08
0,10
0,15
0,20
0,30
0,40
0,50
0,70
1,00
2,00
5,00
10,0
$\pm\infty$
-1,00
-0,50
-0
∞ 10 5 2,0 1,25 1,0 0,8 0,6 0,4 0,2 0
0,2 0,4 0,6 0,8 1,0 1,25 2,0 5 10 ∞

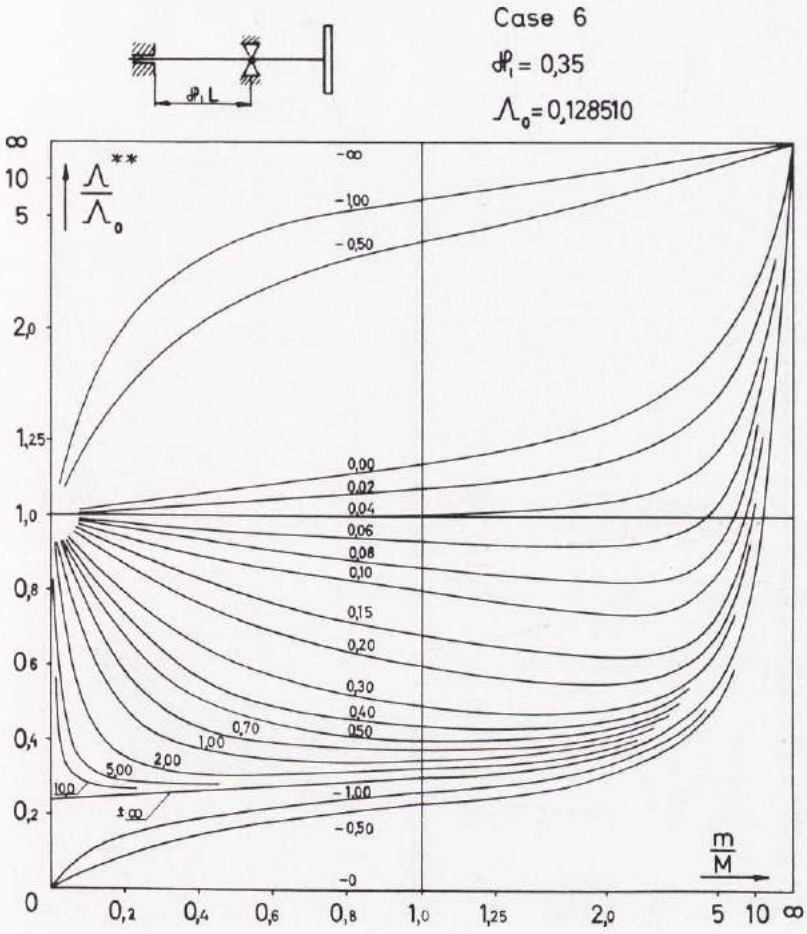
Case 6
$\alpha_1 = 0{,}35$
$\Lambda_0 = 0{,}128510$
$\alpha_1 L$
$\frac{\Lambda^{**}}{\Lambda_0}$
$\frac{m}{M}$
∞
10
5
2,0
1,25
1,0
0,8
0,6
0,4
0,2
0
0,2
0,4
0,6
0,8
1,0
1,25
2,0
5
10
∞
-∞
-100
-0,50
0,00
0,02
0,04
0,06
0,08
0,10
0,15
0,20
0,30
0,40
0,50
0,70
1,00
2,00
5,00
10,0
±∞
-1,00
-0,50
-0

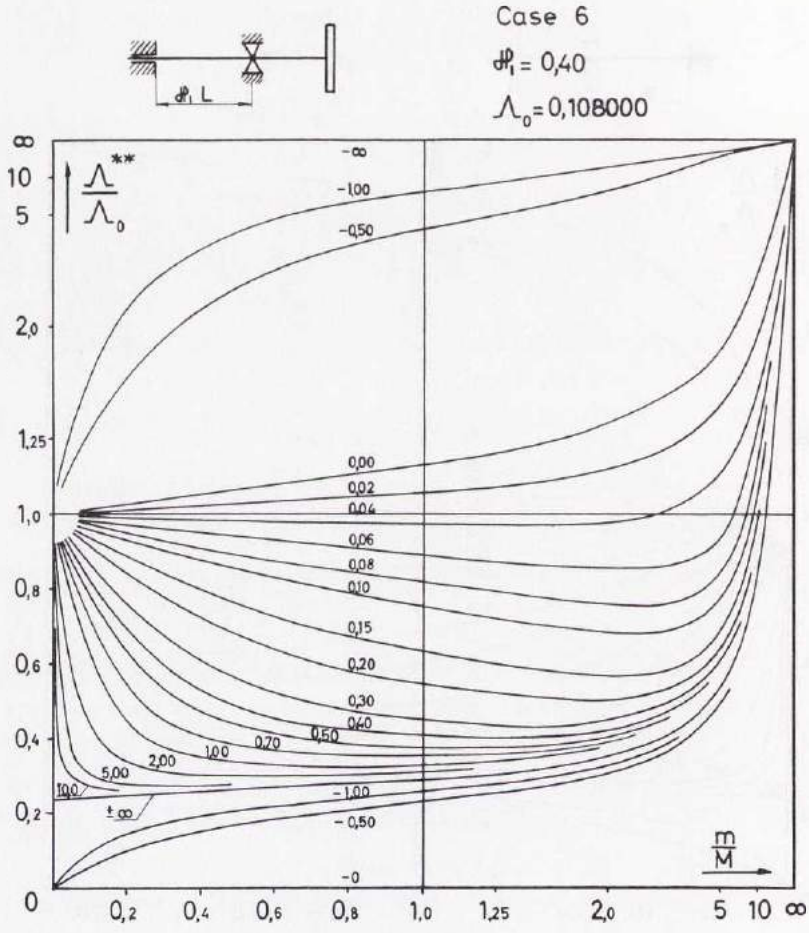
Case 6
$\alpha_1 = 0{,}40$
$\Lambda_0 = 0{,}108000$
$\alpha_1 L$
$\frac{\Lambda^{**}}{\Lambda_0}$
$\frac{m}{M}$
$-\infty$
-1,00
-0,50
0,00
0,02
0,04
0,06
0,08
0,10
0,15
0,20
0,30
0,40
0,50
0,70
1,00
2,00
5,00
10,0
$\pm\infty$
-1,00
-0,50
-0
0
0,2
0,4
0,6
0,8
1,0
1,25
2,0
5
10
∞

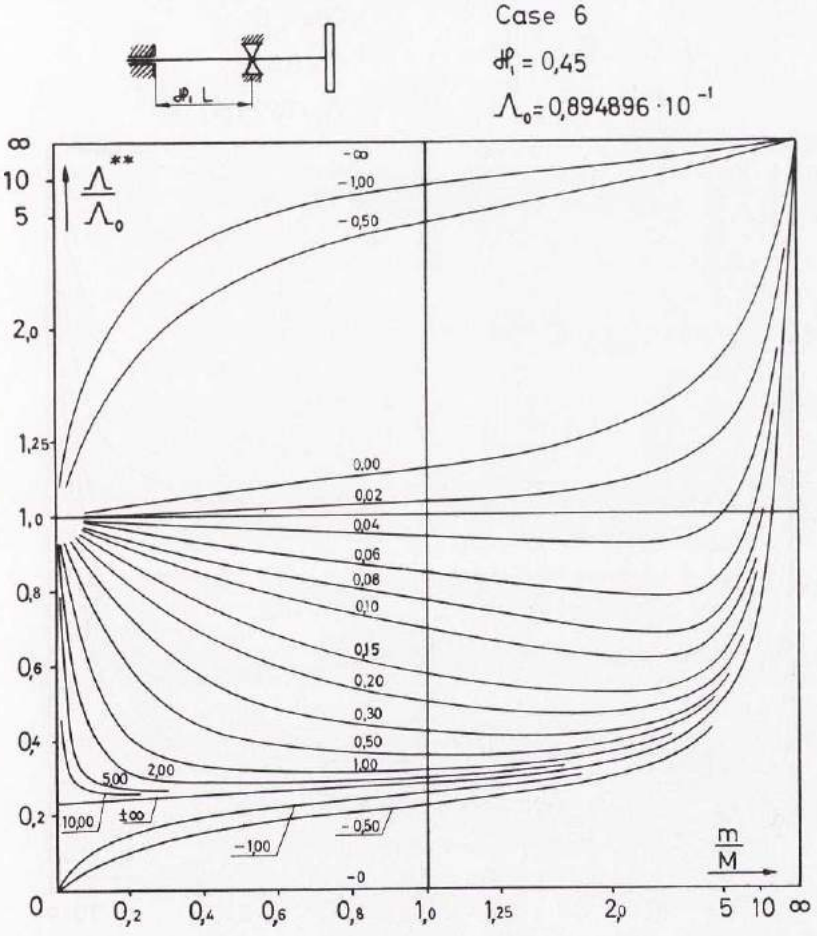
Case 6
$\alpha_1 = 0{,}45$
$\Lambda_0 = 0{,}894896 \cdot 10^{-1}$
$\alpha_1 L$
$\frac{\Lambda^{**}}{\Lambda_0}$
$\frac{m}{M}$
$-\infty$
-1,00
-0,50
0,00
0,02
0,04
0,06
0,08
0,10
0,15
0,20
0,30
0,50
1,00
2,00
5,00
10,00
$\pm\infty$
-1,00
-0,50
-0
∞
10
5
2,0
1,25
1,0
0,8
0,6
0,4
0,2
0
0,2
0,4
0,6
0,8
1,0
1,25
2,0
5
10
∞

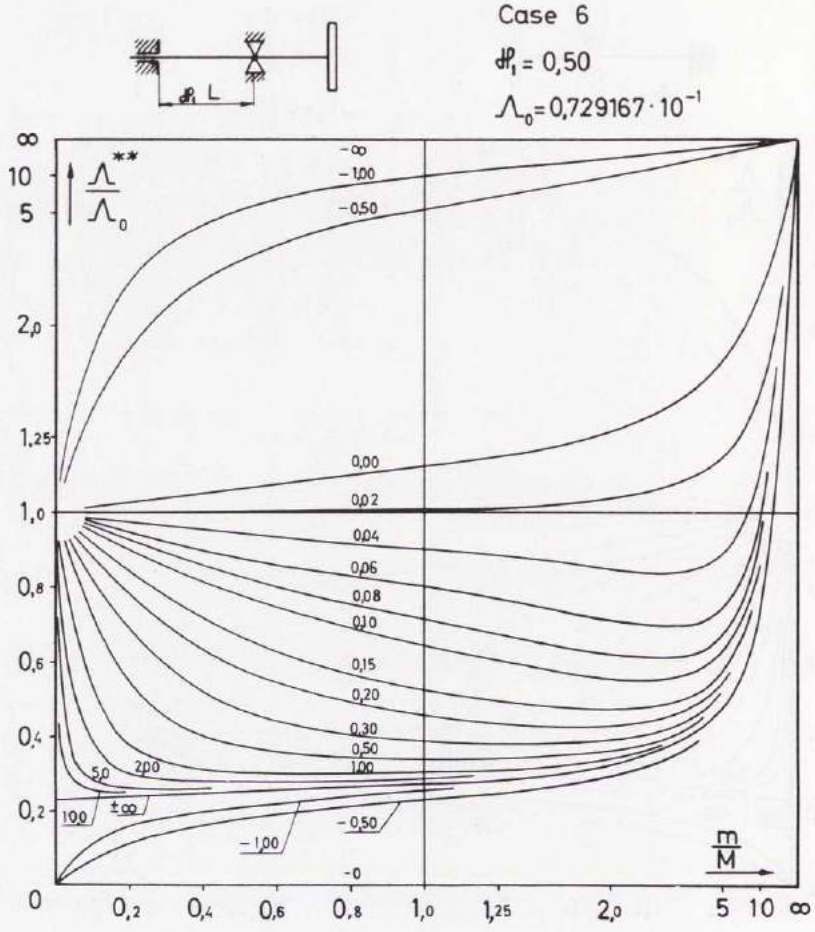
Case 6
$\alpha_1 = 0{,}50$
$\Lambda_0 = 0{,}729167 \cdot 10^{-1}$
$\alpha_1 L$
$\frac{\Lambda^{**}}{\Lambda_0}$
$\frac{m}{M}$
$-\infty$
$-1{,}00$
$-0{,}50$
0,00
0,02
0,04
0,06
0,08
0,10
0,15
0,20
0,30
0,50
1,00
2,00
5,0
100
$\pm\infty$
$-1{,}00$
$-0{,}50$
-0
0
0,2
0,4
0,6
0,8
1,0
1,25
2,0
5
10
∞

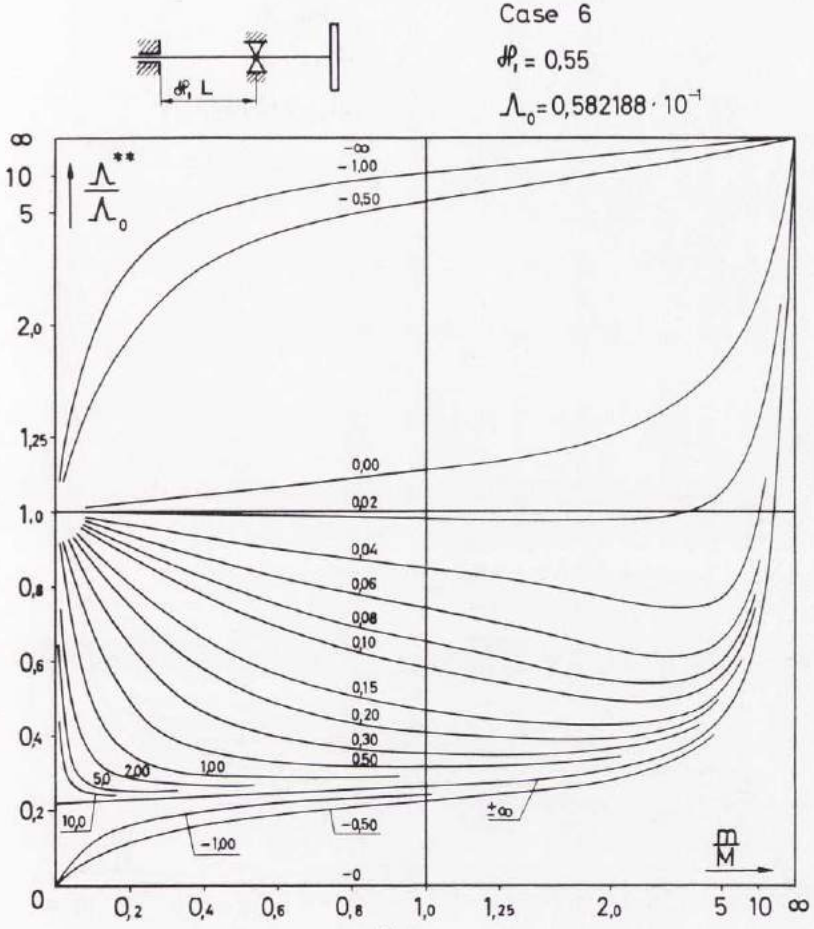
Case 6
$\mathcal{M}_1 = 0{,}55$
$\Lambda_0 = 0{,}582188 \cdot 10^{-1}$
$\mathcal{M}_1$, L
$\frac{\Lambda^{**}}{\Lambda_0}$
$\frac{m}{M}$
$-\infty$
$-1{,}00$
$-0{,}50$
0,00
0,02
0,04
0,06
0,08
0,10
0,15
0,20
0,30
0,50
1,00
2,00
5,0
10,0
$-1{,}00$
$-0{,}50$
-0
$\pm\infty$
0
0,2
0,4
0,6
0,8
1,0
1,25
2,0
5
10
∞

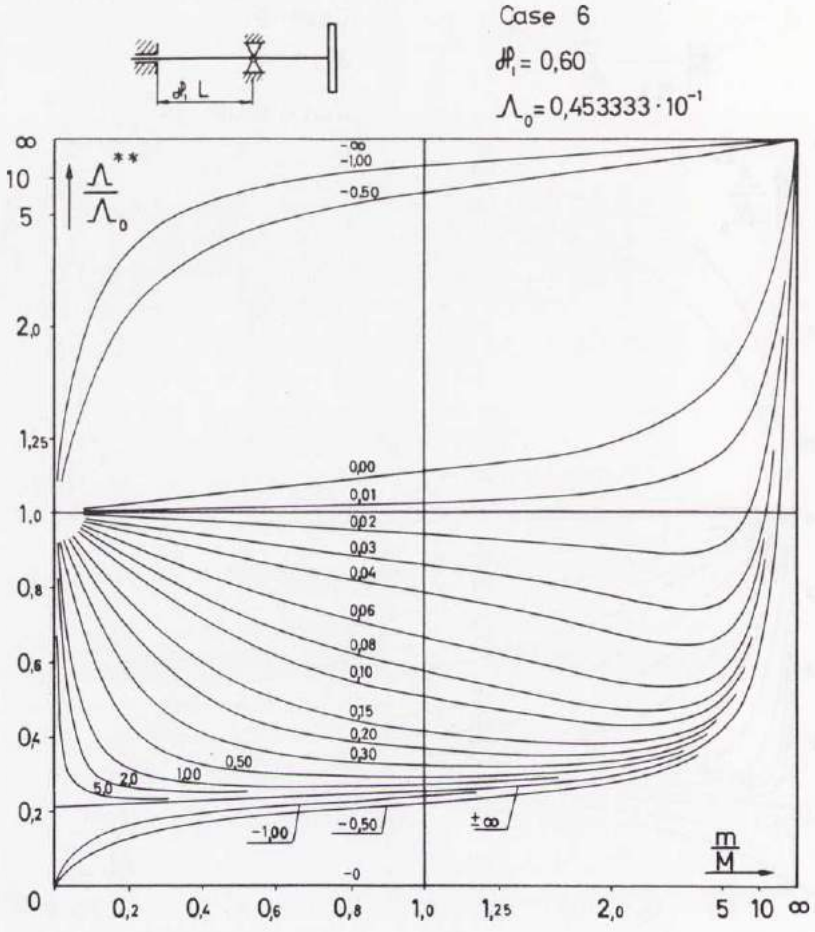
Case 6
$\vartheta_1 = 0{,}60$
$\Lambda_0 = 0{,}453333 \cdot 10^{-1}$
$\vartheta_1 L$
$\frac{\Lambda^{**}}{\Lambda_0}$
$\frac{m}{M}$
-∞
-1,00
-0,50
0,00
0,01
0,02
0,03
0,04
0,06
0,08
0,10
0,15
0,20
0,30
0,50
1,00
2,0
5,0
-1,00
-0,50
-0
±∞
∞
10
5
2,0
1,25
1,0
0,8
0,6
0,4
0,2
0
0,2
0,4
0,6
0,8
1,0
1,25
2,0
5
10
∞

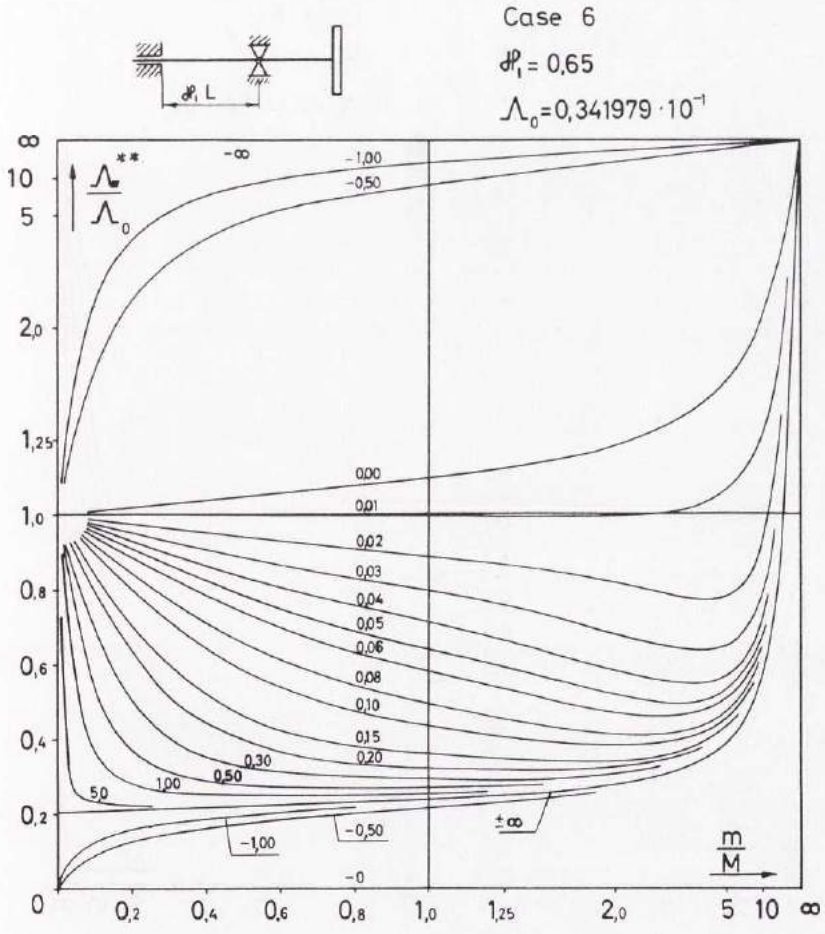
Case 6
$\alpha_1 = 0{,}65$
$\Lambda_0 = 0{,}341979 \cdot 10^{-1}$
α_1, L
$\frac{\Lambda_*}{\Lambda_0}$
**
$-\infty$
-1,00
-0,50
0,00
0,01
0,02
0,03
0,04
0,05
0,06
0,08
0,10
0,15
0,20
0,30
0,50
1,00
5,0
$\pm\infty$
-0
$\frac{m}{M}$
∞
10
5
2,0
1,25
1,0
0,8
0,6
0,4
0,2
0
0,2
0,4
0,6
0,8
1,0
1,25
2,0
5
10
∞

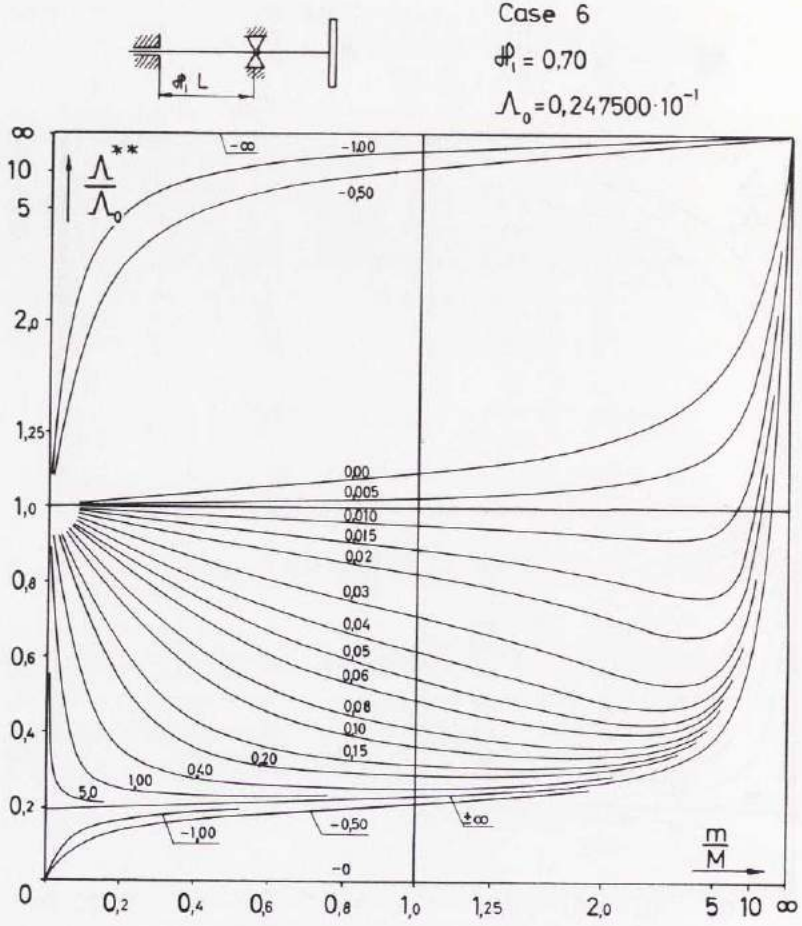
Case 6
$\alpha_1 = 0{,}70$
$\Lambda_0 = 0{,}247500 \cdot 10^{-1}$
$\alpha_1 L$
$\frac{\Lambda}{\Lambda_0}$ **
$\frac{m}{M}$
-∞
-1,00
-0,50
0,00
0,005
0,010
0,015
0,02
0,03
0,04
0,05
0,06
0,08
0,10
0,15
0,20
0,40
1,00
5,0
±∞
-1,00
-0,50
-0
0
0,2
0,4
0,6
0,8
1,0
1,25
2,0
5
10
∞

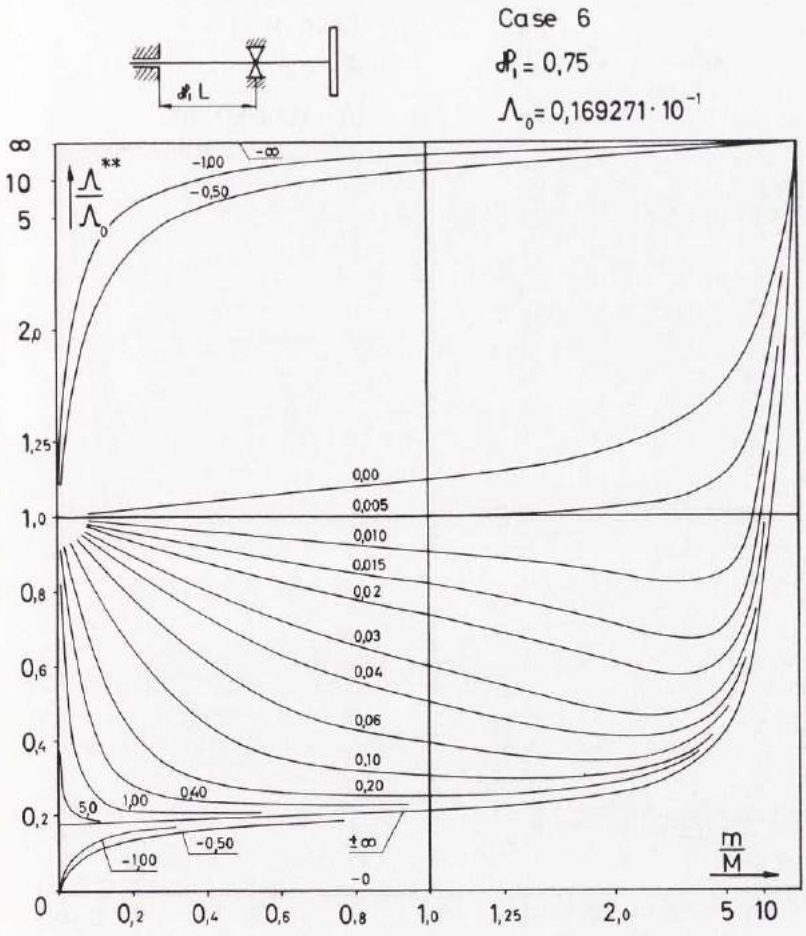
Case 6
$\alpha_1 = 0{,}75$
$\Lambda_0 = 0{,}169271 \cdot 10^{-1}$
$\alpha_1 L$
$\frac{\Lambda^{**}}{\Lambda_0}$
∞
10
5
2,0
1,25
1,0
0,8
0,6
0,4
0,2
0
-1,00
-∞
-0,50
0,00
0,005
0,010
0,015
0,02
0,03
0,04
0,06
0,10
0,20
0,40
1,00
5,0
-1,00
-0,50
±∞
-0
$\frac{m}{M}$
0,2
0,4
0,6
0,8
1,0
1,25
2,0
5
10

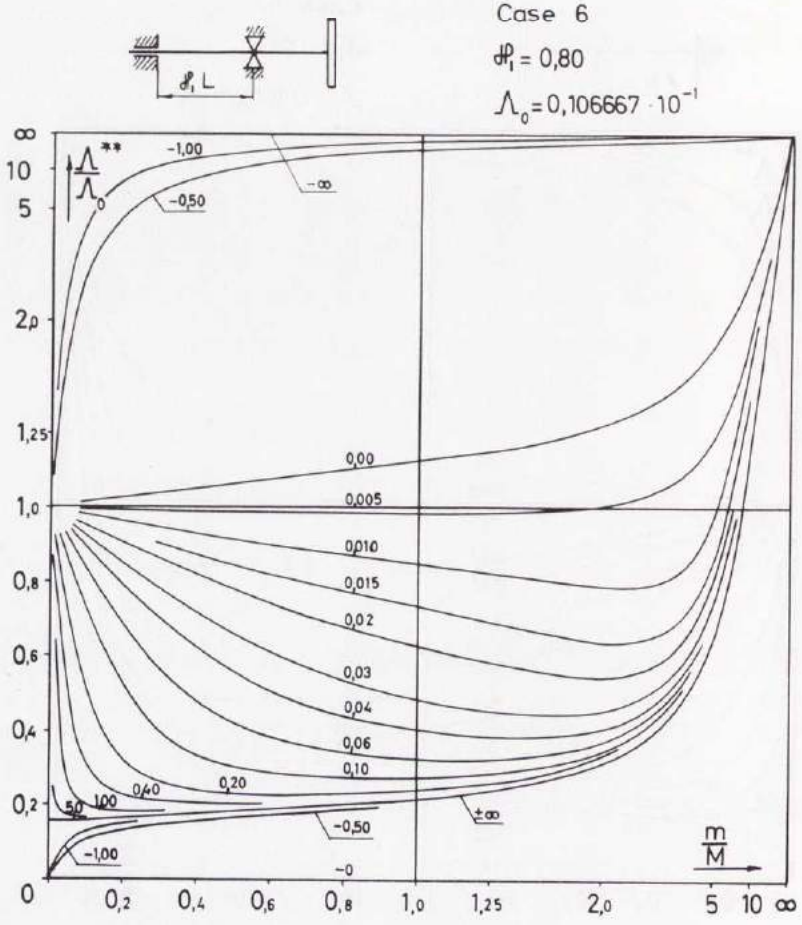
Case 6
$\alpha_1 = 0{,}80$
$\Lambda_0 = 0{,}106667 \cdot 10^{-1}$
$\alpha_1 L$
$\frac{\Lambda}{\Lambda_0}$ **
-1,00
-0,50
-∞
0,00
0,005
0,010
0,015
0,02
0,03
0,04
0,06
0,10
0,20
0,40
1,00
5,0
∞
±∞
-0,50
-1,00
-0
$\frac{m}{M}$
0
0,2
0,4
0,6
0,8
1,0
1,25
2,0
5
10
∞
0,2
0,4
0,6
0,8
1,0
1,25
2,0
5
10
∞

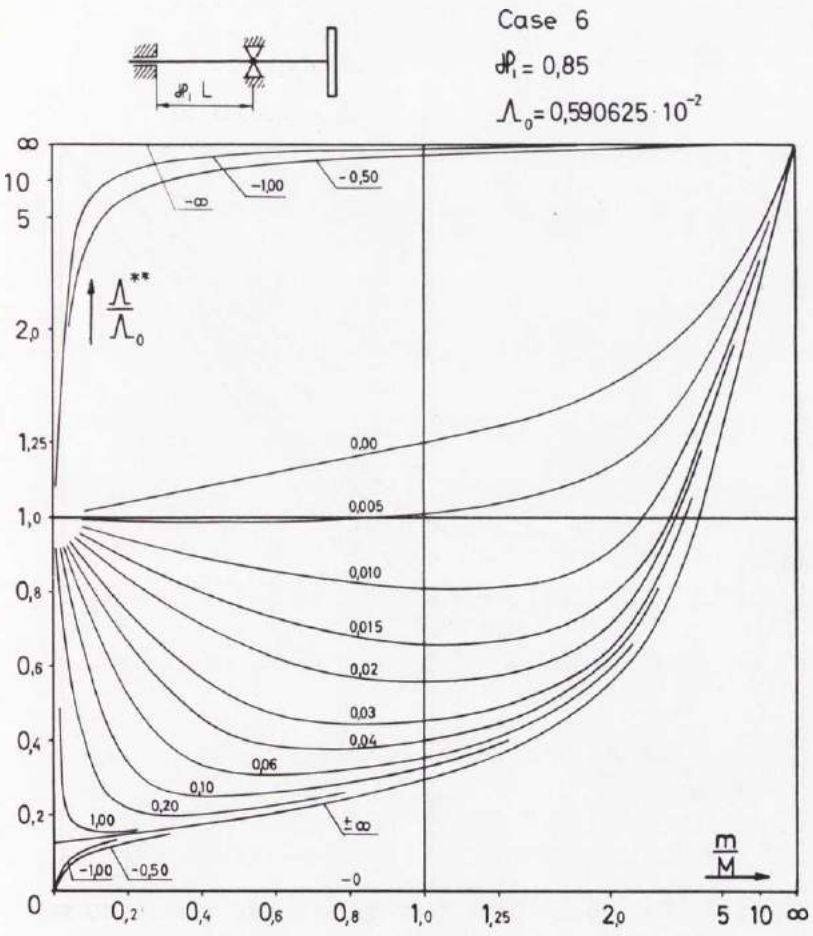
Case 6
$\alpha P_1 = 0{,}85$
$\Lambda_0 = 0{,}590625 \cdot 10^{-2}$
αP_1 L
$\frac{\Lambda^{**}}{\Lambda_0}$
$\frac{m}{M}$
-∞
-1,00
-0,50
0,00
0,005
0,010
0,015
0,02
0,03
0,04
0,06
0,10
0,20
1,00
±∞
-0
-1,00
-0,50
∞
10
5
2,0
1,25
1,0
0,8
0,6
0,4
0,2
0
0,2
0,4
0,6
0,8
1,0
1,25
2,0
5
10
∞

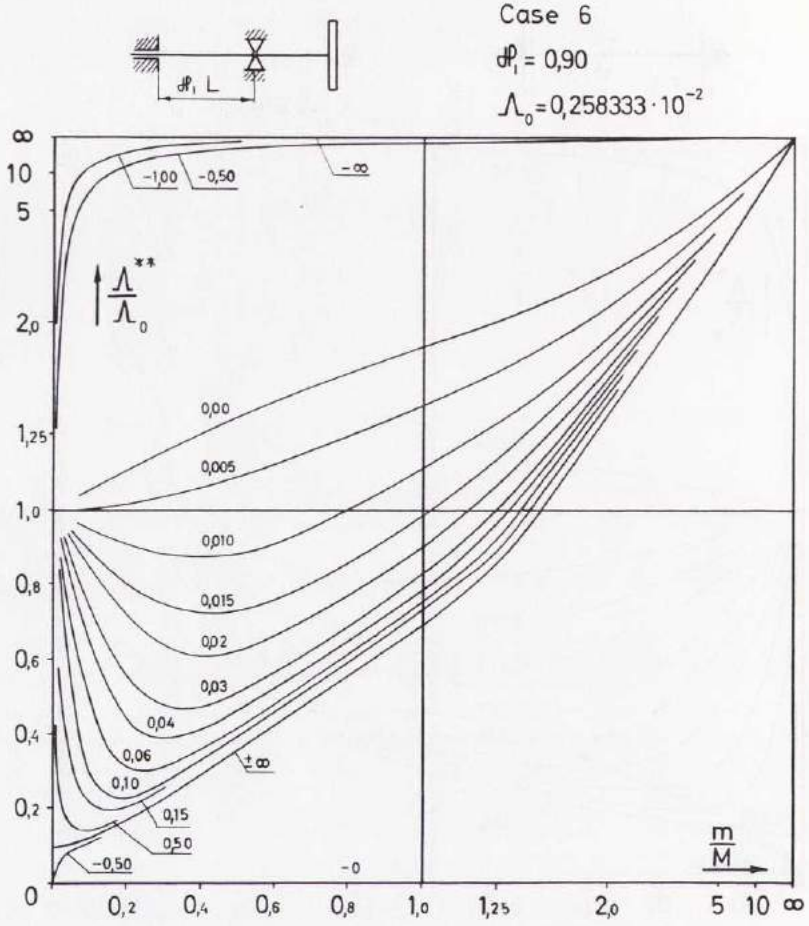
Case 6
dP1 = 0,90
Λ0 = 0,258333 · 10⁻²
dP1 L
Λ**/Λ0
m/M
-1,00
-0,50
-∞
0,00
0,005
0,010
0,015
0,02
0,03
0,04
0,06
0,10
0,15
0,50
±∞
-0,50
-0
∞
10
5
2,0
1,25
1,0
0,8
0,6
0,4
0,2
0
0,2
0,4
0,6
0,8
1,0
1,25
2,0
5
10
∞

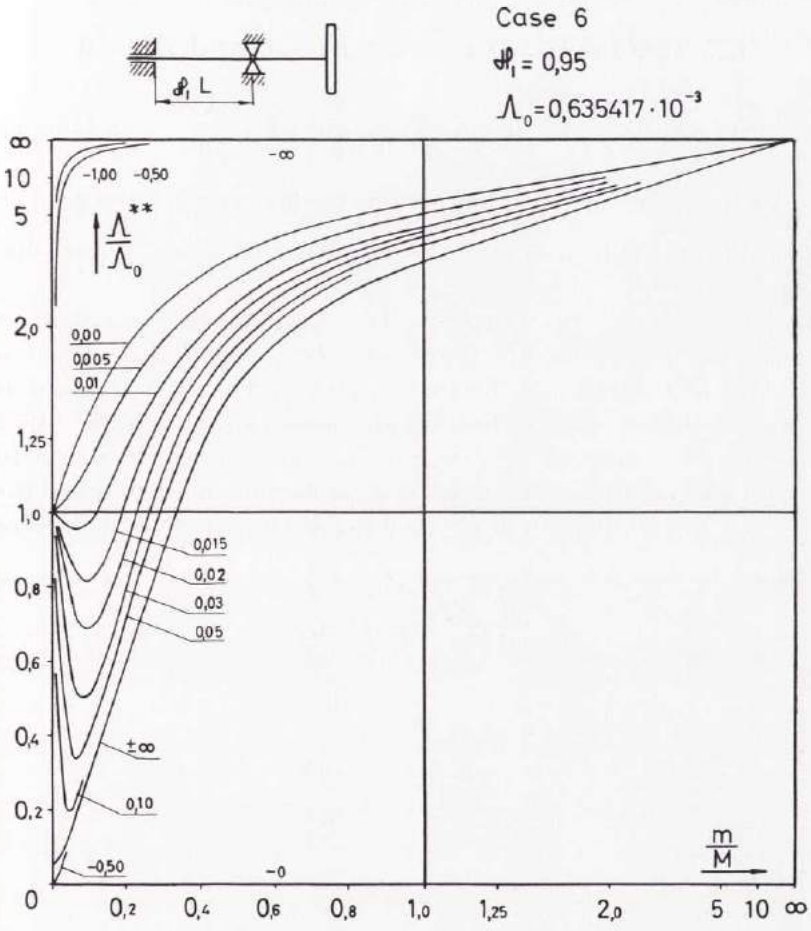
Case 6
$\vartheta_1 = 0{,}95$
$\Lambda_0 = 0{,}635417 \cdot 10^{-3}$
ϑ_1 L
$\frac{\Lambda^{**}}{\Lambda_0}$
-1,00
-0,50
$-\infty$
0,00
0,005
0,01
0,015
0,02
0,03
0,05
$\pm\infty$
0,10
-0,50
-0
$\frac{m}{M}$
0
0,2
0,4
0,6
0,8
1,0
1,25
2,0
5
10
∞

12. Special Diagrams for $m = 0$ and $M = 0$

In the previous chapter diagrams were given for $\frac{\Lambda^{**}}{\Lambda_0}$ as a function of $\frac{m}{M}$. However, the accuracy of the reading is not very good in the vicinity of the boundary of the diagrams. Therefore, special diagrams are drawn for these cases.

Starting with $m = 0$ we may conclude that this means a shaft of no mass but with a certain flexural rigidity, and this condition is prevailing in the chapters before Chapter 9. The critical speed is wanted for the six cases of bearing arrangement shown in fig. 107.1 when the polar moment of inertia of the disc grows from zero to infinity. The parameter Θ^* must not be used because it takes the value ∞ if $m = 0$. Instead of Θ^* we use ν which is already defined as

$$\nu = \left(\frac{\omega}{\Omega} - \frac{I_e}{I_p}\right) \cdot \frac{I_p}{ML^2}$$

or, if

$$\gamma = \frac{1}{2}\left(\frac{\omega}{\Omega} - \frac{I_e}{I_p}\right)$$

we have

$$\nu = \frac{2\gamma I_p}{ML^2} \quad \left(\text{Compare } \Theta^* = \frac{2\gamma I_p}{mL^2}\right)$$

For a shaft with one disc the eq. 110.2 gives

$$\Lambda^* = \frac{\xi_{F11} + \nu\zeta_{M11}}{2} \pm \sqrt{\frac{(\xi_{F11} + \nu\zeta_{M11})^2}{4} + \nu(\xi_{M11}\zeta_{F11} - \xi_{F11}\zeta_{M11})}$$

The values of the different influence numbers depends both on the actual bearing arrangement and on the position of the disc on the shaft. They are all calculated in Chapter 14. Further $\Lambda_0 = \xi_{F11}$ and in general

$$\frac{\Lambda^*}{\Lambda_0} = \frac{1}{2\xi_{F11}} \left\{ \xi_{F11} + \nu\zeta_{M11} \pm \sqrt{(\xi_{F11} + \nu\zeta_{M11})^2 + 4\nu(\xi_{M11}\zeta_{F11} - \xi_{F11}\zeta_{M11})} \right\}$$

Specially $\frac{\Lambda^*}{\Lambda_0} = 1$ for $\nu = 0$ and $\frac{\Lambda^*}{\Lambda_0} = 1 - \frac{\xi_{M11}\zeta_{F11}}{\xi_{F11}\zeta_{M11}}$ for $\nu = \infty$.

This formula was calculated by an electronic computer. The result is collected in six diagrams on page 198 up to and including page 203. The critical angular velocity Ω then is obtained from

$$\Omega^2 = \frac{1}{\Lambda^*} \cdot \frac{EI}{ML^3}$$

For small values of ν one can use the expression

$$\frac{\Lambda^*}{\Lambda_0} = 1 - \nu \left(\frac{\xi_{M11}}{\xi_{F11}} \right)^2$$

Compare the formula by Hahn in Chapter 10 which gives

$$\frac{\Lambda_H}{\Lambda_0} = 1 + \nu \frac{\zeta_{M11}}{\xi_{F11}}$$

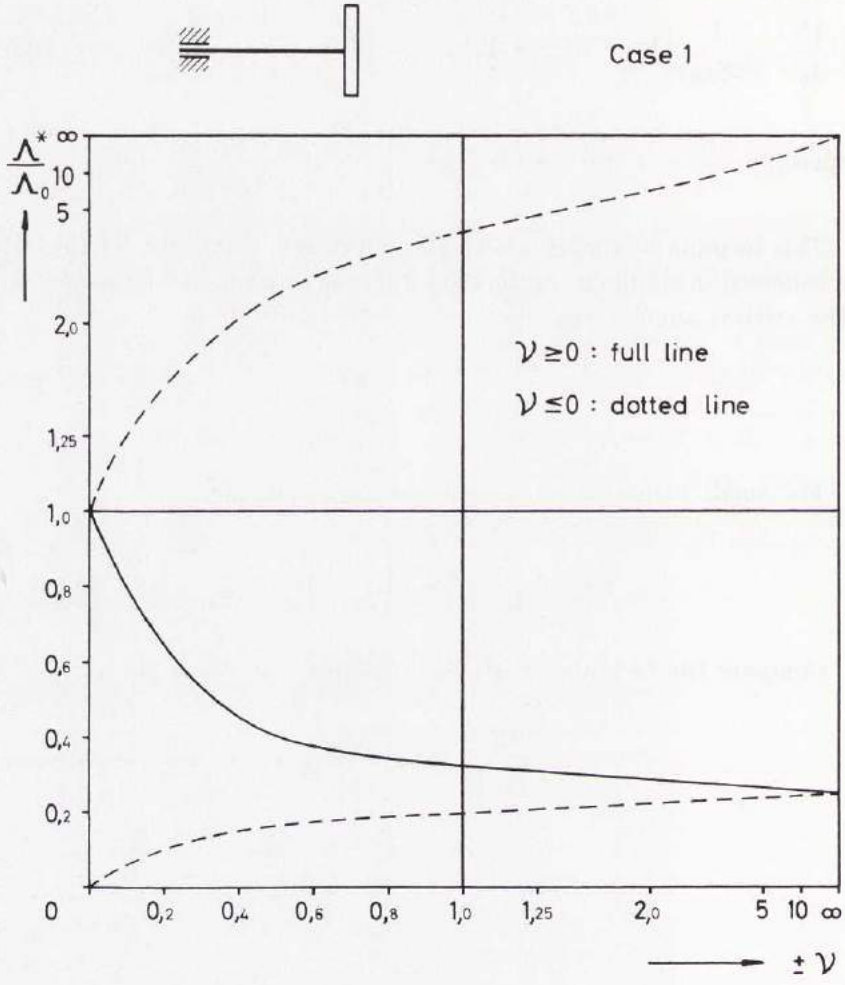
Case 1
$\frac{\Lambda^*}{\Lambda_0}$
∞
10
5
2,0
1,25
1,0
0,8
0,6
0,4
0,2
0
$\nu \geq 0$: full line
$\nu \leq 0$: dotted line
0,2
0,4
0,6
0,8
1,0
1,25
2,0
5
10
∞
$\pm \nu$

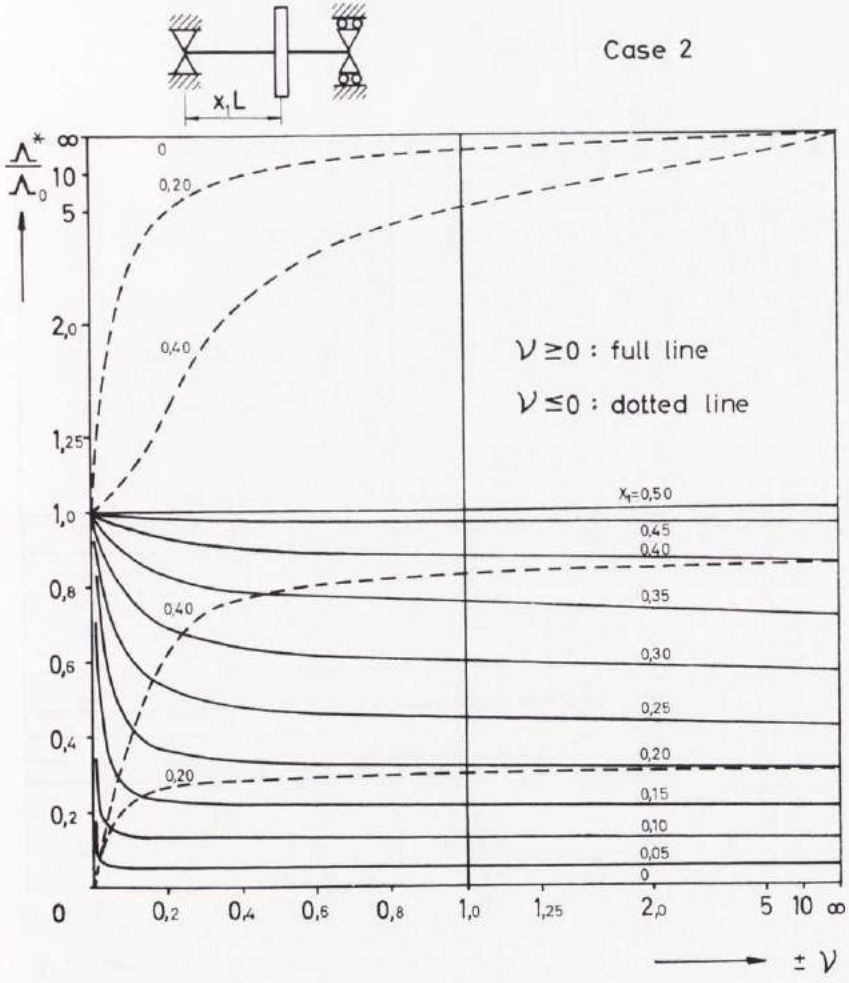
Case 2
x, L
Λ*/Λ0
∞
10
5
2,0
1,25
1,0
0,8
0,6
0,4
0,2
0
0,20
0,40
ν ≥ 0 : full line
ν ≤ 0 : dotted line
x1=0,50
0,45
0,40
0,35
0,30
0,25
0,20
0,15
0,10
0,05
0
0,2
0,4
0,6
0,8
1,0
1,25
2,0
5
10
∞
± ν

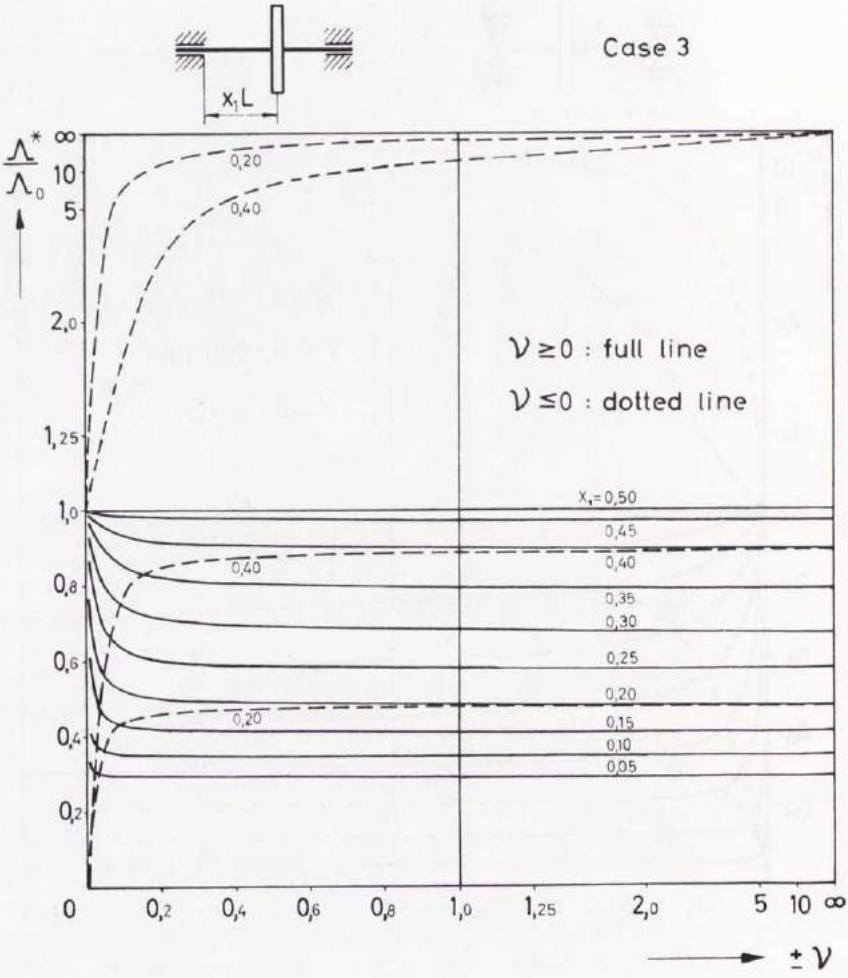
Case 3
x₁L
Λ*/Λ₀
∞
10
5
2,0
1,25
1,0
0,8
0,6
0,4
0,2
0
0,2
0,4
0,6
0,8
1,0
1,25
2,0
5
10
∞
± ν
ν ≥ 0 : full line
ν ≤ 0 : dotted line
0,20
0,40
0,40
0,20
x₁ = 0,50
0,45
0,40
0,35
0,30
0,25
0,20
0,15
0,10
0,05

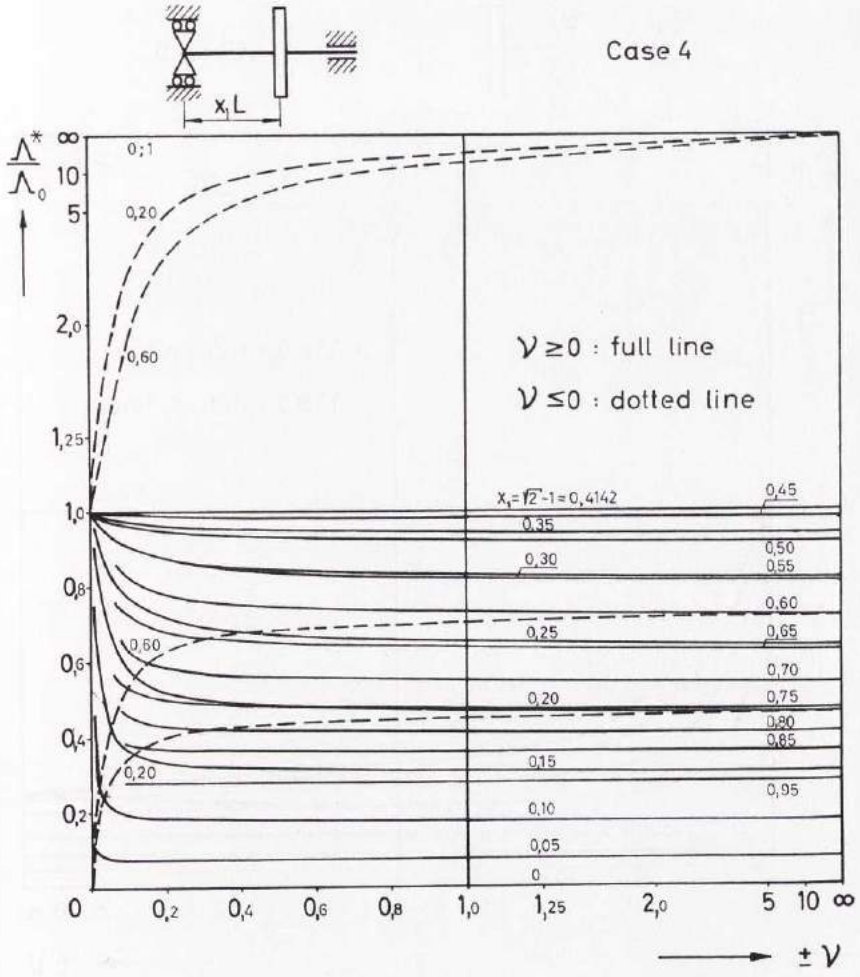
Case 4
x₁L
Λ*/Λ₀
∞
10
5
2,0
1,25
1,0
0,8
0,6
0,4
0,2
0
0;1
0,20
0,60
0,60
0,20
ν ≥ 0 : full line
ν ≤ 0 : dotted line
x₁ = √2 - 1 = 0,4142
0,45
0,35
0,30
0,50
0,55
0,60
0,25
0,65
0,70
0,20
0,75
0,80
0,85
0,15
0,95
0,10
0,05
0
0,2
0,4
0,6
0,8
1,0
1,25
2,0
5
10
∞
± ν

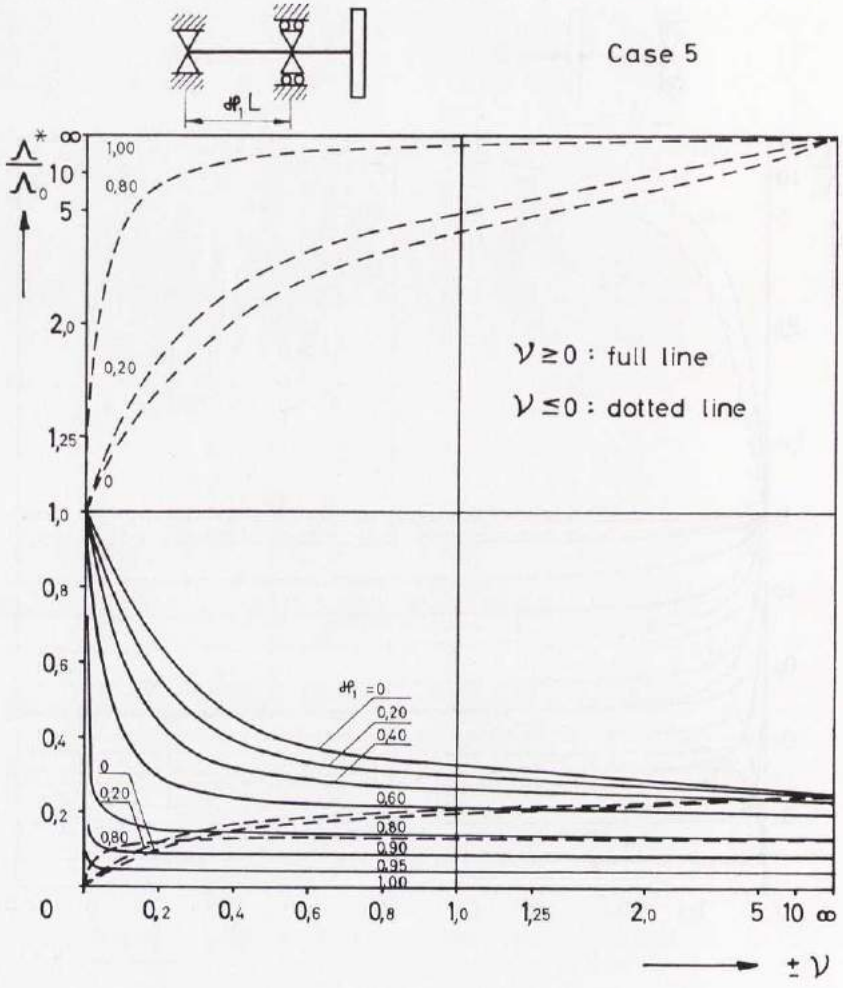
Case 5
dP₁ L
Λ*/Λ₀
∞
10
5
2,0
1,25
1,0
0,8
0,6
0,4
0,2
0
1,00
0,80
0,20
0
ν ≥ 0 : full line
ν ≤ 0 : dotted line
dP₁ = 0
0,20
0,40
0,60
0,80
0,90
0,95
1,00
0
0,20
0,80
0,2
0,4
0,6
0,8
1,0
1,25
2,0
5
10
∞
± ν

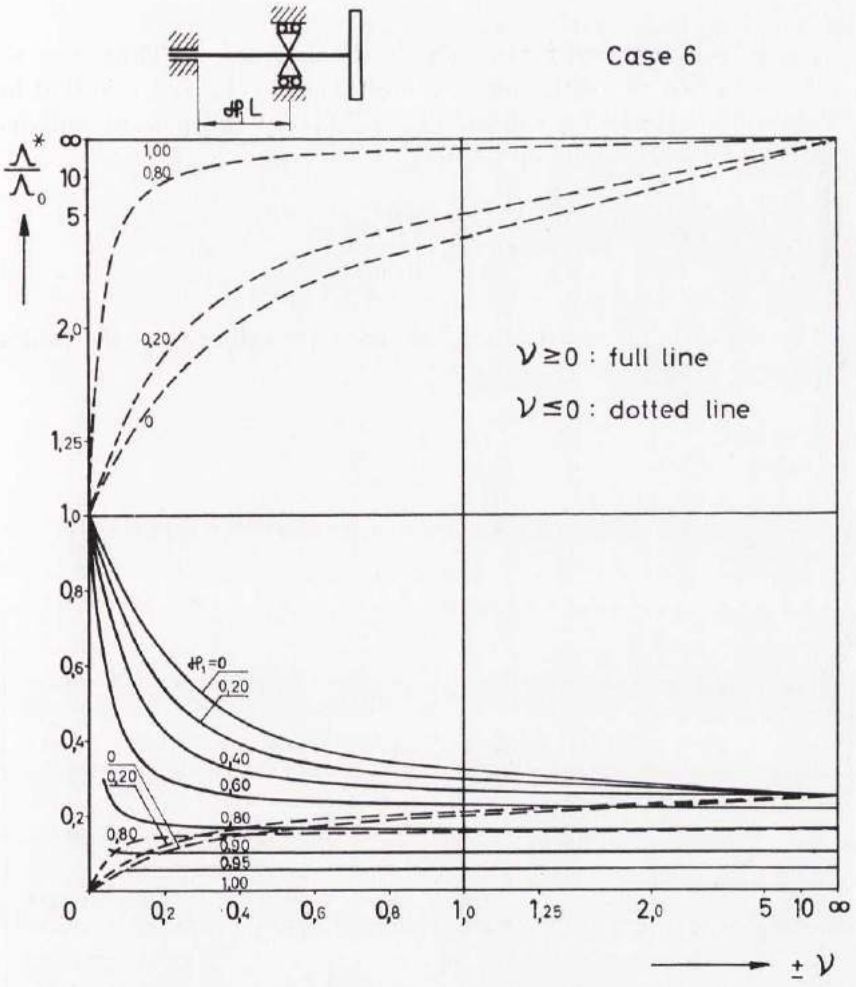
Case 6
dP L
Λ*/Λ0
∞
10
5
2,0
1,25
1,0
0,8
0,6
0,4
0,2
0
1,00
0,80
0,20
0
ν≥0 : full line
ν≤0 : dotted line
dP1=0
0,20
0,40
0,60
0,80
0,90
0,95
1,00
0
0,20
0,80
0,2
0,4
0,6
0,8
1,0
1,25
2,0
5
10
∞
± ν

The other boundary case to be treated is $M = 0$. From the previous chapters we have

$$\frac{m}{M} = \lambda \cdot \frac{A+\Theta B}{C+\Theta D}$$

The condition stated means practically that $\Theta = 0$. Thus $A = \infty$ or $C = 0$ gives the satisfying λ-values. These values can be find in "Tables for Calculating Critical Speeds" [4] by the present author. We may write the critical angular velocity as

$$\Omega = \lambda^2 \sqrt{\frac{EI}{mL^3}}$$

The λ^2-values for the first critical speed are collected in the tables 204.1 and 204.2.

Case	1	2	3	4
λ^2	3,516	9,870	22,373	15,418

Table 204.1

$\varkappa_1$	0,00	0,05	0,10	0,15	0,20	0,25	0,30
Case 5	3,516	3,766	4,050	4,376	4,753	5,193	5,711
Case 6	3,516	3,797	4,117	4,485	4,911	5,408	5,995
$\varkappa_1$	0,35	0,40	0,45	0,50	0,55	0,60	0,65
Case 5	6,327	7,068	7,969	9,071	10,417	12,020	13,746
Case 6	6,695	7,541	8,579	9,870	11,497	13,564	16,157
$\varkappa_1$	0,70	0,75	0,80	0,85	0,90	0,95	1,00
Case 5	15,096	15,371	14,619	13,412	12,130	10,930	9,870
Case 6	19,129	21,526	21,927	20,690	18,892	17,070	15,418

Table 204.2

The result is also shown in fig. 205.1.

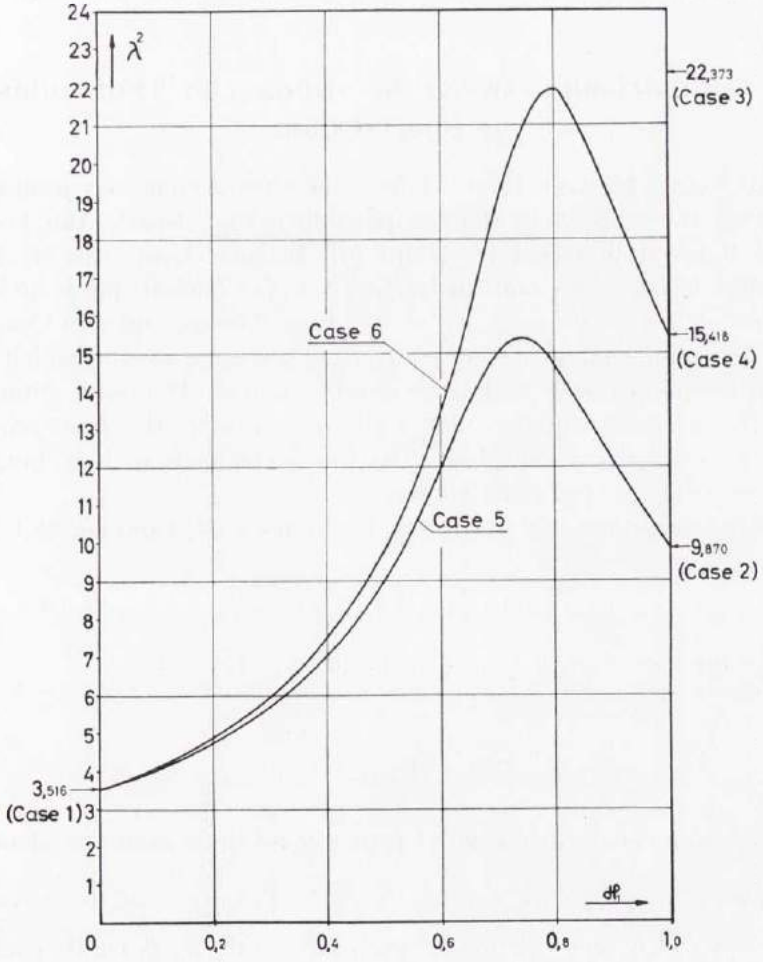
λ²
22,373
(Case 3)
Case 6
15,418
(Case 4)
Case 5
9,870
(Case 2)
3,516
(Case 1)
dP₁
0
0,2
0,4
0,6
0,8
1,0

Fig. 205.1

13. Comparison between the "Dunkerley" Formulas in a Special Case

In Chapter 10 two variants of the Dunkerley formula were proposed. Besides these there is another possibility to calculate the lowest critical speed proposed by Hahn [6]. It was shown that Hahn's formula in some cases failed. It gave complex critical speeds at high values of the inertia moments of the discs. The examples in Chapter 10 had a finite number of discs. Here is treated a case in which the shaft is equipped with an infinite number of discs. The result obtained by the approximate formulas is compared with the first critical speed for a homogenous shaft. The treatment deals with a "hinged-hinged" shaft as fig. 207.1 shows.

For a weightless shaft with one disc of mass M_1 from eq. 25.1

$$A = A_{01} = \xi_{F11}$$

if the gyroscopic effect is neglected and $\mu_1 = 1$. Further

$$\Omega_{01}^2 = \frac{1}{M_1 A_{01}} \cdot \frac{kEI}{L^3}$$

Divide the shaft in fig. 207.1 into s small discs each one of mass $\frac{m}{s}$, where m is the total mass of the shaft. Take away all these masses but one and in spite of this let the shaft retain its flexural rigidity. The critical speed of this arrangement is

$$\Omega_{0i}^2 = \frac{1}{\frac{m}{s} \cdot A_{0i}} \cdot \frac{kEI}{L^3}$$

if the remaining disc has the number of order i.

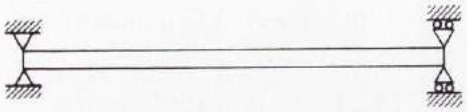

Fig. 207.1

According to Dunkerley's formula the first non-dimensional critical speed for the shaft with s discs can be written

$$(\Lambda_0)_{\text{res}} = \sum_{i=1}^{s} \frac{1}{s} \cdot \Lambda_{0i} \quad \ldots\ldots\ldots\ldots \quad 207.2$$

where

$$\Lambda_{0i} = (\xi_{F11})_i \text{ and } \Omega^2_{\text{res}} = \frac{1}{(\Lambda_0)_{\text{res}}} \cdot \frac{kEI}{mL^3}$$

From Chapter 14 we get for a "hinged-hinged" shaft that

$$(\xi_{F11})_i = \frac{1}{3}(x_1 x_2)^2$$

Choose $k = 48$. Thus

$$(\xi_{F11})_i = 16[x(1-x)]^2$$

where x is a running coordinate. The first attempt is to put all the mass on the middle of the shaft. This gives $\xi_{F11} = 1$ and from eq. 207.2

$$(\Lambda_{01})_{\text{res}} = 1$$

The next attempt is to divide m symmetrically into two masses each one placed at one third of the length of the shaft from the bearings. Thus

$$\xi_{F11} = 16\left(\frac{1}{3} \cdot \frac{2}{3}\right)^2 = \frac{64}{81}$$

and from eq. 207.2

$$(\Lambda_{02})_{\text{res}} = \left(\frac{1}{2} \cdot \frac{64}{81}\right) 2 = \frac{64}{81} \approx 0{,}79$$

Now divide the shaft into an infinite number of small discs. In this case eq. 207.2 gives

$$(\Lambda_{0\infty})_{\text{res}} = 16 \int_0^1 [x(1-x)]^2 dx$$

and

$$(\Lambda_{0\infty})_{\text{res}} = \frac{8}{15} = 0{,}533\ldots.$$

and the corresponding critical speed is $(\Omega_{0\infty})_{\text{res}}$, where

$$(\Omega_{0\infty})^2_{\text{res}} = \frac{48}{\frac{8}{15}} \cdot \frac{EI}{mL^3} = 90 \cdot \frac{EI}{mL^3}$$

Thus the series 207.2 converges to a limiting value. But it remains to scrutinize if this value is a proper value.

For a uniform beam eq. 88.1 gives

$$y = A \sin k_c\lambda x + B \operatorname{sh} k_h\lambda x + C \cos k_c\lambda x + D \operatorname{ch} k_h\lambda x$$

The boundary values are

$$x = 0 \qquad y = 0 \qquad y'' = 0$$

giving

$$C = D = 0$$

and

$$x = 1 \qquad y = 0 \qquad y'' = 0$$

giving

$$\left.\begin{aligned} A \sin k_c\lambda + B \operatorname{sh} k_h\lambda &= 0 \\ -A\left(\frac{k_c}{k_h}\right)^2 \sin k_c\lambda + B \operatorname{sh} k_h\lambda &= 0 \end{aligned}\right\}$$

The condition for non-trivial values of A and B is

$$\sin k_c\lambda \operatorname{sh} k_h\lambda \left\{1 + \left(\frac{k_c}{k_h}\right)^2\right\} = 0$$

Thus $k_c\lambda = 0+n\pi$, where $n = 1, 2, 3 \ldots$. If the gyroscopic effect is neglected is $k_c = 1$ and $\lambda_1 = \pi$. The first critical speed for a homogenous shaft is denoted by Ω_{hom} and from definition is

$$\Omega^2_{\text{hom}} = \pi^4 \cdot \frac{EI}{mL^3}$$

and consequently

$$\frac{(\Omega_{0\infty})_{\text{res}}}{\Omega_{\text{hom}}} = \frac{\sqrt{90}}{\pi^2} = 0{,}9612$$

We can conclude that the limiting value of the series 207.2 is not exactly the right value but it is a rather good approximation.

In a similar manner we now can compare some methods considering the gyroscopic effect.

For a single mass is from eq. 110.2

$$\Lambda^2 - \Lambda(\xi_{F11} + \nu\zeta_{M11}) - \nu(\xi_{M11}\zeta_{F11} - \xi_{F11}\zeta_{M11}) = 0$$

and from page 215 is for this bearing arrangement

$$\xi_{F11} = [x(1-x)]^2 \qquad \xi_{M11} = -x(1-x)\,(1-2x)$$
$$\zeta_{F11} = x(1-x)\,(1-2x) \qquad \zeta_{M11} = 3x(1-x)-1$$

if $k = 3$, and consequently, if here $\Lambda = \Lambda^*$,

$$2\Lambda^* = x^4 - 2x^3 + (1-3\nu)x^2 + 3\nu x - \nu +$$
$$+ \sqrt{\{[x(1-x)]^2 - \nu[1-3x(1-x)]\}^2 + 4\nu[x(1-x)]^3}$$

From eq. 207.2 we can write

$$\Lambda^*_{\text{res}} = \sum_{i=1}^{s} \frac{1}{s} \cdot \Lambda^*_i$$

If $s \to \infty$ is

$$\Lambda^*_{\text{res}} = \int_0^1 \Lambda^*_i dx$$

and in this case

$$\Lambda^*_{\text{res}} = \frac{1-15\nu}{60} + \int_0^{\frac{1}{2}} \sqrt{\{[x(1-x)]^2 - \nu[1-3x(1-x)]\}^2 + 4\nu[x(1-x)]^3}\, dx$$

The last integral is hyperelliptic and was solved numerically. Hahn's value is called $(\Lambda_H)_{\text{res}}$, where

$$(\Lambda_H)_{\text{res}} = \frac{1-15\nu}{30}$$

It consists of the first term in Λ^*_{res} multiplied by two. The usual "Dunkerley value" is Λ_D, where ($\nu = 0$)

$$\Lambda_D = \frac{1}{30}$$

The exact value was obtained above. We had

$$\left.\begin{aligned} k_c\lambda &= n\pi \\ k_c &= \sqrt{\sqrt{1+\left[\frac{\gamma}{2}\left(\frac{r}{L}\right)^2\lambda^2\right]^2} - \frac{\gamma}{2}\left(\frac{r}{L}\right)^2\lambda^2} \end{aligned}\right\}$$

From definition is $\nu = \dfrac{2\gamma I_p}{ML^2} = \dfrac{2\gamma Mr^2}{2ML^2} = \gamma\left(\dfrac{r}{L}\right)^2$. Thus

$$k_c = \sqrt{\sqrt{1+\left(\frac{\nu}{2}\lambda^2\right)^2} - \frac{\nu}{2}\lambda^2}$$

and

$$\left[\sqrt{1+\left(\frac{\nu}{2}\lambda^2\right)^2} - \frac{\nu}{2}\lambda^2\right]\lambda^2 = n^2\pi^2$$

giving

$$\lambda = \frac{n\pi}{\sqrt[4]{1-n^2\nu\pi^2}}$$

If $\nu\pi^2 > 1$ there are no critical speeds. This fact is already stated by Grammel [5]. The condition can also be written as $r > \dfrac{2}{\pi}L \approx 0{,}636L$, if $\dfrac{\omega}{\Omega} = +1$. The thick and short shaft with $r = 0{,}636L$ is shown in fig. 211.1.

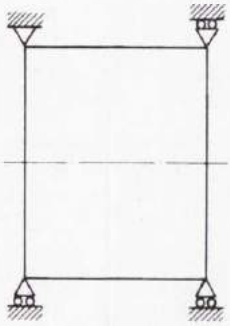

Fig. 211.1

The result can be summarized in the following way:

$\nu \leq 0 \left(\frac{\omega}{\Omega} \leq \frac{1}{2}\right)$ gives an infinite number of critical speeds

$0 < \nu \leq \frac{1}{\pi^2} \left(\frac{\omega}{\Omega} > \frac{1}{2}\right)$ gives a finite number of critical speeds

$\nu > \frac{1}{\pi^2}$ gives no critical speeds.

The corresponding Λ-value for the exact treatment is

$$\Lambda^{**} = \frac{1 - \nu\pi^2}{\pi^4} \quad \text{and} \quad n^{**} = \frac{30\pi}{\sqrt{1 - \nu\pi^2}} \sqrt{\frac{EI}{mL^3}} \text{ (r.p.m.)}$$

The first critical speeds corresponding to the theories by Dunkerley, Hahn and the present author are denoted be n_0, n_H and n^*. The ratios $\frac{n^*}{n^{**}}$, $\frac{n_0}{n^{**}}$ and $\frac{n_H}{n^{**}}$ are studied for different ν-values. See the result in table 212.1.

The Hahn approximation again fails at high gyroscopic effects. However, it is the best one in the range $0 < \nu \lesssim 0{,}04$. The $\frac{n^*}{n^{**}}$-value always lies between the values of the other approximations. Further the "improved approximation" is the best one for negative values of ν and it is rather good for all positive ν-values. Moreover it is the best fitting approximation for high values of ν.

v	$\frac{n_0}{n^{**}}$	$\frac{n^*}{n^{**}}$	$\frac{n_H}{n^{**}}$
−0,20	1,6576	0,8882	0,8288
−0,15	1,5139	0,9022	0,8397
−0,10	1,3549	0,9191	0,8569
−0,05	1,1747	0,9402	0,9033
±0,00	0,9612	0,9612	0,9612
+0,01	0,9126	0,9413	0,9898
+0,02	0,8611	0,9059	1,0293
+0,03	0,8065	0,8608	1,0874
+0,04	0,7478	0,8074	1,1824
+0,05	0,6841	0,7455	1,3682
+0,06	0,6138	0,6742	1,9411
+0,0666	—	—	∞

Table 212.1

14. Survey of Influence Functions

In order to give the reader a possibility to find quickly the influence functions needed for calculating all critical speeds for a shaft with several discs even considering the gyroscopic effect, here is presented a survey of the most common cases. All bearing arrangements with one or two bearings and a special case with three bearings are treated.

The following notations are used

α_{Fij} = the displacement in a point Q_i on the shaft caused by a unit force in a point Q_j.

α_{Mij} = the displacement in a point Q_i caused by a unit bending moment in a point Q_j.

β_{Fij} = the angle in a point Q_i on the shaft caused by a unit force in a point Q_j.

β_{Mij} = the angle in a point Q_i on the shaft caused by a unit moment in a point Q_j.

The signs of the different influence numbers must be interpreted relative a coordinate system with its origin in the left hand side bearing, its axis of abscissae along the centre line of the shaft and its axis of ordinates pointing downwards in the figures on the following pages. Further

$$\xi_{Fij} = \alpha_{Fij} \cdot \frac{EI}{L^3} \qquad \zeta_{Fij} = \beta_{Fij} \cdot \frac{EI}{L^2}$$

$$\xi_{Mij} = \alpha_{Mij} \cdot \frac{EI}{L^2} \qquad \zeta_{Mij} = \beta_{Mij} \cdot \frac{EI}{L}$$

The numbers (or functions) ξ_{Fij}, ξ_{Mij}, ζ_{Fij} and ζ_{Mij} are non-dimensional.

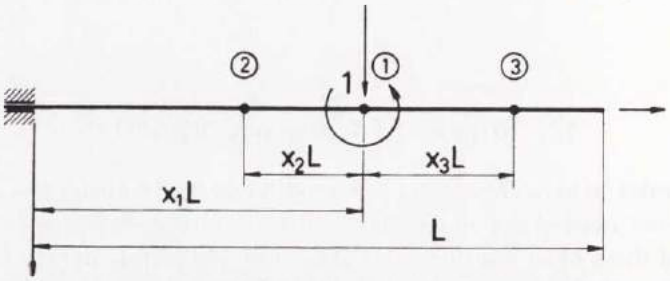

Clamped-free shaft
Case 1

Point	ξ_{Fi1}	ζ_{Fi1}
1	$\frac{1}{3} \cdot x_1^3$	$\frac{1}{2} \cdot x_1^2$
2	$\frac{1}{6}(x_2^3 - 3x_1^2 x_2 + 2x_1^3)$	$\frac{1}{2}(x_1^2 - x_2^2)$
3	$\frac{1}{6} \cdot x_1^2(2x_1 + 3x_3)$	$\frac{1}{2} \cdot x_1^2$

Point	ξ_{Mi1}	ζ_{Mi1}
1	$-\frac{1}{2} \cdot x_1^2$	$-x_1$
2	$-\frac{1}{2}(x_1 - x_2)^2$	$-x_1 + x_2$
3	$-\frac{1}{2} \cdot x_1(x_1 + 2x_3)$	$-x_1$

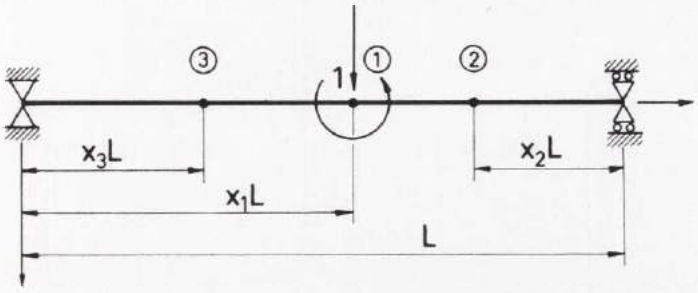

Hinged-hinged shaft
Case 2

Point	ξ_{Fi1}	ζ_{Fi1}
1	$\frac{1}{3}(x_1x_2)^2$	$\frac{1}{3}\cdot x_1x_2(x_2-x_1)$
2	$\frac{1}{6}\cdot x_1x_2(1-x_1^2-x_2^2)$	$-\frac{1}{6}\cdot x_1(1-x_1^2-3x_2^2)$
3	$\frac{1}{6}(1-x_1)x_3[1-(1-x_1)^2-x_3^2]$	$\frac{1}{6}(1-x_1)[1-(1-x_1)^2-3x_3^2]$

Point	ξ_{Mi1}	ζ_{Mi1}
1	$-\frac{1}{3}\cdot x_1x_2(x_2-x_1)$	$x_1x_2-\frac{1}{3}$
2	$\frac{1}{6}\{3(1-x_1-x_2)^2-(1-x_2)^3-$ $-(1-x_2)[3(1-x_1)^2-1]\}$	$\frac{1}{6}[6(1-x_1-x_2)-3(1-x_1)^2-$ $-3(1-x_2)^2+1]$
3	$\frac{x_3}{6}[1-3(1-x_1)^2-x_3^2]$	$-\frac{1}{6}[3(x_1^2+x_3^2)+2(1-3x_1)]$

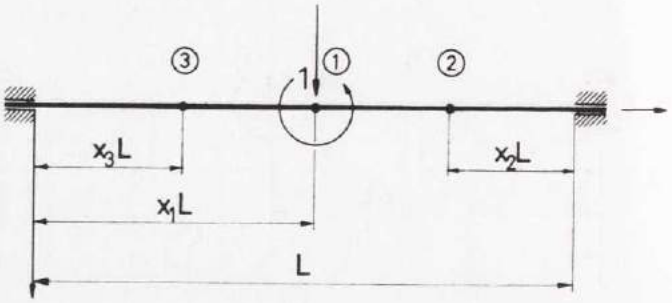

Clamped-clamped shaft
Case 3

Point	ξ_{Fi1}	ζ_{Fi1}
1	$\frac{1}{3}(x_1x_2)^3$	$\frac{1}{2}(x_1x_2)^2(x_2-x_1)$
2	$\frac{1}{6}(x_1x_2)^2[3(1-x_1-x_2)+2x_1x_2]$	$-\frac{1}{2}\cdot x_1^2x_2\{2[1-x_1(1-x_2)]-3x_2\}$
3	$\frac{1}{6}(1-x_1)^2x_3^2(3x_1-x_3-2x_1x_3)$	$\frac{1}{2}(1-x_1)^2x_3(2x_1-x_3-2x_1x_3)$

Point	ξ_{Mi1}	ζ_{Mi1}
1	$-\frac{1}{2}(x_1x_2)^2(x_2-x_1)$	$-x_1x_2(1-3x_1x_2)$
2	$\frac{1}{2}[(1-x_1-x_2)^2-(1-x_1)(1-x_2)^2(1-x_1-2x_1x^2)]$	$1-x_1-x_2-(1-x_1)(1-x_2)(1-3x_1x_2)$
3	$-\frac{1}{2}(1-x_1)x_3^2(1-3x_1+2x_1x_3)$	$-(1-x_1)x_3(1-3x_1+3x_1x_3)$

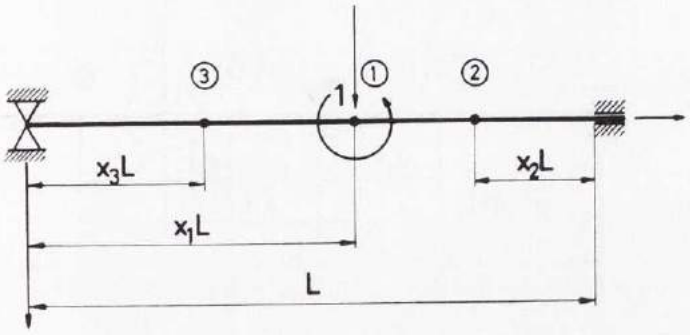

Hinged-clamped shaft
Case 4

Point	ξ_{Fi1}	ζ_{Fi1}
1	$\frac{1}{12}\cdot x_1^2(3+x_1)x_2^3$	$\frac{1}{4}x_1x_2^2(x_1x_2+3x_2-2)$
2	$\frac{1}{6}x_1x_2^2\left[\frac{1}{2}(3-x_1^2)(1-x_2)-x_1^2\right]$	$\frac{1}{4}[2(1-x_1-x_2)^3-2(1-x_1)^2+x_2(1-x_1)^2(2+x_1)(2-x_2)]$
3	$-\frac{1}{12}x_3(1-x_1)^2[x_3^2(2+x_1)-3x_1]$	$\frac{1}{4}(1-x_1)^2[x_1-x_3^2(x_1+2)]$

Point	ξ_{Mi1}	ζ_{Mi1}
1	$-\frac{1}{4}\cdot x_1x_2^2(x_1x_2+3x_2-2)$	$\frac{1}{4}x_2[-4+3x_2(1+x_1)^2]$
2	$\frac{1}{4}[2(1-x_1-x_2)^2-(1-x_1^2)(1-x_2)^3-(1-x_1)(1-3x_1)(1-x_2)]$	$\frac{1}{4}x_2[3(1-x_1^2)(2-x_2)-4]$
3	$\frac{1}{4}(1-x_1)x_3[(1+x_1)(1-x_3^2)-2(1-x_1)]$	$\frac{1}{4}(1-x_1)[(1+x_1)(1-3x_3^2)-2(1-x_1)]$

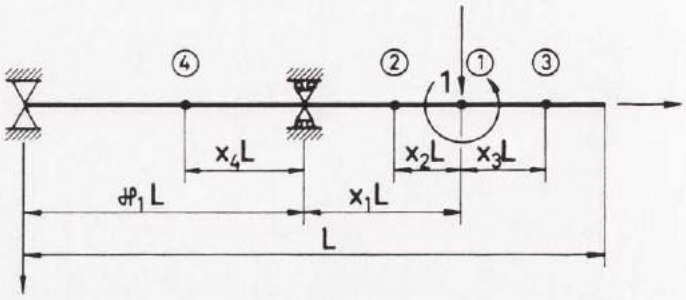

Hinged-hinged-free shaft
Case 5

Point	ξ_{Fi1}	ζ_{Fi1}
1	$\frac{1}{3}x_1^2(x_1+\varkappa_1)$	$\frac{1}{6}x_1(2\varkappa_1+3x_1)$
2	$\frac{1}{6}(x_1-x_2)[2x_1\varkappa_1+3x_1(x_1-x_2)-(x_1-x_2)^2]$	$\frac{1}{6}[x_1(3x_1+2\varkappa_1)-3x_2^2]$
3	$\frac{1}{6}[2x_1\varkappa_1(x_1+x_3)+x_1^2(2x_1+3x_2)]$	$\frac{1}{6}\cdot x_1(2\varkappa_1+3x_1)$
4	$-\frac{1}{6}\cdot\frac{x_1x_4}{\varkappa_1}(\varkappa_1-x_4)(2\varkappa_1-x_4)$	$\frac{1}{6}\cdot\frac{x_1}{\varkappa_1}(2\varkappa_1^2-6\varkappa_1x_4+3x_4^2)$

Point	ξ_{Mi1}	ζ_{Mi1}
1	$-\frac{1}{6}\cdot x_1(2\varkappa_1+3x_1)$	$-\frac{1}{3}(\varkappa_1+3x_1)$
2	$-\frac{1}{6}\cdot(x_1-x_2)[2\varkappa_1+3(x_1-x_2)]$	$-\frac{1}{3}[\varkappa_1+3(x_1-x_2)]$
3	$-\frac{1}{6}[3(x_1+x_3)^2+2\varkappa_1(x_1+x_3)-3x_3^2]$	$-\frac{1}{3}(\varkappa_1+3x_1)$
4	$\frac{1}{6}\cdot\frac{x_4}{\varkappa_1}\cdot(\varkappa_1-x_4)(2\varkappa_1-x_4)$	$-\frac{1}{6\varkappa_1}(2\varkappa_1^2-6\varkappa_1x_4+3x_4^2)$

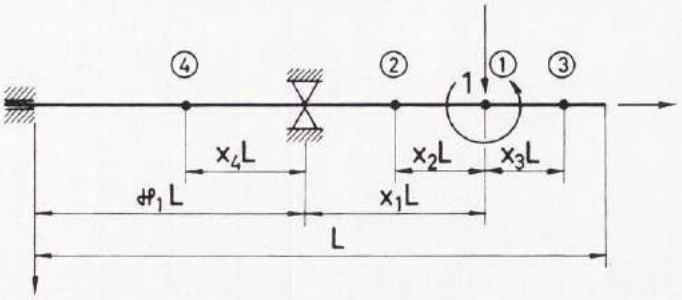

Clamped-hinged-free shaft
Case 6

Point	ξ_{Fi1}	ζ_{Fi1}
1	$\frac{1}{12} \cdot x_1^2(3\varkappa_1+4x_1)$	$\frac{1}{4} \cdot x_1(\varkappa_1+2x_1)$
2	$\frac{1}{12}(x_1-x_2)[2(x_1-x_2)(2x_1+x_2)+3\varkappa_1 x_1]$	$\frac{1}{4}[\varkappa_1 x_1+2(x_1^2-x_2^2)]$
3	$\frac{1}{12}[4x_1^3+6x_1^2x_3+3\varkappa_1 x_1(x_1+x_3)]$	$\frac{1}{4} \cdot x_1(\varkappa_1+2x_1)$
4	$-\frac{1}{4} \cdot \frac{x_1x_4}{\varkappa_1}(\varkappa_1-x_4)^2$	$\frac{1}{4} \cdot \frac{x_1}{\varkappa_1}(\varkappa_1-x_4)(\varkappa_1-3x_4)$

Point	ξ_{Mi1}	ζ_{Mi1}
1	$-\frac{1}{4} \cdot x_1(\varkappa_1+2x_1)$	$-\frac{1}{4}(\varkappa_1+4x_1)$
2	$-\frac{1}{4}[\varkappa_1(x_1-x_2)+2(x_1-x_2)^2]$	$-\frac{1}{4}[\varkappa_1+4(x_1-x_2)]$
3	$-\frac{1}{4}[\varkappa_1(x_1+x_3)+4x_1x_3+2x_1^2]$	$-\frac{1}{4}(\varkappa_1+4x_1)$
4	$\frac{1}{4} \cdot \frac{x_4}{\varkappa_1}(\varkappa_1-x_4)^2$	$\frac{1}{4\varkappa_1}(\varkappa_1-x_4)(3x_4-\varkappa_1)$

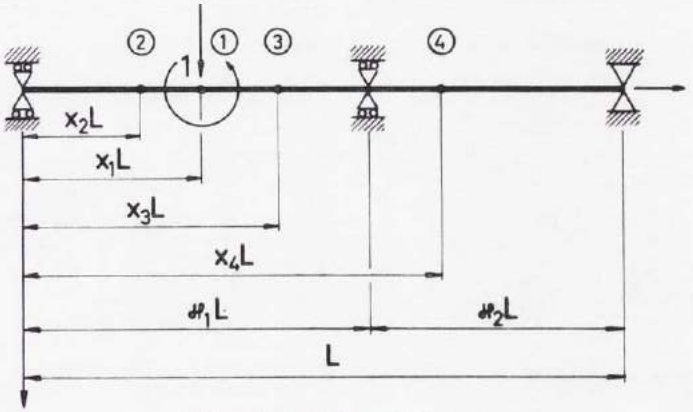

Hinged-hinged-hinged shaft
Case 7

Point	ξ_{Fi1}	ζ_{Fi1}
1	$\frac{1}{12\varkappa_1\varkappa_2}\left\{x_1(\varkappa_1^2-x_1^2)\left[(1-x_1)^3-(1-x_1)\varkappa_2^2-\frac{(\varkappa_1-x_1)^3}{\varkappa_1}\right]-2\varkappa_2 x_1(\varkappa_1-x_1)^3\right\}$	$\frac{1}{12\varkappa_1\varkappa_2}\left\{(\varkappa_1^2-3x_1^2)\left[(1-x_1)^3-(1-x_1)\varkappa_2^2-\frac{(\varkappa_1-x_1)^3}{\varkappa_1}\right]-2\varkappa_2(\varkappa_1-x_1)^3\right\}$
2	$\frac{1}{12\varkappa_1\varkappa_2}\left\{x_2(\varkappa_1^2-x_2^2)\left[(1-x_1)^3-(1-x_1)\varkappa_2^2-\frac{(\varkappa_1-x_1)^3}{\varkappa_1}\right]-2\varkappa_2 x_2(\varkappa_1-x_1)^3\right\}$	$\frac{1}{12\varkappa_1\varkappa_2}\left\{(\varkappa_1^2-3x_2^2)\left[(1-x_1)^3-(1-x_1)\varkappa_2^2-\frac{(\varkappa_1-x_1)^3}{\varkappa_1}\right]-2\varkappa_2(\varkappa_1-x_1)^3\right\}$
3	$\frac{1}{12\varkappa_1\varkappa_2}\left\{x_3(\varkappa_1^2-x_3^2)\left[(1-x_1)^3-(1-x_1)\varkappa_2^2-\frac{(\varkappa_1-x_1)^3}{\varkappa_1}\right]+2\varkappa_1\varkappa_2(x_3-x_1)^3-2\varkappa_2 x_3(\varkappa_1-x_1)^3\right\}$	$\frac{1}{12\varkappa_1\varkappa_2}\left\{(\varkappa_1^2-3x_3^2)\left[(1-x_1)^3-(1-x_1)\varkappa_2^2-\frac{(\varkappa_1-x_1)^3}{\varkappa_1}\right]+6\varkappa_1\varkappa_2(x_3-x_1)^2-2\varkappa_2(\varkappa_1-x_1)^3\right\}$
4	$\frac{1}{12\varkappa_1\varkappa_2}\left\{x_4(\varkappa_1^2-x_4^2)\left[(1-x_1)^3-(1-x_1)\varkappa_2^2-\frac{(\varkappa_1-x_1)^3}{\varkappa_1}\right]-\frac{(x_4-\varkappa_1)^3}{\varkappa_2}\left[-(1-x_1)^3+(1-x_1)(1-\varkappa_1)^3+\frac{(\varkappa_1-x_1)^3}{\varkappa_1}\right]+2\varkappa_1\varkappa_2(x_4-x_1)^3-2\varkappa_2 x_4(\varkappa_1-x_1)^3\right\}$	$\frac{1}{12\varkappa_1\varkappa_2}\left\{(\varkappa_1^2-3x_4^2)\left[(1-x_1)^3-(1-x_1)\varkappa_2^2-\frac{(\varkappa_1-x_1)^3}{\varkappa_1}\right]-\frac{3}{\varkappa_2}(x_4-\varkappa_1)^2\left[-(1-x_1)^3+(1-x_1)(1-\varkappa_1^2)+\frac{(\varkappa_1-x_1)^3}{\varkappa_1}\right]+6\varkappa_1\varkappa_2(x_4-x_1)^2-2\varkappa_2(\varkappa_1-x_1)^3\right\}$

Point	ξ_{Mi1}	ζ_{Mi1}
1	$\frac{1}{12\varkappa_1\varkappa_2}\left\{x_1(\varkappa_1^2-x_1^2)\left[3(1-x_1)^2-\varkappa_2^2-3\cdot\frac{(\varkappa_1-x_1)^2}{\varkappa_1}\right]-6\varkappa_2 x_1(\varkappa_1-x_1)^2\right\}$	$\frac{1}{12\varkappa_1\varkappa_2}\left\{(\varkappa_1^2-3x_1^2)\left[3(1-x_1)^2-\varkappa_2^2-3\cdot\frac{(\varkappa_1-x_1)^2}{\varkappa_1}\right]-6\varkappa_2(\varkappa_1-x_1)^2\right\}$
2	$\frac{1}{12\varkappa_1\varkappa_2}\left\{x_2(\varkappa_1^2-x_2^2)\left[3(1-x_1)^2-\varkappa_2^2-3\cdot\frac{(\varkappa_1-x_1)^2}{\varkappa_1}\right]-6\varkappa_2 x_2(\varkappa_1-x_1)^2\right\}$	$\frac{1}{12\varkappa_1\varkappa_2}\left\{(\varkappa_1^2-3x_2^2)\left[3(1-x_1)^2-\varkappa_2^2-3\cdot\frac{(\varkappa_1-x_1)^2}{\varkappa_1}\right]-6\varkappa_2(\varkappa_1-x_1)^2\right\}$
3	$\frac{1}{12\varkappa_1\varkappa_2}\left\{x_3(\varkappa_1^2-x_3^2)\left[3(1-x_1)^2-\varkappa_2^2-3\cdot\frac{(\varkappa_1-x_1)^2}{\varkappa_1}\right]+6\varkappa_1\varkappa_2(x_3-x_1)^2-6\varkappa_2 x_3(\varkappa_1-x_1)^2\right\}$	$\frac{1}{12\varkappa_1\varkappa_2}\left\{(\varkappa_1^2-3x_3^2)\left[3(1-x_1)^2-\varkappa_2^2-3\cdot\frac{(\varkappa_1-x_1)^2}{\varkappa_1}\right]+12\cdot\varkappa_1\varkappa_2(x_3-x_1)-6\varkappa_2(\varkappa_1-x_1)^2\right\}$
4	$\frac{1}{12\varkappa_1\varkappa_2}\left\{x_4(\varkappa_1^2-x_4^2)\left[3(1-x_1)^2-\varkappa_2^2-3\cdot\frac{(\varkappa_1-x_1)^2}{\varkappa_1}\right]-\frac{1}{\varkappa_2}(x_4-\varkappa_1)^3\left[-3(1-x_1)^2+1-\varkappa_1^2+3\cdot\frac{(\varkappa_1-x_1)^2}{\varkappa_1}\right]+6\varkappa_1\varkappa_2(x_4-x_1)^2-6\varkappa_2 x_4(\varkappa_1-x_1)^2\right\}$	$\frac{1}{12\varkappa_1\varkappa_2}\left\{(\varkappa_1^2-3x_4^2)\left[3(1-x_1)^2-\varkappa_2^2-3\cdot\frac{(\varkappa_1-x_1)^2}{\varkappa_1}\right]-\frac{3}{\varkappa_2}(x_4-\varkappa_1)^2\left[-3(1-x_1)^2+1-\varkappa_1^2+3\cdot\frac{(\varkappa_1-x_1)^2}{\varkappa_1}\right]+12\varkappa_1\varkappa_2(x_4-x_1)-6\varkappa_2(\varkappa_1-x_1)^2\right\}$

15. Summary

In this report methods of calculation of critical shaft speeds are demonstrated. Influence numbers are consequently used both when discussing the nature of the phenomena and in deriving determinants from which the critical speeds may be computed. Different modes of bearing arrangements are treated, viz. rigid and flexible bearings where there may be either no bending moments in them or zero deflection angle. The formulas are carried out to the last stage and the user need not spend any time on derivations. This matter has been the aim in every chapter.

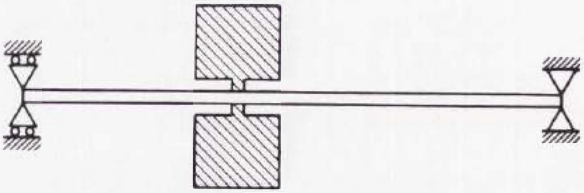

Fig. 222.1

Further the gyroscopic effect is thoroughly scrutinized and various rotational circumstances are discussed. All equations are valid for both forward precessions and reverse precessions of any kind.

The influence of the mass of the shaft on the critical speeds is treated in an exact way for any position of one disc on a shaft for different bearing arrangements at the same time as the gyroscopic effect is taken into account.

Finally two approximate formulas are proposed on the basis of Dunkerley's formula. With the aid of one of these formulas, diagrams and tables [4] the designer has got a tool for calculating the lowest critical speed for the most usual bearing arrangements in an accurate and rapid way. However, tables for other shaft and bearing arrangements are still lacking.

It must be noticed that the results are valid even for thick discs if they are mounted to the shaft over a small range according to fig. 222.1.

The parameters ν and Θ^* in this case are defined as

$$\nu = \left(\frac{\omega}{\Omega} - \frac{I_e}{I_p}\right) \cdot \frac{I_p}{M_{\text{ref}} L^2} \quad \text{and} \quad \Theta^* = \left(\frac{\omega}{\Omega} - \frac{I_e}{I_p}\right) \cdot \frac{I_p}{mL^2}$$

It was to be desired that test results could be shown. Further it would be of great value to scrutinize different bearing arrangements available from the manufacturers concerning spring constants. In this report only lateral springs are considered and bearings giving rise to bending moments proportional to the deflection angles remain to be treated.

16. References

1. Aitken, A. C.: Determinants and Matrices, Oliver and Boyd, 1959.
2. Biezeno-Grammel: Technische Dynamik, Julius Springer, 1939.
3. Den Hartog: Mechanical Vibrations, Mc Graw-Hill, 1956.
4. Fernlund, I.: Tables for Calculating Critical Speeds of a Shaft with Thin Discs. (Available at the Library of Chalmers University of Technology, Gothenburg, Sweden).
5. Grammel, R.: Der Kreisel, Springer-Verlag, 1950.
6. Hahn, E.: Schweiz. Bauztg., Bd 72, 1918.
7. Jakobsson, B.: The Semi-Inverted Diagram, Engineers' Digest January, Volume 5, No. 1, 1948 (or Teknisk Tidskrift, Vol. 77, No. 31, August 2, 1947, pp. 572—573).
8. Malmqvist, Stenström, Danielsson: Matematisk Analys, Natur och Kultur, 1952.
9. Stodola, A.: Dampfturbinen.
10. Zurmühl, R.: Matrizen, Springer-Verlag, 1958.

Forts. fr. omsl. 2:dra sida

202. RÅDE, LENNART, *Sampling planes for acceptance sampling by variables using the range.* 34 s. 1958. Kr. 9: 50. (Avd. Allm. Vetenskaper. 14.)
203. JAKOBSSON, BENGT, AND FLOBERG, LEIF, *The rectangular plane pad bearing.* 44 s. 1958. Kr. 5: —. (Avd. Maskinteknik. 12.)
204. ASPLUND, SVEN OLOF, *Column-beams and suspension bridges analysed by »Green's matrix».* 36 s. 1958. Kr. 7: —. (Avd. Väg- och Vattenbyggnad. Byggnadsteknik. 29.)
205. WILHELMSSON, HANS, *On the properties of the electron beam in the presence of an axial magnetic field of arbitrary strength.* 32 s. 1958. Kr. 7: 50. (Avd. Elektroteknik. 63.)
206. WILHELMSSON, HANS, *The interaction between an obliquely incident plane electromagnetic wave and an electron beam. III.* 17 s. 1958. Kr. 5: —. (Avd. Elektroteknik. 64.)
207. HEDVALL, J. ARVID, *On the influence of pre-treatment and transition processes on the adsorption capacity and the reactivity of various types of glass and silica.* 39 s. 1959. Kr. 8: —. (Institutionen för Silikatkemisk Forskning. 40.)
208. KÄRRHOLM, GUNNAR, *A flow problem solved by strip method.* 22 s. 1959. Kr. 4: 50. (Avd. Allm. Vetenskaper. 15.)
209. GRANHOLM, HJALMAR, *Allmän teori för beräkning av armerad betong.* 228 s. 1959. Kr. 20: —. (Avd. Väg- och Vattenbyggnad. Byggnadsteknik. 30.)
210. LIDIN, LARS G., *On helical-springs suspension.* 75 s. 1959. Kr. 15: —. (Avd. Maskinteknik. 13.)
211. BJÖRK, NILS, *Theory of the indirectly heated thermistor.* 46 s. 1959. Kr. 10: —. (Avd. Elektroteknik. 65.)
212. CARLSSON, ORVAR, *The influence of submicroscopic pores on the resistance of bricks towards frost.* 13 s. 1959. Kr. 3: 50. (Institutionen för Silikatkemisk Forskning. 41.)
213. GRANHOLM, HJALMAR, *KAM 40, KAM 60 och KAM 90.* 41 s. 1959. Kr. 3: 50. (Avd. Väg- och Vattenbyggnad. Byggnadsteknik. 31.)
214. JAKOBSSON, BENGT, AND FLOBERG, LEIF, *The centrally loaded partial journal bearing.* 35 s. 1959. Kr. 7: 50. (Avd. Maskinteknik. 14.)
215. FLOBERG, LEIF, *Experimental investigation of power loss in journal bearings, considering cavitation.* 16 s. 1959. Kr. 3: 50. (Avd. Maskinteknik. 15.)
216. FLOBERG, LEIF, *Lubrication of a rotating cylinder on a plane surface, considering cavitation.* 40 s. 1959. Kr. 8: —. (Avd. Maskinteknik. 16.)
217. TROEDSSON, CARL BIRGER, *The growth of the Western city during the Middle Ages.* 125 s. 1959. Kr. 19: —. (Avd. Arkitektur. 4.)
218. HEDVALL, J. ARVID, *The importance of the reactivity of solids in geological-mineralogical processes.* 11 s. 1959. Kr. 2: 50. (Institutionen för Silikatkemisk Forskning. 42.)
219. CORNELL, ELIAS, *Humanistic inquiries into architecture. I—III.* 112 s. 1959. Kr. 17: —. (Avd. Arkitektur. 5.)
220. GRANHOLM, CARL-ADOLF, *Ekonomiska aluminiumprofiler.* 48 s. 1959. Kr. 5: 50. (Avd. Väg- och Vattenbyggnad. Byggnadsteknik. 32.)
221. LUNDÉN, ARNOLD, CHRISTOFFERSON, STINA, AND LODDING, ALEX, *The isotopic effect of lithium ions in countercurrent electromigration in molten lithium bromide and iodide.* 38 s. 1959. Kr. 7: 50. (Avd. Allm. Vetenskaper. 16.)
222. INGEMANSSON, STIG, AND KIHLMAN, TOR, *Sound insulation of frame walls.* 47 s. 1959. Kr. 8: 50. (Avd. Väg- och Vattenbyggnad. Byggnadsteknik. 33.)
223. HÖGLUND, B., AND RADHAKRISHNAN, V., *A radiometer for the hydrogen line.* 25 s. 1959. Kr. 6: 50. (Avd. Elektroteknik. 66.)
224. JAKOBSSON, BENGT, *Torque distribution, power flow, and zero output conditions of epicyclic gear trains.* 55 s. 1960. Kr. 12: —. (Avd. Maskinteknik. 17.)
225. OLVING, SVEN, *Electromagnetic and space charge waves in a sheath helix.* 91 s. 1960. Kr. 17: —. (Avd. Elektroteknik. 67.)
226. STRÖMBLAD, JOHN, *Beschleunigungsverlauf und Gleichgewichtsdrehzahlen einfacher Planetengetriebe nebst Selbsthemmungsversuche.* 80 s. 1960. Kr. 18: —. (Avd. Maskinteknik. 18.)
227. SANDFORD, FOLKE, *Some current problems concerning brick manufacture.* 20 s. 1960. Kr. 5: —. (Avd. Kemi och Kemisk Teknologi. 35.)
228. OLVING, SVEN, *A new method for space charge wave interaction studies. II.* 40 s. 1960. Kr. 8: —. (Avd. Elektroteknik. 68.)
229. GRANHOLM, HJALMAR, *Le problème de Boussinesq.* 15 s. 1960. Kr. 3: 50. (Avd. Väg- och Vattenbyggnad. Byggnadsteknik. 34.)
230. HIBA, MIODRAG, ET CEDERVALL, KRISTER, *Flambement élastique d'une barre en bois lamellée et cloüée avec le module de déplacement du moyen de liaison constant k.* 22 s. 1960. Kr. 5: —. (Avd. Väg- och Vattenbyggnad. Byggnadsteknik. 35.)
231. FLOBERG, LEIF, *The optimum thrust tilting-pad bearing.* 23 s. 1960. Kr. 5: —. (Avd. Maskinteknik. 19.)

Forts. å omsl. 4:de sida

Forts. fr. omsl. 3:dje sida

232. Floberg, Leif, *The two-groove journal bearing, considering cavitation.* 32 s. 1960. Kr. 6: —. (Avd. Maskinteknik. 20.)
233. Hedvall, J. Arvid, *Heterogeneous catalysis, results and projects for research.* 18 s. 1961. Kr. 5: —. (Avd. Kemi och Kemisk Teknologi. 36.)
234. Floberg, Leif, *Lubrication of two cylindrical surfaces, considering caviation.* 36 s. 1961. Kr. 10: —. (Avd. Maskinteknik. 21.)
235. Floberg, Leif, *Attitude-eccentricity curves and stability conditions of the infinite journal bearing.* 43 s. 1961. Kr. 11: —. (Avd. Maskinteknik. 22.)
236. Ben-Yair, M. P., *Thermometric titrations of zinc. cadmium and mercuric salts.* 11 s. 1961. Kr. 3: —. (Avd. Kemi och Kemisk Teknologi. 37.)
237. Sandford, F., Liljegren, B., and Jonsson, B., *The resistance of bricks towards frost experiments and considerations.* 20 s. 1961. Kr. 5: —. (Avd. Kemi och Kemisk Teknologi. 38.)
238. Floberg, Leif, *Experimental investigation of cavitation regions in journal bearings.* 28 s. 1961. Kr. 6: —. (Avd. Maskinteknik. 23.)
239. Granholm, Hjalmar, *Sandöbrons bågställning.* 128 s. 1961. Kr. 20: —. (Avd. Väg- och Vattenbyggnad. Byggnadsteknik. 36.)
240. Lindblad, Anders, *On the design of lines for merchant ships.* 125 s. Kr. 20: —. (Avd. Skeppsbyggeri. 7.)
241. Lundén, Arnold, *Self diffusion and the structure of molten salts.* 14 s. Kr. 4: —. (Avd. Allm. Vetenskaper. 17.)
242. Larsson, Lars-erik, *Sprickbildning i vattenledningsrör av förspänd betong.* 70 s. 1961. Kr. 15: —. (Avd. Väg- och Vattenbyggnad. Byggnadsteknik. 37.)
243. Asplund, S. O., *A unified analysis of indeterminate structures.* 36 s. 1961. Kr 8: —. (Avd. Väg- och Vattenbyggnad. Byggnadsteknik. 38.)
244. Braunstein, A., *The magnetic field in iron with variable permeability.* 11 s. 1961. Kr. 3: —. (Avd. Elektroteknik. 69.)
245. Fernlund, Ingemar, *A method to calculate the pressure between bolted or riveted plates.* 126 s. 1961. Kr. 25: —. (Avd. Maskinteknik. 24.)
246. Hedvall, J. Arvid, and Karamustafaoglu, Vural, *On the conservation of ancient alabaster objects.* 19 s. 1961. Kr. 5: —. (Avd. Kemi och Kemisk Teknologi. 39.)
247. Ekelöf, Stig, *A theory of the eddy current equivalent winding and its application to the closing of non-delayed telephone relays.* 35 s. 1961. Kr. 7: —. (Avd. Elektroteknik. 70.)
248. Cederwall, Krister, *Beräkning av spikade konstruktioner med hänsyn till förbandens deformationsegenskaper.* 52 s. 1961. Kr. 10: —. (Avd. Väg- och Vattenbyggnad. Byggnadsteknik. 39.)
249. Kärrholm, Gunnar, and Samuelsson, Alf, *Bridge slabs with edge-beams.* 73 s. 1961. Kr. 15: —. (Avd. Väg- och Vattenbyggnad. Byggnadsteknik. 40.)
250. Losberg, Anders, *Design methods for structurally reinforced concrete pavements.* 143 s. 1961. Kr. 30: —. (Avd. Väg- och Vattenbyggnad. Byggnadsteknik. 41.)
251. Ekelöf, Stig, *Primärnormalerna för resistans och spänning vid CTH's institution för elektricitetslära och elektrisk mätteknik.* 20 s. 1961. Kr. 4: —. (Avd. Elektroteknik 71.)
252. Åkesson, Bengt Å., *Rationalization of Lévy's plate solution.* 135 s. 1961. Kr. 25: —. (Avd. Väg- och Vattenbyggnad. Byggnadsteknik. 42.)
253. Brogren, Gösta, *A double-crystal spectrometer for work in vacuum region.* 19 s. 1961. Kr. 4: —. (Avd. Allm. Vetenskaper. 18.)
254. Kihlman, Tor, *Flanktransmissionens inverkan på rumsisolering mot luftljud.* 69 s. 1961. Kr. 14: —. (Avd. Väg- och Vattenbyggnad. Byggnadsteknik. 43.)
255. Svensson, S. Ivar, *The influence of cam curve derivative steps on cam dynamical properties.* 93 s. 1961. Kr. 25: —. (Avd. Maskinteknik. 25.)
256. Hult, Jan, *Mechanics of a beam subject to primary creep.* 20 s. 1962. Kr. 5: —. (Avd. Allm. Vetenskaper. 19.)
257. Sandford, Folke, and Hedvall, J. Arvid, *Concerning the cause of the colour of an amazonite preparation.* 8 s. 1962. Kr. 3: —. (Avd. Kemi och Kemisk Teknologi. 40.)
258. Nilsson, Jan, *On the structure of weak interactions.* 66 s. 1962. Kr. 15: —. (Avd. Allm. Vetenskaper. 20.)
259. Ström, Lars, *An absolute anemometer.* 22 s. 1962. Kr. 6: —. (Avd. Maskinteknik. 26.)

Pris kronor 50: — ELANDERS BOKTRYCKERI AKTIEBOLAG
GÖTEBORG 1962

CHALMERS TEKNISKA HÖGSKOLAS HANDLINGAR
TRANSACTIONS OF CHALMERS UNIVERSITY OF TECHNOLOGY
GOTHENBURG, SWEDEN
Nr 276 (Avd. Maskinteknik 29) 1963

ON THE WHIRLING OF A ROTOR

BY

INGEMAR FERNLUND

Report No. 21 from the Institute of Machine Elements
Chalmers University of Technology
Gothenburg, Sweden
1963

Av Chalmers Tekniska Högskolas Handlingar hava tidigare utkommit:

Fullständig förteckning över Chalmers Tekniska Högskolas Handlingar
lämnas av Chalmers Tekniska Högskolas Bibliotek, Göteborg.

201. KÄRRHOLM, GUNNAR, *Influenced functions of elastic plates divided in strips.* 18 s. 1958. Kr. 4: 50. (Avd. Väg- och Vattenbyggnad. Byggnadsteknik. 28.)
202. RÅDE, LENNART, *Sampling planes for acceptance sampling by variables using the range.* 34 s. 1958. Kr. 9: 50. (Avd. Allm. Vetenskaper. 14.)
203. JAKOBSSON, BENGT, AND FLOBERG, LEIF, *The rectangular plane pad bearing.* 44 s. 1958. Kr. 5: —. (Avd. Maskinteknik. 12.)
204. ASPLUND, SVEN OLOF, *Column-beams and suspension bridges analysed by »Green's matrix».* 36 s. 1958. Kr. 7: —. (Avd. Väg- och Vattenbyggnad. Byggnadsteknik. 29.)
205. WILHELMSSON, HANS, *On the properties of the electron beam in the presence of an axial magnetic field of arbitrary strength.* 32 s. 1958. Kr. 7: 50. (Avd. Elektroteknik. 63.)
206. WILHELMSSON, HANS, *The interaction between an obliquely incident plane electromagnetic wave and an electron beam. III.* 17 s. 1958. Kr. 5: —. (Avd. Elektroteknik. 64.)
207. HEDVALL, J. ARVID, *On the influence of pre-treatment and transition processes on the adsorption capacity and the reactivity of various types of glass and silica.* 39 s. 1959. Kr. 8: —. (Institutionen för Silikatkemisk Forskning. 40.)
208. KÄRRHOLM, GUNNAR, *A flow problem solved by strip method.* 22 s. 1959. Kr. 4: 50. (Avd. Allm. Vetenskaper. 15.)
209. GRANHOLM, HJALMAR, *Allmän teori för beräkning av armerad betong.* 228 s. 1959. Kr. 20: —. (Avd. Väg- och Vattenbyggnad. Byggnadsteknik. 30.)
210. LIDIN, LARS G., *On helical-springs suspension.* 75 s. 1959. Kr. 15: —. (Avd. Maskinteknik. 13.)
211. BJÖRK, NILS, *Theory of the indirectly heated thermistor.* 46 s. 1959. Kr. 10: —. (Avd. Elektroteknik. 65.)
212. CARLSSON, ORVAR, *The influence of submicroscopic pores on the resistance of bricks towards frost.* 13 s. 1959. Kr. 3: 50. (Institutionen för Silikatkemisk Forskning. 41.)
213. GRANHOLM, HJALMAR, *KAM 40, KAM 60 och KAM 90.* 41 s. 1959. Kr. 3: 50. (Avd. Väg- och Vattenbyggnad. Byggnadsteknik. 31.)
214. JAKOBSSON, BENGT, AND FLOBERG, LEIF, *The centrally loaded partial journal bearing.* 35 s. 1959. Kr. 7: 50. (Avd. Maskinteknik. 14.)
215. FLOBERG, LEIF, *Experimental investigation of power loss in journal bearings, considering cavitation.* 16 s. 1959. Kr. 3: 50. (Avd. Maskinteknik. 15.)
216. FLOBERG, LEIF, *Lubrication of a rotating cylinder on a plane surface, considering cavitation.* 40 s. 1959. Kr. 8: —. (Avd. Maskinteknik. 16.)
217. TROEDSSON, CARL BIRGER, *The growth of the Western city during the Middle Ages.* 125 s. 1959. Kr. 19: —. (Avd. Arkitektur. 4.)
218. HEDVALL, J. ARVID, *The importance of the reactivity of solids in geological-mineralogical processes.* 11 s. 1959. Kr. 2: 50. (Institutionen för Silikatkemisk Forskning. 42.)
219. CORNELL, ELIAS, *Humanistic inquiries into architecture. I—III.* 112 s. 1959. Kr. 17: —. (Avd. Arkitektur. 5.)
220. GRANHOLM, CARL-ADOLF, *Ekonomiska aluminiumprofiler.* 48 s. 1959. Kr. 5: 50. (Avd. Väg- och Vattenbyggnad. Byggnadsteknik. 32.)
221. LUNDÉN, ARNOLD, CHRISTOFFERSON, STINA, AND LODDING, ALEX, *The isotopic effect of lithium ions in countercurrent electromigration in molten lithium bromide and iodide.* 38 s. 1959. Kr. 7: 50. (Avd. Allm. Vetenskaper. 16.)
222. INGEMANSSON, STIG, AND KIHLMAN, TOR, *Sound insulation of frame walls.* 47 s. 1959. Kr. 8: 50. (Avd. Väg- och Vattenbyggnad. Byggnadsteknik. 33.)
223. HÖGLUND, B., AND RADHAKRISHNAN, V., *A radiometer for the hydrogen line.* 25 s. 1959. Kr. 6: 50. (Avd. Elektroteknik. 66.)
224. JAKOBSSON, BENGT, *Torque distribution, power flow, and zero output conditions of epicyclic gear trains.* 55 s. 1960. Kr. 12: —. (Avd. Maskinteknik. 17.)
225. OLVING, SVEN, *Electromagnetic and space charge waves in a sheath helix.* 91 s. 1960. Kr. 17: —. (Avd. Elektroteknik. 67.)
226. STRÖMBLAD, JOHN, *Beschleunigungsverlauf und Gleichgewichtsdrehzahlen einfacher Planetengetriebe nebst Selbsthemmungsversuche.* 80 s. 1960. Kr. 18: —. (Avd. Maskinteknik. 18.)
227. SANDFORD, FOLKE, *Some current problems concerning brick manufacture.* 20 s. 1960. Kr. 5: —. (Avd. Kemi och Kemisk Teknologi. 35.)
228. OLVING, SVEN, *A new method for space charge wave interaction studies. II.* 40 s. 1960. Kr. 8: —. (Avd. Elektroteknik. 68.)

Forts. å omsl. 3:dje sida

CHALMERS TEKNISKA HÖGSKOLAS HANDLINGAR
TRANSACTIONS OF CHALMERS UNIVERSITY OF TECHNOLOGY
GOTHENBURG, SWEDEN
Nr 276 (Avd. Maskinteknik 29) 1963

ON THE WHIRLING OF A ROTOR

BY

INGEMAR FERNLUND

Report No. 21 from the Institute of Machine Elements
Chalmers University of Technology
Gothenburg, Sweden
1963

SCANDINAVIAN UNIVERSITY BOOKS
AKADEMIFÖRLAGET-GUMPERTS · GÖTEBORG

SCANDINAVIAN UNIVERSITY BOOKS

Denmark: MUNKSGAARD, *Copenhagen*
Norway: UNIVERSITETSFORLAGET, *Oslo, Bergen*
Sweden: AKADEMIFÖRLAGET-GUMPERTS, *Göteborg*
SVENSKA BOKFÖRLAGET/Norstedts-Bonniers, *Stockholm*

Manuscript received by the Publications Committee,
Chalmers University of Technology, Oct. 4th, 1962

PRINTED IN SWEDEN BY
ELANDERS BOKTRYCKERI AKTIEBOLAG, GÖTEBORG 1963

Preface

Of the research work on elastic rotors that has been carried out by the *Institute of Machine Elements, Chalmers University of Technology, Gothenburg, Sweden*, a report suitable for predicting critical speeds has been published.

The present report is a continuation and it deals with the problem of predicting possible whirlings in machinery.

I wish to express my thanks to Professor *B. Jakobsson*, the Head of the Institute, for his interest in the subject.

Ingemar Fernlund
Tekn. lic.
Research Assistant at the
Institute of Machine Elements

Contents

1. Introduction

In a previous report [5] the gyroscopic bending moments were derived on various conditions of whirling. The angular velocity of the shaft $\omega \frac{\text{rad}}{\text{s}}$ and the angular velocity of the whirling $\Omega \frac{\text{rad}}{\text{s}}$ were assumed to have a certain ratio. Here this ratio is called K and $K = \frac{\omega}{\Omega} = \frac{n}{N}$ where n and N are the corresponding r.p.m. of the two rotations.

It was pointed out that K is usually assumed to have the value $+1$ but that in some cases other K-values have been observed. The following is quoted from "Mechanical Vibrations" by *Den Hartog* [3].

"Now we come to a curious and still partly unexplained phenomenon. It was reported in the classical book on steam turbines of *Stodola* [9] that a rough critical had been observed at the critical speed corresponding to $\omega = -\Omega$. This was called a "reverse whirl", or more eruditely a "retrograde precession". No explanation was given of where the energy comes from. ... Whereas the forward whirl or ordinary critical speed can be observed on every machine, the reverse whirl is extremely rare. The author of this book looked around and asked his friends for fifteen years about it without results and was about ready to conclude that the reverse critical was imaginary, when a case actually occurred. A model was constructed which showed roughness at the calculated speed, and stroboscopic observation showed the whirl to be actually opposite in direction to the rotation. With this model tests were conducted determining the amplitude of vibration at this critical as of function of (1) unbalance and (2) flatness of shaft, and it was conclusively established that neither unbalance nor shaft flatness affects the amplitude, which remained constant throughout. During the tests the apparatus was disassembled several times, and new shafts and discs were used. After every such reassembly the reverse whirl amplitude was different and often entirely absent. Also, roughnesses were observed at other

ratios K than -1, in particular at $K=+\frac{1}{2}$ and $+\frac{1}{3}$. No rational explanation for this behaviour is available, and it is suspected that it is determined by damping or internal friction". (The notations in this quotation are altered to coincide with those in the present report).

In [5] it was shown that every speed ω is a "critical" one (the shaft has an indifferent position if the unbalance is zero) if the angular velocity of the whirl is of a certain value. But in the present report experimental investigations of an unbalanced rotor show that only a few "critical" speeds occur.

As seen there are a lot of curious things in connection with these "unusual" critical speeds. This report treats a number of these phenomena. Only a one-disc rotor is considered.

2. Notation

A	Arbitrary constant. Point
B	Arbitrary constant. Centre of bearing
C	Arbitrary constant. Centre of disc
D	Arbitrary constant
D^*	Non-dimensional coefficient for the damping force
E	Modulus of elasticity in tension and compression
G	Centre of gravity
I	Moment of inertia of a cross section
I_p	Polar moment of inertia of a disc
I_e	Equatorial moment of inertia of a disc
K	"Whirling ratio"
K_y, K_z	Elastic shear forces of a shaft
L	Length of a shaft
M	Mass of a disc. Bending moment. Torque (Index shows the intended thing)
N	R.p.m. of the whirling motion
Q	Arbitrary number
R	Radial position of the centre of gravity
S	Centre of a shaft
Y, Z	Mass forces of the disc
a	Distance
c	Spring constant
d	Diameter of a shaft
e	Eccentricity of a disc
k_i	Radius of inertia
k	Coefficient of damping. Arbitrary constant
m	Mass of a shaft or an arbitrary number
n	R.p.m. of a motor shaft
p	Angular velocity
q_s	Constant depending on s
r	Radius. Deflection of a shaft

r_c	Crookedness of the shaft at the disc
$\boldsymbol{r}_G$	Vector for the centre of gravity of a disc
$\boldsymbol{r}_S = re^{i\varphi}$	Vector for the centre of the shaft
v	Angle
w	Angle
x, y, z	Coordinates
$\Lambda = \dfrac{kEI}{M_{ref}L^3\Omega^2}$	Non-dimensional "critical speed"
Φ	Function
Ω	Angular velocity
α	Angle, influence number concerning diplacements
β	Influence number concerning rotations (angles)
$\gamma = \dfrac{1}{2}\left(\dfrac{\omega}{\Omega} - \dfrac{I_e}{I_p}\right)$	Constant
ε	Ratio or a small number in general
ζ	Coordinate
η	Coordinate
$\nu = \dfrac{2\gamma I_p}{ML^2}$	Non-dimensional "moment of inertia"
ξ	Coordinate. Non-dimensional influence number concerning displacements
$\rho = \dfrac{r}{e}\left(\text{or } \dfrac{r}{r_c}\right)$	Non-dimensional "deflection" of a shaft
$\tau = \Omega_n t$	Non-dimensional "time"
φ	Angle
$\chi = \rho e^{i\varphi}$	Non-dimensional vector for the deflection of the shaft
ψ	Angle
ω	Angular velocity of the shaft of a motor

Indices:

c	With reference to the critical condition
$disc$	With reference to the disc
F	With reference to a force
M	With reference to a moment
n	With reference to the normal (= usual) assumption
g	With reference to a gyroscopic effect
φ	With reference to the whirl velocity $\dot{\varphi}$

3. Input Torque and Gyroscopic Moments of a Rotor

In this chapter we discuss some methods of deriving the input torque and the gyroscopic moment in a rotor with one disc.

In Chapter 7 of [5] the case in fig. 10.1 was treated.

A *rigid* shaft rotates around the line AB with the constant angular velocity $\Omega \frac{\text{rad}}{\text{s}}$ on the same time as the disc rotates around the line $A'B'$ with the constant angular velocity $\omega' \frac{\text{rad}}{\text{s}}$.

The eqs 54.3 in [5] give the moments at the point A'

$$\left.\begin{aligned} M_\xi &= -\Omega \sin\alpha \sin\omega' t \{I_\xi\omega' + (I_p - I_\xi)\omega''\} + \tfrac{1}{2} \times \\ &\quad \times Mea\Omega^2 \sin^2\alpha \sin 2\omega' t \\ M_\eta &= -\Omega \sin\alpha \cos\omega' t \{I_\xi\omega' + (I_p - I_\xi)\omega''\} - Me^2\Omega(\omega' + \omega'') \times \\ &\quad \times \sin\alpha \cos\omega' t + Mea \left\{ \frac{\Omega^2}{2} \sin^2\alpha - (\omega'')^2 \right\} + \frac{1}{2} Mea \times \\ &\quad \times \Omega^2 \sin^2\alpha \cos 2\omega' t \\ M_\zeta &= -Mea\Omega^2 \sin\alpha (a \cos\alpha \sin\omega' t + \tfrac{1}{2} \cdot e \sin\alpha \sin 2\omega' t) \end{aligned}\right\} \quad \ldots 9.1$$

where

$$\left.\begin{aligned} \omega' &= \omega - \Omega \\ \omega'' &= \omega - \Omega(1 - \cos\alpha) \end{aligned}\right\}$$

Notice that the ξ-, η-, and ζ-axis rotates with the disc. By projection

$$\left.\begin{aligned} M_{\xi'} &= M_\xi \cos\omega' t - M_\eta \sin\omega' t \\ M_{\eta'} &= M_\xi \sin\omega' t + M_\eta \cos\omega' t \end{aligned}\right\} \quad \ldots\ldots\ldots\ldots 9.2$$

The ξ'-axis is in the plane $A'B'B$ and the η'-axis is perpendicular to it.

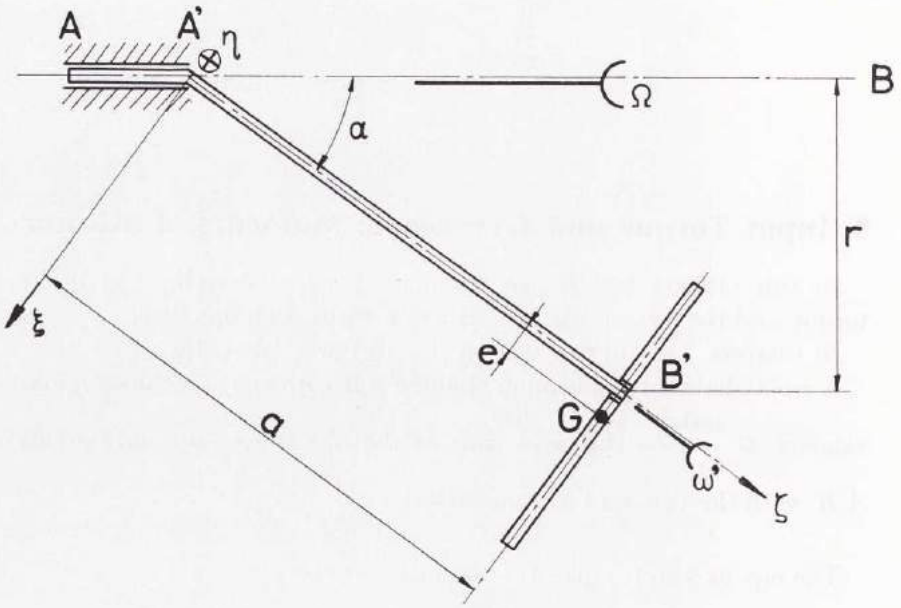

Fig. 10.1

The input torque is

$$M_{in} = M_\zeta \cos \alpha + M_\xi \sin \alpha$$

and by insertion of the expressions in the eqs 9.1 and 9.2

$$M_{in} = Mea \sin \alpha \{(\omega'')^2 - \Omega^2 \cos^2 \alpha\} \sin \omega' t + \\ + Me^2 \omega' \Omega \sin^2 \alpha \sin 2\omega' t \quad \ldots\ldots\ldots\ldots\ldots \quad 10.2$$

or

$$M_{in} = Mer \{(\omega'')^2 - \Omega^2 \cos^2 \alpha\} \sin \omega' t + Me^2 \omega' \Omega \sin^2 \alpha \sin 2\omega' t$$

If $\alpha = 0$ and r is kept constant

$$M_{in} = Mer(\omega^2 - \Omega^2) \sin \omega' t \quad \ldots\ldots\ldots\ldots \quad 10.3$$

This expression is now derived in another way. Consider the point mass in fig. 11.1. It rotates around the point S with the angular velocity $\dot{\psi}\ \frac{\text{rad}}{\text{s}}$ while the point S rotates around the point B. Further, r and e are constant distances.

In fig. 11.2 the forces and the necessary torque are shown.

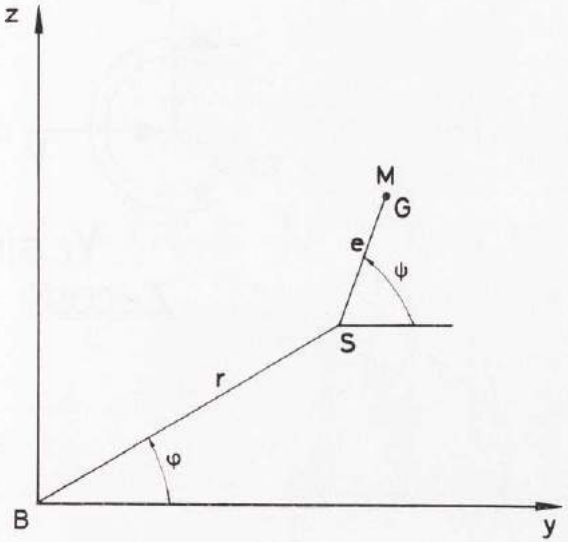

Fig. 11.1

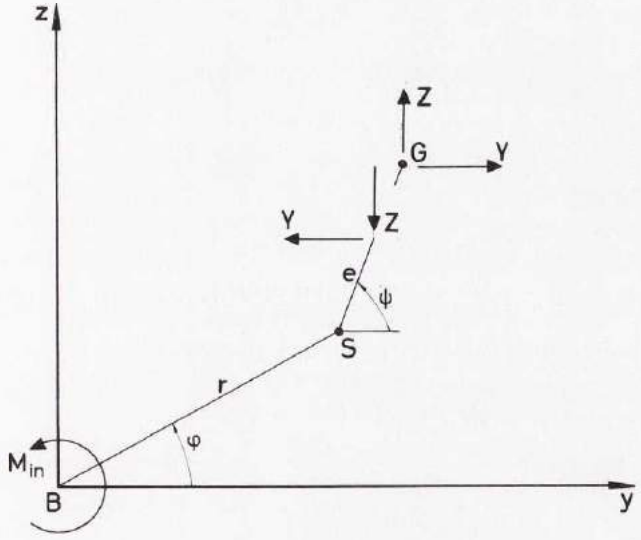

Fig. 11.2

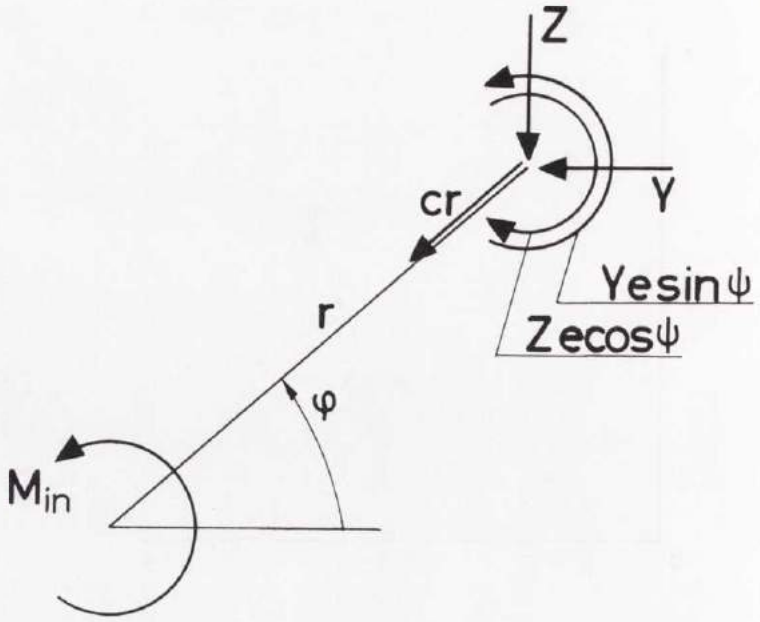

Fig. 12.1

We get for the motion of the centre of gravity

$$\left.\begin{aligned} M\ddot{y} &= Y \\ M\ddot{z} &= Z \\ M_{in} + Yz - Zy &= 0 \end{aligned}\right\}$$

From geometry

$$\left.\begin{aligned} y &= r\cos\varphi + e\cos\psi \\ z &= r\sin\varphi + e\sin\psi \end{aligned}\right\}$$

and these equations give after some calculations

$$M_{in} = Mer(\dot{\varphi}^2 - \dot{\psi}^2)\sin\theta$$

where

$$\theta = \psi - \varphi$$

and the result is the same as in eq. 10.3. Observe that $\omega' t = (\theta - \pi)$.

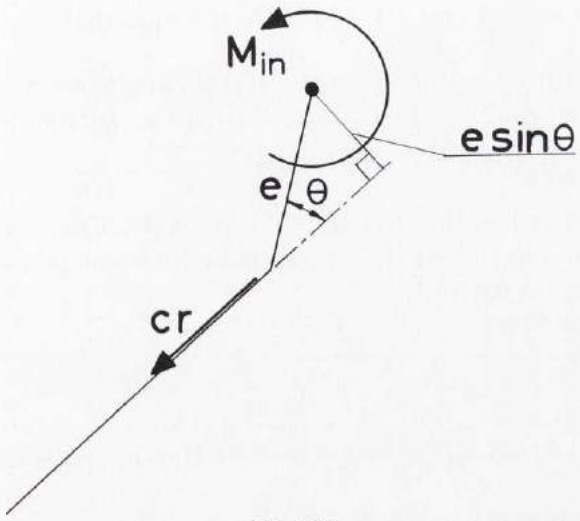

Fig. 13.1

Now we treat the case where in fig. 11.2 r is proportional to the resultant of Y and Z and is directed in its direction. Further, we assume that the shaft is unaffected by gyroscopic moments. With these presumptions the figs 12.1 and 13.1 are drawn.

From fig. 12.1 is obtained

$$M_{in} = Ze \cos \psi - Ye \sin \psi$$

and further

$$\left.\begin{aligned} Y &= -cr \cos \varphi \\ Z &= -cr \sin \varphi \end{aligned}\right\}$$

where c is a spring constant.

Thus

$$M_{in} = cre \sin \theta \quad \ldots\ldots\ldots\ldots\ldots\ldots \quad 13.2$$

which also can be written down directly with the aid of fig. 13.1.

If $K = +1$ the eqs 10.3 and 13.2 give the same torque, viz. $M_{in} = 0$. It is shown later that r always varies if $K \neq +1$.

From the eqs 9.1 and 9.2 we get for the rigid shaft

$$M_{\eta'} = -\Omega \sin\alpha(I_p\omega''-I_e\Omega\cos\alpha)+M(a\sin\alpha)\Omega^2(a\cos\alpha)- \\ -\tfrac{1}{2}Me^2\Omega(\omega'+\omega'')\sin\alpha+Mea\{\Omega^2\sin^2\alpha-(\omega'')^2\}\cos\omega' t- \\ -\tfrac{1}{2}\cdot Me^2\Omega(\omega'+\omega'')\sin\alpha\cos 2\omega' t \quad \ldots\ldots\ldots\ldots\ldots\ldots \quad 14.1$$

$M_{\eta'}$ is an outer moment acting at the point A'. Thus, eq. 10.2 gives the input torque and eq. 14.1 the bending moment perpendicular to r for the case in fig. 10.1.

If $e = 0$ we get

$$\left.\begin{aligned} M_{in} &= 0 \\ M_{\eta'} &= -\Omega\sin\alpha(I_p\omega''-I_e\Omega\cos\alpha)+M(a\sin\alpha)\Omega^2(a\cos\alpha) \end{aligned}\right\}$$

and the bending moment *at the disc* is

$$(M_{\eta'})_{disc} = -\Omega\sin\alpha(I_p\omega''-I_e\Omega\cos\alpha)$$

For small values of α we get

$$(M_{\eta'})_{disc} = -\left(\frac{\omega}{\Omega}-\frac{1}{2}\right)I_p\Omega^2\alpha \quad \ldots\ldots\ldots\ldots \quad 14.2$$

and the gyroscopic moment from the disc is $M_g = -(M_{\eta'})_{disc}$ and thus

$$M_g = (K-\tfrac{1}{2})I_p\Omega^2\alpha \quad \ldots\ldots\ldots\ldots\ldots\ldots \quad 14.3$$

which is the usual value of this moment. Now it must be emphasized that this moment is derived for a perfectly balanced disc. In practice we have $e \neq 0$ and the shaft deflection r will vary.

Now the following assumptions are made for the theoretical treatment in the rest of the report:

The gyroscopic bending moment can approximately be written as in eq. 14.3 if

1) $e^2 \ll \dfrac{I_p}{M}$ and $ea \ll \dfrac{I_p}{M}$

2) r varies according to $(r_0-\Delta r)\leq r\leq(r_0+\Delta r)$, where $\dfrac{\Delta r}{r_0} \ll 1$

3) $\dot\varphi$ varies according to $(\dot\varphi_0-\Delta\dot\varphi)\leq\dot\varphi\leq(\dot\varphi_0+\Delta\dot\varphi)$, where $\dfrac{\Delta\dot\varphi}{\dot\varphi_0} \ll 1$.

4. Basic Equations for the Motion

4,1. Perfect Shaft

Consider a circular shaft on support with an unbalanced disc driven by a motor according to fig. 16.1. The coupling is thought only to transmit a torque.

Further assumptions:

The mass and the gyroscpoic effect of the shaft can be neglected
The friction torques in the bearings can be neglected
The internal damping is zero
The shaft is perfectly elastic
The shaft is vertical.

In fig. 17.1 the cross-section $A-A$ is shown.

In this figure we have the following notations:

B Bearing
S Centre of the shaft
G Centre of gravity
K_y Elastic force in the y-direction
K_z Elastic force in the z-direction
M_x Input torque at the disc
M_{in} Input torque at the motor
e Eccentricity of the disc
r Deflection of the shaft at the disc.

Further, the deflection of the shaft r is split up into two *arbitrary* directions perpendicular to each other, r_1 and r_2.

With notations from [5] we get for the deflections and the angles

$$\left.\begin{aligned} r_1 &= -(\ \ K_y \cos\varphi + K_z \sin\varphi)\alpha_F + 2\gamma I_p \Omega^2 \alpha_M w_1 \\ w_1 &= -(\ \ K_y \cos\varphi + K_z \sin\varphi)\beta_F + 2\gamma I_p \Omega^2 \beta_M w_1 \\ r_2 &= -(-K_y \sin\varphi + K_z \cos\varphi)\alpha_F + 2\gamma I_p \Omega^2 \alpha_M w_2 \\ w_2 &= -(-K_y \sin\varphi + K_z \cos\varphi)\beta_F + 2\gamma I_p \Omega^2 \beta_M w_2 \end{aligned}\right\} \quad \ldots\ . \quad 15.1$$

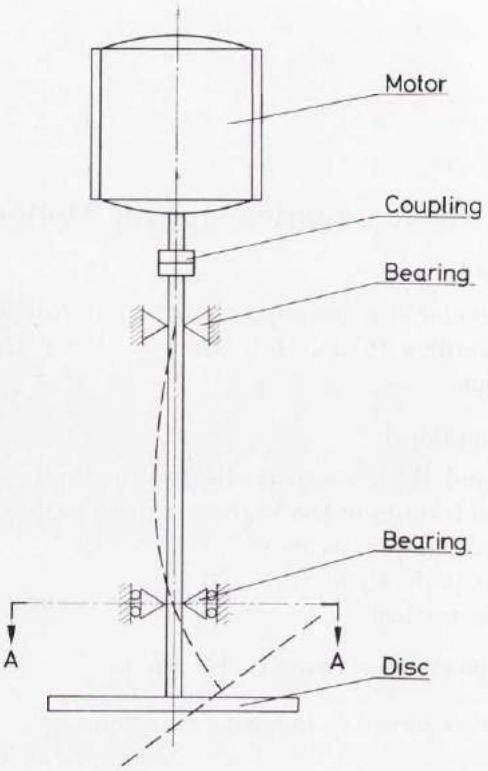

Fig. 16.1

where

$$\gamma = \tfrac{1}{2}(K - \tfrac{1}{2})$$

and w_1 and w_2 are the inclinations of the disc towards the bearing line.

From the eqs 15.1 is obtained

$$\left.\begin{aligned} w_1 &= \frac{-(K_y \cos\varphi + K_z \sin\varphi)}{1 - 2\gamma I_p \Omega^2 \beta_M} \cdot \beta_F \\ w_2 &= \frac{-(-K_y \sin\varphi + K_z \cos\varphi)}{1 - 2\gamma I_p \Omega^2 \beta_M} \cdot \beta_F \end{aligned}\right\}$$

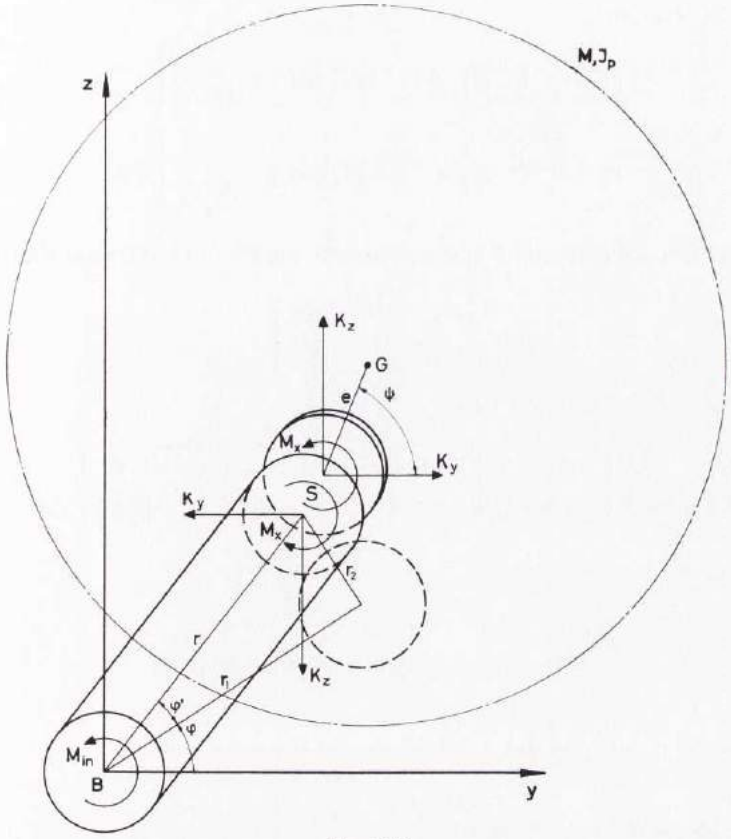

Fig. 17.1

and thus

$$\left.\begin{aligned} r_1 &= -(\quad K_y \cos\varphi + K_z \sin\varphi)\left(\alpha_F + \frac{2\gamma I_p \Omega^2 \alpha_M \beta_F}{1-2\gamma I_p \Omega^2 \beta_M}\right) \\ r_2 &= -(-K_y \sin\varphi + K_z \cos\varphi)\left(\alpha_F + \frac{2\gamma I_p \Omega^2 \alpha_M \beta_F}{1-2\gamma I_p \Omega^2 \beta_M}\right) \end{aligned}\right\}$$

Now define

$$\Omega_g^{-2} = M\alpha_F\left\{1 + \frac{\alpha_M \beta_F}{\alpha_F \beta_M} \cdot \frac{2\gamma I_p \Omega^2 \beta_M}{1-2\gamma I_p \Omega^2 \beta_M}\right\} \quad \ldots\ldots\ 17.2$$

and consequently

$$\left.\begin{aligned} r_1 &= -(\quad K_y \cos\varphi + K_z \sin\varphi)\,\frac{1}{M\Omega_g^2} \\ r_2 &= -(-K_y \sin\varphi + K_z \cos\varphi)\,\frac{1}{M\Omega_g^2} \end{aligned}\right\} \quad \ldots\ldots\ldots \quad 18.1$$

Further, we have (if k is a coefficient for viscous external damping)

$$\left.\begin{aligned} K_y &= M\ddot{y} + k\dot{y} \\ K_z &= M\ddot{z} + k\dot{z} \end{aligned}\right\}$$

and thus, from the eqs 18.1

$$\left.\begin{aligned} -M\Omega_g^2 r_1 &= M(\quad \ddot{y}\cos\varphi + \ddot{z}\sin\varphi) + k(\quad \dot{y}\cos\varphi + \dot{z}\sin\varphi) \\ -M\Omega_g^2 r_2 &= M(-\ddot{y}\sin\varphi + \ddot{z}\cos\varphi) + k(-\dot{y}\sin\varphi + \dot{z}\cos\varphi) \end{aligned}\right\} \quad \ldots\ldots \quad 18.2$$

Geometry gives

$$\left.\begin{aligned} y &= r_1 \cos\varphi - r_2 \sin\varphi + e\cos\psi \\ z &= r_1 \sin\varphi + r_2 \cos\varphi + e\sin\psi \end{aligned}\right\} \quad \ldots\ldots\ldots\ldots \quad 18.3$$

Derivation gives by putting

$$\left.\begin{aligned} \Omega_{g0} &= \frac{\Omega_g}{\Omega_n} \\ \Omega_n^{-2} &= M\alpha_F \\ \frac{r_1}{e} &= \rho_1 \\ \frac{r_2}{e} &= \rho_2 \\ 2D^* &= \frac{k}{M\Omega_n} \end{aligned}\right\}$$

that the eqs 18.2 can be written

$$\left.\begin{aligned} -\rho_1\Omega_{g0}^2 &= \ddot{\rho}_1 - \rho_1\dot{\varphi}^2 - \ddot{\psi}\sin\theta - \dot{\psi}^2\cos\theta - \rho_2\ddot{\varphi} - 2_2\dot{\rho}\dot{\varphi} + \\ &\quad + 2D^*(\dot{\rho}_1 - \dot{\psi}\sin\theta - \rho_2\dot{\varphi}) \\ -\rho_2\Omega_{g0}^2 &= 2\dot{\rho}_1\dot{\varphi} + \rho_1\ddot{\varphi} + \ddot{\psi}\cos\theta - \dot{\psi}^2\sin\theta + \ddot{\rho}_2 - \rho_2\dot{\varphi}^2 + \\ &\quad + 2D^*(\rho_1\dot{\varphi} + \dot{\psi}\cos\theta + \dot{\rho}_2) \end{aligned}\right\} \quad \ldots\ldots\ldots \quad 18.4$$

and in these equations and in the following

$$\dot{\varphi} = \frac{d\varphi}{d(\Omega_n t)}, \quad \ddot{\varphi} = \frac{d^2\varphi}{d(\Omega_n t)^2}, \quad \text{etc.}$$

and we denote $\tau = \Omega_n t$.

The eqs 18.4 can also be written

$$\left.\begin{aligned} &\ddot{\rho}_1 + 2D^*\dot{\rho}_1 + \rho_1(\Omega_{g0}^2 - \dot{\varphi}^2) - \rho_2\ddot{\varphi} - 2\dot{\rho}_2\dot{\varphi} - 2D^*\dot{\varphi}\rho_2 = \\ &\quad = \ddot{\psi}\sin\theta + \dot{\psi}^2\cos\theta + 2D^*\dot{\psi}\sin\theta \\ &\rho_1\ddot{\varphi} + 2\dot{\rho}_1\dot{\varphi} + 2D^*\dot{\varphi}\rho_1 + \ddot{\rho}_2 + 2D^*\dot{\rho}_2 + \rho_2(\Omega_{g0}^2 - \dot{\varphi}^2) = \\ &\quad = -\ddot{\psi}\cos\theta + \dot{\psi}^2\sin\theta - 2D^*\dot{\psi}\cos\theta \end{aligned}\right\} \quad \ldots\ldots\ 19.1$$

Further, the equilibrium of torque gives

$$M_{in} = M_x + K_z y_s - K_y z_s = I_p \frac{d^2\psi}{dt^2} + K_z y - K_y z \quad \ldots\ldots\ 19.2$$

and from the eqs 18.1 we have

$$\left.\begin{aligned} K_y &= -M\Omega_g^2(r_1\cos\varphi - r_2\sin\varphi) \\ K_z &= -M\Omega_g^2(r_1\sin\varphi + r_2\cos\varphi) \end{aligned}\right\}$$

Thus from eq. 19.2 we get

$$M_{in}^* = \ddot{\psi} + \varepsilon^2(\rho_1\sin\theta - \rho_2\cos\theta) \quad \ldots\ldots\ 19.3$$

where

$$\left.\begin{aligned} M_{in} &= I_p\Omega_n^2 M_{in}^* \\ \varepsilon &= \frac{e}{k_i}\cdot\Omega_{g0} \\ I_p &= Mk_i^2 \end{aligned}\right\}$$

The critical whirl speed Ω_c can be determined from eq. 17.2 by putting $\Omega_g = \Omega = \Omega_c$. This can easily be proved by using the results of Chapter 10 of [5].

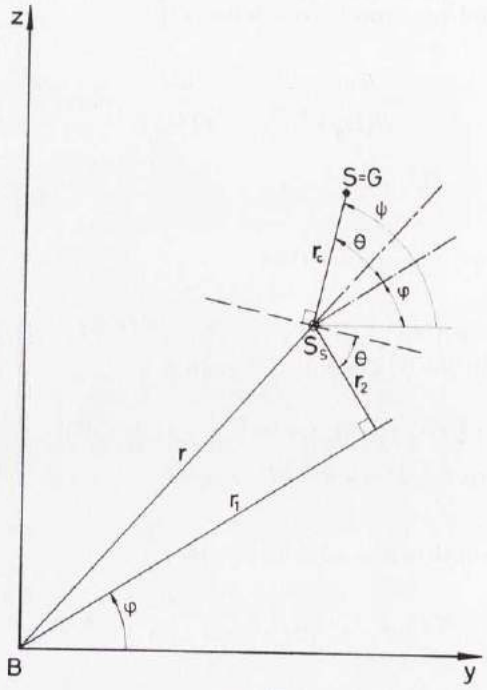

Fig. 20.1

4,2. **Curved Shaft with a Disc without Eccentricity**

In this section it is supposed that the shaft is also at rest slightly curved in one plane. At the disc it has a slope w_c and a deflection r_c. Further, it is assumed that the eccentricity of the disc is zero.

The geometry in this case is shown in fig. 20.1.

In this figure S_s is the point in which the centre of a *straight* shaft would have been at a deflection.

By assuming small angles the eqs 15.1 are replaced by

$$\left.\begin{aligned} r_1 &= -(K_y \cos\varphi + K_z \sin\varphi)\alpha_F + 2\gamma I_p \Omega^2 \alpha_M w_1 \\ w_1 - w_c \cos\theta &= -(K_y \cos\varphi + K_z \sin\varphi)\beta_F + 2\gamma I_p \Omega^2 \beta_M w_1 \end{aligned}\right\}$$

$$\left.\begin{aligned} r_2 &= -(-K_y \sin\varphi + K_z \cos\varphi)\alpha_F + 2\gamma I_p \Omega^2 \alpha_M w_2 \\ w_2 - w_c \sin\theta &= -(-K_y \sin\varphi + K_z \cos\varphi)\beta_F + 2\gamma I_p \Omega^2 \alpha_M w_2 \end{aligned}\right\}$$

and from here

$$\left.\begin{aligned} w_1 &= \frac{-(\quad K_y \cos\varphi + K_z \sin\varphi)\beta_F}{1-2\gamma I_p \Omega^2 \beta_M} + \frac{w_c \cos\theta}{1-2\gamma I_p \Omega^2 \beta_M} \\ w_2 &= \frac{-(-K_y \sin\varphi + K_z \cos\varphi)\beta_F}{1-2\gamma I_p \Omega^2 \beta_M} + \frac{w_c \sin\theta}{1-2\gamma I_p \Omega^2 \beta_M} \end{aligned}\right\}$$

and, further,

$$\left.\begin{aligned} r_1 &= -(\quad K_y \cos\varphi + K_z \sin\varphi)\left(\alpha_F + \frac{2\gamma I_p \Omega^2 \alpha_M \beta_F}{1-2\gamma I_p \Omega^2 \beta_M}\right) + \\ &\quad + \frac{2\gamma I_p \Omega^2 \alpha_M}{1-2\gamma I_p \Omega^2 \beta_M} \cdot w_c \cos\theta \\ r_2 &= -(-K_y \sin\varphi + K_z \cos\varphi)\left(\alpha_F + \frac{2\gamma I_p \Omega^2 \alpha_M \beta_F}{1-2\gamma I_p \Omega^2 \beta_M}\right) + \\ &\quad + \frac{2\gamma I_p \Omega^2 \alpha_M}{1-2\gamma I_p \Omega^2 \beta_M} \cdot w_c \sin\theta \end{aligned}\right\} \quad \ldots\ldots \ 21.1$$

We may write, with notations from [5],

$$\frac{2\gamma I_p \Omega^2 \alpha_M w_c}{1-2\gamma I_p \Omega^2 \beta_M} = \frac{\frac{\nu\zeta_M}{\Lambda} \cdot w_c}{1-\frac{\nu\zeta_M}{\Lambda}} \cdot \frac{\xi_M L}{\zeta_M} = \frac{\nu\zeta_M}{\Lambda-\nu\zeta_M} \cdot \frac{\xi_M}{\zeta_M} \cdot w_c L =$$

$$= \frac{\nu\zeta_M}{\Lambda-\nu\zeta_M} \cdot \frac{\xi_M}{\zeta_M} \cdot \frac{r_c L}{L_c} = \Phi r_c$$

and here is also

$$\left.\begin{aligned} w_c &= \frac{r_c}{L_c} \\ \Phi &= \frac{\nu\zeta_M}{\Lambda-\nu\zeta_M} \cdot \frac{\xi_M}{\zeta_M} \cdot \frac{L}{L_c} \end{aligned}\right\} \quad \ldots\ldots\ldots\ldots \ 21.2$$

where L_c can be positive or negative.

Thus, the eqs 21.1 can be written

$$\left.\begin{aligned} r_1-\Phi r_c\cos\theta &= -(\quad K_y\cos\varphi+K_z\sin\varphi)\cdot\frac{1}{M\Omega_g^2}\\ r_2-\Phi r_c\sin\theta &= -(-K_y\sin\varphi+K_z\cos\varphi)\cdot\frac{1}{M\Omega_g^2}\end{aligned}\right\}$$

Compare with the eqs 18.1. The eqs 18.1 are still valid if r_1 is changed to $(r_1-\Phi r_c\cos\theta)$ and r_2 to $(r_2-\Phi r_c\sin\theta)$.

Geometry gives

$$\left.\begin{aligned} y &= r_1\cos\varphi-r_2\sin\varphi+r_c\cos\psi\\ z &= r_1\sin\varphi+r_2\cos\varphi+r_c\sin\psi\end{aligned}\right\}$$

These equations are the same as the eqs 18.3 if e is replaced by r_c. Now we are able to write the final differential equations at once, viz.

$$\left.\begin{aligned} &\ddot\rho_1+2D^*\dot\rho_1+\rho_1(\Omega_{g0}^2-\dot\varphi^2)-\rho_2\ddot\varphi-2\dot\rho_2\dot\varphi-2D^*\dot\varphi\rho_2=\\ &\quad=\ddot\psi\sin\theta+(\dot\psi^2+\Phi\Omega_{g0}^2)\cos\theta+2D^*\dot\psi\sin\theta\\ &\rho_1\ddot\varphi+2\dot\rho_1\dot\varphi+2D^*\dot\varphi\rho_1+\ddot\rho_2+2D^*\dot\rho_2+\rho_2(\Omega_{g0}^2-\dot\varphi^2)=\\ &\quad=-\ddot\psi\cos\theta+(\dot\psi^2+\Phi\Omega_{g0}^2)\sin\theta-2D^*\dot\psi\cos\theta\end{aligned}\right\}\quad\ldots\ 22.1$$

where

$$\rho_1=\frac{r_1}{r_c},\quad \rho_2=\frac{r_2}{r_c}.$$

Finally, for the input torque we have

$$M_{in}^*=\ddot\psi+\varepsilon^2(\rho_1\sin\theta-\rho_2\cos\theta)$$

where

$$\varepsilon=\frac{r_c}{k_t}\cdot\Omega_{g0}\sqrt{1+\Phi}$$

5. Solutions of the Differential Equations

In this chapter solutions of the differential equations 19.1 are obtained for the assumptions:

$$\dot{\psi} = \dot{\psi}_0 = \text{const.}$$
$$\dot{\varphi} = \dot{\varphi}_0 = \text{const.}$$

The following cases are treated:

Case 1 $K = +1$; $\rho_2 = 0$; $\dot{\psi}_0 \neq \Omega_{g0}$ or $\dot{\psi}_0 = \Omega_{g0}$
Case 2 A special whirling with $\rho_2 = 0$
Case 3 K of any kind: $e = 0$, $D^* = 0$, $\dot{\varphi}_0 = \Omega_{g0}$
Case 4 K of any kind: $e \neq 0$, $D^* = 0$, $\dot{\varphi}_0 \neq \Omega_{g0}$ or $\dot{\varphi}_0 = \Omega_{g0}$

5,1. Case 1

In this section the ordinary whirl with $K = 1$ is treated by considering external damping.

From the eqs 19.1 we get by putting $\rho_2 = 0$, $\rho_1 = \rho$, $\dot{\varphi} = \dot{\psi} = \dot{\psi}_0$, and $\theta = \theta_0$ (= const.)

$$\left.\begin{aligned} \ddot{\rho} + 2D^*\dot{\rho} + (\Omega_{g0}^2 - \dot{\psi}_0^2)\rho &= \dot{\psi}_0^2 \cos\theta_0 + 2D^*\dot{\psi}_0 \sin\theta_0 \\ 2\dot{\rho} + \qquad 2D^*\rho &= \dot{\psi}_0 \sin\theta_0 - 2D^* \cos\theta_0 \end{aligned}\right\} \quad \ldots\ldots \quad 23.1$$

Here we try the solution $\rho = \rho_0$ (= const.). Thus

$$(\Omega_{g0}^2 - \dot{\psi}_0^2)\rho_0 = \dot{\psi}_0^2 \cos\theta_0 + (2D^*)^2(\rho_0 + \cos\theta_0)$$

or

$$\rho_0 = \frac{[\dot{\psi}_0^2 + (2D^*)^2]\cos\theta_0}{\Omega_{g0}^2 - \dot{\psi}_0^2 - (2D^*)^2} \quad \ldots\ldots\ldots\ldots \quad 23.2$$

Further the last equation in 23.1 gives

$$\dot{\psi}_0 \sin\theta_0 = 2D^*\left(\frac{\rho_0}{\cos\theta_0} + 1\right)\cos\theta_0$$

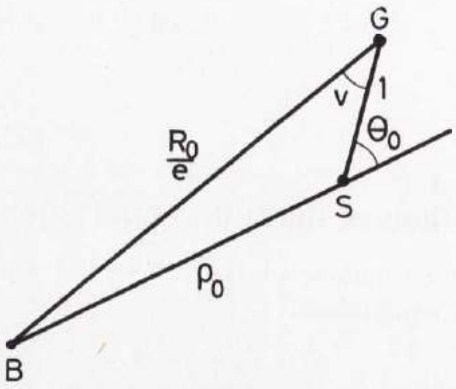

Fig. 24.1

and with the aid of eq. 23.2 is obtained

$$\operatorname{tg} \theta_0 = \frac{2D^*}{\dot{\psi}_0} \cdot \frac{\Omega_{g0}^2}{\Omega_{g0}^2 - \dot{\psi}_0^2 - (2D^*)^2} \quad \ldots\ldots\ldots\ldots \quad 24.2$$

and eq. 23.2 may be written

$$\rho_0 = \frac{\dot{\psi}_0[\dot{\psi}_0^2 + (2D^*)^2]}{\sqrt{(2D^*\Omega_{g0}^2)^2 + \dot{\psi}_0^2[\Omega_{g0}^2 - \dot{\psi}_0^2 - (2D^*)^2]^2}} = \dot{\psi}_0 \sqrt{\frac{\dot{\psi}_0^2 + (2D^*)^2}{(\Omega_{g0}^2 - \dot{\psi}_0^2)^2 + (2D^*\dot{\psi}_0)^2}} \quad 24.3$$

At the critical state for a rotor unaffected by any gyroscopic moments ($\dot{\psi}_0 = \Omega_{g0} = 1$) we get

$$\left.\begin{aligned} \operatorname{tg} \theta_0 &= -\frac{1}{2D^*} \\ \rho_0 &= \frac{\sqrt{1+(2D^*)^2}}{2D^*} \end{aligned}\right\}$$

Now consider fig. 24.1.

We get from above

$$\cos^2 \theta_0 = \frac{1}{1 + \operatorname{tg}^2 \theta_0} = \frac{(2D^*)^2}{1+(2D^*)^2}$$

and

$$\cos \theta_0 = -\frac{2D^*}{\sqrt{1+(2D^*)^2}}$$

Hence $\rho_0 \cos(\pi-\theta_0) = +1$, which means that $v = \frac{\pi}{2}$ rad. independent of the damping.

In the tabs 26.1 and 27.1 ρ_0 and θ_0 are calculated for the same rotor with different values of $\dot{\psi}_0$ and D^*. (The last decimal may be incorrect in some units). For this case we have

$$\left.\begin{aligned} \rho_0 &= \dot{\psi}_0 \sqrt{\frac{\dot{\psi}_0^2+(2D^*)^2}{(1-\dot{\psi}_0^2)^2+(2D^*)^2\dot{\psi}_0^2}} \\ \operatorname{tg}\theta_0 &= \frac{2D^*}{\dot{\psi}_0} \cdot \frac{1}{1-\dot{\psi}_0^2-(2D^*)^2} \end{aligned}\right\}$$

It is remarkable that if $\dot{\psi}_0 < \frac{\sqrt{2}}{2}$ the shaft deflection increases with increasing damping. It can easily be shown with the aid of the cosine theorem that

$$\frac{R_0}{e} = \frac{1}{\sqrt{(1-\dot{\psi}_0^2)^2+(2D^*)^2\dot{\psi}_0^2}}$$

and from this expression it can be concluded that the centre of gravity always decreases its distance from the bearing line when the damping increases.

The maximum shaft deflection is obtained when

$$\dot{\psi}_0^2 = \tfrac{1}{2}\left(1+\sqrt{1+2\alpha}\right)$$

where $\alpha = (2D^*)^2$ for shortness and this gives

$$\left.\begin{aligned} (\rho_0)^2_{max} &= \frac{1+2\alpha+(1+\alpha)\sqrt{1+2\alpha}}{1+2\alpha-(1-\alpha)\sqrt{1+2\alpha}} \\ \left(\frac{R_0}{e}\right)^2 &= \frac{2}{1+2\alpha-(1-\alpha)\sqrt{1+2\alpha}} \end{aligned}\right\}$$

The maximum deflection of the centre of gravity is obtained when

$$\dot{\psi}_0^2 = 1-\frac{\alpha}{2}$$

$\dot{\psi}_0$	$2D^*$ or $2D_m^*$	Damping force in G		Damping force in S		θ_0	
		ϱ_0	θ_0 (rad.)	ϱ_0	θ_0 (rad.)	D.f. in G (°)	D.f. in S (°)
0,25	0,00000000	0,06666667	0,00000000	0,06666667	0,00000000	0,00	0,00
	0,01000000	0,06671980	0,04264519	0,06666647	0,00266665	2,44	0,15
	0,02000000	0,06687873	0,08516302	0,06666574	0,00533325	4,88	0,31
	0,05000000	0,06798089	0,21072816	0,06666078	0,01333249	12,07	0,76
	0,10000000	0,07177668	0,40716657	0,06664301	0,02666024	23,33	1,53
	0,20000000	0,08525382	0,72802400	0,06657208	0,05328266	41,71	3,05
	0,50000000	0,14776353	1,23970007	0,06608186	0,13255131	71,03	7,59
	2,00000000	0,47425045	1,93639870	0,05882353	0,48995716	110,95	28,07
	3,00000000	0,62686037	2,16239627	0,05205792	0,67474069	123,90	38,66
0,50	0,00000000	0,33333333	0,00000000	0,33333333	0,00000000	0,00	0,00
	0,01000000	0,33339263	0,02666379	0,33332596	0,00666653	1,53	0,38
	0,02000000	0,33357032	0,05331104	0,33330377	0,01333249	3,05	0,76
	0,10000000	0,33918174	0,26396394	0,33259505	0,06656794	15,12	3,81
	0,20000000	0,35586173	0,51305787	0,33040933	0,13255131	29,40	7,59
	0,50000000	0,44721359	1,10714895	0,31622776	0,32175075	63,43	18,43
	1,00000000	0,62017367	1,69515109	0,27735010	0,58800284	97,13	33,69
	2,00000000	0,82462112	2,25311265	0,20000000	0,92729532	129,09	53,13
	3,00000000	0,90676470	2,51279635	0,14907120	1,10714895	143,97	63,43
0,75	0,00000000	1,28571428	0,00000000	1,28571428	0,00000000	0,00	0,00
	0,01000000	1,28564006	0,03047360	1,28552580	0,01714111	1,75	0,98
	0,02000000	1,28541619	0,06093243	1,28495940	0,03427216	3,49	1,96
	0,05000000	1,28386073	0,15207329	1,28101721	0,08550505	8,71	4,90
	0,10000000	1,27844342	0,30233004	1,26722878	0,16977816	17,32	9,73
	0,20000000	1,25871707	0,59089997	1,21621641	0,33029753	33,86	18,92
	0,50000000	1,17323083	1,29662863	0,97618707	0,70862626	74,29	40,60
	1,00000000	1,07972362	1,97001698	0,64783417	1,04272182	112,87	59,74
	2,00000000	1,02528045	2,49902797	0,36000000	1,28700197	143,18	73,74
	3,00000000	1,01182598	2,70456621	0,24540384	1,37874833	154,96	79,00
0,90	0,00000000	4,26315604	0,00000000	4,26315606	0,00000000	0,00	0,00
	0,01000000	4,25865049	0,05844349	4,25838763	0,04733286	3,35	2,71
	0,02000000	4,24520687	0,11667326	4,24415909	0,09445468	6,68	5,41
	0,05000000	4,15479379	0,28805569	4,14839693	0,23255707	16,50	13,32
	0,10000000	3,87648806	0,55303164	3,85277842	0,44237398	31,69	25,35
	0,20000000	3,17034685	0,97704644	3,09485158	0,75837772	55,98	43,45
	0,50000000	1,89696903	1,67837909	1,65824930	1,17128096	96,16	67,11
	1,00000000	1,31634869	2,20072142	0,88059085	1,36274014	126,09	78,08
	2,00000000	1,09052712	2,61357255	0,44751381	1,46563045	149,75	83,97
	3,00000000	1,04145519	2,77988125	0,29925995	1,50054199	159,28	85,97

Tab. 26.1

$\dot{\psi}_0$	$2D^*$ or $2D_m^*$	Damping force in G		Damping force in S		θ_0	
		ϱ_0	θ_0 (rad.)	ϱ_0	θ_0 (rad.)	D.f. in G (°)	D.f. in S (°)
	0,00000000	2,77777777	3,14159265	2,77777777	3,14159265	180,00	180,00
	0,01000000	2,77718122	3,12737397	2,77709235	3,11937417	179,19	178,73
	0,02000000	2,77539362	3,11317618	2,77503844	3,09717760	178,37	177,46
	0,05000000	2,76299589	3,07091434	2,76078813	3,03093568	175,95	173,66
1,25	0,10000000	2,72029404	3,00275390	2,71163066	2,92292362	172,05	167,47
	0,20000000	2,57065125	2,88202337	2,53836550	2,72336852	165,13	156,04
	0,50000000	2,00138073	2,68411806	1,85823537	2,30361167	153,79	131,99
	1,00000000	1,45978667	2,66839142	1,13990188	1,99365005	152,89	114,23
	2,00000000	1,15048550	2,80430763	0,60975610	1,79211087	160,67	102,68
	0,00000000	1,80000000	3,14159265	1,80000000	3,14159265	180,00	180,00
	0,01000000	1,79991041	3,13625982	1,79987042	3,12959328	179,69	179,31
	0,02000000	1,79964178	3,13092985	1,79948184	3,11759735	179,39	178,63
	0,05000000	1,79776664	3,11498560	1,79676871	3,08166470	178,48	176,57
	0,10000000	1,79114541	3,08873207	1,78717830	3,02216396	176,97	173,16
1,50	0,20000000	1,76578682	3,03859945	1,75029716	2,90604752	174,10	166,50
	0,50000000	1,62697843	2,92292362	1,54348726	2,60117303	167,47	149,04
	1,00000000	1,38493061	2,85353696	1,15233192	2,26553445	163,50	129,81
	2,00000000	1,15384615	2,89288247	0,69230769	1,96558735	165,75	112,62
	3,00000000	1,07724577	2,94889192	0,48175895	1,84174341	168,96	105,52
	0,00000000	1,48484848	3,14159265	1,48484848	3,14159265	180,00	180,00
	0,01000000	1,48481928	3,13882225	1,48479504	3,13310805	179,84	179,51
	0,02000000	1,48473168	3,13605268	1,48463473	3,12462405	179,68	179,03
	0,03000000	1,48458577	3,13328482	1,48436767	3,11614370	179,52	178,54
	0,04000000	1,48438164	3,13051949	1,48399404	3,10766641	179,37	178,06
1,75	0,05000000	1,48411945	3,12775755	1,48351406	3,09919399	179,21	177,57
	0,10000000	1,48194586	3,11402780	1,47953226	3,05694716	178,42	175,15
	0,20000000	1,47344907	3,08728923	1,46391979	2,97349714	176,89	170,37
	0,50000000	1,42162290	3,01866374	1,36692446	2,74036398	172,96	157,01
	1,00000000	1,30402473	2,95712503	1,13221053	2,43797894	169,43	139,69
	2,00000000	1,14478493	2,95526680	0,75384615	2,10330050	169,32	120,51
	0,00000000	1,33333333	3,14159265	1,33333333	3,14159265	180,00	180,00
	0,01000000	1,33332037	3,13992606	1,33330370	3,13492612	179,90	179,62
	0,02000000	1,33328149	3,13825980	1,33321483	3,12826017	179,81	179,24
	0,05000000	1,33300958	3,13326649	1,33259321	3,10827178	179,52	178,09
2,00	0,10000000	1,33204214	3,12498295	1,33038021	3,07502471	179,05	176,19
	0,20000000	1,32822895	3,10870990	1,32163720	3,00904133	178,12	172,41
	0,50000000	1,30384048	3,06482100	1,26491106	2,81984190	175,60	161,57
	1,00000000	1,24034734	3,01723788	1,10940039	2,55358981	172,87	146,31
	2,00000000	1,13137084	2,99969579	0,80000000	2,21429733	171,87	126,87

Tab. 27.1

giving

$$\left.\begin{aligned} \rho_0^2 &= \frac{4-\alpha^2}{4\alpha-\alpha^2} \\ \left(\frac{R_0}{e}\right)^2_{max} &= \frac{4}{4\alpha-\alpha^2} \end{aligned}\right\}$$

Observe that if α is small

$$(\rho_0)_{max} \quad \text{is obtained for } \dot{\psi}_0^2 = \left(1+\frac{\alpha}{2}\right)$$

$$\left(\frac{R_0}{e}\right)_{max} \text{is obtained for } \dot{\psi}_0^2 = \left(1-\frac{\alpha}{2}\right).$$

The damping force was previously assumed to be applied at the centre of gravity. Because this force is partly caused by air friction it seems reasonable to think that the force is applied at the centre of the disc and this point need not to be the same as the centre of gravity. Due to the manufacturing the centre of the disc in many cases coincides with the centre of the shaft. In these cases the damping force might be applied at the centre of the shaft. The damping coefficients are in these cases called D_m^* (m indicates here: $m$odified).

From the eqs 23.1 we have for a rotor unaffected by any gyroscopic moments

$$\left.\begin{aligned} (1-\dot{\psi}_0^2)\rho_0 &= \dot{\psi}_0^2 \cos\theta_0 \\ 2D_m^*\rho_0 &= \dot{\psi}_0 \sin\theta_0 \end{aligned}\right\}$$

and these equations have the solution

$$\left.\begin{aligned} \rho_0 &= \frac{\dot{\psi}_0^2}{\sqrt{(1-\dot{\psi}_0^2)^2+(2D_m^*\dot{\psi}_0)^2}} \\ \operatorname{tg}\theta_0 &= \frac{2D_m^*\dot{\psi}_0}{1-\dot{\psi}_0^2} \end{aligned}\right\}$$

The maximum shaft deflection is obtained when

$$\dot{\psi}_0^2 = \frac{2}{2-\alpha} \qquad [\alpha = (2D_m^*)^2]$$

and

$$\left.\begin{aligned}(\rho_0)^2_{max} &= \frac{4}{4\alpha-\alpha^2}\\ \left(\frac{R_0}{e}\right)^2 &= \frac{4-\alpha^2}{4\alpha-\alpha^2}\end{aligned}\right\}$$

The maximum deflection of the centre of gravity is obtained when

$$\psi_0^2 = \frac{\sqrt{1+2\alpha}-1}{\alpha}$$

and

$$\left.\begin{aligned}\rho_0^2 &= \frac{\left(\sqrt{1+2\alpha}-1\right)^2}{\left(1+\alpha-\sqrt{1+2\alpha}\right)^2+\alpha^2\left(\sqrt{1+2\alpha}-1\right)}\\ \left(\frac{R_0}{e}\right)^2_{max} &= \frac{\alpha^2}{\alpha^2-2\alpha-2+2\sqrt{1+2\alpha}}\end{aligned}\right\}$$

If α is small one gets that

$$(\rho_0)_{max} \quad \text{is obtained for } \psi_0^2 = \left(1+\frac{\alpha}{2}\right)$$

$$\left(\frac{R_0}{e}\right)_{max} \quad \text{is obtained for } \psi_0^2 = \left(1-\frac{\alpha}{2}\right).$$

This equals the first damping case.

In the tabs 26.1 and 27.1 also the values of ρ_0 and θ_0 for different values of ψ_0 and D_m^* are shown for comparison.

As a matter of fact the difference of the calculated values according to the two methods is very small in practical cases.

If $D^* = 0$ we get from the eq. 24.3

$$\rho_0 = \frac{\psi_0^2}{\Omega_{g0}^2-\psi_0^2} \quad \ldots\ldots\ldots\ldots\ldots\ldots \quad 29.1$$

and

$$\theta_0 = 0 \text{ or } \theta_0 = \pm\pi$$

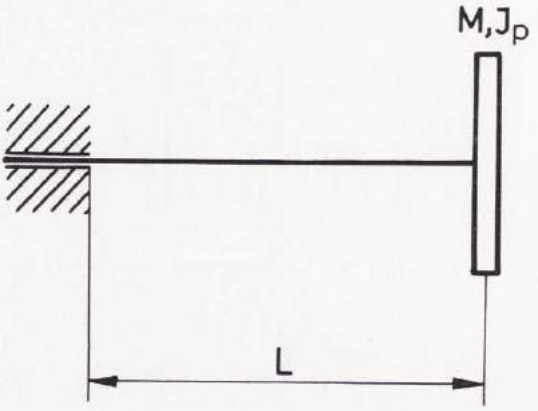

Fig. 30.1

Further, for a rotor unaffected by any gyroscopic moments

$$\rho_0 = \frac{\psi_0^2}{1-\psi_0^2} \quad \ldots\ldots\ldots\ldots\ldots\ldots \quad 30.2$$

which formula is given in many reports on the subject. It is of practical interest to know the error if Ω_{g0} in eq. 29.1 is substituted by $\frac{\Omega_c}{\Omega_n}$, where Ω_c is the critical angular velocity.

This question is treated for a special bearing arrangement, viz. the clamped-free shaft in fig. 30.1.

From definition

$$\Omega_{g0}^{-2} = 1 + \frac{\alpha_M \beta_F}{\alpha_F \beta_M} \cdot \frac{\frac{1}{2} \cdot I_p \Omega^2 \beta_M}{1 - \frac{1}{2} \cdot I_p \Omega^2 \beta_M}$$

Introducing (see also [5])

$$\left.\begin{aligned} \Omega^2 &= \frac{1}{\Lambda} \cdot \frac{6EI}{ML^3} \\ \nu &= \frac{1}{2} \cdot \frac{I_p}{ML^2} \end{aligned}\right\}$$

we get

$$\frac{1}{2} \cdot I_p \Omega^2 \beta_M = \frac{1}{2} \cdot I_p \cdot \frac{1}{\Lambda} \cdot \frac{6EI}{ML^3} \cdot \zeta_M \cdot \frac{L}{6EI} = \frac{\nu \zeta_M}{\Lambda}$$

Further, from [5]

$$\left.\begin{aligned} \xi_F &= 2 \quad \zeta_F = 3 \\ \xi_M &= -3 \quad \zeta_M = -6 \end{aligned}\right\}$$

Thus

$$\Omega_{g0}^2 = 1 + \frac{9\nu}{2\Lambda + 3\nu}$$

At the critical speed $\Lambda = \Lambda_c$ where Λ_c is obtained from the solution of the equation

$$\Omega_{g0}^2 = \psi_0^2$$

Here

$$\psi_0^2 = \frac{\Omega^2}{\Omega_n^2} = M\alpha_F\Omega^2 = M\alpha_F \cdot \frac{1}{\Lambda} \cdot \frac{6EI}{ML^3} = \frac{\xi_F}{\Lambda} = \frac{2}{\Lambda}$$

Thus

$$1 + \frac{9\nu}{2\Lambda_c + 3\nu} = \frac{2}{\Lambda_c}$$

giving

$$\Lambda_c^2 - 2(1-3\nu)\Lambda_c - 3\nu = 0 \quad \ldots\ldots\ldots\ldots \quad 31.1$$

From eq. 29.1

$$\rho_0 = \frac{2\Lambda + 3\nu}{\Lambda^2 - 2(1-3\nu)\Lambda - 3\nu} \quad \ldots\ldots\ldots\ldots \quad 31.2$$

and if Ω_{g0} is replaced by $\frac{\Omega_c}{\Omega_n}$ we get from eq. 29.1

$$\rho_0' = \frac{\Lambda_c}{\Lambda - \Lambda_c}$$

From eq. 31.1 is also obtained

$$\nu = \frac{\Lambda_c(\Lambda_c - 2)}{3(1-2\Lambda_c)} \quad \ldots\ldots\ldots\ldots\ldots \quad 31.3$$

This expression is put into eq. 31.2 and we get

$$\frac{\rho_0}{\rho_0'} = 1 + \frac{1}{\frac{\Lambda_c}{\Lambda}\left(\frac{\Lambda}{2-\Lambda_c} - \frac{1}{1-2\Lambda_c}\right)}$$

From here we get

$$\rho_0 > \rho_0'$$

if

$$\frac{\Lambda}{2-\Lambda_c} - \frac{1}{1-2\Lambda_c} > 0$$

giving

$$\Lambda > \frac{2-\Lambda_c}{1-2\Lambda_c}$$

But from eq. 31.3 is obtained that

$$\tfrac{1}{2} \leq \Lambda_c \leq 2$$

and the limits correspond to $\nu = \infty$ and $\nu = 0$. Thus

$$\frac{2-\Lambda_c}{1-2\Lambda_c} < 0$$

This means that ρ_0 is always greater than ρ_0' except when $\nu = 0$ or $\nu = \infty$. Then $\rho_0 = \rho_0'$.

This fact may be of interest if the eccentricity of a shaft is calculated from

$$e = \frac{r}{\rho}$$

where r is measured at a special speed and ρ is taken from

$$\rho = \rho_0' = \frac{\Omega^2}{\Omega_c^2 - \Omega^2}$$

The calculated eccentricity e will be too great. The correct result is obtained with the aid of the expression

$$\rho = \frac{\Omega^2}{\Omega_g^2 - \Omega^2}$$

Finally, we get from eq. 23.1 for a rotor unaffected by gyroscopic moments and external damping the following expressions at the critical state

$$\left.\begin{aligned} \ddot{\rho} &= \cos\theta_0 \\ 2\dot{\rho} &= \sin\theta_0 \end{aligned}\right\}$$

With the solution

$$\left.\begin{aligned} \rho &= C + \frac{\tau}{2}\sin\theta_0 \\ \theta_0 &= \pm\frac{\pi}{2} \end{aligned}\right\} \quad \ldots\ldots\ldots\ldots\ldots\ldots \quad 33.1$$

Here C is an arbitrary constant. Thus the shaft centre at the disc describes an "Archimedes' spiral". This has also been shown by *Föppl* and *Lorenz*. References are given in [9].

5,2. **Case 2**

In this section a special whirling mode is investigated. The case has

$$\rho_2 = 0;\ \rho_1 = \rho;\ \dot{\psi} = \dot{\psi}_0;\ \dot{\varphi} = \dot{\varphi}_0$$
$$\dot{\psi}_0 \neq \dot{\varphi}_0;\ \theta = (\dot{\psi}_0 - \dot{\varphi}_0)\tau + \theta_0$$

($\dot{\psi}_0$ and $\dot{\varphi}_0$ are constants and $\dot{\psi}_0 = \dfrac{d\psi}{d\tau}$ etc. Further, θ_0 is a constant).

The first of the eqs 19.1 gives

$$\begin{aligned} \rho = {} & C_1 e^{-D^*\tau}\cos p\tau + C_2 e^{-D^*\tau}\sin p\tau + \\ & + \frac{\dot{\psi}_0[(\Omega_{g0}^2 - \dot{\theta}^2 - \dot{\varphi}_0^2)\dot{\psi}_0 - \dot{\theta}(2D^*)^2]}{(\Omega_{g0}^2 - \dot{\theta}^2 - \dot{\varphi}_0^2)^2 + (2D^*\dot{\theta})^2}\cos\theta + \\ & + \frac{2D^*\dot{\psi}_0[\dot{\theta}\dot{\psi}_0 + \Omega_{g0}^2 - \dot{\theta}^2 - \dot{\varphi}_0^2]}{(\Omega_{g0}^2 - \dot{\theta}^2 - \dot{\varphi}_0^2)^2 + (2D^*\dot{\theta})^2}\sin\theta \quad \ldots\ldots\ldots \quad 33.2 \end{aligned}$$

where $p^2 = \{\Omega_{g0}^2 - \dot{\varphi}_0^2 - (D^*)^2\}$ and the second equation gives

$$p = C_3 e^{-D^* \tau} - \frac{\dot{\psi}_0\{\dot{\theta}\dot{\psi}_0 + 2(D^*)^2\}}{2\dot{\varphi}_0[\dot{\theta}^2 + (D^*)^2]} \cos\theta +$$

$$+ \frac{D^*\dot{\psi}_0(2\dot{\varphi}_0 - \dot{\psi}_0)}{2\dot{\varphi}_0[\dot{\theta}^2 + (D^*)^2]} \sin\theta$$

where $C_s (s = 1, 2, 3)$ are arbitrary constants. Further, $p > 0$ and $p \neq \dot{\theta}$.

These solutions must be identical which demands

$$\left.\begin{aligned} \frac{\dot{\psi}_0[(\Omega_{g0}^2 - \dot{\theta}^2 - \dot{\varphi}_0^2)\dot{\psi}_0 - \dot{\theta}(2D^*)^2]}{(\Omega_{g0}^2 - \dot{\theta}^2 - \dot{\varphi}_0^2)^2 + (2D^*\dot{\theta})^2} &= -\frac{\dot{\psi}_0[\dot{\theta}\dot{\psi}_0 + 2(D^*)^2]}{2\dot{\varphi}_0[\dot{\theta}^2 + (D^*)^2]} \\ D^*\dot{\psi}_0 \cdot \frac{2[\dot{\theta}\dot{\psi}_0 + \Omega_{g0}^2 - \dot{\theta}^2 - \dot{\varphi}_0^2]}{(\Omega_{g0}^2 - \dot{\theta}^2 - \dot{\varphi}_0^2)^2 + (2D^*\dot{\theta})^2} &= D^*\dot{\psi}_0 \cdot \frac{2\dot{\varphi}_0 - \dot{\psi}_0}{2\dot{\varphi}_0[\dot{\theta}^2 + (D^*)^2]} \end{aligned}\right\} \quad \ldots\ldots \quad 34.1$$

If $D^* \neq 0$ and $\dot{\psi}_0 \neq 0$ we get

$$\frac{2(\dot{\theta}\dot{\psi}_0 + \Omega_{g0}^2 - \dot{\theta}^2 - \dot{\varphi}_0^2)}{\dot{\psi}_0 - 2\dot{\varphi}_0} = \frac{(\Omega_{g0}^2 - \dot{\theta}^2 - \dot{\varphi}_0^2)\dot{\psi}_0 - \dot{\theta}(2D^*)^2}{\dot{\theta}\dot{\psi}_0 + 2(D^*)^2} = -\frac{(\Omega_{g0}^2 - \dot{\theta}^2 - \dot{\varphi}_0^2)^2 + (2D^*\dot{\theta})^2}{2\dot{\varphi}_0[\dot{\theta}^2 + (D^*)^2]} \quad 34.2$$

From the eqs 34.1 is obtained

$$\dot{\varphi}_0 = \frac{\Omega_{g0}^2 + \dot{\psi}_0^2}{2\dot{\psi}_0}$$

independent of the damping. Insertion into the first of the eqs 34.1 gives the solutions

$$\left.\begin{aligned} \dot{\psi}_0 &= \pm \quad \Omega_{g0} \\ \dot{\psi}_0^2 &= \quad \frac{2\Omega_{g0}^2 - (2D^*)^2}{2} \pm \sqrt{\frac{[2\Omega_{g0}^2 - (2D^*)^2]^2}{4} - \Omega_{g0}^4} \end{aligned}\right\}$$

The first solution gives $K = +1$ which is already treated, and the second gives complex angular velocities for real values of the damping coefficient D^*.

In the special case $D^* = 0$ the eqs 34.1 give

$$\Omega_{g0}^2 - \dot{\theta}^2 - \dot{\varphi}_0^2 = -2\dot{\varphi}_0\dot{\theta}$$

and from here

$$\dot{\varphi}_0 = \frac{\dot{\psi}_0 \pm \Omega_{g0}}{2}$$

or, which is the same,

$$K = 2 \pm \frac{\Omega_{g0}}{\dot{\varphi}_0} \quad \ldots\ldots\ldots\ldots\ldots\ldots \quad 35.1$$

At a critical state $\dot{\varphi}_0 = \Omega_{g0}$ and thus $K = 3$. (The value $K = +1$ is not considered in this section). The corresponding deflection of the shaft is

$$\rho = \rho_3 - \frac{9}{4}\cos\theta \qquad (\rho_3 = \text{const.}) \ldots\ldots\ldots \quad 35.2$$

Thus, it has been shown that if external damping is present the rotor cannot whirl with $\dot{\varphi} = \text{const}$. But if no damping occurs this is possible at the critical state with $K = +3$.

This type of whirl was also theoretically observed by *Kane* [7]. He came to the same result in another manner. He also discussed the stability of this whirl.

5,3. **Case 3**

In this section the perfectly balanced rotor is studied at its critical whirling speed. The external damping is not considered. Hence

$$e = 0; \; D^* = 0; \; \dot{\varphi}_0 = \Omega_{g0}$$

The second of the eqs 19.1 gives with $r_2 = 0$ and $r_1 = r$

$$\frac{1}{r} \cdot \frac{d}{d\tau}(r^2\dot{\varphi}_0) = 0$$

and thus

$$r = r_0 = \text{const.}$$

The first of the eqs 19.1 gives then

$$r_0 \cdot 0 = 0$$

and we may conclude that the value of r_0 at the critical speed is indifferent. This conclusion is valid for all kinds of whirling.

5,4. **Case 4**

In this section an arbitrary whirl is studied. It is assumed that no external damping occurs. Further,

$$\left.\begin{aligned} \dot{\psi} &= \dot{\psi}_0 = \text{const.} \\ \dot{\varphi} &= \dot{\varphi}_0 = \text{const.} \end{aligned}\right\}$$

The eqs 19.1 become

$$\left.\begin{aligned} \ddot{\rho}_1 + \rho_1(\Omega_{g0}^2 - \dot{\varphi}_0^2) - 2\dot{\rho}_2\dot{\varphi}_0 &= \dot{\psi}_0^2 \cos\theta \\ 2\dot{\rho}_1\dot{\varphi}_0 + \ddot{\rho}_2 + \rho_2(\Omega_{g0}^2 - \dot{\varphi}_0^2) &= \dot{\psi}_0^2 \sin\theta \end{aligned}\right\} \quad \ldots\ldots\ldots \quad 36.1$$

Elimination of ρ_2 gives

$$\rho_1^{IV} + 2(\Omega_{g0}^2 + \dot{\varphi}_0^2)\ddot{\rho}_1 + (\Omega_{g0}^2 - \dot{\varphi}_0^2)^2\rho_1 = (\Omega_{g0} + \dot{\theta} - \dot{\varphi}_0)(\Omega_{g0} - \dot{\theta} + \dot{\varphi}_0)\dot{\psi}_0^2 \cos\theta \quad 36.2$$

with the solution, if $\Omega_{g0}^2 \neq \dot{\varphi}_0^2$,

$$\begin{aligned} \rho_1 = {} & A_1 \sin(\Omega_{g0} - \dot{\varphi}_0)\tau + B_1 \cos(\Omega_{g0} - \dot{\varphi}_0)\tau + \\ & + C_1 \sin(\Omega_{g0} + \dot{\varphi}_0)\tau + D_1 \cos(\Omega_{g0} + \dot{\varphi}_0)\tau + \\ & + \frac{\dot{\psi}_0^2}{\Omega_{g0}^2 - \dot{\psi}_0^2} \cos\theta \quad \ldots\ldots\ldots\ldots\ldots\ldots\ldots\ldots \quad 36.3 \end{aligned}$$

and by inserting into the first of the eqs 36.1

$$\begin{aligned} \rho_2 = {} & -A_1 \cos(\Omega_{g0} - \dot{\varphi}_0)\tau + B_1 \sin(\Omega_{g0} - \dot{\varphi}_0)\tau + \\ & + C_1 \cos(\Omega_{g0} + \dot{\varphi}_0)\tau - D_1 \sin(\Omega_{g0} + \dot{\varphi}_0)\tau + \\ & + \frac{\dot{\psi}_0^2}{\Omega_{g0}^2 - \dot{\psi}_0^2} \sin\theta \quad \ldots\ldots\ldots\ldots\ldots\ldots\ldots\ldots \quad 36.4 \end{aligned}$$

The expressions for ρ_1 and ρ_2 are only valid if

$$\left.\begin{aligned} &\Omega_{g0}+\dot{\theta}_0-\dot{\varphi}_0 \neq 0 \\ &\Omega_{g0}-\dot{\theta}_0+\dot{\varphi}_0 \neq 0 \\ &\Omega_{g0} \neq \dot{\psi}_0 \end{aligned}\right\} \quad \ldots\ldots\ldots\ldots\ldots\ldots \quad 37.1$$

The arbitrary constants A_1, B_1, C_1, and D_1 may be determined from the boundary conditions.

At a critical speed $\dot{\varphi}_0 = \Omega_{g0}$ and the eqs 36.1 become

$$\left.\begin{aligned} \ddot{\rho}_1 - 2\dot{\varphi}_0\dot{\rho}_2 &= \dot{\psi}_0^2 \cos\theta \\ 2\dot{\varphi}_0\dot{\rho}_1 + \ddot{\rho}_2 &= \dot{\psi}_0^2 \sin\theta \end{aligned}\right\} \quad \ldots\ldots\ldots\ldots\ldots\ldots \quad 37.2$$

and from here

$$\dddot{\rho}_1 + (2\dot{\varphi}_0)^2\dot{\rho}_1 = (3\dot{\varphi}_0 - \dot{\psi}_0)\dot{\psi}_0^2 \sin\theta \quad \ldots\ldots\ldots\ldots\ldots \quad 37.3$$

If, as an example, $3\dot{\varphi}_0 = \dot{\psi}_0$ $(K = +3)$ we get

$$\rho_1 = \rho_{10} + C_1 \sin 2\dot{\varphi}_0\tau + D_1 \cos 2\dot{\varphi}_0\tau \qquad (\rho_{10} = \text{const.})$$

and from the first of the eqs 37.2

$$\rho_2 = \rho_{20} + C_1 \cos 2\dot{\varphi}_0\tau - D_1 \sin 2\dot{\varphi}_0\tau - \frac{9}{4}\sin\theta \qquad (\rho_{20} = \text{const.})$$

If we choose $D_1 = \left(-\frac{9}{4} + D_1'\right)$ we have

$$\left.\begin{aligned} \rho_1 &= \rho_{10} + C_1 \sin 2\dot{\varphi}_0\tau + D_1' \cos 2\dot{\varphi}_0\tau - \frac{9}{4}\cos\theta \\ \rho_2 &= \rho_{20} + C_1 \cos 2\dot{\varphi}_0\tau - D_1' \sin 2\dot{\varphi}_0\tau \end{aligned}\right\}$$

Further, if $C_1 = D_1' = \rho_{20} = 0$ we get

$$\left.\begin{aligned} \rho_1 = \rho &= \rho_{10} - \frac{9}{4}\cos\theta \\ \rho_2 &= 0 \end{aligned}\right\}$$

and this solution was obtained in the previous section. Hence this is only one of many solutions possible. But this is the only solution giving a perfectly constant whirl velocity.

If, as another example, $\dot{\psi}_0 = -\dot{\varphi}_0$ $(K = -1)$ we get from eq. 37.3 that

$$\ddot{\rho}_1 + (2\dot{\varphi}_0)^2 \dot{\rho}_1 = -4\dot{\varphi}_0^3 \sin 2\dot{\varphi}_0 \tau$$

and find the solution

$$\left.\begin{aligned} \rho_1 &= \rho_{10} + C_1 \sin 2\dot{\varphi}_0\tau + D_1 \cos 2\dot{\varphi}_0\tau + \frac{\dot{\varphi}_0\tau}{2} \sin 2\dot{\varphi}_0\tau \\ \rho_2 &= \rho_{20} + C_1 \cos 2\dot{\varphi}_0\tau - D_1 \sin 2\dot{\varphi}_0\tau + \frac{\dot{\varphi}_0\tau}{2} \cos 2\dot{\varphi}_0\tau \end{aligned}\right\}$$

A whirl with $K \approx -1$ can only be obtained if $\rho_{10} \gg \frac{\dot{\varphi}_0\tau}{2}$, thus only during a short period on "artificial" conditions.

For completeness it may be pointed out that the solutions 36.3 and 36.4 are valid also for $K = +1$ at a non-critical state if we put $\theta = 0$ or $\theta = \pi$. In the case $\Omega_{g0} = \dot{\varphi}_0$ the eq. 37.3 and the first of the eqs 37.2 give

$$\left.\begin{aligned} \rho_1 &= \rho_{10} + C_1 \sin 2\dot{\varphi}_0\tau + D_1 \cos 2\dot{\varphi}_0\tau + \frac{\dot{\varphi}_0\tau}{2} \sin \theta \\ \rho_2 &= \rho_{20} + C_1 \cos 2\dot{\varphi}_0\tau - D_1 \sin 2\dot{\varphi}_0\tau - \frac{\dot{\varphi}_0\tau}{2} \cos \theta \end{aligned}\right\}$$

and we see immediately that the ordinary whirling at its critical speed must have $\theta = \frac{\pi}{2}$.

Summarizing, it has been proved that at a non-critical state only the whirl with $K = +1$ is quite pure and at a critical state only the cases $K = +1$ and $K = +3$ can have quite pure whirlings. (In a pure whirling K is absolutely constant).

Concerning the conditions 37.1 we get for $\Omega_{g0} = \dot{\varphi}_0$

$$\left.\begin{aligned} \dot{\theta}_0 &= 0 \\ \dot{\theta}_0 &= 2\dot{\varphi}_0 \\ \pm\dot{\varphi}_0 &= \dot{\psi}_0 \end{aligned}\right\}$$

which means $K \neq +1$, $K \neq +3$, and $K \neq \pm 1$ respectively. The cases $K = +1$ and $K = +3$ have already been treated and the case $K = -1$ will be specially treated later.

Though the input torques for maintaining the whirls can be derived from eq. 19.3 they are thoroughly investigated in the next chapter.

6. On the Input Torque

It has been shown previously that at each rotational speed the rotor has a critical state if the proper whirl velocity occurs. But experience from practice shows that there are many motor speeds which are not critical, which means that the corresponding whirl speeds do not develope. A very important task is to predict which critical rotational modes a rotor may have. In this chapter a theory about this matter is put forward.

It has been shown in Chapter 4 that the necessary torque for entertaining a pure whirling motion is

$$M_{in} = cre \sin \theta \qquad [\theta = (\omega - \Omega)t]$$

If a motor at a certain speed, besides the constant torque M_0, delivers "torque-tones" so that

$$M_{in} = M_0 + \sum_s M_{1s} \sin q_s \omega t + \sum_s M_{2s} \cos q_s \omega t$$

where q_s are constants belonging to the driving machine, a critical whirl may occur only if

$$\pm q_s \omega_{cs} = \omega_{cs} - \Omega_{cs}$$

The indices cs mean critical speed of order s and hence

$$K = \frac{1}{1 \mp q_s} \qquad \text{39.1}$$

The constant torque M_0 takes care of the load and the term

$$M_{1s} \sin q_s \omega t \text{ or } M_{2s} \cos q_s \omega t = M_{2s} \sin \left(-q_s \omega t + \frac{\pi}{2} \right)$$

sustains the whirl of order s. The other "torque-tones" disturb the "pure" motion.

This can be shown more precisely in the following way. From eq. 19.1 we get, if

$$\left.\begin{aligned} r_1 &= r \\ r_2 &= 0 \\ y_s &= r\cos\varphi \\ z_s &= r\sin\varphi \\ k &= 0 \end{aligned}\right\}$$

that

$$\left.\begin{aligned} \ddot{y}+y_s\Omega_g^2 &= 0 \\ \ddot{z}+z_s\Omega_g^2 &= 0 \end{aligned}\right\} \quad \left(\ddot{y}=\frac{d^2y}{dt^2},\ \ddot{z}=\frac{d^2z}{dt^2}\right) \quad \ldots\ldots\ldots \quad 40.1$$

Further, the torque-equation 19.3 can be written

$$M_{in} = I_p\cdot\frac{d^2\psi}{dt^2}+Me\Omega_g^2(y_s\sin\psi-z_s\cos\psi) \quad \ldots\ldots\ldots \quad 40.2$$

From the eqs 40.1 and 40.2 is obtained by introducing

$$\left.\begin{aligned} \eta_s &= \frac{y_s}{e} \\ \zeta_s &= \frac{z_s}{e} \end{aligned}\right\}$$

the following equations

$$\left.\begin{aligned} \ddot{\eta}_s+\Omega_{g0}^2\eta_s &= -\frac{d^2}{d\tau^2}(\cos\psi) \\ \ddot{\zeta}_s+\Omega_{g0}^2\zeta_s &= -\frac{d^2}{d\tau^2}(\sin\psi) \\ \ddot{\psi} &= M_{in}^*-\varepsilon^2(\eta_s\sin\psi-\zeta_s\cos\psi) \\ \left(\ddot{\eta}_s=\frac{d^2\eta_s}{d\tau^2},\ \ddot{\zeta}_s=\frac{d^2\zeta}{d\tau^2}\right) & \end{aligned}\right\} \quad \ldots\ldots\ldots \quad 40.3$$

By introducing

$$\chi = \eta_s+i\zeta_s$$

we get from the first and the second equations of 40.3 that

$$\ddot{\chi}+\Omega_{g0}^2\chi = -\frac{d^2}{d\tau^2}(e^{i\psi}) \quad \ldots\ldots\ldots\ldots\ldots 41.1$$

Here χ is a vector in origin. Its modulus is the shaft deflection and its argument is the "whirl-angle".

If the "input torque" can be written

$$M_{in}^* = \sum_s M_{1s}^* \sin q_s\psi + \sum_s M_{2s}^* \cos q_s\psi$$

we get

$$\ddot{\psi} = \sum_s M_{1s}^* \sin q_s\psi + \sum_s M_{2s}^* \cos q_s\psi - \varepsilon^2(\eta_s \sin\psi - \zeta_s \cos\psi) \ldots\ldots 41.2$$

If $\varepsilon^2|\chi|$ is much less than $\{\sum_s M_{1s}^* \sin q_s\psi + \sum_s M_{2s}^* \cos q_s\psi\}$ we get

$$\ddot{\psi} = \sum_s M_{1s}^* \sin q_s\psi + \sum_s M_{2s}^* \cos q_s\psi \quad \ldots\ldots\ldots 41.3$$

(This sum may contain one or two terms less than the sum in eq. 41.2 as will be shown later) and after integration

$$\dot{\psi} = \dot{\psi}_0 - \sum_s \frac{M_{1s}^*}{q_s} \cos q_s\psi + \sum_s \frac{M_{2s}^*}{q_s} \sin q_s\psi \quad \ldots\ldots\ldots 41.4$$

The right hand side of eq. 41.1 can be written

$$(\dot{\psi}^2 - i\ddot{\psi})e^{i\psi}$$

which approximately takes the form

$$(\dot{\psi}_0^2 - i\ddot{\psi})e^{i\psi}$$

if $\dot{\psi}_0$ is much greater than the sum of all the other terms in eq. 41.4. The eq. 41.3 can also be written

$$\ddot{\psi} = \tfrac{1}{2}\left[\sum_s (M_{2s}^* e^{iq_s\psi} + M_{2s}^* e^{-iq_s\psi}) - i\sum_s (M_{1s}^* e^{iq_s\psi} - M_{1s}^* e^{-iq_s\psi})\right]$$

and the eq. 41.1 gives

$$\ddot{\chi}+\Omega_{g0}^2\chi = \dot{\psi}_0^2 e^{i\psi} + \tfrac{1}{2}\sum_s [-(M_{1s}^* + iM_{2s}^*)e^{i(1+q_s)\psi} + \\ +(M_{1s}^* - iM_{2s}^*)e^{-i(-1+q_s)\psi}] \quad \ldots\ldots\ldots\ldots\ldots 41.5$$

If $\psi \approx \dot{\psi}_0 \tau$ the particular solution which is of main interest is

$$\chi = \frac{\dot{\psi}_0^2 e^{i\psi}}{\Omega_{g0}^2 - \dot{\psi}_0^2} + \frac{1}{2} \sum_s \frac{-(M_{1s}^* + iM_{2s}^*)}{\Omega_{g0}^2 - (1+q_s)^2 \dot{\psi}_0^2} \cdot e^{i(1+q_s)\psi} +$$

$$+ \frac{1}{2} \sum_s \frac{M_{1s}^* - iM_{2s}^*}{\Omega_{g0}^2 - (-1+q_s)^2 \dot{\psi}_0^2} \cdot e^{-i(-1+q_s)\psi} \quad \ldots\ldots\ldots \quad 42.1$$

Here Ω_{g0} must be nearly constant and

$$\Omega_{g0}^2 \neq \begin{cases} \dot{\psi}_0^2 \\ (1+q_s)^2 \dot{\psi}_0^2 \\ (-1+q_s)^2 \dot{\psi}_0^2 \end{cases} \quad \ldots\ldots\ldots\ldots\ldots \quad 42.2$$

If eq. 42.2 is not fulfilled solutions of another type occur. From eq. 42.1 the following conclusions can be drawn:

1) If $M_{1s}^* = M_{2s}^* = 0$ for all s we get

$$\chi = \frac{\dot{\psi}_0^2}{\Omega_{g0}^2 - \dot{\psi}_0^2} \cdot e^{i\psi}$$

which means that the shaft whirls with $K = +1$ with the deflection $\frac{\dot{\psi}_0^2}{\Omega_{g0}^2 - \dot{\psi}_0^2}$.

2) If $\dot{\psi}_0$ is far from $\pm \frac{\Omega_{g0}}{1+q_s}$ or $\pm \frac{\Omega_{g0}}{-1+q_s}$ and all $M_{0s}^* = [(M_{1s}^*)^2 + (M_{2s}^*)^2]^{\frac{1}{2}}$ are small the shaft will mainly whirl with $K = +1$ and the trace of S is nearly a circle.

3) If $M_{1s}^* \neq 0$, $M_{2s}^* \neq 0$ and if $\dot{\psi}_0$ is near the value $\frac{\Omega_{g0}}{1+q_s}$ the shaft will whirl with $\dot{\varphi}_0 = (1+q_s)\dot{\psi}_0$. Thus $K = \frac{1}{1+q_s}$. Analogously we get if $\dot{\psi}_0$ is near the value $\frac{\Omega_{g0}}{1-q_s}$ a whirl with $\dot{\varphi}_0 = (1-q_s)\dot{\psi}_0$. Thus $K = \frac{1}{1-q_s}$. Hence, one "torque-tone" M_{0s}^* can cause two kinds of whirl.

4) Eq. 17.2 shows that Ω_{g0} is a function of K and $\dot{\psi}_0$. Thus $\Omega_{g0} = \Omega_{g0}(K, \dot{\psi}_0)$. If $\dot{\psi}_0$ is changed very slowly with $K \approx 1$ (which in practice often occurs), at a certain value of $\dot{\psi}_0$, say

$$\dot{\psi}_0 = \frac{\Omega_{g0}}{1+q_s} + \varepsilon$$

where ε is a small number, we get one of the terms in the series very great. This means that the shaft developes a whirl velocity indicated by the argument of this term. In that way K changes from $+1$ to $K = \frac{1}{1+q_s}$. But this gives a new value of Ω_{g0}. But if $[\Omega_{g0}^2 - (1+q_s)\dot{\psi}_0^2]$ is still small the new whirl will remain and further adjustment of $\dot{\psi}_0$ may stabilize the motion.

This thing will only happen if the corresponding "torque-tone" amplitude is different from zero and if the other "torque-tones" do not destroy the whirling. This can happen if the other "torque-tones" are much greater than the "proper" one. In such cases "irregular" whirling must occur which means that $\dot{\varphi}$ varies strongly with the time.

5) A whirling with $K \neq +1$ has in general greater difficulty to be developed if $\dot{\psi}_0$ is near the usual critical speed than when it is far from this speed.

6) When passing a critical speed θ may shift nearly π radians.

7) One special whirl can exist within a narrow motor speed range. The motor speed will vary except at the critical state. However, in general the whirl speed and the shaft deflection vary. The exceptional cases are treated in Sec. 5,4.

8) If, as an example, all "torque tones" besides $M_{12}^* \sin 2\psi$ are zero we get

$$\chi = \frac{\dot{\psi}_0^2}{\Omega_{g0}^2 - \dot{\psi}_0^2} \cdot e^{i\psi} - \frac{1}{2} \cdot \frac{M_{12}^*}{\Omega_{g0}^2 - (3\dot{\psi}_0)^2} \cdot e^{i3\psi} + \frac{1}{2} \cdot \frac{M_{12}^*}{\Omega_{g0}^2 - \dot{\psi}_0^2} \cdot e^{-i\psi} \quad 43.1$$

If $\dot{\psi}_0 \to \frac{\Omega_{g0}}{3}$ we see that the second term dominates over the other ones. In that case $|\chi|$ is nearly a constant and the whirling "pure".

But it never exceeds the value $\frac{M_{12}^*}{\varepsilon^2}$ and thus

$$\lim_{\dot\psi_0 \to \frac{\Omega_{g0}}{3}} \chi \approx \frac{M_{12}^*}{\varepsilon^2} \cdot e^{i3\psi}, \text{ if } \frac{M_{12}^*}{\varepsilon^2} \gg \frac{\dot\psi_0^2}{\Omega_{g0}^2 - \dot\psi_0^2}$$

9) If we, as an example, want to study the case $\dot\psi_0 = \frac{\Omega_{g0}}{3}$ we have "resonance" for both $q_s = 2$ and $q_s = 4$. We get if only these two torques act the exact solution (which is easily shown by insertion into the eqs 40.3)

$$\eta_s + i\zeta_s = \frac{\dot\psi_0^2}{\Omega_{g0}^2 - \dot\psi_0^2} \cdot e^{i\psi} - \frac{1}{\varepsilon^2}(M_{12}^* + iM_{22}^*)e^{3i\psi} + \frac{1}{\varepsilon^2}(M_{14}^* - iM_{24}^*)e^{-3i\psi}$$

or

$$\left.\begin{aligned} \varepsilon^2\eta_s &= \varepsilon^2 \cdot \tfrac{1}{8} \cdot \cos\psi + (-M_{12}^* + M_{14}^*)\cos 3\psi + (M_{22}^* - M_{24}^*)\sin 3\psi \\ \varepsilon^2\zeta_s &= \varepsilon^2 \cdot \tfrac{1}{8} \cdot \sin\psi - (\ \ M_{12}^* + M_{14}^*)\sin 3\psi - (M_{22}^* + M_{24}^*)\cos 3\psi \end{aligned}\right\}$$

and thus the point S does not describe a circle. In that way the assumptions concerning the gyroscopic moments are only exactly valid if $\Omega_{g0} = 1$. Of course, analogously exact solutions also can be obtained for other critical states. It is remarkable that in spite of a varying input torque the angular velocity of the shaft is exactly constant ($\ddot\psi = 0$).

Observe that the whirl has not exactly $K = +\frac{1}{3}$ (any exact K-values besides $K = +1$ and $K = +3$ do not exist at an unbalanced rotor). But if $M_{02}^* \gg M_{04}^*$ and $M_{02}^* \gg \frac{\varepsilon^2}{8}$ the whirling will be fairly "pure".

The previous theory explains all whirlings except for the case when $K = -1$. This whirling must be treated in a special way because $\frac{1}{2} M_{12}^* \ll \dot\psi_0^2$ in many machines (see eq. 43.1).

We have already studied the influence of the so-called external damping. It arises from the friction between the rotating and the stationary parts, which means the external medium, in most cases air. However, there exists another kind of damping called internal damping. This is due to the friction between the rotating parts of the rotor. The action of the different types has a considerable difference as among others *Dimentberg* [4] has shown in the case $K = +1$ and $I_p = 0$. Under certain conditions the internal damping can increase the deflection of the shaft.

In order to make full allowance for the resistance forces due to internal friction, a moving system of coordinates is considered with its origin in the point B (see fig. 11.2) with the axes rotating relative the stationary system with angular velocity $\dot{\varphi}$. Thus, using complex quantities,

$$\left.\begin{aligned} \chi &= \chi_\varphi e^{i\varphi} \\ \dot{\chi} &= (\dot{\chi}_\varphi + i\dot{\varphi}\chi_\varphi)e^{i\varphi} \\ \ddot{\chi} &= (\ddot{\chi}_\varphi + 2i\dot{\varphi}\dot{\chi}_\varphi - \dot{\varphi}^2\chi_\varphi)e^{i\varphi} \end{aligned}\right\} \quad \ldots\ldots\ldots\ldots \quad 45.1$$

By considering external friction the eq. 41.5 can be written

$$\ddot{\chi} + 2D_m^*\dot{\chi} + \Omega_{g0}^2\chi = \psi_0^2 e^{i\psi} + \tfrac{1}{2}\sum[-(M_{1s}^* + iM_{2s}^*)e^{i(1+q_s)\psi} + \\ + (M_{1s}^* - iM_{2s}^*)e^{-i(-1+q_s)\psi}]$$

Insertion of the eqs 45.1 gives if we, moreover, add the term $2D_i^*\dot{\chi}_\varphi e^{i\varphi}$ due to internal friction

$$\{\ddot{\chi}_\varphi + (2i\dot{\varphi} + 2D_i^* + 2D_m^*)\dot{\chi}_\varphi + (-\dot{\varphi}^2 + i2D_m^*\dot{\varphi} + \Omega_{g0}^2)\chi_\varphi\}e^{i\varphi} =$$

$$= \psi_0^2 e^{i\psi} + \tfrac{1}{2}\sum[-(M_{1s}^* + iM_{2s}^*)e^{i(1+q_s)\psi} + (M_{1s}^* - iM_{2s}^*)e^{-i(-1+q_s)\psi}] \ldots \quad 45.2$$

Further, we may write

$$\left.\begin{aligned} \chi_\varphi &= \chi e^{-i\varphi} \\ \dot{\chi}_\varphi &= (\dot{\chi} - i\dot{\varphi}\chi)e^{-i\varphi} \\ \ddot{\chi}_\varphi &= (\ddot{\chi} - 2i\dot{\varphi}\dot{\chi} - \dot{\varphi}^2\chi)e^{-i\varphi} \end{aligned}\right\}$$

and by putting these expressions into the eq. 45.2 we get

$$\ddot{\chi} + 2(D_i^* + D_m^*)\dot{\chi} + (\Omega_{g0}^2 - 2i\dot{\varphi}D_i^*)\chi = \psi_0^2 e^{i\psi} + \\ + \tfrac{1}{2}\sum[-(M_{1s}^* + iM_{2s}^*)e^{i(1+q_s)\psi} + (M_{1s}^* - iM_{2s}^*)e^{-i(-1+q_s)\psi}]$$

Try the complementary solution $\chi = e^{\lambda\tau}$. We get

$$\lambda^2 + 2(D_i^* + D_m^*)\lambda + \Omega_{g0}^2 - 2i\dot{\varphi}D_i^* = 0$$

with the roots

$$\lambda = -(D_i^* + D_m^*) \pm \sqrt{(D_i^* + D_m^*)^2 - \Omega_{g0}^2 + 2i\dot{\varphi}D_i^*}$$

If $(D_i^* + D_m^*) \ll \Omega_{g0}$ we get

$$\lambda = -(D_i^* + D_m^*) \pm \frac{\dot{\varphi} D_i^*}{\Omega_{g0}} \pm i\Omega_{g0}$$

Stable solutions are obtained if

$$\dot{\varphi} < \left(1 + \frac{D_m^*}{D_i^*}\right) \Omega_{g0}$$

For clarity the particular solution is calculated for only one "disturbing" term, which in general can be written $Qe^{im\psi}$ where $m = \begin{cases} 1+q_s \\ 1-q_s \end{cases}$ and Q is an arbitrary amplitude. Thus we get

$$\chi = \frac{Q}{-m^2\dot{\psi}_0^2 + \Omega_{g0}^2 + i2m\dot{\psi}_0 D_m^* + i2D_i^*(m\dot{\psi} - \dot{\varphi})} \cdot e^{im\psi}$$

At a special whirling $(m\dot{\psi} - \dot{\varphi}) = 0$ always and we may conclude that the internal damping never limits the amplitude of the deflection due to the *particular* solution.

For the special case $K = -1$ we can have the solution

$$\chi \cong A' e^{i\left(\psi + \frac{\pi}{2}\right)} + B' e^{-i\left(\psi - \frac{\pi}{2}\right)} - \frac{\dot{\psi}_0}{2D_m^* + 4D_i^*} \cdot e^{i\left(\psi + \frac{\pi}{2}\right)} + \frac{M_{12}^*}{4D_m^* \dot{\psi}_0} \cdot e^{-i\left(\psi - \frac{\pi}{2}\right)}$$

or, if $\boldsymbol{r}_S = e\chi$

$$\boldsymbol{r}_S \cong A\, e^{i\left(\psi + \frac{\pi}{2}\right)} + B\, e^{-i\left(\psi - \frac{\pi}{2}\right)} - \frac{e\dot{\psi}_0}{2D_m^* + 4D_i^*} \cdot e^{i\left(\psi + \frac{\pi}{2}\right)} + \frac{eM_{12}^*}{4D_m^* \dot{\psi}_0} \cdot e^{-i\left(\psi - \frac{\pi}{2}\right)} \quad 46.1$$

where A', B', A, and B are arbitrary constants.

If $A = \frac{e\dot{\psi}_0}{2D_m^* + 4D_i^*}$ we get

$$\boldsymbol{r}_S \cong \left(B + \frac{eM_{12}^*}{4D_m^* \dot{\psi}_0}\right) e^{-i\left(\psi - \frac{\pi}{2}\right)} \quad \ldots\ldots\ldots\ldots \quad 46.2$$

and from this expression it follows that the case $K = -1$ also in theory may exist in spite of the fact that $e \neq 0$.

Now we are capable to follow the events when the whirling changes from $K = +1$ to $K = -1$. Suppose that the shaft whirls with

$K = +1$ near the speed corresponding to the critical state for $K = -1$. Then we have the solution

$$r_S \cong A_1 e^{-D_1\tau} e^{-i\Omega_{g0}\tau} + B_1 e^{-D_2\tau} e^{i\Omega_{g0}\tau} +$$

$$+ \frac{e\dot{\psi}_0^2}{-\dot{\psi}_0^2 + \Omega_{g0}^2 + i2D_m^*\dot{\psi}_0} \cdot e^{i\psi}$$

$$+ \frac{e}{2} \cdot \frac{M_{12}^*}{-\dot{\psi}_0^2 + \Omega_{g0}^2 - i(2D_m^* + 4D_i^*)\dot{\psi}_0} \cdot e^{-i\psi}$$

where

$$\left.\begin{aligned} D_1 &= D_i^* + D_m^* + \frac{\dot{\varphi}}{\Omega_{g0}} \cdot D_i^* \\ D_2 &= D_i^* + D_m^* - \frac{\dot{\varphi}}{\Omega_{g0}} \cdot D_i^* \end{aligned}\right\}$$

Then the shaft is given a disturbance (for instance from the bearings) such as

$$B_1 = \frac{-e\dot{\psi}_0^2}{-\dot{\psi}_0^2 + \Omega_{g0}^2 + i2D_m^*\dot{\psi}_0}$$

During a short time the terms containing the factors $e^{-i\Omega_{g0}\tau}$ and $e^{-i\psi}$ are dominating and the shaft begins to whirl reversely. In that way the value of the function $\Omega_{g0} = \Omega_{g0}(K, \dot{\varphi})$ changes its value and $\Omega_{g0} \to -\dot{\psi}_0$. After a while the solution 46.1 is valid and another disturbance brings the rotor to a whirl described by the expression 46.2. Observe, that the limit of the shaft deflection due to the "torque-tone" at this critical state must be

$$|r_S'| = e \cdot \frac{M_{12}^*}{\varepsilon^2}$$

In other cases the whirling cannot be maintained. It must also be pointed out that if $M_{12}^* = 0$ $|r_S'| = 0$ if $e \neq 0$. If, on the other side, $e = 0$ $|r_S'|$ can have an arbitrary value. The shaft deflection is indifferent. If the external damping is zero, $e \to 0$ and $M_{12}^* \neq 0$ the deflection of the shaft tends to infinity. But in this case the input torque also can settle up variations in the motor speed and hence the shaft deflection is also in this case indifferent.

The internal friction was previously assumed to be viscous. This is a first approximation. The results give a rough orientation of the influence of internal damping.

Dimentberg [4] has carried out a close investigation of the nature of internal damping.

Maybe also the so-called "Magnus-effect" [1] is of some significance.

As the ρ-value at a critical state is limited the eq. 41.3 is justified.

In the undamped case the ordinary whirl has $\theta = 0$ or $\theta = \pi$ at a non-critical state. The eq. 13.2 gives $M_{in} = 0$. Thus this whirl always exists in a rotor which is freely rotating in bearings without friction. At the critical state $\theta \to \frac{\pi}{2}$ when $r \to \infty$. Hence, from eq. 13.2, the rotor demands a steady increasing torque.

From the eqs 33.1 we get for a point-mass rotor

$$\rho = C + \frac{\tau}{2} \text{ or } r = Ce + \frac{e}{2}\omega_c t$$

where C is an arbitrary constant and with eq. 13.2

$$M_{in} = ce^2(C + \tfrac{1}{2}\omega_c t)$$

which gives

$$\frac{dM_{in}}{dt} = \frac{1}{2} ce^2\omega_c$$

or

$$\frac{dM_{in}}{dt} = \frac{1}{2} Me^2\omega_c^3$$

This equation indicates the necessary increase in torque to keep the rotor at the critical state and was shown by *Biezeno* and *Grammel* [2].

If the motor in the undamped case after a while gives

$$\frac{dM_{in}}{dt} < \frac{1}{2} ce^2\omega_c$$

the rotor will take a speed below the critical speed and if

$$\frac{dM_{in}}{dt} > \frac{1}{2} ce^2\omega_c$$

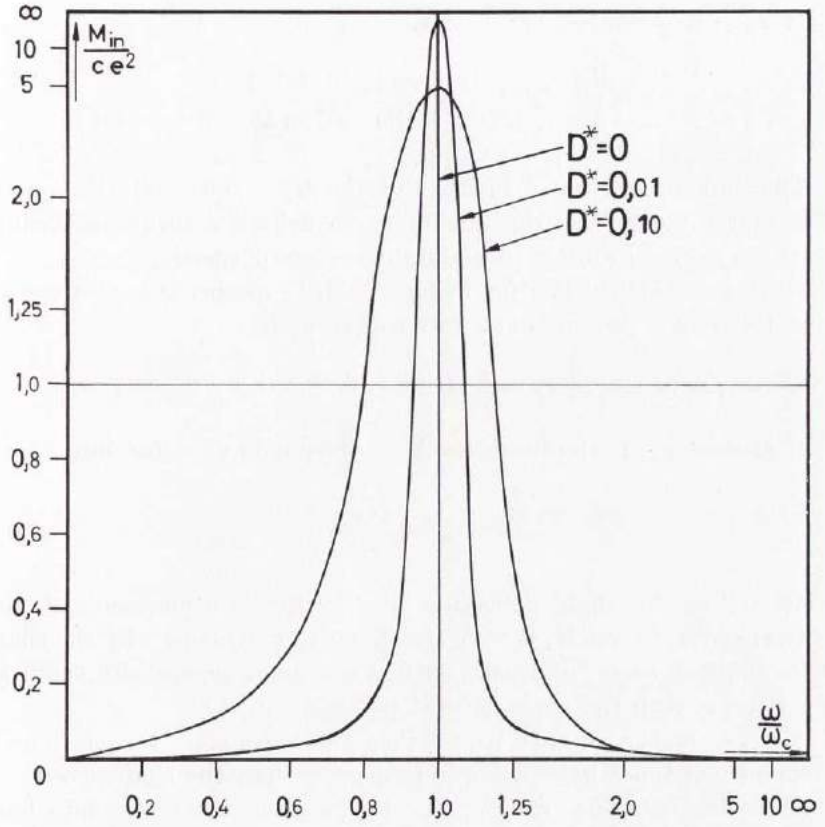

Fig. 49.1

it will pass it. See also [6]. Thus the motor must have a characteristic curve according to fig. 49.1 if the rotor shall be able to stay at every speed with $K = +1$.

For the case with external damping we get from the eqs 13.2, 24.2, and 24.3 that

$$\frac{M_{in}}{ce^2} = \frac{2D^*\Omega_{g0}^2\dot{\psi}_0[\dot{\psi}_0^2+(2D^*)^2]}{(2D^*\Omega_{g0}^2)^2+\dot{\psi}_0^2[\Omega_{g0}^2-\dot{\psi}_0^2-(2D^*)^2]^2}$$

and if $\dot{\psi}_0 = \dot{\varphi}_0 = \Omega_{g0}$ we get

$$\frac{M_{in}}{ce^2} = \frac{\Omega_{g0}}{2D^*}$$

If $I_p = 0$ we have

$$\frac{M_{in}}{ce^2} = \frac{2D^*\psi_0[\psi_0^2+(2D^*)^2]}{(2D^*)^2+\psi_0^2[1-\psi_0^2-(2D^*)^2]^2}$$

This function is drawn in fig. 49.1 for $D^* = 0{,}01$ and $D^* = 0{,}10$. The motor must have the possibility to deliver a torque according to these curves in order to maintain its motor speed.

Such a possibility has for instance a D.C. motor. It is also known that this motor produces "torques-tones" with

$$q_s = s \quad (s = 1, 2, 3 \ldots)$$

If against q_s an amplitude of M_s corresponds we must have

$$r_s' = \frac{M_s}{ce} \quad \ldots\ldots\ldots\ldots\ldots\ldots \quad 50.1$$

where r_s' is the shaft deflection due to the "torque-tone" at the critical speed. Often M_s is very small and this explains why the shaft deflections at such "unusual" critical speeds in general are small in comparison with the shaft deflections at $K = +1$.

An A.C. motor is able to produce sub-harmonic "torque-tones". Hence these tones have a lower frequency than the shaft speed.

Often the couplings split up the torque from the motor into harmonics. This happens for instance in Hooke's coupling (cardan-coupling) and similar couplings if the input and output shafts are not exactly collinear. Especially the "torque-tone" of angular velocity 2ω has a relatively great amplitude which depends upon the amount of this misalignment. According to eq. 39.1 one may expect that such a coupling might excite the critical speeds with $K = -1$ and $K = +\frac{1}{3}$. As a matter of fact just these whirlings are mentioned in literature.

In order to investigate this idea practically the test apparatus shown in fig. 64.2 was rebuilt so that the motor drove the shaft via a Hooke's coupling and the shaft of the motor could be inclined. Tests were carried out with the angles of misalignment 0°, 5°, 20°, and 26° at the speeds corresponding to the critical states with $K = +\frac{1}{3}$ and $K = -1$. The result was, however, that the shaft deflections decreased with increasing angle. Probably this was due to the large variations of the speed of the shaft during every revolution of the shaft.

At these tests great deflection of the shaft was also observed at the speed corresponding to $K = -\frac{2}{3}$. On this occasion the angle of misalignment was 0° or 10°. Only tests at these angles were carried out.

Finally the concept of "secondary critical speed" has to be discussed. It has been seen that a horisontal rotor often is disturbed at a speed equal to half the ordinary critical speed.

If the motor is running with $\dot{\psi}\,\frac{\text{rad}}{\text{s}}$ the gravity force at a horisontal rotor causes an input torque $Mge\cos\psi$ (see fig. 11.2 by assuming the gravity force parallel to the z-axis). Thus, because

$$Mge\cos\psi = Mge\sin\left(-\dot{\psi}t + \frac{\pi}{2}\right)$$

we may get a whirling at $K = +\frac{1}{2}$ according to eq. 39.1. In that case the gyroscopic effect is absent ($\gamma = 0$) and $\Omega_g = \Omega_n$. Thus it may be suspected that the horisontal shaft should be rough at the speed $\frac{\Omega_n}{2}$. The deflection radius r' due to the gravity force consequently can be obtained from the relation

$$cer' = Mge$$

and thus

$$r' = \frac{Mg}{c}$$

The trace of the centre of the shaft can be written (with origin in the "centre of the bearings" B)

$$\boldsymbol{r}_S = \frac{Mg}{c} + \frac{1}{3}e\cdot e^{i\psi} + \frac{Mg}{c}\cdot e^{i\frac{1}{2}\psi}$$

Analogously the trace of the centre of gravity has the equation

$$\boldsymbol{r}_G = \frac{Mg}{c} + \frac{4}{3}e\cdot e^{i\psi} + \frac{Mg}{c}\cdot e^{i\frac{1}{2}\psi}$$

In fig. 52.1 $\boldsymbol{r}_S$ and $\boldsymbol{r}_G$ are shown in the case $\frac{Mg}{c} = \frac{4}{3}e$.

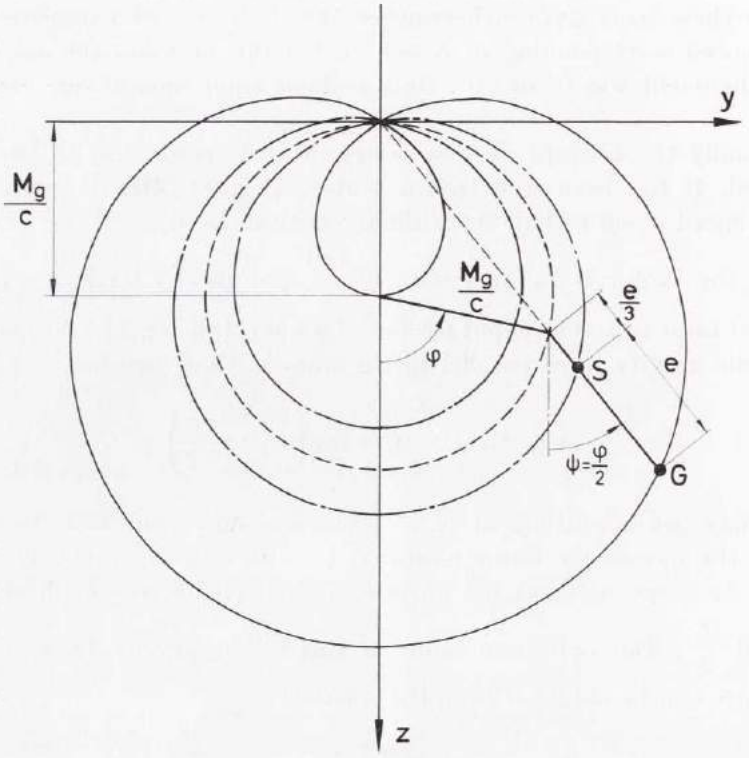

Fig. 52.1

It may also be possible to investigate the harmonics of the torque from a motor by studying the critical states. In that case the coupling between the motor and the shaft must be rigid. Perhaps this is of practical interest because of the fact that it is very difficult to decide the harmonics in an electrical way if the amplitudes are small.

In a dissertation 1924 *Schröder* [8] also found that the critical speeds of the second kind ($K \neq +1$) occur at limited deflections of the shaft. He obtained this result by assuming small variations of a certain kind in the motor speed then and performing a limit analysis at the critical speed.

His solution did not include the case $K = -1$ and nor did he discover the special properties of the case $K = +3$.

In spite of this and the facts that he did not consider the gyroscopic effect, the effect of the damping or perform any own tests, his dissertation must be considered as an important work in this field.

7. Whirl Curves

In practice, it is rather difficult to see how a rotor whirls. If the deflections of a shaft in the y- and z-directions are recorded one can from the chart calculate the angular velocity of the whirl. The motor speed is obtained separately. But the difficulty is to see if the whirl is positive or negative.

However, if the electric signals due to the movements in the y- and z-directions of the disc centre of gravity are led to the x- and y-plates respectively of an oscilloscope one can see the path of this disc centre. Each ratio $K = \dfrac{\omega}{\Omega}$ gives a special curve and with the aid of this curve one can decide the value of K without knowing ω and Ω.

As an example the path of the disc centre if $K = +\frac{1}{3}$ is constructed in fig. 54.1.

In the first position the bearing centre B, the "virtual" shaft centre S^* (here is only concerned with the position of the shaft centre due to one "torque-tone" at resonance which means that $BS^* = r' = \text{const.}$), and the centre of the disc C are collinear and the positions are denoted S_0^* and C_0 respectively. We put $S^*C = e'$ and if $r' > e'$ we have $\rho' = \dfrac{r'}{e'} > 1$. If S_0^* is moved to S_3^*, C_0 is moved to C_3 and the angle between $S_3^*C_3$ and BS_0^* is one third of the angle between the lines BS_3^* and BS_0^*. Thus the line S_3C_3 is parallel to the line $B1$. The final path in this case can be seen in fig. 58.1.

For other values of K the corresponding paths of the disc centre are drawn in figures on page 55 up to page 60.

Observe that if a curve is obtained for $K = K_1$ and $\rho' = \rho_1'$ the same curve is obtained for $K = \dfrac{1}{K_1}$ and $\rho' = \dfrac{1}{\rho_1'}$.

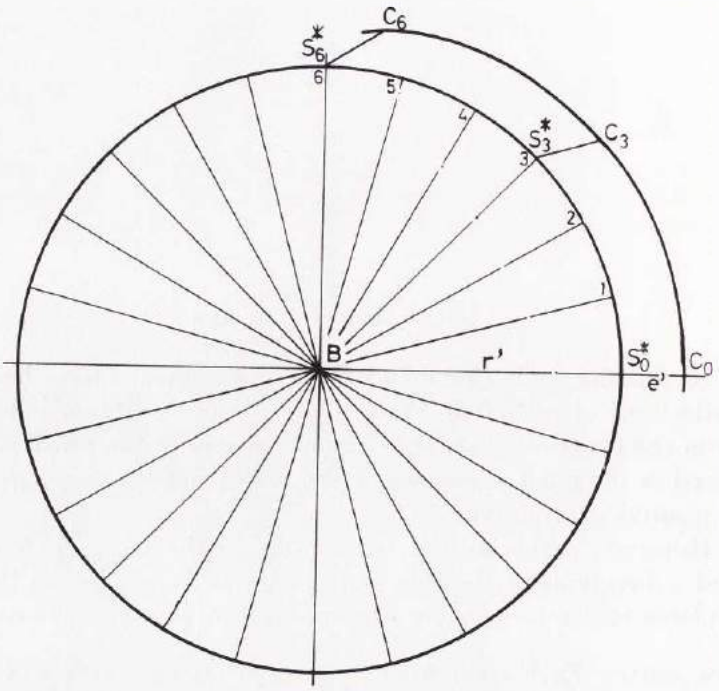

Fig. 54.1

If, during $K = -1$, the shaft deflection changes from $\rho' < 1$ to $\rho' > 1$ the direction of the rotational speed of the point C will be reversed which is easily shown.

Comparison of the oscilloscope screen picture and the figures gives the K-value.

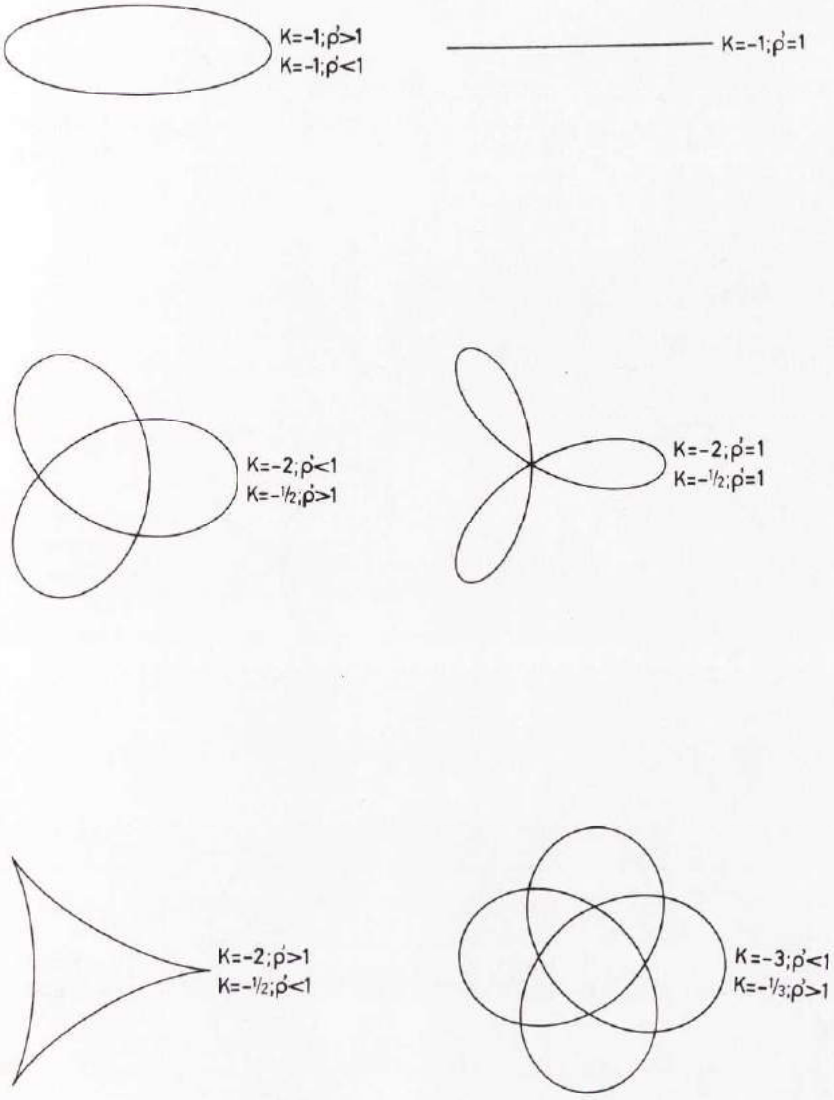

Fig. 55.1

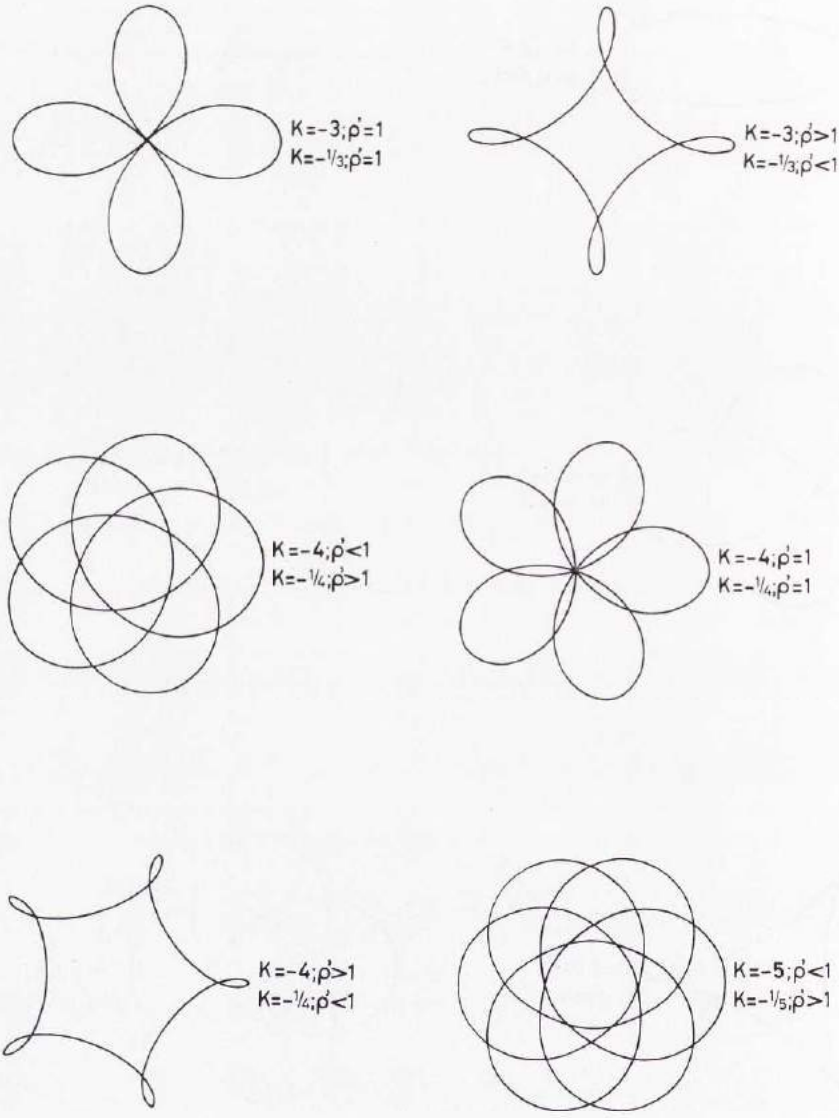
K=-3;ρ'=1
K=-1/3;ρ'=1
K=-3;ρ'>1
K=-1/3;ρ'<1
K=-4;ρ'<1
K=-1/4;ρ'>1
K=-4;ρ'=1
K=-1/4;ρ'=1
K=-4;ρ'>1
K=-1/4;ρ'<1
K=-5;ρ'<1
K=-1/5;ρ'>1

Fig. 56.1

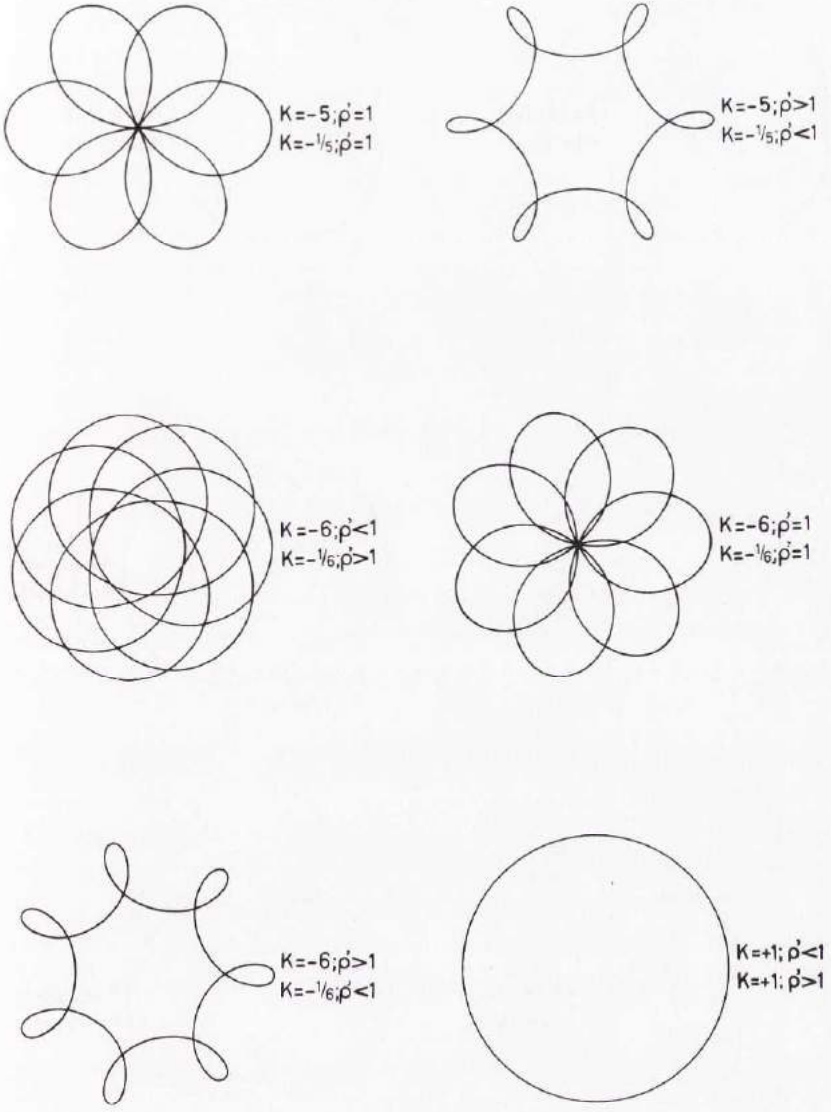
K=-5;ρ'=1
K=-1/5;ρ'=1
K=-5;ρ'>1
K=-1/5;ρ'<1
K=-6;ρ'<1
K=-1/6;ρ'>1
K=-6;ρ'=1
K=-1/6;ρ'=1
K=-6;ρ'>1
K=-1/6;ρ'<1
K=+1; ρ'<1
K=+1; ρ'>1

Fig. 57.1

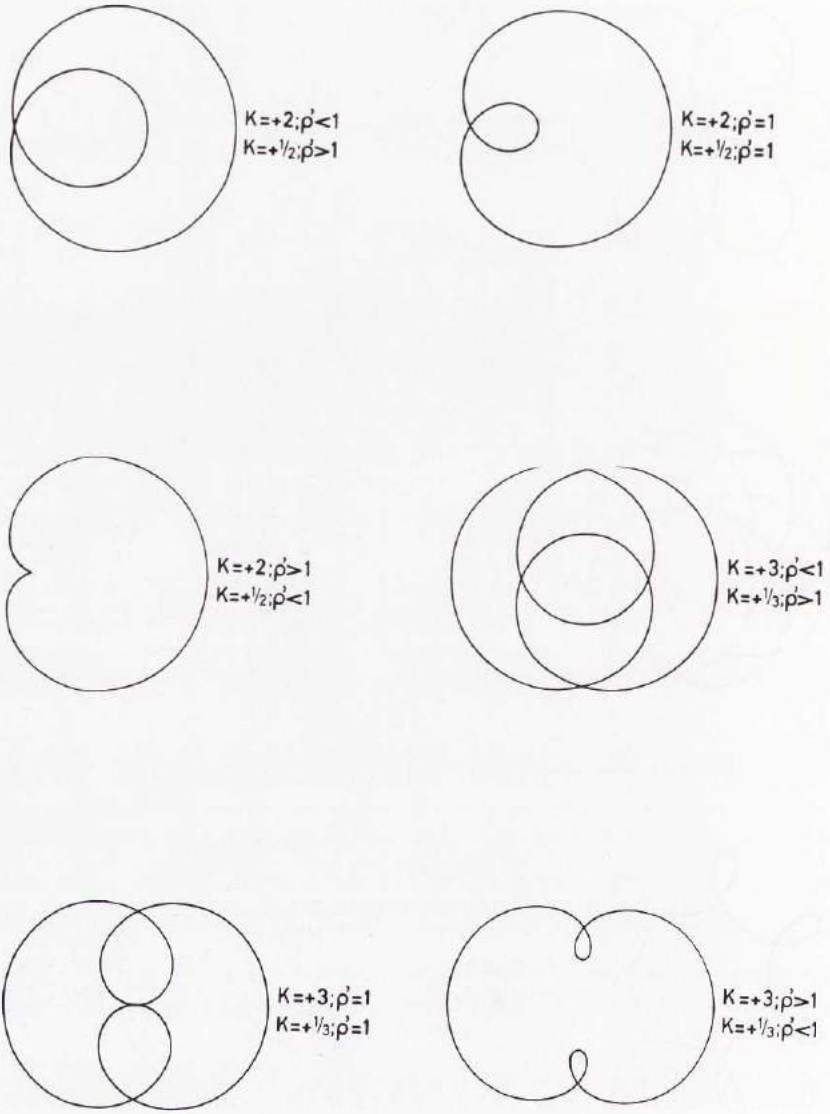
K=+2;ρ'<1
K=+1/2;ρ'>1
K=+2;ρ'=1
K=+1/2;ρ'=1
K=+2;ρ'>1
K=+1/2;ρ'<1
K=+3;ρ'<1
K=+1/3;ρ'>1
K=+3;ρ'=1
K=+1/3;ρ'=1
K=+3;ρ'>1
K=+1/3;ρ'<1

Fig. 58.1

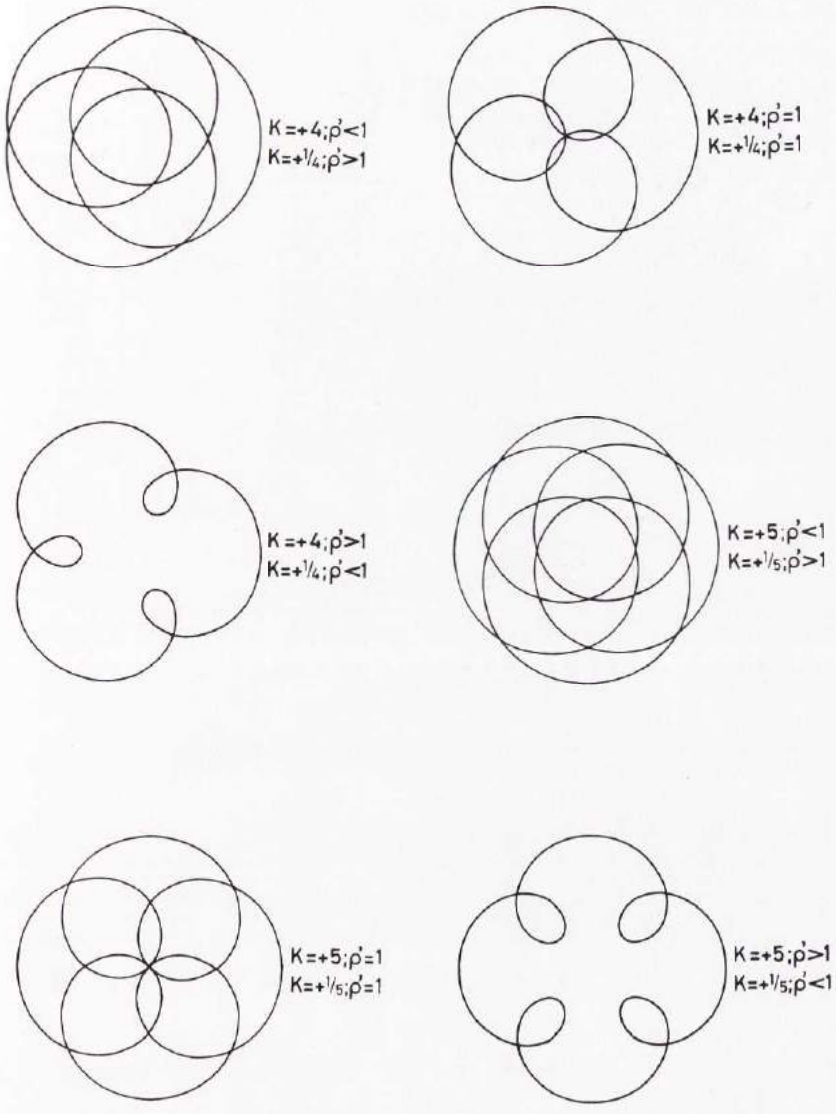
K=+4;ρ'<1
K=+1/4;ρ'>1
K=+4;ρ'=1
K=+1/4;ρ'=1
K=+4;ρ'>1
K=+1/4;ρ'<1
K=+5;ρ'<1
K=+1/5;ρ'>1
K=+5;ρ'=1
K=+1/5;ρ'=1
K=+5;ρ'>1
K=+1/5;ρ'<1

Fig. 59.1

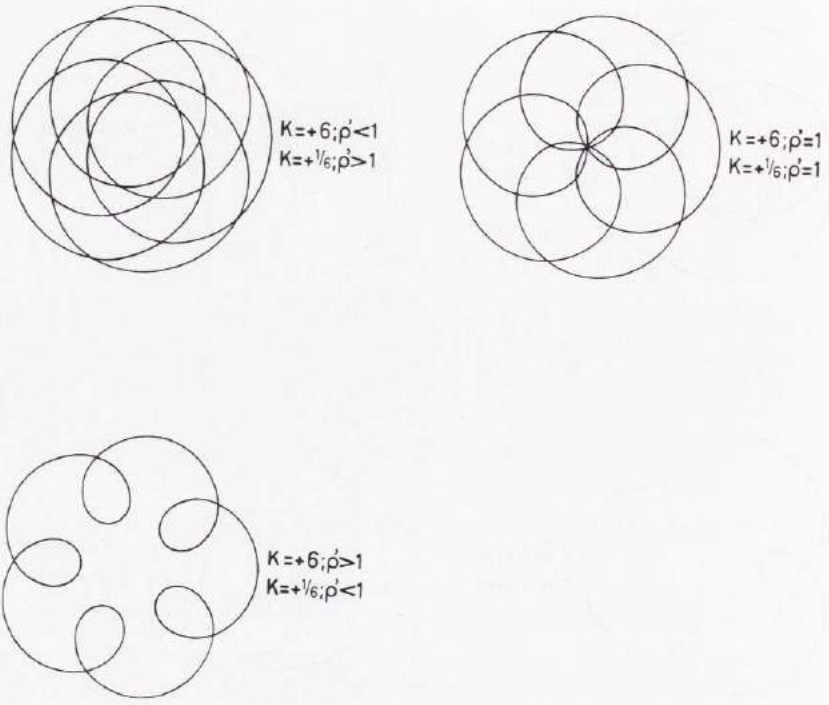

Fig. 60.1

8. Tests of a Rotor with One Disc

In order to investigate the different rotational modes in a rotor a test apparatus was built, the principle of which is shown in fig. 62.1.

The shaft was vertical. Photographs of the apparatus are shown in the figs 64.2 and 64.3.

The electronic equipment can be seen in the figs 64.2, 64.3, and 64.4. The different instruments in fig. 64.4 are:

A. Recorder (Offner). It registered motor speed, input torque, and deflections of the disc in two directions perpendicular to each other.

B. Oscilloscope (Du Mont). It was used as an amplifier for the electric signals from an electromagnetic pickup, T_1 in fig. 64.2 (Philips PR 9262/01). T_1 was mounted very near a gear wheel and in that usual way it served as a "tachometer" for the steered whirling velocity. The whirling was put into the left shaft T_2 in fig. 64.2 by means of a whirl-exciter T_3 driven by the right shaft T_4 in the same figure. The shaft T_4 was driven by an A.C. motor via a variator. These are not shown in the figure. T_2 and T_3 are also shown in fig. 64.3.

C. Calibration Unit (Philips GM 5522) coupled to T_1 in fig. 64.2. (See also under B.)

D. Battery unit for giving one channel in the six-channel-recorder A a prevoltage when measuring and registering the speed of the shaft T_2 in fig. 64.2. It enlarged the deflection on the chart for a given speed because a great amplification could be used.

E. Electronic counter (Hewlett Packard). When it was coupled to B it gave the whirl velocity and when coupled to the frequency-meter T_5 (Hewlett Packard), which obtained electric impulses from the tachometer-generator T_6 (Hewlett Packard) it gave the speed of the shaft T_2 in fig. 64.2.

F. Dual beam oscilloscope (Tetronik) coupled to G.

G. Power supply, reactance converter and amplifier (Disa 51C06 and 51B02). They were used in connection with the capacitive pickups P_1 and P_2 in fig. 64.3 for measuring the deflections of the disc.

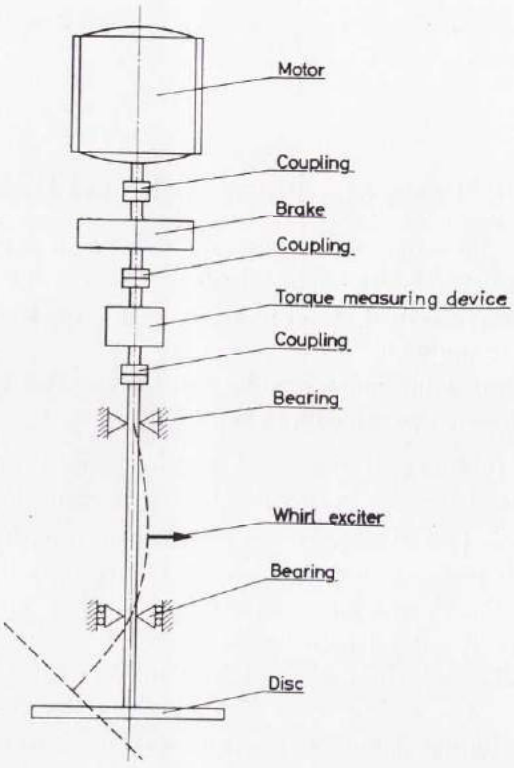

Fig. 62.1

H. Double A.C. bridge (Vibrometer) used together with the torque-measuring-device T_7 in fig. 64.2.

A D.C. motor was driven from a Leonardsystem. (See fig. 72.1. The low frequency generator was not connected.) The arrangement was equipped with a whirl exciter with the aid of which the whirl speed could be varied continuously in the range $160 \leq N \leq 1440$ or $640 \leq N \leq 5760$ (r.p.m.).

The rotor had the following data:

$$\left.\begin{aligned} M &= 9{,}87 \text{ kg} \\ I_p &= 0{,}114 \text{ kgm}^2 \\ L &= 735 \text{ mm} \end{aligned}\right\} \qquad \left.\begin{aligned} d &= 15 \text{ mm} \\ E &= 20{,}3 \cdot 10^{10} \frac{\text{Newton}}{\text{m}^2} \\ m &= 1{,}07 \text{ kg} \end{aligned}\right\}$$

8,1. Tests of a Hinged-Hinged-Free Shaft Driven by a D.C. Motor Coupled to a Common Ward-Leonard System

At first the D.C. motor was driving a hinged-hinged-free arrangement. At the same time the whirl exciter gave a whirling motion to the disc. The arrangement was driven at special values of K for different values of ω and Ω. For each ω-value the corresponding Ω-value was set up and then the whirl exciter was disconnected. In that way it was found that the rotor only at special values of ω kept the same K-value after this uncoupling. These values of ω were the "critical speeds". If the whirl exciter was disconnected and the motor was driven up to one of these critical $\omega(=\omega_c)$ it was seen that the shaft started whirling with the corresponding value of $\Omega(=\Omega_g)$. From the elementary theory (see [5]) one gets that every ω is "critical" if the corresponding value of Ω is developed. This matter was also shown. But a very important thing was that the rotor by itself (which means without whirl exciter) only whirled with $K = -\frac{1}{6}$, $-\frac{1}{5}$, $-\frac{1}{4}$, $-\frac{1}{3}$, $-\frac{1}{2}$, -1, $+\frac{1}{6}$, and $+\frac{1}{3}$ and only in the neighbourhood of the corresponding critical values of ω. This result is in a very good agreement with the theory in Chapter 6.

In the tab. 64.1 the test results are collected. The theoretical values are calculated from eq. 110.2 in [5]. Thus, the influence of the mass of the shaft on the critical speeds is neglected and the bearings are treated as if their lateral stiffness was infinite and their angular stiffness zero.

In two cases the change of θ with π radians when passing the critical speed, viz. $K = -1$ and $K = +\frac{1}{6}$ are shown.

The test results are $(2 \div 8)$ per cent greater than the calculated values which is a good agreement.

The brackets around the $|N|$-values mean that these are not measured. They are calculated from the formula

$$N = \frac{n}{K}$$

and here n is obtained from an electronic counter and the K-value from the figs in Chapter 7. Tests showed that the points G and C practically coincide. This happened because of the fact that the disc was turned in a lathe while it was mounted on the shaft. If the material is homogeneous the points G and C must coincide and the eccentricity must be zero (at least from the practical point of view). Thus

K	Theory		Test		Test figure		Ampl.
	n r.p.m.	$\|N\|$ r.p.m.	n r.p.m.	$\|N\|$ r.p.m.	ϱ'	No	
$-\frac{1}{6}$	131	783	136	[816]	<1	66.3	A
	736	4417					
-6	2393	399					
	16702	2784					
$-\frac{1}{5}$	155	775	162	[810]	<1	66.5	A
	869	4344	877	[4385]	<1	67.1	A
-5	2132	426					
	14125	2825					
$-\frac{1}{4}$	192	768	204	[816]	<1	67.3	A
	1061	4245					
-4	1846	462					
	11537	2884					
$-\frac{1}{3}$	252	755	258	[774]	<1	67.5	A
	1368	4103	1405	[4215]	<1	68.1	A
-3	1522	507					
	8924	2975					
$-\frac{1}{2}$	365	731	378	[756]	<1	68.3	A
	1939	3879					
-2	1143	572					
	6265	3133					
			664	[664]	1	68.5	B
-1	663	663	(712)	(712)	>1	69.3	B
			(738)	(738)	1	69.1	B
	3482	3482					
$+1$	1111	1111	1140	[1140]	>1	69.5	B
$+\frac{1}{6}$	142	851	153	[918]	<1	70.1	A
	957	5742				70.3	
$+6$	13610	2268					
$+\frac{1}{3}$	299	896	322	[966]	<1	70.4	A
	2589	7768					
$+3$	5798	1933					

Tab. 64.1

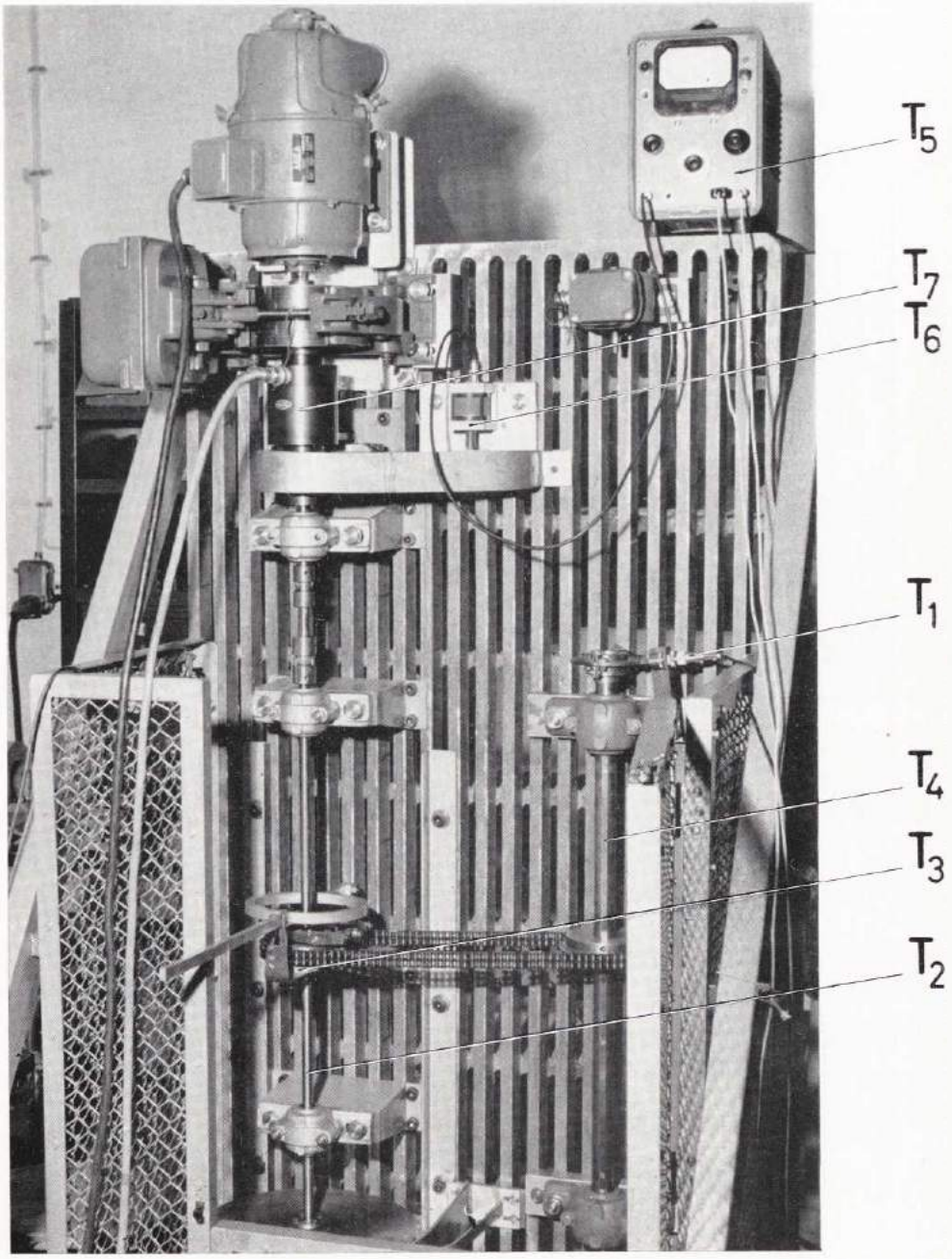

Fig. 64.2

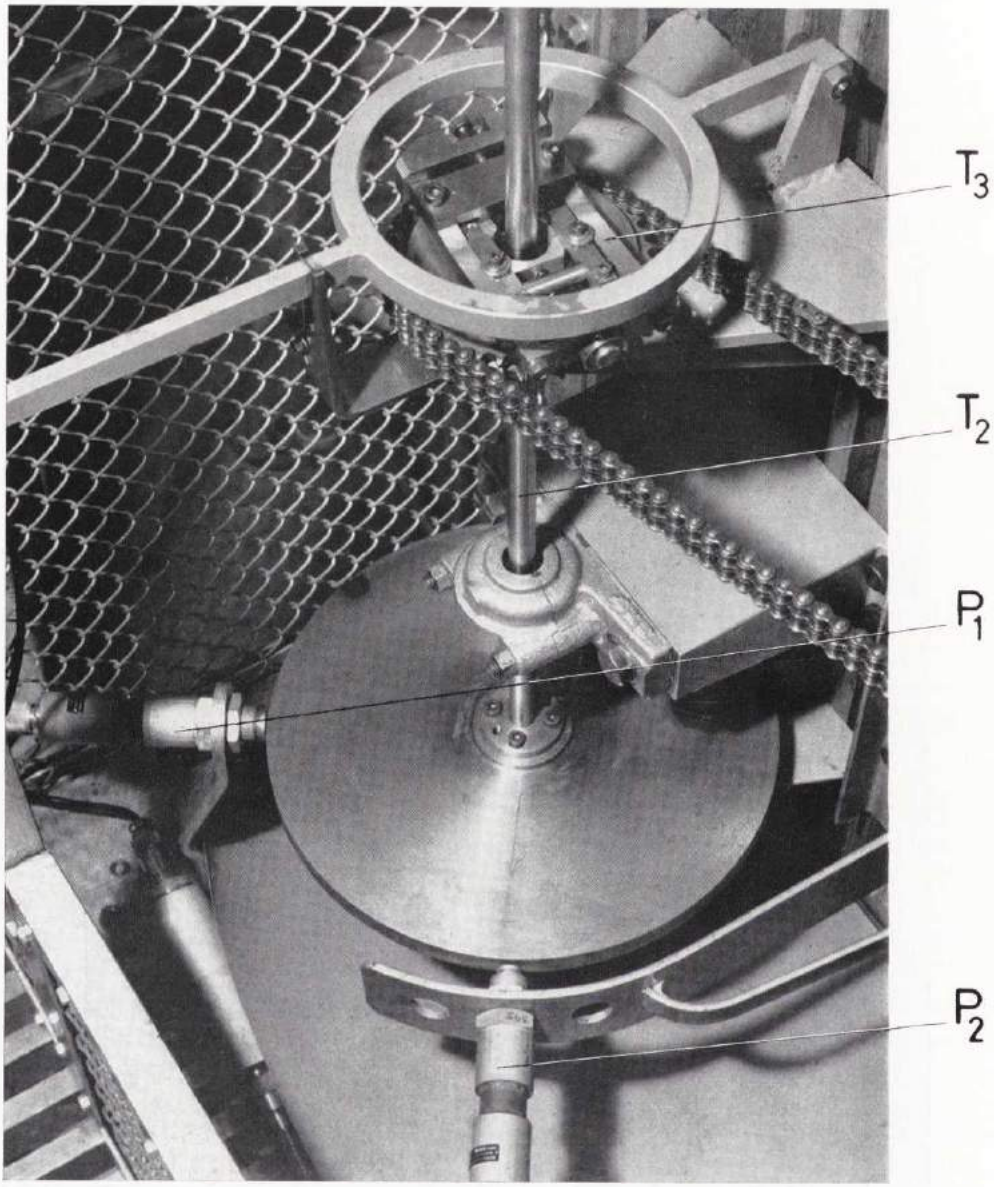

Fig. 64.3

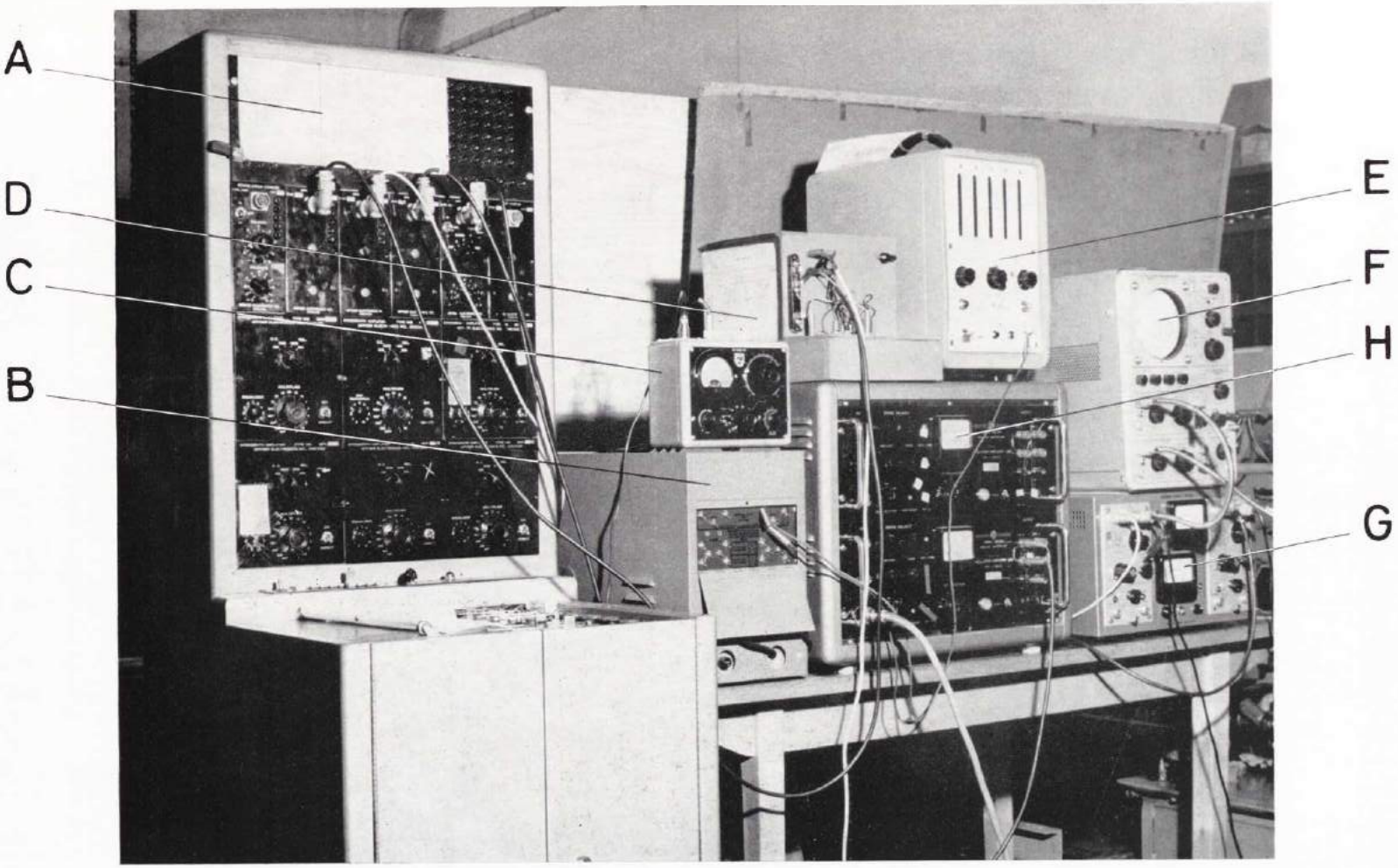

Fig. 64.4

the test apparatus had $e = 0$, but the shaft was slightly curved. In Sec. 4,2 also the theory for this case is outlined and it is derived that the "original" deflection r_c appeared in the differential equations similar to an eccentricity.

The path of the point C was photographed at a very low motor speed and at two different amplifications of the oscilloscope, one of them giving the double picture against the other. Thus the radius in the circle is the deflection r_c on a certain scale. These low speed pictures are shown in fig. 66.1 (amplification A) and fig. 66.2 (amplification B). It can be seen from the tab. 64.1 which amplification was used in the different tests. Further, the photographs from these tests are shown at page 66 up to page 70 and there also the theoretical curves are repeated.

Only critical speeds below the one corresponding to $K = +1$ were sought for (except for $K = -\frac{1}{3}$). The tests and the theory are in good agreement.

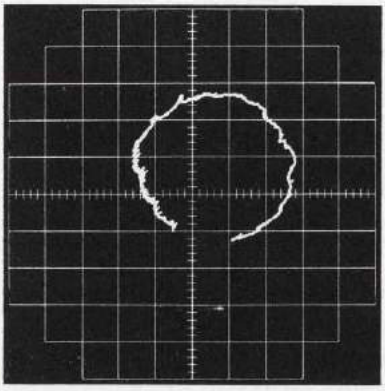

Fig. 66.1

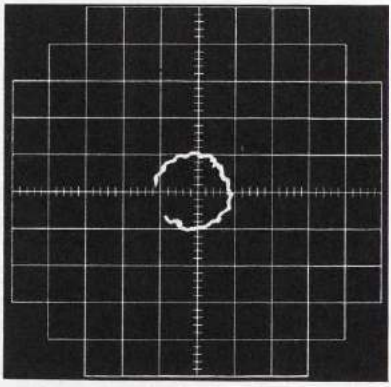

Fig. 66.2

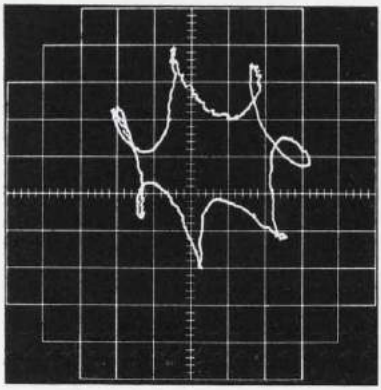

Fig. 66.3

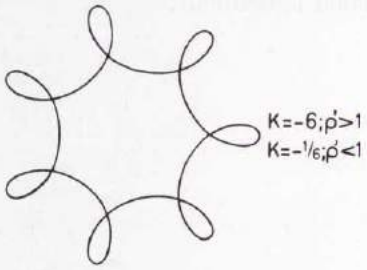

Fig. 66.4

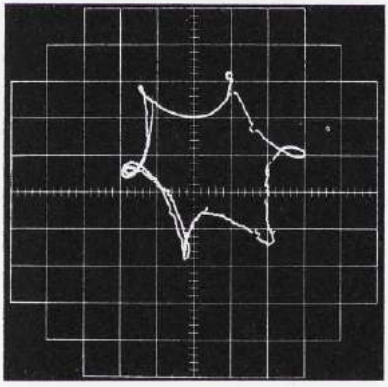

Fig. 66.5

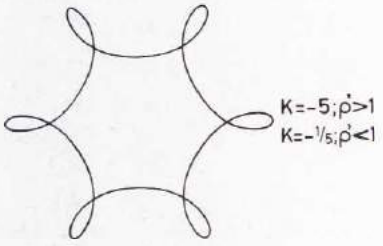

Fig. 66.6

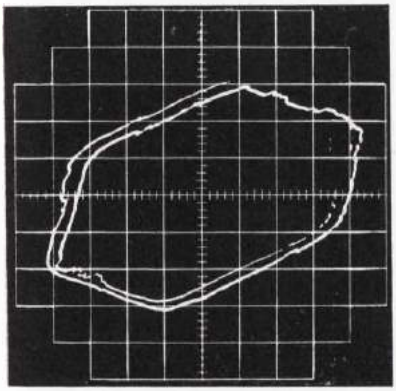

Fig. 67.1

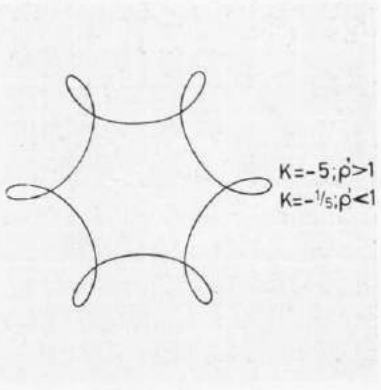

Fig. 67.2

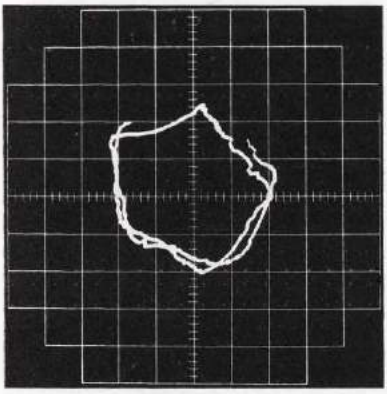

Fig. 67.3

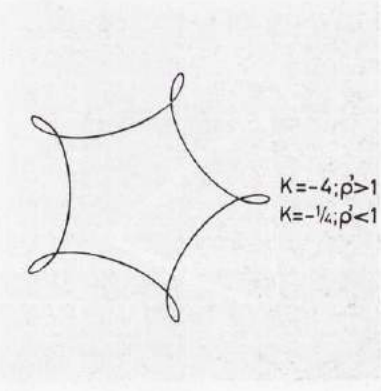

Fig. 67.4

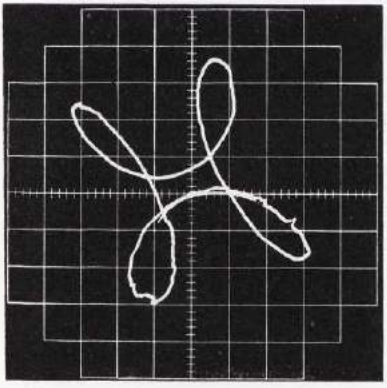

Fig. 67.5

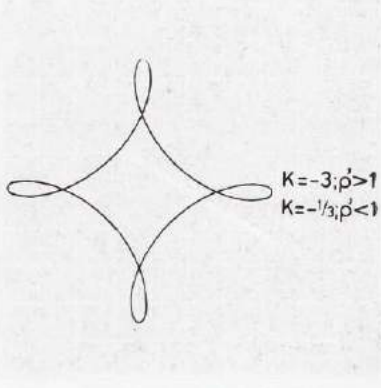

Fig. 67.6

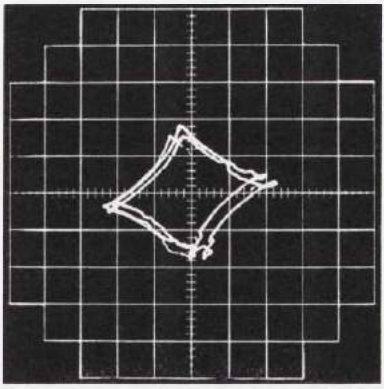

Fig. 68.1

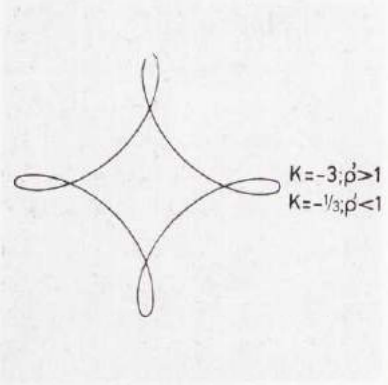

Fig. 68.2

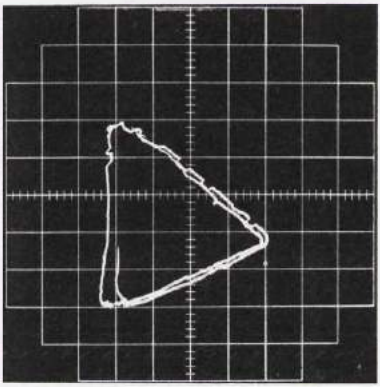

Fig. 68.3

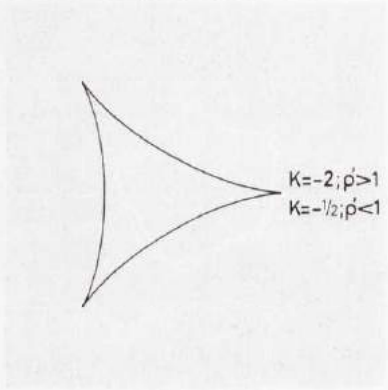

Fig. 68.4

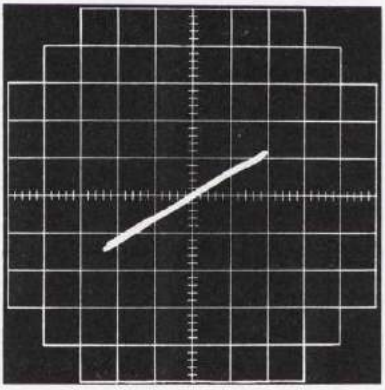

Fig. 68.5

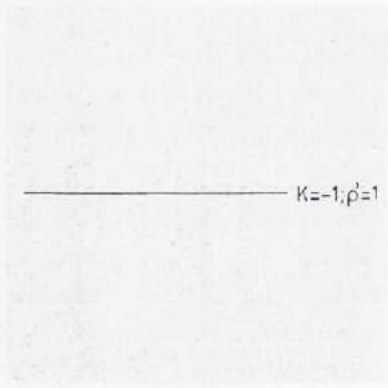

Fig. 68.6

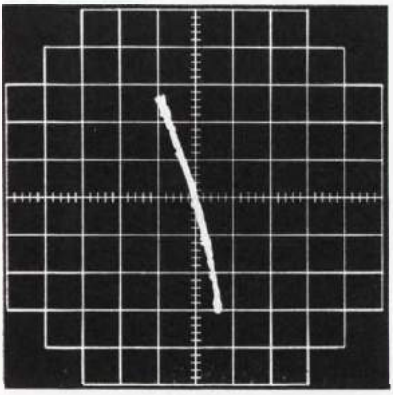

Fig. 69.1

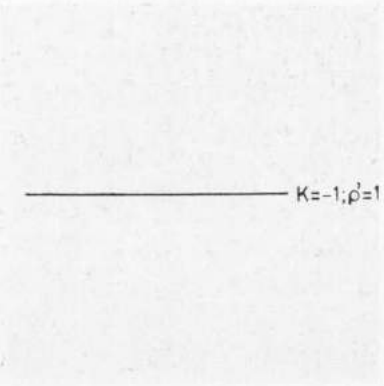

Fig. 69.2

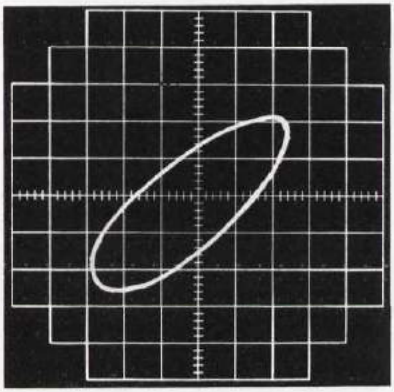

Fig. 69.3

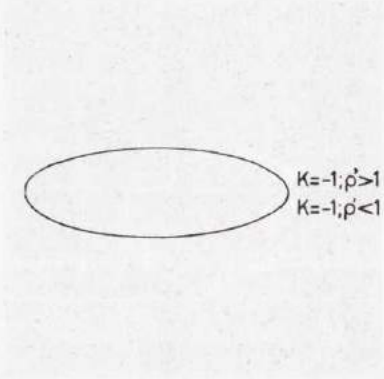

Fig. 69.4

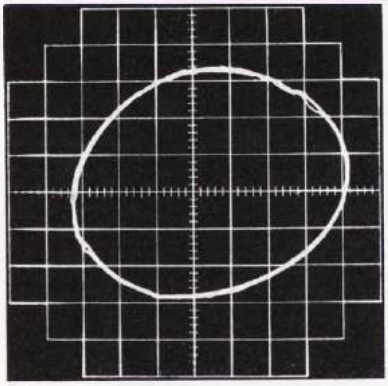

Fig. 69.5

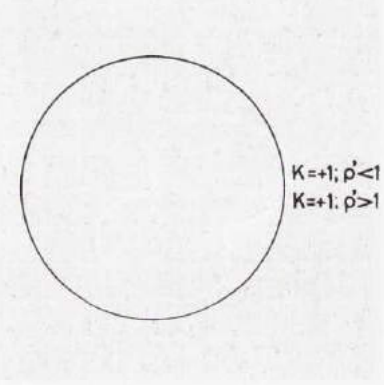

Fig. 69.6

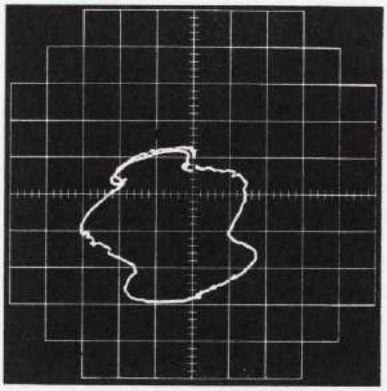

Fig. 70.1

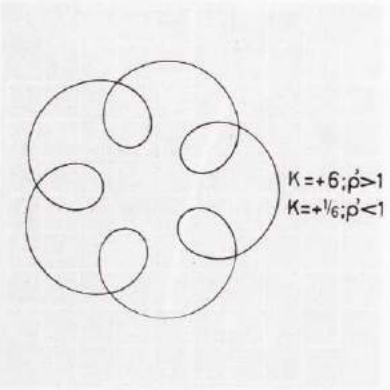

Fig. 70.2

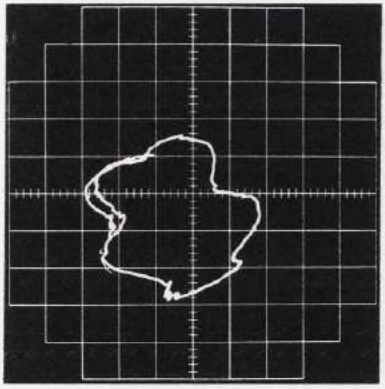

Fig. 70.3

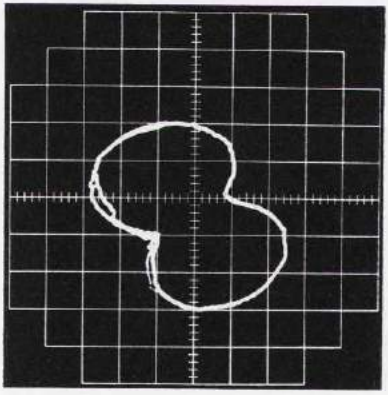

Fig. 70.4

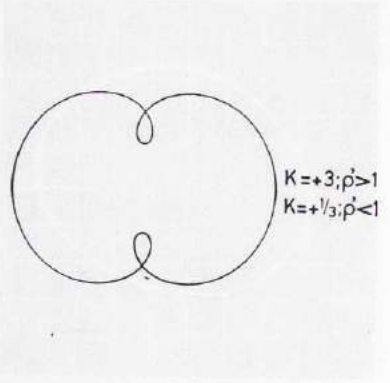

Fig. 70.5

8,2. Tests of a Hinged-Hinged-Free Shaft Driven by a D.C. Motor Coupled to a Special Ward-Leonard System

In this previous section it was shown that the D.C. motor was able to produce different kinds of whirling and this fact depended upon an "unpure" input torque. It became urgent to use an arrangement in which any "torque-tone" could be produced. So the Ward-Leonard-system was changed according to the scheme in fig. 72.1. By means of a signal-generator (Philips Z9.060.69) and its amplifier (Philips GM 5535) a sinusoidal voltage was delivered to the system. In that way it was possible to vary, within some limits, the amplitude and the frequency of a "torque-tone" desired. Thus the frequency of the "torque-tone" must be between 2,8 Hz and about 5 Hz in order to get a "torque-tone" of proper amplitude.

It became evident, with regard to this "torque-frequency", that a hinged-hinged-free rotor with $\varkappa_1 = 0{,}10$ and $x_1 = 0{,}90$ (see p. 218 in [5]) should be suitable. The same disc as before was used and the crookedness r_c of the rotor was 0,12 mm.

The lowest critical speeds for some values of K are shown in tab. 71.1.

K	-1	0	$+1$	$+2$	$+2{,}5$
N r.p.m.	200	205	211	220	228
n r.p.m.	-200	0	211	440	570

Fig. 71.1

Hence, the gyroscopic action is small in this rotor. From eq. 39.1 we get

$$\pm q = \frac{K-1}{K}$$

If $K = 2$ we get $q = \frac{1}{2}$ and the frequency of a proper torque-tone must be $\frac{440}{2 \cdot 60}$ Hz $= 3{,}67$ Hz, which is a suitable value. So this case with $K = +2$ was closely investigated.

In figures on page 73 the input torque in some tests are recorded. They are described in the following.

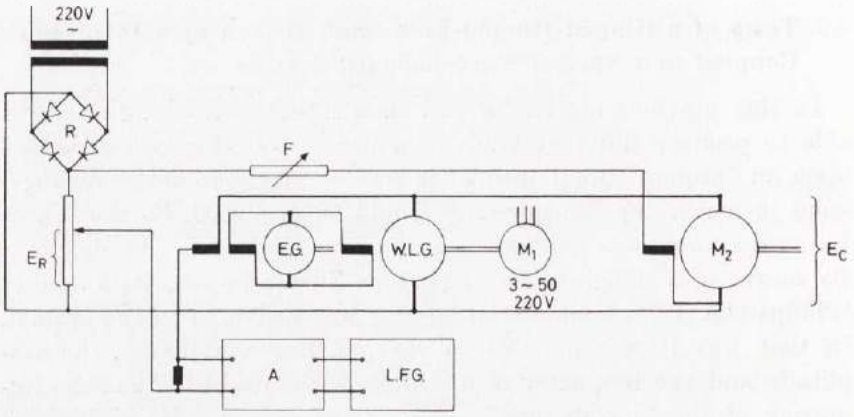

Notation:

E_R	= Reference voltage	M_2	= Motor
E_C	= Controlled voltage	R	= Rectifier
F	= Fine Adjustment	L.F.G.	= Low Frequency Generator (Philips Z9.060.69)
M_1	= Motor		
E.G.	= Exciter Generator	A	= Amplifier (Philips GM 5535)
W.L.G.	= Ward-Leonard Generator		

Fig. 72.1

Test 201. The shaft ran in this test and in the following described tests with 440 r.p.m. The Low Frequency Generator did not supply any torque. It can be seen that the Ward-Leonard-system delivers an output "torque-tone" with the same frequency as the revolution of the shaft. The trace of the centre of the disc was picked up on an oscilloscope and it can be seen on the photos in the figs 75.1, 75.2, and 75.3. From the photos it is clear that the whirl was not quite steady. Here, and in the following, the length of a vertical side of a square on the screen corresponds to a deflection of 0,074 mm of the disc centre and the distance between two adjacent arcs on the charts corresponds to the time 0,05 sec.

Test 202. In this test the Low Frequency Generator gave a slight "torque-tone" of frequency 3,67 Hz to the shaft. In fig. 73.2 can be seen that the period of the input torque was doubled.

The corresponding trace of the centre of the disc is shown in the figs 75.4, 75.5, and 75.6. Compare the figures on page 58 with $K = +2$ and $\rho' < 1$ and $\rho' = 1$ respectively.

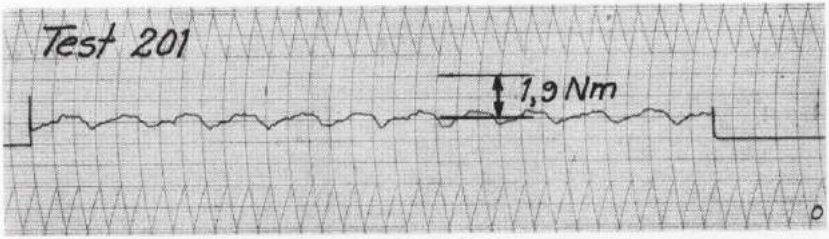

Fig. 73.1

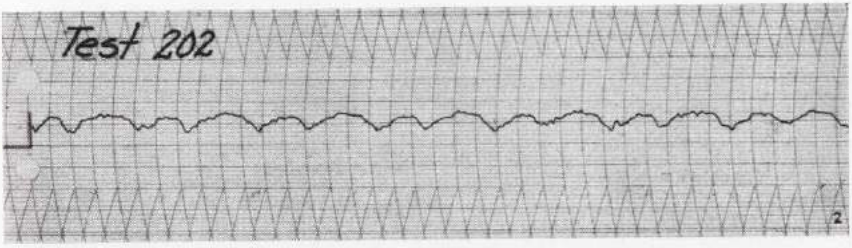

Fig. 73.2

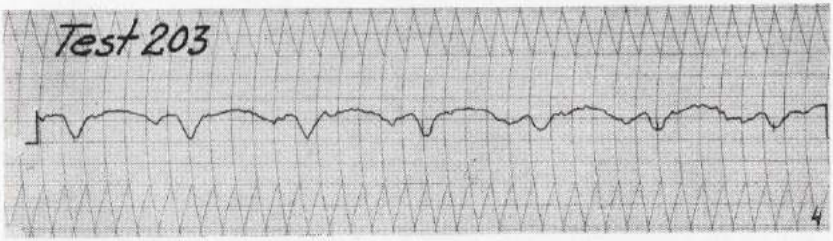

Fig. 73.3

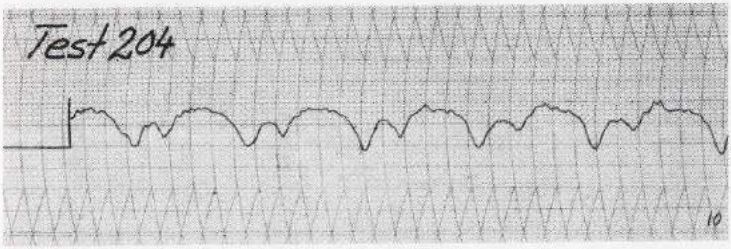

Fig. 73.4

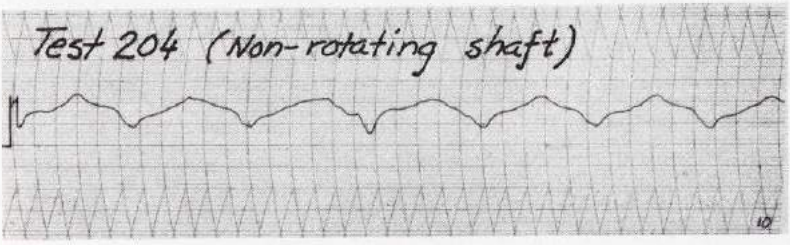

Fig. 73.5

Test 203. In this test the amplitude of the "torque-tone" from the Low Frequency Generator was increased as fig. 73.3 shows. In other respects no changes were done. The trace of the disc centre is shown on the photos in the figs 76.1, 76.2, and 76.3. Compare these photos with the figure with $K = +2$ and $\rho' > 1$ on page 58.

Test 204. The amplitude of the actual "torque-tone" was further increased and the Low Frequency Generator delivered its greatest signal. The torque is recorded in the figs 73.4 and 73.5.

From the tests the measured quantities are collected in tab. 74.1.

Test	Deflection radius of the shaft due to the "torque-tone"		Torque (Nm)
	Measured on figure	Size (mm)	
202	75.4	$0,09 \pm 0,01$	$0,19 \pm 0,04$
203	76.1	$0,19 \pm 0,01$	$0,42 \pm 0,04$
204	76.4	$0,30 \pm 0,01$	$0,61 \pm 0,04$

Tab. 74.1

Theory says that a part of the shaft deflection is directly proportional to the size of the input torque. For the actual deflections in the three tests we have the ratios

$$0,09 : 0,19 : 0,30 = 1 : 2,1 : 3,3$$

and for the amplitudes of the "torque-tones"

$$0,19 : 0,42 : 0,61 = 1 : 2,2 : 3,2 \text{ (mean values)}$$

Concerning the deflections the measured lengths are taken from the figs 75.4, 76.1, and 76.4. At small amplitudes of the torque tone the traces change in size. This coincides with the theory because the varying torque can cause both variations in motor speed and shaft deflection. The "balance" between these effects can easily be disturbed if the input torque is small. Such disturbances may come from the bearings.

Hence theory and tests are in good agreement.

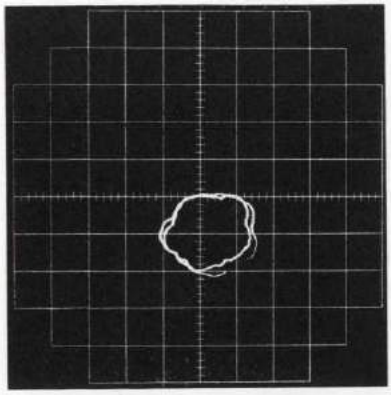

Fig. 75.1 (201)

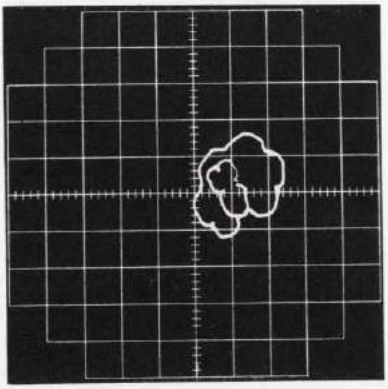

Fig. 75.2 (201)

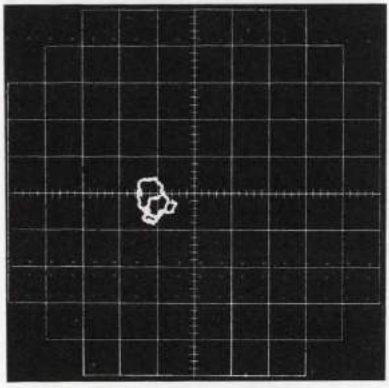

Fig. 75.3 (201)

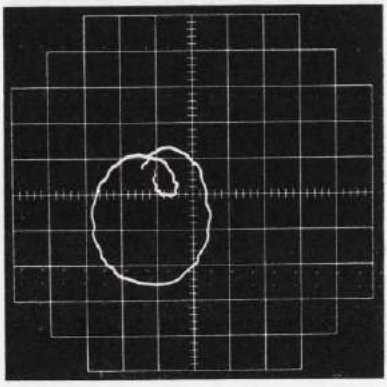

Fig. 75.4 (202)

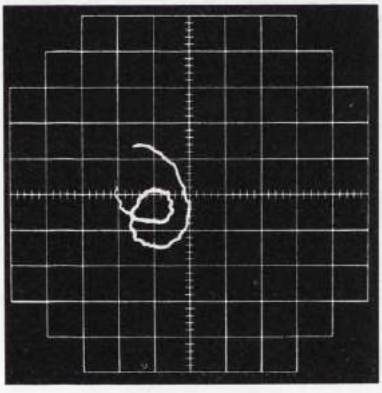

Fig. 75.5 (202)

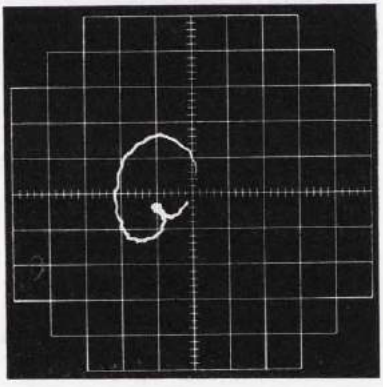

Fig. 75.6 (202)

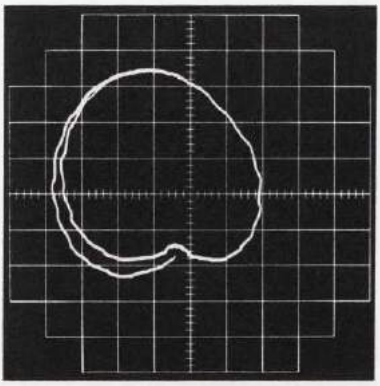

Fig. 76.1 (203)

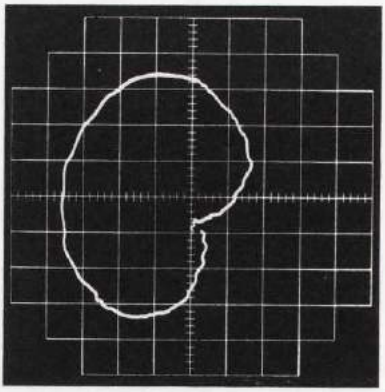

Fig. 76.2 (203)

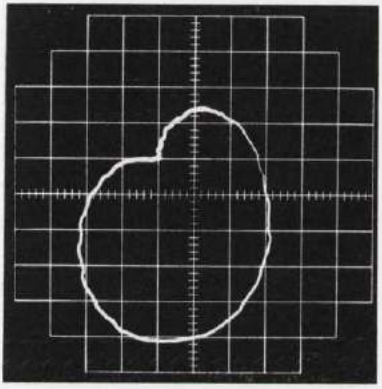

Fig. 76.3 (203)

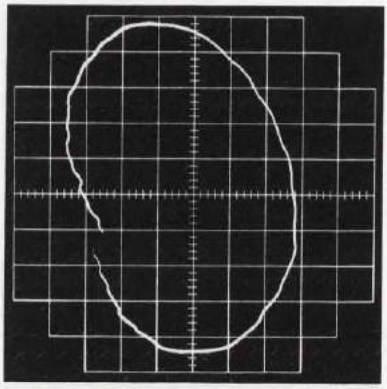

Fig. 76.4 (204)

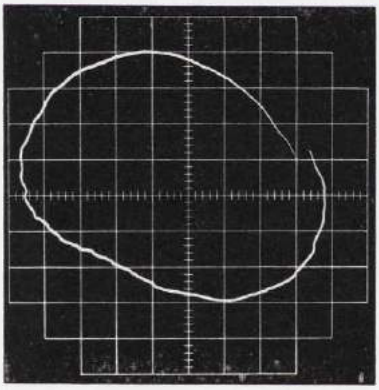

Fig. 76.5 (204)

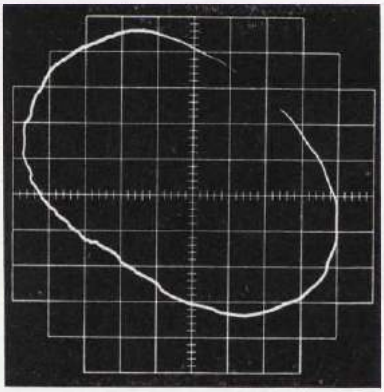

Fig. 76.6 (204)

Test 204 will now be further investigated. Suppose that the amplitude of the actual "torque-tone" is known and we want to determine the shaft deflection r' due to this "torque-tone". In the undamped case we get from eq. 50.1

$$r' = \frac{M_s}{ce} = \frac{0,61}{\left(\frac{\pi}{30} \cdot 205\right)^2 \cdot 9,87 \cdot 0,12 \cdot 10^{-3}} \text{ (m)}$$

and

$$r' = 1,12 \text{ (m)}$$

We can conclude that the external damping is of great importance. From the general expression of χ on page 46 we get

$$D_m^* = \frac{M_s^*}{8 \cdot \frac{r'}{e}} = \frac{0,61}{0,114 \cdot \left(\frac{\pi}{30} \cdot 205\right)^2 \cdot 8 \cdot \frac{0,30}{0,12}}$$

and

$$D_m^* = 0,0006$$

The damping coefficient k_m can also be determined and

$$k_m = 2D_m^* M \Omega_n = 2 \cdot 0,0006 \cdot 9,87 \cdot \frac{\pi}{30} \cdot 205$$

and

$$k_m = 0,25 \left(\frac{\text{Ns}}{\text{m}}\right)$$

9. Summary

In this report the different whirling modes of a rotor are treated. If the shaft is driven by a motor with a speed of $\omega \frac{\text{rad}}{\text{s}}$ the shaft can whirl with another angular velocity $\Omega \frac{\text{rad}}{\text{s}}$. In literature only a few values of $K = \frac{\omega}{\Omega}$ are mentioned. Except the usual value $K = +1$ some other values as $K = -1$, $+\frac{1}{2}$, and $+\frac{1}{3}$ are accounted for. By considering a rotor without eccentricity it is easily shown that every speed ω is a "critical" speed if the proper Ω-value occurs. It means that the shaft deflection is indifferent. But in practice only a few values of K occur and it is urgent to predict these values. Here is shown that the harmonics of the input torque cause these "extra" critical speeds, and further, they can occur even for a rotor with eccentricity.

Many authors derive the expression for the shaft deflection at $K = +1$ as a function of the motor speed. So is also done here, but differently, the gyroscopic effect and the external damping are taken into consideration. Some results at the critical speeds were remarkable.

Thus all whirls except ordinary reverse ($K = -1$) and forward ($K = +1$) whirl can occur at the critical state with a nearly constant deflection of the shaft at zero external damping. But the case $K = +1$ tends to increase the shaft deflection with time and the case $K = -1$ destroys itself. By considering slight external damping also these kinds of whirlings may occur with a constant or nearly constant deflection of the shaft at the critical state.

The deflection of the shaft and the position of the centre of gravity of the disc were theoretically investigated for different kinds of external damping.

Some of the theoretical results are proved in a test apparatus. A method is worked out to determine the K-value by means of an oscilloscope. On the screen of the oscilloscope the trace of the disc

centre could be seen and photographed. With the aid of this method the following "critical" states were observed:

$$K = -\tfrac{1}{6},\ -\tfrac{1}{5},\ -\tfrac{1}{4},\ -\tfrac{1}{3},\ -\tfrac{1}{2},\ -\tfrac{2}{3},\ -1,\ +\tfrac{1}{6},\ +\tfrac{1}{3},\ +1,\ +2,\ +3$$

The word "critical" is startling in an unnecessary way for the designer of rotors. Most of these critical states are totally out of danger. They are caused by the harmonics of the input torque and the shaft deflection due to the harmonic is proportional to the amplitude of the harmonic. Usually these amplitudes are small and so also are the deflections. The main point is that a shaft deflection is unattended by danger as long as the stresses in the shaft do not cause any residual displacements. Hence, the stresses ought to be below the yield point of the shaft material.

The stability of the whirling was investigated both theoretically and practically. In this connection it ought to be said that *Dimentberg* [4] has shown theoretically that the whirling with $K = +1$ is stable below a certain whirl velocity in the post-critical range (both external and internal damping present). Then the gyroscopic effect was neglected. Our tests showed, that in the sub-critical range any other whirl may occur if the proper input torque is delivered to the rotor.

Theoretical results show that at great internal damping the shaft deflection is instable at a whirl just in the neighbourhood of the critical speed. The influence of the gyroscopic action is considered.

10. References

1. Albring, W.: Angewandte Strömungslehre. Verlag von Theodor Steinkopf, Dresden und Leipzig, 1961.
2. Biezeno-Grammel: Technische Dynamik. Julius Springer, 1939.
3. Den Hartog: Mechanical Vibrations. McGraw-Hill, 1956.
4. Dimentberg, F. M.: Flexural Vibrations of rotating Shafts. Butterworths, 1961.
5. Fernlund, I.: Critical Speeds of a Shaft with Thin Discs. Transactions of Chalmers University of Technology, Gothenburg, Sweden.
6. Fernlund, I.: Running Through the Critical Speed of a Rotor. Transactions of Chalmers University of Technology, Gothenburg, Sweden.
7. Kane, T. R.: An Addition to the Theory of Whirling. Journal of Applied Mechanics, September 1961.
8. Schröder, Paul: Die kritischen Zustände zweiter Art raschumlaufender Wellen. Dissertation, Stuttgardt, 1924.
9. Stodola, A.: Dampfturbinen.

Forts. fr. omsl. 2:dra sida

229. GRANHOLM, HJALMAR, *Le problème de Boussinesq.* 15 s. 1960. Kr. 3: 50. (Avd. Väg- och Vattenbyggnad. Byggnadsteknik. 34.)
230. HIBA, MIODRAG, ET CEDERVALL, KRISTER, *Flambement élastique d'une barre en bois lamellée et clouée avec le module de déplacement du moyen de liaison constant k.* 22 s. 1960. Kr. 5: —. (Avd. Väg- och Vattenbyggnad. Byggnadsteknik. 35.)
231. FLOBERG, LEIF, *The optimum thrust tilting-pad bearing.* 23 s. 1960. Kr. 5: —. (Avd. Maskinteknik. 19.)
232. FLOBERG, LEIF, *The two-groove journal bearing, considering cavitation.* 32 s. 1960. Kr. 6: —. (Avd. Maskinteknik. 20.)
233. HEDVALL, J. ARVID, *Heterogeneous catalysis, results and projects for research.* 18 s. 1961. Kr. 5: —. (Avd. Kemi och Kemisk Teknologi. 36.)
234. FLOBERG, LEIF, *Lubrication of two cylindrical surfaces, considering caviation.* 36 s. 1961. Kr. 10: —. (Avd. Maskinteknik. 21.)
235. FLOBERG, LEIF, *Attitude-eccentricity curves and stability conditions of the infinite journal bearing.* 43 s. 1961. Kr. 11: —. (Avd. Maskinteknik 22.)
236. BEN-YAIR, M. P., *Thermometric titrations of zinc, cadmium and mercuric salts.* 11 s. 1961. Kr. 3: —. (Avd. Kemi och Kemisk Teknologi. 37.)
237. SANDFORD, F., LILJEGREN, B., AND JONSSON, B., *The resistance of bricks towards frost experiments and considerations.* 20 s. 1961. Kr. 5: —. (Avd. Kemi och Kemisk Teknologi. 38.)
238. FLOBERG, LEIF, *Experimental investigation of cavitation regions in journal bearings.* 28 s. 1961. Kr. 6: —. (Avd. Maskinteknik. 23.)
239. GRANHOLM, HJALMAR, *Sandöbrons bågställning.* 128 s. 1961. Kr. 20: —. (Avd. Väg- och Vattenbyggnad. Byggnadsteknik. 36.)
240. LINDBLAD, ANDERS, *On the design of lines for merchant ships.* 125 s. Kr. 20: —. (Avd. Skeppsbyggeri. 7.)
241. LUNDÉN, ARNOLD, *Self diffusion and the structure of molten salts.* 14 s. Kr. 4: —. (Avd. Allm. Vetenskaper. 17.)
242. LARSSON, LARS-ERIK, *Sprickbildning i vattenledningsrör av förspänd betong.* 70 s. 1961. Kr. 15: —. (Avd. Väg- och Vattenbyggnad. Byggnadsteknik. 37.)
243. ASPLUND, S. O., *A unified analysis of indeterminate structure.* 36 s. 1961. Kr. 8: —. (Avd. Väg- och Vattenbyggnad. Byggnadsteknik. 38.)
244. BRAUNSTEIN, A., *The magnetic field in iron with variable permeability.* 11 s. 1961. Kr. 3: —. (Avd. Elektroteknik. 69.)
245. FERNLUND, INGEMAR, *A method to calculate the pressure between bolted or riveted plates.* 126 s. 1961. Kr. 25: —. (Avd. Maskinteknik. 24.)
246. HEDVALL, J. ARVID, AND KARAMUSTAFAOĞLU, VURAL, *On the conservation of ancient alabaster objects.* 19 s. 1961. Kr. 5: —. (Avd. Kemi och Kemisk Teknologi. 39.)
247. EKELÖF, STIG, *A theory of the eddy current equivalent winding and its application to the closing of non-delayed telephone relays.* 35 s. 1961. Kr. 7: —. (Avd. Elektroteknik. 70.)
248. CEDERWALL, KRISTER, *Beräkning av spikade konstruktioner med hänsyn till förbandens deformationsegenskaper.* 52 s. 1961. Kr. 10: —. (Avd. Väg- och Vattenbyggnad. Byggnadsteknik. 39.)
249. KÄRRHOLM, GUNNAR, AND SAMUELSSON, ALF, *Bridge slabs with edge-beams.* 73 s. 1961. Kr. 15: —. (Avd. Väg- och Vattenbyggnad. Byggnadsteknik. 40.)
250. LOSBERG, ANDERS, *Design methods for structurally reinforced concrete pavements.* 143 s. 1961. Kr. 30: —. (Avd. Väg- och Vattenbyggnad. Byggnadsteknik. 41.)
251. EKELÖF, STIG, *Primärnormalerna för resistans och spänning vid CTH's institution för elektricitetslära och elektrisk mätteknik.* 20 s. 1961. Kr. 4: —. (Avd. Elektroteknik 71.)
252. ÅKESSON, BENGT Å., *Rationalization of Lévy's plate solution.* 135 s. 1961. Kr. 25: —. (Avd. Väg- och Vattenbyggnad. Byggnadsteknik. 42.)
253. BROGREN, GÖSTA, *A double-crystal spectrometer for work in vacuum region.* 19 s. 1961. Kr. 4 —. (Avd. Allm. Vetenskaper. 18.)
254. KIHLMAN, TOR, *Flanktransmissionens inverkan på rumsisolering mot luftljud.* 69 s. 1961. Kr. 14: —. (Avd. Väg- och Vattenbyggnad. Byggnadsteknik. 43.)
255. SVENSSON, S. IVAR, *The influence of cam curve derivative steps on cam dynamical properties.* 93 s. 1961. Kr. 25: —. (Avd. Maskinteknik. 25.)
256. HULT, JAN, *Mechanics of a beam subject to primary creep.* 20 s. 1962. Kr. 5: —. (Avd. Allm. Vetenskaper. 19.)
257. SANDFORD, FOLKE, AND HEDVALL, J. ARVID, *Concerning the cause of the colour of an amazonite preparation.* 8 s. 1962. Kr. 3: —. (Avd. Kemi och Kemisk Teknologi. 40.)
258. NILSSON, JAN, *On the structure of weak interactions.* 66 s. 1962. Kr. 15: —. (Avd. Allm. Vetenskaper. 20.)
259. STRÖM, LARS, *An absolute anemometer.* 22 s. 1962. Kr. 6: —. (Avd. Maskinteknik. 26.)

Forts. å omsl. 4:de sida

Forts. fr. omsl. 3:dje sida

260. FERNLUND, INGEMAR, *Critical speeds of a shaft with thin discs.* 224 s. 1962. Kr. 50: —. (Avd. Maskinteknik. 27.)
261. FERNLUND, INGEMAR, *On solving Reynold's equation for bearings of finite width with Fourier sine transforms.* 28 s. 1962. Kr. 7: —. (Avd. Maskinteknik. 28.)
262. AURELL, CARL G., *Physical equations from the conceptual point of view.* 52 s. 1962. Kr. 12: 50. (Avd. Elektroteknik. 72.)
263. SMITH, BENGT, *Investigation of reagents for the qualitative analysis of phenols.* 51 s. 1963. Kr. 12: 50. (Avd. Kemi och Kemisk Teknologi. 41.)
264. HULT, JAN, *Primary creep in thickwalled spherical shells.* 26 s. 1963. Kr. 8: —. (Avd. Allm. Vetenskaper. 21.)
265. STRINDEHAG, OVE, *Optimized performance of the vidicon.* 58 s. 1963. Kr. 15: —. (Avd. Elektroteknik. 73.)
266. DUBOIS, J., *An investigation of the S^{34} (p, γ) Cl^{35}-reaction.* 32 s. 1963. Kr. 8: —. (Avd. Allm. Vetenskaper. 22.)
267. DUBOIS J., AND ALBINSSON H., *Radiative proton capture in Ca^{44}.* 22 s. 1963. Kr. 6: —. (Avd. Allm. Vetenskaper. 23.)
268. DUBOIS, J., AND BROMAN L., *The Ca^{42} (p, γ) Sc^{43} reaction and the decay of Sc^{43}.* 31 s. 1963. Kr. 8: —. (Avd. Allm. Vetenskaper. 24.)
269. DUBOIS, J., *Low energy excited levels in some vanadium isotopes.* 28 s. 1963. Kr. 8: —. (Avd. Allm. Vetenskaper. 25.)
270. DUBOIS, J., *The ion beam energy stabilization system of the Van de Graaff generator at Gothenburg.* 16 s. 1963. Kr. 5: —. (Avd. Allm. Vetenskaper. 26.)
271. HEDVALL, J. ARVID, *Surface chemistry and corrosion.* 18 s. 1963. Kr. 6: —. (Avd. Kemi och Kemisk Teknologi. 42.)
272. HEDVALL, J. ARVID, *The chemistry of cement and concrete considered as a facet of the reactivity of solids.* 18 s. 1963. Kr. 6: —. (Avd. Kemi och Kemisk Teknologi. 43.)
273. ASPLUND, SVEN OLOF, *Practical calculation of suspension bridges.* 27 s. 1963. Kr. 8: —. (Avd. Väg- och Vattenbyggnad. Byggnadsteknik. 44.)
274. GRANHOLM, HJALMAR, *Träkonstruktioners brandstabilitet. Symposium vid Chalmers Tekniska Högskola den 18 juni 1962.* 151 s. 1963. Kr. 25: —. (Avd. Väg- och Vattenbyggnad. Byggnadsteknik. 45.)
275. ALBERTSSON, ÅKE, *Vindtryck på skorstenar.* 70 s. 1963. Kr. 18: —. (Avd. Väg- och Vattenbyggnad. Byggnadsteknik. 46.)

Pris kronor 20:—

ELANDERS BOKTRYCKERI AKTIEBOLAG
GÖTEBORG 1963

CHALMERS TEKNISKA HÖGSKOLAS HANDLINGAR
TRANSACTIONS OF CHALMERS UNIVERSITY OF TECHNOLOGY
GOTHENBURG, SWEDEN
Nr 277 (Avd. Maskinteknik 30) 1963

RUNNING THROUGH THE CRITICAL SPEED OF A ROTOR

BY

INGEMAR FERNLUND

Report No. 22 from the Institute of Machine Elements
Chalmers University of Technology
Gothenburg, Sweden
1963

Av Chalmers Tekniska Högskolas Handlingar hava tidigare utkommit:

Fullständig förteckning över Chalmers Tekniska Högskolas Handlingar lämnas av Chalmers Tekniska Högskolas Bibliotek, Göteborg.

201. KÄRRHOLM, GUNNAR, *Influenced functions of elastic plates divided in strips.* 18 s. 1958. Kr. 4: 50. (Avd. Väg- och Vattenbyggnad. Byggnadsteknik. 28.)
202. RÅDE, LENNART, *Sampling planes for acceptance sampling by variables using the range.* 34 s. 1958. Kr. 9: 50. (Avd. Allm. Vetenskaper. 14.)
203. JAKOBSSON, BENGT, AND FLOBERG, LEIF, *The rectangular plane pad bearing.* 44 s. 1958. Kr. 5: —. (Avd. Maskinteknik. 12.)
204. ASPLUND, SVEN OLOF, *Column-beams and suspension bridges analysed by »Green's matrix».* 36 s. 1958. Kr. 7: —. (Avd. Väg- och Vattenbyggnad. Byggnadsteknik. 29.)
205. WILHELMSSON, HANS, *On the properties of the electron beam in the presence of an axial magnetic field of arbitrary strength.* 32 s. 1958. Kr. 7: 50. (Avd. Elektroteknik. 63.)
206. WILHELMSSON, HANS, *The interaction between an obliquely incident plane electromagnetic wave and an electron beam. III.* 17 s. 1958. Kr. 5: —. (Avd. Elektroteknik. 64.)
207. HEDVALL, J. ARVID, *On the influence of pre-treatment and transition processes on the adsorption capacity and the reactivity of various types of glass and silica.* 39 s. 1959. Kr. 8: —. (Institutionen för Silikatkemisk Forskning. 40.)
208. KÄRRHOLM, GUNNAR, *A flow problem solved by strip method.* 22 s. 1959. Kr. 4: 50. (Avd. Allm. Vetenskaper. 15.)
209. GRANHOLM, HJALMAR, *Allmän teori för beräkning av armerad betong.* 228 s. 1959. Kr. 20: —. (Avd. Väg- och Vattenbyggnad. Byggnadsteknik. 30.)
210. LIDIN, LARS G., *On helical-springs suspension.* 75 s. 1959. Kr. 15: —. (Avd. Maskinteknik. 13.)
211. BJÖRK, NILS, *Theory of the indirectly heated thermistor.* 46 s. 1959. Kr. 10: —. (Avd. Elektroteknik. 65.)
212. CARLSSON, ORVAR, *The influence of submicroscopic pores on the resistance of bricks towards frost.* 13 s. 1959. Kr. 3: 50. (Institutionen för Silikatkemisk Forskning. 41.)
213. GRANHOLM, HJALMAR, *KAM 40, KAM 60 och KAM 90.* 41 s. 1959. Kr. 3: 50. (Avd. Väg- och Vattenbyggnad. Byggnadsteknik. 31.)
214. JAKOBSSON, BENGT, AND FLOBERG, LEIF, *The centrally loaded partial journal bearing.* 35 s. 1959. Kr. 7: 50. (Avd. Maskinteknik. 14.)
215. FLOBERG, LEIF, *Experimental investigation of power loss in journal bearings, considering cavitation.* 16 s. 1959. Kr. 3: 50. (Avd. Maskinteknik. 15.)
216. FLOBERG, LEIF, *Lubrication of a rotating cylinder on a plane surface, considering cavitation.* 40 s. 1959. Kr. 8: —. (Avd. Maskinteknik. 16.)
217. TROEDSSON, CARL BIRGER, *The growth of the Western city during the Middle Ages.* 125 s. 1959. Kr. 19: —. (Avd. Arkitektur. 4.)
218. HEDVALL, J. ARVID, *The importance of the reactivity of solids in geological-mineralogical processes.* 11 s. 1959. Kr. 2: 50. (Institutionen för Silikatkemisk Forskning. 42.)
219. CORNELL, ELIAS, *Humanistic inquiries into architecture. I—III.* 112 s. 1959. Kr. 17: —. (Avd. Arkitektur. 5.)
220. GRANHOLM, CARL-ADOLF, *Ekonomiska aluminiumprofiler.* 48 s. 1959. Kr. 5: 50. (Avd. Väg- och Vattenbyggnad. Byggnadsteknik. 32.)
221. LUNDÉN, ARNOLD, CHRISTOFFERSON, STINA, AND LODDING, ALEX, *The isotopic effect of lithium ions in countercurrent electromigration in molten lithium bromide and iodide.* 38 s. 1959. Kr. 7: 50. (Avd. Allm. Vetenskaper. 16.)
222. INGEMANSSON, STIG, AND KIHLMAN, TOR, *Sound insulation of frame walls.* 47 s. 1959. Kr. 8: 50. (Avd. Väg- och Vattenbyggnad. Byggnadsteknik. 33.)
223. HÖGLUND, B., AND RADHAKRISHNAN, V., *A radiometer for the hydrogen line.* 25 s. 1959. Kr. 6: 50. (Avd. Elektroteknik. 66.)
224. JAKOBSSON, BENGT, *Torque distribution, power flow, and zero output conditions of epicyclic gear trains.* 55 s. 1960. Kr. 12: —. (Avd. Maskinteknik. 17.)
225. OLVING, SVEN, *Electromagnetic and space charge waves in a sheath helix.* 91 s. 1960. Kr. 17: —. (Avd. Elektroteknik. 67.)
226. STRÖMBLAD, JOHN, *Beschleunigungsverlauf und Gleichgewichtsdrehzahlen einfacher Planetengetriebe nebst Selbsthemmungsversuche.* 80 s. 1960. Kr. 18: —. (Avd. Maskinteknik. 18.)
227. SANDFORD, FOLKE, *Some current problems concerning brick manufacture.* 20 s. 1960. Kr. 5: —. (Avd. Kemi och Kemisk Teknologi. 35.)
228. OLVING, SVEN, *A new method for space charge wave interaction studies. II.* 40 s. 1960. Kr. 8: —. (Avd. Elektroteknik. 68.)

Forts. å omsl. 3:dje sida

CHALMERS TEKNISKA HÖGSKOLAS HANDLINGAR
TRANSACTIONS OF CHALMERS UNIVERSITY OF TECHNOLOGY
GOTHENBURG, SWEDEN
Nr 277 (Avd. Maskinteknik 30) 1963

RUNNING THROUGH THE CRITICAL SPEED OF A ROTOR

BY

INGEMAR FERNLUND

Report No. 22 from the Institut of Machine Elements
Chalmers University of Technology
Gothenburg, Sweden
1963

SCANDINAVIAN UNIVERSITY BOOKS
AKADEMIFÖRLAGET-GUMPERTS · GÖTEBORG

SCANDINAVIAN UNIVERSITY BOOKS

Denmark: MUNKSGAARD, *Copenhagen*
Norway: UNIVERSITETSFORLAGET, *Oslo, Bergen*
Sweden: AKADEMIFÖRLAGET-GUMPERTS, *Göteborg*
SVENSKA BOKFÖRLAGET/Norstedts–Bonniers, *Stockholm*

Manuscript received by the Publications Committee,
Chalmers University of Technology, Nov. 4th, 1962

PRINTED IN SWEDEN BY
ELANDERS BOKTRYCKERI AKTIEBOLAG, GÖTEBORG 1963

Preface

In earlier works [6] and [7] the present author has treated the problems of finding the critical states of a rotor. Thus only constant values of the motor speed were discussed.

In this report the transition of a rotor through its critical speed is treated. Mathematically this problem is of a complicated nature. The digital computer *Alwac III E* was used and such a help was indeed one of the essential requirements for succeeding in getting numerical results of value for the designer.

I wish to thank the *Swedish Technical Research Council* for its sponsorship and Professor *B. Jakobsson, the Head of the Institute of Machine Elements at Chalmers University of Technology, Gothenburg,* for suggestions and a great deal of valuable comments.

Ingemar Fernlund
Tekn. lic.
Research Assistant at the
Institute of Machine Elements

Contents

1. Introduction

A shaft which is operating beyond the first ordinary critical speed on starting or stopping must pass through this critical speed. This gives rise to the problem of determining the stresses, essentially the flexural stresses, of the shaft. In many machines the speed of the motor is sub-critical because of the fear of designing a rotor which passes through the critical speed and this fear has probably grown from the lack of knowledge about the behaviour of the rotor when passing the critical speed.

The present report gives some new results concerning the behaviour of a rotor with one disc when passing its critical speed, and these results may be of value for the designer of rotors.

In modern machines the shaft often runs in the post-critical range, a so-called high-speed shaft. In design of these machines one has to care for the stability.

2. Notation

A	Reaction force in bearing
B	Bearing line or reaction force in bearing
$C(u)$	Frenel's integral
D^*	Non-dimensional damping coefficient
F	Force
G	Centre of gravity
I	Moment of inertia of a cross section
I_p	Polar moment of inertia of a disc
$K = \frac{\omega}{\Omega}$	Ratio
L	Length
M	Mass. Bending moment
M_{in}	Input torque
N	Normal force in a deflection limiter
R	Deflection of the centre of gravity
S	Notation for shaft centre
$S(u)$	Frenel's integral
a	Angular acceleration
a_1	Arbitrary constant
b_1	Arbitrary constant
c_1	Arbitrary constant
d	Diameter of shaft
e	Eccentricity
f	Function
k	Coefficient of external damping
k_i	Radius of gyration
k_{iu}, k_{iv}	Functions
n	R.p.m. of a motor
q	Constant
r	Deflection of shaft

u	Variable or $u = \dfrac{d\rho}{d\tau}$
v	Angle or $v = \dfrac{d\varphi}{d\tau}$
x	Coordinate
y	Coordinate
z	Coordinate
Δ	Radial clearance in a deflection limiter
θ	Angle, Variable
Ω	Angular velocity of whirling $\left(\dfrac{\text{rad}}{\text{s}}\right)$
α	Constant or Influence number concerning displacements
β	Influence number concerning rotations
$\gamma_G = \dfrac{Mg\alpha_{11}}{e}$	Constant
$\varepsilon = \dfrac{e}{k_i}$	Constant
ζ	Non-dimensional deflection
η	Non-dimensional deflection
$\varkappa = \dfrac{\Omega}{\Omega_n}$	Constant or $\varkappa$ = non-dimensional length
$\lambda = \dfrac{a}{2\Omega_n^2}$	Non-dimensional angular acceleration
μ	Coefficient of friction
ξ	Variable or non-dimensional influence number concerning displacements
ρ	Non-dimensional deflection
σ	Stress
τ	Non-dimensional "time"
φ	"Whirl-angle"
ψ	"Shaft-angle"
ω	Angular velocity of the shaft $\left(\dfrac{\text{rad}}{\text{s}}\right)$

3. Basic Equations for the Motion of a One-Disc Rotor during Transition Through its Critical Speed

Consider a circular shaft in two supports A and B with an unbalanced disc rotating with a variable angular velocity according to fig. 8.1. The shaft is driven by a motor and the deflection of the shaft is limited by a solid ring DL (Deflection Limiter). The coupling C is assumed not to be able to transmit anything but a torque and the weight of it is negligible besides the weight of the disc. Further, the mass of the shaft and the gyroscopic effect are neglected.

In fig. 8.1 the rotor is shown in a position when the three points B', S and G are in the same plane and from [7] it is known that B' is the cross point between the centreline of the bearings and a vertical plane perpendicular to it through the point S, S is the centre of the shaft at the disc, and G is the centre of gravity of the disc.

Thus, the deflection of the shaft is $r = \overline{B'S}$ and the eccentricity of the disc is $e = \overline{SG}$. It is assumed that the deflections are small.

Part of the arrangement is shown projected at the $y-z$-plane in fig. 9.1. Observe that the shaft is bent into two directions and its deflections in these directions are r_1 and r_2 respectively.

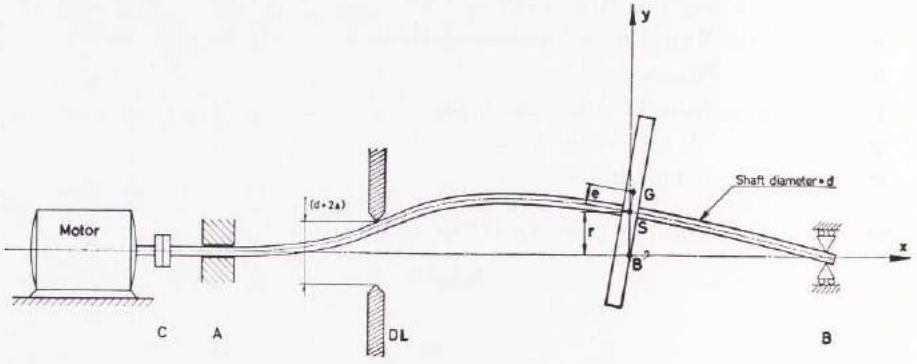

Fig. 8.1.

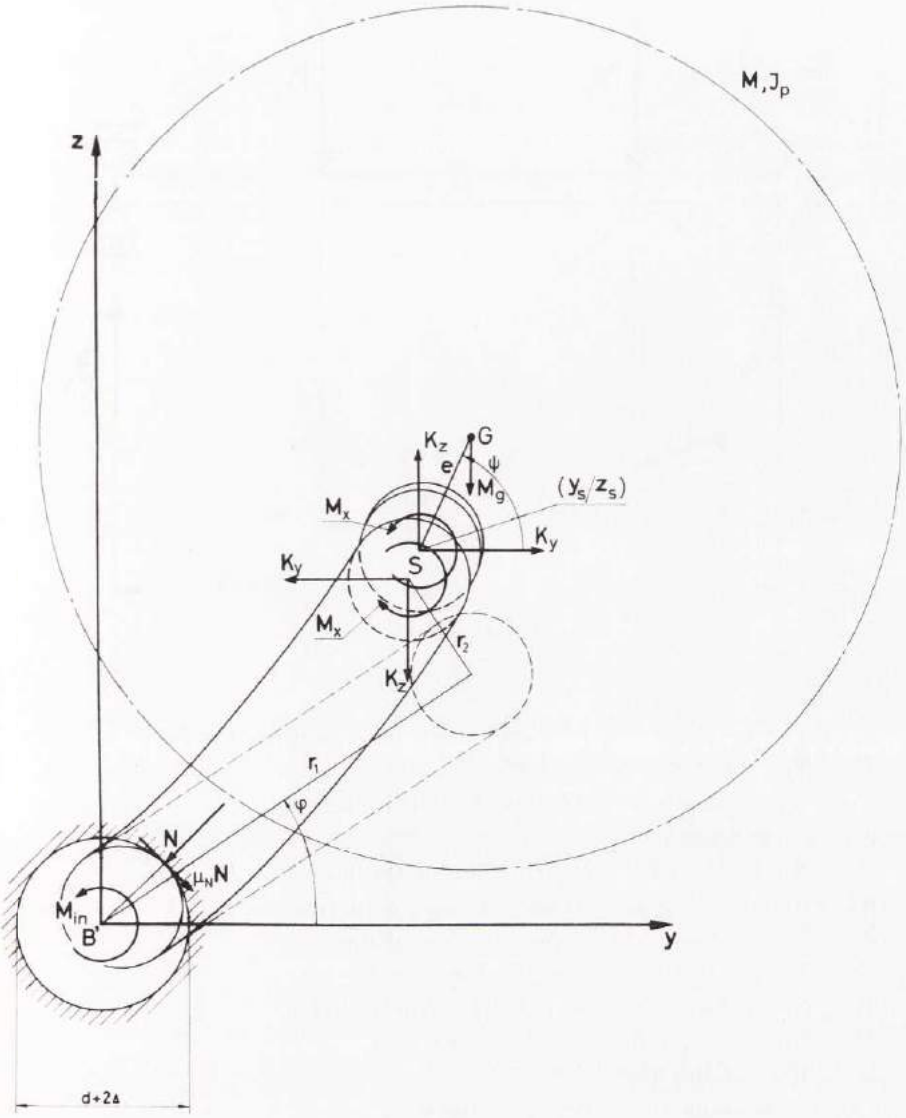

Fig. 9.1.

Notations:

y_s The deflection of the shaft in the y-direction
z_s The deflection of the shaft in the z-direction
y The position of the centre of gravity G in the y-direction
z The position of the centre of gravity G in the z-direction

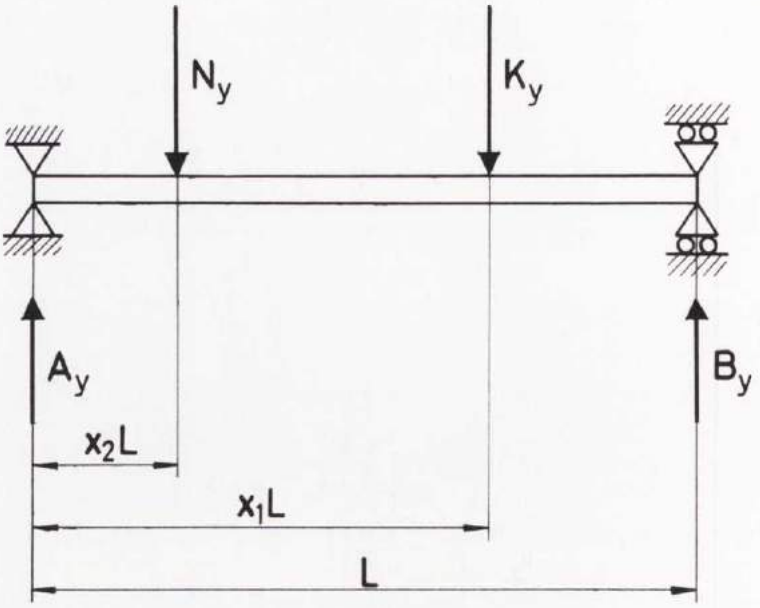

Fig. 10.1

μ_N The coefficient of friction at the deflection limiter DL
d The diameter of the shaft
Δ Radial clearance in the deflection limiter DL
φ "Whirl-angle"
ψ Angle decided by the rotation of the motor
K_y Elastic force in the shaft in the y-direction
K_z Elastic force in the shaft in the z-direction
M_x Torque in the shaft in the x-direction
N Normal force at the deflection limiter DL
M_{in} Outer torque in the x-direction
M Mass of the disc
I_p Polar moment of inertia of the disc

In fig. 10.1 the forces acting on the shaft in the $x-y$-plane are shown and the notations are

A_y Reaction force in bearing A in the y-direction
B_y Reaction force in bearing B in the y-direction
N_y Normal force in the deflection limiter in the y-direction

The equations for the movement of the disc are

$$\left.\begin{aligned} M\ddot{y} &= K_y - k\dot{y} \\ M\ddot{z} &= K_z - k\dot{z} - Mg \\ I_p\ddot{\psi} &= M_x + K_y e \sin\psi - K_z e \cos\psi \end{aligned}\right\} \quad \ldots\ldots\ldots\ 11.1$$

where k is a coefficient for external viscous damping. For the deflections of the shaft at the disc we have

$$\left.\begin{aligned} r_1 &= -(K_y \cos\varphi + K_z \sin\varphi)\alpha_{11} - N_1\alpha_{12} \\ r_2 &= (K_y \sin\varphi - K_z \cos\varphi)\alpha'_{11} - N_2\alpha'_{12} \end{aligned}\right\} \quad \ldots\ldots\ 11.2$$

where α_{11}, α_{12}, α'_{11}, and α'_{12} are influence numbers (See [6]). As a matter of fact $\alpha_{11} \neq \alpha'_{11}$ and $\alpha_{12} \neq \alpha'_{12}$.

Moreover, the forces N_1 and N_2 are projections of the forces N and μN in the directions of r_1 and r_2 respectively.

For the outer torque M_{in} we get

$$M_{in} - M_x + K_y z_s - K_z y_s - \mu_N N\left(\frac{d}{2} + \Delta\right) - (\mu_A A + \mu_B B)\frac{d}{2} = 0 \qquad 11.3$$

where μ_A and μ_B are the coefficients of friction in the bearing A and B respectively.

In this report only cases satisfying the condition $\alpha_{ij} = \alpha'_{ij}$ which means that $r_1 = r$ and $r_2 = 0$ are treated. Hence, the shaft is presumed to be rigid in a torsional point of view but it is still flexible in bending.

Thus

$$\left.\begin{aligned} N_1 &= N \\ N_2 &= \mu_N N \end{aligned}\right\}$$

and we also get

$$\left.\begin{aligned} \Delta\cos\varphi &= -K_y\alpha_{12} - N_y\alpha_{22} \\ \Delta\sin\varphi &= -K_z\alpha_{12} - N_z\alpha_{22} \end{aligned}\right\} \quad \ldots\ldots\ldots\ 11.4$$

where

$$\left.\begin{aligned} N_y &= N(\cos\varphi - \mu_N \sin\varphi) \\ N_z &= N(\sin\varphi + \mu_N \cos\varphi) \end{aligned}\right\} \quad \ldots\ldots\ldots\ 11.5$$

We also have

$$\left.\begin{aligned} y_s &= -K_y\alpha_{11} - N_y\alpha_{12} \\ z_s &= -K_z\alpha_{11} - N_z\alpha_{12} \end{aligned}\right\} \quad \ldots\ldots\ldots\ 11.6$$

and from the eqs 11.4, 11.5, and 11.6 we get

$$N = \frac{r - \Delta \cdot \frac{\alpha_{11}}{\alpha_{12}}}{\frac{\alpha_{11}\,\alpha_{22}}{\alpha_{12}} - \alpha_{12}} \qquad \ldots\ldots\ldots\ldots\ldots\ldots \quad 12.1$$

Further, the eqs 11.6, 11.1 and 11.5 give

$$\left.\begin{aligned} y_s &= -(M\ddot{y}+k\dot{y})\alpha_{11} - N(\cos\varphi - \mu_N \sin\varphi)\alpha_{12} \\ z_s &= -(M\ddot{z}+k\dot{z})\alpha_{11} - N(\sin\varphi + \mu_N \cos\varphi)\alpha_{12} - Mg\alpha_{11} \end{aligned}\right\} \quad \ldots\ldots \quad 12.2$$

and the last of the eqs 11.1, eq. 11.3, 11.5, and 11.6 give

$$\begin{aligned} M_{in} = I_p\ddot{\psi} &+ \frac{1}{\alpha_{11}}[y_s + N(\cos\varphi - \mu_N \sin\varphi)\alpha_{12}]\,z - \\ &- \frac{1}{\alpha_{11}}[z_s + N(\sin\varphi + \mu_N \cos\varphi)\alpha_{12}]\,y + \\ &+ \mu_N N\left(\Delta + \frac{d}{2}\right) + (\mu_A A + \mu_B B)\frac{d}{2} \qquad \ldots\ldots\ldots\ldots\ldots \quad 12.3 \end{aligned}$$

Geometry gives

$$\left.\begin{aligned} y &= y_s + e\cos\psi = r\cos\varphi + e\cos\psi \\ z &= z_s + e\sin\psi = r\sin\varphi + e\sin\psi \end{aligned}\right\}$$

From the eqs 12.2 is then obtained

$$\left.\begin{aligned} r &= y_s\cos\varphi + z_s\sin\varphi = -\alpha_{11}[(M\ddot{y}+k\dot{y})\cos\varphi + \\ &\qquad + (M\ddot{z}+k\dot{z})\sin\varphi] - N\alpha_{12} - Mg\alpha_{11}\sin\varphi \\ 0 &= y_s\sin\varphi - z_s\cos\varphi = -\alpha_{11}[(M\ddot{y}+k\dot{y})\sin\varphi - \\ &\qquad - (M\ddot{z}+k\dot{z})\cos\varphi] + \mu_N N\alpha_{12} + Mg\alpha_{11}\cos\varphi \end{aligned}\right\} \quad 12.4$$

In the previous part

$$\ddot{r} = \frac{d^2r}{dt^2},\quad \ddot{\varphi} = \frac{d^2\varphi}{dt^2},\quad \ddot{\psi} = \frac{d^2\psi}{dt^2} \quad \text{etc.}$$

In the following

$$\ddot{\rho} = \frac{d^2\rho}{d\tau^2},\quad \ddot{\varphi} = \frac{d^2\varphi}{d\tau^2},\quad \ddot{\psi} = \frac{d^2\psi}{d\tau^2} \quad \text{etc.}$$

where

$$\left.\begin{aligned} \rho &= \frac{r}{e} \\ \tau &= \Omega_n t \\ \Omega_n^2 &= \frac{1}{M\alpha_{11}} \end{aligned}\right\} \quad \text{(Observe that } \rho \text{ and } \tau \text{ are non-dimensional)}$$

We introduce the non-dimensional coefficient of damping

$$D^* = \frac{1}{2} \cdot k\alpha_{11}\Omega = \frac{1}{2} \cdot \frac{k}{M\Omega_n}$$

where the case $D^* = 1$ corresponds to the "usual" critical damping. If

$$\left.\begin{aligned} \varepsilon &= \frac{e}{k_i} \\ \gamma_G &= \frac{Mg\alpha_{11}}{e} \\ I_p &= Mk_i^2 \\ d^* &= \frac{d}{e}, \quad \Delta^* = \frac{\Delta}{e} \\ A^* &= \frac{A}{Me\Omega_n^2}, \quad B^* = \frac{B}{Me\Omega_n^2}, \quad N^* = \frac{N}{Me\Omega_n^2} \\ M_{in}^* &= \frac{M_{in}}{I_p\Omega_n^2} \end{aligned}\right\}$$

we, as an example, get

$$\left.\begin{aligned} \frac{\mu_N N\Delta}{I_p\Omega_n^2} &= \mu_N N^*\Delta^*\varepsilon^2 \\ \frac{\mu_A Ad}{I_p\Omega_n^2} &= \mu_A A^* d^*\varepsilon^2 \end{aligned}\right\}$$

and the eqs 12.4 and 12.3 can be written, if $\theta = (\psi - \varphi)$,

$$\left.\begin{aligned}
\ddot{\rho} &= -\rho+\rho\dot{\varphi}^2+\ddot{\psi}\sin\theta+\dot{\psi}^2\cos\theta- \\
&\quad -\frac{\alpha_{12}}{\alpha_{11}}\cdot N^*-2D^*(\dot{\rho}-\dot{\psi}\sin\theta)-\gamma_G\sin\varphi \\
\rho\ddot{\varphi} &= -2\dot{\rho}\dot{\varphi}-\ddot{\psi}\cos\theta+\dot{\psi}^2\sin\theta- \\
&\quad -\mu_N\frac{\alpha_{12}}{\alpha_{11}}N^*-2D^*(\rho\dot{\varphi}+\dot{\psi}\cos\theta)-\gamma_G\cos\varphi
\end{aligned}\right\} \quad .. 14.1$$

$$M_{in}^* = \ddot{\psi}+\varepsilon^2\left\{\rho\sin\theta+N^*\left[\frac{\alpha_{12}}{\alpha_{11}}\sin\theta+\right.\right.$$

$$\left.\left.+\mu_N\left\{\Delta^*+\frac{d^*}{2}-\frac{\alpha_{12}}{\alpha_{11}}(\rho+\cos\theta)\right\}\right]+\frac{d^*}{2}(\mu_A A^*+\mu_B B^*)\right\} \quad 14.2$$

From the eq. 12.1 we obtain

$$N^* = \frac{\alpha_{12}}{\alpha_{22}}\cdot\frac{\rho-\dfrac{\alpha_{11}}{\alpha_{12}}\cdot\Delta^*}{1-\dfrac{\alpha_{12}^2}{\alpha_{11}\alpha_{22}}} \quad \ldots\ldots\ldots\ldots\ldots\ldots\ldots\ldots \quad 14.3$$

Observe that $N^*\geq O$. If $\rho\leq\dfrac{a_{11}}{a_{12}}\cdot\Delta^*$, $N^*=O$.

The reaction forces A^* and B^* can easily be obtained from the equilibrium equations.

4. Running through the Critical Speed with Uniform Acceleration

4,1. The Treatment of the Problem in Literature

F. M. Lewis [10] gave in 1932 an exact solution of the problem of running a system having a single degree of freedom and linear damping through its critical speed from rest at a uniform acceleration. He found an expression for the envelope in which the maximum amplitudes are located. The result was plotted for various rates of acceleration and for various dampings. In this solution integrals of the type

$$\int_0^x e^{a_1\xi} \cos b_1\xi \cos c_1\xi^2 d\xi \quad (a_1,\ b_1, \text{ and } c_1 \text{ are constants})$$

occur. It was pointed out that this integral cannot be reduced to any functions which have been evaluated. He also remarked that when $a_1 = 0$ the integral may be reduced to Fresnel's integrals but he did not treat the case. Here he gives the reason. "The so-called process of contour integration gives a successful method of attack, and even in the case of zero damping furnishes a simpler solution than the one involving Fresnel's integrals".

However, *J. P. Ellington* and *H. Mc Callion* in 1956 [5] presented the solution for the acceleration from rest of an undamped linear mass-spring system when subjected to an exciting force with constant amplitude. They write: "However, this solution (Lewis' solution) is not easy to evaluate, the integrals involved demanding either graphical construction and numerical integration or summation of series. The purpose of the present note then is to show how a solution, in terms of previously known functions, may be obtained for the undamped vibrating system".

These known functions were Fresnel's integrals as was already pointed out by Lewis.

In our days the two methods of solutions are of the same class of serviceableness because of the occurrence of electronic computers.

Dimentberg published in 1961 the solution for the system having two degrees of freedom [3]. (At that time most of the calculations in this

report were already done at the electronic computer *Alwac III E* in Gothenburg). The solution for this is easily obtained from the solution of *Lewis* or *Ellington Mc Callion* as can be seen in Sec. 4,3. *Dimentberg* has plotted the maximum amplitude in a single case. (With the notations in this report he has $\varkappa = 0{,}90$ and $\lambda = 0{,}001$.)

Finally, *Dornig* [4] has also treated the undamped case having a single degree of freedom and *Capello* in [2] hints that the solution can also be applied to an unbalanced disc rotating on a shaft.

4,2. The Treatment of the Problem in this Report

In this report two methods to solve the problem are used. The first method is based on the treatment in [5] and is in its principal features similar to Dimentberg's solution. Because of the fact that this solution makes it possible to reach some general conclusions concerning the amplitude and that Dimentberg did not mention it, a presentation is justified.

However, this solution is not used for getting numerical results. The reason is that a lot of similar calculations of a cumbersome nature ought to be calculated on an electronic computer for getting a correct result in a rapid way. No computer with standard programmes for Fresnel's integrals were placed at the disposal of the institution. Further, it seemed to be very difficult to perform such a programme in a short time. Furthermore, the case of uniform acceleration is a special case of the general case when the acceleration is arbitrary. Because of the fact that this general case was also aimed at, and that a solution in known functions for this case can hardly be found, no special programmes were needed to be done to get results for a uniform acceleration.

Instead the equations of Chapter 3 were used in a step by step method. This method only demands programmes for the simple functions $\sin x$, $\cos x$ and $\sqrt{x}$.

Finally, it ought to be mentioned that the influences of the gravity force and the gyroscopic effects are not further studied.

4,3. Solution with Fresnel's integrals

If no deflection limiter or damping exist the eqs 11.1 and 11.2 give

$$\left.\begin{aligned} M\alpha_{11}\ddot{y}+y &= e\cos\psi \\ M\alpha_{11}\ddot{z}+z &= e\sin\psi \end{aligned}\right\}$$

If $\eta = \frac{y}{e}$, $\zeta = \frac{z}{e}$ and $\Omega_n^2 = \frac{1}{M\alpha_{11}}$ one gets with $\tau = \Omega_n t$

$$\left.\begin{aligned} \ddot{\eta}+\eta &= \cos\psi \\ \ddot{\zeta}+\zeta &= \sin\psi \end{aligned}\right\} \quad \left(\text{Observe } \ddot{\eta} = \frac{d^2\eta}{d\tau^2} \text{ and } \ddot{\zeta} = \frac{d^2\xi}{d\tau^2}\right) \ldots\ldots \quad 17.1$$

The initial conditions are based upon the fact that up to the initial moment for the acceleration the centre of gravity of the disc performs a circular movement with a constant angular velocity ω_0 and here also $\varphi = \psi = \omega_0 t = \varkappa\tau$. Thus, if $\varkappa \neq 1$,

$$\left.\begin{aligned} \eta &= A_{11}\sin\tau + B_{11}\cos\tau + \frac{1}{1-\varkappa^2}\cdot\cos\varkappa\tau \\ \zeta &= A_{21}\sin\tau + B_{21}\cos\tau + \frac{1}{1-\varkappa^2}\cdot\sin\varkappa\tau \end{aligned}\right\} \ldots\ldots\ldots \quad 17.2$$

The solution contains two complementary solutions. The deflection from these solutions is consequently assumed to be zero. Thus

$$\left.\begin{aligned} \eta &= \frac{1}{1-\varkappa^2}\cos\varkappa\tau \\ \zeta &= \frac{1}{1-\varkappa^2}\sin\varkappa\tau \end{aligned}\right\} \qquad \left.\begin{aligned} \dot{\eta} &= \frac{-\varkappa}{1-\varkappa^2}\sin\varkappa\tau \\ \dot{\zeta} &= \frac{\varkappa}{1-\varkappa^2}\cos\varkappa\tau \end{aligned}\right\}$$

At $\varkappa\tau = s\cdot 2\pi$, where s is an integer, we get

$$\left.\begin{aligned} \eta &= \frac{1}{1-\varkappa^2} \\ \zeta &= 0 \end{aligned}\right\} \qquad \left.\begin{aligned} \dot{\eta} &= 0 \\ \dot{\zeta} &= \frac{\varkappa}{1-\varkappa^2} \end{aligned}\right\} \ldots\ldots\ldots\ldots \quad 17.3$$

and at this very moment the acceleration begins. If

$$\left.\begin{aligned} \frac{d^2\psi}{dt^2} &= a \\ \frac{d\psi}{dt} &= at + \omega_0 \\ \psi &= \frac{at^2}{2} + \omega_0 t \end{aligned}\right\} \quad \text{we get} \quad \left.\begin{aligned} \frac{d^2\psi}{d\tau^2} &= \ddot{\psi} = 2\lambda \\ \frac{d\psi}{d\tau} &= \dot{\psi} = 2\lambda\tau + \varkappa \\ \psi &= \lambda\tau^2 + \varkappa\tau \end{aligned}\right\}$$

$$\text{where } \lambda = \frac{a}{2\Omega_n^2}.$$

Insertion into the eq. 17.1 gives

$$\left.\begin{aligned} \ddot{\eta}+\eta &= \cos(\lambda\tau^2+\varkappa\tau) \\ \ddot{\zeta}+\zeta &= \sin(\lambda\tau^2+\varkappa\tau) \end{aligned}\right\}$$

According to *Kamke* [8] the solution is

$$\left.\begin{aligned} \eta &= A_{12}\sin\tau+B_{12}\cos\tau+\int_0^\tau \cos(\lambda x^2+\varkappa x)\sin(\tau-x)dx \\ \zeta &= A_{22}\sin\tau+B_{22}\cos\tau+\int_0^\tau \sin(\lambda x^2+\varkappa x)\sin(\tau-x)dx \end{aligned}\right\}$$

The boundary conditions 17.3 give

$$A_{12}=0 \qquad B_{12}=\frac{1}{1-\varkappa^2}$$

$$A_{22}=\frac{\varkappa}{1-\varkappa^2} \qquad B_{22}=0$$

and consequently

$$\left.\begin{aligned} \eta &= \frac{1}{1-\varkappa^2}\cos\tau+\int_0^\tau \cos(\lambda x^2+\varkappa x)\sin(\tau-x)dx \\ \zeta &= \frac{\varkappa}{1-\varkappa^2}\sin\tau+\int_0^\tau \sin(\lambda x^2+\varkappa x)\sin(\tau-x)dx \end{aligned}\right\} \quad \ldots\ldots \quad 18.1$$

The integrals can be split up into Fresnel's integrals. If

$$I_1 = \int_0^\tau \cos(\lambda x^2+\varkappa x)\sin(\tau-x)\,dx =$$

$$= \sin\tau\int_0^\tau \cos(\lambda x^2+\varkappa x)\cos x\,dx - \cos\tau\int_0^\tau \cos(\lambda x^2+\varkappa x)\sin x dx$$

$$I_{11} = \int_0^\tau \cos(\lambda x^2+\varkappa x)\cos x\,dx$$

$$I_{12} = \int_0^\tau \cos(\lambda x^2 + \varkappa x) \sin x \, dx$$

and

$$I_2 = \int_0^\tau \sin(\lambda x^2 + \varkappa x) \sin(\tau - x) dx =$$

$$= \sin\tau \int_0^\tau \sin(\lambda x^2 + \varkappa x) \cos x \, dx - \cos\tau \int_0^\tau \sin(\lambda x^2 + \varkappa x) \sin x \, dx$$

$$I_{21} = \int_0^\tau \sin(\lambda x^2 + \varkappa x) \cos x \, dx$$

$$I_{22} = \int_0^\tau \sin(\lambda x^2 + \varkappa x) \sin x \, dx$$

we may write with $\alpha_1 = (\varkappa + 1)$ and $\alpha_2 = (\varkappa - 1)$ that

$$\left.\begin{aligned} 2I_{11} &= \int_0^\tau \cos(\lambda x^2 + \alpha_1 x) dx + \int_0^\tau \cos(\lambda x^2 + \alpha_2 x) dx \\ 2I_{12} &= \int_0^\tau \sin(\lambda x^2 + \alpha_1 x) dx - \int_0^\tau \sin(\lambda x^2 + \alpha_2 x) dx \\ 2I_{21} &= \int_0^\tau \sin(\lambda x^2 + \alpha_1 x) dx + \int_0^\tau \sin(\lambda x^2 + \alpha_2 x) dx \\ 2I_{22} &= -\int_0^\tau \cos(\lambda x^2 + \alpha_1 x) dx + \int_0^\tau \cos(\lambda x^2 + \alpha_2 x) dx \end{aligned}\right\}$$

Only two basic types of integrals occur, viz.

$$\left.\begin{aligned} I_I &= \int_0^\tau \cos(\lambda x^2 + \alpha x) dx \\ I_{II} &= \int_0^\tau \sin(\lambda x^2 + \alpha x) dx \end{aligned}\right\}$$

Substitute

$$\left.\begin{aligned} u &= q(\theta + \tfrac{1}{2}) \\ q &= \frac{\alpha}{\sqrt{\lambda}} \\ \theta &= \frac{\lambda x}{\alpha} \end{aligned}\right\}$$

Then

$$\lambda x^2+\alpha x = \lambda x^2 \cdot \frac{\lambda\alpha^2}{\lambda\alpha^2}+\alpha x \cdot \frac{\lambda\alpha}{\lambda\alpha} = \frac{\alpha^2}{\lambda}\cdot\left(\frac{\lambda x}{\alpha}\right)^2 + \frac{\alpha^2}{\lambda}\cdot\frac{\lambda x}{\alpha} =$$

$$= q^2(\theta^2+\theta) = q^2\left[\left(\theta+\frac{1}{2}\right)^2 - \frac{1}{4}\right] = q^2\left[\left(\frac{u}{q}\right)^2 - \frac{1}{4}\right] = u^2 - \frac{q^2}{4}$$

Further

$$dx = \frac{\alpha}{\lambda}\cdot d\theta = \frac{\alpha}{\lambda}\cdot d\left\{\frac{u}{q}-\frac{1}{2}\right\} = \frac{\alpha}{\lambda q}\cdot du = \frac{\alpha^2}{\lambda}\cdot\frac{1}{\alpha q}\cdot du =$$

$$= \frac{q}{\alpha}\cdot du = \frac{du}{\sqrt{\lambda}}$$

and consequently

$$\left.\begin{aligned} I_I &= \frac{1}{\sqrt{\lambda}}\int_{q/2}^{u(\alpha)} \cos\left(u^2-\frac{q^2}{4}\right)du \\ I_{II} &= \frac{1}{\sqrt{\lambda}}\int_{q/2}^{u(\alpha)} \sin\left(u^2-\frac{q^2}{4}\right)du \end{aligned}\right\}$$

where

$$u(\alpha) = q\left(\frac{\lambda\tau}{\alpha}+\frac{1}{2}\right) = \frac{q}{\alpha}\left(\lambda\tau+\frac{\alpha}{2}\right) = \frac{1}{\sqrt{\lambda}}\left(\lambda\tau+\frac{\alpha}{2}\right)$$

Now we may write

$$I_I = \frac{1}{\sqrt{\lambda}}\left\{\cos\frac{q^2}{4}\int_{q/2}^{u(\alpha)}\cos u^2du + \sin\frac{q^2}{4}\int_{q/2}^{u(\alpha)}\sin u^2du\right\} =$$

$$= \frac{1}{\sqrt{\lambda}}\left\{\left[C\left(u(\alpha)\right) - C\left(\frac{q}{2}\right)\right]\cos\frac{q^2}{4} + \left[S\left(u(\alpha)\right) - S\left(\frac{q}{2}\right)\right]\sin\frac{q^2}{4}\right\}$$

and in a similar manner

$$I_{II} = \frac{1}{\sqrt{\lambda}}\left\{\left[S\left(u(\alpha)\right) - S\left(\frac{q}{2}\right)\right]\cos\frac{q^2}{4} - \left[C\left(u(\alpha)\right) - C\left(\frac{q}{2}\right)\right]\sin\frac{q^2}{4}\right\}$$

where Fresnel's integrals are defined as

$$S(u) = \int_0^u \sin x^2 dx \approx \sqrt{\frac{\pi}{8}} - \frac{1}{2} \cdot \frac{\cos u^2}{u} - \frac{1}{4} \cdot \frac{\sin u^2}{u^3}$$

and

$$C(u) = \int_0^u \cos x^2 \, dx \approx \sqrt{\frac{\pi}{8}} + \frac{1}{2} \cdot \frac{\sin u^2}{u} - \frac{1}{4} \cdot \frac{\cos u^2}{u^3}$$

The series are valid for large arguments.

These functions have been computed, see for instance [12], and the primary problem is solved.

Now we turn to a special case. Assuming that the shaft is *started from rest*, we have $\varkappa = 0$, $\alpha_1 = 1$, and $\alpha_2 = -1$. This will give

$$2I_{11} = I_I(\alpha = 1) + I_I(\alpha = -1) = \frac{1}{\sqrt{\lambda}} \left\{ [C(u_1) + C(u_2)] \cos \frac{1}{4\lambda} + \right.$$
$$\left. + [S(u_1) + S(u_2)] \sin \frac{1}{4\lambda} \right\}$$

$$2I_{12} = I_{II}(\alpha = 1) - I_{II}(\alpha = -1) = \frac{1}{\sqrt{\lambda}} \left\{ [S(u_1) - S(u_2)] \cos \frac{1}{4\lambda} - \right.$$
$$\left. - [C(u_1) - C(u_2)] \sin \frac{1}{4\lambda} - 2S\left(\frac{0,5}{\sqrt{\lambda}}\right) \cos \frac{1}{4\lambda} + 2C\left(\frac{0,5}{\sqrt{\lambda}}\right) \sin \frac{1}{4\lambda} \right\}$$

$$2I_{21} = I_{II}(\alpha = 1) + I_{II}(\alpha = -1) = \frac{1}{\sqrt{\lambda}} \left\{ [S(u_1) + S(u_2)] \cos \frac{1}{4\lambda} - \right.$$
$$\left. - [C(u_1) + C(u_2)] \sin \frac{1}{4\lambda} \right\}$$

$$2I_{22} = -I_I(\alpha = 1) + I_I(\alpha = -1) = \frac{1}{\sqrt{\lambda}} \left\{ [-C(u_1) + C(u_2)] \cos \frac{1}{4\lambda} + \right.$$
$$\left. + [-S(u_1) + S(u_2)] \sin \frac{1}{4\lambda} + 2C\left(\frac{0,5}{\sqrt{\lambda}}\right) \cos \frac{1}{4\lambda} + 2S\left(\frac{0,5}{\sqrt{\lambda}}\right) \sin \frac{1}{4\lambda} \right\}$$

where $u_1 = \frac{1}{\sqrt{\lambda}} \left(\lambda\tau + \frac{1}{2}\right)$ and $u_2 = \frac{1}{\sqrt{\lambda}} \left(\lambda\tau - \frac{1}{2}\right)$. When $\tau \to \infty$

$$S(u_1) = S(u_2) = C(u_1) = C(u_2) = \sqrt{\frac{\pi}{8}} \text{ and } \textit{if } \lambda \textit{ is a small number}$$

$$S\left(\frac{0,5}{\sqrt{\lambda}}\right) \cong C\left(\frac{0,5}{\sqrt{\lambda}}\right) \approx \sqrt{\frac{\pi}{8}}.$$

Thus

$$\left.\begin{aligned} I_{11} &= \frac{1}{\sqrt{\lambda}} \cdot \sqrt{\frac{\pi}{8}} \left(\cos\frac{1}{4\lambda} + \sin\frac{1}{4\lambda}\right) \\ I_{12} &= \frac{1}{\sqrt{\lambda}} \cdot \sqrt{\frac{\pi}{8}} \left(-\cos\frac{1}{4\lambda} + \sin\frac{1}{4\lambda}\right) \\ I_{21} &= \frac{1}{\sqrt{\lambda}} \cdot \sqrt{\frac{\pi}{8}} \left(\cos\frac{1}{4\lambda} - \sin\frac{1}{4\lambda}\right) \\ I_{22} &= \frac{1}{\sqrt{\lambda}} \cdot \sqrt{\frac{\pi}{8}} \left(\cos\frac{1}{4\lambda} + \sin\frac{1}{4\lambda}\right) \end{aligned}\right\} \quad \ldots\ldots\ldots \quad 22.1$$

From eq. 18.1 we have

$$\left.\begin{aligned} \eta &= \cos\tau + I_{11}\sin\tau - I_{12}\cos\tau \\ \zeta &= \qquad I_{21}\sin\tau - I_{22}\cos\tau \end{aligned}\right\} \quad \ldots\ldots\ldots \quad 22.2$$

and from here, if $I_{ij} \gg 1$ $(i, j = 1, 2)$,

$$\left(\frac{R_\infty}{e}\right)^2 = \eta^2 + \zeta^2 = (I_{11}^2 + I_{21}^2)\sin^2\tau + (I_{12}^2 + I_{22}^2)\cos^2\tau - \\ - (I_{11}\,I_{12} + I_{21}\,I_{22})\sin 2\tau$$

Insertion of the eqs 22.1 gives

$$\frac{R_\infty}{e} = \frac{1}{2}\sqrt{\frac{\pi}{\lambda}} \quad \ldots\ldots\ldots\ldots\ldots\ldots \quad 22.3$$

The eqs 22.1, 22.2, and 22.3 say that a disc started from rest and accelerated with a constant, rather slow angular acceleration at infinitely high speed whirls with its natural frequency with a constant

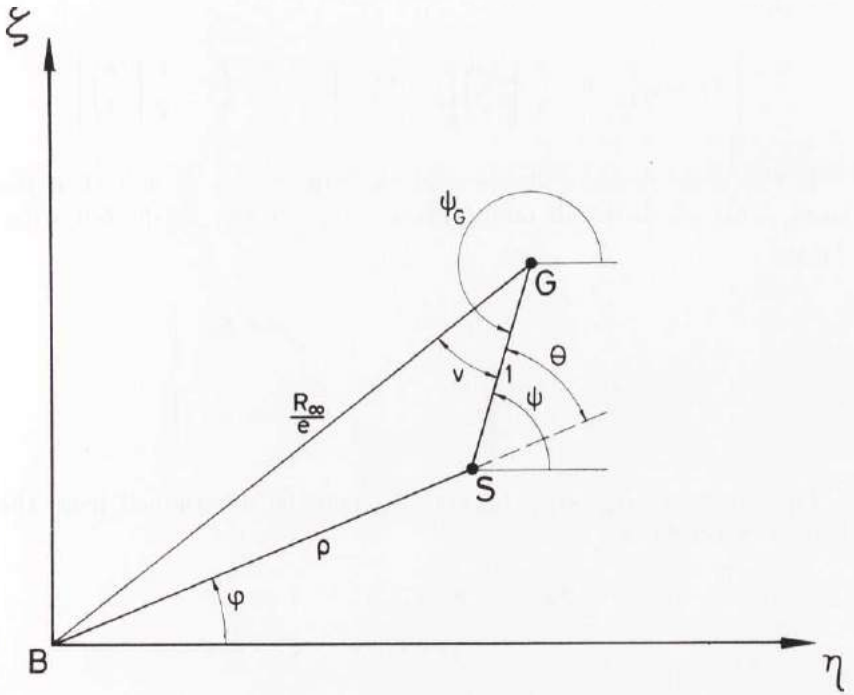

Fig. 23.1

deflection of the centre of gravity. This does not seem to have been mentioned earlier.

It can be shown that if $\lambda<0$ and $\varkappa \gg 1$ the eq. 22.3 still holds as a limiting value of $\frac{R}{e}$ if λ is changed to $|\lambda|$.

From fig. 23.1

$$\psi_G = \pi+\psi$$

and hence

$$\dot{\psi}_G = \dot{\psi}$$

Thus while G moves around B on a circle of radius R_∞ with the natural angular velocity Ω_n the point S whirls around G on a circle of radius e and with the forced angular velocity at. Further

$$\left(\frac{1}{2}\sqrt{\frac{\pi}{\lambda}}-1\right) \leq \rho \leq \left(\frac{1}{2}\sqrt{\frac{\pi}{\lambda}}+1\right)$$

and thus

$$\left[2\lambda+\varepsilon^2\left(-1+\frac{1}{2}\sqrt{\frac{\pi}{\lambda}}\right)\right]\leq M_{in}^{*}\leq\left[2\lambda+\varepsilon^2\left(1+\frac{1}{2}\sqrt{\frac{\pi}{\lambda}}\right)\right]$$

If the acceleration is broken at the "time" $\tau=\tau_s$ and then the shaft is driven so that it maintains $\dot{\psi}=\varkappa_s=$ const. in the following, we get

$$\left.\begin{aligned}\eta &= A_{13}\sin\tau+B_{13}\cos\tau+\frac{1}{1-\varkappa_s^2}\cos\varkappa_s\tau\\ \zeta &= A_{23}\sin\tau+B_{23}\cos\tau+\frac{1}{1-\varkappa_s}\sin\varkappa_s\tau\end{aligned}\right\}$$

The constants A_{13}, B_{13}, A_{23} and B_{23} may be determined from the boundary conditions

$$\begin{aligned}\tau=\tau_s \qquad \lambda=\eta_s \qquad \dot{\eta}=\dot{\eta}_s\\ \zeta=\zeta_s \qquad \dot{\zeta}=\dot{\zeta}_s\end{aligned}$$

However, the deflections due to the complementary solutions in practice may vanish because of external damping and then only the deflection due to the particular solutions remains. Thus

$$\frac{R_s}{e}=\frac{1}{|1-\varkappa_s^2|}$$

If $\varkappa_s\to\infty$, $R_s\to 0$.
The case $\varkappa=\varkappa_s=1$ has the particular solutions

$$\left.\begin{aligned}\eta &= \frac{\tau}{2}\sin\tau\\ \zeta &= -\frac{\tau}{2}\cos\tau\end{aligned}\right\}$$

The following always apply

$$\left.\begin{aligned}\eta &= \rho\cos\varphi+\cos\psi\\ \zeta &= \rho\sin\varphi+\sin\psi\end{aligned}\right\}$$

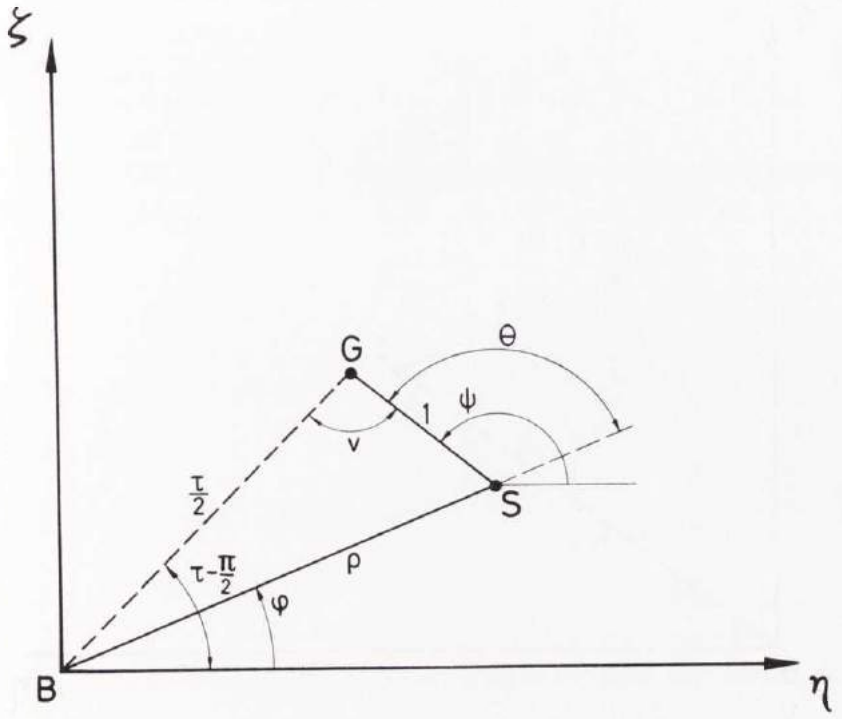

Fig. 25.1

and from here

$$\rho \sin \theta = \eta \sin \psi - \zeta \cos \psi = \left(\frac{\tau}{2} \sin^2 \tau + \frac{\tau}{2} \cos^2 \tau \right) = \frac{\tau}{2} \quad \ldots \; 25.2$$

Further fig. 25.1 gives

$$\sin v = \frac{\rho \sin (\pi - \theta)}{\frac{\tau}{2}} = \frac{\rho \sin \theta}{\frac{\tau}{2}}$$

From eq. 25.2 we get

$$v = \frac{\pi}{2}$$

and

$$\rho = \sqrt{1 + \left(\frac{\tau}{2} \right)^2}$$

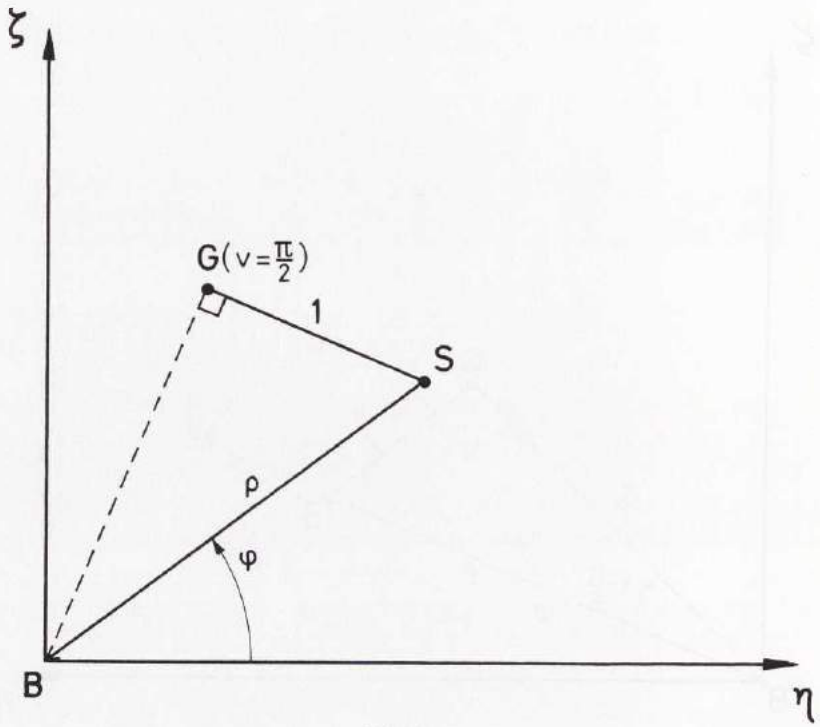

Fig. 26.1

The position of the centre of gravity in this case is shown in fig. 26.1. The "torque" demanded is from eq. 14.2

$$M_{in}^{*} = \varepsilon^2 \rho \sin\theta = \varepsilon^2 \cdot \frac{\tau}{2} \quad \ldots\ldots\ldots\ldots \quad 26.2$$

This "torque" is just enough to keep the shaft moving with the natural angular velocity. The expression 26.2 is derived by *Biezeno-Grammel* [1]. It is also indicated that if, at an increasing deflection,

$$\frac{dM_{in}^{*}}{d\tau} > \frac{\varepsilon^2}{2}$$

the shaft leaves its critical position. The case, however, is hardly taken from practice. See more about this in [7] and Chapter 6 in this report.

In a previous example a very slow acceleration was considered. On the contrary an infinitely rapid acceleration started from rest gives the deflections

$$\left.\begin{aligned} \eta &= \cos\tau \\ \zeta &= 0 \end{aligned}\right\}$$

and hence

$$\frac{R_\infty}{e} = \cos\tau$$

It means that the shaft deflection varies between zero and $2e$.

4,4. Solution with a Step by Step Method

The eqs 14.1 can be written ($\gamma_G = 0$)

$$\left.\begin{aligned} \ddot{\rho} &= -\rho(1-\dot{\varphi}^2)+\ddot{\psi}\sin\theta+\dot{\psi}^2\cos\theta-\frac{\alpha_{12}}{\alpha_{11}}\cdot N^*-2D^*(\dot{\rho}-\dot{\psi}\sin\theta) \\ \ddot{\varphi} &= -\frac{2\dot{\rho}\dot{\varphi}}{\rho}-\frac{\ddot{\psi}}{\rho}\cos\theta+\frac{\dot{\psi}^2}{\rho}\sin\theta-\frac{1}{\rho}\cdot\mu_N\cdot\frac{\alpha_{12}}{\alpha_{11}}N^*- \\ &\qquad -\frac{2D^*}{\rho}(\rho\dot{\varphi}+\ddot{\psi}\cos\theta) \end{aligned}\right\} \quad 27.1$$

The boundary conditions are

$$\left.\begin{aligned} &\tau = 0 \quad \rho = \rho_0 = \frac{\varkappa^2}{|1-\varkappa^2|} \quad \varphi = 0 \quad \psi = \theta_0 \quad \theta = \theta_0 \\ &\qquad \dot{\rho} = 0 \qquad\qquad \dot{\varphi} = \varkappa \quad \dot{\psi} = \varkappa \quad \dot{\theta} = 0 \\ &\qquad\qquad\qquad\quad \varphi = 0 \quad \ddot{\psi} = 2\lambda \quad \ddot{\theta} = 2\lambda \end{aligned}\right\} \quad 27.2$$

The uniform acceleration means that

$$\psi = \lambda\tau^2+\varkappa\tau+\psi_0 \qquad (\psi_0 = \text{const.})$$

Now introduce the notations

$$\dot{\rho} = u,\ \dot{\varphi} = v$$

and the eqs 27.1 can be written

$$\left.\begin{aligned} \dot{u} &= f_1(\rho, u, \theta, v, \tau) \\ \dot{v} &= f_2(\rho, u, \theta, v, \tau) \end{aligned}\right\}$$

Further, we approximately have

$$\left.\begin{aligned} \dot{u} &= \frac{\Delta u}{\Delta \tau} = \frac{k_{iu}}{\Delta \tau} \\ \dot{v} &= \frac{\Delta v}{\Delta \tau} = \frac{k_{iv}}{\Delta \tau} \end{aligned}\right\}$$

At $\tau = \tau_0$, then $u = u_0$, $v = v_0$, $\rho = \rho_0$, and $\theta = \theta_0$. Thus

$$\left.\begin{aligned} k_{0u} &= \Delta\tau\, f_1\,(\rho_0,\, u_0\, \theta_0,\, v_0,\, \tau_0) \\ k_{0v} &= \Delta\tau\, f_2\,(\rho_0,\, u_0,\, \theta_0,\, v_0,\, \tau_0) \end{aligned}\right\}$$

At

$$\tau = \tau_1 = (\tau_0 + \tfrac{1}{2} \cdot \Delta\tau)$$

then

$$\left.\begin{aligned} u_1 &= u_0 + \tfrac{1}{2} \cdot k_{0u} \\ v_1 &= v_0 + \tfrac{1}{2} \cdot k_{0v} \\ \rho_1 &= \rho_0 + \frac{1}{2} \cdot \Delta\tau \cdot \frac{u_0 + u_1}{2} = \rho_0 + \frac{\Delta\tau}{4}(u_0 + u_1) \\ \varphi_1 &= \varphi_0 + \frac{1}{2} \cdot \Delta\tau \cdot \frac{v_0 + v_1}{2} = \varphi_0 + \frac{\Delta\tau}{4}(v_0 + v_1) \\ k_{1u} &= \Delta\tau\, f_1(\rho_1,\, u_1,\, \theta_1,\, v_1,\, \tau_1) \\ k_{1v} &= \Delta\tau\, f_2(\rho_1,\, u_1,\, \theta_1,\, v_1,\, \tau_1) \end{aligned}\right\}$$

At

$$\tau = \tau_2 = (\tau_0 + \tfrac{1}{2} \cdot \Delta\tau)$$

then

$$\left.\begin{aligned} u_2 &= u_0 + \tfrac{1}{2} \cdot k_{1u} \\ v_2 &= v_0 + \tfrac{1}{2} \cdot k_{1v} \\ \rho_2 &= \rho_0 + \frac{\Delta\tau}{4}(u_1 + u_2) \\ \varphi_2 &= \varphi_0 + \frac{\Delta\tau}{4}(v_1 + v_2) \\ k_{2u} &= \Delta\tau f_1(\rho_2,\, u_2,\, \theta_2,\, v_2,\, \tau_2) \\ k_{2v} &= \Delta\tau f_2(\rho_2,\, u_2,\, \theta_2,\, v_2,\, \tau_2) \end{aligned}\right\}$$

At

$$\tau = \tau_3 = (\tau_0 + \Delta\tau)$$

then

$$\left.\begin{aligned} u_3 &= u_0 + k_{2u} \\ v_3 &= v_0 + k_{2v} \\ \rho_3 &= \rho_0 + \frac{\Delta\tau}{4}(u_2 + u_3) \\ \varphi_3 &= \varphi_0 + \frac{\Delta\tau}{4}(v_2 + v_3) \\ k_{3u} &= \Delta\tau f_1(\rho_3, u_3, \theta_3, v_3, \tau_3) \\ k_{3v} &= \Delta\tau f_2(\rho_3, u_3, \theta_3, v_3, \tau_3) \end{aligned}\right\}$$

At

$$\tau = \tau_4 = (\tau_0 + \Delta\tau)$$

then

$$\left.\begin{aligned} u_4 &= u_0 + \tfrac{1}{6}(k_{0u} + 2k_{1u} + 2k_{2u} + k_{3u}) \\ v_4 &= v_0 + \tfrac{1}{6}(k_{0v} + 2k_{1v} + 2k_{2v} + k_{3v}) \\ \rho_4 &= \rho_0 + \frac{\Delta\tau}{12}(u_0 + 3u_1 + 4u_2 + 3u_3 + u_4) \\ \varphi_4 &= \varphi_0 + \frac{\Delta\tau}{12}(v_0 + 3v_1 + 4v_2 + 3v_3 + v_4) \\ k_{4u} &= \Delta\tau f_1(\rho_4, u_4, \theta_4, v_4, \tau_4) \\ k_{4v} &= \Delta\tau f_2(\rho_4, u_4, \theta_4, v_4, \tau_4) \end{aligned}\right\}$$

The values u_4, v_4, ρ_4, φ_4, k_{4u}, and k_{4v} are the final values at the "time" $\tau = (\tau_0 + \Delta\tau)$. Then these values represent the values with indices zero for the new step where $(\tau_0 + \Delta\tau) \leq \tau \leq (\tau_0 + 2\Delta\tau)$. If we start with $\tau_0 = 0$, $u_0 = 0$ $v_0 = \varkappa$, $\rho = \rho_0$, and $\theta = \theta_0$ according to the boundary conditions we can calculate all wanted quantities over a certain time by this step by step method which is a modified *Runge* method [9].

The values of ρ_0 and θ_0 for different values of $\varkappa$ and D^* can be found in the tabs 26.1 and 27.1 in [7].

About the truncation error see Sec. 4, 6.

4,5. Shaft with Damping

For the shaft without friction and damping two solutions are proposed, the exact solution and the numerical step by step solution. From the exact solution some general conclusions were made, namely

$$\left.\begin{aligned} &\frac{R_\infty}{e} = \frac{1}{2}\sqrt{\frac{\pi}{\lambda}} \\ &M_{in}^* = 2\lambda + \varepsilon^2 \rho \sin\theta \\ &\left(\frac{1}{2}\sqrt{\frac{\pi}{\lambda}} - 1\right) \leq \rho \leq \left(\frac{1}{2}\sqrt{\frac{\pi}{\lambda}} + 1\right) \end{aligned}\right\}$$

at infinitely high speed when the shaft is slowly accelerated from rest.

The exact solution was not used to get other results. With the aid of the step by step method some cases with different values of the parameters λ, $\varkappa$ and D^* were calculated. The figs on page 31 up to page 42 show ρ as a function of ψ. In some figures the straight line $\frac{R_\infty}{e} = \frac{1}{2}\sqrt{\frac{\pi}{\lambda}}$ is also marked for comparison. It is seen that this line very well fit to a mean line for cases with $\varkappa$ small enough.

The time τ^* at which $\dot{\psi} = 1$ is $\tau^* = \dfrac{1-\varkappa}{2\lambda}$.

Cases with a uniform deceleration are also treated. After a time $\tau_{br} = -\dfrac{\varkappa}{2\lambda}$, $\dot{\psi} = 0$ and the diagrams are finished there.

It is remarkable that a very rapid braking hardly changes the deflection of the shaft.

The reader may orientate himself quickly in the diagrams by remembering that

1) Each diagram has the same λ-value.

2) There are three D^*-values which correspond to every $\varkappa$.

3) Accelerations have $\lambda > 0$ and decelerations $\lambda < 0$. In the diagrams the time-direction is indicated by an arrow.

4) The ρ-curve for $\lambda = 0$ is also drawn for comparison.

In the figs. 43.1 and 44.1 the variation of $\dot{\varphi}$ is shown for different values of the damping D^* at the values $\lambda = 0{,}001$, $\varkappa = 0{,}90$ and $\lambda = -0{,}001$, $\varkappa = 1{,}25$ respectively. They show that the whirling speed $\dot{\varphi}$ "fastens" at the critical speed at small values of the external damping.

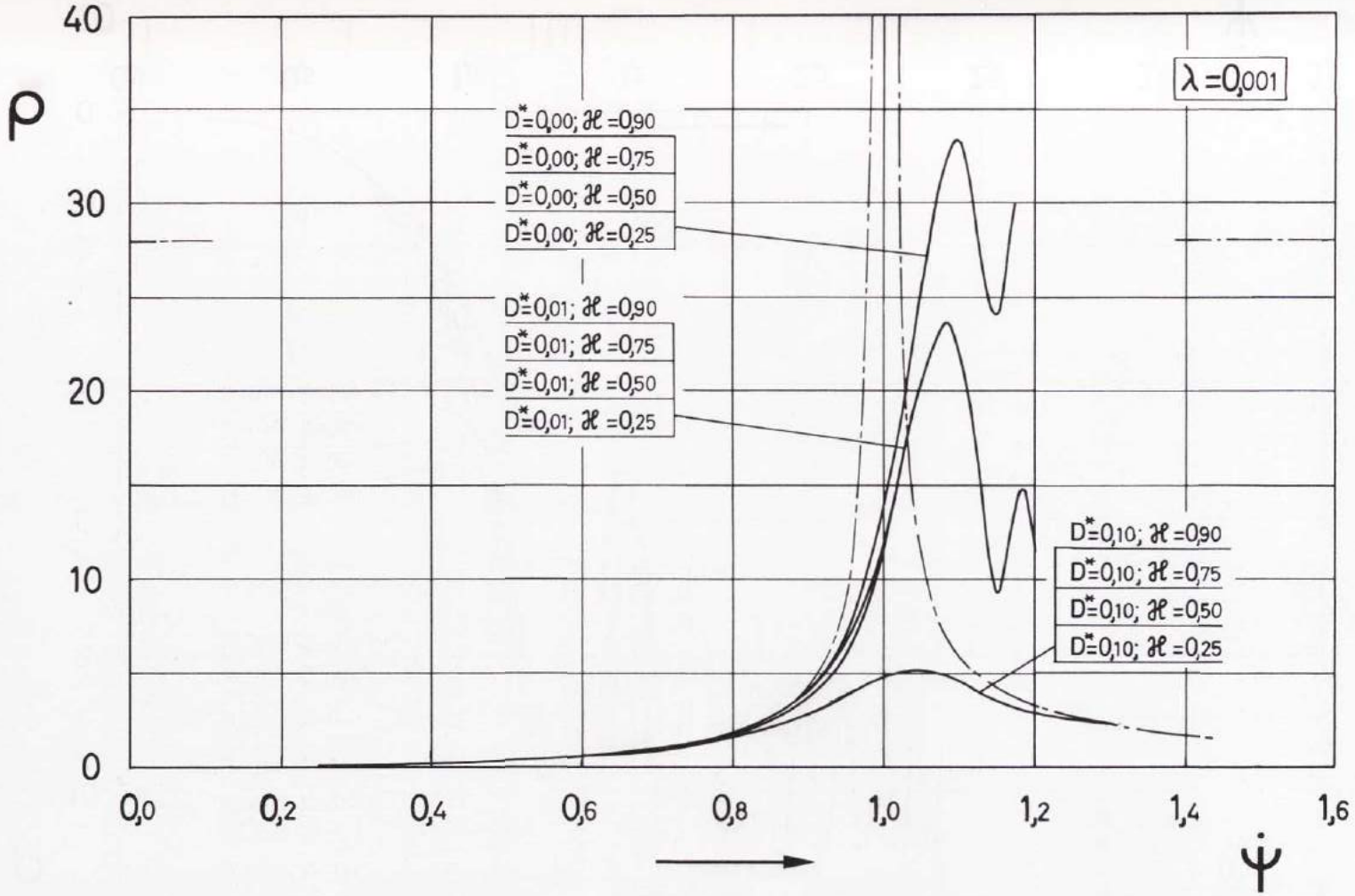
ρ
40
30
20
10
0
0,0
0,2
0,4
0,6
0,8
1,0
1,2
1,4
1,6
ψ
λ =0,001
D*=0,00; ℋ =0,90
D*=0,00; ℋ =0,75
D*=0,00; ℋ =0,50
D*=0,00; ℋ=0,25
D*=0,01; ℋ =0,90
D*=0,01; ℋ =0,75
D*=0,01; ℋ =0,50
D*=0,01; ℋ =0,25
D*=0,10; ℋ =0,90
D*=0,10; ℋ =0,75
D*=0,10; ℋ =0,50
D*=0,10; ℋ =0,25

Fig. 31.1

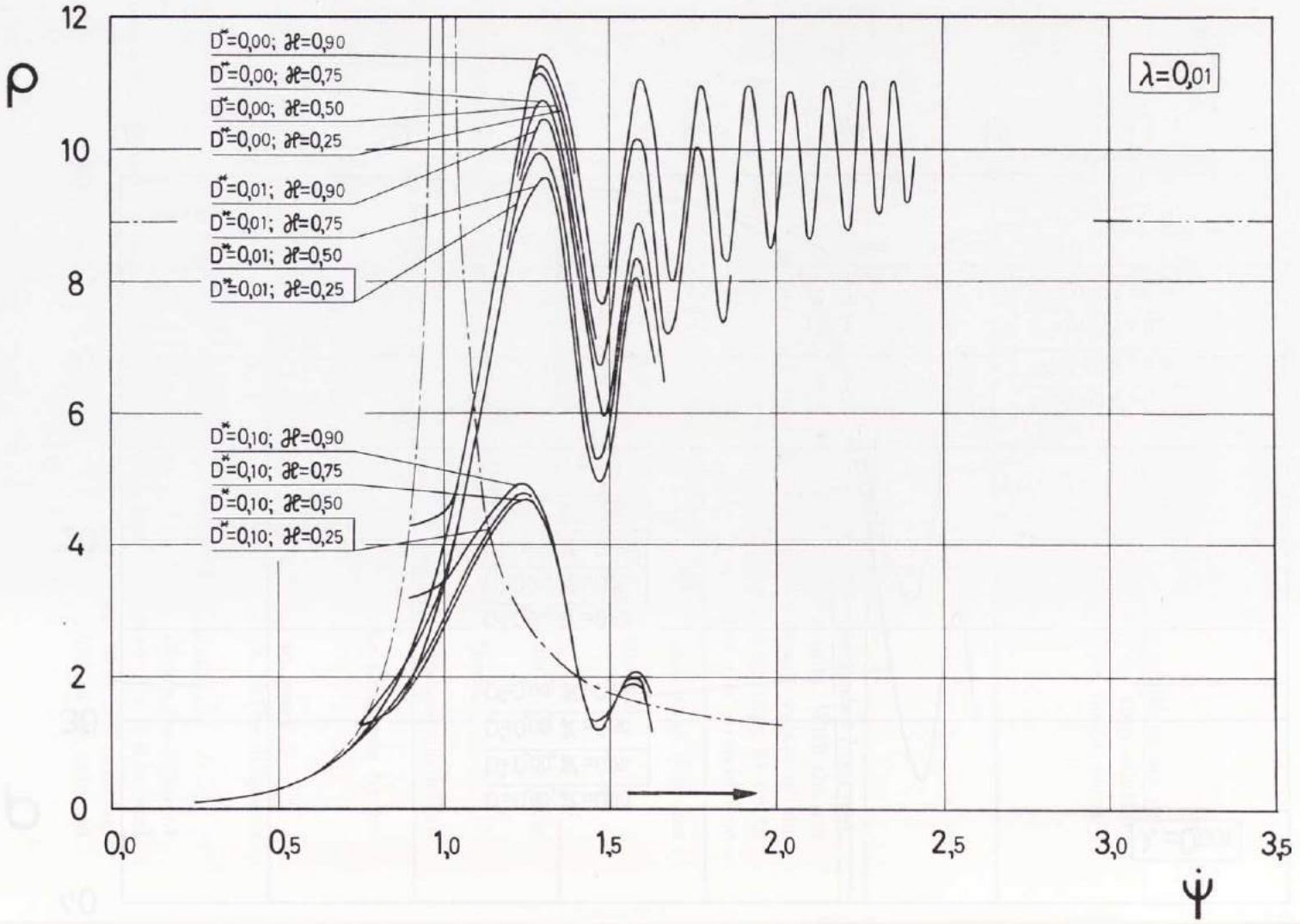
ρ
12
10
8
6
4
2
0
0,0
0,5
1,0
1,5
2,0
2,5
3,0
3,5
ψ
λ=0,01
D*=0,00; ∂ℓ=0,90
D*=0,00; ∂ℓ=0,75
D*=0,00; ∂ℓ=0,50
D*=0,00; ∂ℓ=0,25
D*=0,01; ∂ℓ=0,90
D*=0,01; ∂ℓ=0,75
D*=0,01; ∂ℓ=0,50
D*=0,01; ∂ℓ=0,25
D*=0,10; ∂ℓ=0,90
D*=0,10; ∂ℓ=0,75
D*=0,10; ∂ℓ=0,50
D*=0,10; ∂ℓ=0,25

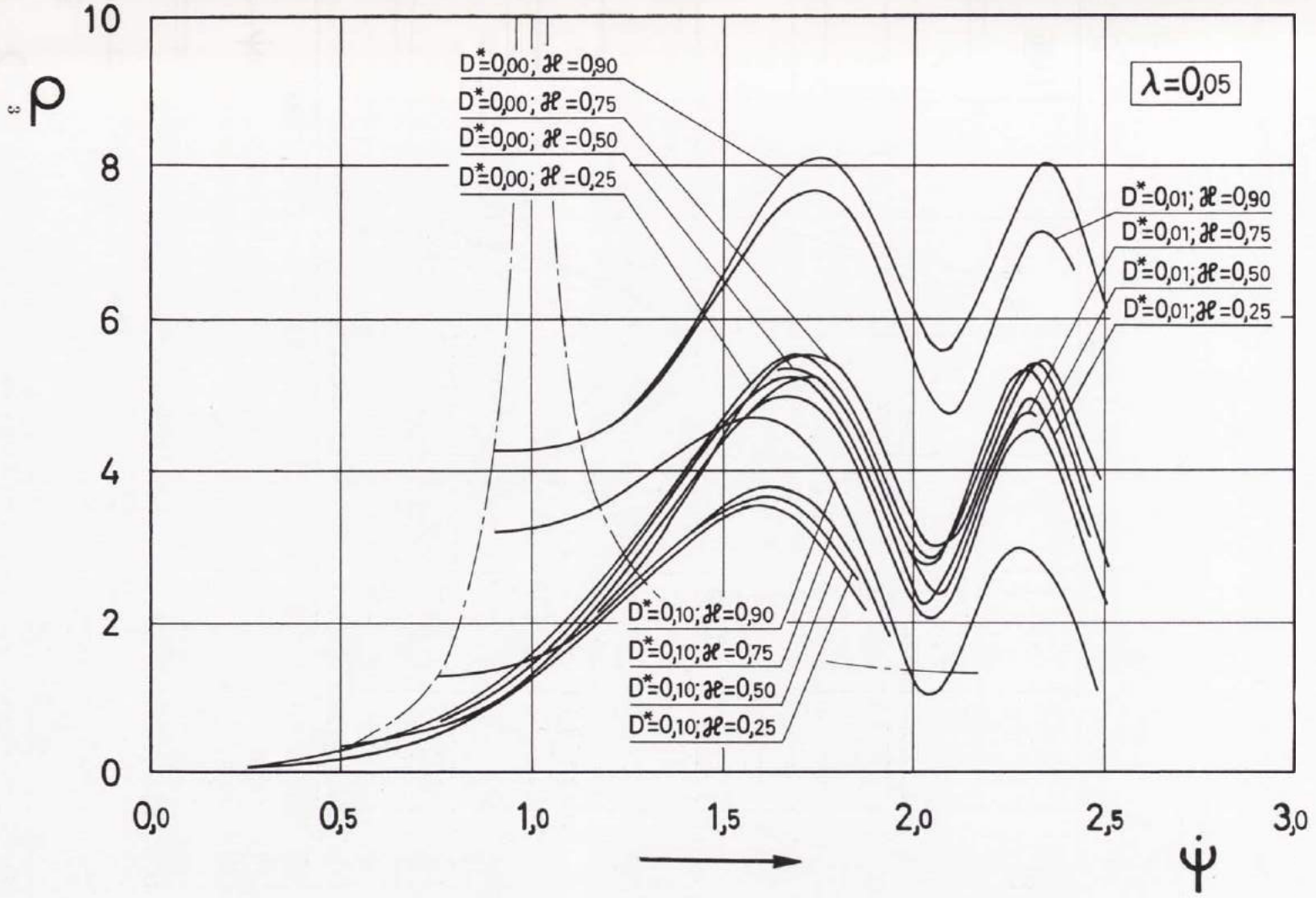
10
8
6
4
2
0
ρ_s
0,0
0,5
1,0
1,5
2,0
2,5
3,0
Ψ
λ=0,05
D*=0,00; ℛ =0,90
D*=0,00; ℛ =0,75
D*=0,00; ℛ =0,50
D*=0,00; ℛ =0,25
D*=0,01; ℛ =0,90
D*=0,01; ℛ =0,75
D*=0,01; ℛ =0,50
D*=0,01; ℛ =0,25
D*=0,10; ℛ =0,90
D*=0,10; ℛ =0,75
D*=0,10; ℛ =0,50
D*=0,10; ℛ =0,25

Fig. 33.1

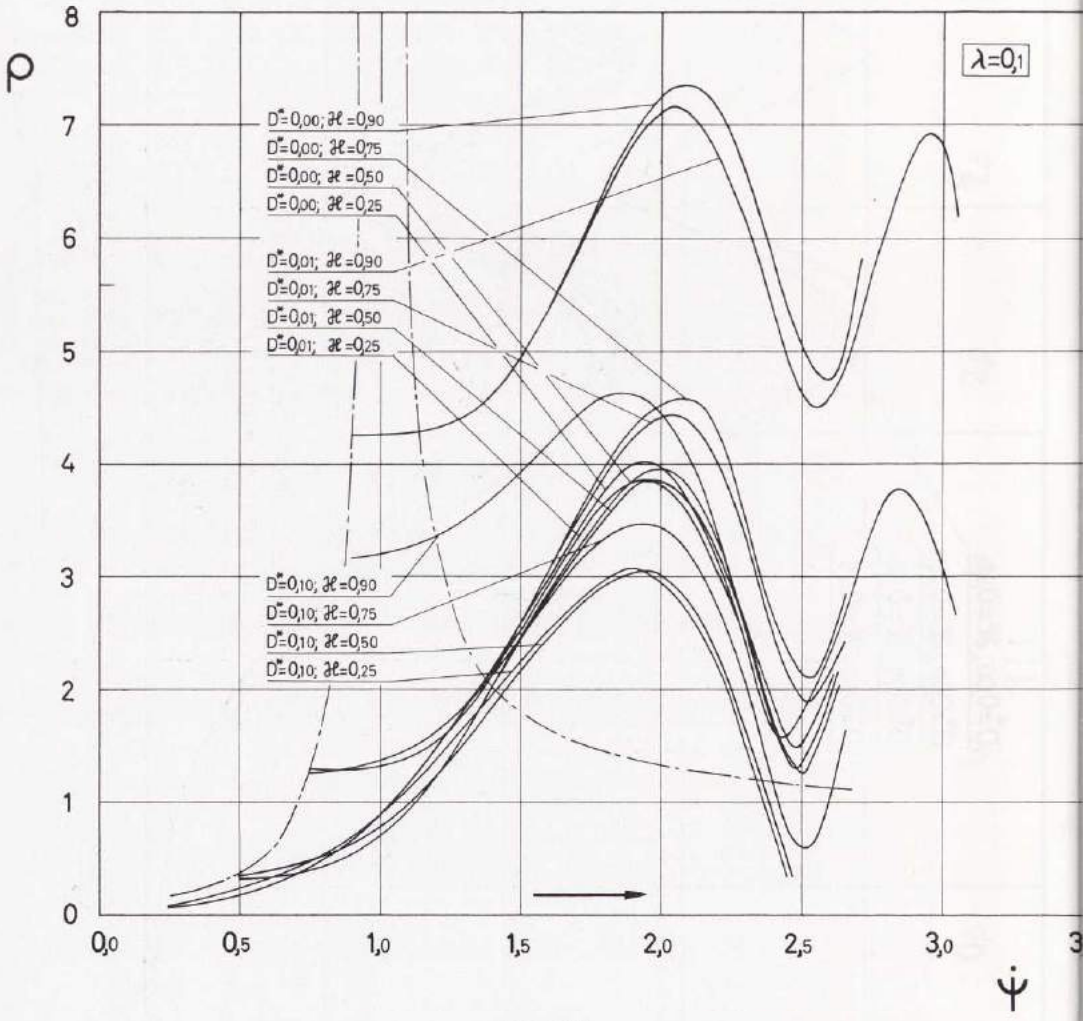
ρ
8
7
6
5
4
3
2
1
0
0,0
0,5
1,0
1,5
2,0
2,5
3,0
ψ
λ=0,1
D*=0,00; ∂ℓ=0,90
D*=0,00; ∂ℓ=0,75
D*=0,00; ∂ℓ=0,50
D*=0,00; ∂ℓ=0,25
D*=0,01; ∂ℓ=0,90
D*=0,01; ∂ℓ=0,75
D*=0,01; ∂ℓ=0,50
D*=0,01; ∂ℓ=0,25
D*=0,10; ∂ℓ=0,90
D*=0,10; ∂ℓ=0,75
D*=0,10; ∂ℓ=0,50
D*=0,10; ∂ℓ=0,25

Fig. 34.1

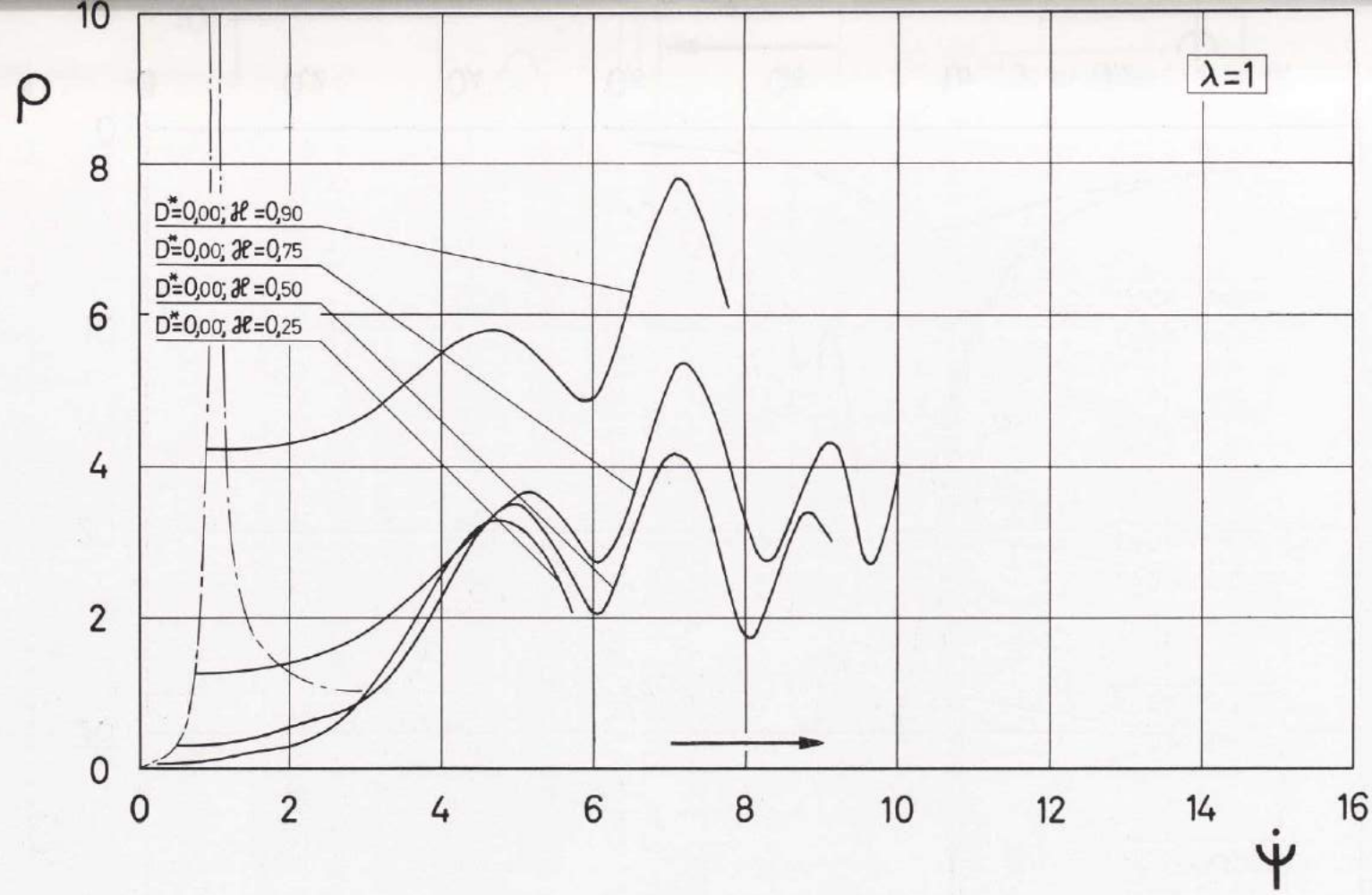
ρ
10
8
6
4
2
0
0
2
4
6
8
10
12
14
16
ψ
λ=1
D*=0,00; ℋ =0,90
D*=0,00; ℋ=0,75
D*=0,00; ℋ=0,50
D*=0,00; ℋ=0,25

Fig 35.1

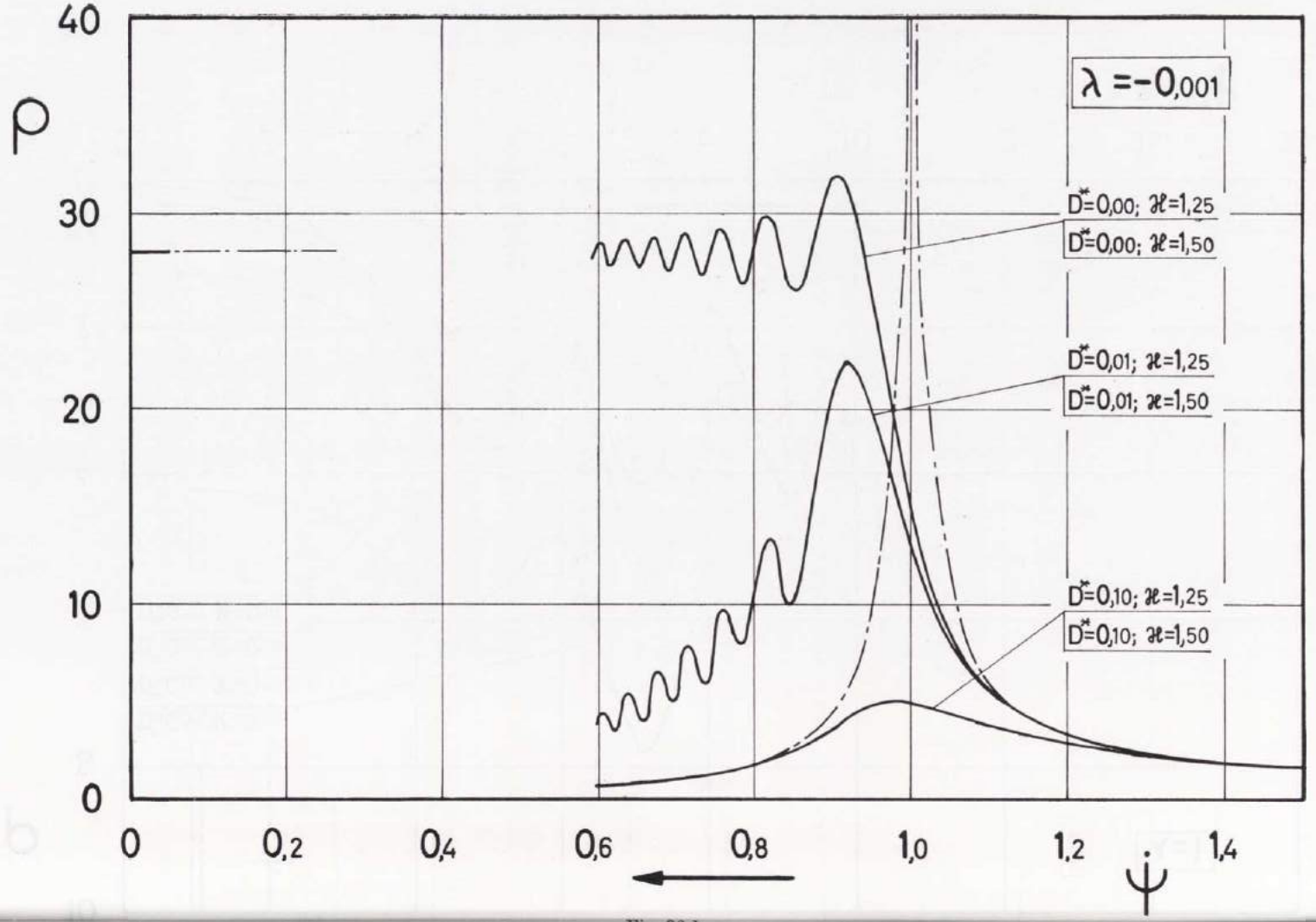
ρ
40
30
20
10
0
0
0,2
0,4
0,6
0,8
1,0
1,2
1,4
ψ
λ =-0,001
D*=0,00; ℋ=1,25
D*=0,00; ℋ=1,50
D*=0,01; ℋ=1,25
D*=0,01; ℋ=1,50
D*=0,10; ℋ=1,25
D*=0,10; ℋ=1,50

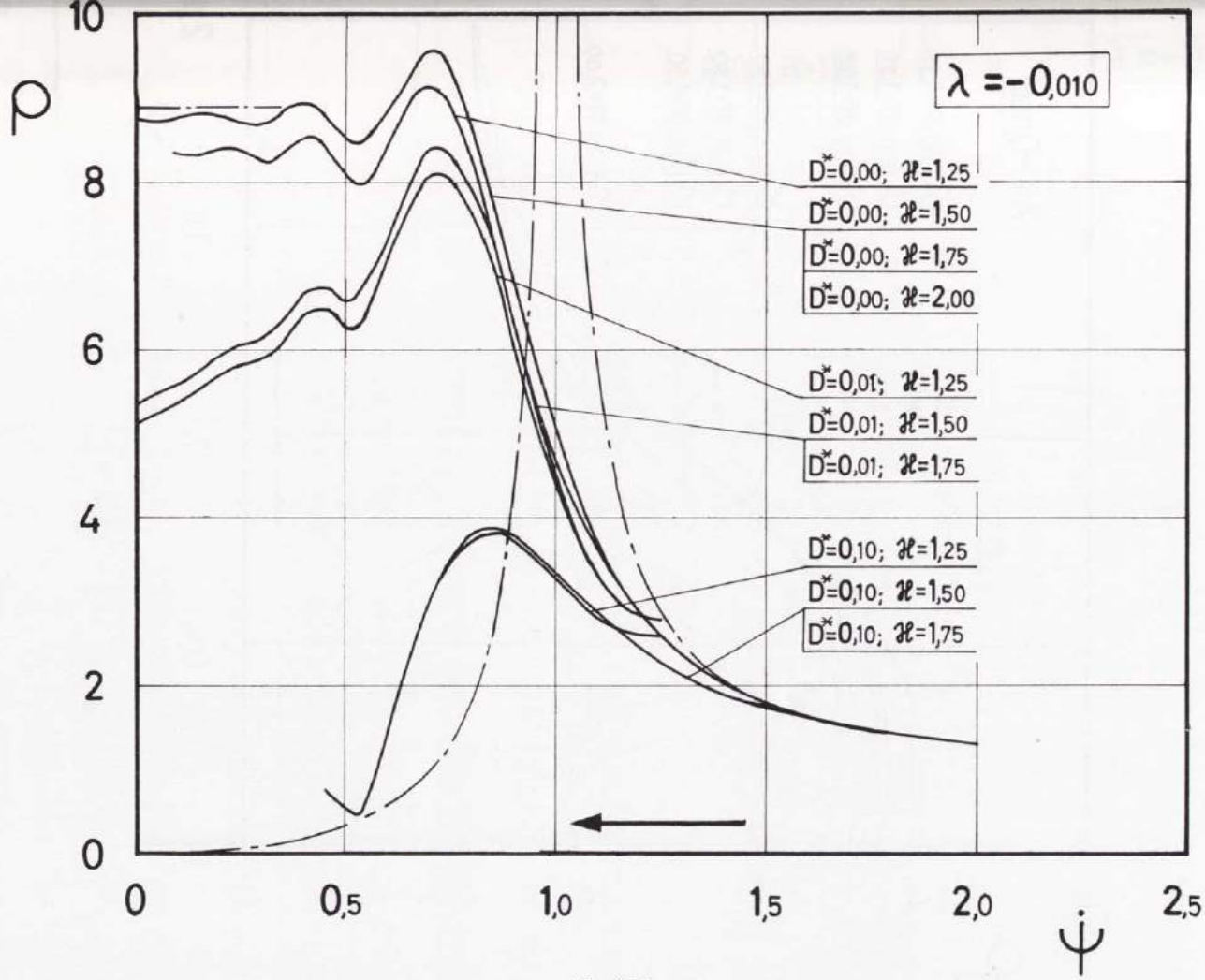
ρ
10
8
6
4
2
0
0
0,5
1,0
1,5
2,0
2,5
ψ
λ =-0,010
D*=0,00; ℋ=1,25
D*=0,00; ℋ=1,50
D*=0,00; ℋ=1,75
D*=0,00; ℋ=2,00
D*=0,01; ℋ=1,25
D*=0,01; ℋ=1,50
D*=0,01; ℋ=1,75
D*=0,10; ℋ=1,25
D*=0,10; ℋ=1,50
D*=0,10; ℋ=1,75

Fig. 37.1

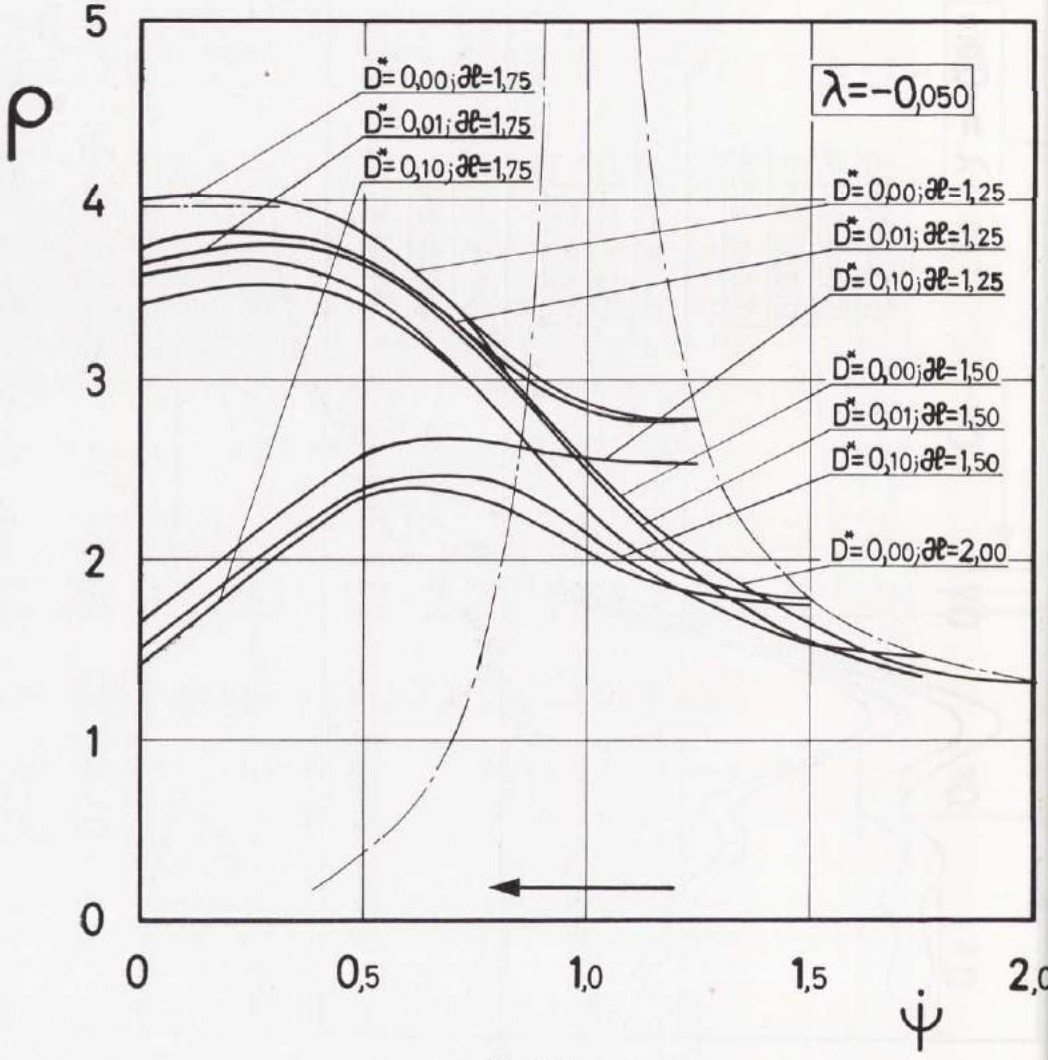
ρ
5
4
3
2
1
0
0
0,5
1,0
1,5
2,0
ψ
λ=−0,050
D*= 0,00; ∂ℓ=1,75
D*= 0,01; ∂ℓ=1,75
D*= 0,10; ∂ℓ=1,75
D*= 0,00; ∂ℓ=1,25
D*= 0,01; ∂ℓ=1,25
D*= 0,10; ∂ℓ=1,25
D*= 0,00; ∂ℓ=1,50
D*= 0,01; ∂ℓ=1,50
D*= 0,10; ∂ℓ=1,50
D*= 0,00; ∂ℓ=2,00

Fig. 38.1

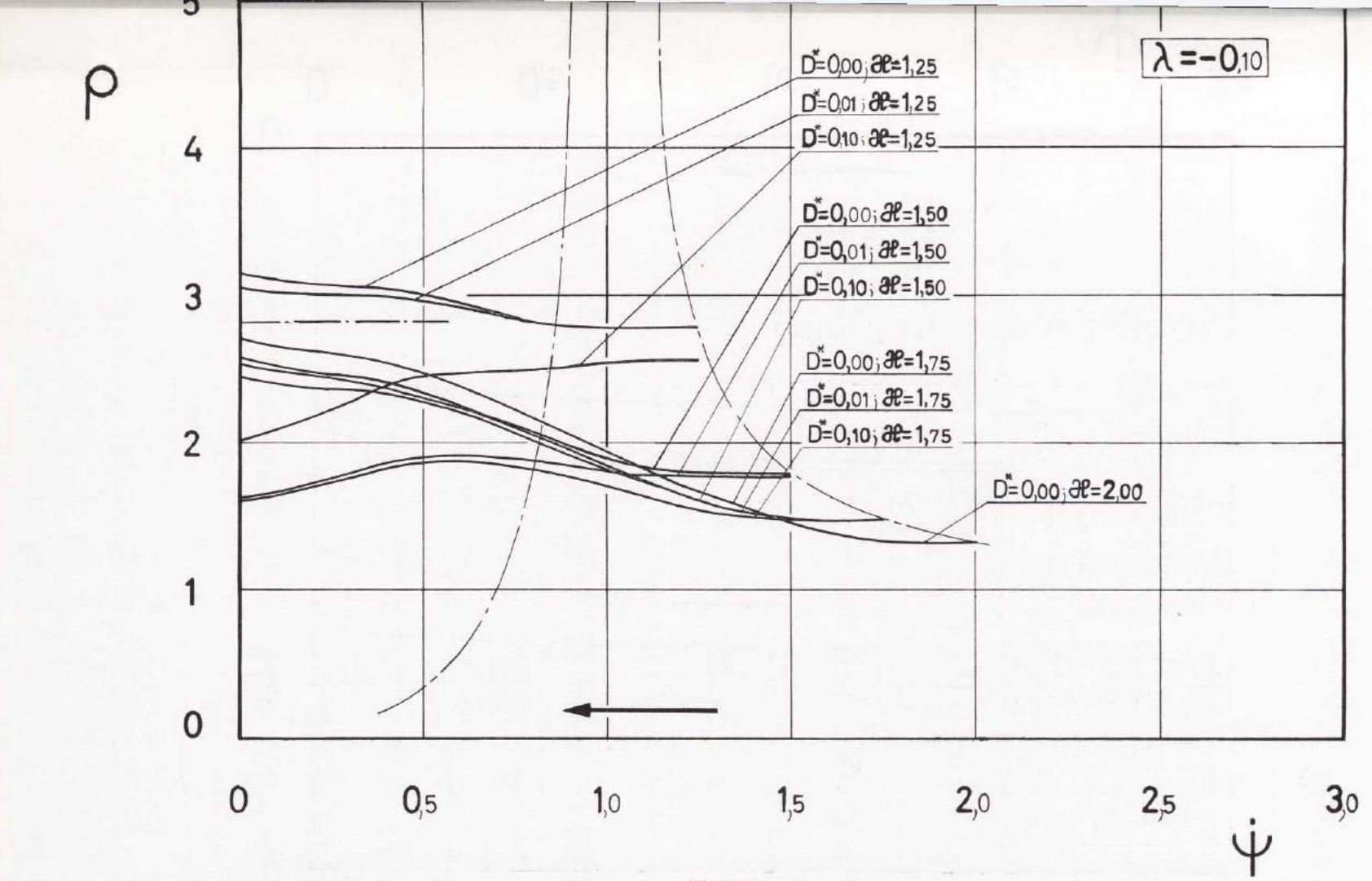
ρ
λ=-0,10
D*=0,00; ∂ℓ=1,25
D*=0,01; ∂ℓ=1,25
D*=0,10; ∂ℓ=1,25
D*=0,00; ∂ℓ=1,50
D*=0,01; ∂ℓ=1,50
D*=0,10; ∂ℓ=1,50
D*=0,00; ∂ℓ=1,75
D*=0,01; ∂ℓ=1,75
D*=0,10; ∂ℓ=1,75
D*=0,00; ∂ℓ=2,00
0
1
2
3
4
0
0,5
1,0
1,5
2,0
2,5
3,0
ψ

Fig. 39.1

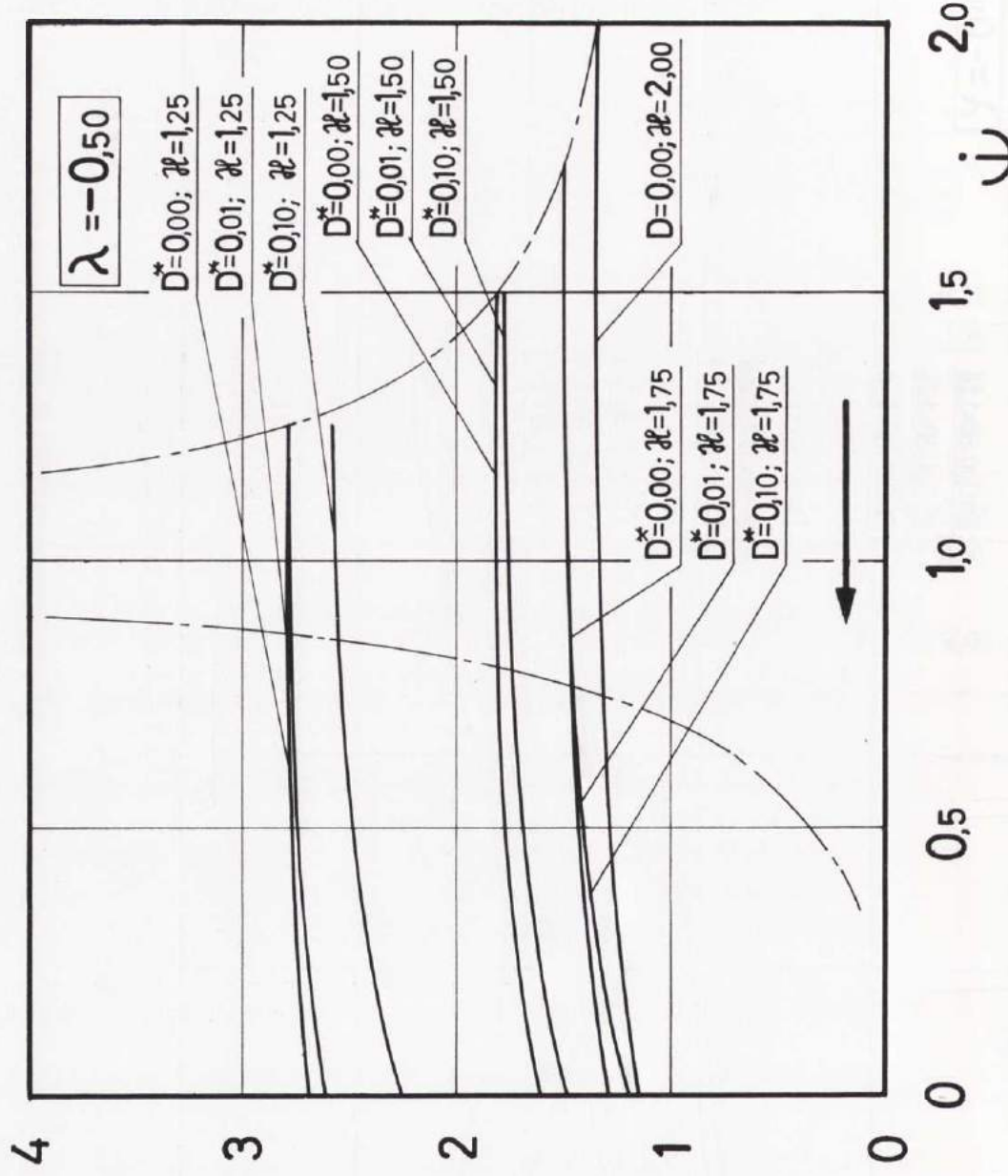
λ = −0,50
D*=0,00; ϰ=1,25
D*=0,01; ϰ=1,25
D*=0,10; ϰ=1,25
D*=0,00; ϰ=1,50
D*=0,01; ϰ=1,50
D*=0,10; ϰ=1,50
D=0,00; ϰ=2,00
D*=0,00; ϰ=1,75
D*=0,01; ϰ=1,75
D*=0,10; ϰ=1,75
ρ
ψ
0
1
2
3
4
0
0,5
1,0
1,5
2,0

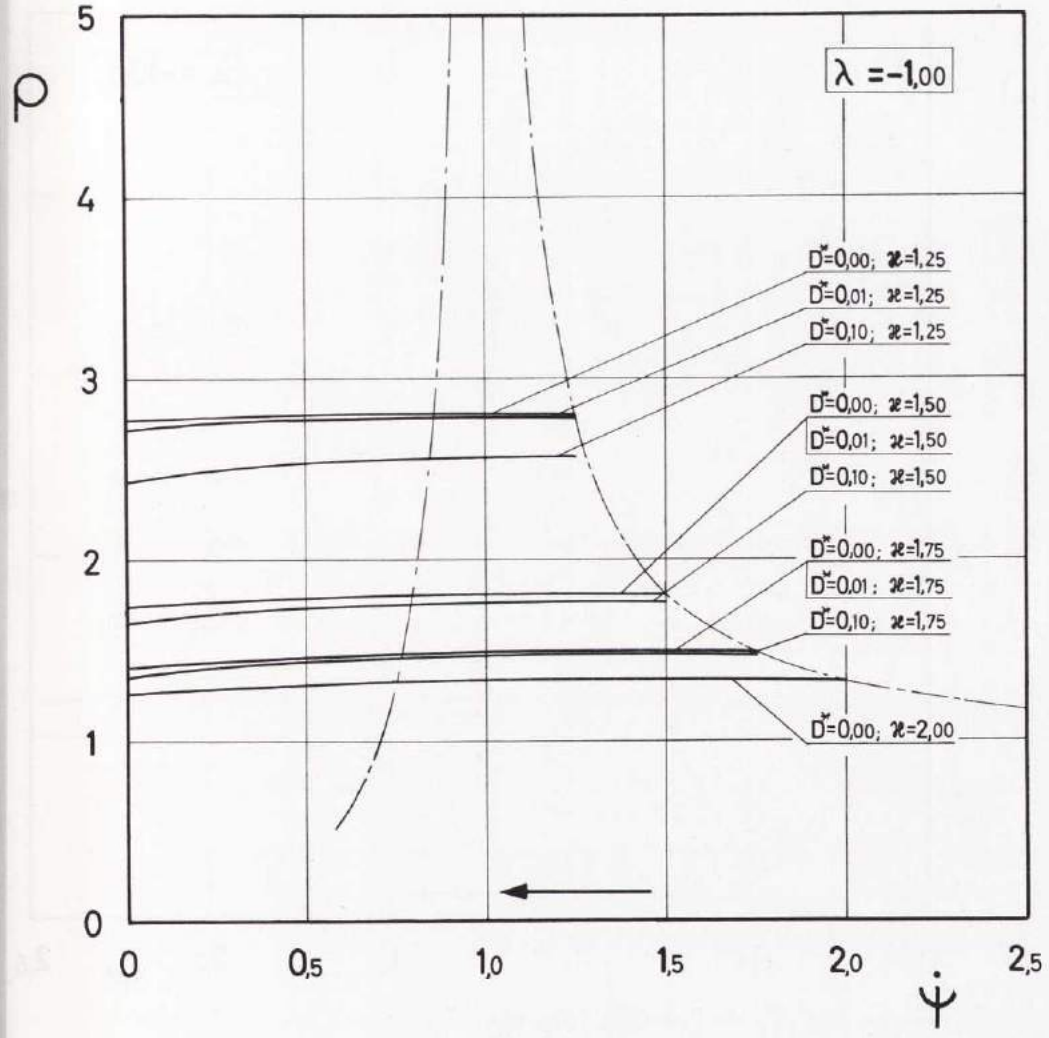
λ =-1,00
D̃=0,00; ϰ=1,25
D̃=0,01; ϰ=1,25
D̃=0,10; ϰ=1,25
D̃=0,00; ϰ=1,50
D̃=0,01; ϰ=1,50
D̃=0,10; ϰ=1,50
D̃=0,00; ϰ=1,75
D̃=0,01 : ϰ=1,75
D̃=0,10; ϰ=1,75
D̃=0,00; ϰ=2,00
ρ
ψ̇
0
1
2
3
4
5
0
0,5
1,0
1,5
2,0
2,5

Fig. 41.1

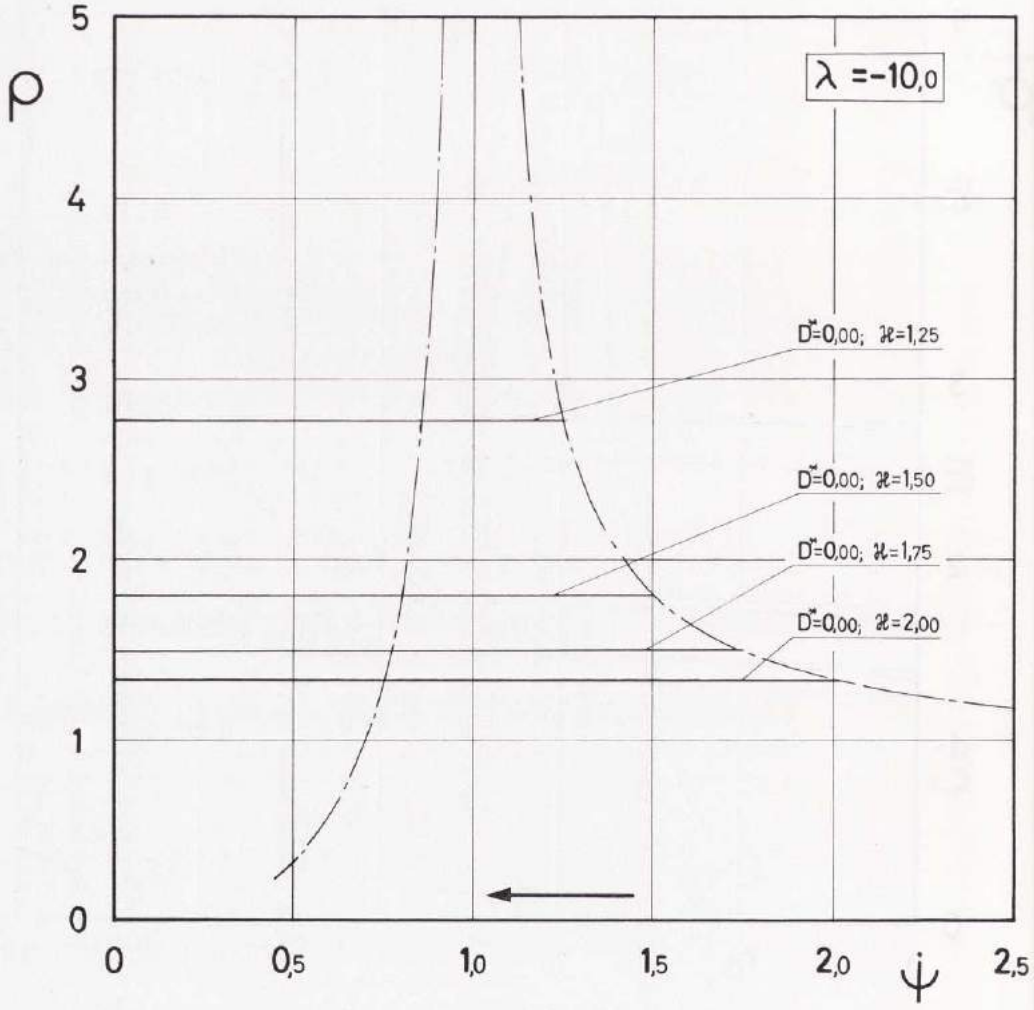
ρ
λ =-10,0
D̃=0,00; ℵ=1,25
D̃=0,00; ℵ=1,50
D̃=0,00; ℵ=1,75
D̃=0,00; ℵ=2,00
0
1
2
3
4
5
0
0,5
1,0
1,5
2,0
2,5
ψ

Fig. 42.1

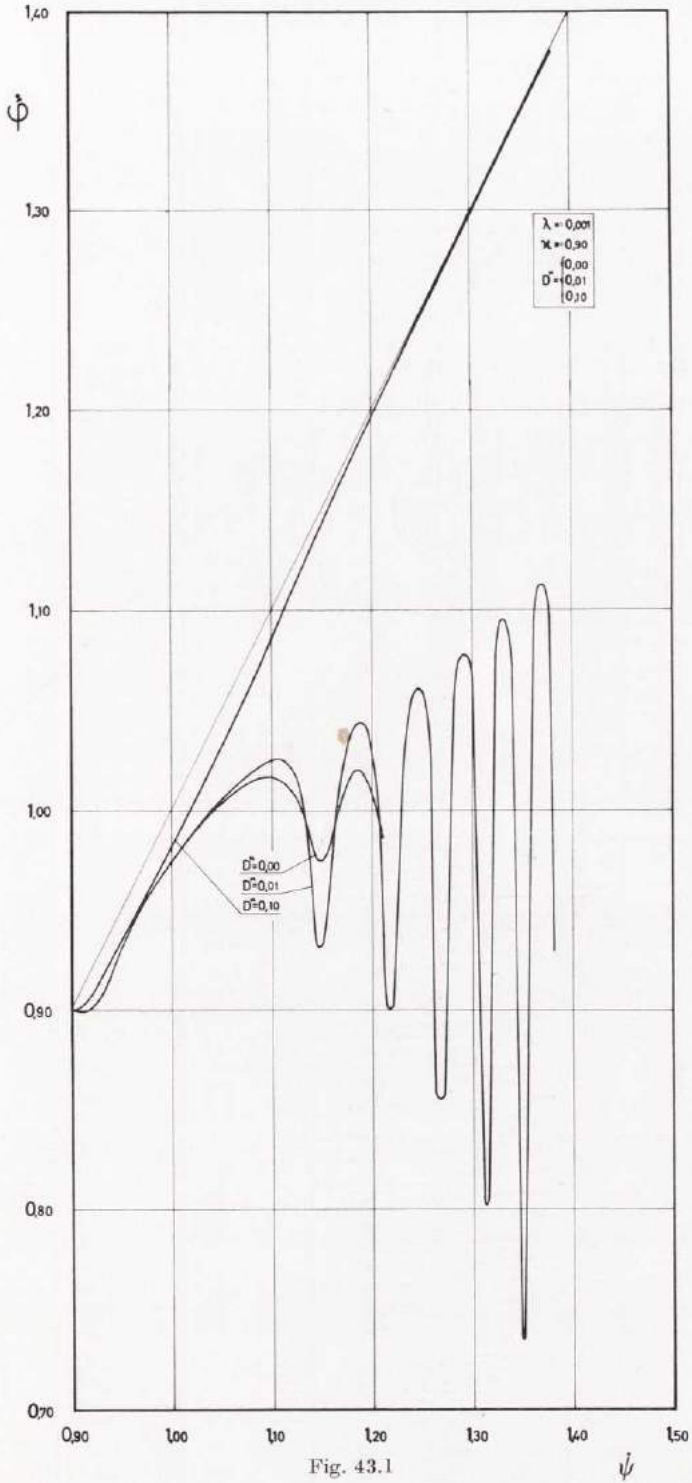
1,40
1,30
1,20
1,10
1,00
0,90
0,80
0,70
φ
0,90
1,00
1,10
1,20
1,30
1,40
1,50
ψ
λ = 0,001
κ = 0,90
D* = 0,00
0,01
0,10
D*=0,00
D*=0,01
D*=0,10

Fig. 43.1

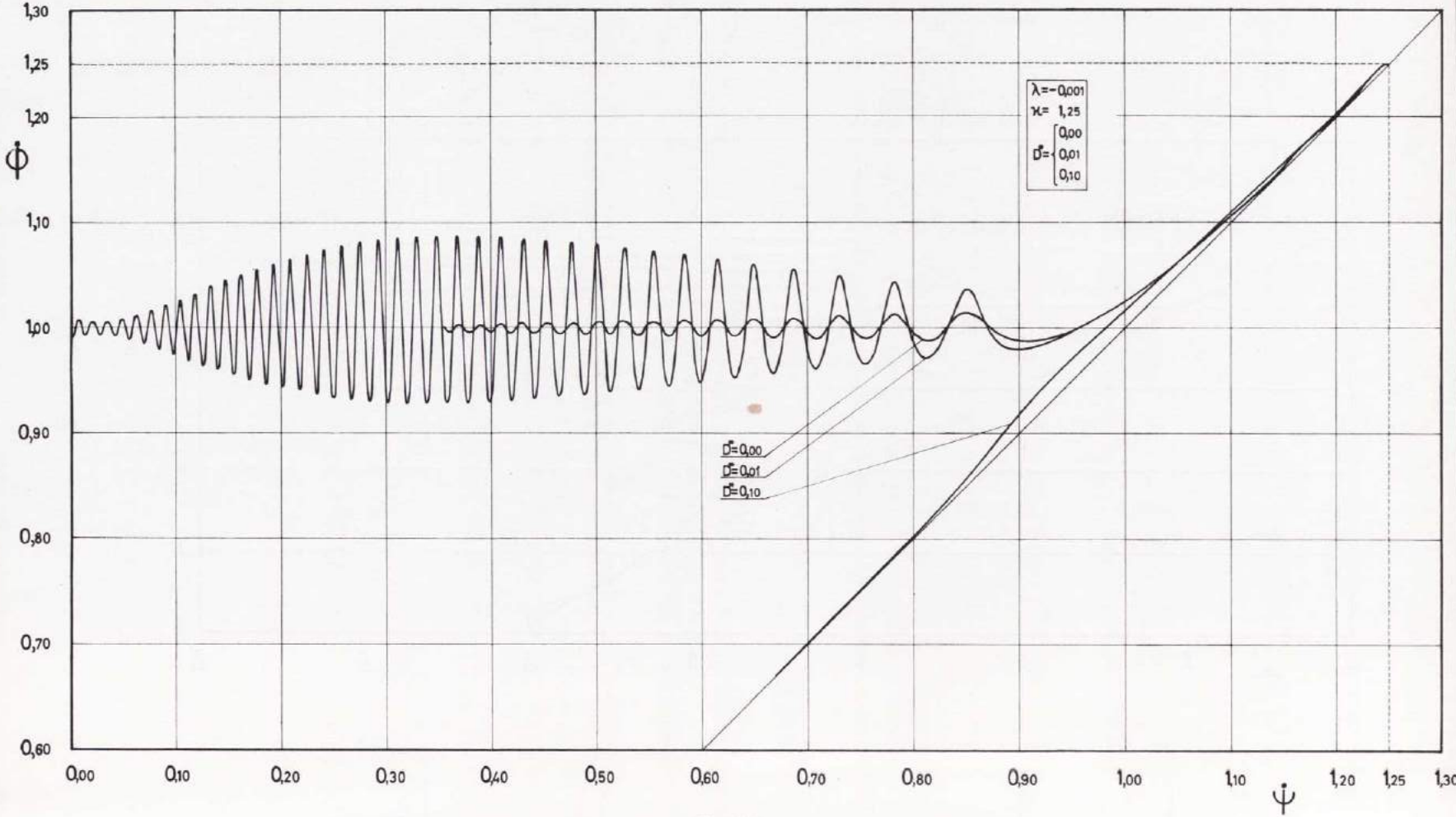
λ=-0,001
κ= 1,25
D*= 0,00
0,01
0,10
D*=0,00
D*=0,01
D*=0,10
Φ
Ψ
1,30
1,25
1,20
1,10
1,00
0,90
0,80
0,70
0,60
0,00
0,10
0,20
0,30
0,40
0,50
0,60
0,70
0,80
0,90
1,00
1,10
1,20
1,25
1,30

Fig. 44.1

4,6. The Truncation Error

By using the method outlined in Sec. 4,4 for solving the differential equations in 27.1 we get after each step an error due to the extrapolation. It is impractical to try to correct for this error after each step in automatic work. However, it is a matter of fact that the error from this source, if uncorrected, tends to grow and accumulate as the solution proceeds. After considerable time the accuracy of any significant figure of the numerical solution might be impaired.

Furthermore, the truncation error does not represent the only source of uncertainty concerning the correctness of the solution. By using a digital computer with a limited capacity there also occurs an accidental error due to the necessity of rounding-off the numbers. It will be pointed out that the truncation error is systematic in nature.

These two kinds of errors co-exist and interact and they will conspire to affect the precision of the solution adversely.

There exists a general method [9] which can be used for following the accumulation of error in numerical solutions of differential equations. This method is, however, hardly suitable for our complicated equations. Instead of using this method some simple calculations were made. In our cases we only wanted to investigate, as an example, the function ρ over a limited range of the running coordinate τ. The conditions at $\tau = 0$ are known and we want to know the variation of ρ over the range in τ. For practical purpose two decimals in ρ are enough and by trying different values of $\Delta\tau$ a value of $\Delta\tau$ could be determined which at least gave the wanted accuracy. The value of ρ of course varied with the value of λ but on the whole the calculations were carried out with $\Delta\psi \approx 1$ radian. By a calculation with $\lambda = 0$, $\varkappa = 0{,}90$, and $D_m^* = 0{,}01$ the value of ρ decreased from $4{,}244158$ to $4{,}244151$ after 40 steps with $\Delta\tau = 1$. In the most cumbersome cases the machine had to compute 350 steps.

It was also possible to compare with the two cases treated by *Dimentberg* [3]. In the first case he has $\varkappa = 0{,}90$, $\lambda = 0{,}001$, $D^* = 0$ and he got the maximum deflection of the centre of gravity G $R_{max} = 33{,}9\,e$ at $\dot{\psi} = 1{,}09$ (this is seen from a diagram). The calculations with the step by step method gave with $\Delta\tau = 1$ that $R_{max} = 32{,}88\,e$ at $\dot{\psi} = 1{,}096$ (interpolated values). Dimentberg also gives results for another damping coefficient $D^* = 0{,}0106$ and he got $R_{max} = 20{,}7\,e$ at $\dot{\psi} = 1{,}075$ (from a diagram). The corresponding values with the step by step method are ($\Delta\tau = 1$) $R_{max} = 22{,}58\,e$ at $\dot{\psi} = 1{,}084$ (interpolated values).

The values from the digital computer are shown in the tabs 46.1 and 46.2.

$\lambda=0{,}001$ $\quad \varkappa=0{,}90$ $\quad D^*=0{,}00$			
$\dot{\psi}$	ϱ	θ (rad)	$\frac{R}{e}$
— — —	— — —	— — —	— — —
1,0700	30,2223	2,25849	29,60
1,0800	32,0597	2,56702	31,22
1,0900	33,1438	2,91278	32,17
1,1000	33,2233	3,30234	32,23
1,1100	32,1322	3,74609	31,32
— — —	— — —	— — —	— — —

Tab. 46.1

$\lambda=0{,}001$ $\quad \varkappa=0{,}90$ $\quad D^*=0{,}01$			
$\dot{\psi}$	ϱ	θ (rad)	$\frac{R}{e}$
— — —	— — —	— — —	— — —
1,0700	22,7276	2,30375	22,07
1,0800	23,3710	2,58755	22,50
1,0900	23,3090	2,90238	22,32
1,1000	22,362	3,25344	21,35
— — —	— — —	— — —	— — —

Tab. 46.2

It ought to be mentioned that the calculations in the present report had not been carried out if a digital computer had not been at our disposal. For computing one step by hand about 16 hours was needed and the machine only needed 40 seconds for the same procedure.

4,7. Photographic Study of the Behaviour of a Rotor During Transition of the Critical Speed

Several questions arise in connection with the behaviour of a rotor when it passes its critical speed.

What is the phase-angle relation during the acceleration (retardation)?

How does the damping influence this relation?

How does the damping influence on the deflections?

How great is the damping in a practical case?

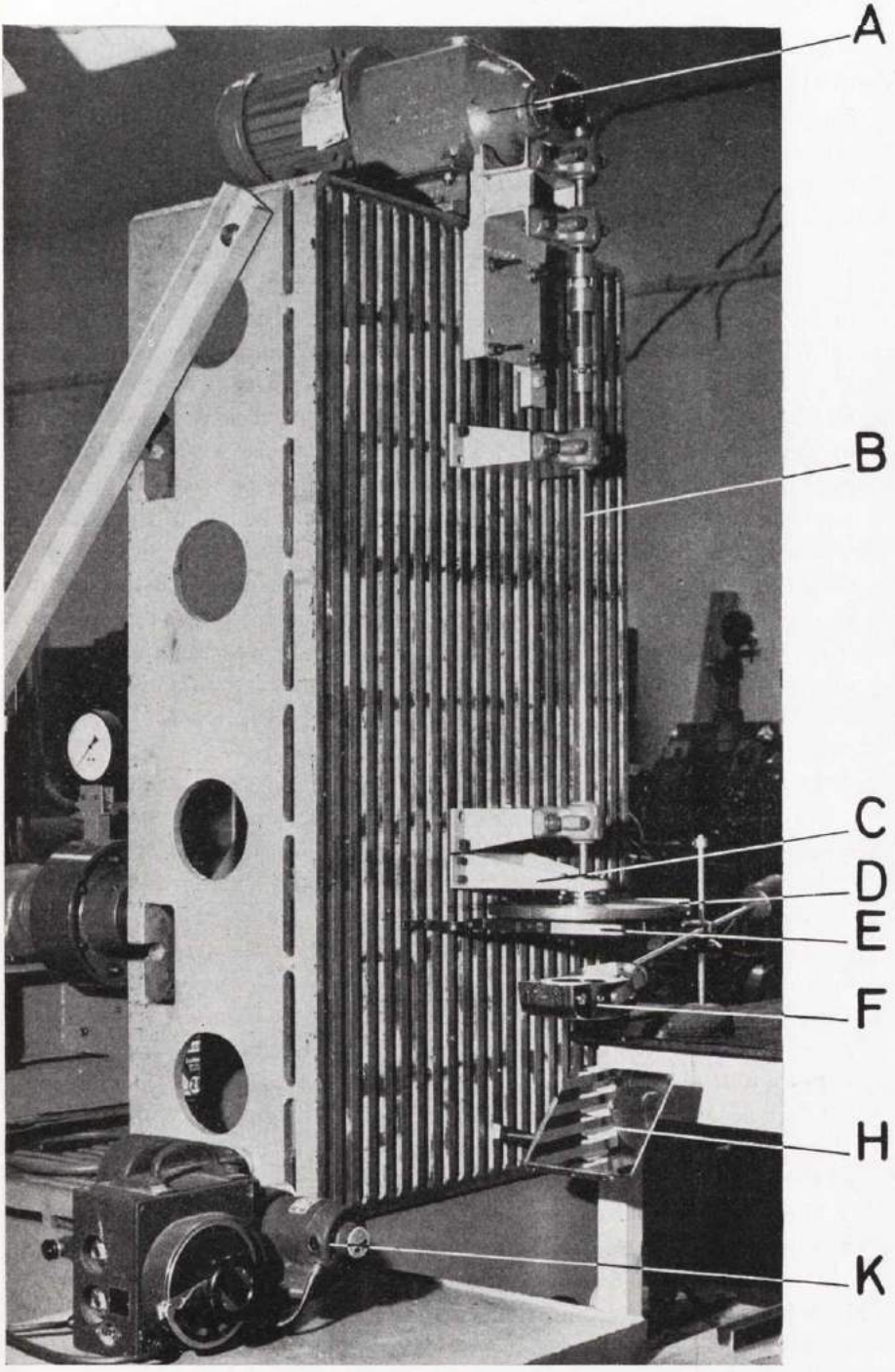

Fig. 47.1

These questions are answered to some degree by the results from the theoretical study in the preceding chapters. However, the theoretical results are of no practical interest if the rotor in practice does not behave in the way predicted. In order to check the theory some experiments were done with the equipment and instrumentation shown in fig. 47.1.

An A.C. motor (A) with a variator turned a 15 mm circular shaft (B). The free end of the shaft carried an unbalanced disc (D). The deflection of the shaft was limited by a collar (C).

The lower side of the disc was painted black and the centre of the shaft (S) was marked by a yellow point. The position of the point S at rest was shown by two thin steel wires painted in a yellow colour in right angles to each other. The carrier of these wires (E) can be seen in fig. 47.1. From the point S a scribed line showed the angular position of the centre of gravity (G) of the disc. The loci of the point S was observed by light reflected from the point S and the steel wires and then the position of the point G could be determined with the aid of the scribed line and the known value of the eccentricity e of the disc.

In an optical way the deflection of the shaft was magnified by a magnifying glass (F) and after a reflection in a mirror (H) the course was filmed by a "slow motion camera" (K). The camera took approx. 3000 photos per second.

At first the camera was calibrated by running the shaft at a constant speed. Then both accelerations and decelerations through the critical speed of the rotor were filmed.

With the aid of a film reading device then all wanted quantities during the course could be obtained.

4,71. Acceleration

In order to analyze the course at acceleration through the critical speed the shaft was driven at a uniform sub-critical speed. Then the camera was started and after one second the rotor was accelerated for four seconds by changing the position of a knob on the variator. During the acceleration the rotor passed its critical speed. Because of this manual operation the acceleration was not uniform.

The critical speed of the rotor was 1158 r.p.m. and the tests were started at 800 r.p.m. and 900 r.p.m. Four films were taken. Because of the cumbersome evaluation of the films only one of these was subjected to a close examination. In this the shaft deflection r and the phase angle shaft θ were determined. Three pieces of the film are

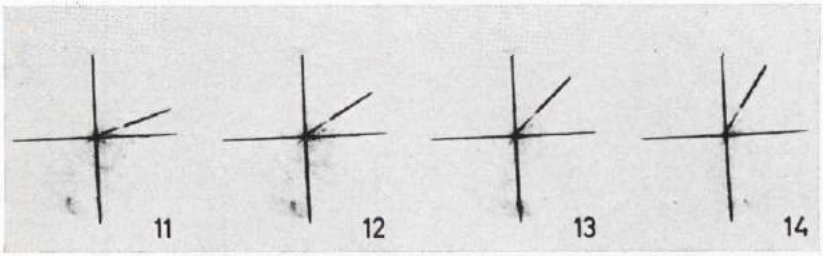

Sub-critical constant speed ($\theta = 0°$) (11 – 14).

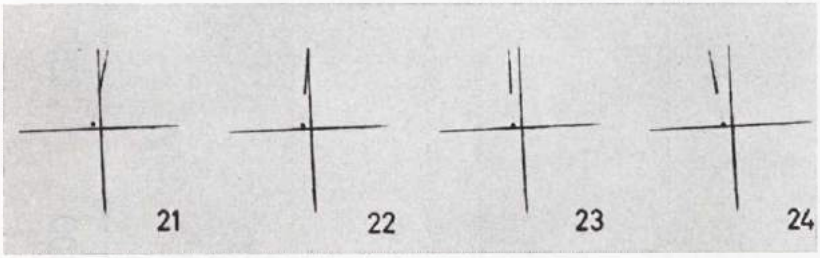

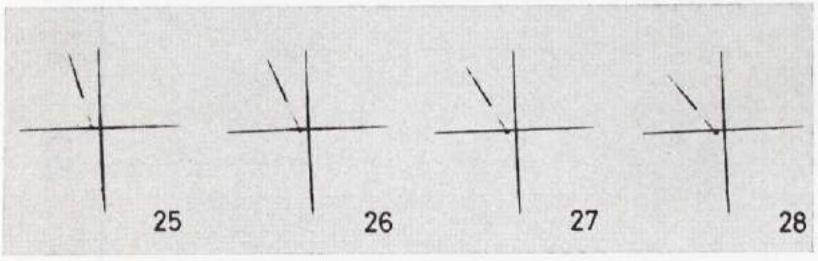

Post-critical speeds just above the critical speed ($\theta \approx 90°$) (21 – 28).

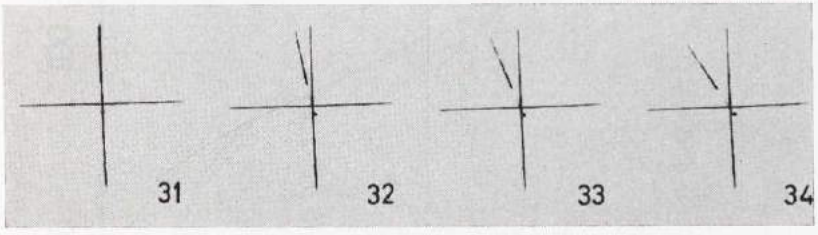

Post-critical constant speed ($\theta = 180°$) (31 – 34).

Fig. 49.1

shown in fig. 49.1. The results are also shown in the figs 50.1 and 51.1.

In these figures also theoretical results are drawn for a mean value of the acceleration.

Further, calculations were carried out for different values of the damping factor D^*.

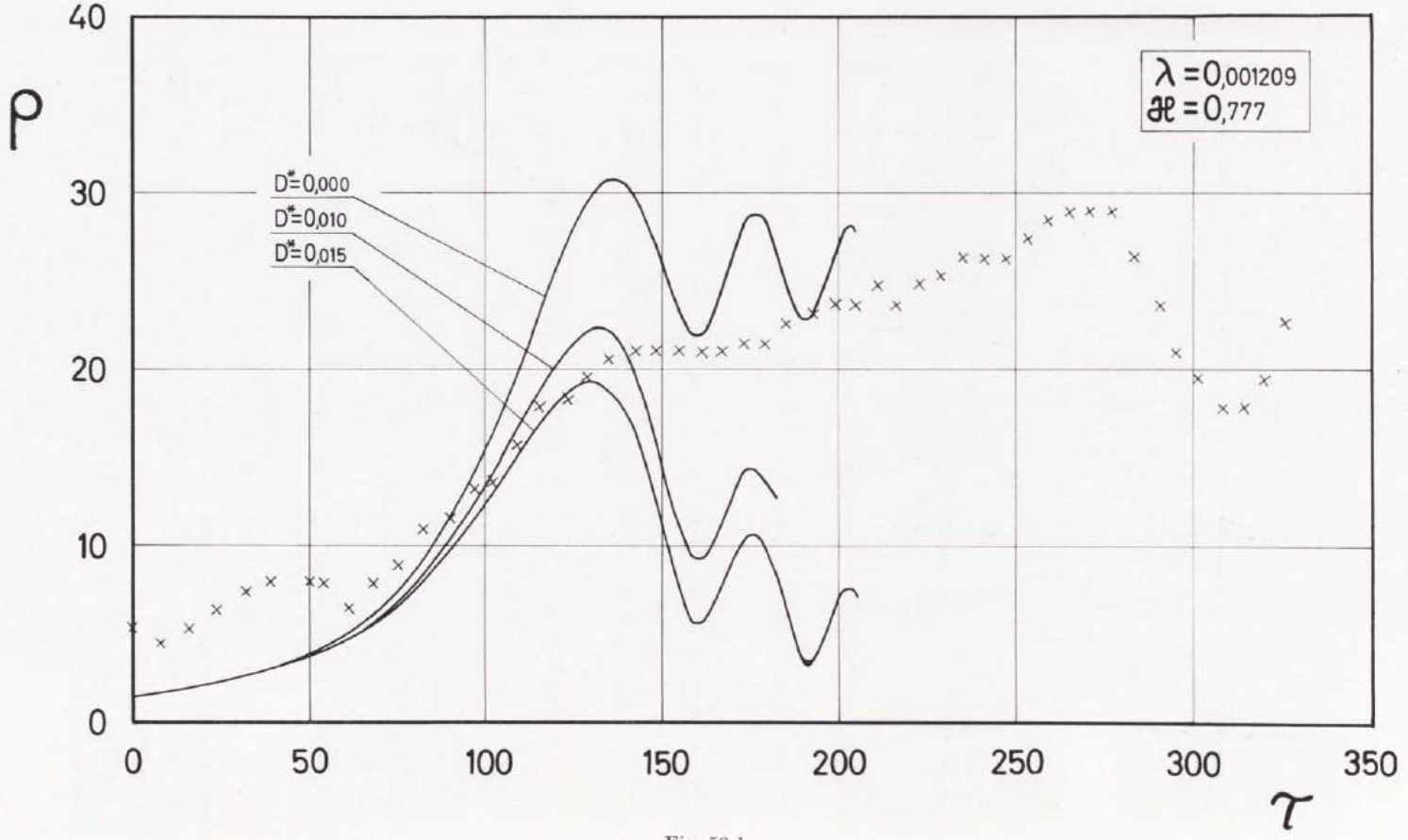
ρ
τ
λ = 0,001209
ℜ = 0,777
D* = 0,000
D* = 0,010
D* = 0,015
0
10
20
30
40
0
50
100
150
200
250
300
350

Fig. 50.1

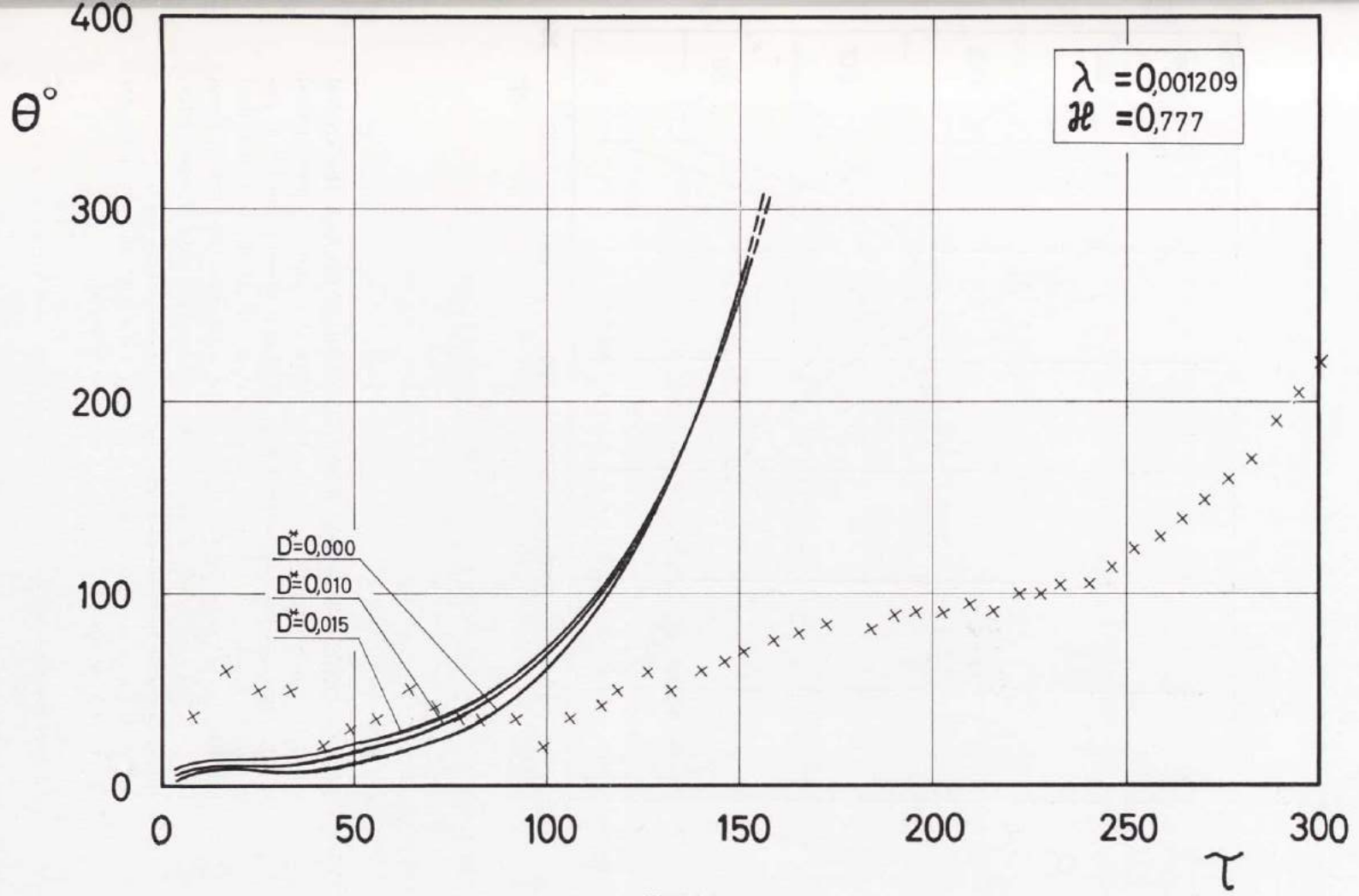
400
θ°
300
200
100
0
0
50
100
150
200
250
300
τ
λ =0,001209
ℋ =0,777
D*=0,000
D*=0,010
D*=0,015

Fig. 51.1

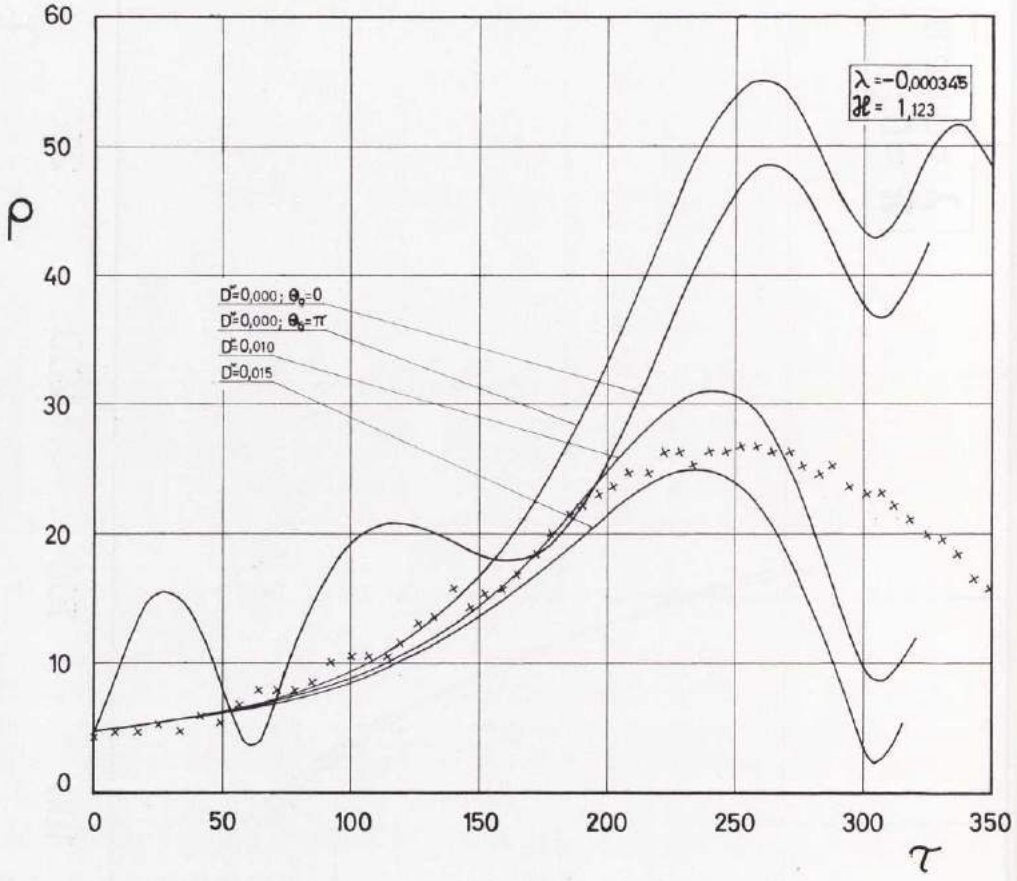

Fig. 52.1

4,72. **Deceleration**

When filming the course during deceleration through the critical speed the motor at first turned the shaft at a uniform post-critical speed. The camera was started and after one second the rotor was manually decelerated through its critical speed. At the test described here the initial value of the speed of the shaft was 1300 r.p.m. From the film the shaft deflection and the phase angle shift θ were determined and the results are shown in the figs 52.1 and 53.1.

The theoretical curves with different values of the damping are calculated for the mean value of the deceleration.

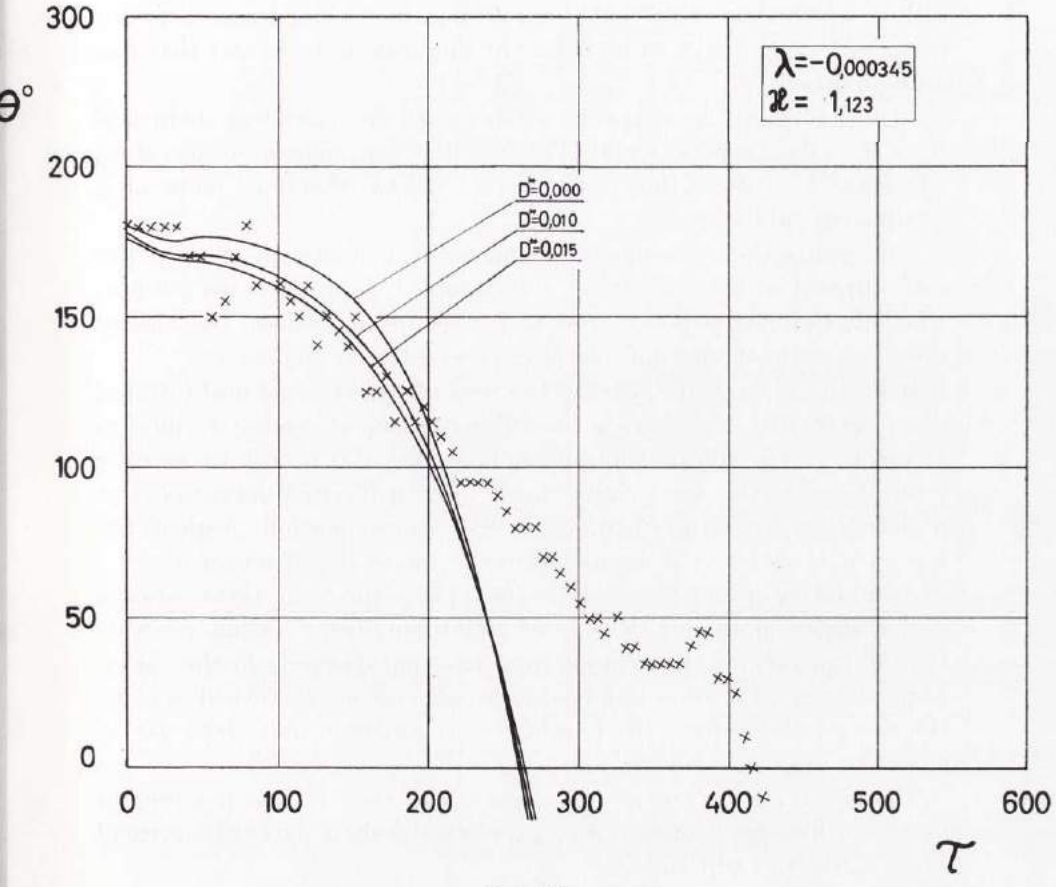

Fig. 53.1

As as curiosity a curve with a faulty assumption concerning the start angle θ is shown. At a constant post-critical speed $\theta = \pi$ always at zero damping but in fig. 52.1 it is also calculated for the case $\theta = 0$. After some violent vibrations the shaft takes a form similar to the correct one.

The test curve also shows such vibrations of small amplitude.

4,73. Conclusions

For practical reasons the tests could not be made with absolutely constant acceleration. In the acceleration tests the λ-value was controlled by hand but in the deceleration tests with the aid of an electri-

cally controlled brake. Thus the accuracy in a comparison between test and theory ought to be better in the braking tests and that has also happened.

In fig. 50.1 can be seen that at the start the shaft was disturbed by a secondary critical speed. This and the non-uniform acceleration cooperate to disturb this test. The results are therefore more of a qualitative nature.

Concerning the D^*-value it ought to be emphasized that in the test apparatus both external and internal damping were present. Further, the disc also gave rise to gyroscopic moments. The theory does not consider internal damping or gyroscopic moments.

It has been shown in [7] that the sum of the external and internal damping coefficients occurs in the differential equations for the motion of the disc. The internal damping, however, also occurs in another term. Because the tests show stable motion (limited deflections) at post-critical speeds one can, as a first approximation, neglect the action of this "internal-damping-term" besides the "sum-term".

As a matter of fact it was shown in [7] that the "sum-term" always causes stable motion if the "internal-damping-term" is not present. On the contrary, if the amount from external damping in the "sum-term" is zero the rotor is unstable at all post-critical whirl speeds. We can therefore, from the braking tests, conclude that $(D_i^* + D^*) \approx (0{,}010 \div 0{,}015)$.

The great advantage of these tests was that it was possible to follow visibly the change of θ and r when the shaft passed its critical speed as the fig. 49.1 shows.

4,8. Experimental Investigation with the Aid of a Recorder

The apparatus shown in fig. 64.2 of [7] was also used for studying the behaviour of the rotor during transition through its critical speed. The electric signals from the capacitive pick-ups in fig. 64.3 of [7] were, after amplifying, rectified and led to a recorder. On the graph was written, besides the deflections of the disc in two directions perpendicular to each other, the speed of the motor and the torque delivered from the motor. The place where the torque was measured can be seen in the fig. 64.2 of [7].

Tests were carried out for both acceleration and deceleration through the critical speed. The shaft was turned by a D.C.motor. The speed of the motor was changed manually during the acceleration tests.

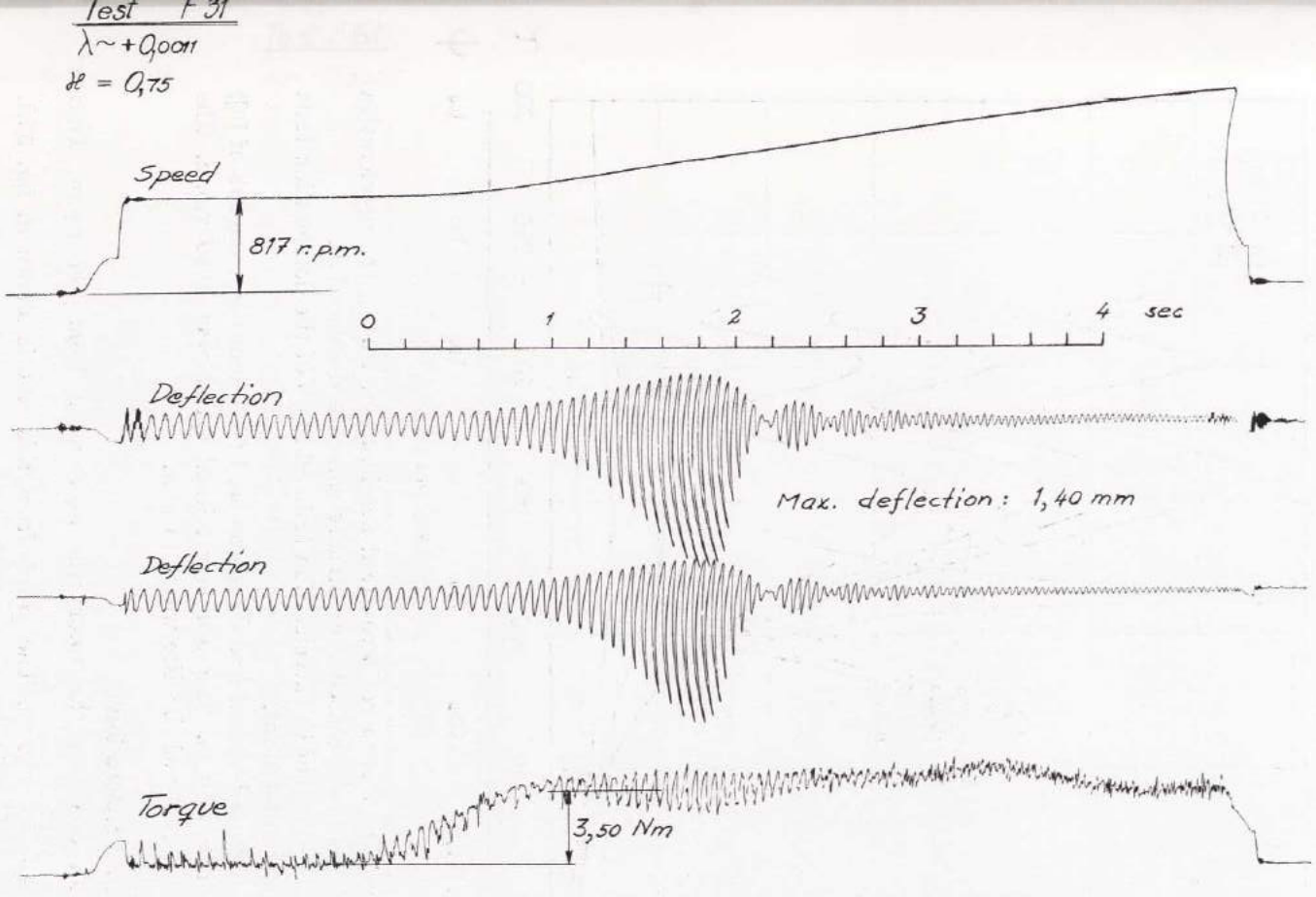
Test F 31
λ ~ +0,0011
μ = 0,75
Speed
817 r.p.m.
0
1
2
3
4
sec
Deflection
Max. deflection: 1,40 mm
Deflection
Torque
3,50 Nm

Fig. 55.1

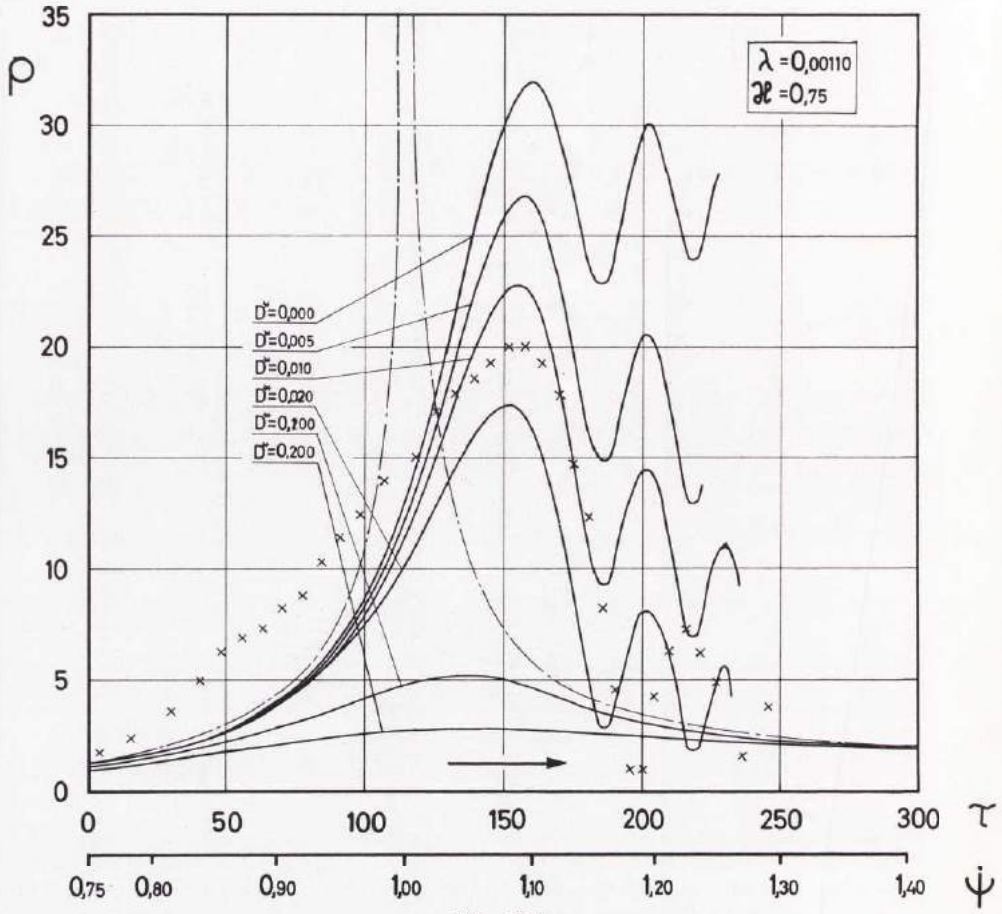

Fig. 56.1

The aim was to get a constant acceleration. During the deceleration tests a brake caused a practically constant deceleration.

Here one of the acceleration tests and two of the deceleration tests are accounted for.

A hinged-hinged-free shaft was used (See figure on page 218 of [6]) and $\varkappa_1 = 0,80$. The ordinary critical speed was 1090 r.p.m. The eccentricity of the disc was 0,13 mm.

4,81. **Acceleration**

In one test the rotor was accelerated from 817 r.p.m. Thus $\varkappa = \frac{817}{1090} = 0,75$. The graph from this test is shown in fig. 55.1.

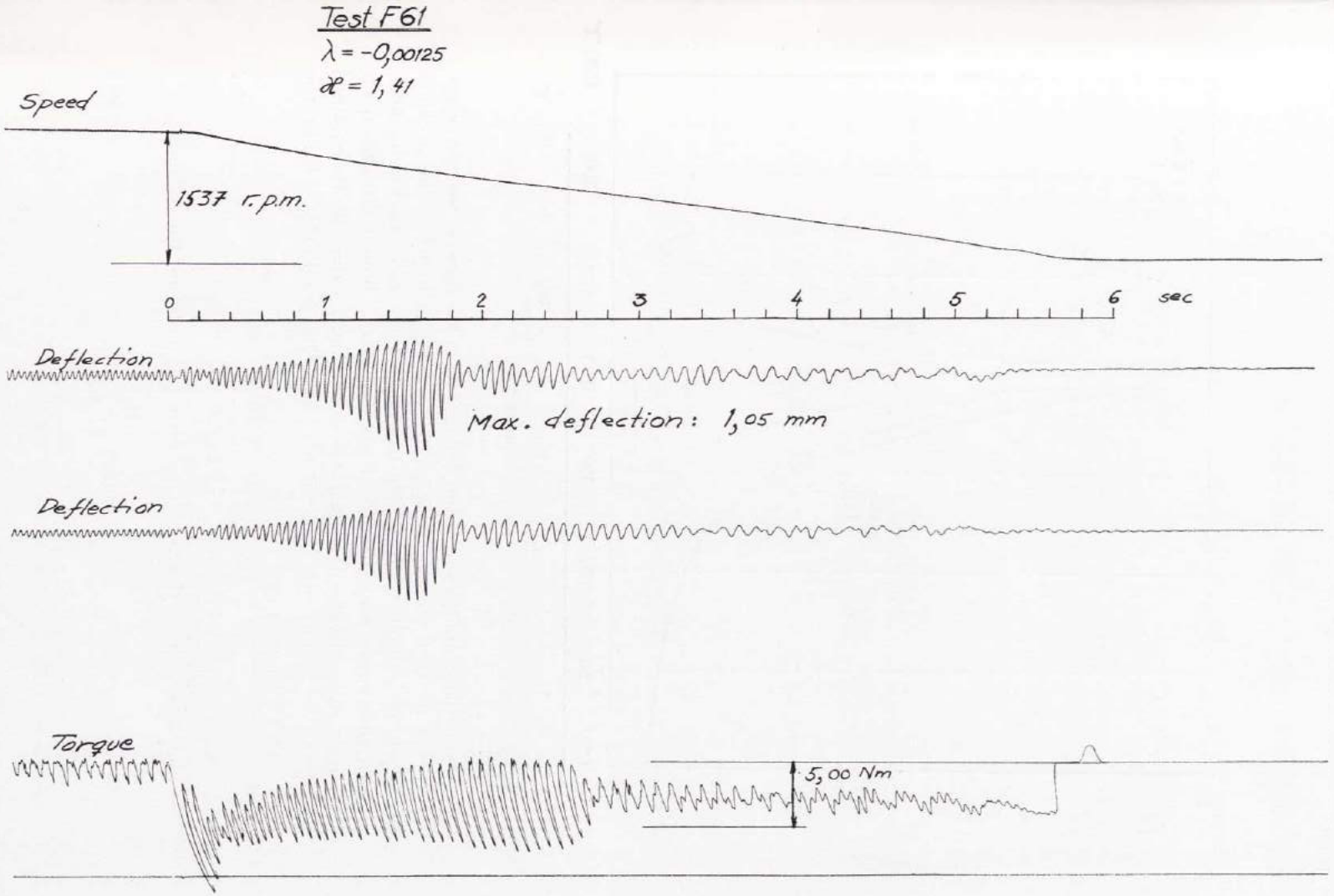
Test F61
λ = -0,00125
α = 1, 41
Speed
1537 r.p.m.
0
1
2
3
4
5
6
sec
Deflection
Max. deflection: 1,05 mm
Deflection
Torque
5,00 Nm

Fig. 57.1

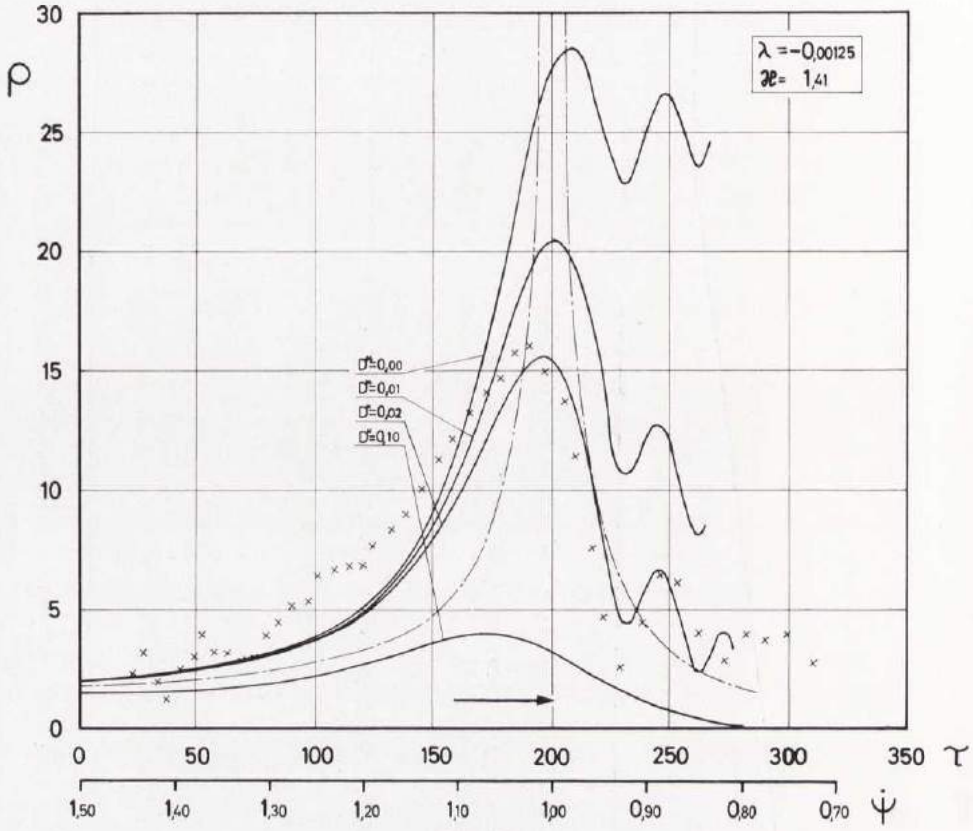

Fig. 58.1

From the graph in which the deflections of the disc centre were registered in two directions perpendicular to each other the ρ-values could be evaluated at different times and they are plotted in fig. 56.1. In this figure also theoretical curves for $\lambda = 0{,}0011$ are drawn for some values of the damping factor D^*. The λ-value can be obtained from the test in two different manners. One possibility is to use the expression

$$\lambda = \frac{a}{2\omega_n^2} = \frac{15}{\pi} \cdot \frac{1}{n_n^2} \cdot \frac{dn}{dt} \quad \ldots\ldots\ldots\ldots\ldots\ldots \quad 58.2$$

and take $\frac{dn}{dt}$ from the test. The other way is to use the formula

$$\lambda \approx \frac{M_{in}}{2I_p\omega_n^2} \quad \ldots\ldots\ldots\ldots\ldots\ldots \quad 58.3$$

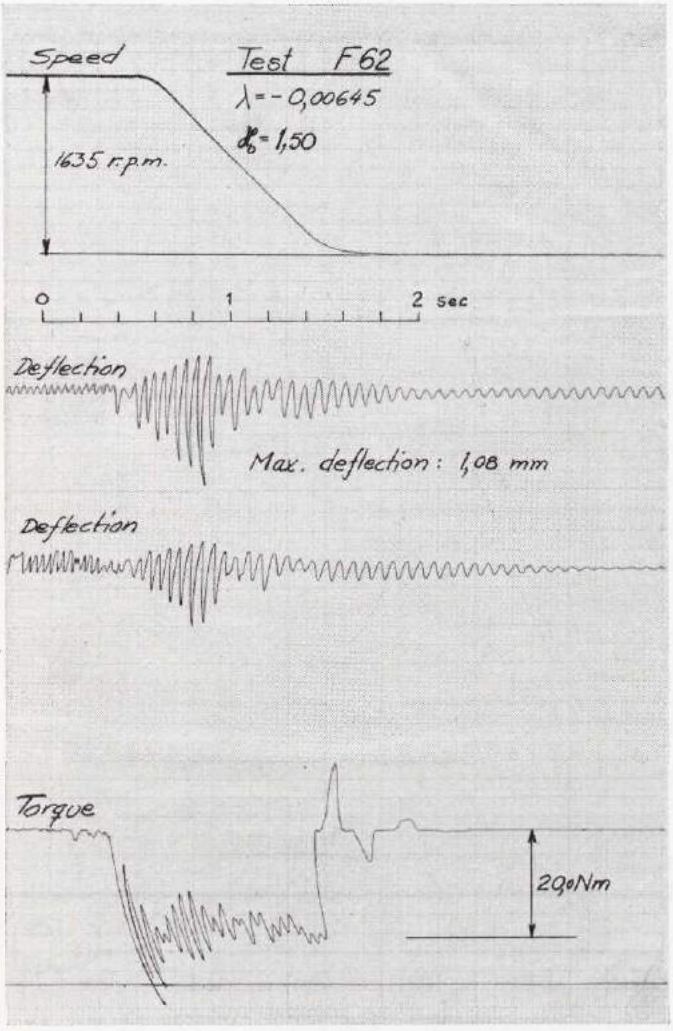

Fig. 59.1

and take M_{in} from the test. (M_{in} is the torque delivered from the motor). The motor did not give a constant torque. Here is the mean torque estimated. The two methods did not give exactly the same value. From eq. 58.2 the λ-value 0,0010 was calculated. The eq. 58.3 gave a higher value, viz. $\lambda = 0{,}0011$. Curves are only drawn for the higher value of λ.

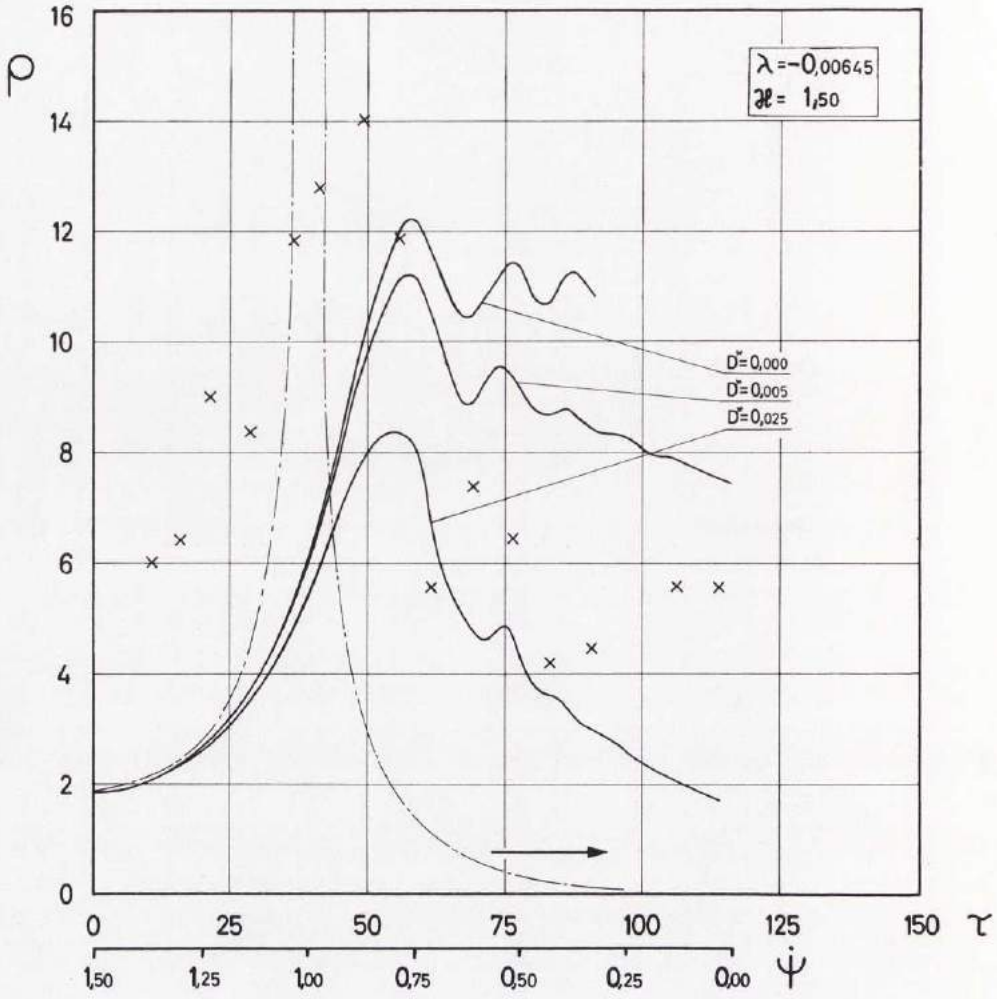

Fig. 60.1

4,82. **Deceleration**

The deceleration tests could be done more accurately than the acceleration tests because the brake gave a very uniform deceleration. Two adjustments of the brake were used. The formulas 58.2 and 58.3 are still applicable for determining the λ-value.

In the first test the graph in fig. 57.1 was obtained and in fig. 58.1 the ρ-values are plotted against the time. In the last figure also theo-

retical curves are drawn for $= \lambda - 0{,}00125$ which is a representative value for this test. Calculations are carried out for some values of the damping factor D^*. Before braking the shaft was turned at 1537 r.p.m. which gives $\varkappa = \frac{1537}{1090} = 1{,}41$.

The second test gave a graph shown in fig. 59.1 and the ρ-values are plotted in fig. 60.1. Theoretical curves are here drawn for $\lambda = -0{,}00645$. In this test $\varkappa = 1{,}50$.

4,83. Conclusions

Also in the tests registered by a recorder the disturbance from secondary critical speeds (or speed) is obvious. Concerning the external and internal damping during the tests the same circumstances as mentioned in Sec. 4,73 were valid.

5. Running through the Critical Speed with Varying Acceleration

From eq. 14.2 we get (if $N^* = \mu_A = \mu_B = 0$) for a rotor with one disc

$$M_{in}^* = \ddot{\psi} + \varepsilon^2 \rho \sin \theta \quad \ldots\ldots\ldots\ldots\ldots \quad 62.1$$

In our test machines $|\ddot{\psi}| > 0,69 \cdot 10^{-3}$, $\varepsilon^2 = 10^{-6}$, and $\rho < 50$. Thus $\varepsilon^2 \rho \ll \ddot{\psi}$ and this probably also holds for most machines in practice. Often the torque-speed-curve for a motor is known. As an example, the induction motor often has a torque-speed curve according to fig. 63.1.

One consequently can say that this curve also represents the variation in λ during the acceleration from the practical point of view. Thus the $M-n$-curves are by changing scales also the $\lambda-\dot{\psi}$-curve ($\ddot{\psi} = 2\lambda$). In order to elucidate what happens at such a varying acceleration some numerical results are presented. Four cases were computed with the assumption that the motor had a $M-n$-curve as in fig. 63.2.

If $0 \leq n \leq n_1$ M is constant

$n_1 \leq n \leq 1,25\ n_1$ M is linearly decreasing.

This can also be expressed as

$$0 \leq \dot{\psi} \leq \dot{\psi}_1 \qquad \lambda = \lambda_0 (= \text{const.})$$

$$\dot{\psi}_1 \leq \dot{\psi} \leq 1,25\ \dot{\psi}_1 \qquad \lambda = \lambda_0 (5\ \dot{\psi}_1 - 4\ \dot{\psi}) \cdot \dot{\psi}_1^{-1}$$

The programme for the digital computer was written in such a way that it could handle varying λ. Moreover, the λ-value was permitted to vary arbitrarily. In the step by step method this is easily done. During each step the λ-value was constant but it varied from one step to another.

The properties of the four cases treated are collected in tab. 68.1.

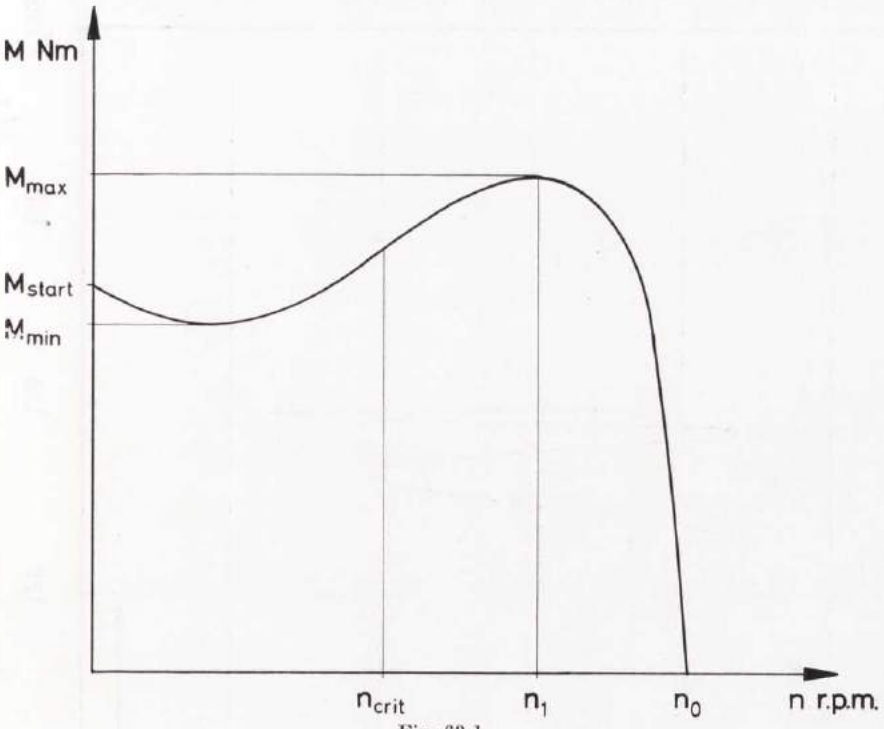

Fig. 63.1

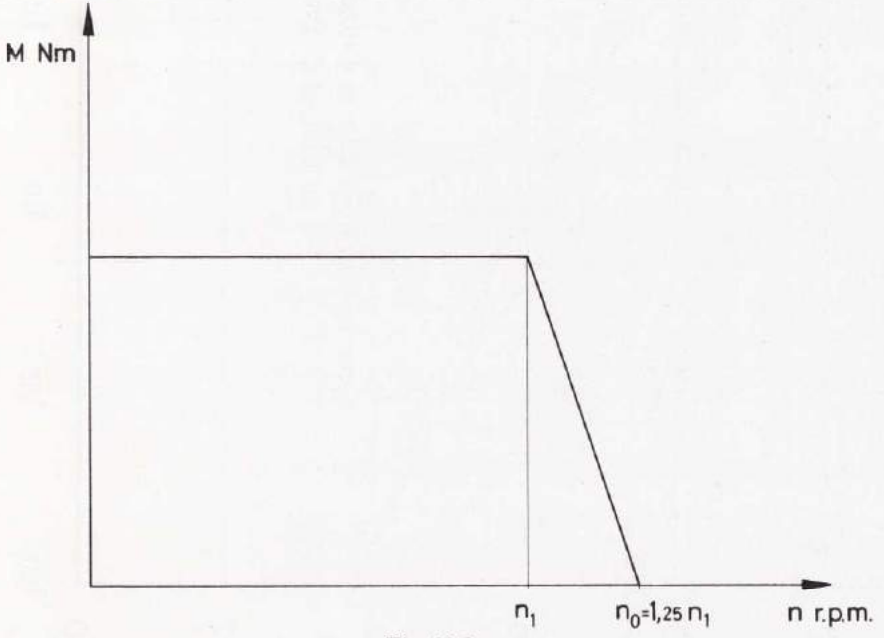

Fig. 63.2

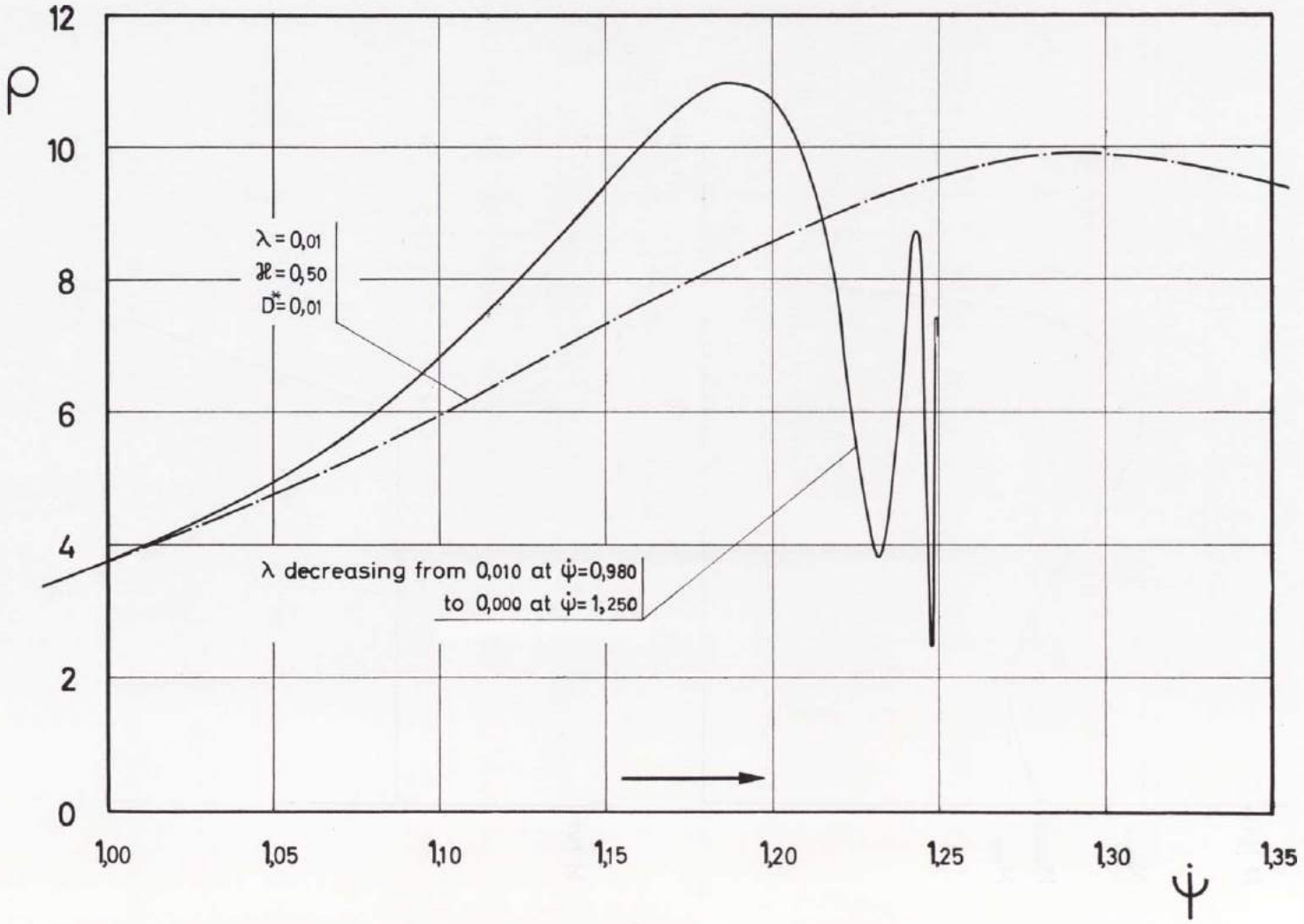
ρ
12
10
8
6
4
2
0
λ = 0,01
ℜ = 0,50
D* = 0,01
λ decreasing from 0,010 at ψ̇=0,980
to 0,000 at ψ̇= 1,250
1,00
1,05
1,10
1,15
1,20
1,25
1,30
1,35
ψ̇

Case 1

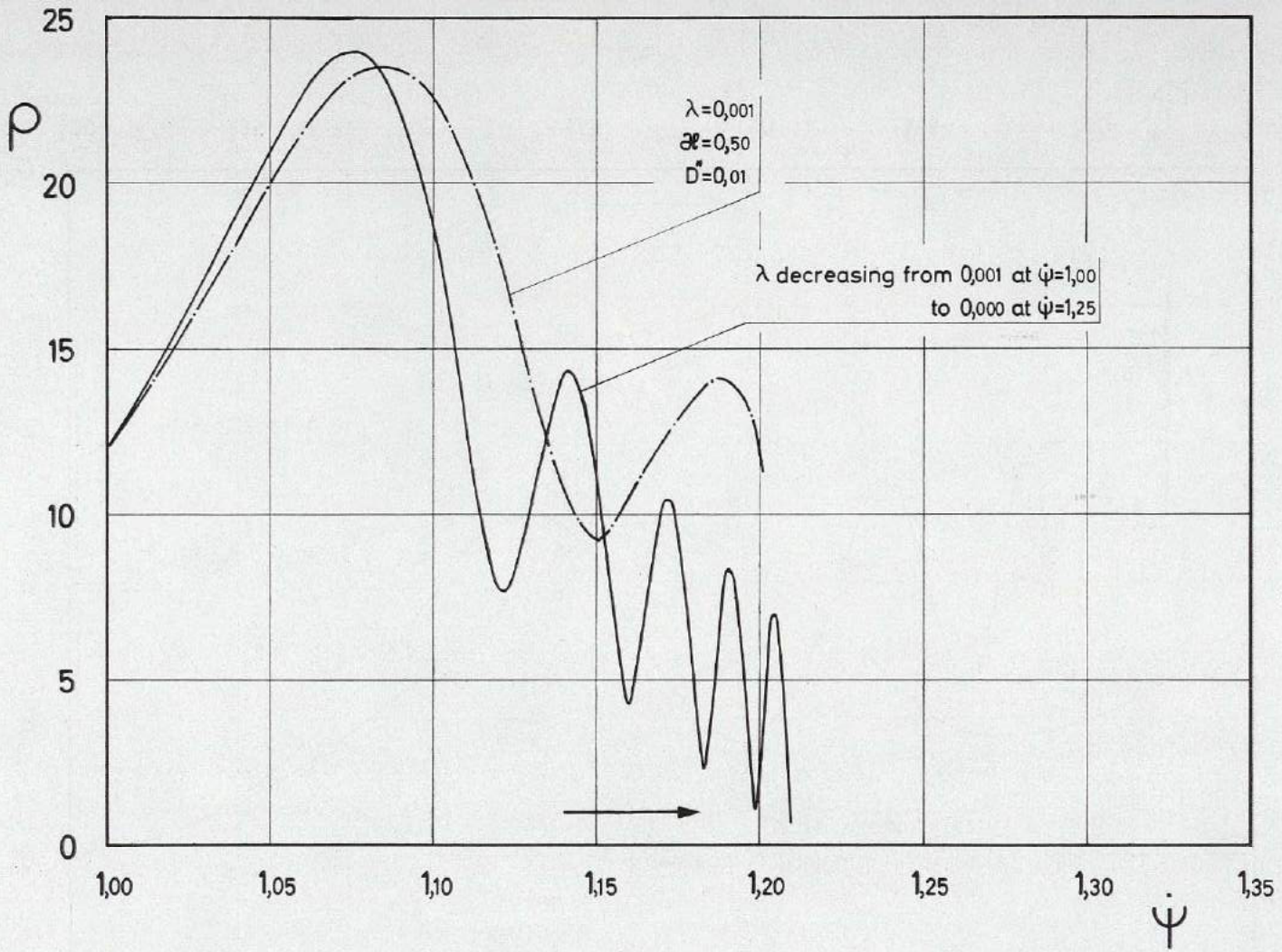

Case 2

Fig. 65.1

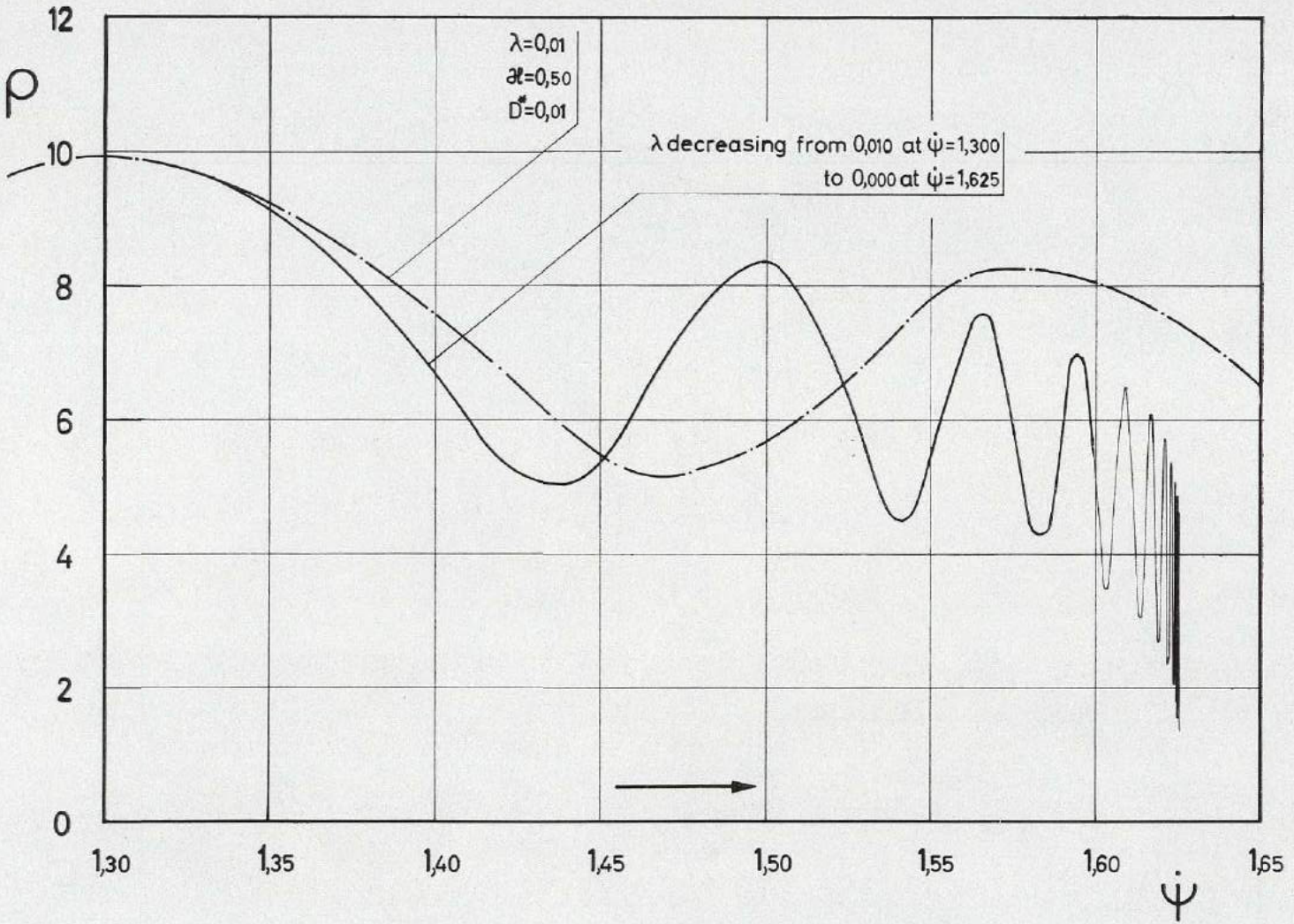

Case 3

Fig. 66.1

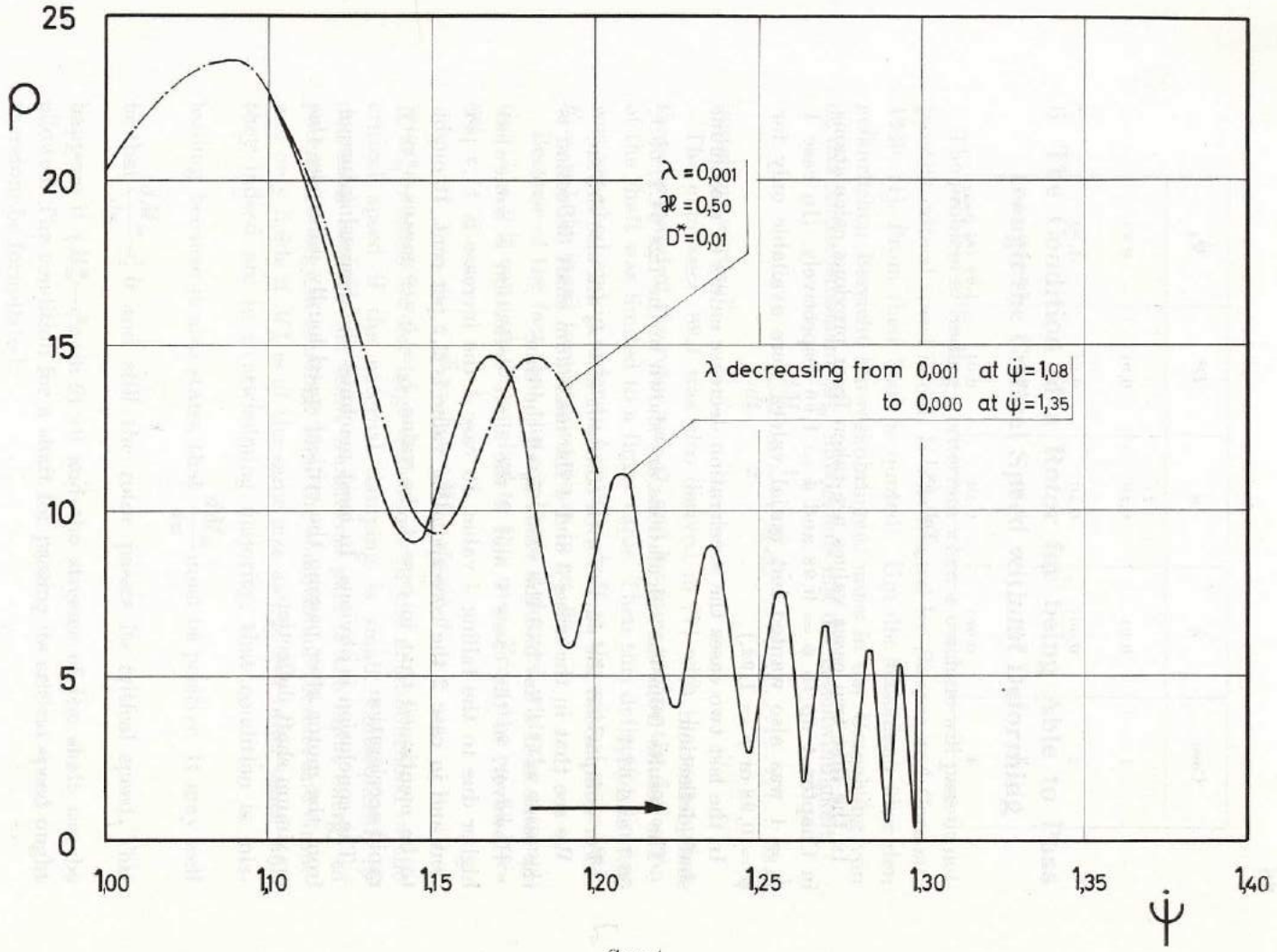

Case 4

Fig. 67.1

Case	λ	$\varkappa$	D^*	$\dot{\psi}_1$
1	0,01	0,50	0,01	0,98
2	0,001	0,50	0,01	1,00
3	0,01	0,50	0,01	1,30 (at ϱ_{max})
4	0,001	0,50	0,01	1,08 (at ϱ_{max})

Tab. 68.1

In the first two cases values are taken from previous calculations in Chapter 4 up to $\dot{\psi} = 0,98$ and $\dot{\psi} = 1,00$ respectively. (In case 1 $\dot{\psi}_1 = 1$ was also wanted but initial values were available only for $\dot{\psi} = 0,98$ or $\dot{\psi} = 1,02$.)

In the last two cases the acceleration decrease enters at maximum shaft deflection.

The results from the calculations are shown in the figs 64.1, 65.1, 66.1, and 67.1.

For comparison the curves with constant $\lambda = \lambda_0$ are also drawn.

We see that in the cases 3 and 4 the maximum shaft deflection is the same as if λ has had the value λ_0 all the time.

However, in the cases 1 and 2 the shaft deflection is somewhat higher due to the falling λ-value. In case 1 the increase is 11,3 per cent and in case 2 the corresponding value is 2,2 per cent. It ought to be mentioned that in case 1 the value $\lambda_0 = 0,010$ means a very rapid acceleration.

The conclusion is obvious. In most machines the decreasing torque from the motor after passing the critical speed hardly influences the maximum shaft deflection.

6. The Condition of a Rotor for being Able to Pass trough the Critical Speed without Deforming

The problem of finding a criterium when a machine will pass or not pass its critical speed is old. It was treated by *Biezeno* and *Grammel* 1939, [1]. From their book is quoted: „Um die Maschinen über den gefährlichen Bereicht hinwegzubringen, muss in der Umgebung von ω_c das Antriebsmoment M_{in} mindestens mit der Geschwindigkeit

$$\frac{dM_{in}}{dt} = \frac{1}{2} \cdot e^2 M \omega_c^3 \quad \ldots\ldots\ldots\ldots\ldots\ldots \quad 69.1$$

gesteigert werden".

The expression 69.1 was also derived in [7] with the assumption that the speed of the rotor was Ω_c and by some means the deflection of the shaft was limited to a finite value. Then this deflection limiter was vanished and in order to keep the shaft at the critical state with $K = +1$ the input torque must be as in eq. 69.1.

Because of the fact that the condition is derived with the assumption $\lambda = 0$ it can only be applied to this case. From the eq. 62.1 we get

$$\ddot{\psi} = 2\lambda = M_{in}^* - \varepsilon^2 \rho \sin \theta$$

If M_{in}^* is small we get large deflections in the neighbourhood of the critical speed if the external damping is small. Consequently $\ddot{\psi}$ decreases because the shaft transforms part of the input energy to potential energy in bending. Thus the condition of Biezeno and Grammel only holds if M_{in}^* is of the same size as $\varepsilon^2 \rho$. For other cases, and they indeed are in overwhelming majority, that condition is misleading because it also states that $\frac{dM_{in}}{dn}$ must be positive. It may well be that $\frac{dM_{in}}{dn} \leq 0$ and still the rotor passes its critical speed. This happens if $(M_{in}^* - \varepsilon^2 \rho \sin \theta) > 0$ and the stresses of the shaft can be allowed. The condition for a shaft for passing its critical speed ought therefore be formulated:

A shaft can run through its critical speed without danger if the maximum deflection does not create plastic deformation of the shaft.

This general rule ought to be drawn up in more concrete terms for convenience in design work. Suppose that in a piece of machinery all geometrical data and the $M-n$-curve are known. At first we calculate the critical speed ω_c. The "mean" value of λ can be calculated from the expression

$$\lambda_m = \frac{M_{in}}{2I_p\,\omega_c^2} \quad (\text{if } \varepsilon^2\rho_{max} \ll M_{in}^* \text{ which must be rechecked at the end of the calculation})$$

where $M_{\min} \leq M_{in} \leq M_{max}$ if $n_c < n_1$ in fig. 63.1 (An analogous discussion can be made for other types of $M-n$-curves).

Then the maximum shaft deflection at the disc during the acceleration through the critical speed can be taken from the curves in Sec. 4,5. If the actual values could not be found there the following approximate formula can give some help:

$$(\rho_{max})_{disc} < 1{,}2\left(\frac{1}{2}\sqrt{\frac{\pi}{\lambda}}\right)$$

This formula gives values, fair enough for practical purposes, if $\varkappa \ll 1$ and $\lambda \leq 0{,}010$. (At deceleration through the critical speed the λ-value is practically constant and one gets

$$\lambda = \frac{M_{br}}{2I_p\,\omega_c^2}$$

where M_{br} is the braking torque. Then the computation is the same as for acceleration). When ρ_{max} has been calculated the corresponding maximum bending stress of the shaft can be expressed with the aid of the eccentricity. Thus, if the force at the disc is F, we get

$$F = e \cdot \frac{(\rho_{max})_{disc}}{(\alpha_F)_{disc}}$$

and the maximum bending moment can be written

$$(M_b)_{max} = FL_M = e \cdot \frac{(\rho_{max})_{disc}}{(\alpha_F)_{disc}} \cdot L_M$$

where L_M is a length characteristic for the kind of support. With the aid of a proper strength theory (for steel the maximum strain energy theory or the maximum shear theory [11]) the maximum allowable value of e can be determined.

In Chapter 8 an actual case is treated.

7. The Action of a Deflection Limiter

It is of great practical interest to know the properties of a deflection limiter of the type shown in fig. 8.1. At first the case with constant speed and $K = +1$ is studied and then the case with acceleration. The presumptions for the arrangement are accounted for in Chapter 3.

7,1. Analysis of the Steady State

Consider the case in fig. 8.1, where the shaft whirls with an angular velocity $\Omega \frac{\text{rad}}{\text{s}}$ and the shaft rotates with the same velocity ($K = +1$).

It is assumed that no external or internal damping exist and the deflection limiter cannot cause any tangential forces.

From the eqs 14.1 and 14.3 the following is obtained

$$\left.\begin{aligned} 0 &= -\rho + \rho\dot{\psi}^2 \pm \dot{\psi}^2 - \frac{\alpha_{12}}{\alpha_{11}} \cdot N^* \\ N^* &= \frac{\alpha_{12}}{\alpha_{22}} \cdot \frac{\rho - \dfrac{\alpha_{11}}{\alpha_{12}} \cdot \Delta^*}{1 - \dfrac{\alpha_{12}^2}{\alpha_{11}\alpha_{22}}} \end{aligned}\right|$$

The upper sign is valid when $\theta = 0$ and the lower one when $\theta = \pi$. From these equations ρ and N^* can be solved and the result is

$$\left.\begin{aligned} \rho &= \frac{\Delta^* \cdot \dfrac{\xi_{12}}{\xi_{22}} \pm \dot{\psi}^2 \left(1 - \dfrac{\xi_{12}^2}{\xi_{11}\xi_{22}}\right)}{1 - \dot{\psi}^2 \left(1 - \dfrac{\xi_{12}^2}{\xi_{11}\xi_{22}}\right)} \\ \frac{N^*}{\Delta^*} &= \frac{\xi_{11}}{\xi_{22}} \cdot \frac{-1 + \dot{\psi}^2 \left(1 \pm \dfrac{\xi_{12}}{\xi_{11}} \cdot \dfrac{1}{\Delta^*}\right)}{1 - \dot{\psi}^2 \left(1 - \dfrac{\xi_{12}^2}{\xi_{11}\xi_{22}}\right)} \end{aligned}\right| \quad \ldots\ldots\ldots \quad 71.1$$

where $\xi_{ij} = \alpha_{ij} \cdot \dfrac{kEI}{L^3}$ (k is an arbitrary constant).

If $\theta = 0$ the eqs 71.1 are only valid if $N^* \geq 0$ which means

$$\frac{1}{1+\frac{\xi_{12}}{\xi_{11}} \cdot \frac{1}{\Delta^*}} \leq \dot{\psi}^2 \leq \frac{1}{1-\frac{\xi_{12}^2}{\xi_{11}\xi_{22}}}$$

and if $\theta = \pi$ a corresponding condition can be determined.

If $N^* = 0$ we of course get $\rho = \frac{\dot{\psi}^2}{|1-\dot{\psi}^2|}$. Now a special case is treated for elucidating the properties of the deflection limiter. Consider the rotor in fig. 8.1, in which $x_1 = 0{,}50$, $x_2 = 0{,}10$, and $\Delta^* = 3{,}55$. For example, with the aid of the influence numbers on page 215 in [6] we get

$$\left.\begin{aligned} \theta &= 0 \\ \rho &= \frac{25{,}028643+\dot{\psi}^2}{3{,}086896-\dot{\psi}^2} \\ N^* &= 27{,}391970 \cdot \frac{-3{,}086896+3{,}344281\,\dot{\psi}^2}{3{,}086896-\dot{\psi}^2} \\ & 0{,}960748 \leq \dot{\psi} \leq 1{,}756956 \end{aligned}\right\}$$

and

$$\left.\begin{aligned} \theta &= \pi \\ \rho &= \frac{25{,}028643-\dot{\psi}^2}{3{,}086896-\dot{\psi}^2} \\ N^* &= 27{,}391970 \cdot \frac{-3{,}086896+2{,}829511\,\dot{\psi}^2}{3{,}086896-\dot{\psi}^2} \\ & 1{,}044492 \leq \dot{\psi} \leq 1{,}756956 \end{aligned}\right\}$$

The ρ-curves are shown in fig. 74.1. Observe that if a curve has the "label" *BSG* it means that on the straight line *BSG* the centre of gravity G lies outside the shaft S and the bearing B. If the "label" is *BGS* the centre of gravity is between B and S. It can also be seen that if the shaft "deflection" ρ is greater than 12 the shaft has contact with the deflection limiter. Further, if

$$1{,}044492 < \dot{\psi} < 1{,}756956$$

the shaft has three possibilities to come into equilibrium, viz.

1) $N^*>0$; G outside B and S
2) $N^*>0$; G between B and S
3) $N^*=0$; G between B and S 73.1

It can also be concluded that the deflection limiter without friction needs external help to reach the lower curve 3) and in that way justify its name. If the rotor is not disturbed the deflection limiter just moves the critical speed to a higher value.

The N^*-curves are drawn in fig. 75.1. An interesting thing is that opposed to the rotor without a deflection limiter in this case we get that the "*BSG*-curves" and "*BGS*-curves" are valid mainly over the same range of the speed. Another thing worth mentioning is that above the speed $\dot{\psi} = 1{,}756956$ the rotor cannot have contact with the deflection limiter.

7,2. Analysis of an Accelerated Rotor

In Sec. 7,1 a special rotor was investigated with respect to the steady state. It was also obtained that the rotor within a special range of the motor speed could take different positions of equilibrium. The case is only theoretical because the absence of friction in the deflection limiter. An important task is to investigate if this friction can force the shaft to take the lower curve 3) in 74.1 after an acceleration through the critical speed. This might be the necessary disturbing factor mentioned in the previous section.

Therefore, the example was further treated. The shaft was supposed to be accelerated with $\lambda = 0{,}001$ from $\varkappa = 0{,}90$. The external damping factor D^* had the value $0{,}01$ which is a "practical" value from the tests in Chapter 4.

Three different values of the coefficient of friction were used, viz. $\mu_N = 0$, $0{,}10$, and $0{,}50$. The ρ- and N^*-curves are shown in the figs 74.1 and 75.1. If $\mu_N = 0$ we get $\rho_{max} = 54{,}1$ and if no deflection limiter had been present fig. 31.1 gives $\rho_{max} = 23{,}5$. Thus the deflection limiter here serves as a "deflection amplifier".

We can consequently make the statement, that the main property of a deflection limiter must be the capability of introducing tangential forces to the whirling of the rotor. From this also follows that the deflection limiter must not necessarily be placed close to the disc.

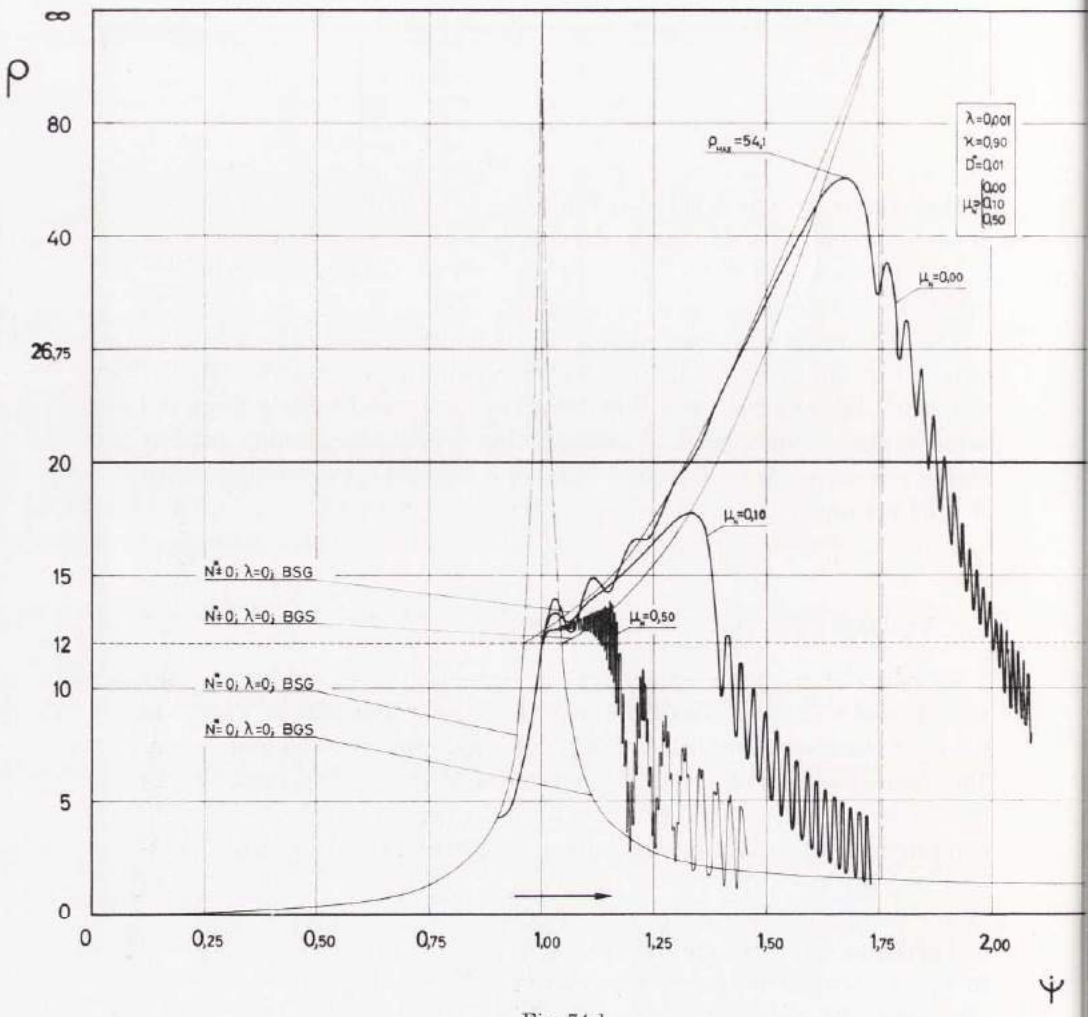

Fig. 74.1

In fig. 76.1 the velocity of the whirling is shown. From this figure and fig. 74.1 it follows that greater variations in $\dot{\varphi}$ give smaller ρ-values which agrees with the statement above. When the shaft has left the deflection limiter after the acceleration through the critical speed it whirls roughly with the critical speed ($\dot{\varphi} \approx 1$). After a long enough time $\dot{\varphi}$ may coincide with $\dot{\psi}$ if the rotor is kept with a constant speed after the acceleration. See more about this matter on page 24.

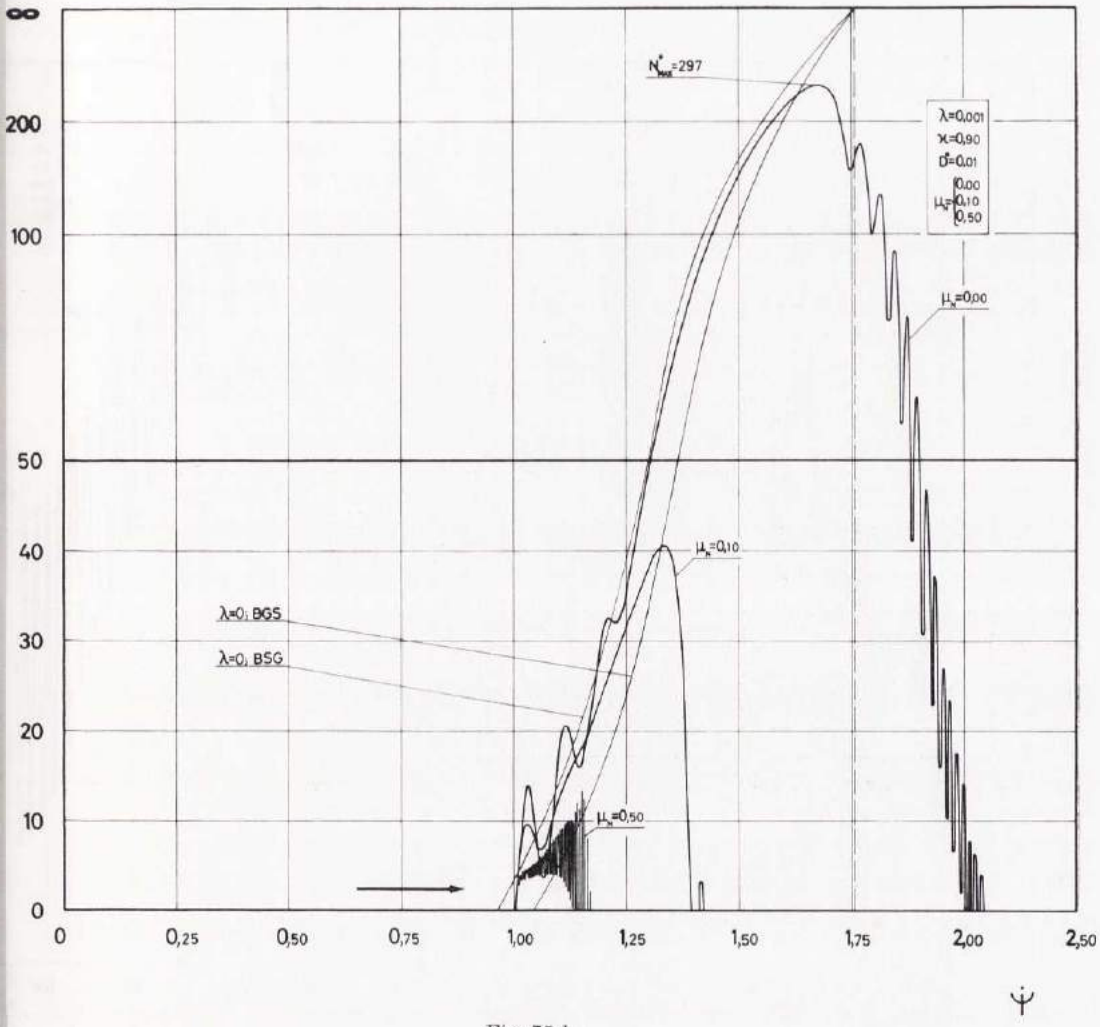
∞
200
100
50
40
30
20
10
0
0
0,25
0,50
0,75
1,00
1,25
1,50
1,75
2,00
2,50
N*max=297
λ=0,001
κ=0,90
D*=0,01
μR=0,00
0,10
0,50
μR=0,00
μR=0,10
μR=0,50
λ=0; BGS
λ=0; BSG

Fig. 75.1

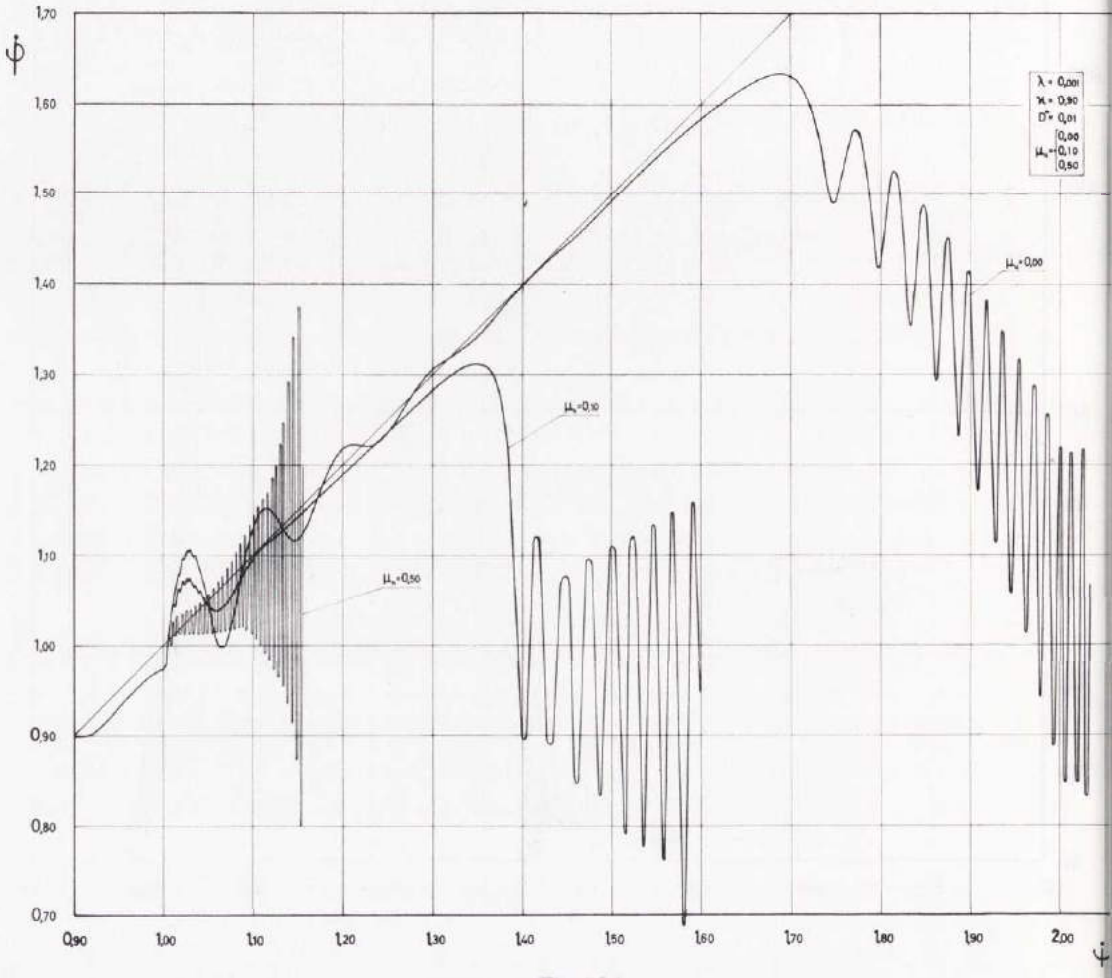
λ = 0,001
ϰ = 0,90
D* = 0,01
μ_a = 0,00 / 0,10 / 0,50
μ_a = 0,00
μ_a = 0,10
μ_a = 0,50
1,70
1,60
1,50
1,40
1,30
1,20
1,10
1,00
0,90
0,80
0,70
0,90
1,00
1,10
1,20
1,30
1,40
1,50
1,60
1,70
1,80
1,90
2,00

Fig. 76.1

8. Experimental Investigation of a Deforming Shaft

In previous parts of the present report the condition for a rotor for being able to pass its critical speed and the action of a deflection limiter have been treated. Here some tests concerning these matters are accounted for. The test apparatus in the figs 64.2, 64.3 and 64.4 in [7] was used with a vertical hinged-hinged shaft with $x_1 = 0,20$ and $x_2 = 0,16$ (See Chapter 14 in [6]). Other data were: $M = 9,87$ kg, $I_p = 0,114$ kgm^2, $e = 0,13$ mm, $L = 729$ mm, $E = 20,3 \cdot 10^{10}$ N/m^2, and $d = 15,00$ mm. The shaft was driven by an A.C. motor and the delivered input torque can be seen in fig. 79.1.

In the first test (Test 103) a deflection limiter was used and the result can be seen in fig. 79.1. After reaching a relatively high speed the shaft became "centred".

In the second test (Test 104) the deflection limiter was taken away. Now it will be checked by the theory developed in Chapter 6 if the rotor will pass its critical speed or not.

The critical speed ($K = +1$) can be calculated to 1260 r.p.m. The motor delivers ≈ 33 Nm up to the critical speed. Thus

$$\lambda_m = \frac{33}{2 \cdot 0,114 \left(\frac{\pi}{30} \cdot 1260 \right)^2} = 0,00825$$

The maximum deflection of the shaft (no damping) is

$$\rho_{max} \simeq 1,2 \left(\frac{1}{2} \sqrt{\frac{\pi}{0,00825}} \right) = 11,7$$

and thus $r_{max} = 11,7 \cdot 0,13$ mm $= 1,52$ mm. For the hinged-hinged shaft the connection between the force F and the deflection r_{max} is (with a new meaning of the notation x_2)

$$F = \frac{3}{(x_1 x_2)^2} \cdot \frac{EI}{L^3} \cdot r_{max}$$

The maximum bending torque is

$$(M_b)_{max} = \frac{3}{x_1 x_2} \cdot \frac{EI}{L^2} \cdot r_{max}$$

and then the maximum bending stress

$$(\sigma_b)_{max} = \frac{1,5}{x_1 x_2} \cdot \frac{dr_{max}}{L^2} \cdot E$$

In our case $(\sigma_b)_{max} = 82 \frac{N}{mm^2}$. For the shear stress we get

$$\tau_{max} = \frac{33 \cdot 10^3}{\frac{\pi \cdot 15^3}{16}} \frac{N}{mm^2} = 50 \frac{N}{mm^2}$$

The press fit between the shaft and the disc gave the pressure $p \approx 55 \frac{N}{mm^2}$. These stresses and the friction stresses on the surface of the shaft cannot result into yielding because the material had its "yield point" at $275 \frac{N}{mm^2}$. From this calculation we would expect the shaft to be able to pass its critical speed without plastic deformation. But this did not happen as the figs 80.1 and 81.1 show. The photo in fig. 81.1 was taken after reassembly.

The explanation may be the following.

It was derived in [7] that a rotor subjected to both external and internal damping got increasing deflections at whirling speeds higher than a certain value. This has also been observed in experimental investigations in our laboratory.

It is remarkable that the deflections of the shaft at speeds in the vicinity of the critical state was comparatively small. Hence, as the criterium stated, the shaft was able to pass the critical speed without any plastic deformation. However, valuable experience was reached. It was not sufficient to control only the possibility of the rotor to

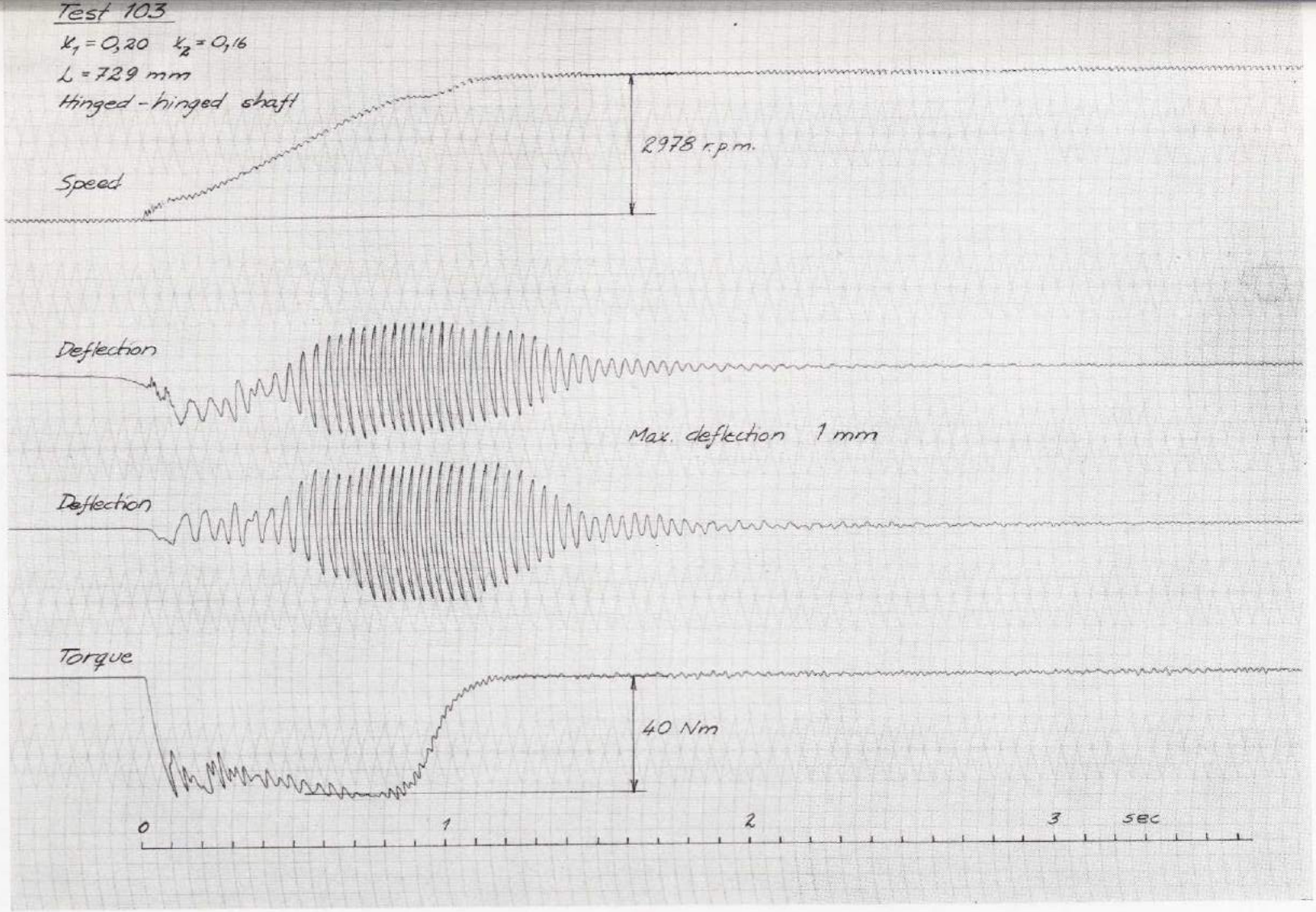
Test 103
$k_1 = 0{,}20$ $k_2 = 0{,}16$
$L = 729$ mm
Hinged - hinged shaft
Speed
2978 r.p.m.
Deflection
Max. deflection 1 mm
Deflection
Torque
40 Nm
0
1
2
3
sec

Fig. 79.1

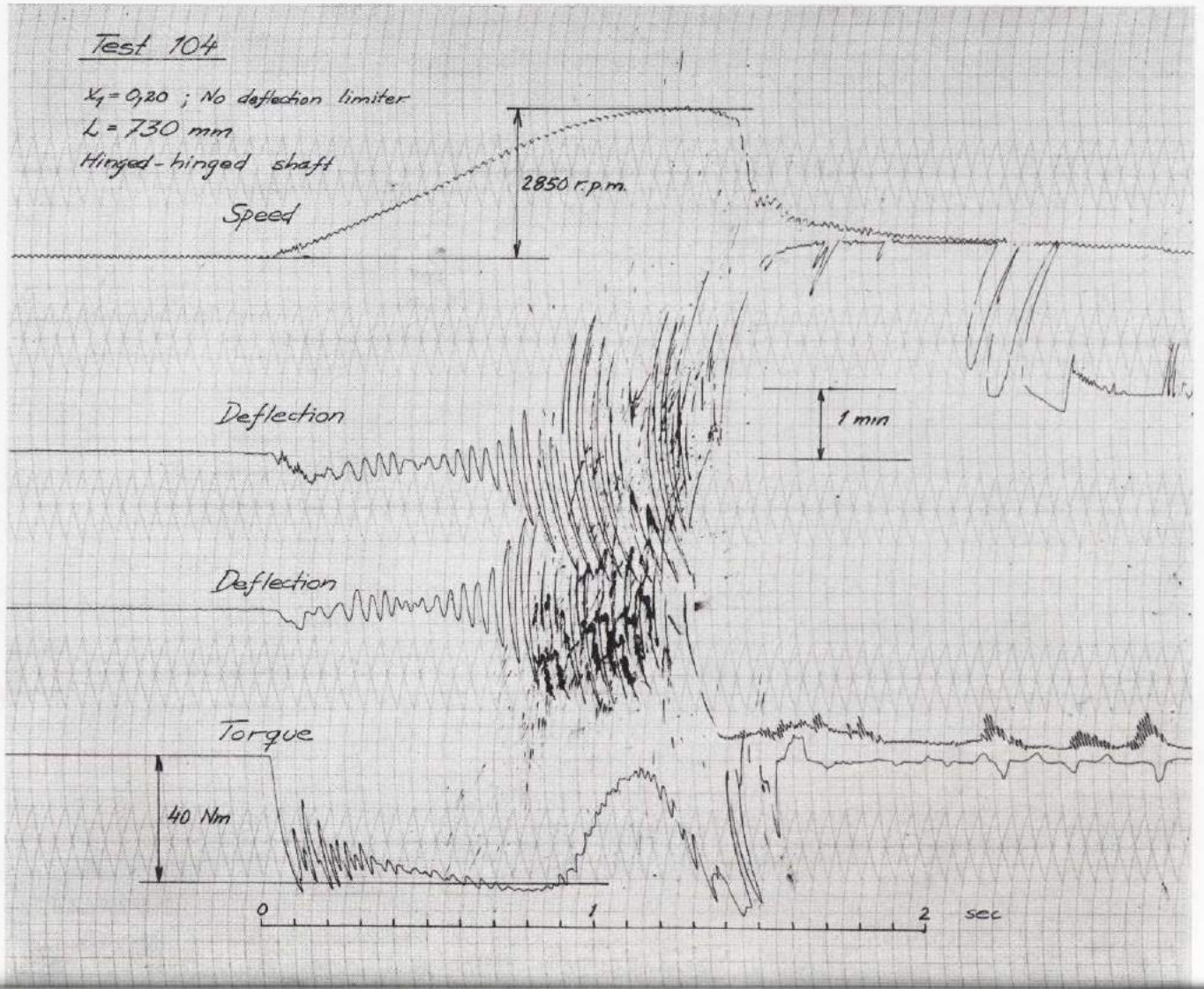
Test 104
$\chi_1 = 0{,}20$; No deflection limiter
L = 730 mm
Hinged - hinged shaft
Speed
2850 r.p.m.
Deflection
1 mm
Deflection
Torque
40 Nm
0
1
2
sec

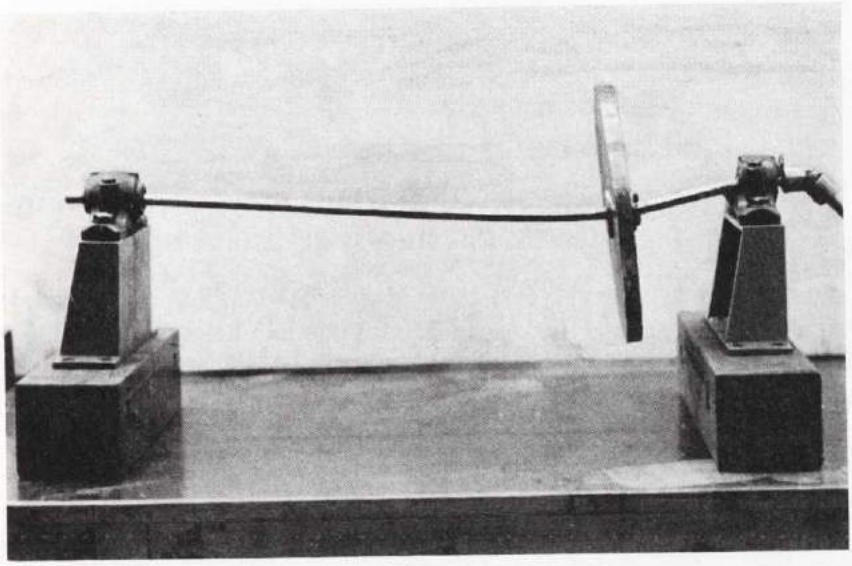

Fig. 81.1

pass the critical speed. The stability of the motion at the actual post-critical whirling speed range must also be checked. Unfortunately, the knowledge of the external and internal damping is still too little to give reliable results concerning the boundary between whirling speed zones with stable or instable motion.

9. Comparison between Two Kinds of External Damping for a Rotor Passing Its Critical Speed

In a previous report [7] two kinds of external damping were treated. This was divided into the cases when on one hand the damping force was applied in the centre of gravity G (damping coefficient denoted D^*) and on the other hand when this force was acting in the centre S of the shaft (damping coefficient denoted D_m^*). The result was that at small damping forces these two kinds gave practically the same deflection to the shaft at a constant whirling with $K = +1$.

In this section a comparison is carried out for one accelerated and one decelerated motion through the critical speed of the shaft. For the acceleration $\lambda = 0{,}001$ and $\varkappa = 0{,}90$ were valid and the corresponding values for the deceleration $\lambda = -0{,}001$ and $\varkappa = 1{,}25$. The results are shown in fig. 83.1. The difference in respect to the shaft deflection could not be shown with the aid of the present scales of the coordinate axis. The numerical values of the deflections are also collected in the tabs 82.1 and 84.1. Hence, the difference between the two damping kinds is negligible.

	$\lambda = 0{,}001$ $\quad \varkappa = 0{,}90$ $\quad \left.\begin{matrix} D^* \\ D_m^* \end{matrix}\right\} 0{,}01$	
ψ	ϱ (Damping force in S)	ϱ (Damping force in G)
0,95	5,976050	5,980778
1,00	11,723789	11,732115
1,05	20,064577	20,074509
1,10	22,368996	22,367781
1,15	9,128763	9,130788
1,20	11,385845	11,374347
1,25	10,317537	10,321366
1,30	7,377784	7,365399
1,35	2,945299	2,964159
1,40	6,205871	6,217445

Tab. 82.1

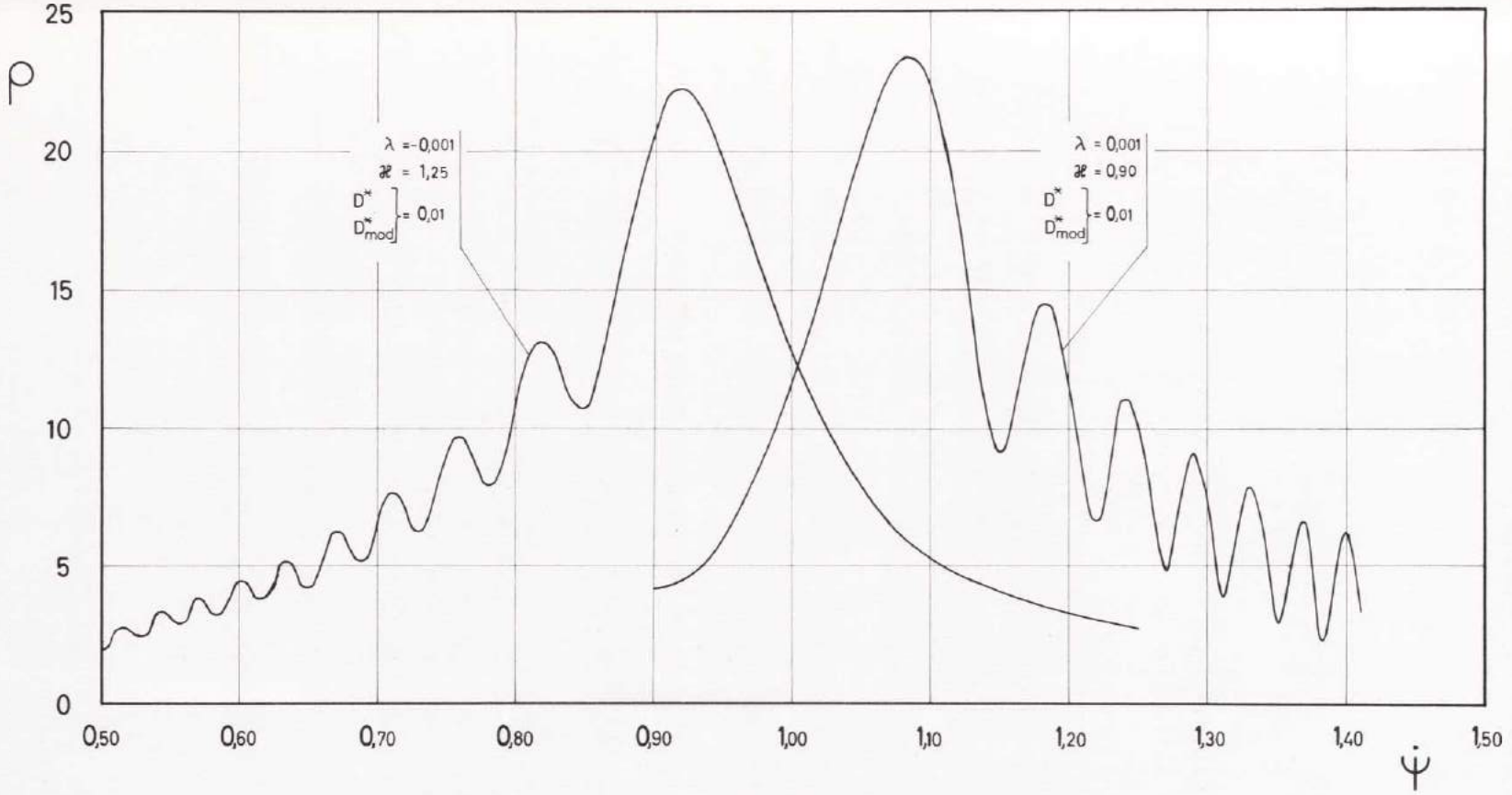
ρ
25
20
15
10
5
0
λ = -0,001
ℜ = 1,25
D*/D*mod = 0,01
λ = 0,001
ℜ = 0,90
D*/D*mod = 0,01
0,50
0,60
0,70
0,80
0,90
1,00
1,10
1,20
1,30
1,40
1,50
Ψ̇

Fig. 83.1

$\lambda = -0{,}001$	$\varkappa = 1{,}25$	$\left.\begin{matrix} D^* \\ D_m^* \end{matrix}\right\}$ 0,01
ψ	ϱ (Damping force in S)	ϱ (Damping force in G)
1,20	3,268027	3,268782
1,15	4,004923	4,006283
1,10	5,321781	5,323937
1,05	7,887847	7,891982
1,00	12,802909	12,810494
0,95	19,809962	19,819563
0,90	21,041432	21,040295
0,85	10,685050	10,686371
0,80	10,862239	10,853999
0,75	9,080750	9,075884

Tab. 84.1

10. Summary

After the introductory chapters the basic equations for the motion of an unbalanced mass point are derived in Chapter 3. Hereby the influences of external damping and a deflection limiter are considered. In Chapter 4 these differential equations are solved for the uniformly accelerated motion. Two kinds of solutions are proposed. The method mainly used in this work is a numerical step-by-step method similar to that by *Runge-Kutta* [9]. By using this method cases with varying acceleration could be treated, as shown in Chapter 5, and cases in which a deflection limiter is present, as shown in Chapter 7. In Chapter 4 a lot of different cases of constant acceleration and constant deceleration are calculated and the results are presented in diagrams which are intended to be of value for the rotor designer.

The rotor which is given a varying acceleration is treated in Chapter 5. It is shown theoretically that when the rotor has passed its critical speed a decreasing input torque hardly affects the maximum deflection of the shaft.

In Chapter 6 the necessary conditions for a rotor to be able to pass its critical speed are discussed. It is shown that the conditions available in literature may be totally misleading.

Chapter 7 deals with the properties of a deflection limiter. The calculations led to the remarkable result that the most important task for such a limiter is to introduce tangential forces to the shaft and in that way influence in the whirling. A deflection limiter without friction forces acts as an "amplifier" for the deflection of the shaft.

Chapter 9 contains a comparison of two kinds of external damping during acceleration or decleration through the critical speed of a rotor.

In the Chapters 4 and 8 experimental results are presented. The behaviour of a rotor in passing through its critical speed was studied. Two methods were used. In some cases the properties of the rotor was studied in a photographic way by means of a "slow motion camera". In that way the phase angle between the "deflection line" BS and the "unbalance line" SG (See fig. 23.1) could be visually shown. Another method for studying different qualities of the rotor was to use a recorder which registered input torque, shaft velocity and shaft deflection.

11. References

1. Biezeno-Grammel: Technische Dynamik. Julius Springer, 1939.
2. Capello, Andrea: Transients in Simple Undamped Oscillators Under Inertial Disturbances. Journal of Applied Mechanics, March, 1960.
3. Dimentberg, F. M.: Flexural Vibrations of Rotating Shafts. Butterworth's, 1961.
4. Dornig, Antongiulio: Transients in Simple Undamped Oscillators Under Inertial Dirturbances. Journal of Applied Mechanics, June, 1959.
5. Ellington, I. P. and Mc Callion, H.: On Running a Machine through its Resonant Frequency. Journal of the Royal Aeronautical Society, September 1956, Vol. 60.
6. Fernlund, I.: Critical Speeds of a Shaft with Thin Discs. Transactions of Chalmers University of Technology, Gothenburg, Sweden, 1962.
7. Fernlund, I.: On the Whirling of a Rotor. Transactions of Chalmers University of Technology, Gothenburg, Sweden, 1963.
8. Kamke, E.: Differential Gleichungen. Akademische Verlagsgesellschaft, Leipzig, 1943.
9. Kopal, Z.: Numerical Analysis. Chapman & Hall Ltd, London, 1932.
10. Lewis, F. M.: Vibration During Acceleration Through a Critical Speed. Transactions of A.S.M.E., 54, 1932.
11. Timoshenko, S.: Strength of Materials, Part II. D. van Nostrand Company, Inc., New York.
12. Watson, G. N.: Bessel Functions. Cambridge, 1944.

Forts. fr. omsl. 2:dra sida

229. GRANHOLM, HJALMAR, *Le problème de Boussinesq.* 15 s. 1960. Kr. 3: 50. (Avd. Väg- och Vattenbyggnad. Byggnadsteknik. 34.)
230. HIBA, MIODRAG, ET CEDERVALL, KRISTER, *Flambement élastique d'une barre en bois lamellée et cloúée avec le module de déplacement du moyen de liaison constant k.* 22 s. 1960. Kr. 5: —. (Avd. Väg- och Vattenbyggnad. Byggnadsteknik. 35.)
231. FLOBERG, LEIF, *The optimum thrust tilting-pad bearing.* 23 s. 1960. Kr. 5: —. (Avd. Maskinteknik. 19.)
232. FLOBERG, LEIF, *The two-groove journal bearing, considering cavitation.* 32 s. 1960. Kr. 6: —. (Avd. Maskinteknik. 20.)
233. HEDVALL, J. ARVID, *Heterogeneous catalysis, results and projects for research.* 18 s. 1961. Kr. 5: —. (Avd. Kemi och Kemisk Teknologi. 36.)
234. FLOBERG, LEIF, *Lubrication of two cylindrical surfaces, considering cavitation.* 36 s. 1961. Kr. 10: —. (Avd. Maskinteknik. 21.)
235. FLOBERG, LEIF, *Attitude-eccentricity curves and stability conditions of the infinite journal bearing.* 43 s. 1961. Kr. 11: —. (Avd. Maskinteknik 22.)
236. BEN-YAIR, M. P., *Thermometric titrations of zinc, cadmium and mercuric salts.* 11 s. 1961. Kr. 3: —. (Avd. Kemi och Kemisk Teknologi. 37.)
237. SANDFORD, F., LILJEGREN, B., AND JONSSON, B., *The resistance of bricks towards frost experiments and considerations.* 20 s. 1961. Kr. 5: —. (Avd. Kemi och Kemisk Teknologi. 38.)
238. FLOBERG, LEIF, *Experimental investigation of cavitation regions in journal bearings.* 28 s. 1961. Kr. 6: —. (Avd. Maskinteknik. 23.)
239. GRANHOLM, HJALMAR, *Sandöbrons bågställning.* 128 s. 1961. Kr. 20: —. (Avd. Väg- och Vattenbyggnad. Byggnadsteknik. 36.)
240. LINDBLAD, ANDERS, *On the design of lines for merchant ships.* 125 s. Kr. 20: —. (Avd. Skeppsbyggeri. 7.)
241. LUNDÉN, ARNOLD, *Self diffusion and the structure of molten salts.* 14 s. Kr. 4: —. (Avd. Allm. Vetenskaper. 17.)
242. LARSSON, LARS-ERIK, *Sprickbildning i vattenledningsrör av förspänd betong.* 70 s. 1961. Kr. 15: —. (Avd. Väg- och Vattenbyggnad. Byggnadsteknik. 37.)
243. ASPLUND, S. O., *A unified analysis of indeterminate structure.* 36 s. 1961. Kr. 8: —. (Avd. Väg- och Vattenbyggnad. Byggnadsteknik. 38.)
244. BRAUNSTEIN, A., *The magnetic field in iron with variable permeability.* 11 s. 1961. Kr. 3: —. (Avd. Elektroteknik. 69.)
245. FERNLUND, INGEMAR, *A method to calculate the pressure between bolted or riveted plates.* 126 s. 1961. Kr. 25: —. (Avd. Maskinteknik. 24.)
246. HEDVALL, J. ARVID, AND KARAMUSTAFAOĞLU, VURAL, *On the conservation of ancient alabaster objects.* 19 s. 1961. Kr. 5: —. (Avd. Kemi och Kemisk Teknologi. 39.)
247. EKELÖF, STIG, *A theory of the eddy current equivalent winding and its application to the closing of non-delayed telephone relays.* 35 s. 1961. Kr. 7: —. (Avd. Elektroteknik. 70.)
248. CEDERWALL, KRISTER, *Beräkning av spikade konstruktioner med hänsyn till förbandens deformationsegenskaper.* 52 s. 1961. Kr. 10: —. (Avd. Väg- och Vattenbyggnad. Byggnadsteknik. 39.)
249. KÄRRHOLM, GUNNAR, AND SAMUELSSON, ALF, *Bridge slabs with edge-beams.* 73 s. 1961. Kr. 15: —. (Avd. Väg- och Vattenbyggnad. Byggnadsteknik. 40.)
250. LOSBERG, ANDERS, *Design methods for structurally reinforced concrete pavements.* 143 s. 1961. Kr. 30: —. (Avd. Väg- och Vattenbyggnad. Byggnadsteknik. 41.)
251. EKELÖF, STIG, *Primärnormalerna för resistans och spänning vid CTH's institution för elektricitetslära och elektrisk mätteknik.* 20 s. 1961. Kr. 4: —. (Avd. Elektroteknik 71.)
252. ÅKESSON, BENGT Å., *Rationalization of Lévy's plate solution.* 135 s. 1961. Kr. 25: —. (Avd. Väg- och Vattenbyggnad. Byggnadsteknik. 42.)
253. BROGREN, GÖSTA, *A double-crystal spectrometer for work in vacuum region.* 19 s. 1961. Kr. 4 —. (Avd. Allm. Vetenskaper. 18.)
254. KIHLMAN, TOR, *Flanktransmissionens inverkan på rumsisolering mot luftljud.* 69 s. 1961. Kr. 14: —. (Avd. Väg- och Vattenbyggnad. Byggnadsteknik. 43.)
255. SVENSSON, S. IVAR, *The influence of cam curve derivative steps on cam dynamical properties.* 93 s. 1961. Kr. 25: —. (Avd. Maskinteknik. 25.)
256. HULT, JAN, *Mechanics of a beam subject to primary creep.* 20 s. 1962. Kr. 5: —. (Avd. Allm. Vetenskaper. 19.)
257. SANDFORD, FOLKE, AND HEDVALL, J. ARVID, *Concerning the cause of the colour of an amazonite preparation.* 8 s. 1962. Kr. 3: —. (Avd. Kemi och Kemisk Teknologi. 40.)
258. NILSSON, JAN, *On the structure of weak interactions.* 66 s. 1962. Kr. 15: —. (Avd. Allm. Vetenskaper. 20.)
259. STRÖM, LARS, *An absolute anemometer.* 22 s. 1962. Kr. 6: —. (Avd. Maskinteknik. 26.)

Forts. å omsl. 4:de sida

Forts. fr. omsl. 3:dje sida

260. FERNLUND, INGEMAR, *Critical speeds of a shaft with thin discs.* 224 s. 1962. Kr. 50: —. (Avd. Maskinteknik. 27.)
261. FERNLUND, INGEMAR, *On solving Reynold's equation for bearings of finite width with Fourier sine transforms.* 28 s. 1962. Kr. 7: —. (Avd. Maskinteknik. 28.)
262. AURELL, CARL G., *Physical equations from the conceptual point of view.* 52 s. 1962. Kr. 12: 50. (Avd. Elektroteknik. 72.)
263. SMITH, BENGT, *Investigation of reagents for the qualitative analysis of phenols.* 51 s. 1963. Kr. 12: 50. (Avd. Kemi och Kemisk Teknologi. 41.)
264. HULT, JAN, *Primary creep in thickwalled spherical shells.* 26 s. 1963. Kr. 8: —. (Avd. Allm. Vetenskaper. 21.)
265. STRINDEHAG, OVE, *Optimized performance of the vidicon.* 58 s. 1963. Kr. 15: —. (Avd. Elektroteknik. 73.)
266. DUBOIS, J., *An investigation of the S^{34} (p, γ) Cl^{35}-reaction.* 32 s. 1963. Kr. 8: —. (Avd. Allm. Vetenskaper. 22.)
267. DUBOIS J., AND ALBINSSON H., *Radiative proton capture in Ca^{44}.* 22 s. 1963. Kr. 6: —. (Avd. Allm. Vetenskaper. 23.)
268. DUBOIS, J., AND BROMAN L., *The Ca^{42} (p, γ) Sc^{43} reaction and the decay of Sc^{43}.* 31 s. 1963. Kr. 8: —. (Avd. Allm. Vetenskaper. 24.)
269. DUBOIS, J., *Low energy excited levels in some vanadium isotopes.* 28 s. 1963. Kr. 8: —. (Avd. Allm. Vetenskaper. 25.)
270. DUBOIS, J., *The ion beam energy stabilization system of the Van de Graaff generator at Gothenburg.* 16 s. 1963. Kr. 5: —. (Avd. Allm. Vetenskaper. 26.)
271. HEDVALL, J. ARVID, *Surface chemistry and corrosion.* 18 s. 1963. Kr. 6: —. (Avd. Kemi och Kemisk Teknologi. 42.)
272. HEDVALL, J. ARVID, *The chemistry of cement and concrete considered as a facet of the reactivity of solids.* 18 s. 1963. Kr. 6: —. (Avd. Kemi och Kemisk Teknologi. 43.)
273. ASPLUND, SVEN OLOF, *Practical calculation of suspension bridges.* 27 s. 1963. Kr. 8: —. (Avd. Väg- och Vattenbyggnad. Byggnadsteknik. 44.)
274. GRANHOLM, HJALMAR, *Träkonstruktioners brandstabilitet. Symposium vid Chalmers Tekniska Högskola den 18 juni 1962.* 151 s. 1963. Kr. 25: —. (Avd. Väg- och Vattenbyggnad. Byggnadsteknik. 45.)
275. ALBERTSSON, ÅKE, *Vindtryck på skorstenar.* 70 s. 1963. Kr. 18: —. (Avd. Väg- och Vattenbyggnad. Byggnadsteknik. 46.)
276. FERNLUND, INGEMAR, *On the whirling of a rotor.* 83 s. 1963. Kr. 20: —. (Avd. Maskinteknik. 29.)

Pris kronor 22: 50

ELANDERS BOKTRYCKERI AKTIEBOLAG
GÖTEBORG 1963

CHALMERS TEKNISKA HÖGSKOLAS HANDLINGAR
TRANSACTIONS OF CHALMERS UNIVERSITY OF TECHNOLOGY
GOTHENBURG, SWEDEN
Nr 278 (Avd. Maskinteknik 31) 1963

NOTES ON CRITICAL SPEEDS

BY

INGEMAR FERNLUND

Report No. 23 from the Institute of Machine Elements
Chalmers University of Technology
Gothenburg, Sweden
1963

Av Chalmers Tekniska Högskolas Handlingar hava tidigare utkommit:

Fullständig förteckning över Chalmers Tekniska Högskolas Handlingar
lämnas av Chalmers Tekniska Högskolas Bibliotek, Göteborg.

201. KÄRRHOLM, GUNNAR, *Influenced functions of elastic plates divided in strips.* 18 s. 1958. Kr. 4: 50. (Avd. Väg- och Vattenbyggnad. Byggnadsteknik. 28.)
202. RÅDE, LENNART, *Sampling planes for acceptance sampling by variables using the range.* 34 s. 1958. Kr. 9: 50. (Avd. Allm. Vetenskaper. 14.)
203. JAKOBSSON, BENGT, AND FLOBERG, LEIF, *The rectangular plane pad bearing.* 44 s. 1958. Kr. 5: —. (Avd. Maskinteknik. 12.)
204. ASPLUND, SVEN OLOF, *Column-beams and suspension bridges analysed by »Green's matrix».* 36 s. 1958. Kr. 7: —. (Avd. Väg- och Vattenbyggnad. Byggnadsteknik. 29.)
205. WILHELMSSON, HANS, *On the properties of the electron beam in the presence of an axial magnetic field of arbitrary strength.* 32 s. 1958. Kr. 7: 50. (Avd. Elektroteknik. 63.)
206. WILHELMSSON, HANS, *The interaction between an obliquely incident plane electromagnetic wave and an electron beam. III.* 17 s. 1958. Kr. 5: —. (Avd. Elektroteknik. 64.)
207. HEDVALL, J. ARVID, *On the influence of pre-treatment and transition processes on the adsorption capacity and the reactivity of various types of glass and silica.* 39 s. 1959. Kr. 8: —. (Institutionen för Silikatkemisk Forskning. 40.)
208. KÄRRHOLM, GUNNAR, *A flow problem solved by strip method.* 22 s. 1959. Kr. 4: 50. (Avd. Allm. Vetenskaper. 15.)
209. GRANHOLM, HJALMAR, *Allmän teori för beräkning av armerad betong.* 228 s. 1959. Kr. 20: —. (Avd. Väg- och Vattenbyggnad. Byggnadsteknik. 30.)
210. LIDIN, LARS G., *On helical-springs suspension.* 75 s. 1959. Kr. 15: —. (Avd. Maskinteknik. 13.)
211. BJÖRK, NILS, *Theory of the indirectly heated thermistor.* 46 s. 1959. Kr. 10: —. (Avd. Elektroteknik. 65.)
212. CARLSSON, ORVAR, *The influence of submicroscopic pores on the resistance of bricks towards frost.* 13 s. 1959. Kr. 3: 50. (Institutionen för Silikatkemisk Forskning. 41.)
213. GRANHOLM, HJALMAR, *KAM 40, KAM 60 och KAM 90.* 41 s. 1959. Kr. 3: 50. (Avd. Väg- och Vattenbyggnad. Byggnadsteknik. 31.)
214. JAKOBSSON, BENGT, AND FLOBERG, LEIF, *The centrally loaded partial journal bearing.* 35 s. 1959. Kr. 7: 50. (Avd. Maskinteknik. 14.)
215. FLOBERG, LEIF, *Experimental investigation of power loss in journal bearings, considering cavitation.* 16 s. 1959. Kr. 3: 50. (Avd. Maskinteknik. 15.)
216. FLOBERG, LEIF, *Lubrication of a rotating cylinder on a plane surface, considering cavitation.* 40 s. 1959. Kr. 8: —. (Avd. Maskinteknik. 16.)
217. TROEDSSON, CARL BIRGER, *The growth of the Western city during the Middle Ages.* 125 s. 1959. Kr. 19: —. (Avd. Arkitektur. 4.)
218. HEDVALL, J. ARVID, *The importance of the reactivity of solids in geological-mineralogical processes.* 11 s. 1959. Kr. 2: 50. (Institutionen för Silikatkemisk Forskning. 42.)
219. CORNELL, ELIAS, *Humanistic inquiries into architecture. I—III.* 112 s. 1959. Kr. 17: —. (Avd. Arkitektur. 5.)
220. GRANHOLM, CARL-ADOLF, *Ekonomiska aluminiumprofiler.* 48 s. 1959. Kr. 5: 50. (Avd. Väg- och Vattenbyggnad. Byggnadsteknik. 32.)
221. LUNDÉN, ARNOLD, CHRISTOFFERSON, STINA, AND LODDING, ALEX, *The isotopic effect of lithium ions in countercurrent electromigration in molten lithium bromide and iodide.* 38 s. 1959. Kr. 7: 50. (Avd. Allm. Vetenskaper. 16.)
222. INGEMANSSON, STIG, AND KIHLMAN, TOR, *Sound insulation of frame walls.* 47 s. 1959. Kr. 8: 50. (Avd. Väg- och Vattenbyggnad. Byggnadsteknik. 33.)
223. HÖGLUND, B., AND RADHAKRISHNAN, V., *A radiometer for the hydrogen line.* 25 s. 1959. Kr. 6: 50. (Avd. Elektroteknik. 66.)
224. JAKOBSSON, BENGT, *Torque distribution, power flow, and zero output conditions of epicyclic gear trains.* 55 s. 1960. Kr. 12: —. (Avd. Maskinteknik. 17.)
225. OLVING, SVEN, *Electromagnetic and space charge waves in a sheath helix.* 91 s. 1960. Kr. 17: —. (Avd. Elektroteknik. 67.)
226. STRÖMBLAD, JOHN, *Beschleunigungsverlauf und Gleichgewichtsdrehzahlen einfacher Planetengetriebe nebst Selbsthemmungsversuche.* 80 s. 1960. Kr. 18: —. (Avd. Maskinteknik. 18.)
227. SANDFORD, FOLKE, *Some current problems concerning brick manufacture.* 20 s. 1960. Kr. 5: —. (Avd. Kemi och Kemisk Teknologi. 35.)
228. OLVING, SVEN, *A new method for space charge wave interaction studies. II.* 40 s. 1960. Kr. 8: —. (Avd. Elektroteknik. 68.)

Forts. å omsl. 3:dje sida

CHALMERS TEKNISKA HÖGSKOLAS HANDLINGAR
TRANSACTIONS OF CHALMERS UNIVERSITY OF TECHNOLOGY
GOTHENBURG, SWEDEN
Nr 278 (Avd. Maskinteknik 31) 1963

NOTES ON CRITICAL SPEEDS

BY

INGEMAR FERNLUND

Report No. 23 from the Institute of Machine Elements
Chalmers University of Technology
Gothenburg, Sweden
1963

SCANDINAVIAN UNIVERSITY BOOKS
AKADEMIFÖRLAGET-GUMPERTS · GÖTEBORG

SCANDINAVIAN UNIVERSITY BOOKS

Denmark: MUNKSGAARD, *Copenhagen*
Norway: UNIVERSITETSFORLAGET, *Oslo, Bergen*
Sweden: AKADEMIFÖRLAGET-GUMPERTS, *Göteborg*
SVENSKA BOKFÖRLAGET/Norstedts-Bonniers, *Stockholm*

Manuscript received by the Publications Committee,
Chalmers University of Technology, Oct. 4th, 1962

PRINTED IN SWEDEN BY
ELANDERS BOKTRYCKERI AKTIEBOLAG, GÖTEBORG 1963

Preface

Of the research on elastic rotors that has been carried out at the *Institute of Machine Elements, Chalmers University of Technology, Gothenburg, Sweden*, three previous reports have been published, [2], [3], and [4].

The present report is a continuation, mainly of the first report, [2].

I wish to express my sincere thanks to the *Swedish Technical Research Council* for their sponsorship and to Professor *B. Jakobsson*, the Head of the Institute, for valuable suggestions and helpful criticism. Some of the calculations have been done on the digital computer *Alwac III E* in Gothenburg.

Ingemar Fernlund
Tekn. lic.
Research Assistent at the Institute
of Machine Elements

Contents

1. Introduction

This report deals with some special problems concerning rotors. In [2] the general equation for a rotating shaft considering the mass and the gyroscopic effect of the shaft was derived. But in the applications the gyroscopic effect of the shaft was neglected. Here this effect is considered for a clamped-free shaft.

In the summary of [2] it was pointed out that "it would be of great value to scrutinize different bearing arrangements available from the manufacturers concerning spring constants". In this report some results in this field are presented.

In [2] a "New Dunkerley formula" was proposed for predicting the lowest critical speed of a rotor in a rapid way. The accuracy of this formula is here narrowly investigated both theoretically and experimentally.

The theoretical treatment is based on the opportunity of using the exact solution for a hinged-hinged shaft with two equal and symmetrically mounted discs. The gyroscopic effect of the shaft being neglected.

In the last chapter the properties of a perfectly balanced rotor are investigated. Especially some energy aspects are closely considered.

2. Notation

A	Arbitrary constant. Force. Bearing
B	Arbitrary constant. Force. Bearing
C	Arbitrary constant. Constant depending on the lateral stiffness of a bearing. Bearing
D	Arbitrary constant
E	Modulus of elasticity in tension and compression. Energy. Bearing
F	Constant. Force. Bearing
$F_1, F_2 \ldots F_5$	Functions
G	Bearing
H_1, H_2, H_3, H_4	Functions
I	Moment of inertia of a cross section $[L^4]$
I_p	Polar moment of inertia of a disc $[ML^2]$
I_e	Equatorial moment of inertia of a disc $[ML^2]$
$K = \frac{\omega}{\Omega}$	Ratio
L	Length of a shaft
M	Mass of a disc. Bending moment. Torque (Index shows the intended thing)
N	R.p.m. of the whirling motion
b	Bearing width
c	Lateral stiffness of a bearing
c_M	Angular stiffness of a bearing
d	Diameter of a shaft
Δd	Diametral clearance of a journal bearing
f, f_1, f_{21}, f_θ	Coefficients
f_1, f_2, f_3, f_4	Functions
i	Number of order
k_c, k_h	Functions of λ
m	Mass of a shaft
n	R.p.m. of a motor

r	Radius
s	Number of order
x	Running coordinate
x_1, x_2, x_3	Non-dimensional lengths
y	Coordinate
$\theta^* = \frac{2\gamma I_p}{mL^2}$	Non-dimensional moment of inertia
$\theta_M = \frac{EI}{cL^3}$	Non-dimensional quantity characteristic for the lateral stiffness of a bearing
$\Lambda = \frac{kEI}{ML^3\Omega^2}$	Non-dimensional critical speed
Ω	Angular velocity of the whirling
$\gamma = \frac{1}{2}\left(\frac{\omega}{\Omega} - \frac{I_e}{I_p}\right)$	Constant
δ	Deflection
$\varkappa_1$	Non-dimensional length
$\varkappa_0 = \frac{EI}{Lc_M}$	Non-dimensional quantity characteristic for the angular stiffness of a bearing
$\lambda = \left(\frac{mL^3\Omega^2}{EI}\right)^{1/4}$	Non-dimensional constant
$\mu_i = M_i/M_{\text{ref}}$	Non-dimensional weight of a disc
$\nu = \frac{2\gamma I_p}{ML^2}$	Non-dimensional moment of inertia
ξ	Non-dimensional influence number concerning displacements
$\varrho = k_c\lambda$	Argument
$\sigma = k_h\lambda$	Argument
$\varphi = x_1\lambda$	Argument
φ_{0i}	Angle of bearing of order i
$\psi = x_3\lambda$	Argument
ω	Angular velocity of a motor (shaft) $\left(\frac{\text{rad}}{\text{s}}\right)$

Indices:

appr	With reference to an approximate value
cc	With reference to a clamped-clamped case
D	With reference to Dunkerley's formula

exact	With reference to an exact value
F	With reference to a force
g	With reference to the gyroscopic effect
hh	With reference to a hinged-hinged case
kin	With reference to kinetic energy
osc	With reference to an oscillation
pot	With reference to potential energy
ref	With reference to a reference mass
rot	With reference to a rotation
*	With reference to values of the critical speeds obtained from an "exact" formula in which the mass and the gyroscopic effect of the shaft are neglected
**	With reference to values of the critical speeds obtained from an "exact" formula in which the gyroscopic effect of the shaft is neglected
1	With reference to a mass of order 1
2	With reference to a mass of order 2

3. Critical Speeds of a Clamped-Free Shaft Considering the Gyroscopic Action of the Shaft

In Chapter 9 of [2] the equation for determining the critical speeds for a clamped-free shaft was derived. However, the action of the gyroscopic effect of the shaft was neglected. In this chapter this matter is considered. The dimensions of the rotor are shown in fig. 10.1.

Notations:

I_p Polar moment of inertia of the disc
L Length of the shaft
m Mass of the shaft
M Mass of the disc
r Constant radius of the shaft

From Chapter 9 in [2] the equation for the elastic line is

$$y = A \sin \lambda k_c \xi + B \operatorname{sh} \lambda k_h \xi + D \cos \lambda k_c \xi + F \operatorname{ch} \lambda k_h \xi$$

where

$$\left.\begin{matrix} k_h \\ k_c \end{matrix}\right\} = \sqrt{\sqrt{1 + \left[\frac{\gamma}{2}\left(\frac{r}{L}\right)^2 \lambda^2\right]^2} \pm \frac{\gamma}{2}\left(\frac{r}{L}\right)^2 \lambda^2} \quad \ldots\ldots\ldots 9.1$$

and

$$\left.\begin{aligned} \gamma &= \frac{1}{2}\left(\frac{\omega}{\Omega} - \frac{1}{2}\right) \\ \lambda^4 &= \frac{mL^3\Omega^2}{EI} \end{aligned}\right\}$$

Further

ω = the angular velocity of the shaft
Ω = the angular velocity of the whirling motion

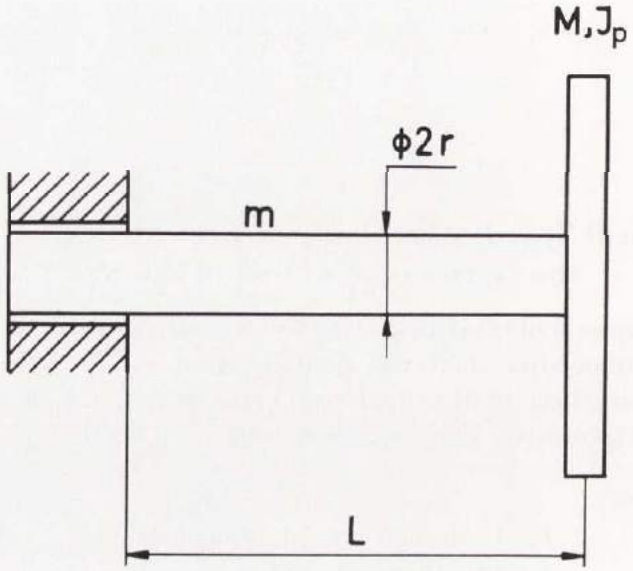

Fig. 10.1

The boundary conditions are

$$\left.\begin{array}{ll} \xi = 0 \quad y = 0 & \\ & \dfrac{dy}{d(\xi L)} = 0 \end{array}\right\} \text{ and } \left.\begin{array}{ll} \xi = 1 \quad EI\dfrac{d^2y}{d(\xi L)^2} + 2\gamma I_p \Omega^2 & \dfrac{dy}{d(\xi L)} = 0 \\ -EI\dfrac{d^3y}{d(\xi L)^3} + \gamma\Omega^2\dfrac{m}{L}r^2 & \dfrac{dy}{d(\xi L)} = My\Omega^2 \end{array}\right\}$$

The conditions at $\xi = 1$ can also be written

$$\left.\begin{array}{l} \dfrac{d^2y}{d\xi^2} + \theta^*\lambda^4 \cdot \dfrac{dy}{d\xi} = 0 \\ -\dfrac{d^3y}{d\xi^3} + \nu\lambda^4 \cdot \dfrac{dy}{d\xi} = \dfrac{M}{m} \cdot \lambda^4 y \end{array}\right\}$$

where

$$\left.\begin{array}{l} \theta^* = \dfrac{2\gamma I_p}{mL^2} \\ \nu = \gamma\left(\dfrac{r}{L}\right)^2 \end{array}\right\}$$

The four boundary conditions give four equations.

The condition for these equations for not having only trivial solutions is

$$\frac{m}{M} = \lambda \cdot \frac{F_1+\theta^*\lambda^3 F_2}{F_3+\nu\lambda^2 F_4+\theta^*\lambda^3 F_5} \quad \ldots\ldots\ldots\ldots \quad 11.1$$

where

$$\left.\begin{aligned}
F_1 &= (k_c^2+k_h^2)\sin\lambda k_c \mathrm{ch}\lambda k_h-(1+k_c^2)\cos\lambda k_c \mathrm{sh}\lambda k_h \\
F_2 &= (k_h-k_c^3)\sin\lambda k_c \mathrm{sh}\lambda k_h+2k_c(1-\cos\lambda k_c \mathrm{ch}\lambda k_h) \\
F_3 &= k_c^3+k_h^3-(k_h-k_c^3)\sin\lambda k_c \mathrm{sh}\lambda k_h+2k_c\cos\lambda k_c \mathrm{ch}\lambda k_h \\
F_4 &= 2k_c\sin\lambda k_c \mathrm{sh}\lambda k_h-(k_h-k_c^3)(1-\cos\lambda k_c \mathrm{ch}\lambda k_h) \\
F_5 &= (1+k_c^4)\sin\lambda k_c \mathrm{ch}\lambda k_h+(k_c^2+k_h^2)\cos\lambda k_c \mathrm{sh}\lambda k_h
\end{aligned}\right\}$$

If the gyroscopic effect of the shaft is neglected we have $\nu = 0$ and thus $k_c = k_h = 1$. In this case eq. 11.1 is transformed into eq. 106.2 in [2].

On the other hand if $M = 0$ and $\theta^* = 0$ we get

$$F_3+\nu\lambda^2 F_4 = 0$$

This equation can also be written

$$2f^2+f(1-f^2)\sin\varrho\mathrm{sh}\sigma+(1+f^4)\cos\varrho\mathrm{ch}\sigma = 0 \quad \ldots\ldots \quad 11.2$$

where

$$\left.\begin{aligned}
f &= \frac{k_c}{k_h} = k_c^2 \\
\varrho &= k_c\lambda \\
\sigma &= k_h\lambda
\end{aligned}\right\}$$

Further from eq. 9.1

$$\sigma^2-\varrho^2 = \nu(\sigma\varrho)^2 \quad \ldots\ldots\ldots\ldots\ldots\ldots \quad 11.3$$

Because of

$$\Omega^2 = (\sigma\varrho)^2 \cdot \frac{EI}{mL^3}$$

the solution can be obtained from the intersection points between the functions 11.2 and 11.3.

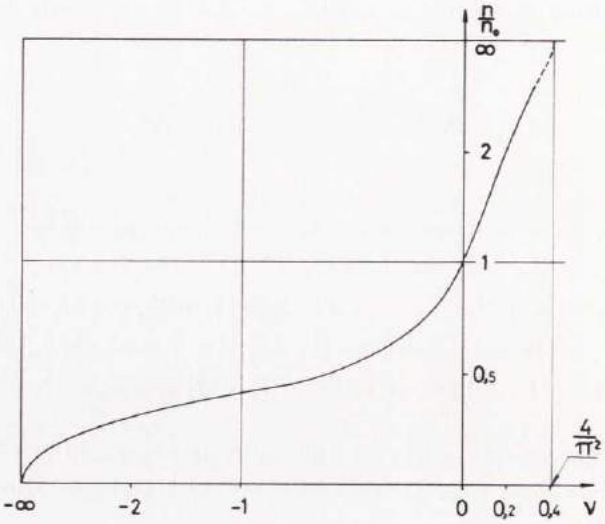

Fig. 12.1

If $\sigma \to \infty$ we get

$$\left.\begin{aligned} \cos \varrho &= 0 \\ \nu &= \frac{1}{\varrho^2} \end{aligned}\right\}$$

and from here $\nu = \left(\frac{2}{\pi}\right)^2$. If $\nu > \left(\frac{2}{\pi}\right)^2$ no solution exists. In Chapter 13 of [2] the corresponding condition for a hinged-hinged shaft was shown to be $\nu > \left(\frac{1}{\pi}\right)^2$ and this condition is in general valid for a shaft with two bearings [6].

With the aid of an electronic computer the eq. 11.2 was solved with ν as a parameter. Only the first critical speed was calculated and the result is shown in fig. 12.1 and tab. 13.1. If $\nu = 0$ the corresponding λ-value and critical speed are denoted λ_0 and n_0 respectively.

When the shaft is equipped with discs the influence of the gyroscopic action of the shaft must be relatively smaller.

In this connection something must be said about the result that no critical speeds will occur if ν exceeds a certain value. In the analysis

ν	λ	n/n_0
−20,0	0,5913	0,0994
−10,0	0,7016	0,1400
− 4,0	0,8763	0,2184
− 2,0	1,0308	0,3022
− 1,8	1,0558	0,3171
− 1,6	1,0842	0,3343
− 1,4	1,1169	0,3548
− 1,2	1,1551	0,3795
− 1,0	1,2009	0,4102
− 0,8	1,2574	0,4497
− 0,6	1,3303	0,5033
− 0,4	1,4305	0,5820
− 0,2	1,5841	0,7137
± 0	1,8751	1,0000
0,02	1,9211	1,0496
0,04	1,9723	1,1064
0,06	2,0298	1,1718
0,08	2,0948	1,2480
0,10	2,1685	1,3374
0,12	2,2523	1,4428
0,14	2,3477	1,5677
0,16	2,4560	1,7156
0,18	2,5783	1,8906
0,20	2,7154	2,0971
0,24	3,0421	2,6321
0,26	3,2407	2,9870
0,30	3,7644	4,0304
0,32	4,1416	4,8786
0,34	4,3148	5,2952

Tab. 13.1

the shear deformation in the infinitely small parts of the shaft was neglected. *Dimentberg* [1] has shown that by taking this deformation into consideration the shaft has an infinitely number of forward and reverse critical states.

4. Influence of the Angular Stiffness of Bearings on Critical Speeds

In this chapter the influence of the angular bearing stiffness is treated for rotors consisting of one disc on a shaft between or outside two bearings. The bearings are rigid in lateral directions and the gyroscopic actions as well as the mass of the shaft are neglected. At first the rotor in fig. 15.1 is studied.

The angular stiffnesses of the bearings are c_{M1} and c_{M2}. Other notations are evident from fig. 15.1. The equilibrium gives

$$\left.\begin{aligned} A+B &= F \\ AL-Fx_2L-c_{M1}\varphi_{01}+c_{M2}\varphi_{02} &= 0 \end{aligned}\right\}$$

The equation for the elastic line gives

$$-EI\,\frac{d^2y}{d(xL)^2} = AxL-c_{M1}\varphi_{01}-\underset{x>x_1}{/}\,FL(x-x_1)$$

The boundary conditions are

$$\left.\begin{aligned} x=0 \quad y=0 \quad \frac{dy}{d(xL)} &= \varphi_{01} \\ x=1 \quad y=0 \quad \frac{dy}{d(xL)} &= -\varphi_{02} \end{aligned}\right\}$$

From this it can be derived that

$$x_{F11} = \frac{1}{6}\left\{-(x_1x_2)^3+3x_1x_2[x_1^2(1+2\varkappa_{01})-(x_1+2\varkappa_{01})]\cdot\frac{x_2^2(1+2\varkappa_{02})-(x_2+2\varkappa_{02})}{1+4(\varkappa_{01}+\varkappa_{02})+12\varkappa_{01}\varkappa_{02}}\right\}\frac{L^3}{EI} \qquad 14.1$$

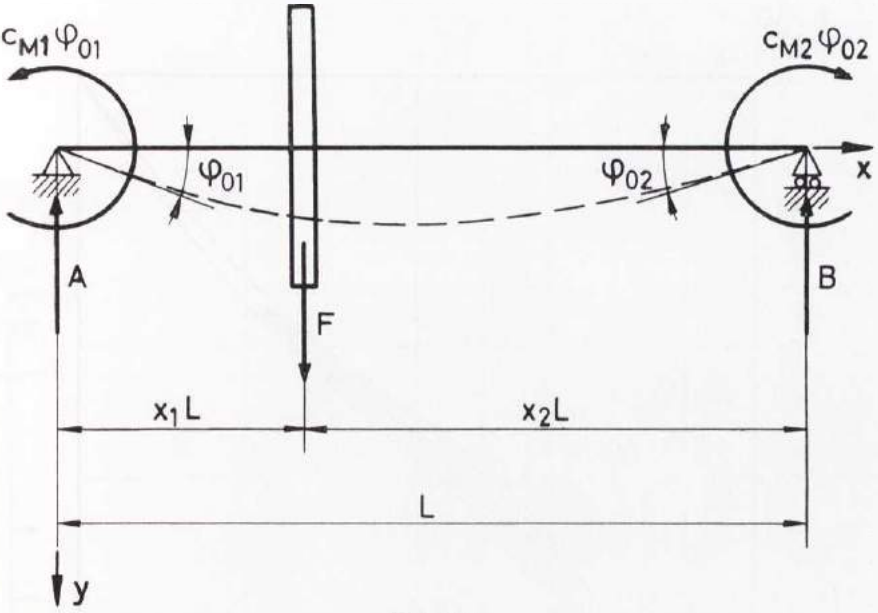

Fig. 15.1

Observe that the same expression is obtained if x_1 and $\varkappa_{01}$ are changed to x_2 and $\varkappa_{02}$ and vice versa. Further

$$\left.\begin{aligned}\varkappa_{01} &= \frac{EI}{Lc_{M1}}\\ \varkappa_{02} &= \frac{EI}{Lc_{M2}}\end{aligned}\right\}$$

If $\xi_{F11} = \alpha_{F11} \cdot \dfrac{EI}{L^3}$, $\varkappa_{01} = \varkappa_{02} = \infty$ we get $\xi_{F11} = \dfrac{(x_1x_2)^2}{3}$, and if $\varkappa_{01} = \infty$ and $\varkappa_{02} = 0$ we get $\xi_{F11} = \dfrac{(x_1x_2)^2}{12}(x_1x_2+3x_2)$ and, finally, if $\varkappa_{01} = \varkappa_{02} = 0$ we get $\xi_{F11} = \dfrac{(x_1x_2)^3}{3}$. These results are in accordance with the results in Chapter 14 of [2]. If $c_{M1} = c_{M2}$ we have $\varkappa_{01} = \varkappa_{02} = \varkappa_0$ and thus

$$f_1 = \frac{\xi_{F11}}{(\xi_{F11})_{\varkappa_0=\infty}} = x_1x_2+3\varkappa_0 \cdot \frac{2(2\varkappa_0+1)(1-x_1x_2)-1}{(2\varkappa_0+1)(6\varkappa_0+1)} \quad \ldots\ldots \text{15.2}$$

This function is drawn in fig. 16.1.

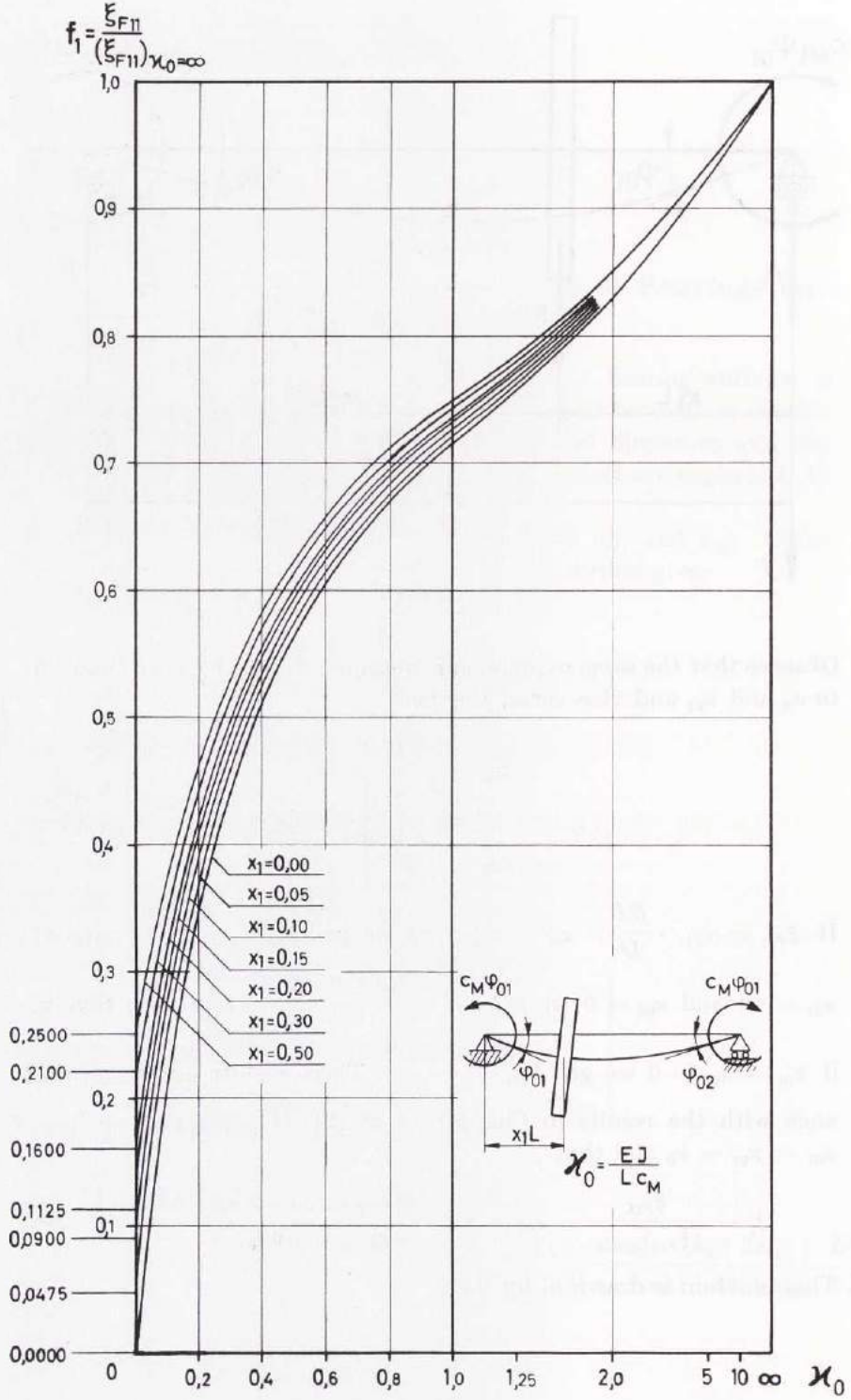
$f_1 = \frac{\xi_{F1}}{(\xi_{F11})_{\varkappa_0=\infty}}$
1,0
0,9
0,8
0,7
0,6
0,5
0,4
0,3
0,2500
0,2100
0,2
0,1600
0,1125
0,1
0,0900
0,0475
0,0000
0
0,2
0,4
0,6
0,8
1,0
1,25
2,0
5
10
∞
$\varkappa_0$
$x_1=0,00$
$x_1=0,05$
$x_1=0,10$
$x_1=0,15$
$x_1=0,20$
$x_1=0,30$
$x_1=0,50$
$c_M\varphi_{01}$
$c_M\varphi_{01}$
φ_{01}
φ_{02}
$x_1 L$
$\varkappa_0 = \frac{EJ}{L c_M}$

Fig. 16.1

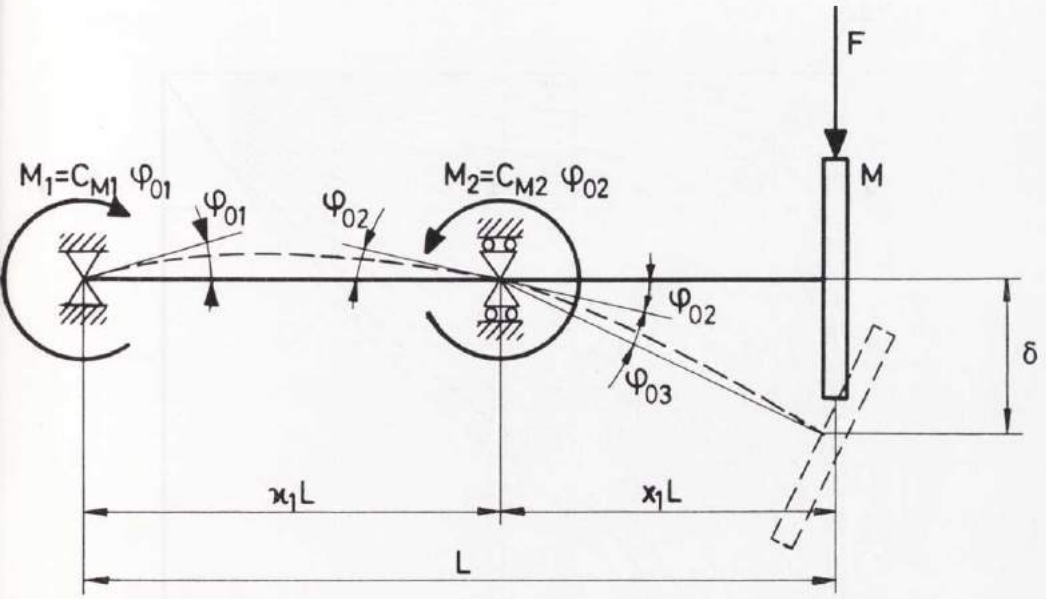

Fig. 17.1

Further, from [2], the critical whirling speed is $\Omega \frac{\text{rad}}{\text{s}}$ where

$$\left.\begin{aligned} \Omega &= \frac{30}{\pi}\sqrt{\frac{1}{A}\cdot\frac{EI}{ML^3}} \\ A &= \xi_{F11} \end{aligned}\right\}$$

Now turn over to the case in fig. 17.1.

From the theory of elasticity we get

$$\left.\begin{aligned} \varphi_{01} &= -\frac{M_1\varkappa_1 L}{3EI} - \frac{(M_2 - Fx_1L)\varkappa_1 L}{6EI} \\ \varphi_{02} &= -\frac{M_1\varkappa_1 L}{6EI} - \frac{(M_2 - Fx_1L)\varkappa_1 L}{3EI} \\ \varphi_{03} &= \frac{F(x_1L)^2}{3EI} \end{aligned}\right\} \quad \ldots\ldots\ldots \quad 17.2$$

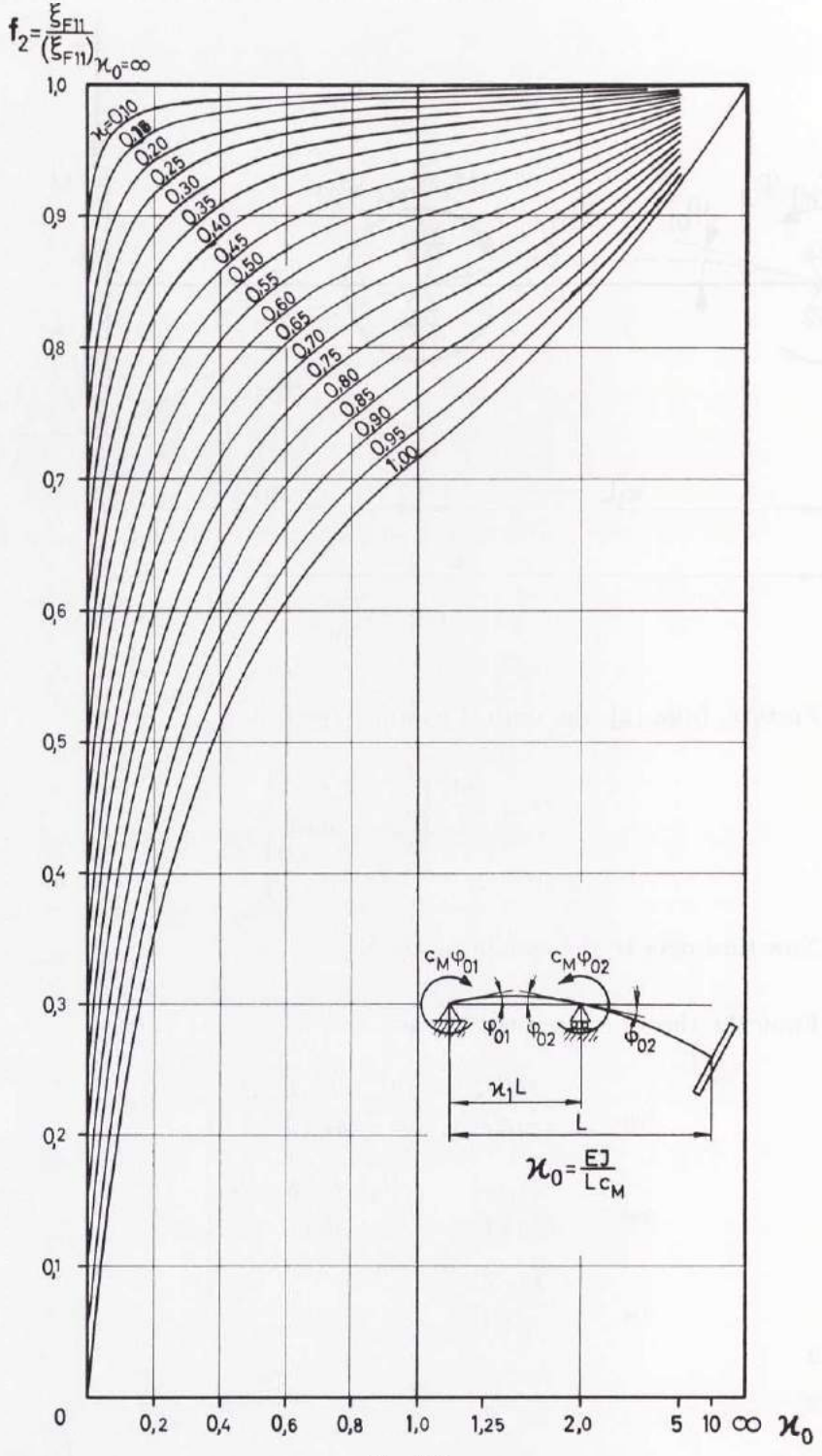
$f_2=\frac{\xi_{F11}}{(\xi_{F11})_{\varkappa_0=\infty}}$
1,0
0,9
0,8
0,7
0,6
0,5
0,4
0,3
0,2
0,1
0
$\varkappa=0,10$
0,15
0,20
0,25
0,30
0,35
0,40
0,45
0,50
0,55
0,60
0,65
0,70
0,75
0,80
0,85
0,90
0,95
1,00
0,2
0,4
0,6
0,8
1,0
1,25
2,0
5
10
∞
$\varkappa_0$
$c_M\varphi_{01}$
$c_M\varphi_{02}$
φ_{01}
φ_{02}
φ_{02}
$\varkappa_1 L$
L
$\varkappa_0=\frac{EJ}{Lc_M}$

Fig. 18.1

Further, we have the deflection

$$\delta = \alpha_{F11} F = \xi_{F11} \cdot \frac{L^3}{EI} \cdot F = (\varphi_{02} + \varphi_{03}) x_1 L$$

With $M_1 = c_{M1}\varphi_{01}$, $M_2 = c_{M2}\varphi_{02}$, and $c_{M1} = c_{M2} = c_M$ we get

$$\xi_{F11} = \frac{x_1^3}{3} + \varkappa_0 \varkappa_1 x_1^2 \cdot \frac{4\varkappa_0 + \varkappa_1}{(2\varkappa_0 + \varkappa_1)(6\varkappa_0 + \varkappa_1)}$$

where $\varkappa_0 = \dfrac{EI}{Lc_M}$. Here is seen that $(\xi_{F11})_{\varkappa_0 = \infty} = \dfrac{x_1^2}{3}$ and thus

$$f_2 = \frac{\xi_{F11}}{(\xi_{F11})_{\varkappa_0 = \infty}} = x_1 + 3\varkappa_1 \varkappa_0 \cdot \frac{4\varkappa_0 + \varkappa_1}{(2\varkappa_0 + \varkappa_1)(6\varkappa_0 + \varkappa_1)}$$

This function is drawn in fig. 18.1.

The results obtained are used in connection with some practical investigations of bearings described in the next chapter.

5. Experimental Investigation of the Angular Stiffness of Some Types of Bearings

In the summary of [2] it was pointed out that it would be valuable to determine the spring constants of different bearing arrangements available from the manufacturers. Here the results from such an investigation are presented. The test apparatus is shown in fig. 21.1.

Notations:

A, B	Tested bearings
C	Disc
D	Variator
E, F	Couplings
G	"Tachometer disc"
K	Capacitive "pick up"
N	Amplifier
O	Optical "pick up"
P	Rectifier, amplifier
R	Recorder

The shaft was driven by an A.C. motor and the speed of the shaft could be changed to any value between 500 r/m and 4300 r/m with the variator. The disc could be mounted anywhere between the bearings or outside bearing B.

The speed of the shaft was measured by an optical pick-up and the deflections of the disc by a capacitive pick-up. The speed of the shaft and the deflection of the disc were registered on a recorder. From the charts also the whirling speed could be calculated.

As has been shown in [4] that the maximum shaft deflection at an acceleration through the critical speed occurs at a higher speed than the critical. Also the whirling speed is slightly higher on that

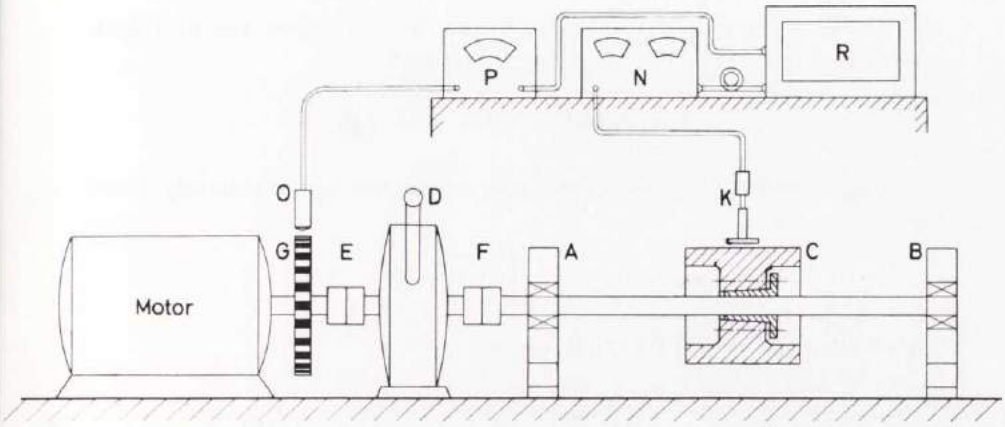

Fig. 21.1

occasion. The best result is obtained by taking an average value of the whirling speed over a range just before the speed corresponding to the maximum shaft deflection.

The bearings were mounted in standard bearing houses from SKF. Only one rough critical speed was obtained in every arrangement which implies that the stiffness of the bearings can be assumed to be the same in all directions.

The following bearings were investigated:

Ⓐ	Single row deep groove ball bearing	SKF	6205
Ⓑ	Cylindrical roller bearing	SKF	NU 205
Ⓒ	Double row angular contact ball bearing	SKF	3205
Ⓓ	Self-aligning ball bearing	SKF	1205
Ⓔ	Spherical roller bearing	SKF	22205
Ⓕ	Full journal bearing	$b/d = 1$; $\psi = \frac{\Delta d}{d} = 3{,}54\ ‰$	
Ⓖ	Full journal bearing	$b/d = 2$; $\psi = \frac{\Delta d}{d} = 3{,}87\ ‰$	

(b = width of the bearing; d = diameter of the bearing; Δd = diametral clearance).

At first there is discussion of the case when the disc is mounted between two similar bearings. From Chapter 6 in [2] it is found that

the non-dimensional critical speed for a rotor with one disc and with lateral springs at the bearings can be written

$$\Lambda = \theta_M[x_1C_2 - x_2(x_1 - C_1)] + \xi_F$$

If we consider a slight gyroscopic action we approximately have to add the term

$$-\nu\xi_F\left(\frac{\xi_M}{\xi_F}\right)^2$$

(See Chapter 12 in [2]). Thus we get

$$\Lambda = \xi_F - \xi_F\nu\left(\frac{\xi_M}{\xi_F}\right)^2 + \theta_M[x_1C_2 - x_2(x_1 - C_1)]$$

If the effect of angular stiffness is also taken into account from eq. 15.2 we get

$$\Lambda = f_1\xi_F - \xi_F\nu\left(\frac{\xi_M}{\xi_F}\right)^2 + \theta_M[x_1C_2 - x_2(x_1 - C_1)]$$

If $\varkappa_0 = \infty$, $\theta_M = 0$, and $\nu = 0$ we have

$\Lambda = \Lambda_{hh} = \xi_F$ (Indices hh refer to *h*inged-*h*inged shaft).

Thus, because of $\frac{\Lambda}{\Lambda_{hh}} = \left(\frac{n_{hh}}{n}\right)^2 = f$,

$$f = f_1 - \nu\left(\frac{\xi_M}{\xi_F}\right)^2 + \theta_M \cdot \frac{x_1C_2 - x_2(x_1 - C_1)}{\xi_F}$$

Denote $f_\theta = \frac{x_1C_2 - x_2(x_1 - C_1)}{\xi_F}$ and we have

$$f_1 = f + \nu\left(\frac{\xi_M}{\xi_F}\right)^2 - \theta_M f_\theta \quad \ldots\ldots\ldots\ldots\ldots \quad 22.1$$

In the tests the following data were valid:

$M = 10{,}0$ kg, $I_p = 3{,}81 \cdot 10^4$ kg mm², $d = 15{,}0$ mm, and $L = 750$ mm. Thus

$$\nu = \frac{1}{2} \cdot \frac{I_p}{ML^2} = \frac{1}{2} \cdot \frac{381}{10{,}0 \cdot (75{,}0)^2} = 0{,}0034$$

In tab. 23.1 the ratio $|\xi_M/\xi_F|$ is shown for the six basic bearing arrangements in Chapter 14 of [2].

	Case 1	Case 2	Case 3	Case 4	Case 5	Case 6
$\left\|\frac{\xi_M}{\xi_F}\right\|$	$\left\|\frac{3}{2}\cdot\frac{1}{x_1}\right\|$	$\left\|\frac{1}{x_1}-\frac{1}{x_2}\right\|$	$\left\|\frac{3}{2}\left(\frac{1}{x_1}-\frac{1}{x_2}\right)\right\|$	$\left\|\frac{3(x_1x_2-3x_1+1)}{(x_1+3)x_1x_2}\right\|$	$\frac{1}{2}+\frac{1}{x_1}$	$\frac{3(1+x_1)}{x_1(3+x_1)}$

Tab. 23.1

In tab. 23.2 the term $(\xi_M/\xi_F)^2$ is given for the actual values x_1.

x_1	$\left(\frac{\xi_M}{\xi_F}\right)^2$					
	Case 1	Case 2	Case 3	Case 4	Case 5	Case 6
0,10	225,0	—	—	—	110,3	113,3
0,20	56,25	14,06	31,64	10,76	30,25	31,64
0,25	36,00	7,111	16,00	4,639	20,25	21,30
0,50	9,000	0,000	0,000	0,7347	6,250	6,612
0,75	4,000	7,111	16,00	20,55	3,361	3,424
0,80	3,516	14,06	31,64	37,43	3,063	3,155
0,90	2,778	—	—	—	2,596	2,637

Tab. 23.2

Now turn to the lateral spring effect. From [2] we have

$$\left.\begin{aligned} \theta_M &= \frac{EI}{cL^3} \quad (\text{if } k=1) \\ \frac{1}{c} &= \frac{1}{c_1}+\frac{1}{c_2} \\ C_1 &= \frac{c}{c_1};\ C_2 = \frac{c}{c_2} \end{aligned}\right\}$$

If $c_1 = c_2$ we have $c = \frac{c_1}{2}$, $C_1 = C_2 = \frac{1}{2}$. For a *hinged-hinged* shaft is $\xi_F = \frac{(x_1 x_2)^2}{3}$. In that way we get

$$\left.\begin{aligned} f_\theta &= \frac{3}{2} \cdot \frac{1-2x_1x_2}{(x_1x_2)^2} \\ \theta_M &= 2 \cdot \frac{EI}{c_1 L^3} \end{aligned}\right\} \quad \ldots\ldots\ldots\ldots\ldots\ldots \quad 24.1$$

In tab. 24.2 the actual values of f_θ are shown.

x_1	0,20	0,25	0,50
f_θ	39,59	26,50	12,00

Tab. 24.2

If $c_1 = \frac{c_2}{2}$ we instead get $c = \frac{c_1}{1,5}$, $C_1 = \frac{2}{3}$, $C_2 = \frac{1}{3}$ with the corresponding

$$\left.\begin{aligned} f_\theta &= \frac{1+x_2-3x_1x_2}{(x_1x_2)^2} \\ \theta_M &= 1,5 \cdot \frac{EI}{c_1 L^3} \end{aligned}\right\} \quad \ldots\ldots\ldots\ldots\ldots\ldots \quad 24.3$$

In formula 22.1 f can be determined because n_{hh} can be calculated and n obtained from the test. With the aid of the tab. 23.2 the term $\nu \left(\frac{\xi_M}{\xi_F}\right)^2$ can be estimated and from the eq. 24.1 or 24.3 the factor f_θ. However, θ_M cannot be calculated with any degree of accuracy. The spring constant c_1 is of a complicated nature because it is composed of spring effects in the bearing itself, in the bearing house, and in the support of the bearing house. Thus from eq. 22.1 we want to calculate f_1, but θ_M is unknown. If we carry out two tests we can determine θ_M because of the fact that we use the same $\varkappa_0$ in the two cases. We consequently have to solve a system of equations with two unknowns. The solution procedure is simplified by using fig. 16.1.

The results from the tests with the disc between the bearings are shown in tab. 26.1. It also contains the critical speed for a hinged-

hinged shaft (n_{hh}) and for a clamped-clamped shaft (n_{cc}). With the aid of these values, which are boundary values for a rotor laterally rigidly supported, one gets a conception of the accuracy of these common methods to calculate the critical speeds. Further, we need n_{hh} to get f in eq. 22.1.

For every assembly the critical speed was experimentally determined five times. In the table only the minimum, the maximum, and the mean value are shown together with the standard deviation.

If, as an example, we study bearing arrangement Ⓐ we get three equations (f is calculated from the mean values of n and n_{hh}). The gyroscopic term is choosen according to Case 2 in tab. 23.2. Thus

$$\left.\begin{aligned} f_1(x_1 = 0{,}50) &= 0{,}620 - 12{,}0\theta_M \\ f_1(x_1 = 0{,}25) &= 0{,}731 - 26{,}5\theta_M \\ f_1(x_1 = 0{,}20) &= 0{,}732 - 39{,}6\theta_M \end{aligned}\right\}$$

Combining the first and the second equations one gets $\varkappa_0 = 0{,}25$, $\theta_M = 0{,}010$, and from the first and the third equation $\varkappa_0 = 0{,}35$, $\theta_M = 0{,}005$, and finally from the second and the third equation $\varkappa_0 = 0{,}90$, $\theta_M = 0{,}000$.

The same procedure was carried out for the other bearings and the result can be seen in tab. 25.1.

Bearing case Ⓐ		Bearing case Ⓑ		Bearing case Ⓓ		Bearing case Ⓔ	
$\varkappa_0$	θ_M	$\varkappa_0$	θ_M	$\varkappa_0$	θ_M	$\varkappa_0$	θ_M
0,90	0,000	2,0	0,005	2,0	0,005	8,7*	0,002
0,35	0,005	1,7	0,008	1,7	0,008	1,7	0,007
0,25	0,010	1,0	0,008	0,52	0,012	0,93	0,015

Tab. 25.1

For bearing Ⓔ the $\varkappa_0$-value 8,7 differs very much from the others. If instead of the average values of n_{hh} and n the maximum and the minimum values respectively are used we get $\varkappa_0 = 1{,}7$ and $\theta_M = 0{,}006$. Hence $\varkappa_0$ may vary very much for small changes of f. Further, it seems practically reasonable that θ_M may vary slightly between the different types of bearing as also can be seen from the table. That is why the mean value $\theta_M = 0{,}005$ is used in the following for bearing Ⓐ and $\theta_M = 0{,}007$ for the other ball and roller bearings. These values are used when calculating $\varkappa_0$ in the tables. The last figure in $\varkappa_0$ is not granted.

Bearing arrangement	x_1	n_{min} n_{mv} n_{max}	Standard deviation	n_{hh} n_{cc}	$\varkappa_0$	c_M Nm/rad
Ⓐ SKF 6205 ($\theta_M = 0{,}005$)	0,50	883 908 923	16	715 ± 8 1430 ± 15	0,36	1830
	0,25	1121 1133 1145	8	953 ± 14 2201 ± 39	0,48	1370
	0,20	1330 1351 1365	13	1117 ± 14 2792 ± 61	0,36	1830
Ⓑ SKF NU 205 ($\theta_M = 0{,}007$)	0,50	745 751 758	4	715 ± 8 1430 ± 15	1,61	408
	0,25	962 985 1000	16	953 ± 14 2201 ± 39	1,05	626
	0,20	1073 1097 1112	15	1117 ± 14 2792 ± 61	1,37	480
Ⓒ SKF 3205 ($\theta_M = 0{,}007$)	0,50	1023 1080 1124	35	715 ± 8 1430 ± 15	0,11	5970
Ⓓ SKF 1205 ($\theta_M = 0{,}007$)	0,50	750 757 770	7	715 ± 8 1430 ± 15	1,46	450
	0,25	991 999 1008	8	953 ± 14 2201 ± 39	1,05	626
	0,20	1086 1094 1100	5	1117 ± 17 2792 ± 61	1,51	435
Ⓔ SKF 22205 ($\theta_M = 0{,}007$)	0,50	738 749 777	15	715 ± 8 1430 ± 15	1,69	389
	0,25	956 959 960	2	953 ± 14 2201 ± 39	1,77	371
	0,20	1100 1123 1135	12	1117 ± 17 2792 ± 61	1,14	576

Tab. 26.1

If the disc is mounted outside the bearings the eq. 22.1 is still valid but now instead

$$f_\theta = \frac{3}{2} \cdot \frac{1+x_1^2}{(x_1 \varkappa_1)^2} \quad \ldots\ldots\ldots\ldots\ldots\ldots \quad 27.1$$

This expression is correct only if the lateral stiffness is the same in both of the bearings and it can be derived from formula 41.1 in [2] if l_1 is replaced by $\frac{1}{\varkappa_1}$. In this case $\xi_F = \frac{x_1^2}{3}$ (see Chapter 14 in [2]). The gyroscopic term is calculated according to Case 6 in tab. 23.2. and also here θ_M is estimated to be 0,005 for bearing Ⓐ and 0,007 for the other bearings if the disc is mounted relatively far from the bearings.

The results of these tests are shown in tab. 28.1. When the disc is mounted near one end of the shaft the forces on the bearings are relatively great at the critical speed. Because the SKF bearings have progressive spring constants (see [7]) the total spring constant will also increase in value.

In the tables consequently the θ_M-value is decreased by 50 % when $x_1 = 0,10$. Because of the fact that the results obtained in that way seem to coincide with the previous values this estimate seems reasonable.

No journal bearings were used in the previous tests because of the difficulty in mounting them properly when they were situated far from each other. Instead they were tested together with a self-aligning ball bearing. At one end of the shaft the self-aligning ball bearing was mounted and at the other end the test bearing. The preceding tests have shown that the self-aligning bearing has a tendency to cause small bending moments in the shaft. Here for simplicity this property of this bearing is not taken into account and all angular stiffness is referred to the journal bearing. Further, the journal bearing with $b/d = 1$ is estimated to have $\theta_M = 0,007$ (as the self-aligning ball bearing) and the journal bearing with $b/d = 2$ half the value. With these assumptions one can get a rough conception of the journal bearings with respect to their property of causing bending moments in the shaft.

At first interest is turned to the case when the disc is mounted between the bearings. By putting $\varkappa_{01} = \infty$ and $\varkappa_{02} = \varkappa_0$ in eq. 14.1 we get

$$f_{11} = \frac{\xi_F}{(\xi_F)_{\varkappa_{01}=\infty}} = 1 + \frac{1}{4} \cdot \frac{x_2(x_1+3)-4}{1+3\varkappa_0}$$

Bearing arrangement	x_1	n_{min} n_{mv} n_{max}	Standard deviation	n_{hhf} n_{cf}	$\varkappa_0$	c_M Nm/rad
Ⓐ SKF 6205	0,25	795 817 852	24	715±12 1430±28	0,73	900
	0,20	897 911 925	9	893±16 1998±44	0,27	2430
Ⓑ SKF NU 205	0,25	703 720 728	9	715±12 1430±28	0,55	1190
	0,20	955 968 975	8	893±16 1998±44	0,21	3130
	0,10	2015 2047 2073	26	1787±45 5651±230	0,25 (θ_M=0,0035)	2630
Ⓓ SKF 1205	0,25	720 734 742	8	715±12 1430±28	0,45	1460
	0,20	833 843 851	19	893±16 1998±44	0,95	692
	0,10	1930 1994 2014	28	1787±45 5651±230	0,30 (θ_M=0,0035)	2190
Ⓔ SKF 22205	0,25	701 705 711	3	715±12 1430±28	0,51	1290
	0,20	976 978 986	4	893±16 1998±44	0,19	3460
	0,10	1938 1960 1998	23	1787±45 5651±230	0,35 (θ_M=0,0035)	1880

Tab. 28.1

and from here

$$\varkappa_0 = \frac{4f_{11} - x_1 x_2 - 3x_2}{12(1-f_{11})} \quad \ldots\ldots\ldots\ldots\ldots\ldots \quad 28.2$$

Further, the eq. 22.1 is still valid if f_1 is now replaced by f_{11}. The gyroscopic term is estimated as a mean value from the cases 2 and

4 in tab. 23.2. Thus f_{11} can be determined at first and then $\varkappa_0$ is obtained from eq. 28.2.

The results from these tests are shown in tab. 29.2. Finally, tests were carried out for the same bearing combinations but the disc was mounted outside the journal bearing. From the eqs 17.2 we get with $M_1 = 0$ that

$$f_{21} = \frac{\xi_F}{(\xi_F)_{\varkappa_0=\infty}} = \frac{x_1^2}{3}\left(1 - \frac{\varkappa_1^2}{\varkappa_1+3\varkappa_0}\right)$$

and from here

$$\varkappa_0 = \frac{\varkappa_1[\varkappa_1-(1-f_{21})]}{3(1-f_{21})} \quad \ldots\ldots\ldots\ldots\ldots\ldots \quad 29.1$$

Also in this case eq. 22.1 is valid if f_1 is replaced by f_{21} and f_θ is taken from eq. 27.1. The gyroscopic term is estimated as a mean value from the cases 1 and 5 in tab. 23.2. At first f_{21} is determined and then $\varkappa_0$ is calculated from eq. 29.1. The results are shown in the tabs 29.2 and 30.1.

Bearing arrangement	x_1	n_{min} n_{mv} n_{max}	Standard deviation	n_{hh} n_{hc}	$\varkappa_0$	c_M Nm/rad
Ⓕ and Ⓓ	0,50	962 974 984	8	715± 8 1081±13	0,014	47000
	0,75	1340 1367 1390	5	953±14 1969±35	0,057	11500
	0,80	1605 1618 1630	9	1117±17 2562±51	0,046	14300
Ⓖ and Ⓓ	0,50	1011 1022 1034	8	715± 8 1081±13	−0,004	∞
	0,75	1648 1657 1655	7	953±14 1969±35	0,002	329000
	0,80	2103 2110 2115	6	1117±17 2562±51	−0,001	∞

Tab. 29.2

Bearing arrangement	x_1	n_{min} n_{mv} n_{max}	Standard deviation	n_{hhf} n_{cf}	$\varkappa_0$	c_M Nm/rad
Ⓕ	0,25	1072 1091 1115	14	715±12 1430±28	−0,013	∞
and						
Ⓓ	0,20	1242 1280 1334	30	893±16 1998±44	0,003	219000
Ⓖ	0,25	1022 1038 1058	14	715±12 1430±28	0,027	24300
and						
Ⓓ	0,20	1425 1454 1515	31	893±16 1998±44	−0,016	∞

Tab. 30.1

5,1. **Conclusions**

The results from the different tests are collected in tab. 30.2. Only the mean values are shown.

c_M in Nm/rad for the bearing						
Ⓐ	Ⓑ	Ⓒ	Ⓓ	Ⓔ	Ⓕ	Ⓖ
1830	408	5970	450	389	47000	∞
1370	626	—	626	371	11500	329000
1830	480	—	435	576	14300	∞
900	1190	—	1460	1290	∞	24300
2430	3130	—	692	3460	219000	∞
—	2630	—	2190	1880	—	—

Tab. 30.2

The bearings Ⓑ, Ⓓ, and Ⓔ seem to have a progressive "angular" spring stiffness. The high values were obtained when the disc was mounted outside the bearings and in these cases the inclination of the shaft at the bearing at the critical speed was also higher than in the cases when the disc was mounted between the bearings. This effect cannot be seen so clearly from the tests for bearing Ⓐ. However, somewhat surprisingly, this bearing was stiffer than the bearings Ⓑ, Ⓓ,

and Ⓔ when the disc was mounted between the bearings. The bearing Ⓒ had the greatest stiffness of the SKF bearings. It is remarkable that the bearings Ⓐ, Ⓑ, Ⓓ, and Ⓔ on the whole give rise to bending moment. This may, to some extent, depend on the gyroscopic effects of the balls and the rollers.

Finally, the journal bearings seem to have a nearly infinite angular stiffness. It can also be seen that this property of the journal bearing increases in strength with increasing b/d-value.

In the treatment of the test results the factor θ_M in many cases was estimated to 0,007. This value corresponds to a spring constant of about 335 $\frac{N}{mm}$ which is very low in comparison with that of an SKF bearing alone [7]. The grease film between moving parts in the bearings is probably of great influence on the lateral spring stiffness.

6. Influence of the Simultaneous Action of the Mass of the Shaft and the Gyroscopic Effect of the Discs in a Rotor with Two Discs

In [2] the critical speeds for a rotor with one disc were determined considering the mass of the shaft and the gyroscopic action of the disc. In this chapter the critical speeds for a rotor with two equal discs are determined with the same considerations. The arrangement is shown in fig. 32.1.

Notations:

I_p Polar moment of inertia of the disc
L Length of the shaft
m Mass of the shaft
M Mass of one disc

The two discs are symmetrically placed on the shaft. We limit ourselves to symmetrical deflection modes of the shaft.

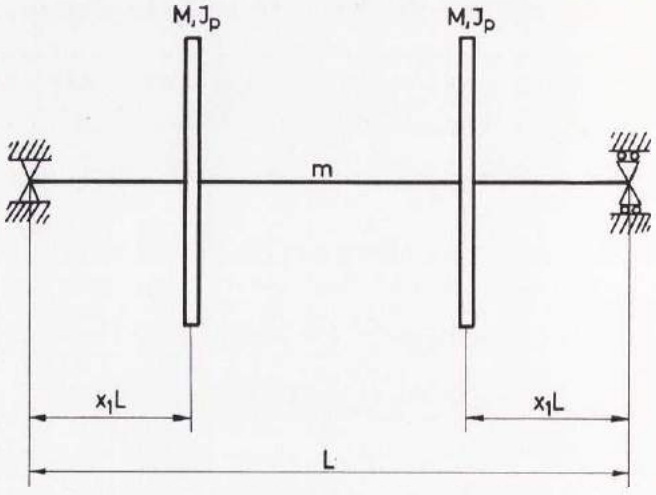

Fig. 32.1

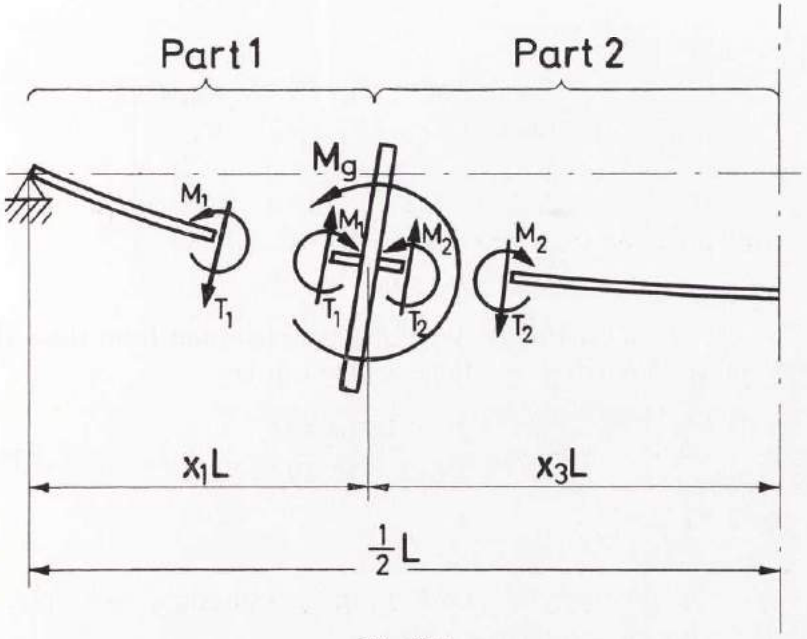

Fig. 33.1

In fig. 33.1 the forces and moments on a disc are drawn at the first critical speed.

The equation for the elastic line of part 1 is (see [2])

$$y_1 = A_1 \sin \lambda\xi_1 + B_1 \mathrm{sh}\lambda\xi_1 + D_1 \cos \lambda\xi_1 + E_1 \mathrm{ch}\lambda\xi_1$$

and for part 2

$$y_2 = A_2 \sin \lambda\xi_2 + B_2 \mathrm{sh}\lambda\xi_2 + D_2 \cos \lambda\xi_2 + E_2 \mathrm{ch}\lambda\xi_2$$

The boundary conditions are

$$\left.\begin{aligned} \xi_1 = 0 \quad y_1 &= 0 \\ \frac{d^2 y_1}{d\xi_1^2} &= 0 \end{aligned}\right\}$$

$$\left.\begin{aligned} \xi_2 = 0 \quad \frac{dy_2}{d\xi_2} &= 0 \\ \frac{d^3 y_2}{d\xi_2^3} &= 0 \end{aligned}\right\}$$

and

$$\left.\begin{aligned} \xi_1 &= x_1 & T_1+T_2 &= My_1\Omega^2 \\ \xi_2 &= x_3 = \tfrac{1}{2}-x_1 & M_1-M_2 &= M_g \\ & & y_1 &= y_2 \\ & & \frac{dy_1}{d\xi_1} &= -\frac{dy_2}{d\xi_2} \end{aligned}\right\}$$

The boundary conditions give eight equations and from them the condition for non-trivial solutions is found to be

$$\frac{m}{M} = \frac{\lambda}{2} \cdot \frac{H_1+\frac{1}{2}\theta^*\lambda^3 H_2}{H_3+\frac{1}{2}\theta^*\lambda^3 H_4} \qquad \ldots\ldots\ldots\ldots \quad 34.1$$

where

$$\left.\begin{aligned} H_1 &= \operatorname{tg}\varphi \cot\psi(\operatorname{tg}\operatorname{h}\varphi+\cot\operatorname{h}\psi)+\operatorname{tg}\operatorname{h}\varphi\cot\operatorname{h}\psi(\operatorname{tg}\varphi-\cot\psi) \\ H_2 &= (\operatorname{tg}\varphi-\operatorname{tg}\operatorname{h}\psi)(\cot\psi+\cot\operatorname{h}\psi) \\ H_3 &= (\cot\psi-\operatorname{tg}\varphi)(\operatorname{tg}\operatorname{h}\varphi+\cot\operatorname{h}\psi) \\ H_4 &= -\operatorname{tg}\varphi+\operatorname{tg}\operatorname{h}\varphi+\cot\psi+\cot\operatorname{h}\psi \end{aligned}\right\}$$

and

$$\left.\begin{aligned} \varphi &= x_1\lambda \\ \psi &= x_3\lambda \end{aligned}\right\} \quad \theta^* = \frac{2\gamma I_p}{mL^2}$$

For a shaft without discs we have $M = 0$ and $\theta^* = 0$. Thus from eq. 34.1

$$H_3 = 0$$

giving

$$\cot\psi = \operatorname{tg}\varphi$$

or

$$\frac{\pi}{2}-\psi+s\pi = \varphi \quad (s = 0, 1, 2, 3\ldots)$$

and

$$\lambda = \pi+s\cdot 2\pi \quad (s = 0, 1, 2, 3\ldots)$$

This result coincides with that from Chapter 13 in [2]. Only the values for symmetrical deflections are obtained. Further we have from definitions that

$$\Omega^2 = \lambda^4 \cdot \frac{EI}{mL^3}$$

or

$$\Omega^2 = \frac{1}{\Lambda^{**}} \cdot \frac{EI}{ML^3}$$

where

$$\Lambda^{**} = \frac{m}{M\lambda^4} = f_1(x_1,\ \theta^*,\ \lambda)$$

We may also write

$$\frac{m}{M} = f_2(x_1,\ \theta^*,\ \lambda)$$

If the mass of the shaft and the gyroscopic effect of the disc are neglected we may write

$$\Omega^2 = \Omega_0^2 = \frac{1}{\Lambda_0} \cdot \frac{EI}{ML^3}$$

where Λ_0 is the elementary non-dimensional critical speed and

$$\Lambda_0 = f_3(x_1) = \tfrac{1}{6} \cdot x_1^2(3-4x_1)$$

Thus we have

$$\left.\begin{aligned} \frac{\Lambda^{**}}{\Lambda_0} &= \left(\frac{n_0}{n}\right)^2 = \frac{f_1(x_1,\ \theta^*,\ \lambda)}{f_3(x_1)} = f_4(x_1,\ \theta^*,\ \lambda) \\ \frac{m}{M} &= f_2(x_1,\ \theta^*,\ \lambda) \end{aligned}\right\} \quad \ldots\ldots \text{ 35.1}$$

By supposing that x_1 and θ^* are known the eqs 35.1 express the function

$$\frac{\Lambda^{**}}{\Lambda_0} = f\left(x_1,\ \theta^*,\ \frac{m}{M}\right) \quad \ldots\ldots\ldots\ldots \text{ 35.2}$$

in parameter form. These functions are drawn in the diagrams on page 36 up to and including page 42. The curves are drawn after values from calculations with the electronic computer *Alwac III E* in Gothenburg. The calculated values can be found in [5], Volume VIII.

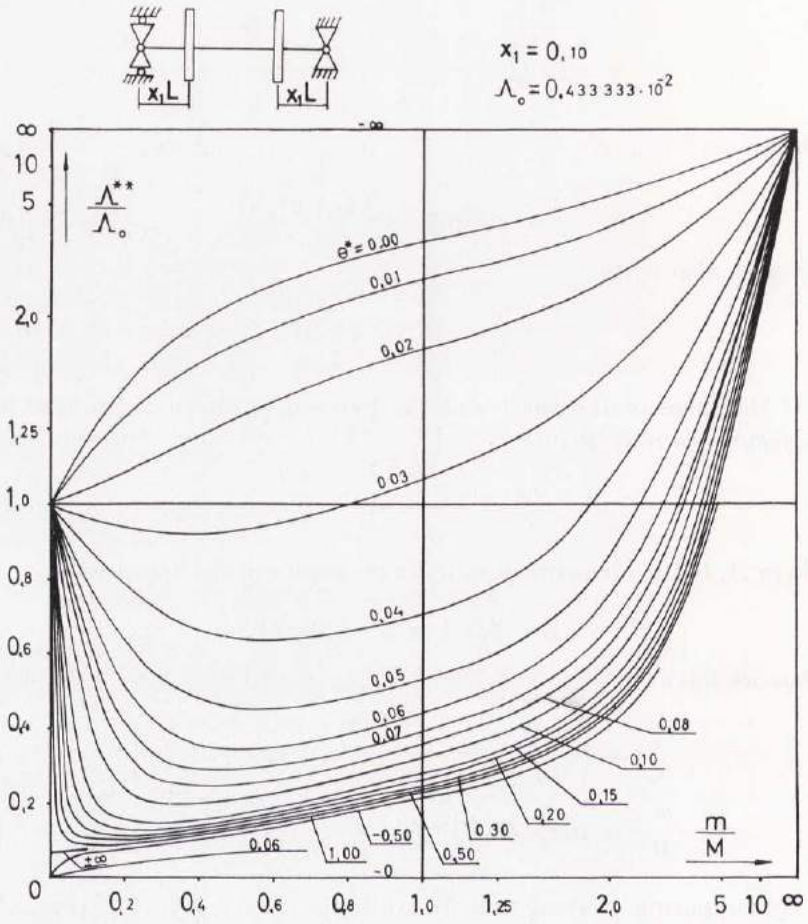
x1 L
x1 L
x1 = 0,10
Λo = 0,433 333 · 10^-2
Λ**/Λo
∞
10
5
2,0
1,25
1,0
0,8
0,6
0,4
0,2
0
-∞
θ* = 0,00
0,01
0,02
0,03
0,04
0,05
0,06
0,07
0,08
0,10
0,15
0,20
0,30
0,50
-0,50
1,00
0,06
±∞
-0
0,2
0,4
0,6
0,8
1,0
1,25
2,0
5
10
∞
m/M

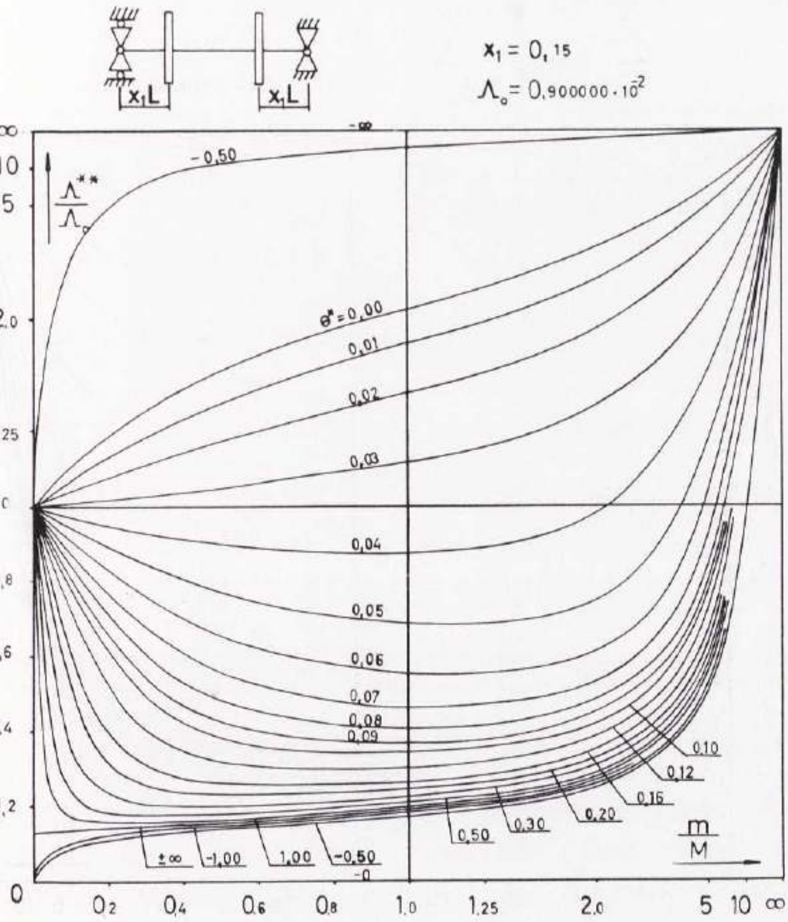

x₁L
x₁L
$x_1 = 0{,}15$
$\Lambda_o = 0{,}900000 \cdot 10^{-2}$
$\frac{\Lambda^{**}}{\Lambda_o}$
$-\infty$
$-0{,}50$
$\Theta^* = 0{,}00$
0,01
0,02
0,03
0,04
0,05
0,06
0,07
0,08
0,09
0,10
0,12
0,16
0,20
0,30
0,50
$\pm\infty$
-1,00
1,00
-0,50
-0
$\frac{m}{M}$
∞
10
5
2,0
1,25
1,0
0,8
0,6
0,4
0,2
0
0,2
0,4
0,6
0,8
1,0
1,25
2,0
5
10
∞

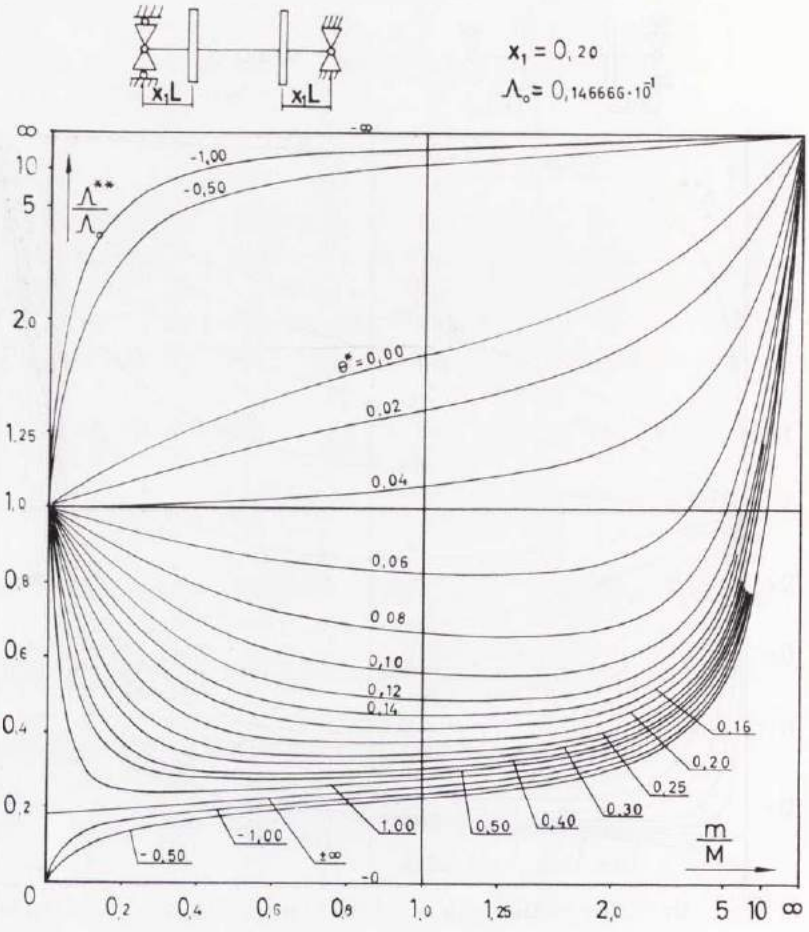
x1L
x1L
x1 = 0,20
Λo = 0,146666·10⁻¹
Λ**/Λo
-∞
∞
10
5
2,0
1,25
1,0
0,8
0,6
0,4
0,2
0
-1,00
-0,50
θ* = 0,00
0,02
0,04
0,06
0,08
0,10
0,12
0,14
0,16
0,20
0,25
0,30
0,40
0,50
1,00
±∞
-0
-0,50
-1,00
m/M
0,2
0,4
0,6
0,8
1,0
1,25
2,0
5
10
∞

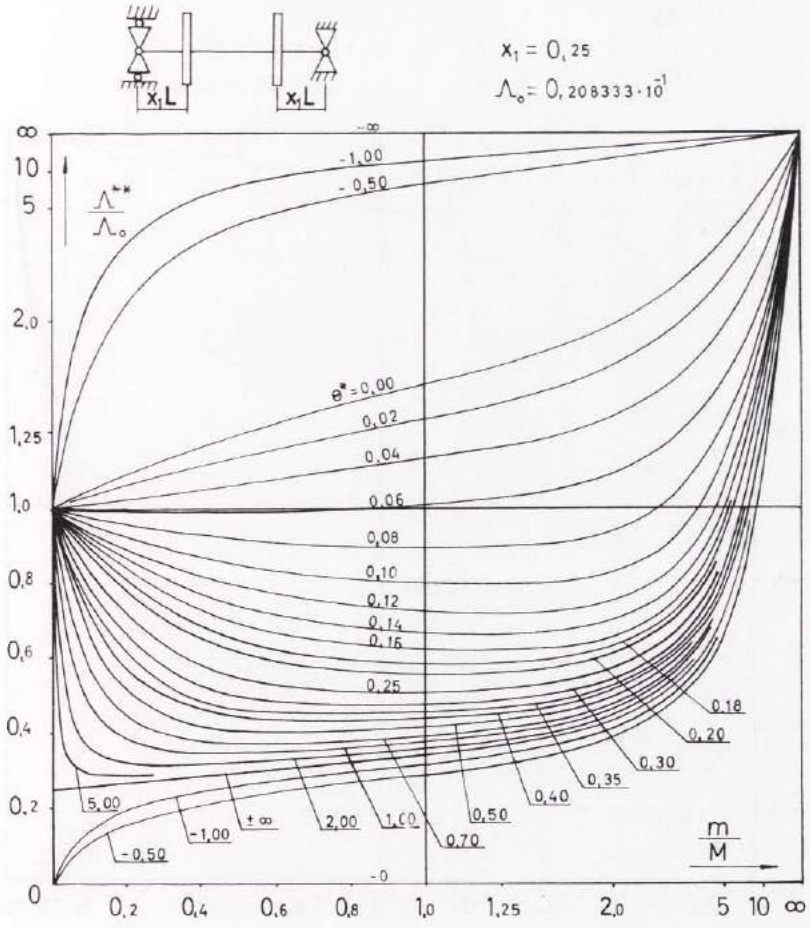
x1 L
x1 L
x1 = 0,25
Λ0 = 0,208333·10⁻¹
Λ**/Λ0
-1,00
-0,50
θ* = 0,00
0,02
0,04
0,06
0,08
0,10
0,12
0,14
0,16
0,25
0,18
0,20
0,30
0,35
0,40
0,50
0,70
1,00
2,00
±∞
-1,00
-0,50
5,00
-0
m/M
∞
10
5
2,0
1,25
1,0
0,8
0,6
0,4
0,2
0
0,2
0,4
0,6
0,8
1,0
1,25
2,0
5
10
∞

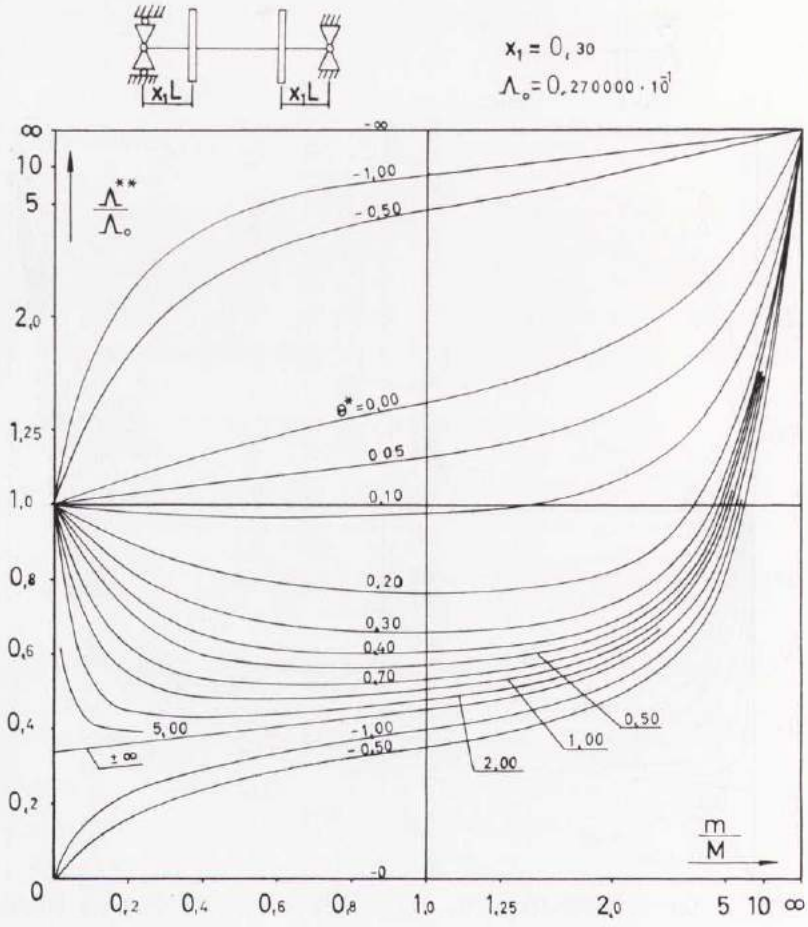
x1L
x1L
x1 = 0,30
Λo = 0,270000 · 10⁻¹
Λ**/Λo
-∞
-1,00
-0,50
θ* = 0,00
0,05
0,10
0,20
0,30
0,40
0,70
5,00
±∞
-1,00
-0,50
0,50
1,00
2,00
-0
m/M
∞
10
5
2,0
1,25
1,0
0,8
0,6
0,4
0,2
0
0,2
0,4
0,6
0,8
1,0
1,25
2,0
5
10
∞

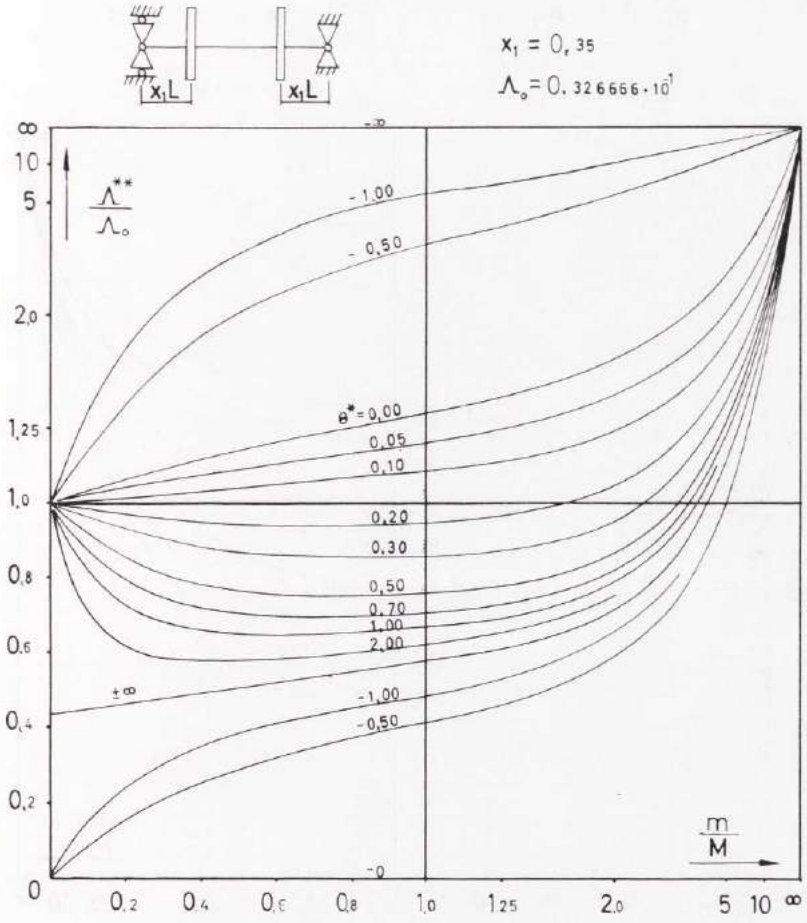
x1L
x1L
x1 = 0,35
Λo = 0.326666·10⁻¹
Λ**/Λo
-∞
-1,00
-0,50
θ* = 0,00
0,05
0,10
0,20
0,30
0,50
0,70
1,00
2,00
±∞
-1,00
-0,50
-0
m/M
∞
10
5
2,0
1,25
1,0
0,8
0,6
0,4
0,2
0
0,2
0,4
0,6
0,8
1,0
1,25
2,0
5
10
∞

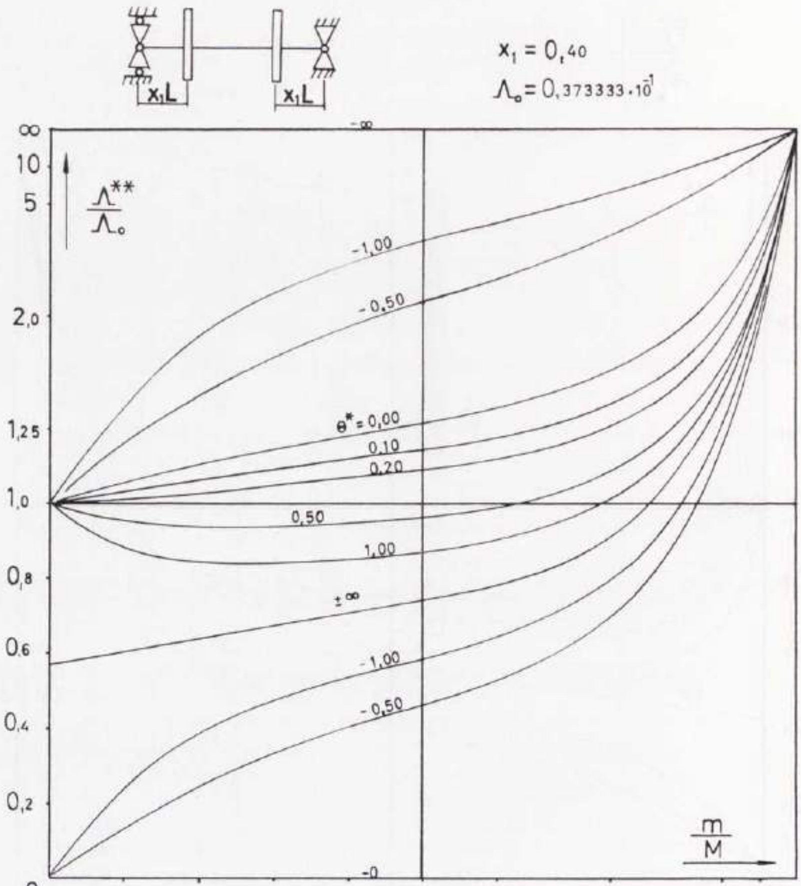
x₁L
x₁L
x₁ = 0,40
Λ₀ = 0,373333·10⁻¹
Λ**/Λ₀
m/M
∞
10
5
2,0
1,25
1,0
0,8
0,6
0,4
0,2
0
0,2
0,4
0,6
0,8
1,0
1,25
2,0
5
10
∞
-∞
-1,00
-0,50
θ* = 0,00
0,10
0,20
0,50
1,00
±∞
-1,00
-0,50
-0

7. Theoretical Tests of the "New Dunkerley Formula"

In Chapter 10 of [2] a "New Dunkerley formula" was proposed. It considers both the mass of the shaft and the gyroscopic effect from the discs. The eq. 114.1 in [2] gives

$$\Lambda^{**}_{\text{appr}} = \sum_{i=1}^{s} \mu_i \varkappa_i^3 \cdot \frac{\Lambda_i^{**}}{\Lambda_{0i}} \cdot \Lambda_{0i} \quad \ldots\ldots\ldots\ldots \quad 43.1$$

where

$$\left.\begin{aligned} \mu_i &= \frac{M_i}{M_{\text{ref}}} \\ \varkappa_i &= \frac{L_i}{L} \end{aligned}\right\}$$

Then Ω is calculated from

$$\Omega^2 = \frac{1}{\Lambda^{**}_{\text{appr}}} \cdot \frac{EI}{M_{\text{ref}} L^3}$$

The index appr refers to approximate. This formula is checked for the rotor in fig. 32.1. For that case eq. 43.1 can be written

$$\Lambda^{**}_{\text{appr}} = 2\Lambda_1^{**}$$

because of

$$\mu_1 = \mu_2 = 1, \text{ if } M_{\text{ref}} = M$$

and

$$\varkappa_i = 1 \quad (i = 1,\ 2)$$

Further, Λ_1^{**} can be found in [5], Volume II, or it can be determined from the diagrams in Chapter 11 of [2]. But in Chapter 6 of the present report the exact solution is obtained and the exact non-

dimensional critical speed is called $\Lambda^{**}_{\text{exact}}$. Against $\Lambda^{**}_{\text{appr}}$ and $\Lambda^{**}_{\text{exact}}$ the values N_{appr} and N_{exact} correspond and they denote the critical whirling velocity of the shaft in r.p.m. Thus

$$\frac{N_{\text{appr}}}{N_{\text{exact}}} = \sqrt{\frac{\Lambda^{**}_{\text{exact}}}{\Lambda^{**}_{\text{appr}}}}$$

An investigation is carried out for different values of x_1 and θ^*. The result is collected in the tables 45.1 and 45.2. Further, two limiting cases are studied. First, if $x_1 = 0{,}50$ we have $\frac{N_{\text{appr}}}{N_{\text{exact}}} = 1$. Second, if $\theta^* = m = 0$, the exact solution is

$$\Lambda^{**}_{\text{exact}} \ (\theta^* = 0, \ m = 0) = (\Lambda_0)_{\text{exact}}$$

where Λ_0 can be calculated from eq. 25.1 in [2]. With

$$\left.\begin{aligned} \xi_{11} &= \frac{x_1^2}{3}(1-x_1)^2 \\ \xi_{12} &= \tfrac{1}{6} \cdot x_1^2(1-2x_1^2) \end{aligned}\right\}$$

we get for the lowest critical speed

$$(\Lambda_0)_{\text{exact}} = \tfrac{1}{6} \cdot x_1^2(3-4x_1)$$

and with Dunkerley's usual formula

$$(\Lambda_0)_{\text{appr}} = \tfrac{2}{3} \cdot x_1^2(1-x_1)^2$$

Thus

$$\frac{(N_0)_{\text{appr}}}{(N_0)_{\text{exact}}} = \frac{\sqrt{3-4x_1}}{2(1-x_1)}$$

If $x_1 = \frac{1}{2}$ we get $\frac{(N_0)_{\text{appr}}}{(N_0)_{\text{exact}}} = 1$ and if $x_1 = 0$ we get $\frac{(N_0)_{\text{appr}}}{(N_0)_{\text{exact}}} = \frac{\sqrt{3}}{2} = 0{,}866$. Observe that if $x_1 = 0$ we have both $(N_0)_{\text{appr}}$ and $(N_0)_{\text{exact}}$ equal to zero but their ratio is $\frac{\sqrt{3}}{2}$.

We may conclude that the error in the approximate formula is small if the discs are far from the bearings and if the gyroscopic action is small.

$\frac{m}{M}$	θ^*											($x_1 = 0{,}10$)
	0			0,05			0,10			∞		
	Λ^{**}_{appr}	Λ^{**}_{exact}	$\frac{N_{appr}}{N_{exact}}$	Λ^{**}_{appr}	Λ^{**}_{exact}	$\frac{N_{appr}}{N_{exact}}$	Λ^{**}_{appr}	Λ^{**}_{exact}	$\frac{N_{appr}}{N_{exact}}$	Λ^{**}_{appr}	Λ^{**}_{exact}	$\frac{N_{appr}}{N_{exact}}$
0,02	0,005704	0,004520	0,890	0,005280	0,004153	0,886	0,004864	0,003799	0,885	0,000670	0,000336	0,709
0,05	0,006186	0,004807	0,881	0,005132	0,003888	0,870	0,004148	0,003023	0,852	0,000685	0,000341	0,705
0,10	0,007030	0,005284	0,866	0,005962	0,003476	0,764	0,003264	0,002069	0,796	0,000743	0,000351	0,688
1,00	0,024824	0,014320	0,758	0,011116	0,002295	0,454	0,007896	0,001386	0,419	0,005699	0,000977	0,414

Tab. 45.1

$\frac{m}{M}$	θ^*											($x_1 = 0{,}30$)
	0			0,05			0,10			∞		
	Λ^{**}_{appr}	Λ^{**}_{exact}	$\frac{N_{appr}}{N_{exact}}$	Λ^{**}_{appr}	Λ^{**}_{exact}	$\frac{N_{appr}}{N_{exact}}$	Λ^{**}_{appr}	Λ^{**}_{exact}	$\frac{N_{appr}}{N_{exact}}$	Λ^{**}_{appr}	Λ^{**}_{exact}	$\frac{N_{appr}}{N_{exact}}$
0,02	0,029768	0,027205	0,956	0,029651	0,027071	0,956	0,029560	0,026939	0,955	0,016840	0,009105	0,735
0,05	0,030340	0,027510	0,952	0,030075	0,027179	0,951	0,029809	0,026851	0,949	0,017079	0,009155	0,731
0,10	0,031292	0,028021	0,946	0,030770	0,027362	0,942	0,030248	0,026718	0,940	0,017498	0,009305	0,730
1,00	0,048908	0,037232	0,873	0,043589	0,031110	0,845	0,039680	0,026385	0,815	0,025069	0,012119	0,695

Tab. 45.2

8. Tests of a Rotor with Two Equal and Symmetrically Mounted Discs

In order to test the theoretical results in Chapter 6 the apparatus in fig. 64.2 of [3] was used. Two equal discs were mounted as fig. 32.1 shows. The rotational mode of the rotor was studied on the screen of an oscillograph. This method is outlined in Chapter 7 of [3]. It may be noticed that in these tests the whirling with $K = +\frac{1}{2}$ existed within a rather wide range for $x_1 = 0{,}20$ and $x_1 = 0{,}25$. The range decreased when x_1 increased. For comparison the critical speeds are calculated also with some other methods outlined previously. The notations are

n^{**} = critical speed of the shaft calculated from eq. 35.2

n^{*} = critical speed of the shaft calculated from eq. 59.1 in [2]. ("Exact" value by considering $m = 0$)

n_D^{**} = critical speed of the shaft calculated from an approximate formula 114.1 in [2]. ("New Dunkerley formula")

n_D = critical speed of the shaft calculated from eq. 112.2 in [2]. ("Usual" Dunkerley formula, which only can be properly used for $K = +\frac{1}{2}$)

n_0 = critical speed of the shaft, if $I_p = 0$ and $m = 0$.

x_1	$K=\frac{\omega}{\Omega}$	θ^*	Test values r.p.m.	n^{**} r.p.m.	n^* r.p.m.	n_D^{**} r.p.m.	n_D r.p.m.	n_0 r.p.m.
0,20	+1	+0,1087	988±32	965	995	864	845	911
0,25	+1	+0,1087	840±6	756	804	720	695	738
	−1	−0,3261	705±6	654	667	621	–	–
0,30	$+\frac{1}{2}$	0	354±10	329	336	312	–	–
	+1	+0,1087	717±3	677	690	636	645	672
	−1	−0,3261	657±3	611	620	587	–	–

Tab. 46.1

The results are shown in tab. 46.1. Observe that in the case $x_1 = 0,30$ the values of n_D and n_0 as a matter of fact are whirling speeds for the whirling $K = +\frac{1}{2}$, which gives no gyroscopic action for a rotor with thin discs.

All the time the values of n^* best fit to the testvalues which are always greater. The reason must be that in the tests the bearings had angular stiffnesses. These are not considered in the theory on this occasion. The shaft was supported in self-aligning ball bearings from SKF.

9. Investigation of a Perfectly Balanced Rotor

In this chapter the behaviour of a perfectly balanced rotor is treated. In Sec. 5,3 of [3] was shown that such a rotor whirls at its critical states with an indifferent position of the disc. Consider the perfectly balanced rotor in fig. 49.1. The mass of the shaft is neglected.

The equations of motion are

$$\left.\begin{aligned} M\ddot{y}+cy &= 0 \\ M\ddot{z}+cz &= 0 \end{aligned}\right\}$$

with the notations

M	Mass of the point mass
c	Spring constant of the shaft

and with the solutions

$$\left.\begin{aligned} y &= A_1 \sin \Omega_n t + B_1 \cos \Omega_n t \\ z &= A_2 \sin \Omega_n t + B_2 \cos \Omega_n t \end{aligned}\right\}$$

where

$$\Omega_n = \sqrt{\frac{c}{M}} \quad \ldots\ldots\ldots\ldots\ldots\ldots \quad 48.1$$

and A_1, B_1, A_2, and B_2 are arbitrary constants.

From here

$$(A_2^2+B_2^2)y^2+(A_1^2+B_1^2)z^2-2(A_1A_2+B_1B_2)yz-(A_1B_2-A_2B_1)^2 = 0$$

and this equation can mean

$$\left.\begin{aligned} &1) \text{ an ellips} \\ &2) \text{ a circle} \\ &3) \text{ a straight line} \end{aligned}\right\} \quad \ldots\ldots\ldots\ldots\ldots\ldots \quad 48.2$$

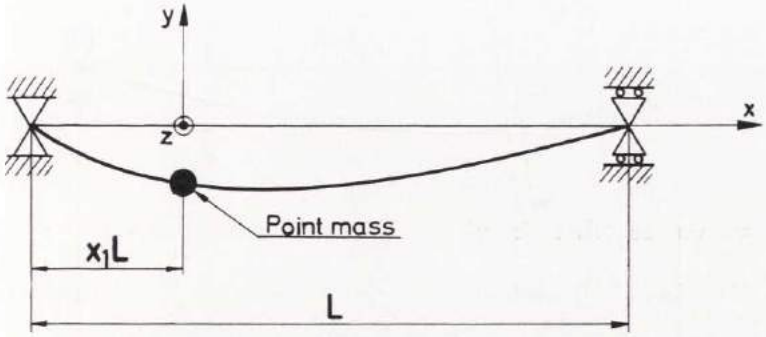

Fig. 49.1

and the kind of the whirl figure is determined by the boundary conditions. In case 3 we get lateral oscillations in one direction and in the first two cases in two directions simultaneously. Observe that the speed of the motor has no influence on the behaviour of the rotor.

The expression 48.1 can also be written

$$\frac{cr^2}{2} = \frac{M(r\Omega_n)^2}{2} \qquad \text{49.2}$$

where r is an arbitrary constant radial deflection of the shaft at the mass. On the left hand we have the expression for the potential energy and on the right hand the expression for the kinetic energy. Thus we have shown that in a perfectly balanced point-mass-rotor the kinetic energy E_{kin} is equal to the potential energy E_{pot}. The total energy is $(E_{tot})_{rot}$ where

$$(E_{tot})_{rot} = E_{kin} + E_{pot} = 2E_{kin} = 2E_{pot}$$

However, there is another possibility to enterprete eq. 49.2. At the steady whirling with the constant shaft deflection r the mass is affected by the "centrifugal force" $F = Mr\Omega_n^2$.

Then look at a beam affected by the force F. The potential energy in the beam is

$$E_{pot} = \frac{Fr}{2} = \frac{M(r\Omega_n)^2}{2}$$

Thus eq. 49.2 can also be looked upon as two ways to write the potential energy of the shaft.

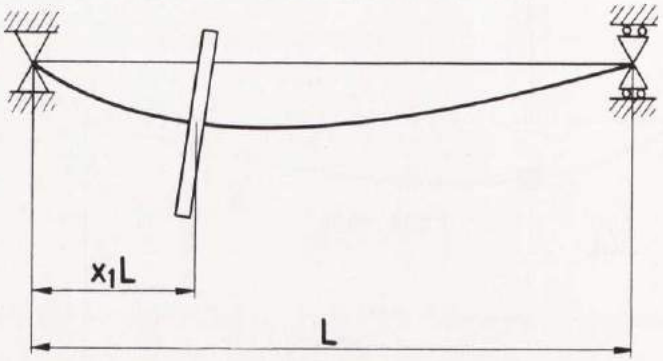

Fig. 50.1

If, instead, we turn over to case 3) in 48.2 we can interprete eq. 49.2 in the following way.

Suppose that the lateral oscillation has its maximum deflection equal to r. Then $\frac{cr^2}{2}$ represents the total energy $(E_{tot})_{osc}$ at the maximum deflection and $\frac{1}{2} \cdot M(r\Omega_n)^2$ represents the same thing at zero deflection. Thus

$$(E_{tot})_{osc} = \tfrac{1}{2} \cdot (E_{tot})_{rot}$$

Now consider the rotor in fig. 50.1 where the point mass is replaced by a disc.

The rotor is whirling with the angular velocity $\Omega \frac{\text{rad}}{\text{s}}$ and at the same time the motor speed is $\omega \frac{\text{rad}}{\text{s}}$. The shaft deflection is r and it has already been shown in [2] that the shaft is subjected to a bending moment due to the gyroscopic effect. For this rotor the kinetic energy can be written

$$E_{kin} = \tfrac{1}{2}(I_\xi \omega_\xi^2 + I_\eta \omega_\eta^2 + I_\zeta \omega_\zeta^2)$$

where all notations can be seen in Chapter 7 of [2]. Thus

$$2E_{kin} = (I_e + Ma^2)(\Omega \sin \alpha \cos \omega' t)^2 + (I_e + Ma^2)(-\Omega \sin \alpha \sin \omega' t)^2 + \\ + I_p(\Omega \cos \alpha + \omega')^2$$

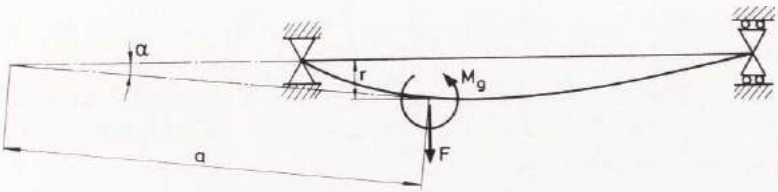

Fig. 51.1

and

$$\omega' = \omega - \Omega$$

and these expressions can be simplified to

$$2E_{kin} = (I_e + Ma^2)\Omega^2 \sin^2\alpha + I_p[\Omega(\cos\alpha - 1) + \omega]^2$$

If α is a small angle we have $\sin\alpha \cong \alpha$, $(\cos\alpha - 1) \cong -\frac{\alpha^2}{2}$ and thus, by putting $r = a\sin\alpha$,

$$E_{kin} = \tfrac{1}{2} \cdot I_p\omega^2 + \tfrac{1}{2} \cdot M(r\Omega)^2 - \gamma I_p\Omega^2\alpha^2 \quad \ldots\ldots\ldots \quad 51.2$$

$$\left[\gamma = \frac{1}{2}\left(\frac{\omega}{\Omega} - \frac{1}{2}\right)\right]$$

The shaft is subjected to the force $F = Mr\Omega^2$ and the gyroscopic moment $M_g = 2\gamma I_p\Omega^2\alpha$ which is shown in fig. 51.1.

The elastic energy in the shaft according to fig. 51.1 can be written

$$E_{pot} = \tfrac{1}{2} \cdot Fr - \tfrac{1}{2} \cdot M_g\alpha$$

or

$$E_{pot} = \tfrac{1}{2} \cdot M(r\Omega)^2 - \gamma I_p\Omega^2\alpha^2 \quad \ldots\ldots\ldots\ldots \quad 51.3$$

By differentiating the eqs 51.2 and 51.3 we get

$$dE_{kin} = dE_{pot} = Mr\Omega dr - 2\gamma I_p\Omega^2\alpha d\alpha$$

which means that the change in the kinetic energy when the rotor changes its position (r_1, α_1) to another (r_2, α_2) is equal to the change in the potential energy. The total energy is E_{tot}, where

$$E_{tot} = E_{kin} + E_{pot} = \tfrac{1}{2} \cdot I_p\omega^2 + 2\{\tfrac{1}{2} \cdot M(r\Omega)^2 - \gamma I_p\Omega^2\alpha^2\} \quad \ldots\ldots \quad 51.4$$

As has been pointed out previously the shaft may have any position. But the eq. 51.4 shows that the total energy changes with the position. If the shaft shall change its position additional energy has to be put into the rotor. This work cannot be supplied from the motor, because (see [3])

$$M_{in} = cer \sin \theta$$

and for a perfectly balanced rotor $e = 0$. The necessary amount of energy therefore must be delivered by outer forces acting on the disc. Suppose that on the rotor in fig. 49.1 a tangential force K_φ is applied at the point mass. From the eq. 19.1 in [3] it is clear that

$$\left.\begin{aligned} \ddot{r} + r(\Omega_n^2 - \dot{\varphi}^2) &= 0 \\ r\ddot{\varphi} + 2\dot{r}\dot{\varphi} &= \frac{K_\varphi}{M} \end{aligned}\right\} \quad \ldots\ldots\ldots\ldots\ldots\ldots \quad 52.1$$

Now we seek such a force K_φ which at $\dot{\varphi} = \Omega_n$ changes the deflection of the shaft from $r = 0$ to $r = r_1$. We get from the first eq. in 52.1

$$\left.\begin{aligned} \ddot{r} &= 0 \\ \dot{r} &= C_1 \\ r &= C_1 t + C_2 \end{aligned}\right\} \quad \ldots\ldots\ldots\ldots\ldots\ldots \quad 52.2$$

Here we have $C_1 = \text{const.}$ and due to the boundary condition $C_2 = 0$. From the second eq. in 52.1 we have $K_\varphi = 2\Omega_n C_1 M$ and from the third eq. of 52.2 $r = \dfrac{C_1}{\Omega_n} \cdot \varphi$ which means an Archimedes' spiral. The tangential force delivers the energy $E_\varphi = \int_0^{(r_1)} K_\varphi (r\Omega_n dt) = M(r_1\Omega_n)^2$. The total energy E_{tot} can be written $E_{\text{tot}} = E_\varphi = M(r_1\Omega_n)^2$.

As the kinetic energy is $E_{\text{kin}} = \dfrac{M(r_1\Omega_n)^2}{2}$ we get also in this way that the kinetic energy is equal to the potential energy.

Thus it has been shown how through a constant tangential force K_φ the rotor changes its deflection from zero to an arbitrary value at a constant whirling velocity.

Summarizing, we have shown the following facts for a perfectly balanced rotor at any critical state:

1) The disc may have any radial position.

2) An outer force is needed for changing the radial position of the disc.

3) The motor cannot deliver energy to change the radial deflection.

4) Without disturbances the shaft runs at its critical speed with zero deflection. In this case this speed presents no danger at all.

5) As disturbances occur they settle the size of the shaft deflection.

6) The change in kinetic energy is equal to the change in potential energy when the disc changes its position.

10. Summary

During some years research work on critical speeds has been carried out at the Institute of Machine Elements, Chalmers University of Technology, Gothenburg. Three reports are previously published, viz. [2], [3], and [4]. The present report deals with some special questions and is a supplement to the previous reports.

Chapter 3 gives the solution to the problem of calculating the critical speeds for a clamped-free rotor with one disc considering the gyroscopic effects from both the shaft and the disc and the mass of the shaft simultaneously. The general solution is specialized to a shaft without disc.

Chapter 4 analyzes the effect of bearing angular stiffness on the critical speed. The results are shown in diagrams for quick computation in practical cases.

Chapter 5 gives some experimental data on the measurements of critical speeds for a rotor supported by SKF bearings as well as journal bearings.

Chapter 6 is concerned with the problem of determining the critical speeds for a rotor with two equal discs symmetrically mounted. The influence of the simultaneous action of the mass of the shaft and the gyroscopic effect of the discs is taken into consideration. Diagrams over the results are drawn and they are meant as a tool for the engineer in practice to compute the critical speeds for this rotor in an accurate but still rapid way.

Chapter 7 deals with theoretical studies of the "New Dunkerley Formula" presented in [2]. This approximate formula is checked in cases exactly computed for the rotor treated in Chapter 6.

Chapter 8 contains results from tests with the rotor considered in Chapter 6.

Chapter 9 treats the properties of a perfectly balanced rotor. Some remarkable results concerning the energy of the rotor are derived.

11. References

1. Dimentberg, F. M.: Flexural Vibrations of Rotating Shafts. Butterworths, London, 1961.
2. Fernlund, I.: Critical Speeds of a Shaft with Thin Discs. Transactions of Chalmers University of Technology, Gothenburg, Sweden, 1962.
3. Fernlund, I.: On the Whirling of a Rotor. Transactions of Chalmers University of Technology, Gothenburg, Sweden, 1963.
4. Fernlund, I.: Running Through the Critical Speed of a Rotor. Transactions of of Chalmers University of Technology, Gothenburg, Sweden, 1963.
5. Fernlund, I.: Tables for Calculating Critical Speeds of a Shaft with Thin Discs, Volume I, II, . . . VIII. (Available only at the Library of Chalmers University of Technology, Gothenburg, Sweden).
6. Grammel, R.: Der Kreisel. Springer-Verlag, 1950.
7. Palmgren, A.: Ball and Roller Bearing Engineering. Philadelphia, 1959.

Forts. fr. omsl. 2:dra sida

229. Granholm, Hjalmar, *Le problème de Boussinesq.* 15 s. 1960. Kr. 3: 50. (Avd. Väg- och Vattenbyggnad. Byggnadsteknik. 34.)
230. Hiba, Miodrag, et Cedervall, Krister, *Flambement élastique d'une barre en bois lamellée et clouée avec le module de déplacement du moyen de liaison constant k.* 22 s. 1960. Kr. 5: —. (Avd. Väg- och Vattenbyggnad. Byggnadsteknik. 35.)
231. Floberg, Leif, *The optimum thrust tilting-pad bearing.* 23 s. 1960. Kr. 5: —. (Avd. Maskinteknik. 19.)
232. Floberg, Leif, *The two-groove journal bearing, considering cavitation.* 32 s. 1960. Kr. 6: —. (Avd. Maskinteknik. 20.)
233. Hedvall, J. Arvid, *Heterogeneous catalysis, results and projects for research.* 18 s. 1961. Kr. 5: —. (Avd. Kemi och Kemisk Teknologi. 36.)
234. Floberg, Leif, *Lubrication of two cylindrical surfaces, considering cavitation.* 36 s. 1961. Kr. 10: —. (Avd. Maskinteknik. 21.)
235. Floberg, Leif, *Attitude-eccentricity curves and stability conditions of the infinite journal bearing.* 43 s. 1961. Kr. 11: —. (Avd. Maskinteknik 22.)
236. Ben-Yair, M. P., *Thermometric titrations of zinc, cadmium and mercuric salts.* 11 s. 1961. Kr. 3: —. (Avd. Kemi och Kemisk Teknologi. 37.)
237. Sandford, F., Liljegren, B., and Jonsson, B., *The resistance of bricks towards frost experiments and considerations.* 20 s. 1961. Kr. 5: —. (Avd. Kemi och Kemisk Teknologi. 38.)
238. Floberg, Leif, *Experimental investigation of cavitation regions in journal bearings.* 28 s. 1961. Kr. 6: —. (Avd. Maskinteknik. 23.)
239. Granholm, Hjalmar, *Sandöbrons bågställning.* 128 s. 1961. Kr. 20: —. (Avd. Väg- och Vattenbyggnad. Byggnadsteknik. 36.)
240. Lindblad, Anders, *On the design of lines for merchant ships.* 125 s. Kr. 20: —. (Avd. Skeppsbyggeri. 7.)
241. Lundén, Arnold, *Self diffusion and the structure of molten salts.* 14 s. Kr. 4: —. (Avd. Allm. Vetenskaper. 17.)
242. Larsson, Lars-Erik, *Sprickbildning i vattenledningsrör av förspänd betong.* 70 s. 1961. Kr. 15: —. (Avd. Väg- och Vattenbyggnad. Byggnadsteknik. 37.)
243. Asplund, S. O., *A unified analysis of indeterminate structure.* 36 s. 1961. Kr. 8: —. (Avd. Väg- och Vattenbyggnad. Byggnadsteknik. 38.)
244. Braunstein, A., *The magnetic field in iron with variable permeability.* 11 s. 1961. Kr. 3: —. (Avd. Elektroteknik. 69.)
245. Fernlund, Ingemar, *A method to calculate the pressure between bolted or riveted plates.* 126 s. 1961. Kr. 25: —. (Avd. Maskinteknik. 24.)
246. Hedvall, J. Arvid, and Karamustafaoğlu, Vural, *On the conservation of ancient alabaster objects.* 19 s. 1961. Kr. 5: —. (Avd. Kemi och Kemisk Teknologi. 39.)
247. Ekelöf, Stig, *A theory of the eddy current equivalent winding and its application to the closing of non-delayed telephone relays.* 35 s. 1961. Kr. 7: —. (Avd. Elektroteknik. 70.)
248. Cederwall, Krister, *Beräkning av spikade konstruktioner med hänsyn till förbandens deformationsegenskaper.* 52 s. 1961. Kr. 10: —. (Avd. Väg- och Vattenbyggnad. Byggnadsteknik. 39.)
249. Kärrholm, Gunnar, and Samuelsson, Alf, *Bridge slabs with edge-beams.* 73 s. 1961. Kr. 15: —. (Avd. Väg- och Vattenbyggnad. Byggnadsteknik. 40.)
250. Losberg, Anders, *Design methods for structurally reinforced concrete pavements.* 143 s. 1961. Kr. 30: —. (Avd. Väg- och Vattenbyggnad. Byggnadsteknik. 41.)
251. Ekelöf, Stig, *Primärnormalerna för resistans och spänning vid CTH's institution för elektricitetslära och elektrisk mätteknik.* 20 s. 1961. Kr. 4: —. (Avd. Elektroteknik 71.)
252. Åkesson, Bengt Å., *Rationalization of Lévy's plate solution.* 135 s. 1961. Kr. 25: —. (Avd. Väg- och Vattenbyggnad. Byggnadsteknik. 42.)
253. Brogren, Gösta, *A double-crystal spectrometer for work in vacuum region.* 19 s. 1961. Kr. 4 —. (Avd. Allm. Vetenskaper. 18.)
254. Kihlman, Tor, *Flanktransmissionens inverkan på rumsisolering mot luftljud.* 69 s. 1961. Kr. 14: —. (Avd. Väg- och Vattenbyggnad. Byggnadsteknik. 43.)
255. Svensson, S. Ivar, *The influence of cam curve derivative steps on cam dynamical properties.* 93 s. 1961. Kr. 25: —. (Avd. Maskinteknik. 25.)
256. Hult, Jan, *Mechanics of a beam subject to primary creep.* 20 s. 1962. Kr. 5: —. (Avd. Allm. Vetenskaper. 19.)
257. Sandford, Folke, and Hedvall, J. Arvid, *Concerning the cause of the colour of an amazonite preparation.* 8 s. 1962. Kr. 3: —. (Avd. Kemi och Kemisk Teknologi. 40.)
258. Nilsson, Jan, *On the structure of weak interactions.* 66 s. 1962. Kr. 15: —. (Avd. Allm. Vetenskaper. 20.)
259. Ström, Lars, *An absolute anemometer.* 22 s. 1962. Kr. 6: —. (Avd. Maskinteknik. 26.)

Forts. å omsl. 4:de sida

Forts. fr. omsl. 3:dje sida

260. FERNLUND, INGEMAR, *Critical speeds of a shaft with thin discs.* 224 s. 1962. Kr. 50: —. (Avd. Maskinteknik. 27.)
261. FERNLUND, INGEMAR, *On solving Reynold's equation for bearings of finite width with Fourier sine transforms.* 28 s. 1962. Kr. 7: —. (Avd. Maskinteknik. 28.)
262. AURELL, CARL G., *Physical equations from the conceptual point of view.* 52 s. 1962. Kr. 12: 50. (Avd. Elektroteknik. 72.)
263. SMITH, BENGT, *Investigation of reagents for the qualitative analysis of phenols.* 51 s. 1963. Kr. 12: 50. (Avd. Kemi och Kemisk Teknologi. 41.)
264. HULT, JAN, *Primary creep in thickwalled spherical shells.* 26 s. 1963. Kr. 8: —. (Avd. Allm. Vetenskaper. 21.)
265. STRINDEHAG, OVE, *Optimized performance of the vidicon.* 58 s. 1963. Kr. 15: —. (Avd. Elektroteknik. 73.)
266. DUBOIS, J., *An investigation of the* S^{34} (p, γ) Cl^{35}*-reaction.* 32 s. 1963. Kr. 8: —. (Avd. Allm. Vetenskaper. 22.)
267. DUBOIS J., AND ALBINSSON H., *Radiative proton capture in* Ca^{44}. 22 s. 1963. Kr. 6: —. (Avd. Allm. Vetenskaper. 23.)
268. DUBOIS, J., AND BROMAN L., *The* Ca^{42} (p, γ) Sc^{43} *reaction and the decay of* Sc^{43}. 31 s. 1963. Kr. 8: —. (Avd. Allm. Vetenskaper. 24.)
269. DUBOIS, J., *Low energy excited levels in some vanadium isotopes.* 28 s. 1963. Kr. 8: —. (Avd. Allm. Vetenskaper. 25.)
270. DUBOIS, J., *The ion beam energy stabilization system of the Van de Graaff generator at Gothenburg.* 16 s. 1963. Kr. 5: —. (Avd. Allm. Vetenskaper. 26.)
271. HEDVALL, J. ARVID, *Surface chemistry and corrosion.* 18 s. 1963. Kr. 6: —. (Avd. Kemi och Kemisk Teknologi. 42.)
272. HEDVALL, J. ARVID, *The chemistry of cement and concrete considered as a facet of the reactivity of solids.* 18 s. 1963. Kr. 6: —. (Avd. Kemi och Kemisk Teknologi. 43.)
273. ASPLUND, SVEN OLOF, *Practical calculation of suspension bridges.* 27 s. 1963. Kr. 8: —. (Avd. Väg- och Vattenbyggnad. Byggnadsteknik. 44.)
274. GRANHOLM, HJALMAR, *Träkonstruktioners brandstabilitet. Symposium vid Chalmers Tekniska Högskola den 18 juni 1962.* 151 s. 1963. Kr. 25: —. (Avd. Väg- och Vattenbyggnad. Byggnadsteknik. 45.)
275. ALBERTSSON, ÅKE, *Vindtryck på skorstenar.* 70 s. 1963. Kr. 18: —. (Avd. Väg- och Vattenbyggnad. Byggnadsteknik. 46.)
276. FERNLUND, INGEMAR, *On the whirling of a rotor.* 83 s. 1963. Kr. 20: —. (Avd. Maskinteknik. 29.)
277. FERNLUND, INGEMAR, *Running through the critical speed of a rotor.* 86 s. 1963. Kr. 22:50. (Avd. Maskinteknik. 30.)

Pris kronor 12: — ELANDERS BOKTRYCKERI AKTIEBOLAG
GÖTEBORG 1963